

# On the classification of time series and cross wavelet phase variance.

by

Marc Pienaar

Thesis Presented for the Degree of

DOCTOR OF PHILOSOPHY

in the

Faculty of Engineering and the Built Environment

Department of Electrical Engineering

UNIVERSITY OF CAPE TOWN

Supervisor: Dr Fred Nicolls

June 2016

The copyright of this thesis vests in the author. No quotation from it or information derived from it is to be published without full acknowledgement of the source. The thesis is to be used for private study or non-commercial research purposes only.

Published by the University of Cape Town (UCT) in terms of the non-exclusive license granted to UCT by the author.

# Declaration of Authorship

I, MARC PIENAAR, declare that this thesis titled, ‘On the classification of time series and cross wavelet phase variance’ and the work presented in it are my own. I confirm that:

- This work was done wholly or mainly while in candidature for a research degree at this University.
- Where any part of this thesis has previously been submitted for a degree or any other qualification at this University or any other institution, this has been clearly stated.
- Where I have consulted the published work of others, this is always clearly attributed.
- Where I have quoted from the work of others, the source is always given. With the exception of such quotations, this thesis is entirely my own work.
- I have acknowledged all main sources of help.
- Where the thesis is based on work done by myself jointly with others, I have made clear exactly what was done by others and what I have contributed myself.

Signed:



---

Date: June 2016

---

*“Reading made Don Quixote a gentleman. Believing what he read made him mad.”*

George Bernard Shaw

UNIVERSITY OF CAPE TOWN

# *Abstract*

Faculty of Engineering and the Built Environment  
Department of Electrical Engineering

Doctor of Philosophy

by Marc Pienaar

The continuous wavelet transform (CWT) is arguably one of the best tools to explore underlying characteristic features of time series data. Its application in large time series classification experiments, however, has been severely limited due to the large amount of redundant associated information. By extending the capabilities of the CWT to perform cross wavelet analysis (CWA), common frequency behaviour between two time series is highlighted, and the potential to extract amplitude modulated (AM) and frequency modulation (FM) characteristics in an automated way is possible. Characterisation of AM is relatively straightforward and can be resolved by any number of Euclidean based techniques in both the time and frequency domains. FM on the other hand, is somewhat more difficult as it transcends multiple wavelet scales. In this study, linear combinations of scales are used to extract both AM similarity (derived from global wavelet power spectra) and FM coherency, using a new method developed called cross wavelet phase variance (CWPV). The methodology is applied to large scale classification problems (using benchmark time series), in which the method clearly outperforms other common distance-based measures. Lastly, the approach provides a powerful framework in which AM and FM characteristics common between time series can be explicitly mapped to their corresponding scales, and with some initial optimisation, can be applied to any classification problem.

# *Acknowledgements*

A PhD is a task that needs funding, time, and dedication. On the funding side, I was fortunate enough to have parts funded by my organisation; other parts funded by my parents, but also self-funded parts. On the time (and support) side, my family gets the biggest thanks — my wife Fiona and daughters Imogen and Jane often made weekends available or sacrificed school holidays to allow ‘PhD’ time. In a similar way my parents (Fay and Jacus) and Fiona’s parents (Bev and Bob) were also instrumental by helping to look after children, provide advice (where possible), and simply by providing continued support and encouragement. On the dedication side, some thanks must go to initial supervisors and study advisors: Dr Jon Tapson, Dr Stephan Woodborne, and Dr Terrence Van Zyl, but by far the biggest thanks go to Fred. Dr Fred Nicolls played a major role in getting this thesis out the door, at some point during the study he adopted me as a student, and in doing so took on the role of study supervisor. He helped formalise thoughts and ideas into a publishable and worthy study and took on the task of editor. Lastly, to all those, including work colleagues who motivated me with persuasive words of encouragement such as “Get the bloody thing done!”.

# Contents

<b>Declaration of Authorship</b>	<b>i</b>
<b>Abstract</b>	<b>iii</b>
<b>Acknowledgements</b>	<b>iv</b>
<b>Figures</b>	<b>viii</b>
<b>Tables</b>	<b>xiii</b>
<b>Information Boxes</b>	<b>xv</b>
<b>Abbreviations</b>	<b>xvi</b>
<b>Notation</b>	<b>xviii</b>
<b>1 Introduction</b>	<b>1</b>
1.1 Motivation . . . . .	1
1.2 Aim . . . . .	2
1.3 Structure of this thesis . . . . .	3
1.4 Conclusion . . . . .	5
<b>2 Before we begin</b>	<b>6</b>
2.1 Overview . . . . .	7
2.2 Preliminaries and modern notation . . . . .	7
2.3 Historical antecedents . . . . .	9
2.3.1 Setting the scene . . . . .	9
2.3.2 Genesis of trigonometric series . . . . .	11
2.3.2.1 ‘Vibrating Strings’ . . . . .	12
2.4 The Fourier series . . . . .	13
2.5 The origins of wavelets . . . . .	15
2.6 Conclusion . . . . .	17

---

<b>3</b>	<b>Mathematical background to wavelets</b>	<b>18</b>
3.1	Overview . . . . .	19
3.2	The Fourier transform (FT) . . . . .	19
3.2.1	The discrete Fourier transform (DFT) . . . . .	21
3.2.2	The fast Fourier transform (FFT) . . . . .	24
3.2.3	The short time Fourier transform (STFT) . . . . .	26
3.2.4	Sampling and other considerations . . . . .	27
3.3	The wavelet transform (WT) . . . . .	32
3.3.1	The continuous wavelet transform (CWT) . . . . .	34
3.3.2	The discrete wavelet transform (DWT) . . . . .	39
3.3.3	The wavelet power spectrum . . . . .	41
3.3.4	The cross wavelet spectrum . . . . .	44
3.4	Worked examples of the CWT . . . . .	46
3.5	Conclusion . . . . .	58
<b>4</b>	<b>Background to time series classification</b>	<b>59</b>
4.1	Overview . . . . .	60
4.1.1	Before we begin: the birth of machine learning . . . . .	60
4.2	The data mining process . . . . .	66
4.2.1	Preprocessing methods . . . . .	66
4.2.2	Classification . . . . .	70
4.2.3	Examples of Euclidean-based techniques . . . . .	73
4.2.4	Examples of high level representation techniques . . . . .	77
4.3	Concluding remarks . . . . .	80
<b>5</b>	<b>Methodology: matching similarities using cross wavelet analysis</b>	<b>82</b>
5.1	Introduction . . . . .	83
5.2	Method . . . . .	84
5.2.1	The CWPV term . . . . .	86
5.3	Defining the similarity framework . . . . .	87
5.4	Worked example to calculate CWS . . . . .	92
5.5	Conclusion . . . . .	98
<b>6</b>	<b>Experiments, results, and discussion</b>	<b>99</b>
6.1	Introduction . . . . .	100
6.2	Data . . . . .	101
6.3	Experiment one . . . . .	102
6.3.1	Aim . . . . .	102
6.3.2	Method . . . . .	104
6.3.3	Results . . . . .	107
6.3.4	Analysis and discussion . . . . .	111
6.4	Experiment two . . . . .	115
6.4.1	Aim . . . . .	117
6.4.2	Method . . . . .	117
6.4.3	Results . . . . .	117



---

6.4.4	Analysis and discussion . . . . .	123
6.5	Conclusion . . . . .	139
<b>7</b>	<b>Conclusion</b>	<b>140</b>
<b>A</b>	<b>UCR data summary</b>	<b>143</b>
A.1	UCR data examples . . . . .	143
<b>B</b>	<b>Experiment two summary of parameterisation</b>	<b>156</b>
B.1	Summary of the CWS, CWPV, and CWED parameterisation . . . . .	156
<b>C</b>	<b>Experiment two summary of the training and test results</b>	<b>237</b>
C.1	Summary of the CWS, CWPV, and CWED training and test results . . .	237
<b>D</b>	<b>Source code listings</b>	<b>249</b>
D.1	Code examples . . . . .	250
<b>E</b>	<b>Application papers</b>	<b>289</b>
E.1	A new approach to finding similarities between time series using Cross Wavelet Phase Variance . . . . .	289
	<b>Bibliography</b>	<b>296</b>

# Figures

1.1	Schematic of main topics discussed in this thesis . . . . .	5
3.1	Radix-2 FFT interlaced decomposition using BIT reversal . . . . .	25
3.2	Comparison between the STFT and the wavelet transform in the time frequency plane . . . . .	29
3.3	Example of an alias signal . . . . .	30
3.4	Example of the Gibbs effect . . . . .	31
3.5	Example of spectral leakage . . . . .	33
3.6	Morlet wavelet and its Fourier transform . . . . .	35
3.7	Example of the Haar wavelet . . . . .	41
3.8	Tree of DWT coefficients . . . . .	42
3.9	Comparison between time and frequency convolutions using the Morlet wavelet with $\omega_0 = 2\pi$ . . . . .	43
3.10	Comparison between the CWT using a Morlet wavelet with $\omega_0 = 2\pi$ with 4 and 30 voices. . . . .	44
3.11	Example of the continuous wavelet transform (CWT), and the cross wavelet modulus and phase . . . . .	45
3.12	Worked example of the Morlet wavelet. . . . .	51
3.13	Scaled and translated example of the Morlet wavelet. . . . .	52
3.14	Fourier transform of the Morlet wavelet using a Heaviside step function. . . . .	53
3.15	Signal comprising 5Hz, 10Hz and 25Hz components . . . . .	54
3.16	CWT worked example generated using Equation (3.26) (p. 38). . . . .	55
3.17	CWT worked example generated using the FFT of the Morlet wavelet. . . . .	56
3.18	CWT worked example generated using the time convolution of the Morlet wavelet. . . . .	57
4.1	Graphic representation of the one-to-one Euclidean distance mapping . . . . .	72
4.2	Example of matching phase differences using dynamic time warping . . . . .	76
4.3	Dynamic time warping path through the cumulative distance matrix $\gamma$ with global constraint examples . . . . .	76
5.1	Simple example of CWS framework . . . . .	85
5.2	Cross Wavelet Phase Variance (CWPV) example . . . . .	88
5.3	Theoretical phase variance vector . . . . .	89
5.4	Example of AM and FM behaviour . . . . .	91

5.5	CWT and cross wavelet phase modulus representing AM and FM behaviour	93
5.6	Simple example of scale set combinations used during CWS computation	94
5.7	Worked example of CWS framework . . . . .	95
5.8	Worked example of CWS framework highlighting scale ranges . . . . .	96
6.1	Ordered phase variance vector . . . . .	106
6.2	Box plot comparing techniques from experiment one . . . . .	109
6.3	Box plot comparing CWPV variations from experiment one . . . . .	111
6.4	Analysis of Coffee, Lightning 2, and Lightning 7 classification problems .	112
6.5	Coffee database classes . . . . .	113
6.6	Cross wavelet modulus and CWPV of time series extracted from the Coffee database . . . . .	114
6.7	Detailed analysis of the Coffee and Beef classification problems . . . . .	116
6.8	Box plot of UCR training results for experiment two comparing all techniques.	119
6.9	UCR experiment two model test results comparing CWS against Euclidean distance and DTW. . . . .	122
6.10	UCR experiment two model test results comparing CWPV against Euclidean distance and DTW. . . . .	123
6.11	UCR experiment two model test results comparing CWED against Euclidean distance and DTW. . . . .	124
6.12	UCR experiment two model test results comparing CWS, CWPV and CWED. . . . .	125
6.13	Box plot of UCR experiment two model test results comparing all techniques.	126
6.14	Comparison of train and test results from experiment two. . . . .	127
6.15	Summary comparing train and test results for the Wafer classification problem using the CWS, CWPV and CWED techniques with 1-7 voices and three $\omega_0$ values. . . . .	128
6.16	Summary comparing train and test results for the Olive Oil classification problem using the CWS, CWPV and CWED techniques with 1-7 voices and three $\omega_0$ values. . . . .	129
6.17	Summary comparing train and test results for the Lightning 2 classification problem using the CWS, CWPV and CWED techniques with 1-7 voices and three $\omega_0$ values. . . . .	130
6.18	Texas sharpshooter plot of CWS vs Euclidean distance and DTW. . . . .	133
6.19	Texas sharpshooter plot of CWPV vs Euclidean distance and DTW. . . . .	134
6.20	Texas sharpshooter plot of CWED vs Euclidean distance and DTW. . . . .	135
6.21	Summary of results for the Beef classification problem comparing CWS, CWPV and CWED methods using 1-7 voices and three $\omega_0$ values. . . . .	137
6.22	Summary of results for the Trace classification problem comparing CWS, CWPV and CWED methods using 1-7 voices and three $\omega_0$ values. . . . .	138
A.1	Synthetic control examples . . . . .	144
A.2	Gun point examples . . . . .	144
A.3	CBF examples . . . . .	145
A.4	Face (all) examples . . . . .	145

A.5	OSU Leaf examples . . . . .	146
A.6	Swedish Leaf examples . . . . .	147
A.7	50words examples . . . . .	148
A.8	Trace examples . . . . .	149
A.9	Two patterns examples . . . . .	149
A.10	Face (four) examples . . . . .	150
A.11	Lightning 2 examples . . . . .	150
A.12	Lightning 7 examples . . . . .	151
A.13	ECG200 examples . . . . .	151
A.14	Adiac examples . . . . .	152
A.15	Yoga examples . . . . .	152
A.16	Fish examples . . . . .	153
A.17	Beef examples . . . . .	154
A.18	Coffee examples . . . . .	154
A.19	Olive oil examples . . . . .	155
B.1	Summary of results for the Synthetic Control classification problem comparing CWS, CWPV, CWED methods using 1-7 voices and three $\omega_0$ values. . . . .	157
B.2	Summary of results for the Gun Point classification problem comparing CWS, CWPV, CWED methods using 1-7 voices and three $\omega_0$ values. . . . .	159
B.3	Summary of results for the CBF classification problem comparing CWS, CWPV, CWED methods using 1-7 voices and three $\omega_0$ values. . . . .	161
B.4	Summary of results for the Face (all) classification problem comparing CWS, CWPV, CWED methods using 1-7 voices and three $\omega_0$ values. . . . .	163
B.5	Summary of results for the OSU Leaf classification problem comparing CWS, CWPV, CWED methods using 1-7 voices and three $\omega_0$ values. . . . .	165
B.6	Summary of results for the Swedish Leaf classification problem comparing CWS, CWPV, CWED methods using 1-7 voices and three $\omega_0$ values. . . . .	167
B.7	Summary of results for the 50words classification problem comparing CWS, CWPV, CWED methods using 1-7 voices and three $\omega_0$ values. . . . .	169
B.8	Summary of results for the Trace classification problem comparing CWS, CWPV, CWED methods using 1-7 voices and three $\omega_0$ values. . . . .	171
B.9	Summary of results for the Two Patterns classification problem comparing CWS, CWPV, CWED methods using 1-7 voices and three $\omega_0$ values. . . . .	173
B.10	Summary of results for the Wafer classification problem comparing CWS, CWPV, CWED methods using 1-7 voices and three $\omega_0$ values. . . . .	175
B.11	Summary of results for the Face (four) classification problem comparing CWS, CWPV, CWED methods using 1-7 voices and three $\omega_0$ values. . . . .	177
B.12	Summary of results for the Lightning2 classification problem comparing CWS, CWPV, CWED methods using 1-7 voices and three $\omega_0$ values. . . . .	179
B.13	Summary of results for the Lightning7 classification problem comparing CWS, CWPV, CWED methods using 1-7 voices and three $\omega_0$ values. . . . .	181
B.14	Summary of results for the ECG200 classification problem comparing CWS, CWPV, CWED methods using 1-7 voices and three $\omega_0$ values. . . . .	183

B.15 Summary of results for the Adiac classification problem comparing CWS, CWPV, CWED methods using 1-7 voices and three $\omega_0$ values. . . . .	185
B.16 Summary of results for the Yoga classification problem comparing CWS, CWPV, CWED methods using 1-7 voices and three $\omega_0$ values. . . . .	187
B.17 Summary of results for the Fish classification problem comparing CWS, CWPV, CWED methods using 1-7 voices and three $\omega_0$ values. . . . .	189
B.18 Summary of results for the Plane classification problem comparing CWS, CWPV, CWED methods using 1-7 voices and three $\omega_0$ values. . . . .	191
B.19 Summary of results for the Car classification problem comparing CWS, CWPV, CWED methods using 1-7 voices and three $\omega_0$ values. . . . .	193
B.20 Summary of results for the Beef classification problem comparing CWS, CWPV, CWED methods using 1-7 voices and three $\omega_0$ values. . . . .	195
B.21 Summary of results for the Coffee classification problem comparing CWS, CWPV, CWED methods using 1-7 voices and three $\omega_0$ values. . . . .	197
B.22 Summary of results for the Olive Oil classification problem comparing CWS, CWPV, CWED methods using 1-7 voices and three $\omega_0$ values. . . . .	199
B.23 Summary of results for the CinC_ECG _Torso classification problem comparing CWS, CWPV, CWED methods using 1-7 voices and three $\omega_0$ values.	201
B.24 Summary of results for the Chlorine Concentration classification problem comparing CWS, CWPV, CWED methods using 1-7 voices and three $\omega_0$ values. . . . .	203
B.25 Summary of results for the Diatom Size Reduction classification problem comparing CWS, CWPV, CWED methods using 1-7 voices and three $\omega_0$ values. . . . .	205
B.26 Summary of results for the ECG Five Days classification problem comparing CWS, CWPV, CWED methods using 1-7 voices and three $\omega_0$ values.	207
B.27 Summary of results for the Faces UCR classification problem comparing CWS, CWPV, CWED methods using 1-7 voices and three $\omega_0$ values. . . . .	209
B.28 Summary of results for the Haptics classification problem comparing CWS, CWPV, CWED methods using 1-7 voices and three $\omega_0$ values. . . . .	211
B.29 Summary of results for the Inline Skate classification problem comparing CWS, CWPV, CWED methods using 1-7 voices and three $\omega_0$ values. . . . .	213
B.30 Summary of results for the Italy Power Demand classification problem comparing CWS, CWPV, CWED methods using 1-7 voices and three $\omega_0$ values. . . . .	215
B.31 Summary of results for the Medical Images classification problem comparing CWS, CWPV, CWED methods using 1-7 voices and three $\omega_0$ values.	217
B.32 Summary of results for the Mote Strain classification problem comparing CWS, CWPV, CWED methods using 1-7 voices and three $\omega_0$ values. . . . .	219
B.33 Summary of results for the SonyAIBORobot SurfaceII classification problem comparing CWS, CWPV, CWED methods using 1-7 voices and three $\omega_0$ values. . . . .	221
B.34 Summary of results for the SonyAIBORobot Surface classification problem comparing CWS, CWPV, CWED methods using 1-7 voices and three $\omega_0$ values. . . . .	223

---

B.35	Summary of results for the Symbols classification problem comparing CWS, CWPV, CWED methods using 1-7 voices and three $\omega_0$ values. . . . .	225
B.36	Summary of results for the Two Lead ECG classification problem comparing CWS, CWPV, CWED methods using 1-7 voices and three $\omega_0$ values.	227
B.37	Summary of results for the Word Synonyms classification problem comparing CWS, CWPV, CWED methods using 1-7 voices and three $\omega_0$ values.	229
B.38	Summary of results for the Cricket_X classification problem comparing CWS, CWPV, CWED methods using 1-7 voices and three $\omega_0$ values. . .	231
B.39	Summary of results for the Cricket_Y classification problem comparing CWS, CWPV, CWED methods using 1-7 voices and three $\omega_0$ values. . .	233
B.40	Summary of results for the Cricket_Z classification problem comparing CWS, CWPV, CWED methods using 1-7 voices and three $\omega_0$ values. . .	235

# Tables

3.1	Fourier transform properties. . . . .	22
5.1	Summary of classification results using the Euclidean distance between global wavelet power spectra and phase variance calculated for all scales. . . . .	92
6.1	Summary of the original UCR datasets used for model testing and analysis in experiment one . . . . .	102
6.2	Summary of updated UCR datasets used in experiment two . . . . .	103
6.3	Experiment one results . . . . .	108
6.4	CWPV variations comparison . . . . .	110
6.5	Summary of training results for experiment two. . . . .	120
6.6	Summary of model test results for experiment two. . . . .	121
6.7	Wilcoxon signed-rank test . . . . .	132
B.1	Summary of results for the Synthetic Control classification problem. . . . .	158
B.2	Summary of results for the Gun Point classification problem. . . . .	160
B.3	Summary of results for the CBF classification problem. . . . .	162
B.4	Summary of results for the Face (all) classification problem. . . . .	164
B.5	Summary of results for the OSU Leaf classification problem. . . . .	166
B.6	Summary of results for the Swedish Leaf classification problem. . . . .	168
B.7	Summary of results for the 50words classification problem. . . . .	170
B.8	Summary of results for the Trace classification problem. . . . .	172
B.9	Summary of results for the Two Patterns classification problem. . . . .	174
B.10	Summary of results for the Wafer classification problem. . . . .	176
B.11	Summary of results for the Face (four) classification problem. . . . .	178
B.12	Summary of results for the Lightning2 classification problem. . . . .	180
B.13	Summary of results for the Lightning7 classification problem. . . . .	182
B.14	Summary of results for the ECG200 classification problem. . . . .	184
B.15	Summary of results for the Adiac classification problem. . . . .	186
B.16	Summary of results for the Yoga classification problem. . . . .	188
B.17	Summary of results for the Fish classification problem. . . . .	190
B.18	Summary of results for the Plane classification problem. . . . .	192
B.19	Summary of results for the Car classification problem. . . . .	194
B.20	Summary of results for the Beef classification problem. . . . .	196
B.21	Summary of results for the Coffee classification problem. . . . .	198

B.22	Summary of results for the Olive Oil classification problem. . . . .	200
B.23	Summary of results for the CinC_ECG_torso classification problem. . .	202
B.24	Summary of results for the Chlorine Concentration classification problem.	204
B.25	Summary of results for the Diatom Size Reduction classification problem.	206
B.26	Summary of results for the ECG Five Days classification problem. . . . .	208
B.27	Summary of results for the Faces UCR classification problem. . . . .	210
B.28	Summary of results for the Haptics classification problem. . . . .	212
B.29	Summary of results for the Inline Skate classification problem. . . . .	214
B.30	Summary of results for the Italy Power Demand classification problem. .	216
B.31	Summary of results for the Medical Images classification problem. . . . .	218
B.32	Summary of results for the Mote Strain classification problem. . . . .	220
B.33	Summary of results for the SonyAIBORobot SurfaceII classification problem.	222
B.34	Summary of results for the SonyAIBORobot Surface classification problem.	224
B.35	Summary of results for the Symbols classification problem. . . . .	226
B.36	Summary of results for the Two Lead ECG classification problem. . . . .	228
B.37	Summary of results for the Word Synonyms classification problem. . . . .	230
B.38	Summary of results for the Cricket_X classification problem. . . . .	232
B.39	Summary of results for the Cricket_Y classification problem. . . . .	234
B.40	Summary of results for the Cricket_Z classification problem. . . . .	236
C.1	Summary of parameters according to the results presented in Table 6.5 (p. 120) . . . . .	239
C.2	Summary of model test results and parameters according to the same map- ping presented in Table 6.5 (p. 120) . . . . .	244



# Information Boxes

2.1	Some notable advances in trigonometry outside of Europe.....	10
3.1	Complex representation .....	20
3.2	Convolution .....	22
3.3	An example of the discrete Fourier transform .....	24
3.4	Heisenberg's inequality .....	28
3.5	Common window functions .....	32
3.6	Examples of continuous wavelet functions .....	37
4.1	Machine learning or pattern recognition .....	61
4.2	Unsupervised, reinforced and supervised learning .....	66
4.3	Dimensionality reduction .....	67
4.4	Statistical forecasting models .....	69
4.5	Classification using FFT amplitude coefficients .....	80

# Abbreviations

<b>AI</b>	<b>a</b> rtificial <b>i</b> ntelligence
<b>AM</b>	<b>a</b> mplitude <b>m</b> odulation
<b>CWA</b>	<b>c</b> ross <b>w</b> avelet <b>a</b> nalysis
<b>CWC</b>	<b>c</b> ross <b>w</b> avelet <b>c</b> oherency
<b>CWED</b>	<b>g</b> lobal power <b>c</b> ontinuous <b>w</b> avelet <b>E</b> uclidean <b>d</b> istance
<b>CWPV</b>	<b>c</b> ross <b>w</b> avelet <b>p</b> hase <b>v</b> ariance
<b>CWS</b>	<b>c</b> ross <b>w</b> avelet <b>s</b> imilarity
<b>CWT</b>	<b>c</b> ontinuous <b>w</b> avelet <b>t</b> ransform
<b>DFT</b>	<b>d</b> iscrete <b>F</b> ourier <b>t</b> ransform
<b>DSTFT</b>	<b>d</b> iscrete <b>s</b> hort <b>t</b> ime <b>F</b> ourier <b>t</b> ransform
<b>DTW</b>	<b>d</b> ynamic <b>t</b> ime <b>w</b> arping
<b>DWT</b>	<b>d</b> iscrete <b>w</b> avelet <b>t</b> ransform
<b>Ed</b>	<b>E</b> uclidean <b>d</b> istance
<b>FFT</b>	<b>f</b> ast <b>F</b> ourier <b>t</b> ransform
<b>FFT-A</b>	<b>E</b> uclidean distance between <b>f</b> ast <b>F</b> ourier <b>t</b> ransform <b>a</b> mplitudes
<b>FFTW</b>	<b>f</b> astest <b>F</b> ourier <b>t</b> ransform in the <b>w</b> est
<b>FM</b>	<b>f</b> requency <b>m</b> odulation
<b>FT</b>	<b>F</b> ourier <b>t</b> ransform
<b>k-NN</b>	<b>k</b> nearest <b>n</b> eighbour
<b>KDD</b>	<b>k</b> nowledge <b>d</b> iscovery in <b>d</b> atabases
<b>LOOCV</b>	<b>l</b> eave- <b>o</b> ne- <b>o</b> ut <b>c</b> ross <b>v</b> alidation

<b>ML</b>	<b>m</b> achine <b>l</b> earning
<b>PAA</b>	<b>p</b> iecewise <b>a</b> ggregate <b>a</b> pproximation
<b>PCA</b>	<b>p</b> rincipal <b>c</b> omponent <b>a</b> nalysis
<b>PLA</b>	<b>p</b> iecewise <b>l</b> inear <b>a</b> pproximation
<b>STFT</b>	<b>s</b> hort <b>t</b> ime <b>F</b> ourier <b>t</b> ransform
<b>SVD</b>	<b>s</b> ingular <b>v</b> alue <b>d</b> ecomposition
<b>WFT</b>	<b>w</b> indowed <b>F</b> ourier <b>t</b> ransform
<b>WT</b>	<b>w</b> avelet <b>t</b> ransform

# Notation

$\mathbb{C}$	set of all complex numbers $\{x + iy\}$ for $x$ and $y$ in $\mathbb{R}$
$C_\psi$	Calderón's admissibility condition
$\delta$	Dirac impulse
$\Delta t \Delta \omega \geq \frac{1}{4\pi}$	Heisenberg's inequality
$e^{i\omega t}$	Euler's formula ((complex) equivalent to $\cos(\omega t) + i \sin(\omega t)$ )
$f = ma$	Newton's 2 <sup>nd</sup> Law of motion ( <i>force = mass · acceleration</i> )
$f$	frequency
$f_0$	fundamental frequency
$f_s$	sampling frequency
$f(t)$	time series
$\hat{f}(\omega)$	Fourier transform at frequency $\omega$
$\hat{f}(\frac{n}{tN})$	Discrete Fourier Transform of $t$
$H$	Hilbert space
$h$	Planck's constant = $6.626 \times 10^{-34}$ J <sup>-s</sup> (exact)
Hz	Hertz = 1 cycle per second
$i$	imaginary number = $\sqrt{-1}$
$Im$	imaginary part
$k$	time measure index
$L^2(\mathbb{R})$	infinite-dimensional Hilbert space
$\mathbb{N}$	set of all positive integers (i.e. natural)
$N$	total number of samples in a sequence

---

$n$	sample index in a sequence
octave ( $s$ )	wavelet scales at $s_j \sim 2^j$ , where $j$ is the sequence $[1 : 2^{\log_2(\frac{n}{2})}]$
$\omega$	angular frequency in $\text{rads}^{-1}$ ( $\omega = 2\pi f$ )
$\phi$	Wavelet scaling function (father wavelet)
$\pi$	ratio of a circle's circumference to its diameter (constant)
$\psi$	mother wavelet
$\mathbb{R}$	set of all real numbers $x$ , $-\infty < x < \infty$
$R^2(u, s)$	cross wavelet coherency
$Re$	real part
scale ( $s$ )	wavelet dilation parameter or scale (scales in the wavelet domain $= \frac{1}{f}$ )
$S_N f(x)$	$N_{th}$ partial sum of the Fourier series of $x$
$t$	time
$\theta(u, s)$	cross wavelet phase
$u$	wavelet translation parameter (time in the wavelet domain)
voice ( $s$ )	intermediate wavelet scales between octaves
$W(u, s)$	continuous wavelet transform
$W_m(u, s)$	normalised continuous wavelet transform
$ W(u, s) ^2$	local wavelet power spectrum
$W_{x,y}(u, s)$	wavelet cross spectrum
$\mathbb{Z}$	set of all integers
$\frac{1}{2} \int_0^{2\pi}  f(x) ^2 dx$	mean energy of a function
$2f_s$	Nyquist rate
$\frac{f_s}{2}$	Nyquist frequency
$\star$	convolution operator
$*$	complex conjugate
$\langle \cdot, \cdot \rangle$	inner product
$ \cdot $	norm

*To my wife Fiona and daughters Imogen and Jane*

*"It is sometimes said that the great discovery of the nineteenth century was that the equations of nature were linear, and the great discovery of the twentieth century is that they are not."*

T. W. Körner

# 1

## Introduction

### 1.1 Motivation

Wavelets have become an increasingly common tool in the natural sciences due to their ability to identify the energy spread of time-based functions, and their frequency components at different scales<sup>†</sup> [1]. They need no background knowledge of underlying fundamental mechanisms before analysis, and it is possible to highlight common “non-linear” processes between time series using cross wavelet analysis (CWA) [2, 3] that would otherwise not be possible using classical time series approaches.

---

<sup>†</sup>The term ‘time-scale’ is used in the cartographic sense: denoting the best possible approximation of frequencies for a given *atom* within frequency space, where *atom*, as its name suggests, is the simplest element of a function space [1].

Traditionally, the continuous wavelet transform (CWT) is preferred over its discrete counterpart during the exploratory stages of time series analysis, but due to the large amount of needless information associated with its transform, it also calls for a large degree of manual interpretation to separate out redundant from real information. The rapid rate at which observable data are growing, combined with the increase in computational theories and tools to help in the extraction of useful information, now calls for some automation when dealing with larger datasets.

In this thesis, the utility and versatility of CWA is explored in time series classification problems, by defining a new approach to identifying similarities between time series using the variance of phase of the cross wavelet and the more traditional power relationships between global wavelet power spectra. The intent is to identify and separate out common frequency information, specifically frequency modulation (FM) and amplitude modulation (AM) at their corresponding scales. An algorithm is developed and applied in a metric space whereby any statistical inferences made from other classifier measures are overcome, and success can be assessed according to the ability to classify (and in this case characterise) benchmark time series against other common techniques. Moreover, any characteristic behaviour that delineates the system according to AM or FM unanimity, may be extracted and used to decide on a substitute classifier measure best suited for further application in the classification problem.

## 1.2 Aim

The aim of this thesis is to test whether CWA, which is superior to traditional Fourier based techniques in describing the relationships between individual time series in time frequency space, can be automated to a sufficient degree to be useful in large time series classification problems. The goal is to define an algorithm that matches similarities using both cross wavelet phase variance (CWPV) and continuous wavelet power to separate out, as much as possible, the degree to which FM and AM behaviour influences the classification problem. To facilitate FM, the CWPV term is introduced as a new method in which the variance of phase (used as a measure of coherency) is assessed over the



combination of wavelet scales that best describe similar behaviour using an iterative algorithm. The specific sub-goals are:

- to test whether its possible to separate out AM and FM behaviour and if so, to determine to what degree such behaviour would influence results obtained using different classifier distance measures; and,
- to test whether there are any gains in accuracy using this approach.

### 1.3 Structure of this thesis

The context of this thesis is structured to follow a natural progression between topics from elementary knowledge in Chapters 2 up to the development of CWA at the end of Chapter 3. In Chapter 4, background on time series analysis and specifically classification is given. In Chapter 5 the methodology is presented, and in Chapter 6 the application and results are discussed. Chapter 7 is the conclusion. Below is a general overview of the contents of each chapter:

- Chapter 1: **Introduction.** What this thesis is about and the outlay (this chapter).
- Chapter 2: **Before we begin.** In this chapter, preliminary concepts and notation are given followed by a brief review of the historical setting from which such notation evolved. A general history of wavelets, their precursor the Fourier transform (FT), and the events that led to the formulation of the FT are given. The chapter ends with some recent mathematical developments in wavelet theory. The purpose of the chapter is not only to introduce the basic concepts and mathematical preliminaries, but also to provide a general context through a historical setting starting some 2000 years ago.
- Chapter 3: **Mathematical background to wavelets.** This chapter provides a more in-depth mathematical background, including properties of the FT and the wavelet transform. It links wavelet analysis to Fourier analysis through the short

time Fourier transform (STFT) and ends with an explanation of the cross wavelet spectrum — the starting point for the methodology presented in Chapter 5.

- Chapter 4: **Background to time series classification.** This chapter provides a general background to time series analysis, with a focus on the classification framework (including examples and techniques).
- Chapter 5: **Methodology: matching similarities using cross wavelet analysis.** This chapter presents the methodology developed in this thesis. The approach is algorithmic and uses both the variance of cross wavelet phase and the Euclidean distance of global wavelet power spectra to provide a similarity measure between time series based on AM and FM characteristics.
- Chapter 6: **Experiments: results and discussion.** In this chapter, the approach described in Chapter 5 is applied and its performance is compared to common techniques used in distance-based classification experiments on a benchmark time series database from the University of California Riverside (UCR) [4, 5]. Two experiments are performed, one in which the CWPV term is explored and the results analysed, and the other in which the analysis from first experiment helped to provide the algorithms necessary for a full mapping of AM and FM characteristics, which are presented and discussed.
- Chapter 7: **Conclusion.** This is the conclusion. A small chapter summarising the thesis and suggesting future avenues of research.
- Appendix A: **UCR data summary.** Provides examples and explanations of the UCR time series database (with examples of different classes in each dataset) used in the classification experiments of this thesis.
- Appendix B: **Experiment two summary of analysis.** Provides a more in-depth comparison of results (comparing AM, FM and a mixture of the two) obtained using the classification method developed in this thesis, and applied to the UCR time-series database.
- Appendix D: **Code listings.** Provides examples of code (in Java) used and developed in this thesis.

- Appendix E: **Application papers.** Published conference proceeding [6] relating to the preliminary analysis and results performed in experiment one in Chapter 6.

## 1.4 Conclusion

The analyses and algorithms presented throughout this thesis use the Morlet wavelet as a basis function. To understand the methodology that is developed, one first has to understand the CWT, which in itself is a coalescence of advanced mathematical concepts, and to understand wavelets some elementary knowledge is needed. To facilitate a smooth transition between chapters, a schematic (representing the natural progression of topics) is presented at the beginning of each chapter to aid the reader by highlighting the central themes relevant to that chapter in black. This schematic is shown in Figure 1.1 (p. 5). In some chapters there are also supporting concepts or ideas that are relevant, but not central to the main topic being addressed, and are therefore presented as information boxes as not to distract from the main context.

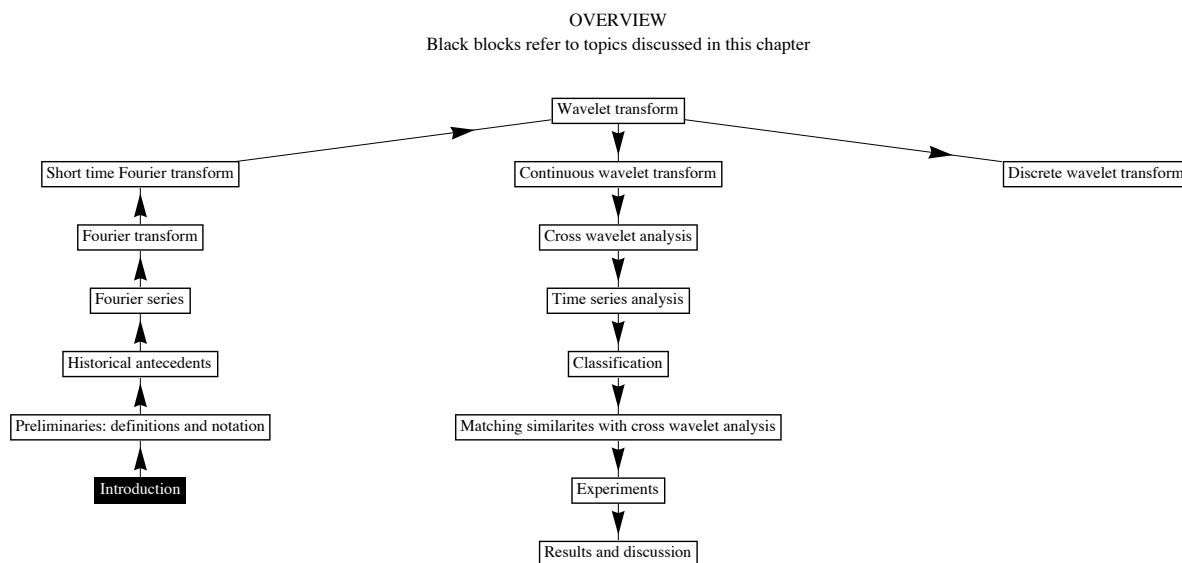


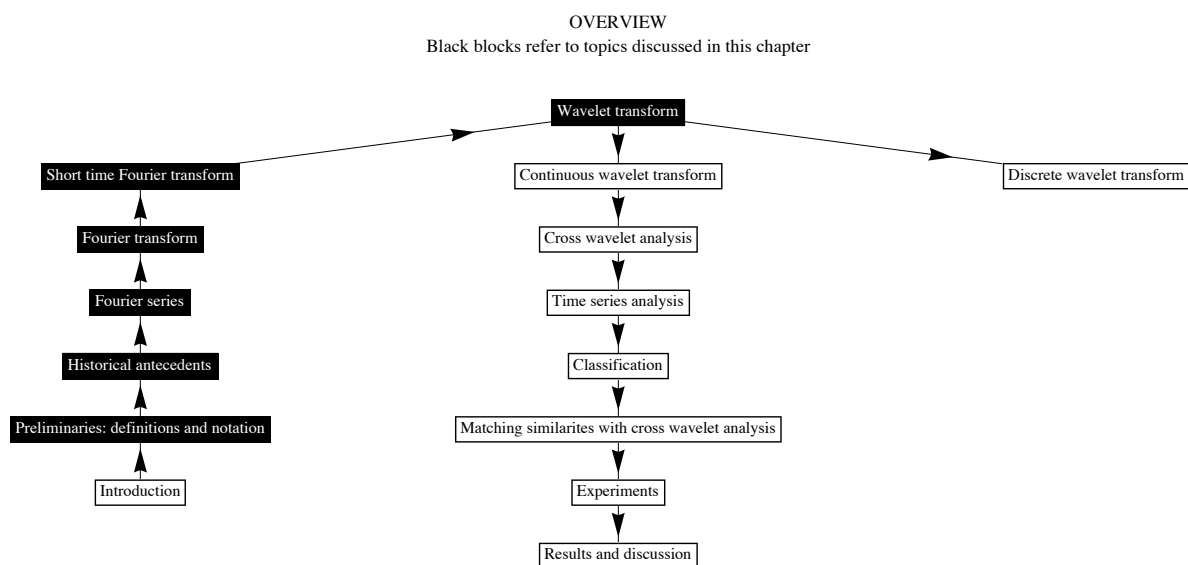
FIGURE 1.1: Schematic of main topics discussed in this thesis. The above flowchart provides a rough outlay of the order in which topics are presented and discussed. The same flowchart is presented in the beginning of each chapter, but with the main topics relevant to that chapter highlighted in black.

*"Since the ancients (as we are told by Pappus), made great account of the science of mechanics in the investigation of natural things; and the moderns, laying aside substantial forms and occult qualities, have endeavoured to subject the pheanomena of nature to the laws of mathematics, I have in this treatise cultivated mathematics so far as it regards philosophy.... If I have been able to see further, it was only because I stood on the shoulders of giants."*

Isaac Newton (AD 1642-1727)

# 2

Before we begin



## 2.1 Overview

The Fourier transform is one of the fundamental techniques used in physics, engineering, and mathematics. It reveals the frequency content of any function, which allows the processing of many aspects of modern technology such as television, digital cinema, computer graphics, space exploration and similar technologies. Since its conception some two centuries ago by Jean Baptiste Joseph Fourier (21 March 1768 – 16 May 1830) [7], many related mathematical concepts have been introduced. On the one hand, rigorous investigation into the mathematical properties of the frequency domain has resulted in the modern definitions of function [8] and integral [9, 10], the inception of the mathematical theory of sets [11], and the formation of functional analysis [10, 12, 13]. On the other hand, the inevitable progression to time-frequency analysis [14] resulted in the development of wavelets [15].

## 2.2 Preliminaries and modern notation

Here we give a very brief review of some fundamental concepts. We begin with the most fundamental concept of all: the mathematical theory of sets from which nearly all of mathematics can be derived [11]. A set is a well-defined collection of objects, encompassing nearly all mathematical definitions including functions. The basic properties of sets and the procedures for performing calculations on their operators are described by the algebra of sets. Sets are usually denoted by capital letters:  $A, B, C, \dots, Z$  and their elements by lower-case letters:  $a, b, c, \dots, z$ . The elements of a set are the distinct objects that make up the set. If  $x$  is an element of  $A$ , we use the symbol  $\in$  to denote that  $x \in A$ . Conversely, if  $x$  is not an element of set  $A$ , we write  $x \notin A$ . If set  $B = \{1, 2, \{x, y\}\}$ , and set  $C = \{x, y\}$ , then the elements of  $B$  are the numbers 1 and 2, and the subset  $C$ . We denote that  $C$  is a subset of  $B$  as  $C \subset B$ , and conversely  $B \not\subset C$ . We use the symbols  $\cap$  and  $\cup$  for the logic operations “and” and “or” respectively. An empty set with no elements is denoted by  $\emptyset$ . The standard notation for sets of integers, real numbers, and complex numbers are:

- $\mathbb{N} = \{1,2,3,\dots\}$  is the set of all positive integers (i.e. natural),
- $\mathbb{Z} = \{0,\pm 1,\pm 2,\pm 3,\dots\}$  is the set of all integers,
- $\mathbb{R}$  is the set of all real numbers  $x$ ,  $-\infty < x < \infty$ , and
- $\mathbb{C}$  is the set of all complex numbers  $\{x + iy\}$  for  $x$  and  $y$  in  $\mathbb{R}$ , and  $i = \sqrt{-1}$ .

The properties and relations of a set and its subsets define which space they belong to. A topological space is a generalisation of the concept of space, so that a set  $X$  with a collection of subsets  $T$  satisfy certain axioms<sup>†</sup> that define the topology of the set. A topological space whose elements are functions is called a function space. For example, the notation  $A^B$  describes the mapping between  $B$  and  $A$  as  $f : B \mapsto A$ , where the elements of  $A$  denoted  $\{A_1, A_2, \dots, A_n\}$  are a collection of functions  $\{f(1), f(2), \dots, f(n)\}$ . The space of all  $n$ -sequences of elements or  $n$ -tuples of real numbers  $(x_1, x_2, x_3, \dots, x_n)$  is Euclidean  $n$ -space, and is usually denoted as  $\mathbb{R}^n$ , where  $\mathbb{R}^n$  is called a vector space  $V$  with  $n$ -vectors. The Lebesgue measure is the standard way to assign a measure to Euclidean  $n$ -space, where a measure is defined as a non-negative real function.  $\mathbb{R}^n$  is measurable only if its domain is also measurable, so that if  $x \in \mathbb{R}$  in  $f(x)$  then  $x$  belongs to domain  $\mathbb{R}$ , and is measurable over a closed sequence. We use  $[a, b]$  to denote a closed interval and  $(a, b)$  to denote an open interval.

The vectors  $ai$  and  $bj$  in  $V = ai + bj$  are orthogonal if  $\langle i, j \rangle = \langle j, i \rangle = 0$ , where  $\langle \cdot, \cdot \rangle$  is the inner product. For  $V = ai + bj$ , we call  $i$  and  $j$  the bases of  $\mathbb{R}^2$ : i.e two functions are orthogonal to each other if  $\int_{-\infty}^{\infty} f_1(t)f_2(t)dt = 0$ , and orthonormal if they are orthogonal and  $\int_{-\infty}^{\infty} f_i(t)f_i(t)dt = 1$ , for  $i = 1,2$ . The norm of  $V = ai + bj$  is defined as  $\sqrt{a^2 + b^2}$ , and denoted as  $|V|$ . A complete vector space is called a Banach space.  $L^p$  functions integrable by  $p$  for  $p \geq 1$  form part of a Banach space, and are defined on the measure space  $X$  as

$$|f|_{L^p} = \left( \int_X |f|^p \right)^{1/p}. \quad (2.1)$$

A special example of a Banach space is a Hilbert space  $H$ , with an inner product  $\langle f, g \rangle$ , and a norm defined as  $|f| = \sqrt{\langle f, f \rangle}$ . The set of  $L^p$  functions with  $p = 2$  is denoted

<sup>†</sup>Axioms are a set of logical statements that are assumed to be true.

$L^2(\mathbb{R})$ , and is an infinite-dimensional Hilbert space, where  $f : X \mapsto \mathbb{R}$  on the measurable space  $X$ , and the integral of  $f^2$  over  $\mathbb{R}$  is finite. The inner product is given as

$$\langle f, g \rangle = \int_{-\infty}^{\infty} f(x)g(x)dx. \quad (2.2)$$

A  $L^p$  function with  $p \neq 2$  is not a Hilbert space, but is a Banach space. All functions are  $L^2$  square integrable if their Fourier series are convergent. This is known as the Riesz-Fischer Theorem:

$$\lim_{N \rightarrow \infty} \|S_N f - f\|_2 = 0, \quad (2.3)$$

where  $\|\cdot\|_2$  is the  $L^2$  norm, and  $S_N f$  is the  $N^{\text{th}}$  partial sum of the Fourier series given as

$$S_N f(x) = \frac{a_0}{2} + \sum_{n=1}^N [a_n \cos(nx) + b_n \sin(nx)], \quad N \geq 0. \quad (2.4)$$

## 2.3 Historical antecedents

### 2.3.1 Setting the scene

We are told that Thales of Miletos and Pythagoras of Samos introduced the principles of geometry to the Greco-Roman world through interaction with the Egyptian and Mesopotamian cultures [16]. It was here in the Greco-Roman world that the principles of harmonic analysis were defined between  $\sim 400$  BC – AD 200. Aristotle ( $\sim 384$  – 322 BC), a pupil of Plato, provided the basis for the scientific method. Euclid of Alexandria ( $\sim 365$  – 275 BC) synthesized the principles of modern geometry in the *Elements* [17]. Archimedes of Syracuse ( $\sim 262$  – 190 BC) introduced the principles of calculus using infinitesimals<sup>†</sup> and calculated an accurate approximation of  $\pi$ . Appolonius of Perga ( $\sim 262$  – 190 BC) proposed the hypothesis of eccentric orbits and planetary motions, which led Hipparchus of Nicaea ( $\sim 190$  – 120 BC) to develop trigonometry as a separate discipline, and in doing so made the first trigonometric tables. Claudius Ptolemaeus (Ptolemy) ( $\sim$

---

<sup>†</sup>Refers to endless terms. Archimedes calculated the area of irregular shapes by summing a series of smaller more calculable shapes whose areas converge to the larger shape.

AD 87 – 165) synthesized a treatise on astronomy in the *Almagest* [18], whereby complex planetary motions could be explained by a series of simpler motions (the very essence of harmonic series). Then, in AD 476, Rome fell (marking the beginning of the ‘Dark Ages’ in Europe) and the mathematical advancements of ‘Hellenistic culture’ were continued outside Europe (see Information Box 2.1 (p. 10)) [16, 19].

INFORMATION BOX 2.1: Some notable advances in trigonometry outside of Europe

Some of the major developments in the fields of trigonometry and astronomy occurred outside of Europe after the fall of Rome. Here we mention three notable persons:

- **Aryabhata** (AD 476 – 550) of India, who provided the first reference to the terms sines and cosines in the *Aryabhatiya*; which in turn makes extensive reference to the *Surya Siddhanta*, a treatise on Indian astronomy. It is from the translation of the Sanskrit words *ḥyā* and *koti-ḥyā*, that the words sine and cosine are derived [16, 19].
- **Abū’ Abdallāh Muhammed ibn Mūsā al-Khwārizmī** (AD 780 - 850) of Persia introduced the concept of Algebra, and pioneered spherical trigonometry. The words Algebra and Algorithm are derived from his name.
- **Abū al-Wafā’ Būzjānī** (AD 940 – 998) of Persia is credited with the tangent (*tan*) function [16, 19].

During medieval times, Europe was reintroduced to some fundamental works on astronomy and trigonometry through the translations of Arabic, Indian, and Greek texts back into Latin [16]<sup>†</sup>. Along with these translations came the Hindu-Arabic numeral system, the extension of the number field to include negative numbers, and symbolic representation of different operations such as addition and subtraction. [20]. With the fall of Constantinople in AD 1453 and the newly invented printing press Regiomontanus (Johann Müller)<sup>†</sup> translated and disseminated, on a large scale, the works of Archimedes, Appolonius, Ptolemy and others back into mainstream literate society. During this time, a contemporary of Regiomontanus, Nicolaus Copernicus (AD 1473 – 1543), completed *De revolutionibus orbium coelestium (On the Revolutions of the Heavenly Spheres)* in

<sup>†</sup>For example: Levi ben Gerson (*Gersonides*) (AD 1288 - 1344) wrote on *On Sines, Chords and Arcs*, with the aid of a whole Arabic treatise translated by his father.

<sup>†</sup>He is known for his work *De triangulis Omnimodis*, marking the rebirth of trigonometry in Europe [19].



AD 1543 which ended Ptolemy’s astronomical reign by contesting his geocentric model [21]. The work became a cornerstone of the ‘scientific revolution’<sup>†</sup>, which grew into the concepts of modern mathematics with the advancement of symbolic algebra by Viéte, the development of logarithms by Napier, Galileo’s science of dynamics, Kepler’s laws of planetary motion, and the development of analytical geometry through the works of Descartes and Pascal [16, 19]. Towards the end of the 17th century calculus, started by Archimedes, was given its modern formulation by Gottfried Wilhelm von Leibniz (AD 1646 – 1716) and Isaac Newton (AD 1642 – 1727) [16, 19].

### 2.3.2 Genesis of trigonometric series

For much of the history of mathematics before the 18th century, trigonometry was mostly applied to the mechanics of astronomy. This changed with the laws of nature proposed in the *Principia* [22] and the ability to use calculus to investigate them. In the 18th century, solutions to differential and partial differential equations on sound and heat propagation were given much attention. However, the notions of function and integration had not yet received a precise definition and great controversy surrounded the mathematical representability of such solutions [23–25]. It was within this environment that Jean Baptiste Joseph Fourier proposed a general solution for the heat equation by trigonometric series [7]. The use of trigonometric series in analysis originates with the works of Euler, and the developments that led to Fourier’s assertion began with the wave equation [26]. In 1715, Brook Taylor (AD 1685 – 1731)(after whom the Taylor series is designated), in his book *De methodo incrementorum*, suggested that pure sounds emerging from vibrating strings may be described by  $\sin(x)$  over  $(0, \pi)$  [23]. The problem of the ‘vibrating strings’ captivated the minds of several prominent mathematicians of the era including Daniel Bernoulli (AD 1700 – 1782); Leonhard Euler (AD 1707 – 1783); Jean le Rond d’Alembert (AD 1717 – 1783); Joseph-Louis LaGrange (AD 1736 – 1813) [27]; Alexis Claude de Clairaut (AD 1713 – 1765); Siméon Denis Poisson (AD 1781 – 1840); Augustin-Lois Cauchy (AD 1789 – 1857); and Fourier [23]. So it began, with the propagation of sound.

---

<sup>†</sup>We use the term ‘scientific revolution’ here for classification purposes, as most developments do not simply happen at a single moment, but are rather the result of gradual development over time.

### 2.3.2.1 ‘Vibrating Strings’

The ancient Greeks are credited with the early study of vibrating strings (the initial concept of harmonics). It was through Newton’s 2<sup>nd</sup> Law of motion ( $f = ma$ ),<sup>†</sup> however, that a mathematical solution was possible. The speed of the wave depends on the tension of the string and its mass density, and when the string is plucked, the vibrations are governed by the one dimensional wave equation. In 1747, d’Alembert derived the wave equation for a vibrating string [26], given in modern form as

$$\frac{\partial^2 y}{\partial t^2} = c^2 \frac{\partial^2 y}{\partial x^2}, \quad (2.5)$$

where  $t$  is time,  $x$  denotes the position along the string,  $y$  is the string height (amplitude), and  $c$  is a constant equal to the propagation speed of the wave. The boundary conditions are  $y(0, t) = y(\ell, t) = 0$  with ( $t \geq 0$ ) (the string is fixed at  $x = 0$  and  $x = \ell$ ). Given the initial shape and velocity as

$$\begin{aligned} y(x, 0) &= \varphi(x) \\ \frac{\partial}{\partial t} y(x, 0) &= \psi(x), \end{aligned} \quad (2.6)$$

a general solution to the wave equation is

$$y(x, t) = A(x - ct) + B(x + ct), \quad (2.7)$$

where  $A$  and  $B$  are any functions of one variable over the interval  $[0, \pi]$  that represent two waveforms travelling in opposite directions. The search for suitable ‘functions’ to solve the wave equation (Equation (2.5) (p. 12)) started a famous controversy among d’Alembert, Daniel Bernoulli, and Leonhard Euler [23] from which the antecedents to the notion of Fourier series emerged. Bernoulli recognised the concept of fundamental frequency and its harmonics [28]. He saw the solution to the vibrating strings as a superposition of harmonically related waves defined by the appropriate coefficients for  $A_n$  in the form

$$y(x, t) = \sum_{n=1}^{\infty} A_n \sin \frac{n\pi x}{\ell} \cos \frac{n\pi ct}{\ell}. \quad (2.8)$$

---

<sup>†</sup> *Force = Mass · Acceleration.* Probably the most utilised formula in physics.

At the time the question about whether a function may be expanded as a sum of sines and cosines was at the heart of the debate. Euler disagreed as the series involves ‘continuous’ functions, whereas  $\varphi$  and  $\psi$  given in Equation (2.6) (p. 12) can be discontinuous, and according to Euler the juxtaposition of two functions could not be written as the sum of single functions [29]. As far as Fourier was concerned, the notions of his series were already evident. Despite the apparent contradictions and controversies, Fourier proposed a solution by using Bernoulli’s method ( $\phi(x)\psi(y)$ ) (now called the ‘separation of variables’) as a combination of  $a_n e^{nx} \cos ny$  and  $b_n e^{ny} \sin(nx)$  with the arbitrary coefficients  $a_n$  and  $b_n$  for the heat equation [7], which is a direct model of the wave equation [26]. Fourier was awarded the annual prize of the French Academy of Sciences in 1811 for his work [30], but Bernoulli, Euler, and LaGrange raised concerns on the mathematical grounds of convergence towards a finite limit and algebraic periodicity [27].

## 2.4 The Fourier series

The fundamental idea of the Fourier series is that any  $2\pi$  periodic function  $f(x)$  can be expanded into a trigonometrical series of harmonically related orthogonal sine and cosine functions (components). Fourier asserted that a  $2\pi$  periodic function  $y = f(x)$  may be represented by a trigonometric series of the form

$$f(x) = \frac{a_0}{2} + \sum_{n=1}^{\infty} (a_n \cos nx + b_n \sin nx), \quad (2.9)$$

where  $n =$  integer multiples of the fundamental frequency. The coefficients  $a_0$ ,  $a_n$  and  $b_n$ , are defined as

$$a_0 = \frac{1}{\pi} \int_{-\pi}^{\pi} f(x) dx, \quad (2.10)$$

$$a_n = \frac{1}{\pi} \int_{-\pi}^{\pi} f(x) \cos(nx) dx, \quad n \geq 0 \quad \text{and} \quad (2.11)$$

$$b_n = \frac{1}{\pi} \int_{-\pi}^{\pi} f(x) \sin(nx) dx, \quad n \geq 1. \quad (2.12)$$

The coefficient  $a_0$  provides the mean amplitude, and the coefficients  $a_n$  and  $b_n$  (proposed earlier by Clairaut and Euler) give the amplitude of the cosine and sine waves. If  $f$  is either an odd or even function, then  $a_n$  and  $b_n$  become zero respectively, and fall away from Equation (2.9) (p. 13). The Fourier series converges if the sequence of its partial sums approaches a finite limit. Fourier did not provide rigorous proof or justifications that his series point-wise converges to  $f(x)$  at  $x$ . The first confirmation on the convergence of Fourier series was provided by Peter Gustav Lejeune-Dirichlet (AD 1805 – 1859) who provided the definition of a function  $y = f(x)$  as  $y = c$  when  $x$  is rational and  $y = d \neq c$  when  $x$  is irrational over the interval  $[-\pi, \pi]$  [8]. Dirichlet, and later in 1880, Dini [31] proved that if  $f$  is  $2\pi$  periodic and satisfies

$$\int_0^\pi \left| \frac{f(x_0 + t) + f(x_0 - t)}{2} - \ell \right| \frac{dt}{t} < \infty \quad (2.13)$$

then the partial Fourier sums converge to  $\ell$ . Further interplay on the convergence of Fourier series resulted in enough rigorous support to provide the basis for the field of functional analysis, the two most important contributions before the 20<sup>th</sup> century being the introduction of the Riemann integral in his thesis of 1854 [32], and the introduction of set theory in the 1870s by Cantor [11]. The abstraction of functional spaces within analysis begins with the introduction of the modern theory of integration by Fredholm [9] and Henri Lebesgue [10]. All further developments in functional analysis stem from this. The most important, and certainly the most relevant to signal processing, is the invention of infinite-dimensional space (later called Hilbert spaces) by David Hilbert in the first decade of the 20<sup>th</sup> century [13]. The Hilbert space  $L^2(\mathbb{R})$  was given prominence in signal processing by Frigyes Riesz and Ernst Sigismund Fischer who provided proof for the Plancherel / Parseval identity on the convergence of Fourier series [33, 34]. Later developments in abstract spaces (*viz.* functional analysis) stem from the ground work of Hilbert and Fréchet [12] (Fréchet was the first person to use the term ‘space’), and the first whole treatise was given in 1922 by Stephan Banach [35].

## 2.5 The origins of wavelets

The story of wavelets begins with a student of Hilbert, Alfred Haar, who introduced a series of orthogonal piecewise basis functions on the interval  $[0, 1]$  as an alternative solution to Fourier series convergence problems [36]. In 1938, Marcinkiewics showed that the Haar basis provides the simplest decomposition for  $L^p[0, 1], 1 < p < \infty$  [37]. A characteristic of the Haar basis function is that it can be translated in time, and scaled into different intervals, which (though unknown at the time) are the first and simplest orthonormal wavelets [38]. In the 1930s, Paul Levy found the Schauder basis (a primitive of the Haar basis) [39, 40] to be superior to the Fourier series in the study of local regularities such as those found in Brownian motion [41]. Another study in the 1930s, led by Littlewood and Paley [42–44], characterised the energy distribution of the Fourier transform according to the dilation parameter  $2^j$  in terms of dyadic blocks  $\Delta_j f(x)$  (i.e. blocks that scale by a factor of 2, which is equivalent to an octave), given as

$$\Delta_j f(x) = \sum_{2^j \leq k < 2^{j+1}} (a_k \cos kx + b_k \sin kx), \quad (2.14)$$

where the Fourier series in terms of dyadic blocks is given as:

$$\begin{aligned} f(x) &= a_0 + \sum_{k=1}^{\infty} (a_k \cos kx + b_k \sin kx) \\ &= a_0 + \sum_{j=1}^{\infty} \Delta_j f(x). \end{aligned} \quad (2.15)$$

Other groundwork during the 1930s includes the works of Antoni Zygmund, Phillip Franklin, and Nikolai Lusin [45]. The triumph for time-frequency analysis was in the 1940s, when Dennis Gabor introduced the short time Fourier transform (STFT)<sup>†</sup> [14]. In 1948, Jean Ville proposed another time frequency decomposition according to energy density as the Wigner-Ville transform [46, 47]:

$$P_v f(t, \omega) = \int_{-\infty}^{+\infty} f\left(t + \frac{T}{2}\right) f^*\left(t - \frac{T}{2}\right) e^{-iT\omega} dT. \quad (2.16)$$

---

<sup>†</sup>Alternatively called the windowed Fourier transform or Gabor transform.

The STFT developed by Gabor prescribes one approach to time-frequency analysis; the other, as noted by Jean Ville in 1948, is to analyse individual frequencies according to scale, then synthesise their energy content to create a time-frequency representation [47]. The second approach is the one adopted by wavelets.

The introduction of the continuous wavelet transform (CWT) in the early 1980s, albeit not entirely a new idea,<sup>†</sup> is owed to Jean Morlet. Morlet was a geophysicist for the French oil company Elf-Aquitaine, who during the 1970s and 1980s sought a better way to prospect for oil [24]. At the time, the STFT imposed major time-frequency limits, which made it difficult to numerically piece together the general structure of the underlying rocks. The main limitation was the dependence on a fixed scale for each analysing window. To create a scale independent approach he independently re-introduced the notions of time scale analysis, which, with the aid of theoretical physicist Alex Grossman, resulted in the continuous wavelet transform [49]. Morlet was motivated by the work of Dennis Gabor [14], but instead of maintaining a constant window size and filling it with eigenfunctions which, translated over time, would resolve the frequency content, he did the opposite. He kept the oscillations inside each window constant and simply scaled the size of the window proportionally. He called his analysing function  $\psi(t)$  ‘wavelets of constant shape’ [15], which later became known as the Morlet wavelet.

Similarly, in the early 1980s Strömberg rediscovered the orthonormal wavelet basis function, first introduced by Haar in 1910. The relationship between the above and connected approaches was synthesised into a ‘Wavelet Theory’ by Yves Meyer and Stephane Mallat [50–54]. Mallat developed multi-resolution analysis as framework in which to apply fast algorithms using filter banks and wavelet scaling. In 1988, Ingrid Daubechies adopted the multi-resolution approach and developed a series of orthonormal basis functions, which have become the cornerstone of modern discrete wavelet analysis [55].

---

<sup>†</sup>In the 1960s, Alberto Calderón formulated a reproducing formula for ‘atomic’ decompositions of  $f \in L^2(\mathbb{R})$  [48], which was independently rediscovered by Grossman and Morlet in the 1980s.

## 2.6 Conclusion

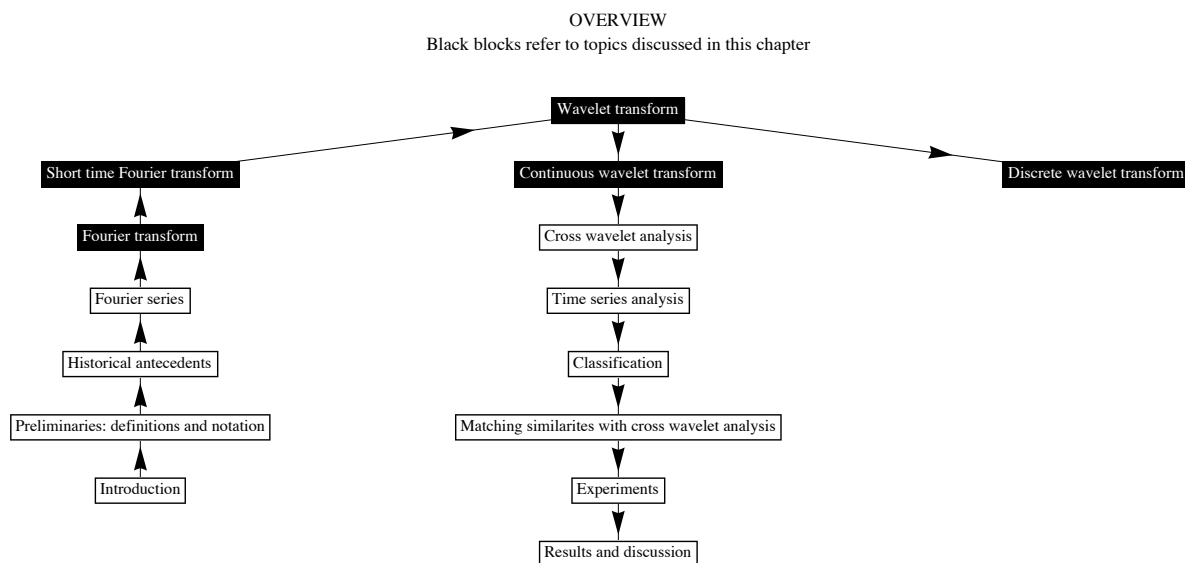
This chapter ended with a brief overview on the origins of wavelets. Although, in practice the discrete wavelet transform (DWT) is often preferred over its continuous counterpart, primarily because of its compact support in the frequency domain, the drawback is that there is less room to explore the frequency content. The CWT, on the other hand, produces too much information (further aggravated by a computational overhead), but also provides more freedom to explore the frequency content and find hidden information. A main advantage therefore of using the CWT over the DWT is that it is easier to interpret and explore the information associated with its transform, which lends itself to the development and testing of the methodology presented in Chapter 5. In the following chapter more detailed information is given specifically relating to the mathematical properties of the FT, the STFT, and the CWT in order to provide the necessary understanding and background for the main methodology.

*"It is sometimes said that one can't localise a signal simultaneously in time and frequency. This can be misleading. It's not that we can't localise the signal in time and frequency. The signal itself can't be concentrated simultaneously in time and frequency. The Heisenberg uncertainty principle does not limit what we can know about reality; it describes that reality. The shorter-lived a function, the wider the band of frequencies given by its Fourier transform; the narrower the band of frequencies of its Fourier transform, the more the function is spread out in time."*

Barbara Burke Hubbard

# 3

## Mathematical background to wavelets





## 3.1 Overview

Wavelets, like their predecessor the Fourier transform (FT), have had a profound application in society. Wavelets are essentially a time-frequency version of the FT — they obey the same mathematical rules and have identical properties — unlike the short time Fourier transform (STFT); however, they use a scaling function to translate and dilate the analysing window to map time-frequency coefficients. In this chapter, the natural progression from the FT to wavelets is presented beginning with a detailed discussion of the FT and its properties, which leads into a discussion on the STFT as a precursor to wavelets, and ending with a detailed section on the continuous wavelet transform; the cross wavelet modulus and phase and some worked examples. The background provides enough important information to understand the methodology presented in Chapter 5.

## 3.2 The Fourier transform (FT)

In modern use, the Fourier series is represented in the frequency domain as a frequency spectrum, whereby frequencies are plotted on the  $x$  axis and a description of the frequencies such as amplitude (the modulus of the FT) or phase on the  $y$  axis. The frequency coefficients (components) are presented as  $n$  integer multiples of the fundamental frequency  $\omega_0$ , which may be expressed as eigenvectors to represent the series for  $f(t)$  according to Euler's formula  $e^{i\omega t} = \cos(\omega t) + i \sin(\omega t)$  in the form

$$f(t) = \sum_{n=-\infty}^{\infty} \hat{f}(\omega) e^{i\omega t}. \quad (3.1)$$

Here,  $i = \sqrt{-1}$  is an imaginary unit, which is combined in the form  $i \sin(\omega t)$  with the function  $\cos(\omega t)$  to produce a complex representation of the series<sup>†</sup> (see Information Box 3.1 (p. 20) for more information on complex representation). The complex Fourier

---

<sup>†</sup>Note that  $a_0$  has been dropped from Equation (3.1) (p. 19) as  $n = 0$ , which is associated with the mean offset and is included in the range  $[-\infty$  to  $\infty]$ .

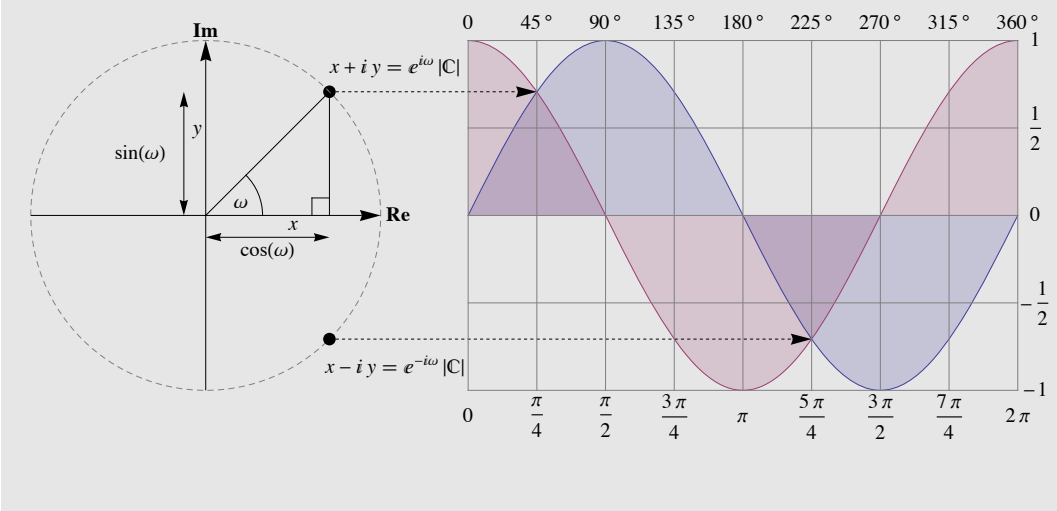
coefficients  $\hat{f}(\omega)$  in Equation (3.1) (p. 19) are calculated as the inner product

$$\hat{f}(\omega) = \frac{1}{2\pi} \int_{-\infty}^{\infty} f(t) e^{-i\omega t} dt, \quad (3.2)$$

where for each frequency  $\omega$ , amplitude =  $\sqrt{[\text{Re } \hat{f}(\omega)]^2 + [\text{Im } \hat{f}(\omega)]^2}$  and phase  $\phi_\omega = \tan^{-1}(\text{Im } \hat{f}(\omega)/\text{Re } \hat{f}(\omega))$ . A generalised form of  $\hat{f}(\omega)$  is called the Fourier transform.

### INFORMATION BOX 3.1: Complex representation

Complex numbers have a real (Re) and imaginary (Im) part that have an orthogonal relationship to each other. The figure below provides a geometric representation of Euler's equation, presented in the complex plane. Such a representation is often called a phasor and allows amplitude, phase, and frequency to be calculated in an algebraic fashion simultaneously using the complex component. A complex component is of the form  $\mathbb{C} = x + iy$ , where  $i$  is the imaginary unit equal to  $\sqrt{-1}$ .  $\mathbb{C}$  corresponds to the coordinate  $(x, y)$  in the cartesian plane, and may be represented in polar coordinates as  $\mathbb{C} = |\mathbb{C}|(\cos \omega + i \sin \omega) = |\mathbb{C}|e^{i\omega}$ . For the complex Fourier series the Fourier components are derived using  $\mathbb{C} = |\mathbb{C}|(\cos \omega n + i \sin \omega n) = |\mathbb{C}|e^{i\omega n}$ , where  $-\infty < n < \infty$ . The coefficients  $a_n$  and  $b_n$  are derived from the exponent of the exponential  $e^{i\omega n}$ . The cosine and sine coordinates (phase) are represented by the complex modulus  $|\mathbb{C}|$ , and the phase may be obtained simultaneously by  $\mathbb{C} = \omega = \tan^{-1} \frac{y}{x}$ .



An important property of the Fourier transform is that the energy<sup>†</sup> is preserved. This allows reconstruction back to its original form in the time domain. Energy is preserved

<sup>†</sup>energy is proportional to the amplitude squared.

when the Fourier transform is bounded so that in the functional space  $L^1$ ,

$$|\hat{f}(\omega)| \leq \int_{-\infty}^{\infty} |f(t)| dt < \infty. \quad (3.3)$$

If  $f \in L^1(\mathbb{R})$  and  $\hat{f} \in L^1(\mathbb{R})$ , then  $\hat{f}$  is also integrable and the inverse Fourier transform is given as

$$f(t) = \frac{1}{2\pi} \int_{-\infty}^{\infty} \hat{f}(\omega) e^{i\omega t} d\omega. \quad (3.4)$$

For discontinuous functions that are not integrable,  $f$  is extended to the Hilbert space  $L^2(\mathbb{R})$  with a finite energy  $\int_{-\infty}^{+\infty} |f(t)|^2 dt$ . The Plancherel theorem in Equation (3.5) (p. 21), which is equivalent to Parseval's theorem in Equation (3.6) (p. 21), allows energy preservation up to a factor of  $2\pi$  [56, 57]. Given the functions  $f(t)$  and  $g(t)$  with the corresponding Fourier transforms  $\hat{f}(\omega)$  and  $\hat{g}(\omega)$ , if  $f$  and  $g$  are in  $L^1(\mathbb{R}) \cap L^2(\mathbb{R})$  then

$$\int_{-\infty}^{\infty} |f(t)|^2 dt = \frac{1}{2\pi} \int_{-\infty}^{\infty} |\hat{f}(\omega)|^2 d\omega \quad (3.5)$$

and

$$\int_{-\infty}^{\infty} f^*(t)g(t) dt = \frac{1}{2\pi} \int_{-\infty}^{\infty} \hat{f}^*(\omega)\hat{g}(\omega) d\omega, \quad (3.6)$$

where  $*$  is the complex conjugate. Extension into  $L^2$  space allows manipulation of the inner product of  $f$ , which satisfies the convolution theorem in Table 3.1 (p. 22) (see Information Box 3.2 (p. 22) for a more detailed explanation). Convolution takes two signals and produces a third. It may be characterised by the relationship  $f[n] \star h[n] = y[n]$  between an input signal  $f[n]$ , an impulse response  $h[n]$ , and an output signal  $y[n]$ , where  $\star$  represents the convolution. Given the functions  $f(t)$  and  $g(t)$  with the corresponding Fourier transforms  $\hat{f}(\omega)$  and  $\hat{g}(\omega)$ , the basic properties of the Fourier transform are summarised in Table 3.1 (p. 22).

### 3.2.1 The discrete Fourier transform (DFT)

In the real world it is not feasible to apply the Fourier transform presented in Equation (3.2) (p. 20) to a signal. Observed signals are a reduction of a continuous (analog)

TABLE 3.1: Fourier transform properties. Slightly modified from [58] to match notation used in this thesis.

Property	Time domain	Frequency domain
Inverse	$\hat{f}(t)$	$\leftrightarrow 2\pi f(-\omega)$
Linearity	$\alpha f(t) + \beta g(t)$	$\leftrightarrow \alpha \hat{f}(\omega) + \beta \hat{g}(\omega)$
Time convolution	$f(t) \star g(t)$	$\leftrightarrow \hat{f}(\omega) \hat{g}(\omega)$
Frequency convolution	$f(t) g(t)$	$\leftrightarrow \frac{1}{2\pi} \hat{f}(\omega) \star \hat{g}(\omega)$
Time translation	$f(t - u)$	$\leftrightarrow e^{i\omega u} \hat{f}(\omega)$
Frequency translation (Modulation)	$e^{i\omega_0 t} f(t)$	$\leftrightarrow \hat{f}(\omega - \omega_0)$
Scaling	$f(at)$	$\leftrightarrow \frac{1}{ a } \hat{f}\left(\frac{\omega}{a}\right)$
Time derivatives	$f^{(n)}(t)$	$\leftrightarrow (i\omega)^n \hat{f}(\omega)$
Frequency derivatives	$(-it)^n f(t)$	$\leftrightarrow \hat{f}^{(n)}(\omega)$
Complex conjugate	$f^*(t)$	$\leftrightarrow \hat{f}^*(-\omega)$
Hermitian symmetry	$f(t)$	$\leftrightarrow \hat{f}(-\omega) = \hat{f}^*(\omega)$

## INFORMATION BOX 3.2: Convolution

The characteristic of a signal  $f(t)$  is decided for any point at  $t$  when it is convolved with the simplest impulse, a Dirac impulse, or unit impulse ( $\delta$ ). The Dirac impulse is a normalised impulse wherein sample zero has a value of one and all other samples are zeros. Diracs are useful in transforming continuous functions into discrete sequences by convolving against a Dirac at  $t$  so that

$$f(t) = \int_{-\infty}^{+\infty} f(n)\delta_n(t)dn, \quad (3.7)$$

where  $\delta_n(t) = \delta(t - n)$ . If  $h$  is the impulse response of  $\delta$  then

$$f(t) = \int_{-\infty}^{+\infty} f(n)h(t - n)dn = \int_{-\infty}^{+\infty} h(n)f(t - n)dt = h \star f(t), \quad (3.8)$$

where  $\star$  is the convolution, and  $h(t - n)$  proves time-invariance. It follows that all impulses may be represented as a shifted and scaled Dirac function  $\delta[n]$  (square brackets are used to represent a discrete sequence) in that the impulse response of  $f(t) = \lambda f(t - n)$  is  $h(t) = \lambda\delta(t - n)$ , so that an impulse  $a[t]$  which, for example, has a value of 5 at sample number 10 may be represented as  $a[t] = 5\delta[t - 10]$ . The following three properties summarises the basics of convolution products:

- Commutativity —  $f \star h(t) = h \star f(t)$
- Differentiation —  $\frac{d}{dt}(f \star h)(t) = \frac{df}{dt} \star h(t) = f \star \frac{dh}{dt}(t)$
- Dirac convolution —  $f \star \delta_n(t) = f(t - n)$ .

signal to a discrete (digital) signal. A discrete signal is characterised by its sampling frequency  $f_s$ , sample time  $t$  (which is the inverse of  $f_s$ ), the total number of samples  $N$ ,

and the length of the sequence  $T$  (which is the product of  $t$  and  $N$ ). The discrete Fourier transform (DFT) may be applied by assuming periodicity over  $N$  samples (a requirement of the Fourier transform), in which the total sample period represents the fundamental frequency ( $f_0 = f_s/N$ ). These assumptions are necessary to derive the Fourier coefficients. In this way the components  $n$  are resolved as harmonic integer multiples of  $f_0$  and the  $n^{\text{th}}$  harmonic is expressed as  $n$  times  $f_0$ . The DFT calculation requires that each harmonic is multiplied  $N$  times to derive a reconstructible frequency spectrum  $|\hat{f}(\frac{n}{tN})|^2$ , resulting in  $N^2 + N$  arithmetic operations. For discrete signals indexed by the time measure  $k$  the equation becomes

$$\sum_{k=0}^{N-1} |f(kt)|^2 = \sum_{k=0}^{N-1} |\hat{f}(\frac{k}{tN})|^2. \quad (3.9)$$

The division by  $N$  is used to normalise all the values. The function  $\hat{f}(\frac{k}{tN})$  is the DFT defined as

$$\hat{f}(\frac{k}{tN}) = \sum_{k=0}^{N-1} f(kt)e^{-i2\pi\frac{n}{N}k}, \quad (3.10)$$

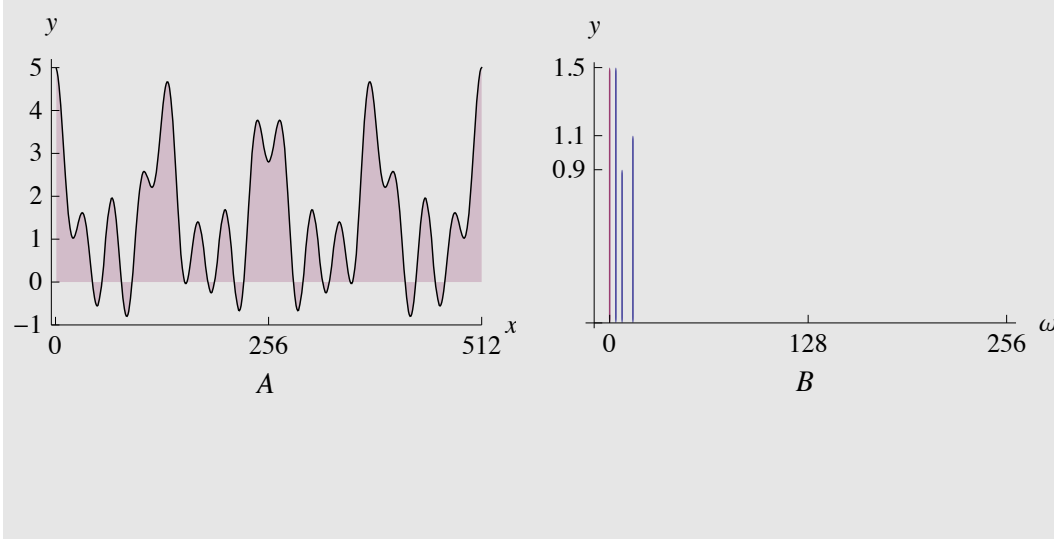
where  $2\pi\frac{n}{N}$  is the discrete frequency  $\omega_n$ . The inverse is given as

$$f(kt) = \frac{1}{N} \sum_{n=0}^{N-1} \hat{f}(\frac{k}{tN})e^{-i2\pi\frac{n}{N}k}. \quad (3.11)$$

Consider the DFT  $\hat{f}(\frac{n}{tN})$  defined in Equation (3.10) (p. 23). The coefficient  $a_0$  in Equation (2.9) (p. 13) is equal to  $\hat{f}(\omega_0)$  and is calculated from the symmetry of a sinusoidal signal about the  $x$ -axis for one full period. Therefore, by assuming a signal is a superposition of sinusoidal waves, any integration over a full period should be zero. Deviation from zero is attributed to the mean offset or  $a_0$ . The complex coefficients  $e^{i\omega t}$  are calculated simultaneously using complex notation, where a real part (Re) is the cosine coordinates on the complex plane and the imaginary part (Im) is calculated from the sine coordinates on the complex plane. The DFT calculation successively multiplies  $f(t)$  by sine ( $a_n$ ) and cosine ( $b_n$ ) waves at  $n$  times the fundamental frequency. These act as narrow-band frequency filters whose product should be zero, unless the signal contains a frequency that matches one of the harmonics. The sine and cosine waves used in the DFT are commonly called the DFT basis functions. In practice, the DFT often introduces the phenomena of

INFORMATION BOX 3.3: An example of the discrete Fourier transform

The signal presented in the figure below (A) is made up of 512 samples and represents the superposition of three cosine waves ( $1.5 \cos\left(\frac{\pi x}{64}\right) + 0.9 \cos\left(\frac{\pi x}{32}\right) + 1.1 \cos\left(\frac{15\pi x}{256}\right) + 1.5$ ). The DFT coefficients are presented as a bar graph in figure B representing amplitude / magnitude and frequency. The DFT example below was calculated using  $N^2 + N = 512^2 + 512 = 262656$  arithmetic operations. The coefficient  $a_0$  represents the mean  $= \frac{1}{512} \sum(f(x)) = 0.001953125 \times 768 = 1.5$  and is shown as the first bar. The coefficients  $a_n$  (Re) and  $b_n$  (Im) are derived by sequentially multiplying the signal by sin and cos Im functions  $n$  times the fundamental frequency (i.e.  $\text{Re}_n = \text{Re} + f(x) \cos(2\pi nx) \dots$ ,  $\text{Im}_n = \text{Im} - \sin(2\pi nx) \dots$ , where  $n = 1, 2, 3 \dots N$ ). The magnitudes are normalised as  $\frac{2}{N} \sqrt{(\text{Re})^2 + (\text{Im})^2} = 0, 0, 0, 1.1, 0, 0, 0, 1.5, 0, 0, 0, 0, 0, 0, 0.9 \dots N$ , and their position along the  $x$ -axis defines the frequencies that they represent (i.e. 4, 8, and 15).



‘spectral leakage’ as well as aliasing, which are caused by discontinuities in the observed signal and violation of the Nyquist–Shannon sampling theorem [59, 60] (discussed further in Section 3.2.4). An example of the appropriate steps that are required to implement the DFT is given in Information Box 3.3 (p. 24).

### 3.2.2 The fast Fourier transform (FFT)

The DFT calculation is very straightforward and easy to compute. However, the time required to calculate the coefficients increases as the signal increases in sample size. The FFT is an optimised version of the DFT that allows the computation of a  $N$  point DFT

in  $O(n \log_2 n)$  operations. Therefore, a signal comprising 512 samples would require 2304 calculations using the FFT, as opposed to 262 656 using the DFT. Early implementations of the FFT are accredited to Gauss [61], Yates [62] and Danielson and Lanczos [63]. The most common form is the radix-2 DIT (decimation in time) Cooley-Tukey FFT algorithm [64]. This algorithm recursively divides a signal in  $\log_2 N$  stages, so that each stage is interleaved into even and odd numbered samples. This re-ordering of the samples in a signal can be done in machine code using a bit reversal sorting algorithm. This provides the proper sequence for which a series of smaller DFTs is done and re-synthesised into a frequency spectrum. Figure 3.1 (p. 25) illustrates this interlaced decomposition of a 16 point signal.

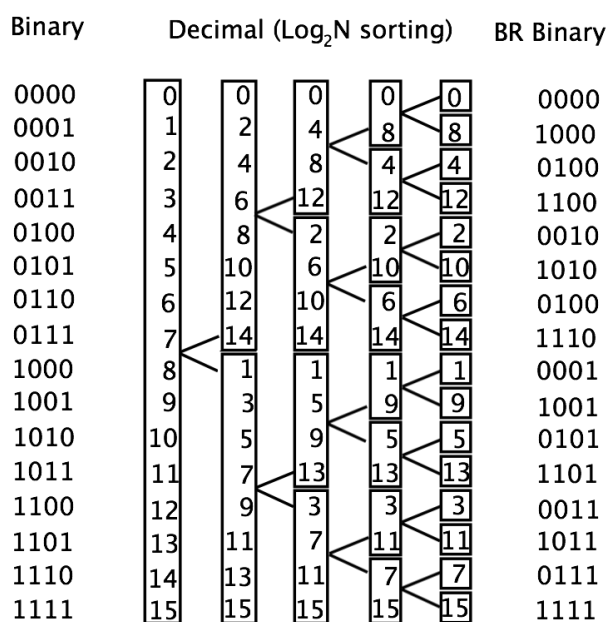


FIGURE 3.1: Radix-2 FFT interlaced decomposition. The above illustration represents the radix-2 DIT (decimation in time) Cooley-Tukey FFT algorithm [64] using a bit reversal sorting algorithm.

One major drawback of the FFT is that, owing to the interlaced breakdown, samples are required to have lengths with base 2. Although the radix-2 DIT is the most common there are many fast algorithms to calculate the DFT, including many options to transform samples with natural order lengths using mixed radix algorithms for example. The main approaches to formulating efficient algorithms include multidimensional index mapping by using either an index map or polynomial reduction, factoring the DFT operators into sparse factors, converting prime-length DFTs into cyclic convolution and recursive

evaluation of the basis function by half-length DFTs. These approaches culminated in 1997 in the development of the FFTW (fastest Fourier transform in the west) [65, 66].

### 3.2.3 The short time Fourier transform (STFT)

A drawback of the Fourier transform is that the frequency information is global, with the underlying assumption that processes responsible for change in the observed signal over time are periodic. Time-frequency analysis, however, provides a means to time localise the processes responsible for change, but at the expense of the frequency content. In 1946, Hungarian born engineer Dennis Gabor provided the first time-frequency solution called the short-time Fourier transform (STFT) or windowed Fourier transform (WFT) [14, 67]. The STFT offers time localisation by calculating the Fourier transform for a series of sliding time windows as

$$\text{STFT}(b, \omega) = \int_{-\infty}^{+\infty} f(t)w^*(t - b)e^{-i\omega t} dt \quad (3.12)$$

where  $w(t)$  is the time window interval centred around a point in time  $b$ , and  $*$  is the complex conjugate. The STFT may be written in discrete form as

$$\text{DSTFT}(b, \omega) = \sum_{n=-\infty}^{+\infty} f(n)w(n - b)e^{-i\omega n}, \quad (3.13)$$

where a new Fourier coefficient is calculated for every  $b$  and  $\omega$ . In this manner, the window function localises the Fourier transform for a position centred around  $b$ , then shifts the window to a new position and calculates a new set of Fourier coefficients, and so on. It is preferable to overlap the windowing functions to provide a continuous representation, and increase the accuracy of separate frequency components. The STFT provides a good tool for analysis but one not wholly suited for synthesis. This is because the inversion back to the time domain is equivalent to the convolution of the transform of the signal and the window function. Any deviation in the reconstructed signal is, therefore, dependent on the choice of synthesis window and the percentage overlap between window samples.



The inverse STFT is calculated as

$$f(t) = \int_{-\infty}^{+\infty} STFT(t, \omega) e^{i\omega t} d\omega. \quad (3.14)$$

The main shortcoming of the STFT is that the size of each window is fixed, whereby the oscillating term  $e^{i\omega t}$  is modulated to resolve all possible frequencies that exist within the time window. The size of the analysing window, therefore, is application specific depending which compromise in the time frequency plane is desired (see Information Box 3.4 (p. 28) for further information). An optimal solution to overcome such a compromise is the analysis of signals using wavelets. Wavelets are similar to the STFT, in that frequency  $\omega$  is calculated for time  $f(t)$  locally using an envelope function to represent a time window. The major advantage of wavelets lies in the scaling function (called the father wavelet  $\phi$ ), which replaces modulation of the oscillating term  $e^{i\omega t}$  with a scaled and translated basis function called the mother wavelet  $\psi$ . The mother wavelet, therefore, provides frequency bands resolvable only at the scale of the time window by scaling the wavelet appropriately. Figure 3.2 (p. 29) illustrates a comparison of the time-frequency decomposition of the STFT and the wavelet transform.

### 3.2.4 Sampling and other considerations

The sampling theorem (also known as the Nyquist–Shannon sampling theorem) describes both the sampling into the discrete domain and reconstruction back into the continuous domain (analog) [59, 60]. The theorem shows that a discrete signal  $f(kt)$  can be perfectly reconstructed to  $f(t)$  using the Nyquist rate [59] ( $2f_s$ ), provided the frequency content of the signal (bandwidth) is limited (band-limited). In other words, we need twice as many samples as the highest embedded frequency. A practical consideration is that a band-limited signal has to be continuous and therefore cannot truly exist in the discrete world. Alternatively, if  $f_s$  is known then the upper frequency limit to allow reconstruction is the Nyquist frequency [59] ( $\frac{f_s}{2}$ ), not to be confused with the Nyquist rate. This state also implies that the signal is bandlimited, which again is practically impossible. We note, therefore, that when the signal deviates from a  $2\pi$  periodic process, redundant

## INFORMATION BOX 3.4: Heisenberg's inequality

The support of a function in both the frequency and time domain is related to its energy. We know from Planck that frequency is related to energy by

$$E = \frac{h}{2\pi}\omega, \quad (3.15)$$

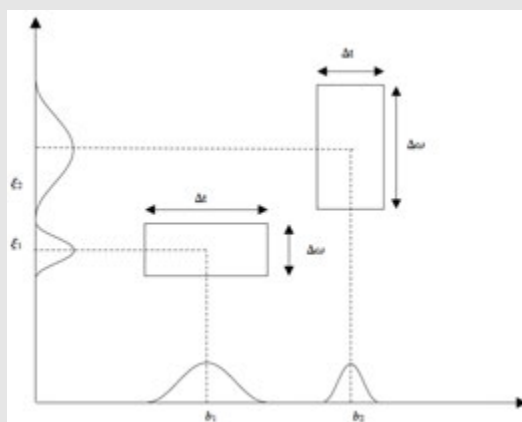
where  $h = 6.626 \times 10^{-34} \text{ J}^{-\text{s}}$  is Planck's constant. This notion is based on a related concept described in Heisenberg's uncertainty principle [68], in that compromise between time and frequency occurs in proportional directions in the spectral representation of time / amplitude based data. The minimum requirement for energy preservation<sup>†</sup> in both time and frequency is given by Heisenberg's inequality

$$\Delta t \Delta \omega \geq \frac{1}{4\pi} \quad (3.16)$$

where  $\Delta t$  is the time spread, and  $\Delta \omega$  is the frequency spread of a function. To explain in more detail, the centre of the analysing window ( $\mu_t$ ) must satisfy  $\int_{-\infty}^{+\infty} t|w(t)|^2 dt$ . A measure for the concentration of  $w$  around  $\mu_t$  is given as

$$\Delta_t = \left\{ \int_{-\infty}^{+\infty} (t - \mu_t)^2 |w(t)|^2 dt \right\}^{\frac{1}{2}}. \quad (3.17)$$

The analysing window is located in the time frequency plane by the bounding coordinates  $[\mu_t - \Delta_t, \mu_t + \Delta_t] \times [\mu_\omega - \Delta_\omega, \mu_\omega + \Delta_\omega]$ , and  $w$  is localised around the point  $[\mu_t, \mu_\omega]$ . The figure below (modified from [58] p 86) illustrates the energy spread in the time frequency plane according to Heisenberg's inequality for the mother wavelet  $\psi$  at two different scales.



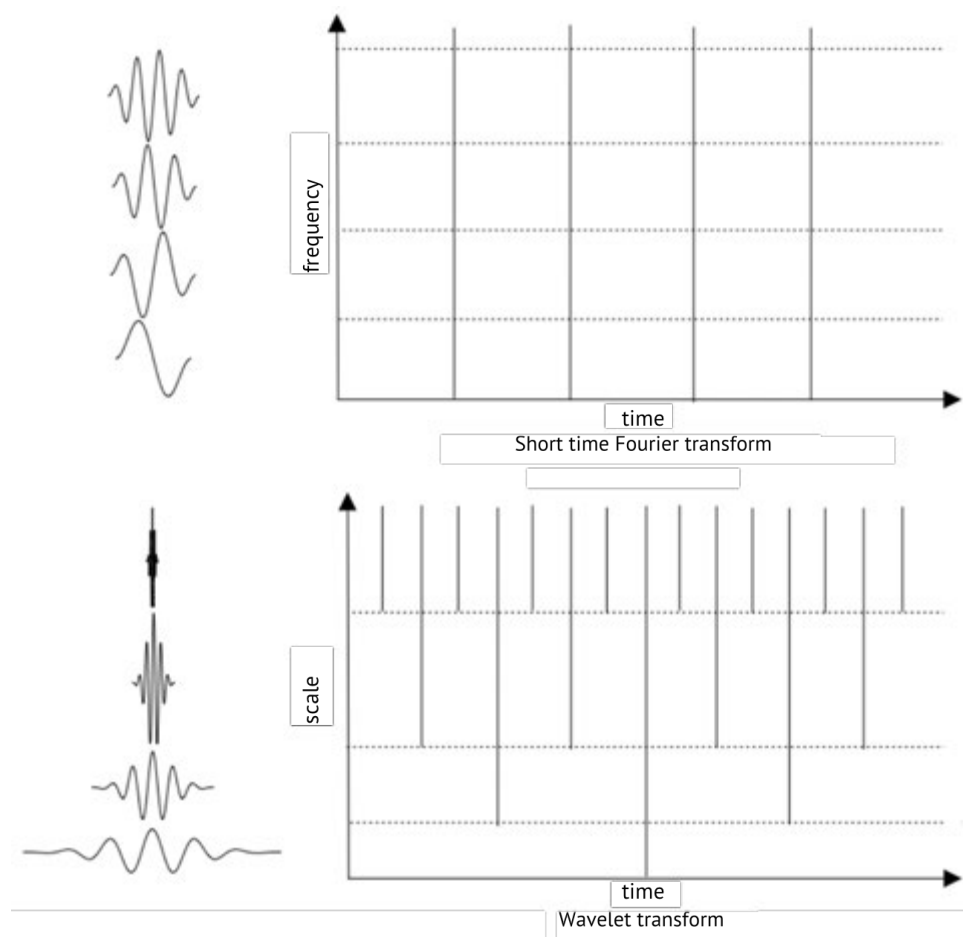


FIGURE 3.2: Comparison between the STFT and the wavelet transform in the time frequency plane. The wavelet transform offers an optimised time frequency decomposition over the STFT. The analysing scheme for the wavelet transform is in dyadic intervals  $2^j$ , and is proportionally localised in the time frequency direction.

or additional frequencies are represented to account for discontinuity. In addition, any deviation from the Nyquist frequency results in alias signals at frequencies lower than the required sampling rate. For example, consider one of the components  $(0.9 \cos(\frac{\pi x}{32}))$  of the signal presented in Information Box 3.3 (p. 24) represented in Figure 3.3 (p. 30) as a 9 Hz<sup>†</sup> signal sampled at 11 Hz. If we were to sample this signal at less than the required sampling rate ( $2f_s = 18$  Hz), then the alias signal represented Figure 3.3 (p. 30) is produced and it is impossible to confirm which signal the underlying function represents.

The sampling theorem gives the conditions for a  $2\pi/T$  periodic Fourier transform that allows for reconstruction of a given signal. Note that the Fourier transform of piecewise

<sup>†</sup>1 Hz = 1 cycle per second.

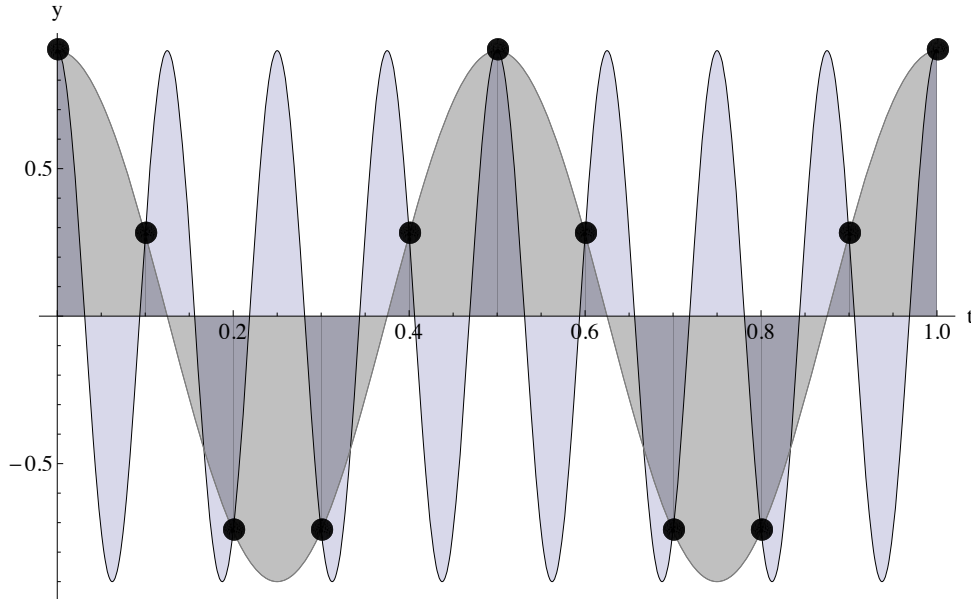


FIGURE 3.3: Example of an alias signal. The above illustration represents a 9 Hz signal sampled at less than  $2f_s$  (11 Hz). The result is an alias signal that is indistinguishable from the original signal.

functions is problematic, and inversion back to the time domain is not possible because of divergence of its Fourier coefficients at discontinuities. This phenomenon is known as the Gibbs effect and relates to a non-finite support of energy in the frequency domain [69–71]. The Gibbs effect is demonstrated in Figure 3.4 (p. 31) by partial Fourier sums for a square wave. Equation (3.18) (p. 30) provides a modified Fourier sum that would minimise the Gibbs effects by adding a sinc term to the equation:

$$\frac{1}{2}a_0 + \sum_{n=1}^{m-1} \text{sinc}\left(\frac{n\pi}{2m}\right)[a_n \cos(n\omega) + b_n \sin(n\omega)] \quad (3.18)$$

where  $m$  is the last term, and  $\text{sinc}(x)$  terms in Equation (3.18) (p. 30) are the Lanczos sigma factors. The extra coefficients associated with the Gibbs effect are known as ‘spectral leakage’. Spectral leakage is most commonly associated with discontinuities at the edges of discrete samples (recall that an assumption of the DFT is that the signal is  $2\pi$  periodic), which results in additional Fourier coefficients required for reconstruction. Leakage can be minimized by multiplying the signal by a window function, which dampens the edge amplitudes towards zero. The Gaussian is a good choice because it is well localised in both space and frequency. Figure 3.5 (p. 33) demonstrates the use of a

window function to reduce the spectral leakage associated with edge discontinuities of a discrete signal (see Information Box 3.5 (p. 32) for some common window functions).

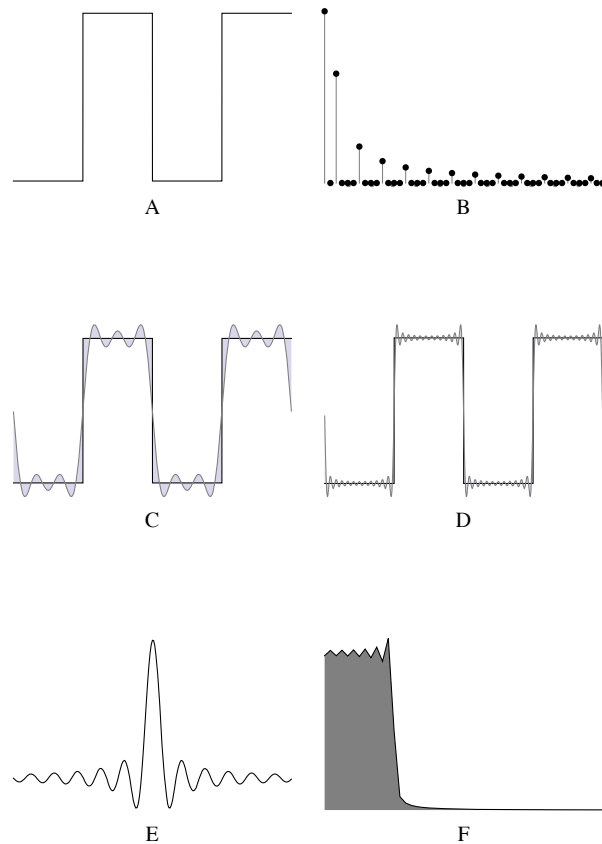
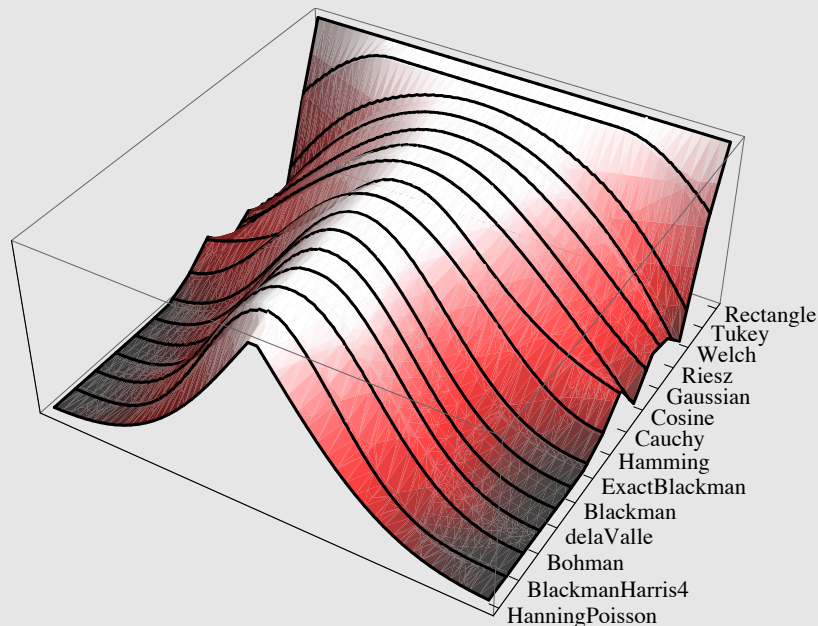


FIGURE 3.4: Example of the Gibbs effect. The Gibbs effect describes the overshooting of a Fourier series at discontinuities within a signal. These overshoots diverge at jumps within the signal as demonstrated for the square wave presented in A above. In the above figure A is an example of a square wave signal. B is the frequency spectrum of A derived using the DFT. C shows the partial Fourier sum of A with  $n = 12$ . Similarly, D is the partial Fourier sum of A with  $n = 48$ . E is an example of a sinc function =  $\text{sinc}(x)$ , and F is the frequency spectrum of E, which closely resembles the data presented in A. The effects of the Gibbs phenomenon are reduced by adding the Lanczos sigma Factor (a sinc function) to the Fourier sum as in Equation (3.18) (p. 30).

## INFORMATION BOX 3.5: Common window functions

A window function is designed to taper towards zero outside a chosen interval in order to minimise edge discontinuities. There are many types of window functions available, each with their own advantages and disadvantages. The values in each window function range between 0 and 1, therefore by multiplying a rectangular window of unit 1 with the data would lead to no change to the input signal. To minimise spectral leakage the window function's main lobe should be narrow, and the side lobes must be suppressed to dampen discontinuities. The figure below shows a visual comparison between a few of the more common window functions.



### 3.3 The wavelet transform (WT)

Wavelets are short finite interval oscillating functions that can be scaled and translated to extract the local time and frequency information from any signal. The term ‘wavelet’ is derived from the French word ‘*ondelette*’ — meaning small wave. It was officially first cited in an appendix by Alfred Haar in the early 1900s [36], but only really became conventional in the early 1980s [15, 49, 72]. The wavelet transform uses two basic parameters: scaling ( $s$ ) and translation ( $u$ ). Using these two parameters, the analysing function  $\psi$  (called the mother wavelet) returns the local time frequency content of a signal through a series of dilations (scalings) and time translations. This allows the signal to be processed at different time and frequency resolutions. If the wavelet function is

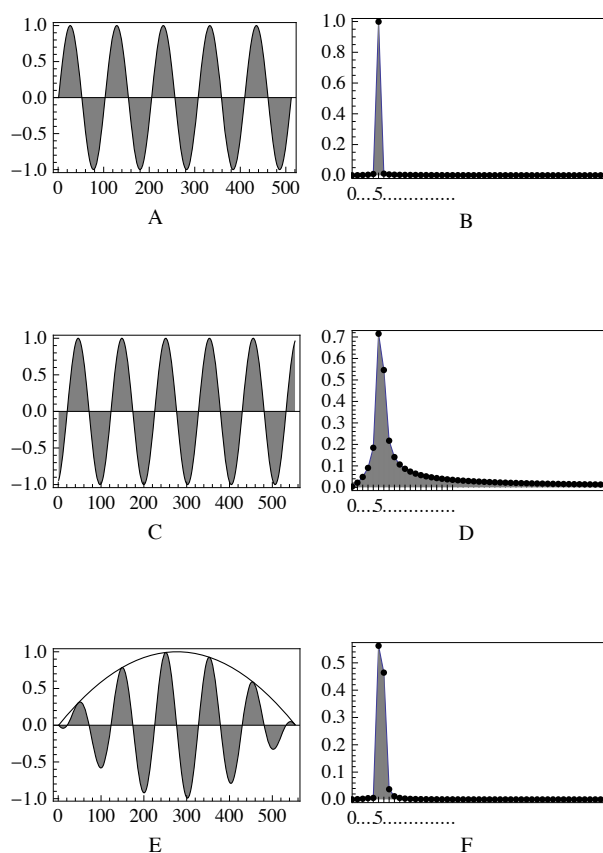


FIGURE 3.5: Example of spectral leakage. Multiplying the input signal by a window function helps taper the discontinuities at the ends of a finite signals. Figures A and B represent a continuous function and its Fourier Amplitudes. Figure C represent the same signal in A, but sampled over an interval that results in discontinuities at either end of the signal. Figure D is the frequency spectrum of C which highlights spectral leakage associated with the discontinuities in C. Figure E represents the data multiplied by a simple Welch window, and F demonstrates the minimisation of the spectral leakage by use of a window function. The Welch window is defined as  $1 - \left(\frac{x-N/2}{N/2}\right)^2$ .

stretched, then frequency localisation increases and the time localisation decreases, and *vice versa*. The many wavelet functions that exist today are amassed into functions conceptually belonging to either the continuous wavelet transform (representing a signal across all its available frequency bands), or the discrete wavelet transform (representing a discrete subset of wavelet coefficients that meet the minimum requirements for signal reconstruction).

### 3.3.1 The continuous wavelet transform (CWT)

Continuous wavelet transform families (daughter wavelets) are derived as the product of a mother wavelet at scales  $s$  and time translations  $u$ , and take the following form:

$$\psi(u, s)(t) = \frac{1}{\sqrt{s}} \psi^* \left( \frac{t-u}{s} \right), u > 0, s > 0, s \in \mathbb{R}. \quad (3.19)$$

The normalisation parameter  $\frac{1}{\sqrt{s}}$  is to ensure that all scales are comparable to each other. A common choice for the mother wavelet  $\psi$  in Equation (3.19) (p. 34) is the Morlet, defined as

$$\psi_0(t) = \pi^{\frac{1}{4}} \cos(t\pi\sqrt{2/\log(2)}) \exp\left(-\frac{t^2}{2}\right). \quad (3.20)$$

The complex Morlet wavelet  $\psi \in L^2(\mathbb{R})$  with a zero average is called the Gabor wavelet, and is defined as

$$\psi_0(t) = \pi^{\frac{1}{4}} \exp(i\omega_0 t) \exp\left(-\frac{t^2}{2}\right). \quad (3.21)$$

Here  $\omega_0$  is the central frequency parameter taken as  $> 5$  to satisfy Calderón's admissibility condition[48],  $t$  represents a non-dimensional time parameter, and  $i = \sqrt{-1}$  is an imaginary number which denotes that the Morlet is a complex wavelet. The parameter  $\omega_0$  determines the compromise between time and frequency: a large value for  $\omega_0$  would lead to better frequency and worse time resolution; a small value for  $\omega_0$  would lead to good time resolution but bad frequency resolution (see Figure 3.9 (p. 43) for an example and see Information Box 3.6 (p. 37) for some examples of different continuous wavelet functions). The admissibility condition implies that the Fourier transform of the wavelet vanishes at zero frequency and is defined as

$$C_\psi = \int_{-\infty}^{+\infty} \frac{|\hat{\psi}(\omega)|^2}{\omega} d\omega < \infty, \quad (3.22)$$

where  $\hat{\psi}(\omega)$  is the Fourier transform of  $t\omega$ , and satisfies the unit energy condition

$$\sum_{-\infty}^{\infty} |\hat{\psi}(t\omega)|^2 \frac{dt}{t} = 1. \quad (3.23)$$



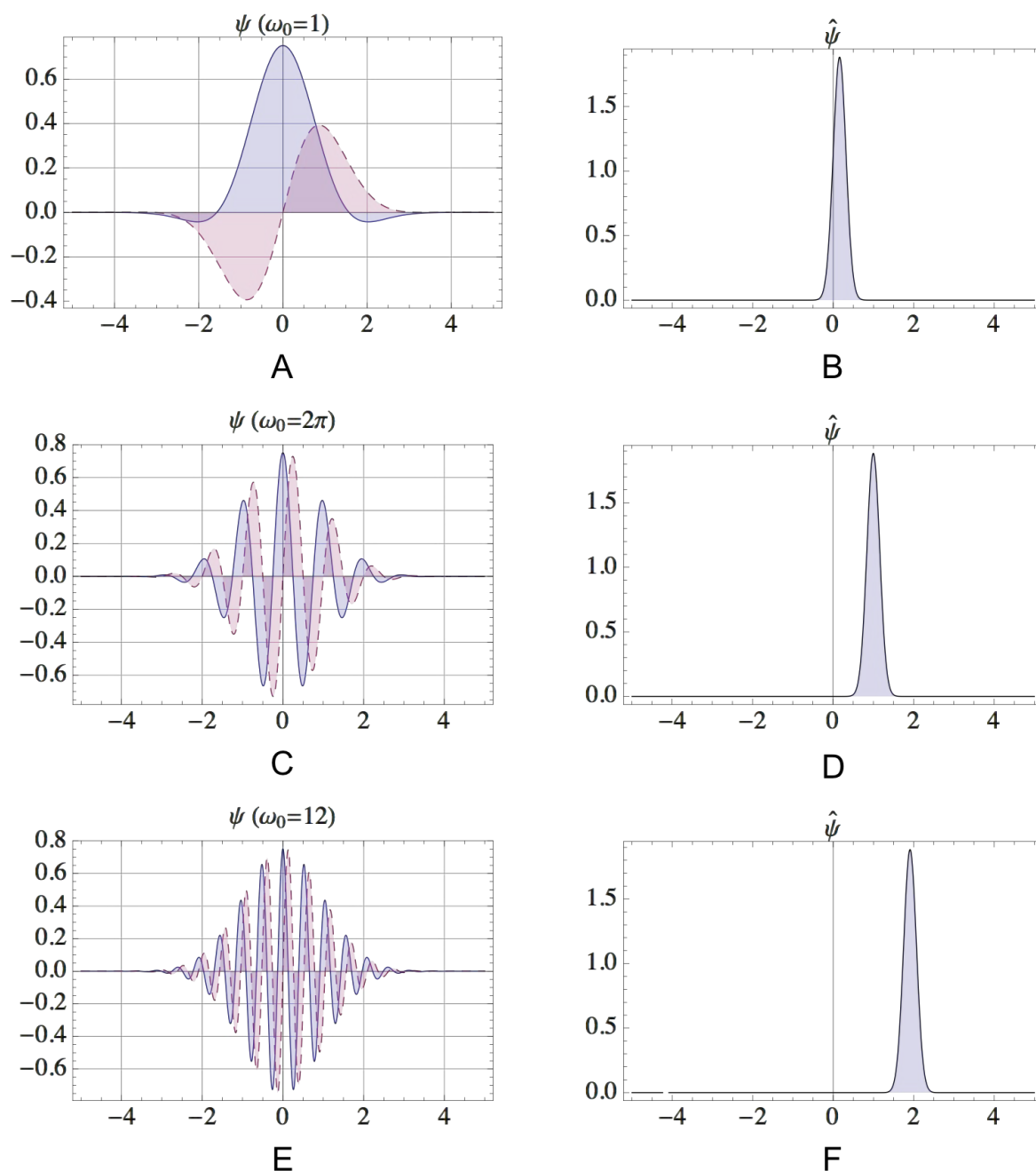


FIGURE 3.6: Graphical representation of the Morlet wavelet  $\psi$  and its Fourier transform  $\hat{\psi}$ . For A and B  $\omega_0 = 1$ , for C and D  $\omega_0 = 2\pi$ , and for D and E  $\omega_0 = 12$ . The dashed line represents the imaginary part. Figure 3.9 (p. 43) gives an example of performing the CWT using the Morlet wavelet presented above using the same three values for  $\omega_0$ .

Figure 3.6 gives an example of the Morlet wavelet and its Fourier transform for  $\omega_0 = 1$ ,  $\omega_0 = 2\pi$ , and  $\omega_0 = 12$ . According to [3] the choice of wavelet is often arbitrary, but should reflect as much as is possible the underlying features of the data being analysed and be selected according to its properties. For good time localisation, for example, a narrower wavelet function should be used, where the folding time of the wavelet amplitude is fast

(decays to zero relatively quickly – note the comparison between the Paul wavelet and the mexican hat wavelet in Information Box 3.6 (p. 37) for an example). For stepwise signals with sharp jumps and discontinuities, boxlike functions like the Haar wavelet could be a good choice. In this thesis, the complex Morlet is used as the mother wavelet function. The wavelet has to be complex in order to return both phase and power (amplitude) coefficients, and the wavelet has to represent a balanced compromise between time and frequency (which the Morlet does) to be useful over a wide variety of time series. A good choice for  $\omega_0$  when using the Morlet is  $2\pi$ , which ensures that scale ( $\frac{N}{frequency}$ ) is directly comparable to frequency ( $\frac{N}{scale}$ ).

The CWT is used to derive the time frequency content of a signal through the convolution of  $f(t)$  with a scaled and translated version of the mother wavelet  $\psi(t)$  as

$$W(u, s) = \frac{1}{\sqrt{s}} \int_{-\infty}^{\infty} f(t) \psi^* \left( \frac{t-u}{s} \right) dt, \quad (3.24)$$

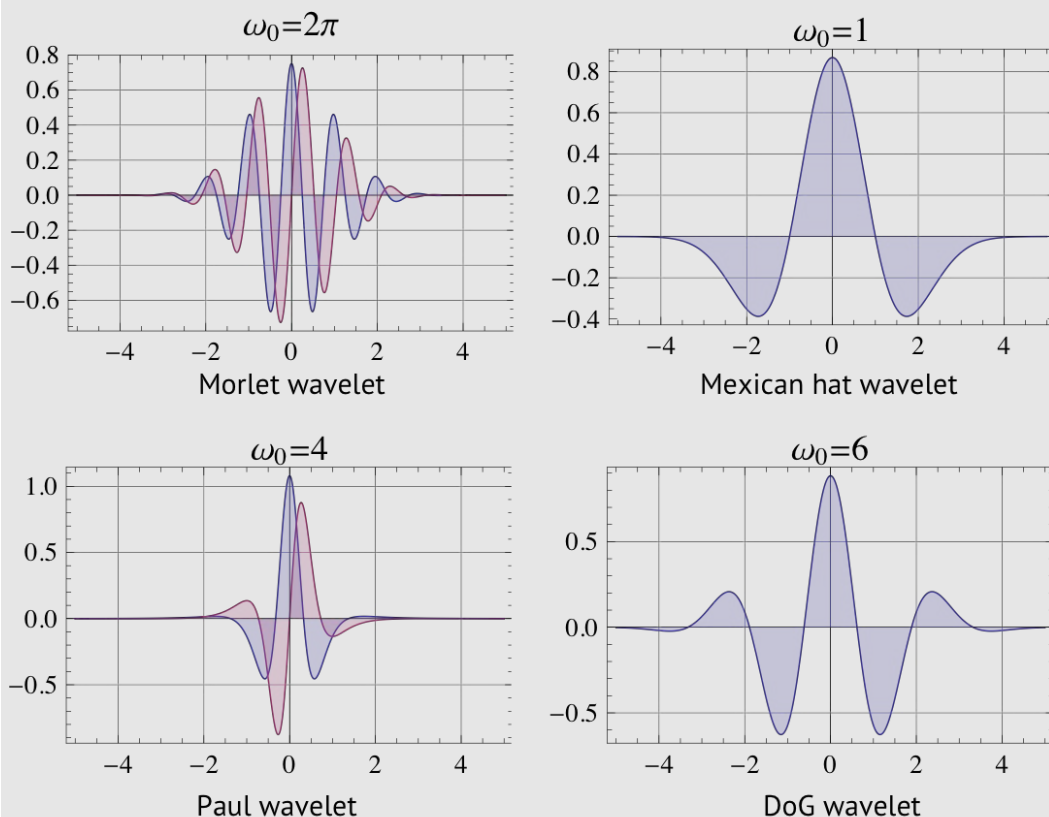
where  $\psi$  is the mother wavelet, \* indicates the complex conjugate, and  $u$  and  $s$  are the translation and scaling parameters. The subscript 0 for  $\psi$  has been dropped to indicate that the wavelet is normalised. The wavelet must be translated by a distance  $u$  to analyse the signal at time  $u$ . In a similar way, the wavelet must be dilated (scaled in time) by  $s$ , to analyse the properties of the signal at scale  $s$ . If you add or subtract a constant  $t_0$  from the independent variable  $t$ , then the translation occurs in the shift parameter  $u$ .

Similarly, the CWT is also covariant under dilation; therefore, if you multiply the independent variable by a constant  $s$  then both the scaling parameter  $s$  and the shift parameter  $u$  are multiplied by  $s$  and the CWT is divided by  $s$ . To approximate the CWT, the convolution should be done  $n$  times for each scale  $s$ . However, according to the convolution theorem, the CWT convolution can be applied  $n$  times to the data simultaneously for each scale  $s$  in Fourier space using the FFT. According to the theorem the complex correlation in Equation (3.24) (p. 36) maintains a duality with the Fourier transform and can be computed as the inverse Fourier transform of the product of the Fourier transform of the signal and the Fourier transform of the mother wavelet. To compute the CWT using the FFT, Equation (3.24) (p. 36) becomes

## INFORMATION BOX 3.6: Examples of continuous wavelet functions

The function  $\psi(t)$  is called the ‘mother wavelet’ and satisfies  $\int \psi(t) dx = 0$ , and  $\int |\psi(t)|^2 dx = 1$ . Each mother wavelet function  $\psi(t)$  decomposes a signal into different frequency components, matched to its scale. These wavelet families adhere to Heisenberg’s uncertainty principle [68], whereby compromise between frequency and time is introduced by the scaling and translation parameters. The continuous wavelet families are typically shifted and scaled in dyadic intervals (octaves), and smaller intermittent intervals (voices) to provide a smooth representation of the underlying function. Reconstruction of  $f(t)$  via the CWT is somewhat cumbersome and may need many wavelet coefficients (derived by using more voices), making the process very computationally intensive. An advantage of the CWT is that additional information about the signal may be procured; the disadvantage is that there is also much redundant information.

The Morlet / Gabor wavelet defines a family of complex non-orthogonal wavelets given by  $\psi(t) = \frac{1}{\sqrt{4\pi}} \exp(i\omega_0 t) \exp\left(-\frac{t^2}{2}\right)$ . Both the derivative of Gaussian (DoG) wavelet defined as  $\frac{(-1)^{n+1}}{\sqrt{\Gamma(n+\frac{1}{2})}} \frac{\partial^n}{\partial t^n} \exp\left(-\frac{t^2}{2}\right)$  and the the mexican hat wavelet, defined as  $-\frac{2e^{-\frac{t^2}{2}}(-1+r^2)}{\sqrt{3\pi^{1/4}}}$  (which is the DoG wavelet with a central frequency of 2) are real valued. The Paul wavelet  $\frac{(2i)^n n!}{\sqrt{\pi} \sqrt{(2n)!}} (1-ir)^{-n-1}$  is similar to the DoG wavelet but like the Morlet / Gabor wavelet is complex. The figure below represents these four common choices for the CWT basis function.



$$W(u, s) = \frac{1}{\sqrt{s}} \int_{-\infty}^{\infty} \hat{f}(t) \hat{\psi}^*(\omega s) dt, \quad (3.25)$$

where  $\hat{f}(t)$  is the Fourier transform of  $t$ ,  $*$  represents the complex conjugate,  $\omega$  is angular frequency, and  $\hat{\psi}^*(\omega s)$  is the Fourier transform of the mother wavelet at scale  $s$ , which is defined for the Morlet as

$$\psi(\omega s) = \pi^{0.25} H(\omega) \exp\left(-\frac{s(\omega - \omega_0)^2}{2}\right), \quad (3.26)$$

where  $\omega_0$  is the central frequency parameter and  $H(\omega)$  is the Heavyside step function equal to 1 for  $\omega \geq 0$  and 0 for  $\omega < 0$ . The angular frequency  $\omega$  is defined over the time index  $n$  as

$$\omega_n = \begin{cases} \frac{2\pi n}{N} & \text{if } n \leq \frac{N}{2} \\ -\frac{2\pi n}{N} & \text{if } n > \frac{N}{2}. \end{cases} \quad (3.27)$$

By calculating the CWT convolution in Fourier space, edge effects and other unwanted signals are reduced through proper sampling, and computation time is significantly improved.

The inverse CWT may be synthesised if Equation (3.22) (p. 34) is satisfied, and is given by Calderón's reconstruction formula as

$$f(t) = \frac{1}{C_\psi} \int_{-\infty}^{+\infty} \int_{-\infty}^{+\infty} W(u, s) \psi_{u;s}(t) \frac{du ds}{u^2}, \quad (3.28)$$

where  $C_\psi$  is the admissibility criterion. Note that the quality of the reconstruction depends on the resolution of scales (number of octaves and voices). In practice, dyadic scales are used to represent octaves (the doubling or halving of frequencies), and the scales in between the octaves are called voices. The number of voices are typically 'user-defined', where more voices provide a better frequency localisation between two octaves and subsequently increases the 'smoothness' of the frequency transitions between octaves. Caution

should be taken, however, when increasing the voice resolution, as each additional voice results in an exponential increase in the wavelet calculation. The largest scale (and therefore the largest octave) is given as  $2^{\log_2(\frac{n}{2})}$ , where  $\log_2(\frac{n}{2})$  defines the number of octaves, and  $n$  is the length of the signal or time series being analysed.

### 3.3.2 The discrete wavelet transform (DWT)

The discrete version of the CWT is called the discrete wavelet transform (DWT) and decomposes a signal in dyadic scales ( $s_j \sim 2^j$ ) with no overlap in time translation, which provides enough information for both the analysis and synthesis of a signal without the large amount of redundancy associated with the CWT. Discrete wavelets may be distinguished by orthonormal wavelet bases and non-orthonormal redundant discrete systems (frames) [38]. The orthonormal wavelet base has the form

$$\psi_{j,k}(t) = 2^{j/2} \psi(2^j t - k), \quad j, k, \in \mathbb{Z}. \quad (3.29)$$

The DWT is best computed using multi-resolution analysis [52–54]. Multi-resolution analysis is a decomposition of  $L^2(\mathbb{R})$  into *levels* of coarser and finer subspaces  $v_j \subset L^2(\mathbb{R}), j \in \mathbb{Z}$ . During computation, the frequency response of both the wavelet function  $\psi(x)$  and the scaling function  $\phi(x)$  act as low and high pass filters to get coarse and detailed resolution coefficients for each scale. The Haar wavelet  $\psi(x)$  is an example of the simplest of the orthonormal wavelet bases, defined as

$$\psi(x) = \begin{cases} 1 & \text{if } 0 \leq x < 1/2 \\ -1 & \text{if } 1/2 \leq x < 1 \\ 0 & \text{otherwise} \end{cases} \quad (3.30)$$

and scaled into different intervals by

$$\phi(x) = \begin{cases} 1 & 0 \leq x < 1 \\ 0 & \text{otherwise.} \end{cases} \quad (3.31)$$

The Haar wavelet function  $\psi(x)$  has only one vanishing moment ( $\int x^k \psi(x) dx = 0$ ) and is symmetric with compact support of length 1. The wavelet function  $\psi(x)$  is orthogonal to  $\phi(x)$  at the same scale  $\int \psi(x)\phi(x) dx = 0$ . The wavelet coefficients are found using the recursive equations  $2 \sum_n a_n \phi(2t - n)$  for  $\phi(x)$ , and  $2 \sum_n b_n \phi(2t - n)$  for  $\psi(x)$ , where  $\sum_k a_k = 1$  and  $\sum_k b_k = 0$ ; therefore  $\int \phi(x) dx = 1$  and  $\int \psi(x) dx = 0$ ; thus  $\sum_k a_k b_k = 0$  is orthogonal. Figure 3.7 (p. 41) gives an example of Haar scaling function  $\phi(x)$  and Haar wavelet function  $\psi(x)$ , along with their Fourier transforms and frequency response. The filtering process is done via the convolution of the frequency response of the scaling and dilating functions and the signal, from which we can define the coarse low pass filter coefficients  $c_{j,n}$ , and the detailed high pass filter coefficients  $d_{j,n}$  for every scale  $j$ . These coefficients may be represented as a tree, with  $c_{0,n} = x_n$  representing the input signal in Figure 3.8 (p. 42).

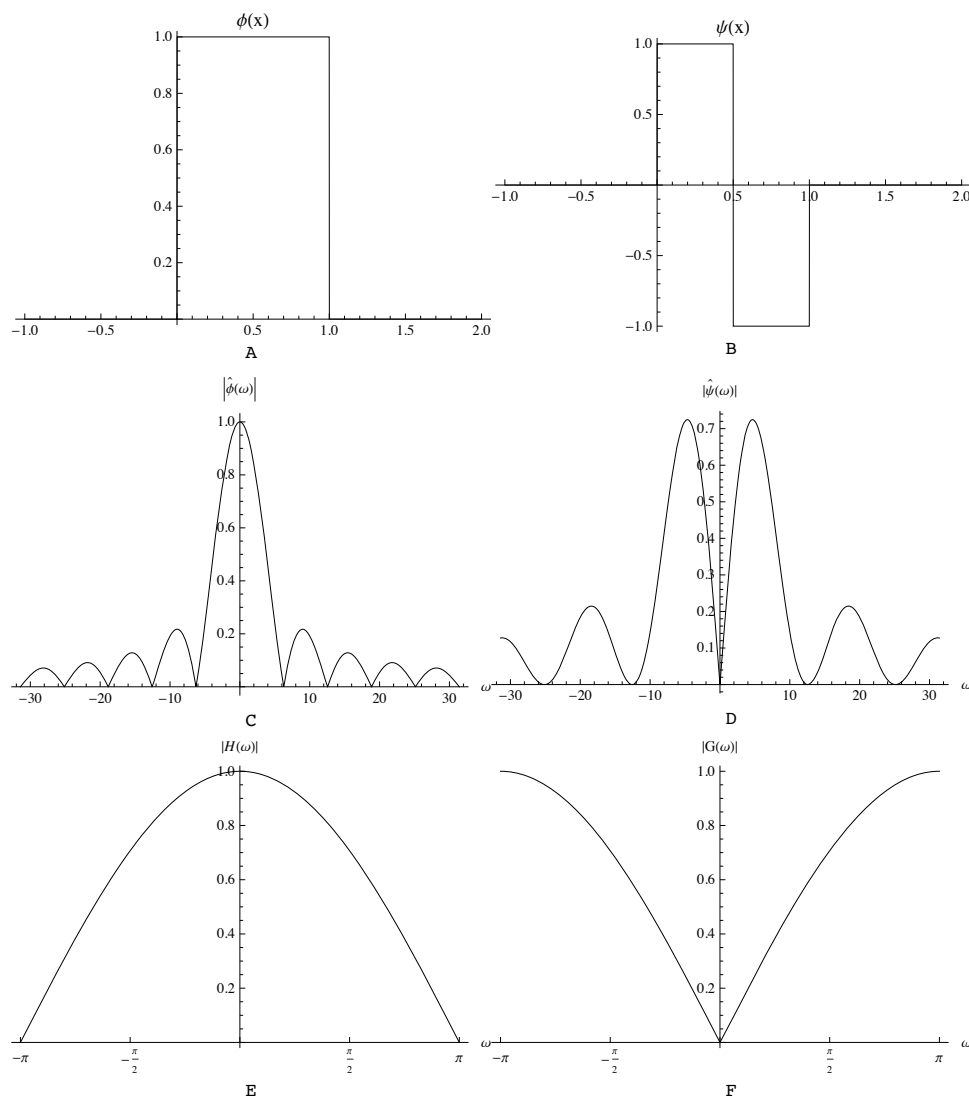


FIGURE 3.7: Example of the Haar wavelet. The scaling function A, and wavelet B do not have good support in the frequency domain, as shown in C and D. The frequency response of the scaling parameter (E) acts as a low pass cut-off filter, and the frequency response of the wavelet function (F) acts as a high pass cut-off filter from which coarse and finer resolution DWT coefficients are derived.

### 3.3.3 The wavelet power spectrum

The CWT coefficients are often displayed as a smoothed contour plot (scalogram) in which the translation convolution of  $f(t)$  comprises a series of overlapping wavelets uniformly shifted by the sampling frequency of the signal. In practice, dyadic scales (octaves with ‘user-defined’ voices) are used to transform a signal, with the default number of scales  $= 2^{\log_2(\frac{n}{2})}$  (where  $\log_2(\frac{n}{2})$  defines the octave). The square of the absolute value of the coefficients  $|W(u, s)|^2$  represents the local wavelet power spectrum energy at a particular

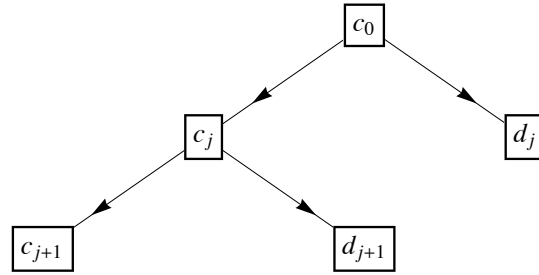


FIGURE 3.8: A DWT tree of coarse wavelet coefficients  $c_{j,n}$ , and detailed coefficients  $d_{j,n}$  for each level  $j$ . The values  $c_{0,n}$  represent the input signal  $x_n$ . The DWT is calculated by  $c_{j+1,n} = \sqrt{2} \sum_m a_{m-2n+2} c_{j,m}$ , and  $d_{j+1,n} = \sqrt{2} \sum_m b_{m-2n+2} c_{j,m}$ , where  $a_i$  and  $b_i$  are low and high pass filter coefficients. The inverse is given by  $c_{j,n} = \sqrt{2} (\sum_m a_{n-2m+2} c_{j+1,n} + \sum_m b_{n-2m+2} d_{j+1,m})$ . The image in the above figure and the description are taken from [73].

point in time and frequency. Time averaging the scales (global wavelet power spectrum) provides a good estimator of the Fourier spectrum over time, but the energy distribution is normalised by scale<sup>†</sup> [3]. To compare better with the Fourier spectrum, the coefficients are normalised in this thesis according to

$$W_M(u, s) = \frac{a \sqrt{|W(u, s)|^2}}{N \sqrt{s}}, \quad (3.32)$$

where  $W_M(u, s)$  represents the normalised modulus, and  $a$  represents a scalar that can be determined analytically by performing the CWT on a cosine wave of known frequency and amplitude and finding the relationship between the global wavelet power spectrum and the Fourier amplitude of the cosine wave.

Figure 3.9 (p. 43) shows a comparison of a time-based convolution and the CWT computed using Equation (3.25) (p. 38) using different values for  $\omega_0$  of a signal comprising 10Hz, 25Hz, 50Hz, and 75Hz represented by  $\sin(20\pi t)$ ,  $\sin(50\pi t)$ ,  $\sin(100\pi t)$ , and  $\sin(150\pi t)$  for  $0 \leq t < \frac{1}{4}$ ,  $\frac{1}{4} \leq t < \frac{1}{2}$ ,  $\frac{1}{2} \leq t < \frac{3}{4}$ , and  $\frac{3}{4} \leq t \leq 1$  respectively over 1000 ms. Figure 3.10 (p. 44) shows a comparison of the CWT using a different number of voices computed with Equation (3.25) (p. 38) using a Morlet wavelet with  $\omega = 2\pi$  on the same signal presented in Figure 3.9 (p. 43).

<sup>†</sup>Note that several methods do exist to reduce excessive information including a wavelet ridge algorithm [74] and *wavelet maxima* calculation[75].



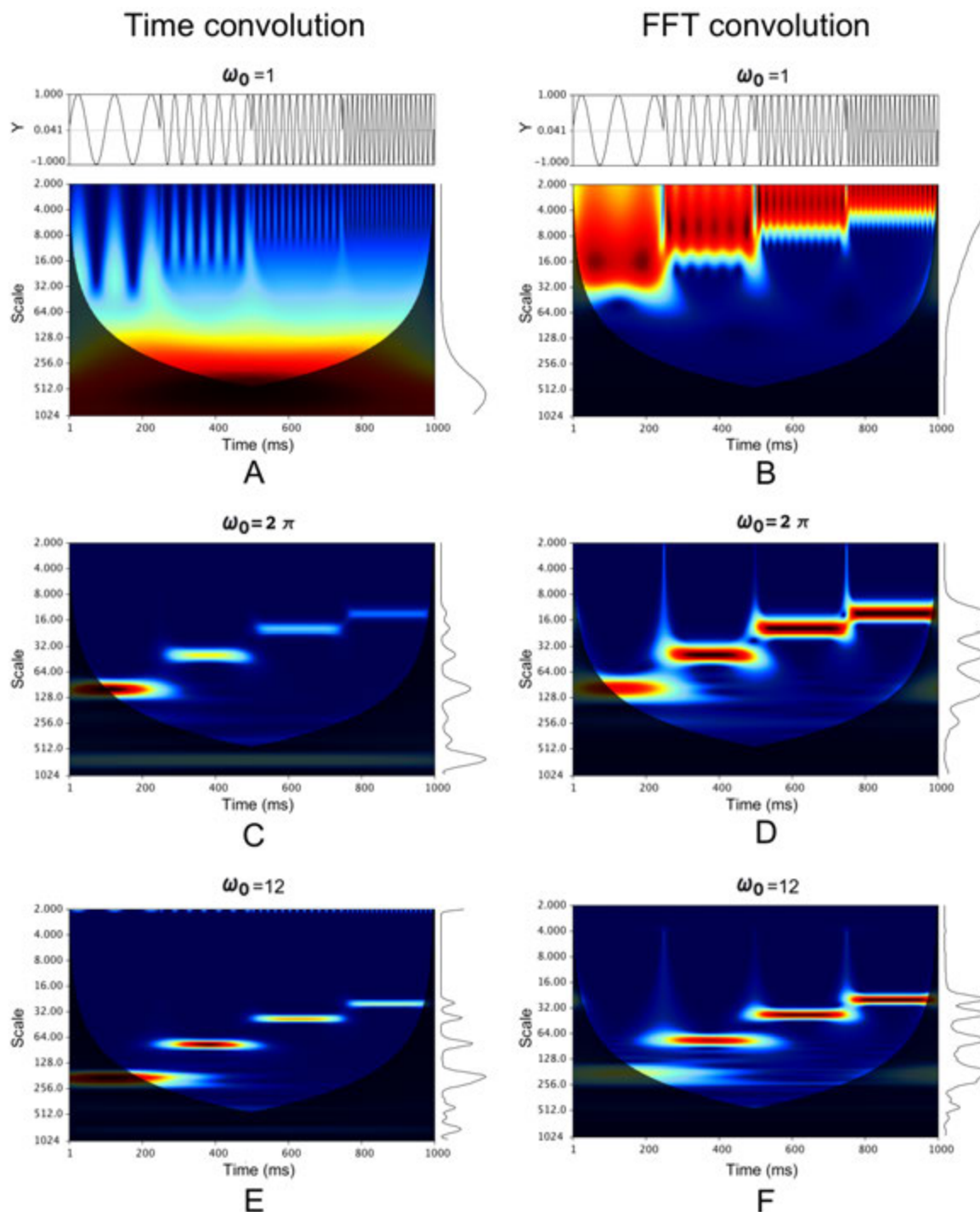


FIGURE 3.9: Comparison between time and frequency convolutions using the Morlet wavelet (presented in Figure 3.6 (p. 35)) with  $\omega_0 = 1, 2\pi$ , and 12. Each scalogram has 144 scales comprising nine octaves with 16 voices each. Figure 3.10 (p. 44) shows a comparison between using 4 and 30 voices for D above. All coefficients are normalised according to Equation (3.32) (p. 42) and plotted inside a cone of influence (COI) — the scale-time decay of  $\frac{1}{e^2}$  — or region which does not suffer from edge effects. In the above example the signal is a piecewise function comprising 10Hz, 25Hz, 50Hz, and 75Hz components represented by  $\sin(20\pi t)$ ,  $\sin(50\pi t)$ ,  $\sin(100\pi t)$ , and  $\sin(150\pi t)$  for  $0 \leq t < \frac{1}{4}$ ,  $\frac{1}{4} \leq t < \frac{1}{2}$ ,  $\frac{1}{2} \leq t < \frac{3}{4}$ , and  $\frac{3}{4} \leq t \leq 1$  respectively. Smaller values of  $\omega_0$  have better time localisation but worse frequency localisation and *vice versa*. The FFT convolution (B, D, and F) improves on energy leakage through proper sampling.

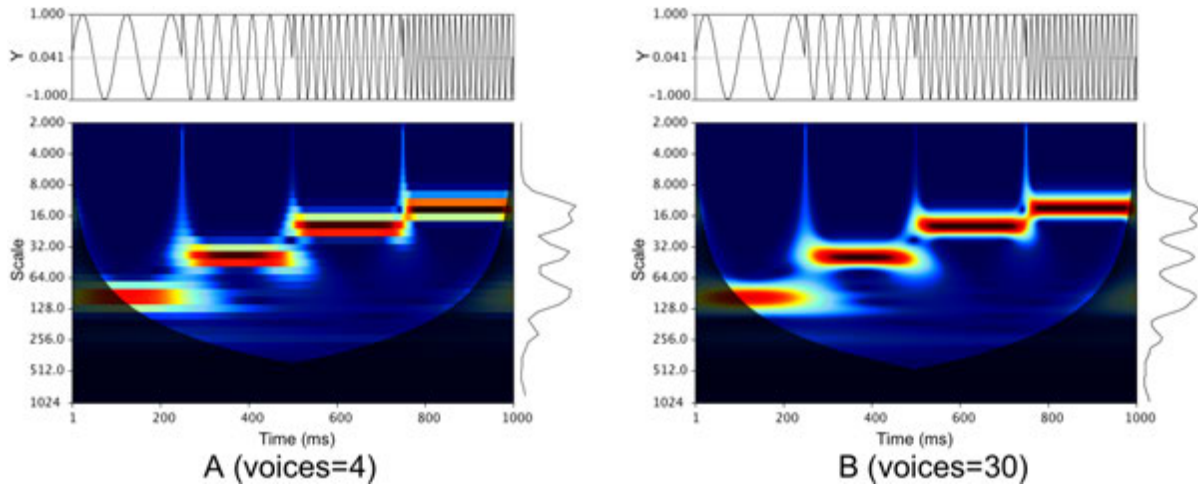


FIGURE 3.10: Comparison between the CWT using a Morlet wavelet with  $\omega_0 = 2\pi$  with 4 and 30 voices. Both A and B represent the CWT presented in Figure 3.9 D (p. 43) but use a different number of voices to compute the CWT. In A there are a total of 36 scales (nine octaves with 4 voices in each) and in B there are 144 scales (nine octaves with 16 voices each). The coefficients in both scalograms are normalised according to Equation (3.32) (p. 42) and plotted inside a cone of influence (COI) — the scale-time decay of  $\frac{1}{\epsilon^2}$  — or region which does not suffer from edge effects. In the above example, the signal is a piecewise function comprising 10Hz, 25Hz, 50Hz, and 75Hz components represented by  $\sin(20\pi t)$ ,  $\sin(50\pi t)$ ,  $\sin(100\pi t)$ , and  $\sin(150\pi t)$  for  $0 \leq t < \frac{1}{4}$ ,  $\frac{1}{4} \leq t < \frac{1}{2}$ ,  $\frac{1}{2} \leq t < \frac{3}{4}$ , and  $\frac{3}{4} \leq t \leq 1$  respectively.

### 3.3.4 The cross wavelet spectrum

To obtain the frequency correlations between two signals, cross wavelet analysis (CWA) [2] is done. The cross spectrum identifies regions of common power by reinforcing the covariance found in the power spectrum of independent variables according to scale. The cross spectrum is defined as

$$W_{xy}(u, s) = W_x^*(u, s)W_y(u, s), \quad (3.33)$$

where  $*$  is the complex conjugate, and  $x$  and  $y$  represent two independent signals. The phase is provided by the argument of the cross-wavelet ( $\arg[W_{xy}]$ ) from which it is possible to derive lead and lag times for each scale.

The phase is calculated as

$$\theta(u, s) = \tan^{-1} \frac{\text{Im}[W_{xy}(u, s)]}{\text{Re}[W_{xy}(u, s)]}, \quad (3.34)$$

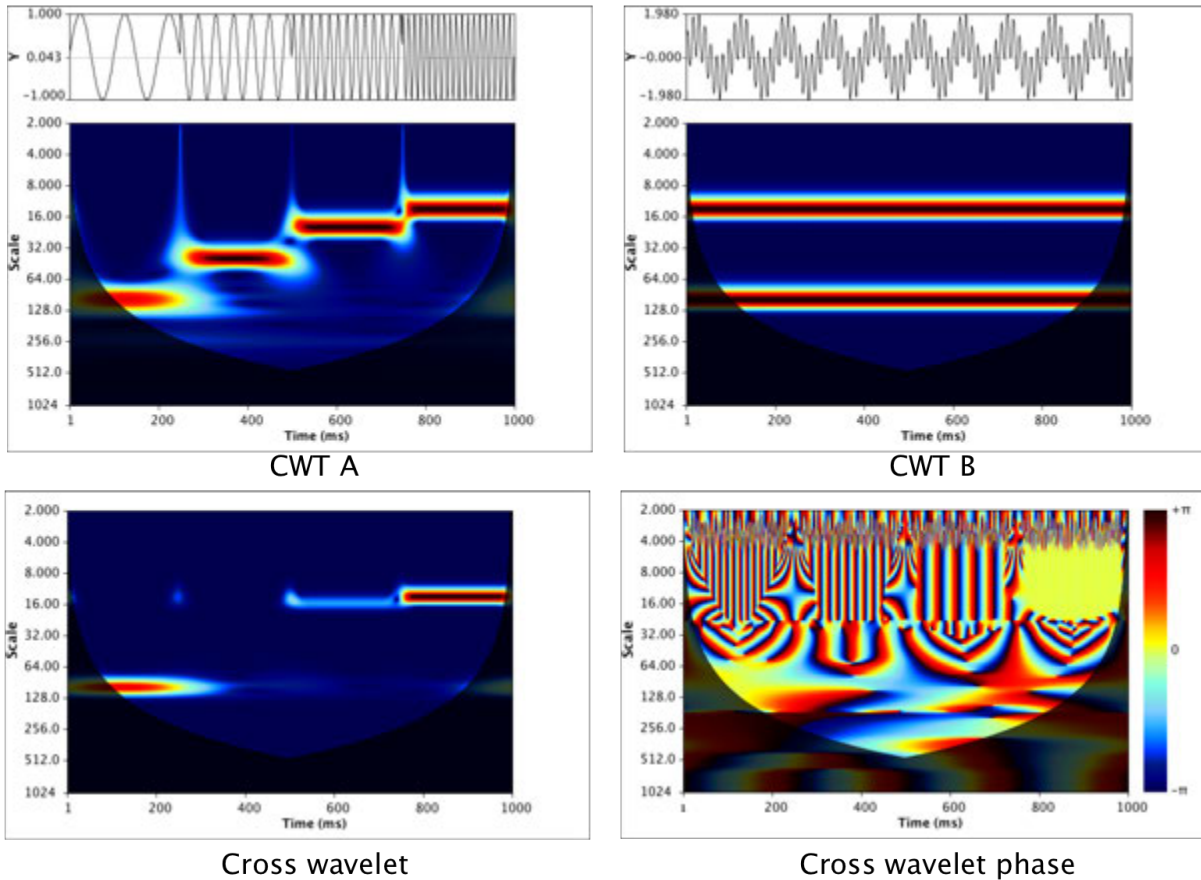


FIGURE 3.11: Example of the continuous wavelet transform (CWT), and the cross wavelet modulus and phase. Each scalogram represents 144 scales (9 octaves with 16 voices per octave) plotted inside a cone of influence (COI). Signal A is a piecewise function comprising 10Hz, 25Hz, 50Hz, and 75Hz components represented by  $\sin(20\pi t) + \sin(50\pi t) + \sin(100\pi t) + \sin(150\pi t)$  for  $0 \leq t < \frac{1}{4}$ ,  $\frac{1}{4} \leq t < \frac{1}{2}$ ,  $\frac{1}{2} \leq t < \frac{3}{4}$ , and  $\frac{3}{4} \leq t \leq 1$  respectively. Signal B is the superposition of a 10Hz and 75Hz signal ( $\sin(20\pi t) + \sin(150\pi t)$ ). The cross wavelet spectrum highlights common power between the 10Hz and 75Hz components of both signals for the time periods that overlap. The cross wavelet phase shows the phase locking ("coherency" and phase shift) behaviour of these frequencies normalised between  $-\pi$  and  $+\pi$ .

where  $\text{Im}[W_{xy}(u, s)]$  and  $\text{Re}[W_{xy}(u, s)]$  represent the imaginary and real parts of the cross wavelet. The cross wavelet modulus represents common power between two signals, whereas the phase represents the coherency as a function of frequency. Figure 3.11 (p. 45) shows an example of the the CWT for two signals and depicts the cross wavelet and cross wavelet phase. The instantaneous time-lag between two signals is calculated using the phase angle  $\theta(u, s)$  as

$$\Delta T_{xy}(u, s) = \frac{\theta_{xy}(u, s)}{2\pi\omega(u)}. \quad (3.35)$$

The phase correlation between two signals implies that the oscillations across a unique

set of wavelengths which characterise the similarity between the time series are phase locked. Similar phase behaviour therefore suggests a causal relationship (provided there is a good basis therefor) defined by lead or lag times (ranging between  $-\pi$  and  $+\pi$ ) for each scale. A useful measure of coherency is called cross wavelet coherency, which provides a normalised covariance (as values in the range 0–1) modulus. It is defined as the square of the cross spectrum normalised by the individual power spectra [3, 76–79] as

$$R^2(u, s) = \frac{|S(W_{xy}(u, s))|^2}{S(|W_x(u, s)|^2)S(|W_y(u, s)|^2)}, \quad (3.36)$$

where  $S$  is a smoothing operator (which smooths across both the scale and time axes). It is important to smooth, otherwise all values would be equal to 1. The utility lies in the ability to show phase correlation between time series even when low power relationships are present.

In Chapter 5, the methodology is developed to use both cross wavelet phase to measure the degree of coherency at each scale using the variance of phase over a time period being compared (the notion is similar to cross wavelet coherency, but a different approach is developed) and CWT power.

### 3.4 Worked examples of the CWT

The following section provides a series of simple worked examples to illustrate how the CWT can be calculated using the Morlet wavelet. Algorithm 3.4.1 (p. 47) demonstrates how to calculate the Morlet wavelet given in Equation (3.21) (p. 34) and Equation (3.26) (p. 38). The same code can be used to generate the Morlet wavelet shown in Figure 3.6 (p. 35). Algorithm 3.4.2 (p. 48), with the sub-functions presented in Algorithms 3.4.3 (p. 49) and 3.4.4 (p. 50) can be used to calculate the CWT. The CWT calculation is performed on the time series presented in Figure 3.15 (p. 54) (which represents a signal comprising 5Hz, 10Hz and 25Hz components superimposed over 1000 ms as  $\sin(10\pi t) + \sin(20\pi t) + \sin(50\pi t)$ , where  $t = 1000ms$ ), and the output comparison using different

CWT computations is shown in Figure 3.16 (p. 55), Figure 3.17 (p. 56), and Figure 3.18 (p. 57).

**Algorithm 3.4.1:** MORLET\_BASE( $t[1, \dots, n], \omega[1, \dots, n], s, u, \omega_0, type$ )

*% t and  $\omega$  are a time index and angular frequency array*

*% s and u are the scale and time translation parameters*

*%  $\omega_0$  is the central frequency parameter*

*% type = 1 or 2 uses Equation (3.21)(p. 34) or Equation (3.26)(p. 38)*

$N = \text{length}(t);$

$T = t;$  *% create the translation and scaling parameter*

**if**  $type == 1$  *% Equation (3.21)(p. 34)*

$Re = [0, N];$  *% create Re and fill it with zeros*

$Im = [0, N];$  *% create Im and fill it with zeros*

$daughter = [N][2];$  *% create an empty output variable*

**for**  $i \leftarrow 1$  **to**  $\text{length}(t)$

$T_i = (t_i - u)/s;$  *% translate and scale the time index*

$Re_i = \pi^{\frac{1}{4}} * \cos(\omega_0 * t_i) * \exp(-\frac{T_i^2}{2});$

$Im_i = \pi^{\frac{1}{4}} * \sin(\omega_0 * t_i) * \exp(-\frac{T_i^2}{2});$

$daughter_{i,1} = Re_i;$

$daughter_{i,2} = Im_i;$

**if**  $type == 2;$  *% Equation (3.26)(p. 38)*

$mother = [0, \text{length}(\omega)];$  *% create mother and fill it with zeros*

$daughter = [0, N];$  *% create the output and fill it with zeros*

**for**  $i \leftarrow 1$  **to**  $\text{length}(\omega)$

$mother_i = \pi^{\frac{1}{4}} * \exp(-\frac{(s*\omega_i - \omega_0)^2}{2}) * \sqrt{N} * 2 * \sqrt{s * \frac{(2*\pi i)}{N}};$

**for**  $i \leftarrow 2$  **to**  $\text{length}(\omega) + 1$

$daughter_i = mother_{i-1};$  *%Heavyside step output*

**return** ( $daughter$ )

**Algorithm 3.4.2:** CWT( $x[1, \dots, n], \omega_0, \text{voices}, \text{option}$ )

```

% This algorithm demonstrates how to calculate the CTW
% x is the input signal.
%  $\omega_0$  is the central frequency parameter.
% voices determines the resolution of the scales (sub – scales).
% option = "FFT", "DFT" or "TIME".
% Note that "FFT" uses Equation (3.26)(p. 38), whereas "DFT" calculates
% the FFT (or DFT) on the wavelet in Equation (3.21)(p. 34) for each
% scale.
N = length(x);
octaves =  $\frac{\log(N)}{\log(2)} - 1$ ; % the number of octaves
scale = [0, 1 : (octaves * voices)]; % the scale vector filled with zeros
for i ← 0 to (octaves * voices)
    { scalei+1 = 2 * 2( $\frac{i}{\text{voices}}$ );
% call the appropriate function and return the modulus and the real
% and imaginary wave arrays
if type = "FFT" % Equation (3.26)(p. 38), Algorithm 3.4.3(p. 49)
    { CWT_FOURIER(x,  $\omega_0$ , scale, "FFT") ← (modulus, waveRe, waveIm)
if type = "DFT" % Equation (3.21)(p. 34), Algorithm 3.4.3(p. 49)
    { CWT_FOURIER(x,  $\omega_0$ , scale, "DFT") ← (modulus, waveRe, waveIm)
if type = "TIME" % Equation (3.21)(p. 34). Algorithm 3.4.4(p. 50)
    { CWT_TIME(x,  $\omega_0$ , scale) ← (modulus, waveRe, waveIm)
FFT(x) ← amplitudes; % FFT power spectrum.
a =  $\frac{\text{amplitudes}}{\max(\text{Modulus})}$ ; % get parameter a (Equation (3.32)(p. 42)).
% normalise the modulus to match Fourier amplitudes.
for i ← 1 to length(scale)
    { for j ← 1 to N
      { Modulusi,j = a * Modulusi,j;
return (modulus, waveRe, waveIm, scale); %Plot the Modulus

```

**Algorithm 3.4.3:** CWT\_FOURIER( $x[1, \dots, n], \omega_0, scale[1, \dots, n], option$ )

*% x is the input signal.*

*%  $\omega_0$  is the central frequency parameter.*

*% scale is the scale vector.*

*% option = "FFT" or "DFT"*

$N = \text{length}(x);$

$t\_index = [1 : N];$  *% time index from 1 to N*

$\omega = [0, 1 : N/2];$  *% the angular frequency array filled with zeros*

**for**  $i \leftarrow 1$  **to**  $N/2$

$\left\{ \omega_i = (2 * \pi * i) / N;$

$data = \text{FFT}(x);$  *% (or DFT) of the data*

*% Define the wavelet arrays and fill with zeros*

$waveRe = [0, 1 : N][0, 1 : \text{length}(scale)];$  *% the real wavelet array*

$waveIm = [0, 1 : N][0, 1 : \text{length}(scale)];$  *% the imaginary wavelet array*

$modulus = [0, 1 : N][0, 1 : \text{length}(scale)];$  *% the wavelet modulus*

**for**  $s \leftarrow 1$  **to**  $\text{length}(scale)$

$\left\{ \text{if } option = \text{"FFT"}$

$\left\{ \text{MORLET\_BASE}(t\_index, \omega, scale_s, 0, \omega_0, 2) \leftarrow daughter;$

$\left\{ product = daughter * data;$

$\text{if } option = \text{"DFT"}$

$\left\{ \text{MORLET\_BASE}(t\_index, null, scale_s, N/2, \omega_0, 1) \leftarrow daughter;$

$\left\{ \text{FFT}(daughter) \leftarrow amplitudes$  *% get the FFT amplitudes.*

$\left\{ product = amplitudes * data;$

*% compute the inverse FFT (or DFT) of product.*

$output = \text{IFFT}(product);$

**for**  $j \leftarrow 1$  **to**  $N$

$\left\{ waveRe_{j,s} = product_j \leftarrow real;$

$\left\{ waveIm_{j,s} = product_j \leftarrow imaginary;$

$\left\{ modulus_{j,s} = \frac{\sqrt{waveRe_{j,s}^2 + waveIm_{j,s}^2}}{N * \sqrt{scale_s}};$

**return**  $(modulus, waveRe, waveIm);$

**Algorithm 3.4.4:** CWT\_TIME( $x[1, \dots, n], \omega_0, \text{scale}[1, \dots, n]$ )

*% x is the input signal.*

*%  $\omega_0$  is the central frequency parameter.*

*% scale is the scale vector.*

$N = \text{length}(x);$

$t\_index = [1 : N];$  *% the time index filled with 1 to N*

*% Define the wavelet arrays and fill with zeros*

$\text{waveRe} = [0, 1 : N][0, 1 : \text{length}(\text{scale})];$  *% the real wavelet array*

$\text{waveIm} = [0, 1 : N][0, 1 : \text{length}(\text{scale})];$  *% the imaginary wavelet array*

$\text{modulus} = [0, 1 : N][0, 1 : \text{length}(\text{scale})];$  *% the wavelet modulus*

**for**  $s \leftarrow 1$  **to**  $\text{length}(\text{scale})$

$\left\{ \begin{array}{l} \text{for } u \leftarrow 1 \text{ to } N \\ \left\{ \begin{array}{l} \text{MORLET\_BASE}(t\_index, \text{null}, \text{scale}_s, u, \omega_0, 1) \leftarrow \text{daughter}; \\ \text{for } i \leftarrow 1 \text{ to } N \\ \left\{ \begin{array}{l} \text{real} = \text{daughter}_{i,1} * x_i; \\ \text{imaginary} = \text{daughter}_{i,2} * x_i; \end{array} \right. \\ \text{waveRe}_{u,s} = \sum \text{real}; \\ \text{waveIm}_{u,s} = \sum \text{imaginary}; \\ \text{modulus}_{u,s} = \frac{\sqrt{\text{waveRe}_{u,s}^2 + \text{waveIm}_{u,s}^2}}{N * \sqrt{\text{scale}_s}}; \end{array} \right. \end{array} \right.$

**return** ( $\text{modulus}, \text{waveRe}, \text{waveIm}$ );



To illustrate Algorithm 3.4.1 (p. 47) consider the following example shown in Figure 3.12 (p. 51). In this example the time-based Morlet (*type 1*) wavelet is shown using  $t = [-\pi, \dots, \pi]$  with a sampling interval  $\frac{2\pi}{511}$ ,  $\omega = 0$ ,  $s = 1$ ,  $u = 0$ ,  $\omega_0 = (1, \pi, 2\pi, \text{ and } 4\pi)$ , and *type* = 1. To generate any of the plots shown in Figure 3.12 (p. 51) the function is called using the appropriate value for  $\omega_0$  and the plot is of the real (column 1) and imaginary (column 2) outputs with the  $x$  axis set to  $[-\pi : \pi]$ .

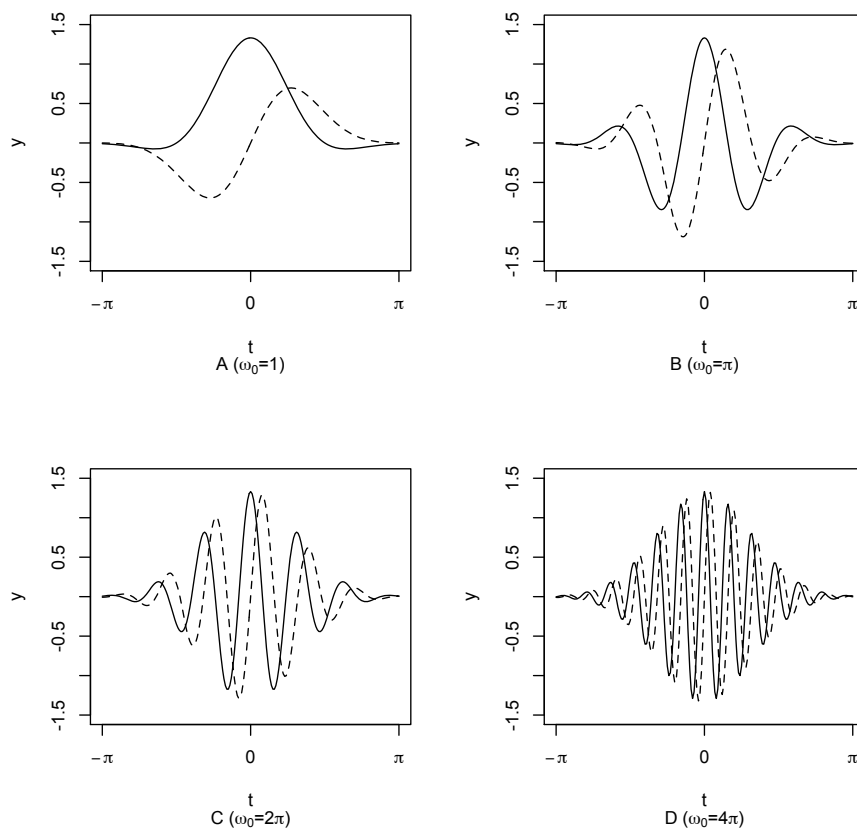


FIGURE 3.12: Worked example of the Morlet wavelet. In the above example the same analysing wavelet is presented and generated using the pseudocode presented in Algorithm 3.4.1 (p. 47), but each subplot uses a different value for  $\omega_0$ . In A  $\omega_0 = 1$ , in B  $\omega_0 = \pi$ , in C  $\omega_0 = 2\pi$ , and in D  $\omega_0 = 4\pi$ . The solid line represents the real (Re) component and the dashed line represents the imaginary (Im) component.

In Figure 3.13 (p. 52) four examples are given using different scale  $s$  and time translation  $u$  values using a time index of  $t = [1, \dots, 200]$  with a sampling interval of 1. In Figure 3.14 (p. 53) an example of two FFT Morlet functions are shown for  $s=4, 8, \text{ and } 16$ . The first function is the Heaviside step function ( $\omega = (2\pi \frac{t[1, \dots, t/2]}{N})$ ) from Equation (3.26) (p. 38), and the second is the FFT power spectrum of the Morlet wavelet (using *type*=2 from

Algorithm 3.4.1 (p. 47)). These two functions are used in Algorithm 3.4.3 (p. 38) with the options “FFT” and “DFT”<sup>†</sup>.

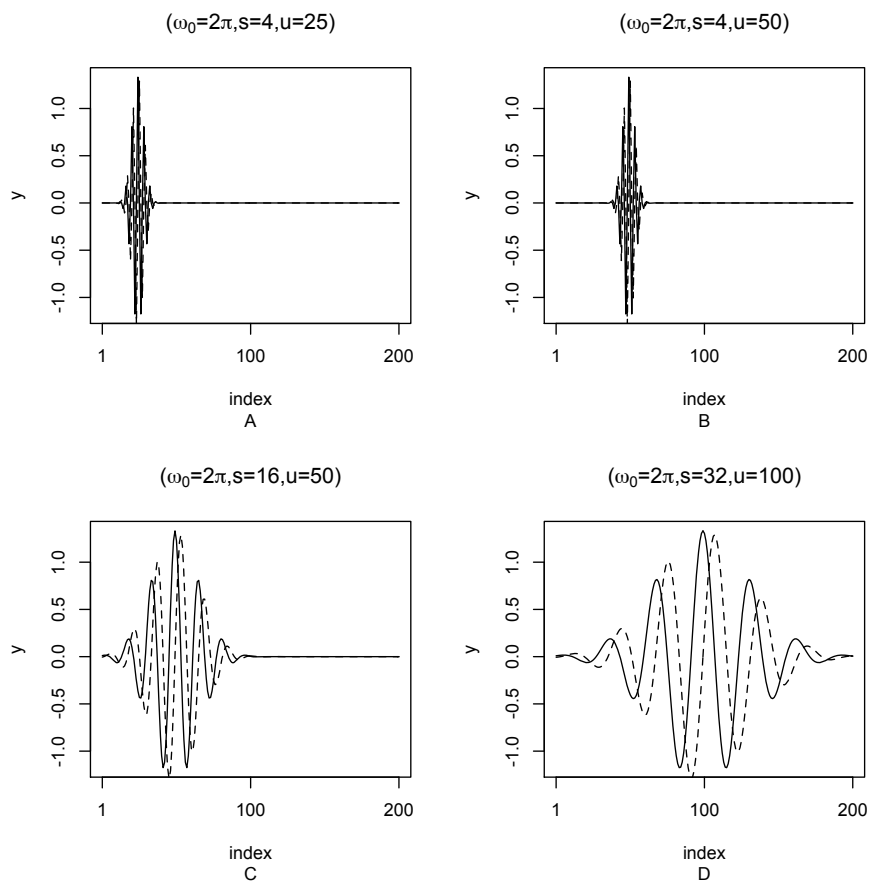


FIGURE 3.13: Scaled and translated example of the Morlet wavelet. In the above example the Morlet wavelet with  $\omega_0 = 2\pi$  is presented, generated using the pseudocode presented in Algorithm 3.4.1 (p. 47). The time index is taken as  $t = [1, \dots, 200]$  with the sampling interval 1. A and B above both use  $s = 4$ , but in A  $u = 25$  and in B  $u = 50$ . In C  $s = 16$  and  $u = 50$  and in D  $s = 32$  and  $u = 100$ . The solid line represents the real (Re) component and the dashed line represents the imaginary (Im) component.

<sup>†</sup>FFT refers to the Heavyside step function used to represent the FFT of the Morlet and the term DFT is used to distinguish between the first option, but refers to either the DFT or FFT of the time based Morlet wavelet.

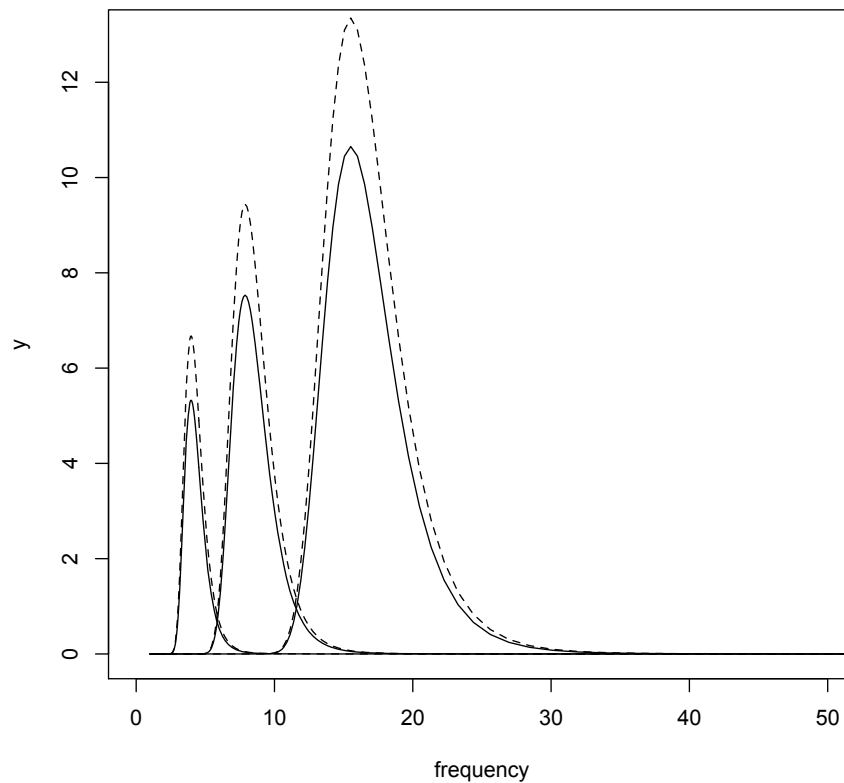


FIGURE 3.14: Fourier transform of the Morlet wavelet using a Heaviside step function. In the above example the Fourier transform of the the Morlet wavelet is shown with  $\omega_0 = 2\pi$  and  $s = 4, 8,$  and  $16$  generated using the pseudocode presented in Algorithm 3.4.1 (p. 47). The time index is taken as  $t = [1, \dots, 512]$  with the sampling interval 1. The  $x$  axis is shown as the first 50 frequencies ( $\frac{N}{t}$ ). The solid line represents the Fourier transform of the Morlet using a Heaviside step function where  $\omega = (2\pi \frac{t[1, \dots, t/2]}{N})$ , and the dashed line represents the amplitudes of the Fourier transform of the time based Morlet wavelet (Algorithm 3.4.1 (p. 47),  $type=1$ ), where amplitude  $= \frac{1}{\sqrt{s}} * \sqrt{Re^2 + Im^2}$ .

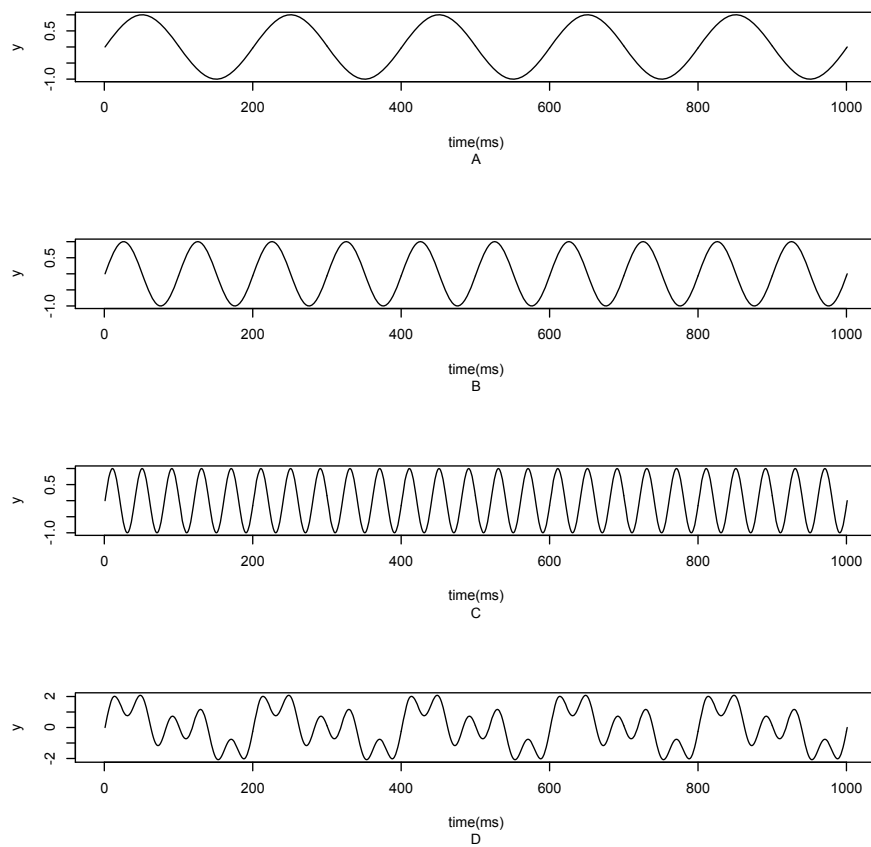


FIGURE 3.15: Signal comprising 5Hz, 10Hz and 25Hz components. In the above example A is  $\sin(10\pi t)$ , B is  $\sin(20\pi t)$ , C is  $\sin(50\pi t)$ , and D is the superposition of A, B and C in the form  $\sin(10\pi t) + \sin(20\pi t) + \sin(50\pi t)$ .

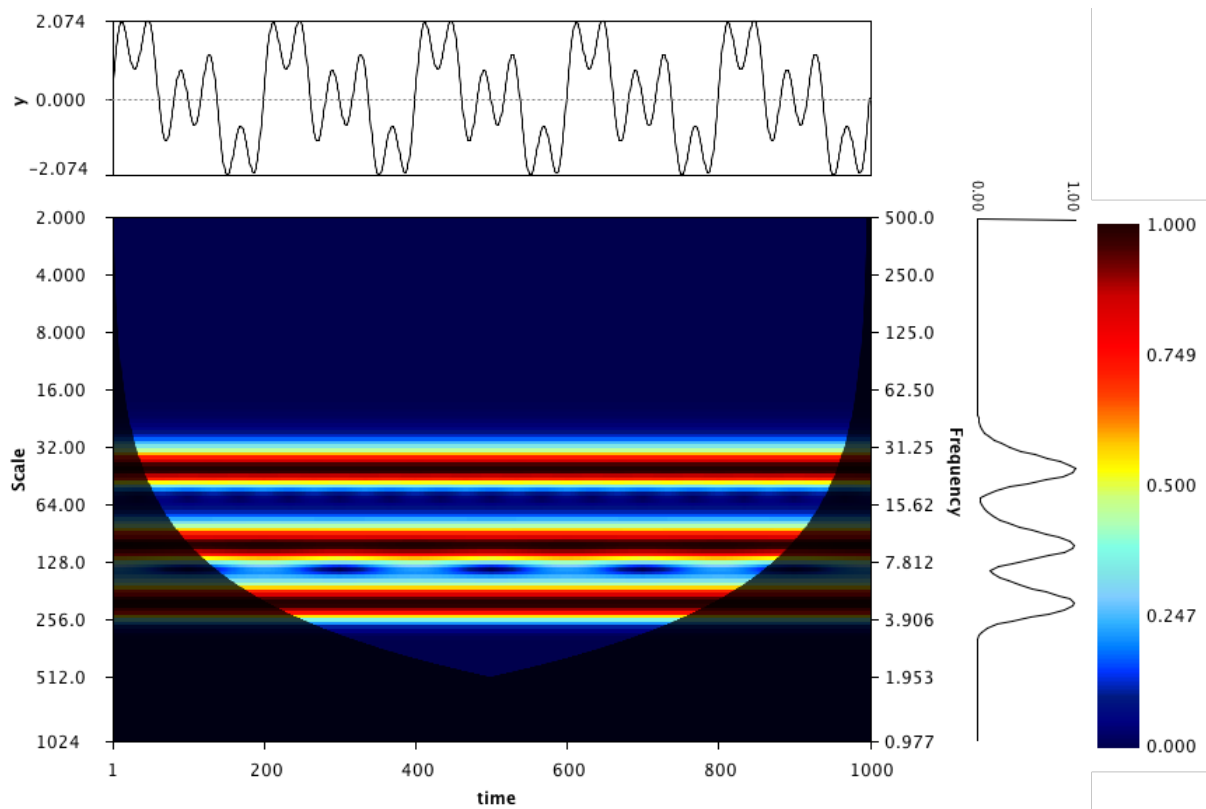


FIGURE 3.16: CWT worked example generated using Equation (3.26) (p. 38). In the above example the CWT was generated using a Morlet wavelet with  $\omega_0 = 2\pi$  and calculated using the pseudocode presented in Algorithm 3.4.2 (p. 48) with 16 voices per octave. The shaded area is the cone of influence and the graph on the right hand side represents the global wavelet power spectrum.

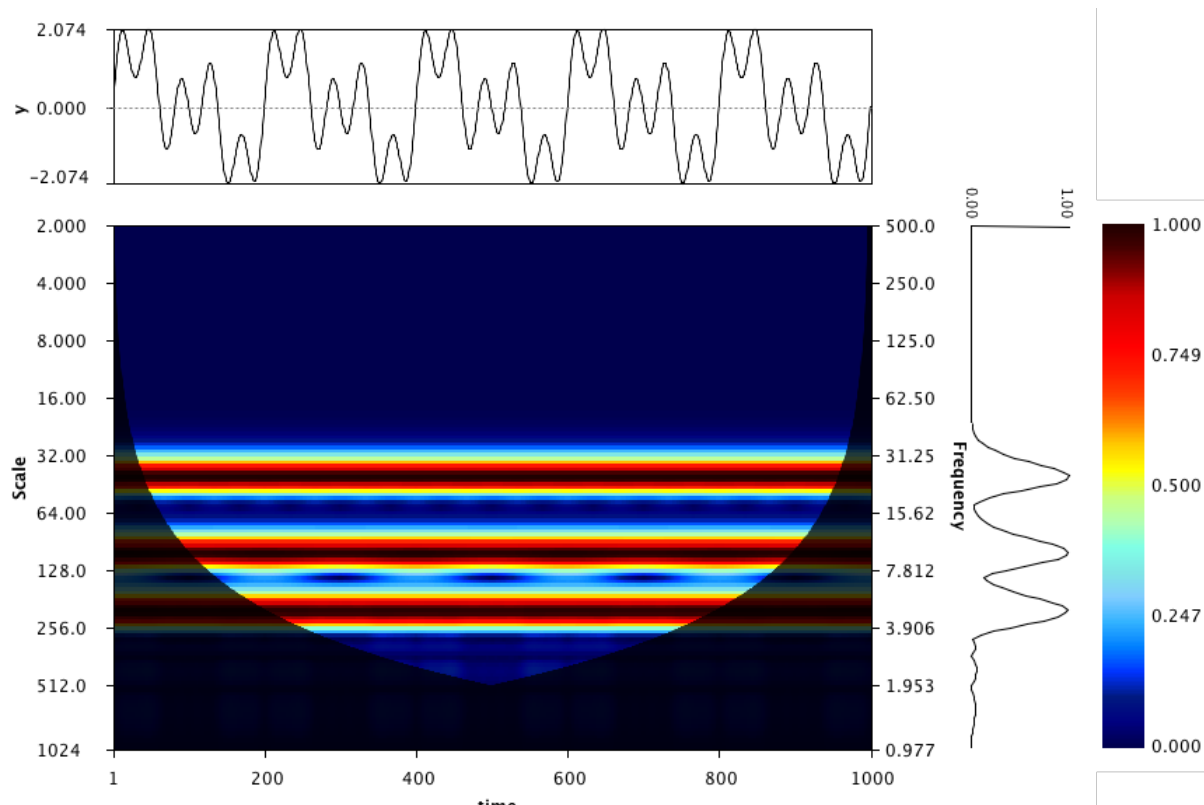


FIGURE 3.17: CWT worked example generated using the FFT of the Morlet wavelet. In the above example the CWT was generated using a Morlet wavelet with  $\omega_0 = 2\pi$  and calculated using the pseudocode presented in Algorithm 3.4.2 (p. 48) with 16 voices per octave. The modulus is the product of the FFT of the signal and the FFT of the Morlet wavelet presented in Equation (3.21) (p. 34). The shaded area is the cone of influence and the graph on the right hand side represents the global wavelet power spectrum.

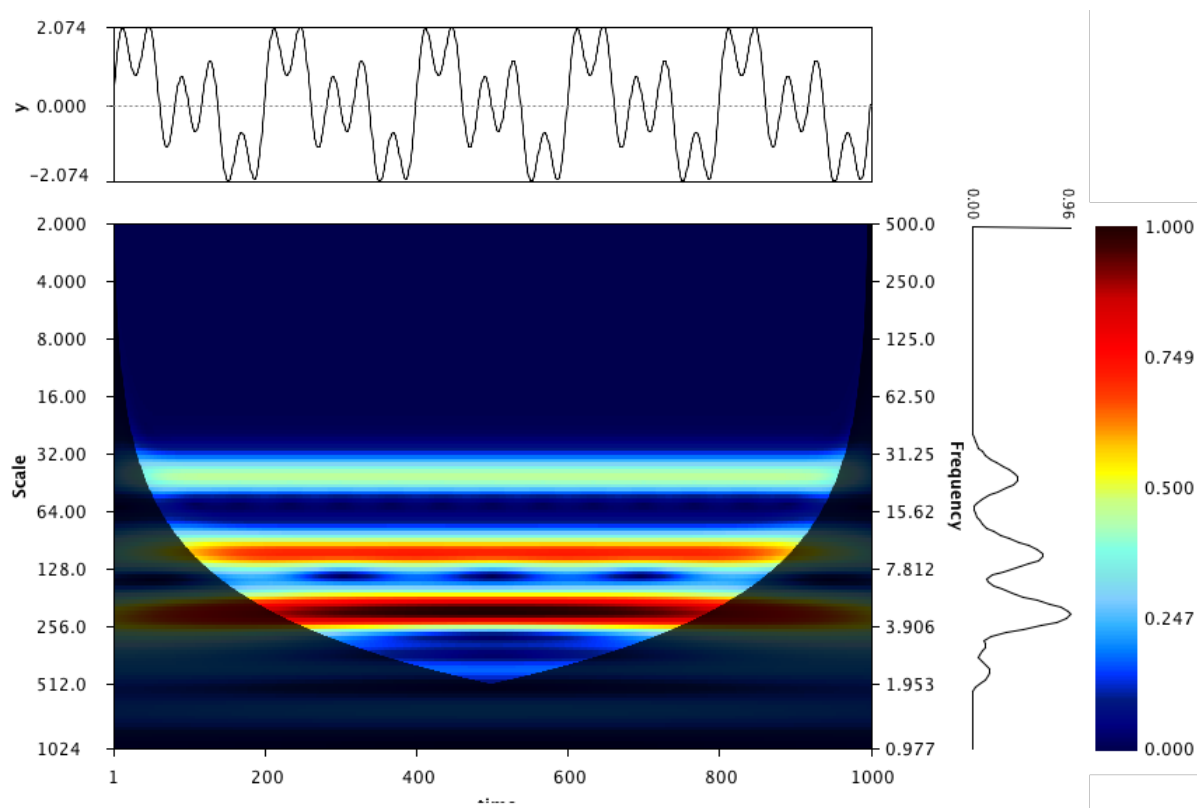


FIGURE 3.18: CWT worked example generated using the time convolution of the Morlet wavelet. In the above example the CWT was generated using a Morlet wavelet with  $\omega_0 = 2\pi$  and calculated using the pseudocode presented in Algorithm 3.4.2 (p. 48) with 16 voices per octave. The modulus is the time convolution of the Morlet wavelet presented in Equation (3.21) (p. 34) and the signal. The shaded area is the cone of influence and the graph on the right hand side represents the global wavelet power spectrum.

## 3.5 Conclusion

This chapter concludes all the relevant background information needed to understand the methodology presented in Chapter 5. The last section provided some simple algorithms and worked examples that convey how the CWT can be calculated using different computations for the Morlet wavelet. In the following chapter a brief overview of time series classification, with some recent trends in machine learning classification techniques, is presented to provide some context to the classification experiments presented in the results section.

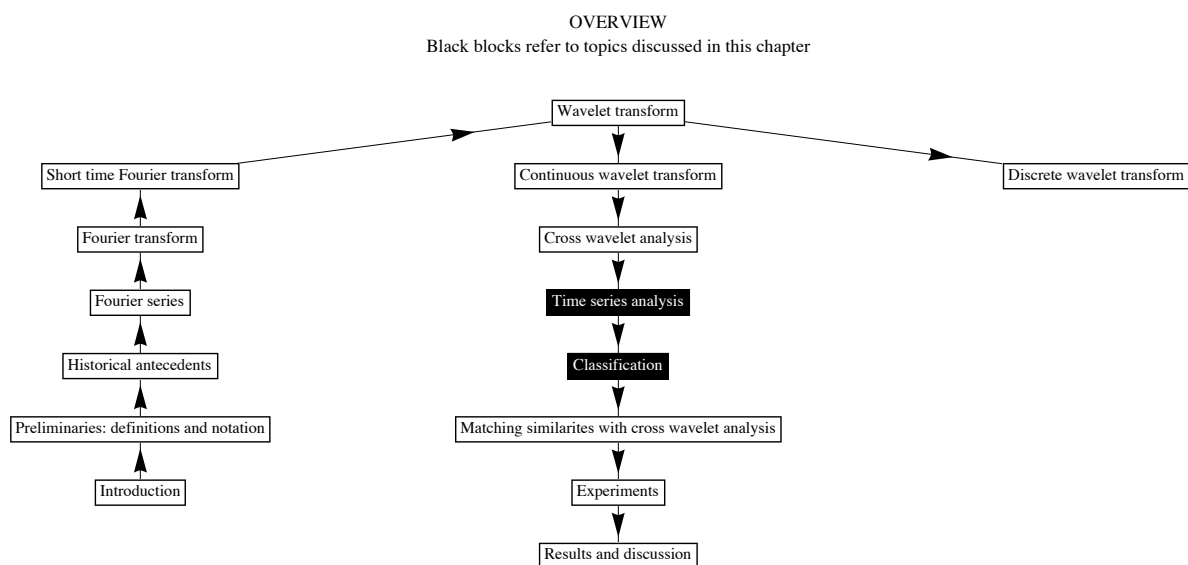


*"The classification of facts, the recognition of their sequence and relative significance is the function of science, and the habit of forming a judgment upon these facts unbiased by personal feeling is characteristic of what may be termed the scientific frame of mind"*

Karl Pearson (AD 1857-1936)

# 4

## Background to time series classification



## 4.1 Overview

Time series observations capture layers of information that represent processes and interactions which exceed both the long and short-term limits of the observation period, but still contain many clues to the underlying nature of the system. Numerous mathematical and statistical methods are used to analyse these data to extract meaning or produce statistics to better characterise the underlying features. There are many broad categories of application each comprising countless methods; these are collectively grouped under the term time series analysis. Generally speaking, time series classification coalesces at the intersection of pattern recognition, statistics and artificial intelligence (AI) and machine learning (ML) tasks, which further down the historical road evolved out of approaches that belong to methods found in either the frequency domain, or from statistically-based time-domain techniques.

One of the most appealing categories of application in time series classification comes as part of the data mining process by implementing new algorithms or adapting existing ones during classification training [80]. Here, classification typically involves supervised learning using algorithms that group time series with similar features or underlying characteristics together according to pre-defined criteria. The common thread is the computer algorithm, which brings together all the connected disciplines associated with classification (see Information Box 4.1 (p. 61) for some basic information on the links between machine learning and pattern recognition for example). This chapter begins with a short narrative on the origin of ML through the development of associated technology to set the scene for the emergence of various data mining techniques that emerged after the 1990s, in which the main techniques compared in the experiments section of this thesis are discussed, with a general overview of other prominent techniques presented.

### 4.1.1 Before we begin: the birth of machine learning

There are many taxonomic terms that describe computer learning tasks that have been developed over the years. As with most taxonomic systems, however, these are constantly being updated or have slightly different definitions according to different sources. From

## INFORMATION BOX 4.1: Machine learning or pattern recognition

Due to the interdisciplinary nature of classification algorithms no single discipline can claim an authoritative position on its origins — the central theme, however, is the computer algorithm. The framework on which modern computers rely can arguably be attributed to Gottfried Wilhelm von Leibniz (AD 1646 – 1716) who created the modern binary number system, which was later endorsed by George Boole (AD 1815 – 1864) who in the 1840s promoted the use of simple logic operators using the binary system [81]. By the 1940s, Alan Mathison Turing (AD 1912 – 1954) had identified ML as a pre-condition for smart systems [82], while in the 1950s Claude Elwood Shannon (AD 1916 – 2001) was providing similar expressions in the engineering world [83], and in 1953 the first computational learning experiments were developed by Christopher Strachey [84]. By the 1960s, developments in ML could be distinguished by either classifiers that could predict unseen data based on pre-classified training sets or by engineering rule-based software — consequently, in 1967 the first pattern recognition program was developed using a nearest neighbour algorithm [85].

Machine learning (ML) as a recognised field, however, evolved out of the promotion of artificial intelligence (AI) — principally in origin, when in 1955 John McCarthy *et al.* [86] proposed a small study to explore whether aspects of learning or intelligent features of conjecture can be simulated by a machine. Early investigations were mostly self-organising and based on artificial neural network theory of incremental change, but because of computational restraints at the time research was mostly theoretical with a focus on the development of mathematical biophysics using logic to model natural processes [87–94]. An influential pioneer in AI was Frank Rosenblatt (AD 1928 – 1971) who introduced the term perceptrons — later called artificial neural networks — that had the potential to recognise patterns of similarity between new data and data already seen (creating the foundation for machine training and recognition through supervision) [95]. According to Carbonell [96], pattern recognition formed as a sub-discipline of AI from its roots in engineering and computer vision, but there seemed to exist a clear distinction between the two fields as represented by the establishment of the the journal *Pattern recognition* in 1968 and the *AI journal* in 1970. However, by 1979 the *IEEE transactions on Pattern Analysis and Machine Intelligence* was established including both fields.

the 1950s onwards, ML as a discipline went through three broad periods of activity, namely: exploration during the 1950s and 1960s; growth of implementing algorithms in the 1970s; and the explosion of research and applications (or other approaches that are not neural networks) from the 1980s till present [97–99]. To set the scene for the explosion of ML as a discipline in the 1980s, the following notable chronological milestones and achievements can be mentioned:

- **1623.** Wilhelm Schickard (AD 1559 – 1635) builds the first automatic calculator (the official start of the long history of computers) [100].
- **1642.** Blaise Pascal (AD 1623 – 1662) invents one of the earliest mechanical calculators (often called the Pascaline) that can be used to add and subtract numbers automatically [101].
- **1694.** Gottfried Wilhelm (von) Leibniz (AD 1646 – 1716) produces his adding machine and creates the modern binary system [98].
- **1767.** Thomas Bayes (AD 1701 – 1761) publishes his theory [102], which becomes a fundamental ideology to data mining as it allows understanding of complex realities based on estimated probabilities.
- **Early 1800s.** Adrien-Marie Legendre (AD 1752 – 1833) and Johann Carl Friedrich Gauss (AD 1777 – 1855) develop least squares regression analysis [103, 104], one of the key analytical tools in data mining and ML. In 1805, the Stanhope Square Demonstrator is also developed as one of the first logic machines [105]. Also, Joseph-Marie Jacquard (AD 1752 – 1834) develops the earliest programmable loom with the ability to store information [106].
- **1832.** Charles Babbage (AD 1791 – 1871) [107] develops the world's first real 'programmable machine'.
- **1843.** Ada Lovelace (AD 1815 – 1852) creates the first algorithm to be solved by Babbage's computer [107].
- **1854.** George Boole (AD 1815 – 1864) publishes *an Investigation of the Laws of Thought on Which Are Founded the Mathematical Theories of Logic and Probabilities* [108], which promotes the use of symbolic logic.
- **1879.** Friedrich Ludwig Gottlob Frege (AD 1848 – 1925) proposes a notational system for mechanical reasoning — a forerunner to predicate calculus systems later used in AI [109].

- **1890.** Herman Hollerith (AD 1860 – 1929) develops the electromechanical punched card tabulator, and forms the *Tabulating Machine Company*, which today (after many iterations and name changes) is called IBM [110].
- **1925.** Vannevar Bush (AD 1890 – 1974) invents the first analog computer, which is built at MIT in 1930 [111].
- **1931.** Kurt Friedrich Gödel (AD 1906 – 1978) defines the foundations of theoretical computer science through his work on universal languages [112, 113].
- **1936.** Alan Mathison Turing (AD 1912 – 1954) publishes a theoretical model of a computer in *On computable numbers, with an application to the Entscheidungsproblem* [114] — consequently, 1936 is often cited as the dawn of the computer age.
- **1937.** Sir Ronald Aylmer Fisher (AD 1890 – 1962) proposes linear discriminant analysis (LDA) as a new classification method, which is the first linear classifier to be performed in a supervised environment [115]. LDA was proposed to solve a 2-class taxonomic classification problem (later generalised to enable multi-class or multiple discriminant analysis (MDA) [116]) in a similar way to principal components analysis (PCA) [117] or statistical regression, but is performed in a supervised environment (see Information Box 4.2 (p. 66) for more information on supervised learning) by retaining the class-discriminatory information that describes or maximises the differences in a dataset. Today, it is widely used as a dimensionality reduction step (see Information Box 4.3 (p. 67) for more information on dimensionality reduction) before classification in the ML environment.
- **Early 1940s.** John V. Atanasoff (AD 1903 – 1995) and Clifford Berry (AD 1918 – 1963) develop the first electronic ‘non-programmable’ computer in 1940. In 1941, Konrad Zuse (AD 1910 – 1995) develops a programmable electronic computer, and later in 1945 develops the first high-level computer language called Plankalkul [118]. In 1943 Warren Sturgis McCulloch (AD 1898 – 1969) and Walter Harry Pitts Jr. (AD 1923 – 1969) publish *A logical calculus of the ideas immanent in nervous activity*, which promotes the idea of neural-network architectures [88]. Finally, in 1944 Howard Hathaway Aiken (AD 1900 – 1973) develops the first American

computer — the IBM Harvard Mark I and in later years he helps develop the Mark II, II, and IV. [118].

- **1946.** John von Neumann (AD 1903 – 1957) starts computer research at the Institute for Advanced Study in Princeton. In the same year John Adam Presper Eckert (AD 1919 – 1995) and John William Mauchl (AD 1907 – 1980) develop the first commercial programmable computer called *Electronic Numerical Integrator And Computer* or ENIAC, which weighed about 30 tonnes and was 1000 faster than the Mark I [118].
- **1948.** Claude Elwood Shannon (AD 1916 – 2001) publishes *A Mathematical Theory of Communications* [119] popularising the term ‘bit’, coined by John Wilder Tukey (AD 1915 – 2000) in 1947 (also famous for Cooley Tukey FFT algorithm published in 1965 [64]). Norbert Wiener (AD 1894 – 1964) also publishes his seminal work on information theory in 1948 called *Cybernetics: Or Control and Communication in the Animal and the Machine* [120].
- **1949.** Sir Maurice Vincent Wilkes (AD 1913 – 2010) builds the world’s first electronic stored-program computer (EDSAC) [118].
- **1950s.** Claude Shannon develops a proposal for a computer chess program; the first learning program (based on checkers) is created by Arthur Lee Samuel [121]; IBM’s first scientific computer is marketed; the first AI program (IPL-II) is developed, and the term AI is adopted at Dartmouth College [86]; the computer languages FORTRAN, LISP, and COBOL are invented; the perceptron model is invented by Frank Rosenblatt [95]; and finally the first artificial intelligence laboratory is founded at MIT [118].

During the 1950s and 1960s, many theories and computer analogies to both natural and human biological systems were developed (see Information Box 4.1 (p. 61) for example). At the same time pattern recognition came into its own right, machine translations of natural language and programs able to recognise patterns based on a nearest neighbour algorithm were developed [85, 122], and geometric representations and many other heuristic problems were also developed. It was in the 1970s, however, that real world

implementations began to emerge, specifically in the areas of speech recognition, signals and database queries, and improved computer vision (see [98] for an excellent overview). What is important throughout this period is that three fundamentally different categories emerged on which almost all ML algorithms are developed, namely unsupervised, supervised, and reinforced learning tasks (see Information Box 4.2 (p. 66) for a general description of these three categories).

In the 1980s, ML (mostly represented by artificial neural network algorithms before this) emerged as an independent memory-based learning discipline. At this stage, technology for optical character recognition and natural language products already represented a \$180 million dollar industry, while imaging systems were being widely adopted in medical research [118]. It is also worth noting that an automated fingerprint identification system (AFIS) and robotic vision systems worth over \$300 million dollars were developed in Japan making it one of the wealthiest nations on the planet. In 1981 multi-layer neural networks are proposed [123] using a back-propagation algorithm [124]. In 1986 an algorithm called ID3 (commonly known as decision trees) [125, 126] was proposed as a new model (and along with its derivatives like ID4, regression-trees, etc., became a major application field especially in financial sciences).

In 1989 the term ‘data-mining’ was coined as a trademark of HNC (a San Diego-based company) [127], and the term ‘Knowledge Discovery in Databases’ (KDD) was coined by Gregory Piatetsky-Shapiro who also organised the first KDD workshop [128]. After 1990, when the world-wide-web (WWW) was invented [129], the ML community saw an expansion in research bringing in the age of ‘big data’, which prompted more automatic systems of analysis, and in 1995 the support-vector machine (SVM) [130] was proposed to fill this gap and allow for the creation of non-linear classifiers. To summarize, many parallel methods and technologies have been developed and many new ones are developed each day, which has resulted in the widespread adoption of ML, pattern recognition, and data mining applications in almost every field of application that exists.

**INFORMATION BOX 4.2: Unsupervised, reinforced and supervised learning**

**Unsupervised learning** does not use pre-defined criteria on which to make data predictions. Its primary goal is to explore the data and find similar structures (clustering techniques for example would fall into this category).

**Reinforced learning** is a type of algorithm that learns from its mistakes in a repetitive simulation-based environment. It differs from both unsupervised and supervised learning in that an absolute correct output is never sought, but rather the set of optimal outputs. It is often used in gaming, robotic and navigation environments.

**Supervised learning** involves training and testing an algorithm using a pre-defined set of examples that have a direct feedback in terms of known label categories. Here, the learning algorithm receives inputs and learns by comparing its classification with the correct outputs in order to make predictions on new or unseen data.

## 4.2 The data mining process

Data mining time series is based on similarity measures that provide a comparison between two or more time series or sequences. Generally, the data mining process seeks to discover new knowledge through preprocessing (representation, indexing, etc.) and mining (similarity methods for classification, clustering, etc.). The preprocessing stage can be broken down into different ‘categories’ such as: representation; indexing; segmentation; visualisation; and choice or design of a similarity measure that will be best suited to the mining task. The mining task is performed according to a desired outcome i.e clustering, classification, knowledge discovery (through patterns), rule discovery, or prediction [131].

### 4.2.1 Preprocessing methods

Representation techniques (preprocessing) become important when computer technology is limited to handle raw data that is particularly large in order to reduce its dimensionality (see Information Box 4.3 for more information on dimensionality reduction) into something smaller. Here, raw time series often need much storage and processing power



to characterise each point in the time series (they are high in dimensionality), and techniques are proposed to ‘transform’ the data into a set of feature coefficients or reduce the length of the original time sequence(s) and index it into something more manageable. One way in which to categorise these methods is according to ‘adaptive’ or ‘non-adaptive’ representations [131, 132], or model based representations — as is true for many statistical approaches. Non-adaptive representation refers to techniques whose representation does not provide enough underlying information for a proper reconstruction of the original data, whereas adaptive representation refers to techniques that include enough underlying information in their representation to provide minimal error during reconstruction. Hence, by adding more parameters to a non-adaptive representation it effectively becomes more adaptive in its reconstruction [133].

#### INFORMATION BOX 4.3: Dimensionality reduction

High dimensionality calls for some form of dimension reduction when dealing with a dataset to effectively reduce the search space to allow for effective processing of all objects (i.e. classifying, clustering, segmenting, and indexing). The frequency domain provides a good functional space to reduce dimensionality, in which the coefficients may be subset into features that are characteristic of the problem at hand before processing. The first algorithm to implement dimensionality reduction in this context is the F-index [134], which requires only a few Fourier coefficients to successfully classify the data. In recent years, many data mining algorithms have been introduced that reduce dimensionality, whereby the random variables under consideration are divided into characteristic features before processing. In the frequency domain, these are usually restricted to applications which use the discrete wavelet transform (DWT) [135–139] or the discrete Fourier transform (DFT) [134, 140–143]. In the time domain, commonly used methods include: piecewise aggregate approximation (PAA) [144]; piecewise linear approximation (PLA) [145, 146]; Chebyshev polynomials (CP) [147]; and singular value decomposition (SVD) [148–153].

Principal component analysis (PCA) [117, 154], is one of the oldest ‘dimensionally reduction’ technique used for multivariate data, which lends itself perfectly to the representation process. It provides linear combinations of the original variables (features) that co-vary in time, of which some (components) are retained and less important ones discarded to provide a reduced representation of the original [155, 156]. To overcome phase differences in time series using a PCA approach, Li [157] proposed the use of time-invariant techniques (such as dynamic time warping (DTW)) to be implemented before

performing PCA. Singular value decomposition (SVD) [148–153] — also used in latent semantic indexing [158] — is another favored technique related to PCA.

Techniques that propose simpler numerical solutions to find representative coefficients are often based on discretising the original sequence into smaller segments in the time domain to derive characteristic features. A common approach is to use the mean [144]. A common technique in this category is piecewise aggregate approximation (PAA) [159], whose coefficients represent time average segments based on either equal sized windows, or variable window sizes, as happens with adaptive piecewise constant approximation (APCA) [160]. Common variations of a time-based segmentation approach, according to [161], include: the segmented sum of variation (SSV) [162]; piecewise linear approximation (PLA) [145, 159], which represents the data as interpolated lines between the end points of each segment; best fit linear regression between subsequences [163]; or techniques that only retain prominent data points, for example perceptually important points (PIP) [164].

Another group of representation techniques represent the subsequences symbolically [165]. A prominent technique in the literature is symbolic aggregate approximation (SAX) [166], which is essentially an adaptation of PAA. It reduces the dimensionality of the data by assigning symbols (like letters for example) to PAA coefficients (an average of the average if you will) which according to its authors, outperforms most other dimensionality reduction techniques [166, 167] — a modified version is indexable symbolic aggregate approximation (iSAX) [168], which speeds up the algorithm even further. Other symbolic representation techniques that discretise time series include: fuzzy neural network clustering based on symbolic features [169]; multiresolution vector quantized (MVQ) [170]; the persist algorithm (based on a multiresolution symbolic representation) [171]; and shapelets that essentially capture the ‘shape’ of small subsequences of a time series [172]. In contrast, some authors propose that instead of reducing the original time series to a smaller feature set, it is possible to represent it with proxies, such as ‘bits’ instead of real values to reduce storage space [173, 174].

Model-based representation, however, takes on a parametric form. One of the key

paradigms developed in the 1920s in this regard, particularly relevant to univariate<sup>†</sup> forecast models (see Information Box 4.4 (p. 69) for more information), proposes that any time series is the superposition of three main components: a trend component, a cyclical or repetitive seasonal component, and a random noise component [175]. Although this notion holds true for nearly all time series applications, many models are heavily criticised because of assumptions of linearity and stationarity [176]. Statistical approaches for time series classification can be divided into a ‘classical’ phase based on derivatives of Fisher’s linear discriminant [115, 116], and a ‘modern’ phase based on the distribution of features within classes that generally rely on a more Bayesian probabilistic underlying model such as hidden Markov models (HMM) [177].

#### INFORMATION BOX 4.4: Statistical forecasting models

In statistical time series analysis most methods are based on correlation theory (focusing on the auto-covariance or cross-covariance functions of a series) [175], and use techniques to forecast future values of the original series based on predictions of the separate components (particularly the seasonal component). Both univariate and multivariate forecast models have been developed, using both stationary and non-stationary methodologies. The most common methods for univariate analysis are based on the auto-regressive (AR) and moving average (MA) class of models [175]. While a multivariate approach may use similar methodologies, it usually requires a link function (such as a linear transfer function (LTF)) to allow explanatory variables from other time series to be used.

Most statistical models assume stationarity and focus on either the noise or seasonal components to make their predictions (adding the trend afterwards). Long-term trends are usually removed via differencing before analysis. In the 1970s, Box and Jenkins [178] proposed the ARIMA (autoregressive integrated moving average) methodology, which has become one of the predominant forecasting models in time series analysis. ARIMA models are particularly useful when analysing autocorrelation within the series, such as seasonality or local seasonality (data related to specific seasons as opposed to others) [179, 180], and are a very powerful tool for forecasting econometric indices or crop yields, etc. For most univariate applications, the typical procedure is to first identify an appropriate model, estimate the model using different parameters, and then test the model using appropriate significance testing or other probabilistic methods. A simple test for model fit is Akaike’s information criterion (AIC), which ensures a balance between complexity and accuracy by penalising the model based on the number of parameters it uses [181].

In terms of the frequency domain, one of the first examples of a representation approach is given by Agrawal *et al.*, [134] who proposed the F-Index, which uses an R-tree algorithm

<sup>†</sup>The analysis of a single time series.

[182, 183] to index the main characteristic coefficients of the DFT to identify similarities between time series based on the Euclidean distance of Fourier amplitudes. Janacek *et al.*, [184] however, proposed statistical likelihood measures instead of using the Euclidean distance. The DWT is another favoured decomposition technique used from the frequency domain, where approaches often retain a few wavelet coefficients that have significant energy. A common choice is the Haar wavelet [1, 135, 185, 186], but other wavelet bases have also been used for dimensionality reduction [138, 139, 187, 188].

## 4.2.2 Classification

There are many tasks related to data mining, but the topic that concerns this thesis is time series classification. Algorithms include: linear (such as logistic regression [189]); support vector machines [130]; decision trees; neural networks; Bayesian networks; hidden Markov models; and kernel estimations (such as a *k nearest neighbour (kNN)*), or even combinations of many algorithms to best identify dominant features [190]. The key underlying element in which to test a new classification technique is based on the notion of the metric space. The metric space defines a mathematical space in which model comparisons can be evaluated using any number of functions or algorithms calculated using appropriate classifier algorithms, such as nearest neighbours or R-trees [182]. The common classifier choice is the *k nearest neighbour (kNN)* algorithm, which offers a simple and accurate approach to perform classification with no underlying assumption on the data, and can accommodate a wide range of distance measures, but also provides no clear training during the classification process. It follows that the simplest nearest neighbour classifier is the *1-nearest neighbour (1NN) or simply NN*, which uses all the training sets for testing during classification. In comparison decision trees are highly rule based, while the Bayes class of classifiers is highly parametric requiring many parameters to produce probabilistic models.

Within the metric space, a set of time series data known to share a common pattern can be grouped into a single class or category, whereas data that are the result of processes that cause a greater variability (for certain time periods or at certain frequencies) between two or more time series are classified into alternative classes or categories — collectively

forming a multi-class database. The time series database  $X$  takes the form of a  $m \times n$  matrix

$$X = \begin{pmatrix} x_1^{(1)} & x_1^{(2)} & \cdots & x_1^{(j)} & \cdots & x_1^{(n)} \\ x_2^{(1)} & x_2^{(2)} & \cdots & x_2^{(j)} & \cdots & x_2^{(n)} \\ \vdots & \vdots & \cdots & \vdots & \cdots & \vdots \\ x_i^{(1)} & x_i^{(2)} & \cdots & x_i^{(j)} & \cdots & x_i^{(n)} \\ \vdots & \vdots & \cdots & \vdots & \cdots & \vdots \\ x_m^{(1)} & x_m^{(2)} & \cdots & x_m^{(j)} & \cdots & x_m^{(n)} \end{pmatrix} = \begin{pmatrix} x_1 \\ x_2 \\ \vdots \\ x_m \end{pmatrix}, \quad (4.1)$$

where  $x_1, x_2, \dots, x_m$  are the different variables that make up the time series data  $x_i^{(1)}$  till  $x_i^{(n)}$ . A common approach in designing a new distance measure function to be used in machine learning is to build a model on a set of training samples and assess its ability to predict or classify previously unseen data. The performance of the measure, where the function is a distance measure, is evaluated by determining the percentage of objects identified correctly.

Simple, but also possibly the most extensively used, time-domain techniques are based on  $L^p$  norm functions such as the Euclidean distance ( $Ed$ ), or variants thereof such as Root Mean Square Distance — which is simply  $\frac{Ed}{n}$ , or the Mikowski distance — a generalisation of  $Ed$ ). The Euclidean distance  $Ed$  is the square root of the sum of the squared differences

$$Ed = \sqrt{\sum_i (x_i - y_i)^2}. \quad (4.2)$$

Figure 4.1 (p. 72) provides an illustration of how the Euclidean distance is calculated using a one-to-one mapping to produce the inner product of all samples between two time series.

To define a metric space for a time series database  $X$ , the distance function  $d$ , where  $d = Ed$  for example, must give the distance between every two time series  $\forall x_1, x_2 \in X$  as a non-negative real number ( $d(x_1, x_1) \geq 0, d(x_1, x_2) \geq 0$ ). If in addition the following

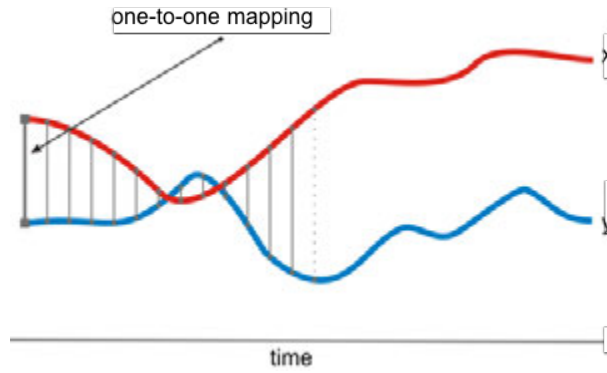


FIGURE 4.1: Graphic representation of the one-to-one Euclidean distance mapping. The graphic is modified from [191] and illustrates how the inner product of time series  $x$  and  $y$  is calculated using a one-to-one distance mapping.

are satisfied

$$d(x_1, x_2) = d(x_2, x_1); \quad (4.3)$$

$$\forall x \in X, d(x, x) = 0; \quad (4.4)$$

$$\forall x, y, z \in X, d(x, y) \leq d(x, z) + d(z, y); \quad (4.5)$$

then  $(d, X)$  may be called a metric space [192]. The most important assessment criterion is the error rate. The most common way of estimating the error rate, and therefore the model, is through a cross-validation approach and includes:

- **Hold-out method.** In this approach, the dataset is randomly divided into a training and test set (often two-thirds training and one third test); the classifier is built on the training set, and error is calculated as the miscalculation rate of the classifier on the test set. Sometimes the hold-out method is randomly resampled  $k$  times, and the error is taken as the average of all  $k$  iterations [193].
- **$k$ -fold cross-validation.** In  $k$ -fold cross-validation, a dataset of  $N$  examples is randomly split into  $k$  subsets of about equal size; the classifier is iteratively tested on each  $k$ -fold and trained using the remaining  $k - 1$  folds, and the error is taken as the complete number of miscalculations for all  $k$  iterations, divided by  $N$  [194]. A variation is the stratified cross-validation in which the class distribution of the

samples in each subset is stratified to be approximately the same as the initial dataset [193].

- **Leave-one-out cross validation (LOOCV).** This approach is very similar to  $k$ -fold cross-validation, but with  $k = N$ . In each  $k$  iteration, the classifier is trained on  $k - 1$  samples and tested with the remaining sample, and so on, until each sample has been tested [193].

Leave-one-out cross validation provides the most reliable and consistent error estimate, but also requires the most computational resources. It is important to note that during the classification process false clustering could occur when similar items in a dataset have been grouped together incorrectly, whereas false dismissals imply that not all the items with the same characteristics have been returned [140, 192]. If the classifier cannot accommodate the classification problem, then an alternative classifier is called for, or more likely an alternative distance function is needed.

### 4.2.3 Examples of Euclidean-based techniques

Over the years, numerous algorithms have been developed in both the time and frequency domain with the purpose of being generic enough distance measures to be useful for a wide range of time series problems. Broadly speaking, however, almost all time series classification techniques are divided into two categories: techniques that provide direct measurements between time series points, and techniques that use global or local features to provide high level representations of characteristic features [195]. One of the most common algorithms that performs well over a wide range of scientific domains using direct measurements between time series points is dynamic time warping (DTW), which replaces the one-to-one mapping of the Euclidean distance by a one-to-many mapping to overcome the limits of phase changes or time shifts in the time domain.

DTW provides a more robust similarity computation by distorting the time axis of one of the sequences to match samples in the other. It was introduced in the 1970s for speech recognition [196, 197] as a way to compensate for different rates of speaking, but since

the mid 1990s [198] has become a common choice in many machine learning experiments [199–206]. A recent study, which compares DTW to other common techniques [207], showed that DTW is one of the most difficult techniques to beat over a wide range of scientific disciplines. One drawback of DTW, however, is that outside the classification application little information is available to understand the relationship between common features.

The DTW algorithm relies on finding the optimal warping path in a underlying distance matrix. Given the two time series  $x = \{x_1, x_2, \dots, x_n\}$  and  $y = \{y_1, y_2, \dots, y_m\}$  of length  $n$  and  $m$ , the distance matrix is given as

$$\text{distMatrix} = \begin{pmatrix} d(x_1, y_1) & d(x_1, y_2) & \cdots & d(x_1, y_m) \\ d(x_2, y_1) & d(x_2, y_2) & & \\ \vdots & & \ddots & \\ d(x_n, y_1) & & & d(x_n, y_m) \end{pmatrix}, \quad (4.6)$$

where  $\text{distMatrix}(i, j)$  corresponds to the distance of  $i^{\text{th}}$  point of  $x$  and  $j^{\text{th}}$  point of  $y$  as  $d(x_i, y_j)$ , with  $1 \leq i \leq n$  and  $1 \leq j \leq m$  [191]. The DTW algorithm can then be expressed as

$$\text{DTW}(x, y) = \min \left( \sqrt{\sum_{k=1}^K W_k} \right), \quad (4.7)$$

where  $W$  is a warping path through the distance matrix computed by creating a cumulative distance matrix  $\gamma$  of the same dimension as  $\text{distMatrix}$  to store  $(i, j)$  values (typically the Euclidean distance between individual points) (shown in Figure 4.3 (p. 76) and given as

$$\gamma(i, j) = d(x_i, y_j) + \min(\gamma(i-1, j-1), \gamma(i-1, j), \gamma(i, j-1)). \quad (4.8)$$

The computation speed of the DTW algorithm can be increased by using threshold values to limit the path search area (in the horizontal and vertical direction) and thus reduce the complexity of the calculation. The solution for the path through the distance matrix is calculated using dynamic programming (solving and storing for a subgroup of point



comparisons prior to moving on to the next position in the path). The most common constraints are summarised according to the following conditions:

- a **monotonic condition**, in which the  $i$  and  $j$  positions stay the same or increase (but never decrease);
- a **continuity condition**, in which the path advances one step at a time;
- the **boundary condition**, starting at the bottom left and ending at the top right of the distance matrix;
- a **window adjustment condition**, whereby the distance the path is allowed to wander from the diagonal is restricted by the window; and
- a **slope constraint condition** which limits the angle the path is allowed to take relative to the diagonal.

By applying these conditions the DTW algorithm computation cost remains realistic and the number of possible paths is limited. Figure 4.2 (p. 76) gives an example of how DTW can be used to effectively match phase differences between a noisy sine and cosine function over the range  $[0, 2\pi]$  by finding the best warping path, while Figure 4.3 (p. 76) illustrates two common global constraints that can be applied to the warping path.

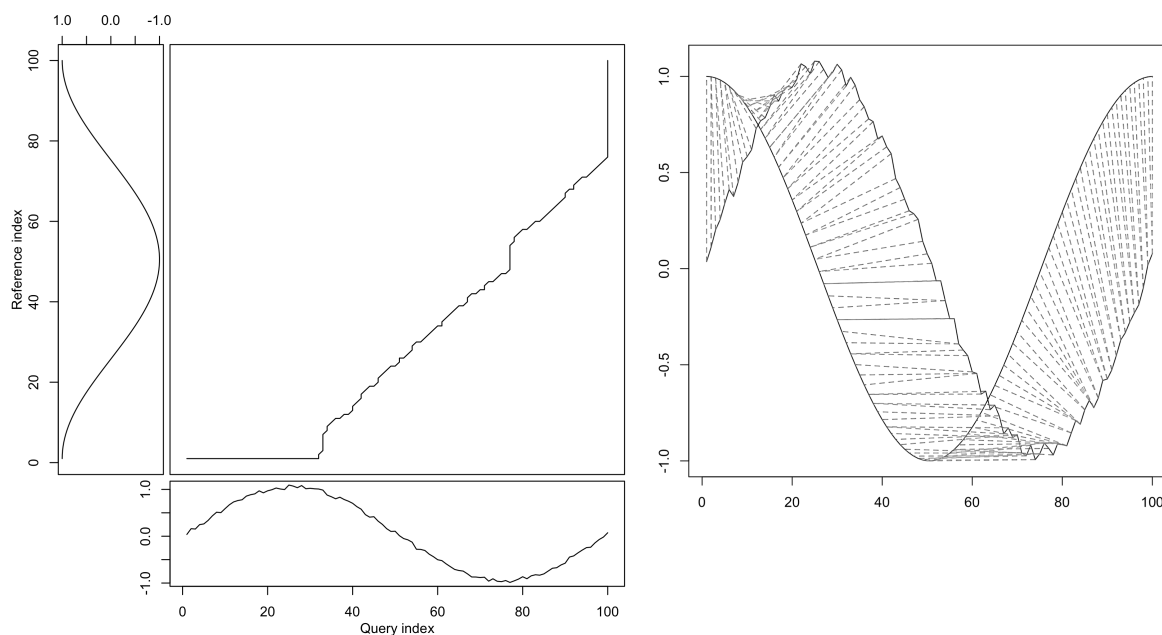


FIGURE 4.2: Example of matching phase differences using dynamic time warping (from [208]). The image on the left illustrates the ‘path’ a one-to-many mapping function used by the DTW algorithm would produce when the data is phase shifted. The path would otherwise be the one-to-one diagonal line when using a one-to-one mapping such as Euclidean distance (shown in Figure 4.1 (p. 72)).

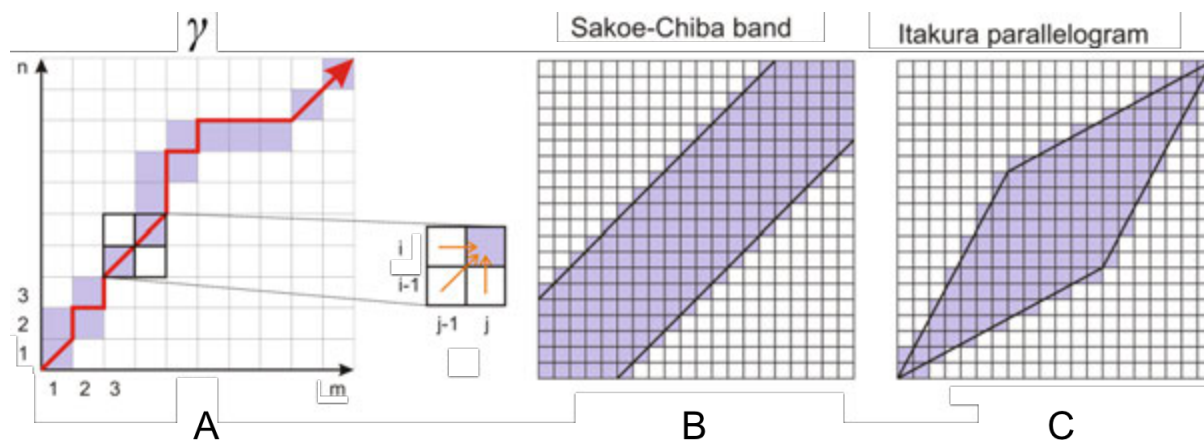


FIGURE 4.3: Dynamic time warping path through the cumulative distance matrix  $\gamma$  with global constraint examples modified from [191]. In Figure A the coloured blocks refer to the warping path and demonstrates how the minimum value from positions  $(i - 1, j - 1)$ ,  $(i - 1, j)$  and  $(i, j - 1)$  is selected. Figure B and C show examples of the global constraints Sakoe-Chiba band and Itakura parallelogram respectively, with coloured blocks referring to the search area of the warping path.

The majority of DTW applications found in the literature implement the Sakoe-Chiba band (shown on Figure 4.3 (p. 76)) with a 10% global window constraint. To test the effect the warping window size could have on accuracy, Ratanamahatana and Keogh

[209] ran an experiment with window sizes (relative to the diagonal) ranging from 0% (the traditional Euclidean distance) to 100% (unconstrained warping path) on seven time series classification problems. They concluded that the best accuracies obtained were all within a global window size of 10% or less. The lucky time warping (LTW) distance [210] (another derivative of DTW) provides a much faster algorithm by evaluating only certain DTW elements in the warping path, with a reasonable trade off between speed and accuracy as well.

It starts to become intuitive that any number of experiments can be performed to test different variations of the DTW algorithm regarding its warping path and ways to speed up computation. It also becomes clear that one classification problem might be optimised using highly constrained conditions while another might require slightly less stringency, the outcome of both determined through empirical means. To better account for the relative importance of phase shifts between time series, for example, weighted DWT (WDTW) [211] can be used. Here, the method penalises points according to the phase difference, where smaller phase differences get lower weights and *vice versa* using a modified logistic weight function

$$w_{(i)} = \left[ \frac{w_{max}}{1 + \exp(-g(i - m_c))} \right], \quad (4.9)$$

where  $i = 1, \dots, m$ ,  $w_{max}$  is the upper bound of the weight,  $g$  is a constant,  $m$  is the length of the sequence, and  $m_c$  is the midpoint of the sequence. Jeong *et al.*, [211] found that this approach yields improved results over standard DTW.

#### 4.2.4 Examples of high level representation techniques

A popular technique, which lends itself to the representation class of time series classification, is symbolic aggregate approximation or SAX, originally introduced by Lin *et al.*, [166] as a dimensionality reduction distance measure. The technique provides a symbolic extension to PAA [159], where PAA is calculated according to average window segments

$\bar{c}_i$  on normalised time series as

$$\bar{c}_i = \frac{w}{n} \sum_{j=\frac{n}{w}(i-1)+1}^{\frac{n}{w}i} c_j. \quad (4.10)$$

Here  $\bar{c}_i$  is the mean of a segment of the points in a time series  $c_j$  based on  $w$  equal sized time windows. To get the SAX representation, the PAA coefficients are further divided into predetermined equal sized ranges of their distribution and each range is assigned a letter. The corresponding distance between the letters or ‘words’ is obtained using a classifier such as Euclidean distance, which uses a lookup table to correspond each letter to a corresponding range. Many variations of SAX have been proposed since its inception, including similar methods such as textual approximation (TAX) [212, 213]. Other examples include: the use of SAX for new pattern discovery [214]; or by combining it with different algorithms, for example genetic programming algorithms, to find even more complex patterns [215]; or classic vector space models (VSM) [216] to weight ‘words’ into class characteristic vectors [195] — although in some instances overfitting SAX models leads to worse performance during testing [217].

A similar approach is the bag of patterns [218], which follows on from SAX by converting overlapping subsequence ‘patterns’ into a vector space. In both instances either a Euclidean distance or cosine distance classifier is most often used for the actual classification. A more flexible variation on the bag of patterns is proposed by Baydogan *et al.*, [219], called bag of features, which considers fixed and variable length intervals and includes shape-based features such as the slope and variance. The latter two provide more insight into pattern distribution through histograms of feature frequencies.

Shapelets [172] are another common technique in the literature, which capture specific local features of ‘object-derived’ time series subsequences. Many techniques exist to characterise similar shapelets for class identification [220]. The technique is chiefly used to cluster and create labelled classification datasets, but is often criticised for being time-consuming. Rakthanmanon and Keogh [221] proposed a faster algorithm, called fast shapelets, while Wistuba *et al.*, [222] proposed the ultra fast shapelet which speeds up the process by up to three orders of magnitude with minimal loss in accuracy.

Recurrence plots [223] have also been suggested as useful time series classifiers. The basic idea behind the recurrence plot is to graphically reveal similar repetitive patterns in time series. Silva *et al.*, [224] proposed the use of recurrence plots using the Campana-Keogh (CK-1) distance measure [225] and found that it outperformed the traditional Euclidean distance and DTW on a large number of benchmark time series.

The frequency domain also provides a set of related techniques for feature extraction and indexing by finding and matching a set of similar frequency patterns; specifically, the DFT and DWT have received a lot of attention in this regard.

The first example is the often-cited F-index of Agrawal *et al.*, [134] who used the Euclidean distance between the first few Fourier coefficients (which represent the low frequencies of the time series) to index time series, while [140] extended the work to handle subsequence matching by using sliding time windows to perform the DFT. Other follow up work includes moving averages in an F-index [141] and using the last  $k$  coefficients according to the symmetric property of the DFT for more efficient storage during indexing [142]. Wu *et al.*, [136] proposed the use of the largest coefficients to better retain the general energy, but noted that the additional computational overhead of using a different feature set for each time series was a disadvantage when using the technique for indexing purposes (see Information Box 4.5 (p. 80) for a general description of using the FFT to match similarities using Euclidean distance). Morchen [226] suggested the use of the same mean energy  $k$  coefficients to partly overcome this problem.

The Haar DWT has been suggested as an alternative to the DFT [135, 152, 186] (including the use of DTW for a similarity measure [227]), which not only provides time frequency decomposition using a faster computation, but has also been shown to have comparable energy preservation [136]. Popivanov and Miller [138] showed that a wide array of wavelet bases that have exact reconstruction properties could be used for feature extraction, for example [228, 229], while others have proposed the use of cross wavelet analysis for classification [6, 230, 231]. Keogh and Kasetty [232] claim that generally more sophisticated techniques such as DWT and DFT perform no better than Euclidean distance.

**INFORMATION BOX 4.5: Classification using FFT amplitude coefficients**

The Fourier transform converts a time-domain function into its frequency domain representation. The FFT provides all the coefficients that describe the function as a feature vector, whereby each coefficient (amplitude and phase) corresponds to a physical meaning in the time domain. By filtering the coefficients that provide the best correlation (using the Euclidean distance between amplitude coefficient vectors) of two time series, it is possible to filter the feature space before further analysis. Optimisation during a classification experiment provides the mapping of the characteristic amplitudes that describe the problem in the frequency domain, and allows further classification to be performed using only a few selected DFTs. Alternatively, if computational time is no constraint, and the classification problem is mainly described by similarities in AM, then the similarity can be taken as the Euclidean distance of all the amplitude coefficients (as the effects of smaller amplitude coefficients would be negligible).

### 4.3 Concluding remarks

A general overview of classification was presented in this chapter with the intent that the experiments performed in Chapter 6 are based on a comparison between Euclidean distance, DTW, and the Euclidean distance of FFT amplitude coefficients, as well as the method developed in this thesis — presented later in Chapter 5. The choice of comparison is plain: the Euclidean distance (despite its antiquity) provides a benchmark technique (both in speed and precision); DTW on the other hand provides an optimised version of the Euclidean distance [207] by using a one-to-many mapping algorithm; and the Euclidean distance of FFT amplitude coefficients provides a direct AM frequency-domain comparison. The goal in this thesis is not speed of computation, but rather a full exploration of characteristic features and classification accuracy. The following points are worth noting:

- The Euclidean distance provides one of the simplest yet purest time-domain techniques used to classify similar AM, but due to its one-to-one mapping it also has many shortcomings. The most obvious is that any phase shift (such as lead and lag) present between time series would most likely result in an inaccurate classification. Alternatively, if the classification problem is characterised by both AM and FM (or FM only), then it is very unlikely that the Euclidean distance will be able to correctly classify all inputs.

- Similarly, the Euclidean distance between FFT amplitudes (FFT-A) provides an AM classification technique well suited to the frequency-domain. The advantage that this approach has over its time-domain counterpart is that lead and lag times become irrelevant. The FFT-A approach is chosen so that frequency ranges can be explored simultaneously during the classification experiments in Chapter 6 and compared to the wavelet methodology developed in this thesis and presented in Chapter 5. However, similarities characterised by amplitude invariance could lead to incorrect classification.
- In contrast, DTW does account for both AM and FM, but has no easy way of communicating the underlying characteristics of the classification problem.

In the following chapter a method called cross wavelet similarity (CWS) is developed to characterise both AM and FM during the classification experiment. The CWS function comprises two terms. The first is designed to match AM by using the Euclidean distance between global wavelet power spectra (a term called CWED) in a similar way to traditional DFT approaches, but by using wavelet energy rather than Fourier frequencies. The second term, which is totally unique to this study, is called cross wavelet phase variance (CWPV) and is used to characterise FM similarities. The CWS function uses the product of these two terms (this approach is described in detail in Chapter 5) to find the optimal combination of similar AM and FM between time series.

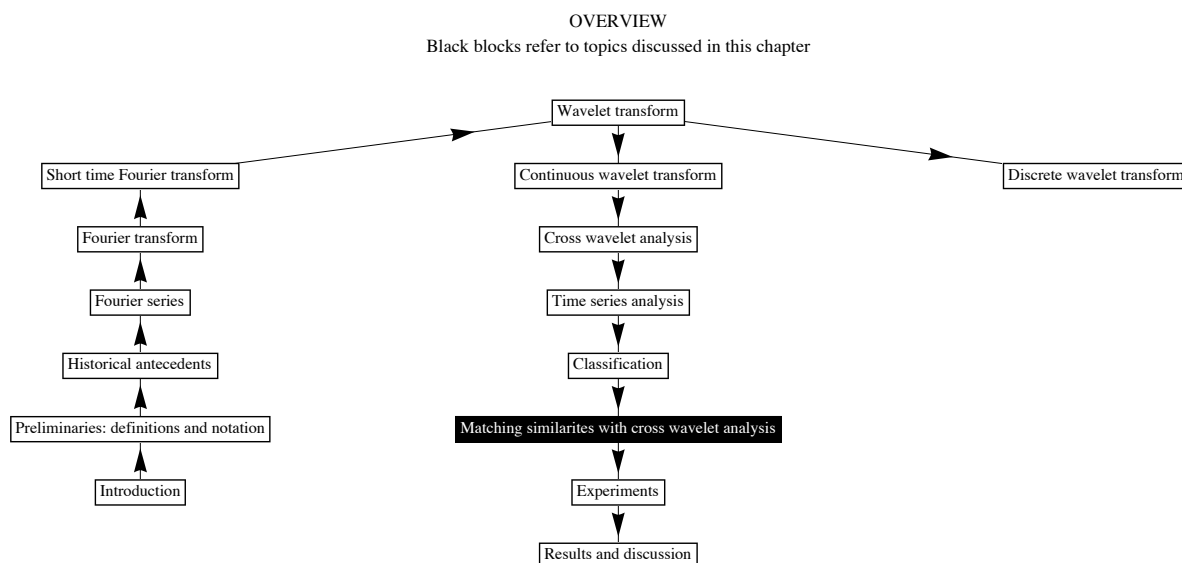
*"...comparing the capacity of computers to the capacity of the human brain, I've often wondered, where does our success come from? The answer is synthesis, the ability to combine creativity and calculation, art and science, into a whole that is much greater than the sum of its parts"*

Garry Kasparov (AD 1963 -)

# 5

Methodology: matching similarities using  
cross wavelet analysis





## 5.1 Introduction

In this chapter, a methodology is developed to exploit global wavelet power spectra and cross wavelet phase to separate out different correlations that best describe the classification problem according to similar underlying amplitude modulated (AM) and frequency modulated (FM) behaviour. Here, similar AM and FM behaviours are calculated for sets of scales (representing different frequency bands) using separate terms designed to extract these characteristics. The first term called CWED (continuous wavelet Euclidean distance) compares AM relationships by calculating the Euclidean distance between global wavelet power spectra of individual time series. The second term is called CWPV (cross wavelet phase variance) and provides a useful measure of FM coherency across a range of scales. The CWPV term is based on a similar notion to cross wavelet coherency [3, 76–79], but is used here to compare the phase difference between time series for a specified set of scales. A ‘global phase vector’ is created (where each value is the variance of phase for a specific scale over time), from which any value, or combination of values, can be summed to provide a metric of ‘local’ phase variability to be compared to other samples during the classification experiment. Here, the minimum value in the comparison represents the best degree of phase coherency between two samples. The cross wavelet phase is amplitude invariant and therefore the less the variability over a set of scales, the more similar the FM behaviour — despite lead or lag times. The scales that best describe similar AM and

the scales that best describe similar FM behaviour (which could be from different scale sets) are assigned during classification training according to the classification result.

During the experiment, the cross wavelet is computed and the CWED and CWPV terms are used to calculate the results that correspond to different scale sets  $S$ . These sets are made up of different linear combinations of scales  $[s]$ . For example, if the wavelet comprises only three scales in total, then the sets  $S_i$  for which the CWED and the CWPV terms are calculated are made up of:  $S_1 = [s_1]$ ;  $S_2 = [s_1, s_2]$ ;  $S_3 = [s_1, s_2, s_3]$ ;  $S_4 = [s_2]$ ;  $S_5 = [s_2, s_3]$ ; and  $S_6 = [s_3]$ . Figure 5.1 (p. 85) provides a simple graphic to help better explain this scenario. Each set contains two result values, one for the CWED term and one for the CWPV term. To find the best combination of these two they are multiplied by each other (during classification training) using the function CWS to form a  $AM_i \times FM_j$  product matrix, where the smallest value within the matrix represents the best combination of scales (according to the least amount of AM and FM differences between samples). The position in the CWS matrix (see Figure 5.1 (p. 85) for example) represents the features that best describe the classification problem according to this approach. To accommodate FM only or AM only possibilities, a comparison with the best AM and FM only classification results is also performed. The methodology also provides a powerful framework to assess if the performance of alternate classifiers differ because of AM or FM characteristics (based on the CWED or CWPV results).

## 5.2 Method

If the frequency characteristics such as the wavelength band of the classification problem are known then no optimisation is required prior to analysis. However, without *a priori* knowledge of the structure of the data in the frequency domain it is not possible to determine the best wavelength range to compare without iteratively assessing the results in a supervised environment. The function cross wavelet similarity (CWS) in Equation (5.1) is used to create a distance matrix that delineates common AM and FM behaviour between time series — based on the comparisons of classification results using different

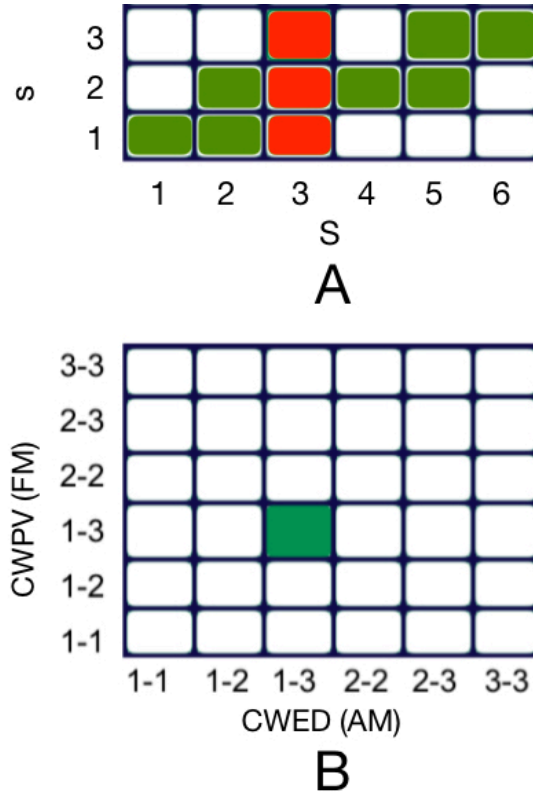


FIGURE 5.1: Simple example of CWS framework. In this example only three scales are used for illustrative purposes. The units coloured in green and red in A are all the permutations or sets  $[S]$  of the scales 1,2,and 3. The  $x$  and  $y$  axes in B represent these sets corresponding to the CWED ( $x$ ) and CWPV ( $y$ ) terms, where the values represent  $AM_{xi} \times FM_{yj}$ . The position highlighted in green in B is an example of set  $S_3$  (coloured in red in A) having the lowest value, suggesting that similar AM and FM behaviour both occur in the scale ranges 1-3 for the CWED and CWPV terms.

combinations of scales:

$$\text{CWS}(x, y, s, u) = \text{CWPV}(x, y, s, u) \times \text{CWED}(x, y, s, u) \quad (5.1)$$

where  $x$  and  $y$  are the individual time series being compared,  $u$  is the time window to be analysed and  $s$  is a set of arbitrary scales. The CWPV term stands for cross wavelet phase variance, developed specifically for this study to compare amplitude invariant frequency ranges calculated using Equation (5.2) (p. 86). The term CWED (given in Equation (5.3) (p. 86)) is the Euclidean distance between the global wavelet power spectra of individual wavelet transforms, and provides a useful measure of AM similarity (in a similar way as the Euclidean distance of FFT amplitude coefficients does). The CWPV term has the

following functional form:

$$\text{CWPV} = \sum_{s \in S} \frac{\sum_{u \in U} (\theta(u, s) - \overline{\theta(u, s)})^2}{N - 1}, \quad (5.2)$$

where  $\theta(u, s)$  is the phase of the cross wavelet,  $U$  represents the analysing interval (which in this case is taken as the length of the time series), and  $S$  is a discrete set of scales in a minimum to maximum range over which to compute the variance of phase. The term CWED in Equation (5.1) (p. 85) is the Euclidean distance between the global wavelet power spectrum of  $W_{Mx}(u, s)$  and  $W_{My}(u, s)$  and may be written out as

$$\text{CWED} = \sqrt{\frac{\sum_{u \in U} (\sum_{s \in S} (W_{Mx}(u, s)) - (W_{My}(u, s)))^2}{N - 1}}, \quad (5.3)$$

where  $W_{Mx}(u, s)$  and  $W_{My}(u, s)$  are the normalised wavelet modulus of  $x$  and  $y$  respectively.

### 5.2.1 The CWPV term

Consider a CWT scalogram (a 2D plot of the wavelet coefficients, where  $x$  represents time,  $y$  represents scale, and  $z$  the coefficient values). If the underlying coefficients are represented as wavelet energy (amplitudes), then the average of any ‘horizontal slice’ along the  $y$ -axis would represent some measure of the local power spectrum for that specific scale. By repeating this procedure for all scales (every point on the  $y$ -axis), the resulting vector becomes the global wavelet power spectrum. The global power spectrum then is comparable to a Fourier spectrum, in the sense that the energy represents the mean amplitude according to the wavelet scales at which they occur. When computing the CWPV term, phase coefficients derived from the cross wavelet are used, and instead of taking the average for each  $y$ -axis scale, the variance is taken to represent the degree of phase synchronicity between samples at that scale. Here, the coefficients do not need to co-vary at the same points in time. They could co-vary according to lead or lag times as long as phase offset and any FM behaviour is the same, in which case we can say there is good phase coherency at those scales.

To illustrate this, consider the example in Figure 5.2 (p. 88), which represents the continuous wavelet power spectrum, cross wavelet modulus and cross wavelet phase of arbitrary time series, here represented by weekly rainfall and temperature (between 1999 and 2005) for Beira, Mozambique. In both Figure 5.2 A (rainfall) and Figure 5.2 B (temperature) there is power at the 52 week period, indicative of the seasonal periodicity associated with meteorological data. The cross spectrum (Figure 5.2 C) reinforces the seasonal covariance of both time series (the same common pattern exists in both transforms), and the phase difference (represented by the range  $-\pi$  to  $\pi$ ) in Figure 5.2 D is virtually zero for every point in time across the 52-week period (indicating here that there is no lead or lag time in seasonal behaviour between the two time series); consequently, the variance calculated across the scales representing this period (shown in the right hand graph of Figure 5.2 D and expanded and transposed in Figure 5.2 E) is justifiably low. In this example, the sum of the entire variance vector should provide an overall measure of the phase coherency between the two time series, while the sum of the variance vector, for example over periods 32 to 52, provides a degree of similarity for those particular scales. If this were to be done (summing the variance vector) for a set of time series in the same metric space, for example, then the two time series that have the lowest summed phase variance would theoretically be more similar than time series with higher summed phase variance.

### 5.3 Defining the similarity framework

The CWS function is performed without prior knowledge on which wavelengths will characterise the similarity between different datasets, and the algorithm performs an empirical iterative-based approach during classification training to determine the scales which are the most similar. Therefore, the larger the training set the more accurate the characterisation will be. To explain the concept, consider the theoretical vector in Figure 5.3 A (p. 89), which represents a hypothetical phase variance vector. Here, 20 arbitrary scales are used for explanation purposes. If the set of scales  $S$  is taken as  $s(\min)=10$  and  $s(\max)=15$  in Equation (5.2) (p. 86), for example, then the sum (representing the sum of variance over  $S$ ) would be higher than if  $S$  is taken as  $s(\min)=5$  and  $s(\max)=6$ .

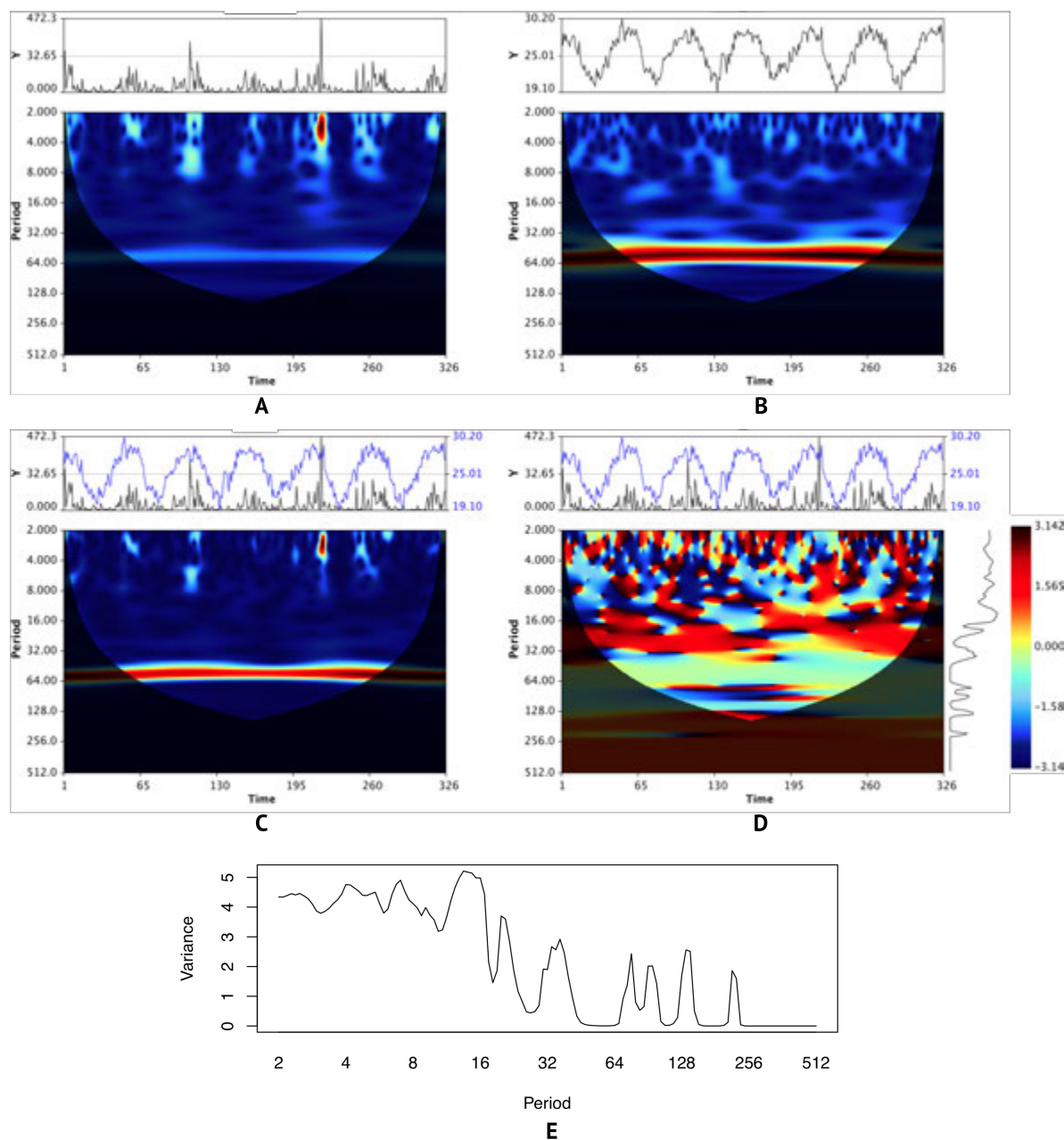


FIGURE 5.2: Cross Wavelet Phase Variance (CWPV) example. The power spectrum of the CWT for weekly rainfall and temperature time series (between 1999 and 2005) for Beira, Mozambique are shown in Figure 5.2 A & B respectively. The cross wavelet (Figure 5.2 C) illustrates power in the frequency domain that is common to the two time series. The CWPV (Figure 5.2 D & E) provides an index of similar phase behaviour between the time series by calculating the variance of the cross wavelet phase as a function of time (shown as a graph on the right hand side of Figure 5.2 D, and expanded in Figure 5.2 E). In this example, the two time series have a near zero phase shift for the seasonal scales (centred on 52) (roughly a zero  $\pi$  shift as shown in the colour legend) of Figure 5.2 D, and consequently the phase variability taken over the time window  $u$  is near zero. In general, low variance values indicate good coherency (similar FM between the time series for those periods or scales), whereas, high values are associated with phase differences in the time series.

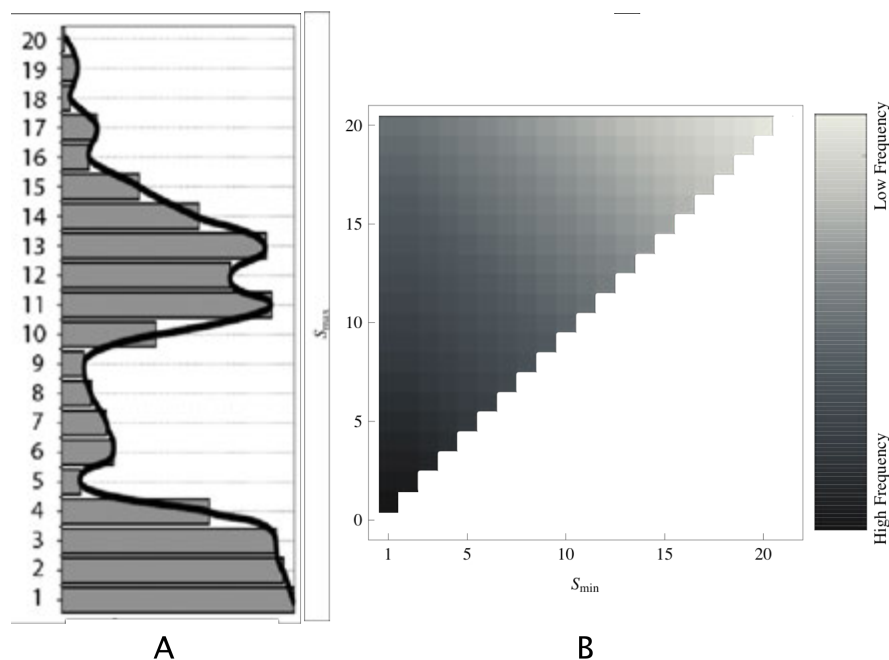


FIGURE 5.3: Theoretical vector representing either phase variance or global wavelet power spectra. The vector is represented as a bar-graph (A). By integrating over different frequency ranges the resulting value will emphasise either similarities or differences. B represents all possible linear combinations between  $s_{min}$  and  $s^{max}$  (i.e. the set of scales that will be evaluated over), and the broad frequency ranges that these combinations represent.

Here, Figure 5.3 B (p. 89) provides the conceptual framework in which to search for the best set of linear combinations<sup>†</sup> of scales, where their corresponding frequency range is defined by the set  $s$  (min) to  $s$  (max) in Equation (5.2) (p. 86). If for example the optimal set of scales was found to be  $s$  (min)=1 and  $s$  (max)=5 for the CWPV term during the classification experiment, then these effectively define the  $FM_j$  or ‘CWPV index’ or  $S$  values for the CWPV term in the CWS equation, which implies that FM similarity occurs in the higher frequency range.

Similarly, if Figure 5.3 A (p. 89) would hypothetically represent the global wavelet power spectrum of a single time series, and the Euclidean distance over a set  $S$  for the CWED term and another global wavelet power spectrum (not represented in Figure 5.3 (p. 89)) returned the best results for  $S$  as  $s$  (min) =15 and  $s$  (max)=20 during classification, then the AM similarity (the  $AM_i$  or ‘CWED index’ or  $S$  for the CWED term in the CWS equation) would be in the low frequency range. On the other hand, if only  $s$  (min)=1

<sup>†</sup>The linear combinations of the CWPV vector take the form  $\text{for}(i \text{ in } 1:N)\{\text{for}(j \text{ in } i:N)\{\sum_i^j CWPV\}\}$

and  $s$  (max)=5 was found to yield the best results, with the exclusion of any CWED coefficients, then the problem could be classified as a pure FM related problem and *vice versa*.

In its simplest form, with little optimisation or similarity searching for characteristic features, the implementation of the CWS function presented in Equation (5.1) (p. 85) can be applied by using a single time window  $u$  that covers all the points in the time series and  $S$  represents all the wavelet scales  $s$  used in both the CWPV and CWED terms. In this approach computation time is controlled by the resolution (number) of scales (or number of octaves (the dyadic scales) and voices (the intermediate scales between octaves)). If the classification results are good, then common similarities would be associated with both good phase coherency (similar FM) and similar AM across all frequencies. With a good understanding of the frequency characteristics of the problem, however, for example if the problem was purely related to FM, then the CWED term in Equation (5.3) (p. 86) may be dropped to speed up the search; alternatively, if the classification problem is characterised by AM similarities, then only the CWED term could be implemented. To demonstrate the methodology, consider the four time series in Figure 5.4 (p. 91), where  $N = 1000$  and A, B, C, and D have the following functional forms:

- $A = \sin\left(\frac{60\pi x^2}{N^2}\right) + \sin\left(\frac{12\pi x}{N}\right),$
- $B = \frac{1}{125}x \sin\left(\frac{60\pi x^2}{N^2} + 200\right) + \sin\left(\frac{12\pi x}{N}\right),$
- $C = \sin\left(\frac{30\pi x^2}{N^2}\right) + \sin\left(\frac{12\pi x}{N}\right),$
- $D = \frac{1}{125}x \sin\left(\frac{30\pi x^2}{N^2} + 200\right) + \sin\left(\frac{12\pi x}{N}\right).$

Both A & B in Figure 5.4 (p. 91) have the same FM characteristics, but different phase shifts. Similarly, C & D have the same functional forms as A & B, but at a lower sampling frequency. Contrariwise, A & C and B & D have similar AM behaviour. If the classification problem were FM related we would expect A & B to be classified as one class and C & D as another, whereas if the classification problem were AM then A & C would form one class and B & D the other. Table 5.1 (p. 92) gives the results of the Euclidean distance between the global wavelet power spectra and the phase variance



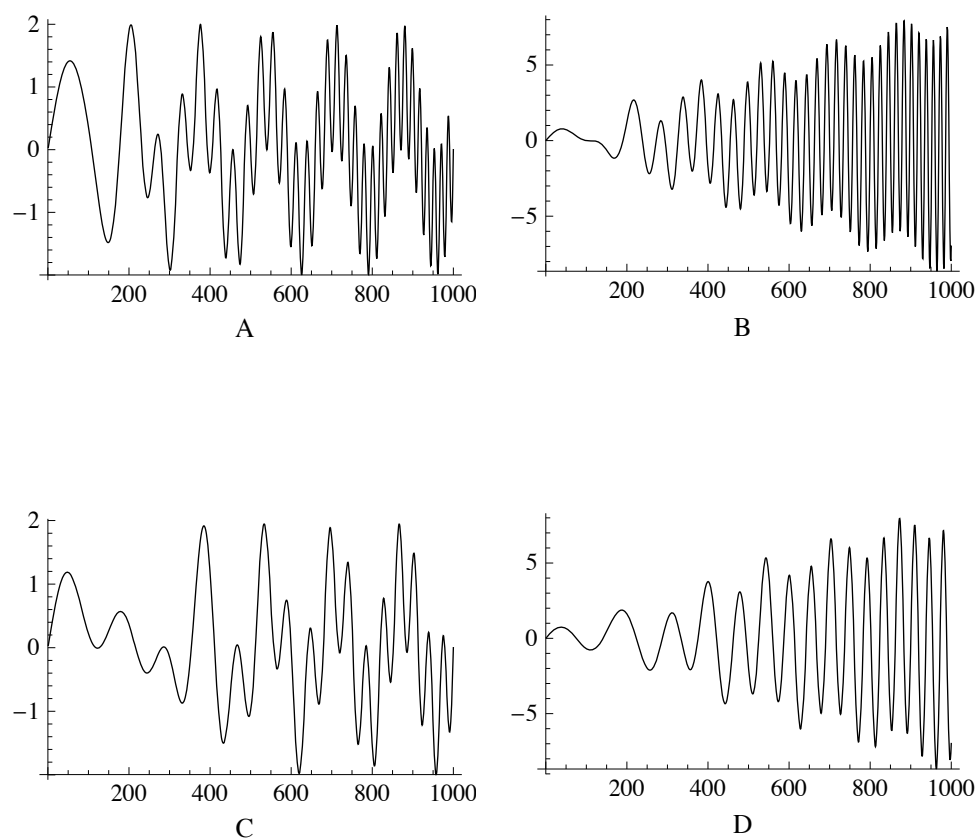


FIGURE 5.4: Example of AM and FM behaviour in time series. Both A & B have the same sampling frequencies, but different phase shifts. C & D have the same functional forms as A & B, but have a lower sampling frequency. Contrariwise, A & C and B & D have the same AM behaviour .

for these four time series computed over all the scales, and behaves exactly as expected. Figure 5.5 (p. 93) shows the wavelet scalograms (with the global wavelet power spectrum) for each time series, and the cross wavelet phase (with the associated variance vector) corresponding to the horizontal, vertical and diagonal combinations (in relation to the layout of A, B, C, and D in Figure 5.5 (p. 93) of each wavelet transform.

TABLE 5.1: Summary of classification results using the Euclidean distance between global wavelet power spectra and phase variance calculated for all scales.

Euclidean distance of global wavelet power spectra				
	A	B	C	D
A				
B	1074.944			
C	602.964	1162.632		
D	1189.257	851.720	856.351	
Phase variance				
	A	B	C	D
A				
B	9.937			
C	67.927	33.127		
D	33.406	74.379	8.441	

## 5.4 Worked example to calculate CWS

In Chapter 6, the approach described in this chapter is applied through a series of controlled experiments based on classification problems from the UCR benchmark time series database [4, 5]. In this worked example, the parameterisation of the CWS, CWED, and CWPV terms are done on the training set taken from the Coffee problem of the ‘updated’ UCR benchmark time series database [5]. The Morlet wavelet with a central frequency of  $2\pi$  is used, with one voice per octave. The total number of scales in this example is nine, and the total number of permutations or linear combinations of scales is 45. Figure 5.6 (p. 94) is a simple graphic representation of these combinations, and Figure 5.7 (p. 95) is the CWS similarity matrix representing the average error according to different combinations of CWED scale range sets  $\times$  CWPV scale range using LOOCV to assess the error. In Figure 5.8 (p. 96), Figure 5.6 and Figure 5.7 are combined to better highlight which scale ranges in both the CWED and CWPV terms are representative of the best error, and gives a good indication that a certain range of frequencies in this problem are attributable to AM and a certain range to FM.

To minimise the confusion of having to choose from multiple scale sets that characterise the AM and FM behaviour of the problem with the same error, the largest continuous cluster is used. This is accomplished by subtracting the minimum from the maximum scale in each set for both axes and adding these results together. To illustrate this,

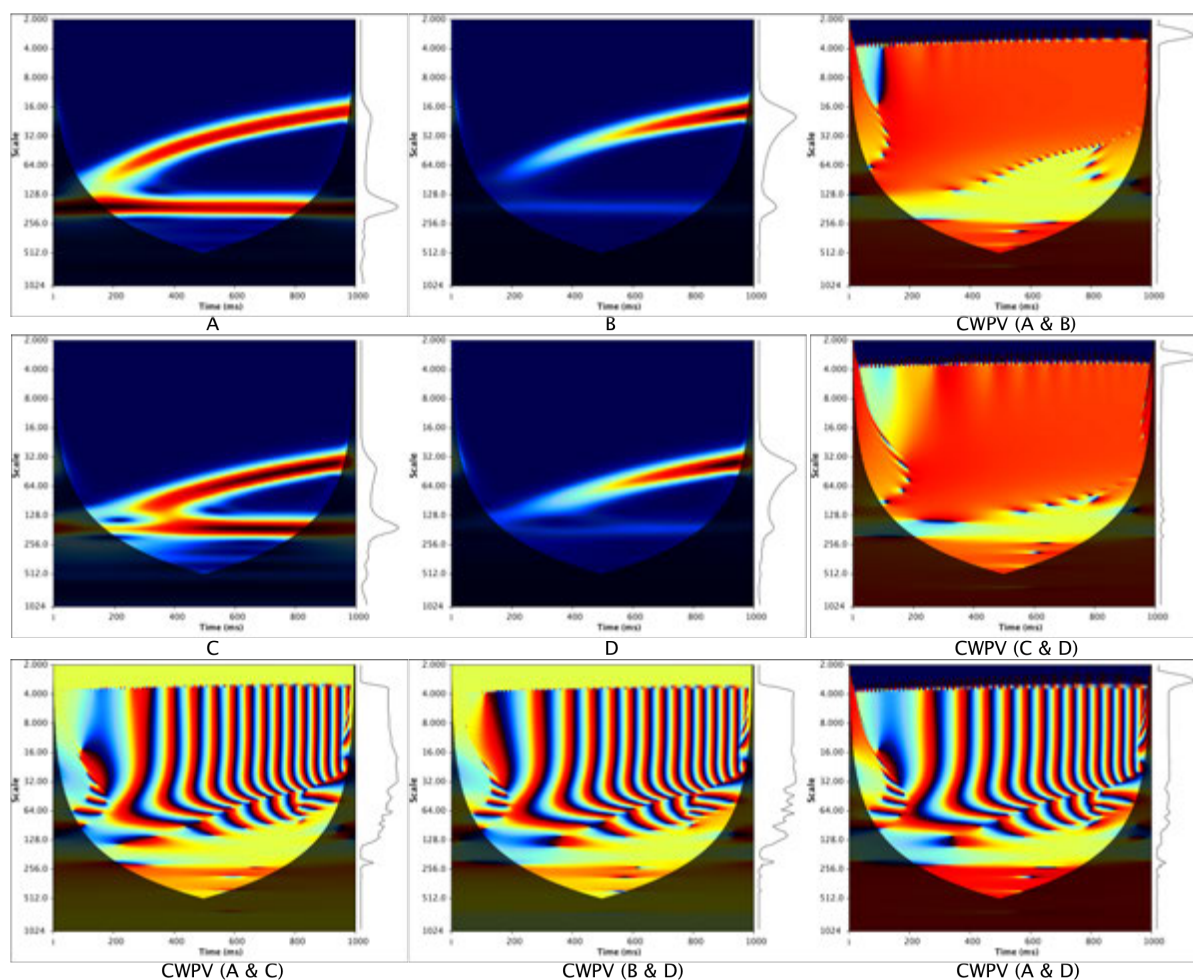


FIGURE 5.5: CWT and cross wavelet phase modulus representing AM and FM behaviour of signals presented in Figure 5.4 (p. 91). The power modulus of the individual wavelets represents the global wavelet power spectrum (shown on the right of each figure). The phase modulus corresponds to the horizontal, vertical and diagonal combinations of each wavelet transform. The variance of the phase is calculated for all scales and shown as a vector on the right. Low variance values over a set of a scales represents good phase locking behaviour.

consider the  $x$ -axis in Figure 5.7 (p. 95). Here, the largest continuous scale range (corresponding to the best error) would be at position 5 (i.e.  $s(\max)=6-s(\min)=1=5$ ), which coincides with the largest continuous range on the  $y$ -axis at position 39 (from top to bottom) (i.e.  $s(\max)=9-s(\min)=6=3$ ) — which summed is 8 (i.e.  $5+3$ ). The parameters used to describe the classification in Equation (5.1) (p. 85) in this example, and which could be used for further testing, therefore become CWPV scales =  $[6, \dots, 9]$ , CWED scales =  $[1, \dots, 6]$ , and voices = 1.

The pseudocode in 5.4.1 (p. 97) is given to allow the reader the ability to design their

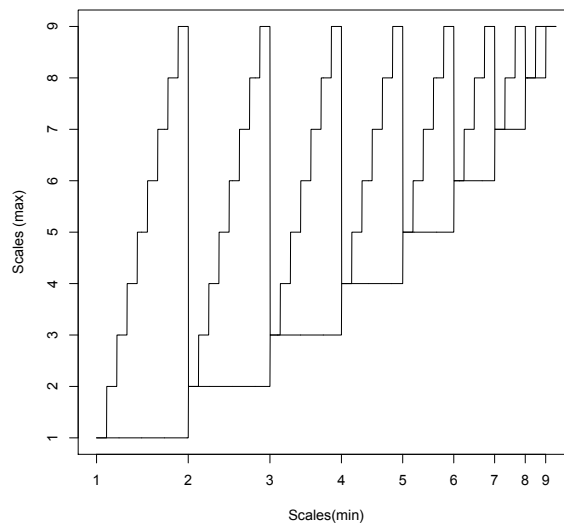


FIGURE 5.6: Simple example of scale set combinations used during CWS computation

own experiments. The code calculates the CWS function over the specified scale ranges for the CWPV and CWED terms. In this form the function would need to be repeated using all the scale combinations (model parameters) to build up the CWS matrix<sup>†</sup> (see Appendix D for more detailed and functional code listings). This pseudocode example also ends off the chapter. The results and analysis of the methodology (applied to the UCR time series database) are provided in the following chapter.

---

<sup>†</sup>Note that during the actual computation, it is better to return all the scale combinations and assess the performance simultaneously to speed up the approach.

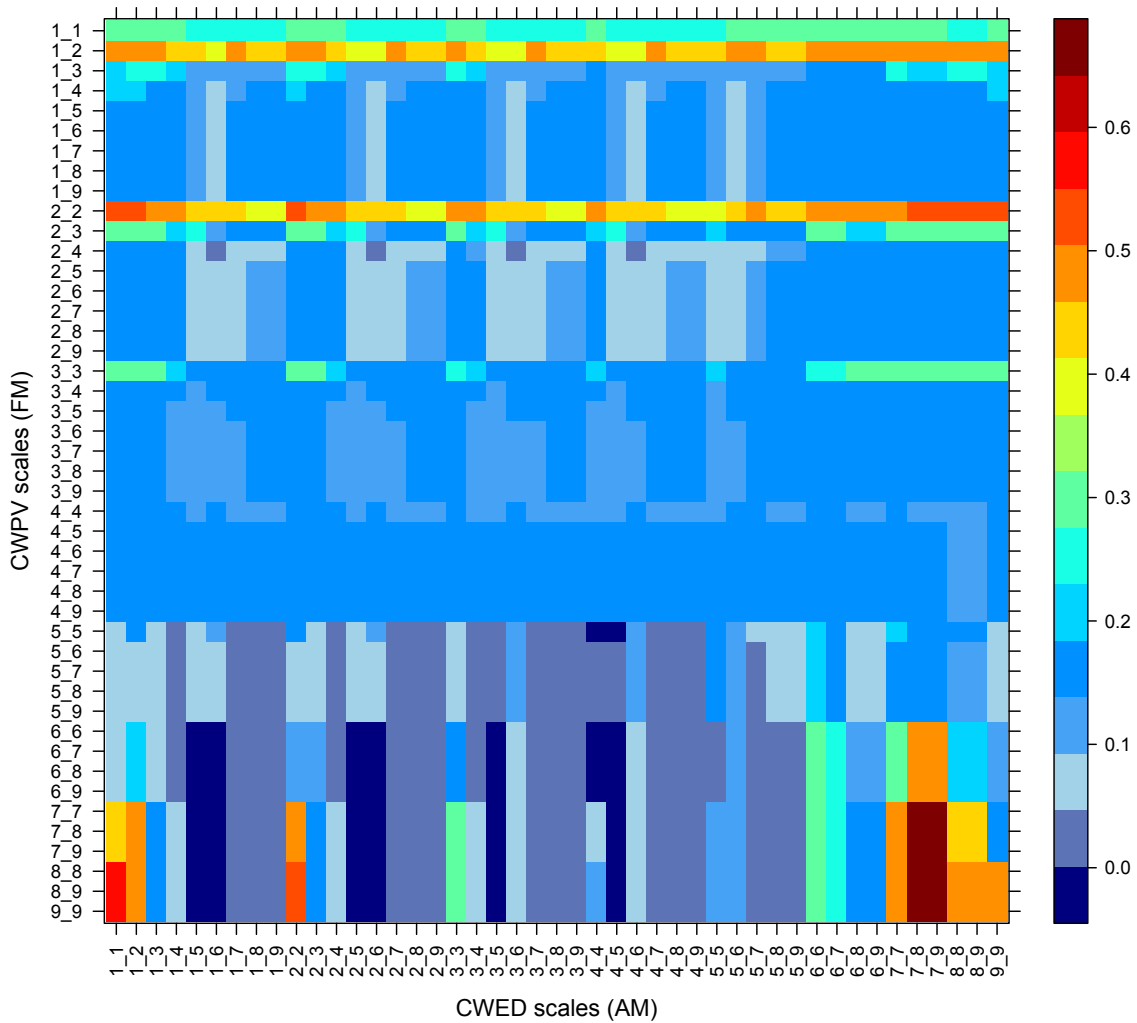


FIGURE 5.7: Worked example of CWS framework. Each block represents the results for a specific combination of  $AM \times FM$  (derived from the CWED and CWPV terms) determined using LOOCV.

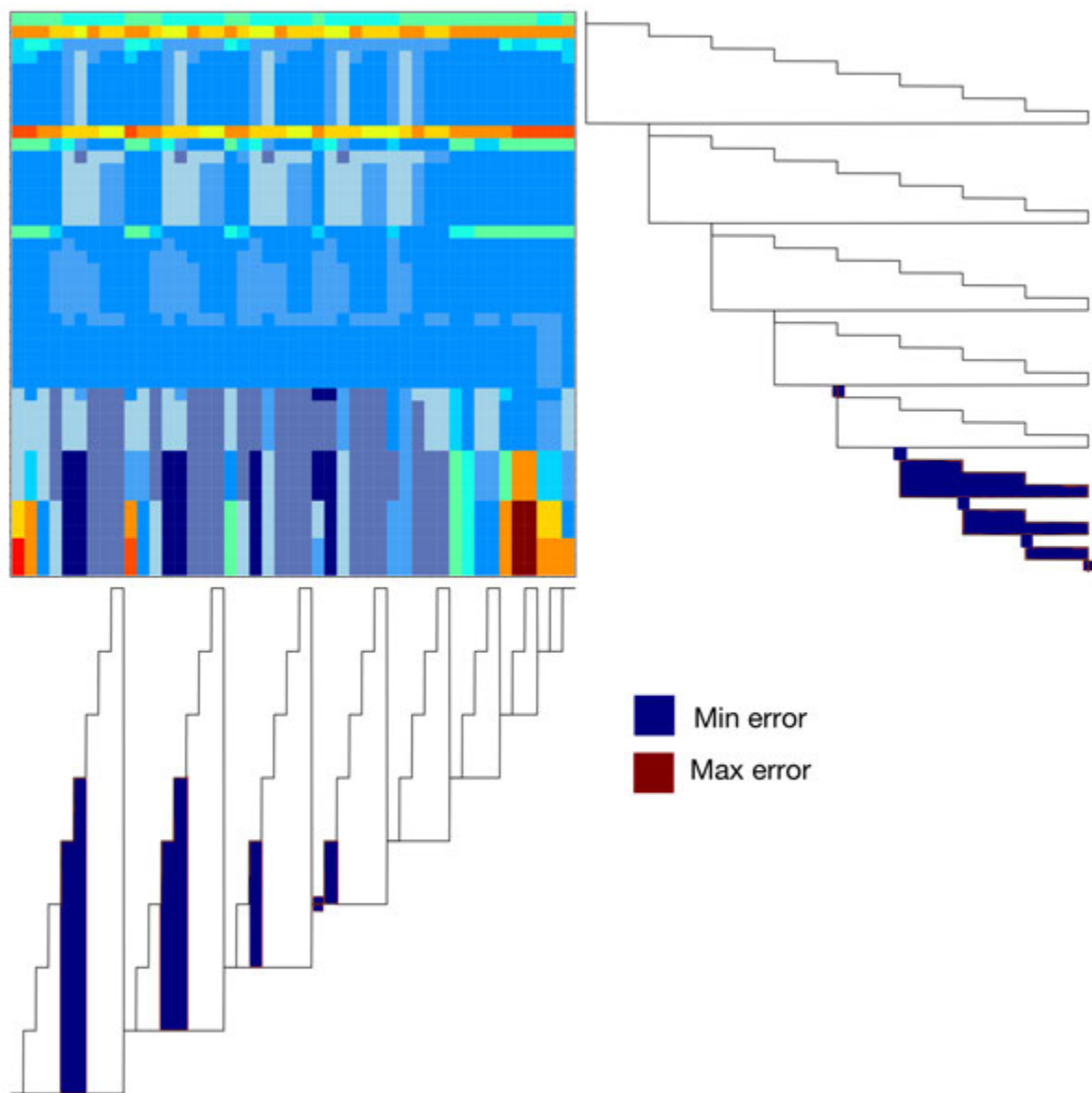


FIGURE 5.8: Worked example of CWS framework highlighting scale ranges. Each block represents the results for a specific combination of  $AM \times FM$  (derived from the CWED and CWPV terms) determined using LOOCV.

**Algorithm 5.4.1:**  $CWS(x[1, \dots, n], y[1, \dots, n], voices, sx_1, sx_2, sy_1, sy_2)$

*% This algorithm calls the CTW function in 3.4.2 (p. 48)*

*% The CWT returns the modulus, real, imaginary and scale*

$w1 = CWT(x, 2\pi, voices, 'FFT') \leftarrow (modulus, waveRe, waveIm, scale)$

$w2 = CWT(y, 2\pi, voices, 'FFT') \leftarrow (modulus, waveRe, waveIm, scale)$

*% create the wavelet scales again*

$N = length(x);$

$scale = w1(scale);$  *% get a scale vector*

*% Calculate the cross wavelet phase*

**for**  $i \leftarrow 1$  **to**  $N$

**do**  $\left\{ \begin{array}{l} \text{for } j \leftarrow 1 \text{ to } length(scale) \\ \text{do } \left\{ \begin{array}{l} cosp_{i,j} = (w1(waveRe_{i,j}) * w2(waveRe_{i,j})) \\ \quad + (w1(waveIm_{i,j}) * w2(waveIm_{i,j})); \\ quad_{i,j} = (w1(waveIm_{i,j}) * w2(waveRe_{i,j})) \\ \quad (w1(waveRe_{i,j}) * w2(waveIm_{i,j})); \\ phase_{i,j} = atan2(quad_{i,j}, cosp_{i,j}); \end{array} \right. \end{array} \right.$

*% Get the phase variance and global power vectors*

**for**  $i \leftarrow 1$  **to**  $length(scale)$

**do**  $\left\{ \begin{array}{l} \text{for } j \leftarrow 1 \text{ to } N \\ \text{do } \left\{ \begin{array}{l} vector_j = phase_{i,j}; \\ P1_j = w1(modulus)_{i,j}; \\ P2_j = w2(modulus)_{i,j}; \end{array} \right. \\ phase\_variance_i = variance(vector) \text{ % variance vector}; \\ GP1_i = \sum P1 \text{ % global wavelet power spectrum for } x; \\ GP2_i = \sum P2 \text{ % global wavelet power spectrum for } y; \end{array} \right.$

*% calculate the CWPV for a specified scale range*

$CWPV = \sum phase\_variance[sx_1, \dots, sx_2];$

*% calculate the CWED for a specified scale range*

$CWED = Euclidean\_distance(GP1[sy_1, \dots, sy_2], GP2[sy_1, \dots, sy_2]);$

$CWS\_result = CWPV * CWED;$

**return**  $(CWS\_result, CWPV, CWED, voices, sx_1, sx_2, sy_1, sy_2)$

## 5.5 Conclusion

In this chapter the methodology for this thesis was presented. The last section provides some simple pseudo code that can be used to train and test the technique. In the following chapter a set of different experiments are done that helped develop the methodology presented here. It should be noted, however, that experiment one was based on the original version of the UCR time series data [4], while experiment two is performed on an ‘updated’ (z-normalised) version that became the new standard at some point during the finalising stages of this thesis [5].

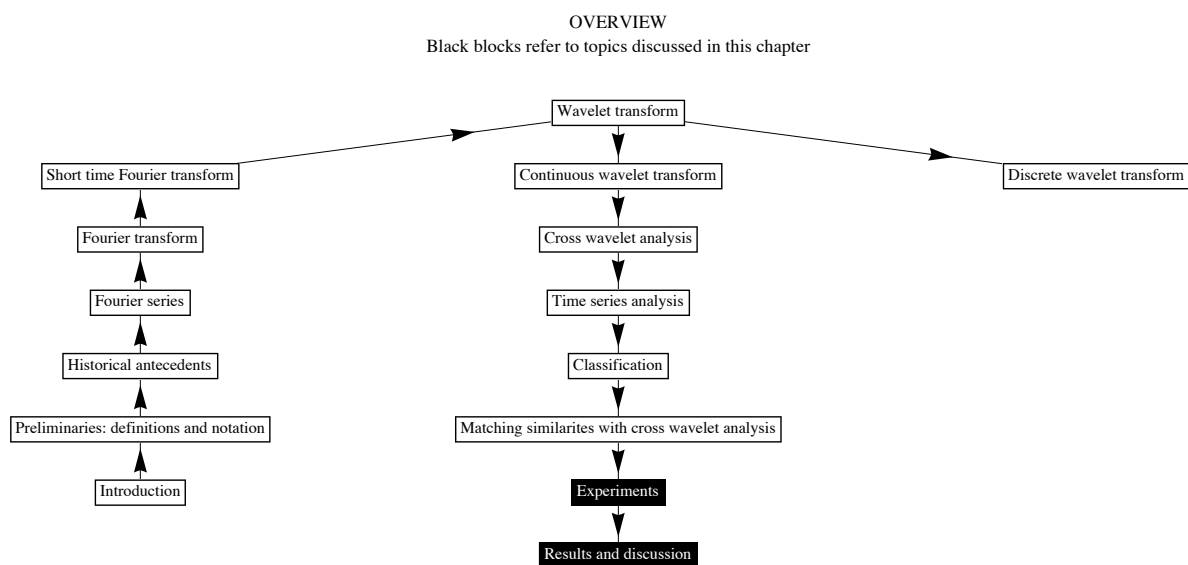


*"As in Mathematicks, so in Natural Philosophy, the investigation of difficult things by the method of analysis, ought ever to precede the method of composition. This analysis consists in making experiments and observations, and in drawing general conclusions from them by induction, and admitting of no objections against the conclusions, but such as are taken from experiments, or other certain Truths. For hypotheses are not to be regarded in experimental Philosophy"*

Isaac Newton (AD 1642-1727)

# 6

## Experiments, results, and discussion



## 6.1 Introduction

A problem with correlation-based approaches to classifying time series data, especially when using time-domain techniques, is the strong autocorrelation inherent in seasonal-based data. One of the main advantages of using a wavelet approach is that lead and lag times (phase differences) between time series become irrelevant in the classification experiment (but could be calculated for further analysis if needed). The strong autocorrelation problem is also partially overcome by assessing features over a broad range of wavelengths.

In this chapter, two experiments are performed. The first experiment was performed on 20 benchmark time-series classification problems from the University of California Riverside (UCR) [4] and the second on an updated set of 40 classification problems from the University of California Riverside (UCR) [5]. The first experiment was designed to test and improve upon the methodology presented in the previous chapter. The second experiment was done to include some newer classification problems that became available during the course of this study. It should be noted, however, that the newer UCR dataset [5] prescribes z-normalisation on all the data, and while the methodology in this thesis makes no explicit assumptions on the underlying data, it has been noted [233] that some of the problems from the original set were not z-normalised and this step does sometimes affect results using Euclidean based techniques. It is assumed that these data represent a good mix of classification problems to test the methodology on.

The UCR repository represents one of the most used publicly available ‘labelled’ time series databases in the world [207, 234]. The experiments presented here were designed to test both the skill (accuracy) of the methodology set out in Chapter 5, as well as the AM and FM characterisation abilities. In these experiments results are compared with other common techniques such as Euclidean distance, the Euclidean distance between FFT amplitude coefficients, and DTW. The second experiment compares CWS with Euclidean distance and DTW.

In the first experiment, several variations of the CWPV function were tested including combinations comprising the Euclidean distance between FFT amplitude coefficients

multiplied by the CWPV vector, as well as testing whether a re-ordering of variance coefficients from best to worst and summing different parts of the resulting vector would yield better results. The experiment was investigative, designed purely to test for accuracy gains using different variations. The analysis of the results became important in designing the methodological framework described in Chapter 5 and implemented in experiment two. It is noted, however, that while the analysis was carried out on the original dataset from the UCR repository, the assumptions were based on amplitude differences between classes prior to them being z-normalised in the new UCR repository [5].

In the second experiment, the aim was to test for an improvement in the skill of the methodology (described in Chapter 5), but also to test whether AM and FM characterisation could be described. Both the CWPV and CWED terms were used, and the results were compared. The results from the second experiment performed well and outperform those obtained in experiment one. In this experiment the parameters that varied were the central frequency ( $\omega_0 = 1\pi, 2\pi, \text{ or } 3\pi$ ) and voice resolution (between 1 and 7 to increase or decrease the amount of frequency content of the wavelet transform). Each classification problem was split into approximately two thirds for training and one third for testing. Stratified 10-fold cross-validation was done for both model training (parameterisation) and for model testing. Code listings for the methods are given in Appendix D (p. 249).

## 6.2 Data

The classification problems presented in Table 6.1 (p. 102) (from the original UCR database [4]) was used for the first experiment. A summary description of these datasets including class examples can be found in Appendix A (p. 143). The classification problems presented in Table 6.2 (p. 103) were used in experiment two where all data was z-normalised.

TABLE 6.1: Summary of the original UCR datasets [4] used for model testing and analysis in experiment one. Each dataset is divided into prescribed classes that can be used to verify the performance of a classifier.

Problem	Classes	Total Samples	Length	Training samples	test samples
Synthetic Control	6	600	60	300	300
Gun-Point	2	200	150	50	150
CBF	3	930	128	30	900
Face (all)	14	2250	131	560	1690
OSU Leaf	6	442	427	200	242
Swedish Leaf	15	1125	128	500	625
50words	50	905	270	450	455
Trace	4	200	275	100	100
Two Patterns	4	5000	128	1000	4000
Wafer	2	7174	152	1000	6174
Face (four)	4	112	350	24	88
Lightning-2	2	121	637	60	61
Lightning-7	7	133	319	70	73
ECG200	2	200	96	100	100
Adiac	37	781	176	390	391
Yoga	2	3300	426	300	3000
Fish	7	350	463	175	175
Beef	5	60	470	30	30
Coffee	2	56	286	28	28
OliveOil	4	60	570	30	30

### 6.3 Experiment one

In this experiment empirical results of different variations of the CWPV term (see Equation (5.2) (p. 86)) are reported using a Morlet wavelet basis function with central frequency of six and 20 voices per octave. The initial results for this experiment [6] (see attached paper in Appendix E (p. 289)), led to further exploration and development of the methodology presented in Chapter 5.

#### 6.3.1 Aim

The aim of this experiment was to empirically investigate if the classification results obtained could be improved by using different combinations of wavelet scales during the classification experiment, as well as different combinations of functions. Specifically, the experiment was designed not to characterise common behaviour, but rather to test

TABLE 6.2: Summary of updated UCR datasets [5] used in experiment two.

Problem	Classes	Total Samples	Length
Synthetic Control	6	600	60
Gun-Point	2	200	150
CBF	3	930	128
Face (all)	14	2250	131
OSU Leaf	6	442	427
Swedish Leaf	15	1125	128
50words	50	905	270
Trace	4	200	275
Two Patterns	4	5000	128
Wafer	2	7174	152
Face (four)	4	112	350
Lightning-2	2	121	637
Lightning-7	7	133	319
ECG	2	200	96
Adiac	37	781	176
Yoga	2	3300	426
Fish	7	350	463
Plane	7	210	144
Car	4	120	577
Beef	5	60	470
Coffee	2	56	286
OliveOil	4	60	570
CinC_ECG_torso	4	1420	1639
ChlorineConcentration	3	4307	166
DiatomSizeReduction	4	322	345
ECGFiveDays	2	884	136
FacesUCR	14	2250	131
Haptics	5	463	1092
InlineSkate	7	650	1882
ItalyPowerDemand	2	1096	24
MedicalImages	10	1141	99
MoteStrain	2	1272	84
SonyAIBORobot SurfaceII	2	980	65
SonyAIBORobot Surface	2	621	70
Symbols	6	1020	398
TwoLeadECG	2	1162	82
WordsSynonyms	25	905	270
Cricket_X	12	780	300
Cricket_Y	12	780	300
Cricket_Z	12	780	300

whether a selected set of scales whose variance of phase has better coherency (least variation) would yield better results when reported alone or combined with the Euclidean distance between FFT amplitudes to partially account for AM similarities.

### **6.3.2 Method**

The classification error rate in this experiment is taken as the miscalculation rate between the training and test set using the hold out method (see Chapter 4 for more information on the hold out method) on the predefined train and test splits that come with the UCR database (presented in Table 6.1 (p. 102)). The classification algorithm used is a  $k$ -NN algorithm which can be performed using the following pseudocode (slightly modified from [4]) :

**Algorithm 6.3.1:** PERFORMANCE(*train, test*)

```

train_class_labels = train(:,1); %class labels
train(:,1) = []; %remove class labels
test_class_labels = test(:,1); %class labels
test(:,1) = []; %remove class labels
correct = 0; %Initialise
for i ← 1 to length(test_class_labels)
    {
    predicted = CLASSIFY(train, train_class_labels, test(i,:));
    do {
        if predicted == test_class_labels(i)
            then {
                correct = correct + 1;
            }
    }
error = (length(test_class_labels) - correct)/length(test_class_labels);
return (error)

```

**Algorithm 6.3.2:** CLASSIFY(*train, train\_class\_labels, unknown\_object*)

```

best_so_far = inf;
predicted = null;
for i ← 1 to length(train_class_labels)
    {
    %here we use three CWPV variations for distance_function
    distance = distance_function(train(i,:), unknown_object)
    do {
        if distance < best_so_far
            then {
                predicted = train_class_labels(i);
                best_so_far = distance;
            }
    }
return (predicted)

```

In the above pseudocode the three CWPV variations were:

- **CWPV<sub>1</sub> (full)**, calculated using a default of eight octaves per classification problem and the results are the simple sum of all variance coefficients over all scales;
- **CWPV<sub>2</sub> (full)**, calculated using a default of seven octaves per classification problem, and multiplied by the Euclidean distance of FFT amplitude coefficients as a

first attempt to test whether combining AM and FM approaches would yield better results, and;

- $\text{CWPV}_2 (\frac{1}{2})$ , which is also calculated using a default of seven octaves and is also the product of the Euclidean distance of FFT amplitude coefficients and CWPV minima, but the variance coefficients were first ordered from lowest to highest and only the first half of the resulting curve was summed. The assumption is that these would represent better coherency within these scales than the entire set of variance coefficients. Figure 6.1 (p. 106) illustrates this variation. A problem with this approach, however, is that some discrepancies such as alias signals or low frequency cycles (one cycle or less) could also yield low variances, and as such are also often included in the calculation.

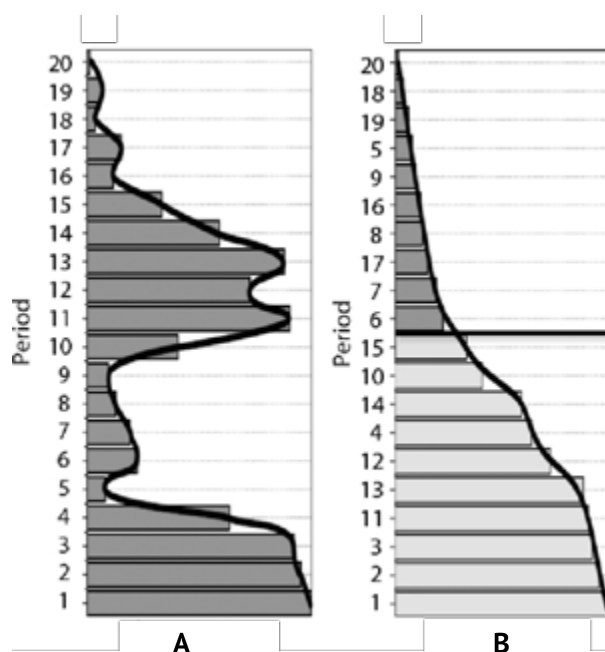


FIGURE 6.1: Ordered phase variance vector. The vector is represented as a bar-graph (A). By integrating over different frequency ranges the resulting value will emphasise either similarities or differences. B represents a reordered curve in which an arbitrary threshold (here  $\frac{1}{2}$ ) is chosen and summed, representing arbitrary combinations of scales without the ability to characterise according to frequency range.



### 6.3.3 Results

All the results are reported as time series that are assigned incorrect classification (errors) divided by the total number of time series in a classification dataset. Table 6.3 (p. 108) and Figure 6.2 (p. 109) present the results as a comparison between Euclidean distance, DTW, the Euclidean distance of FFT amplitude coefficients (FFT-A), and the best two variations of the CWPV approach in this experiment. Table 6.4 (p. 110) and Figure 6.3 (p. 111) provides more detailed comparison between the Euclidean distance of FFT amplitude coefficients and the three CWPV variations.

The results are partially intuitive; by focusing on the whole range of wavelengths when summing the phase variance, the metric is measuring both the similar and the dissimilar components of the time series that are being compared. By focusing on limited wavelength ranges however, it is more likely that the summed variance is reflecting either the similar or the dissimilar components of the time series compared. It is also clear from Table 6.4 (p. 110) that the CWPV<sub>2</sub> ( $\frac{1}{2}$ ) variation outperforms the other variations, suggesting that an approach which includes both AM and FM characteristics is required. The following examples are noted for analyses regarding performance, specifically Lightning 2 and 7, which in the case of FFT-A perform better and the same as the CWPV<sub>2</sub> ( $\frac{1}{2}$ ) approach, and Coffee and Beef which perform better for the CWPV<sub>1</sub> (full) approach. An overall discussion on the reasons for such performance is presented in the following section, which highlights the justification for further experimentation carried out in experiment two.

TABLE 6.3: Experiment one results. Ed stands for Euclidean distance, and FFT-A is the Euclidean distance of the FFT amplitude coefficients. DTW\_1 stands for dynamic time warping, DTW\_2 stands for dynamic time warping with the best warping window, and CWPV<sub>2</sub> (full) and CWPV<sub>2</sub> ( $\frac{1}{2}$ ) are two variations of the CWPV term. The best results are highlighted in bold.

Problem	Ed	DTW_1	DTW_2	FFT-A	CWPV <sub>2</sub> (full)	CWPV <sub>2</sub> ( $\frac{1}{2}$ )
Synthetic Control	0.120	0.120	<b>0.007</b>	0.397	0.150	0.100
Gun-Point	0.087	0.087	0.093	0.027	<b>0.013</b>	0.027
CBF	0.147	0.004	<b>0.003</b>	0.387	0.266	0.148
Face (all)	0.287	<b>0.192</b>	<b>0.192</b>	0.257	0.243	0.228
OSU Leaf	0.479	<b>0.384</b>	0.409	0.430	0.442	0.413
Swedish Leaf	0.211	0.157	0.210	0.147	<b>0.123</b>	0.144
50words	0.369	<b>0.242</b>	0.310	0.411	0.371	0.341
Trace	0.250	0.010	<b>0.000</b>	0.140	0.140	0.120
Two Patterns	0.094	0.002	<b>0.000</b>	0.496	0.457	0.280
Wafer	0.005	0.005	0.020	0.003	<b>0.002</b>	<b>0.002</b>
Face (four)	0.216	0.114	0.170	0.239	0.125	<b>0.068</b>
Lightning-2	0.246	<b>0.131</b>	<b>0.131</b>	0.148	0.213	0.230
Lightning-7	0.425	0.288	<b>0.274</b>	0.301	0.315	0.301
ECG	0.120	0.120	0.230	0.160	0.110	<b>0.100</b>
Adiac	0.389	0.391	0.396	0.263	0.263	<b>0.261</b>
Yoga	0.169	0.155	0.164	0.160	0.147	<b>0.140</b>
Fish	0.217	0.160	0.167	0.229	0.154	<b>0.131</b>
Beef	0.467	0.467	0.500	0.500	0.433	<b>0.367</b>
Coffee	0.250	0.179	0.179	0.357	0.214	<b>0.107</b>
OliveOil	<b>0.133</b>	0.167	<b>0.133</b>	0.200	0.233	<b>0.133</b>

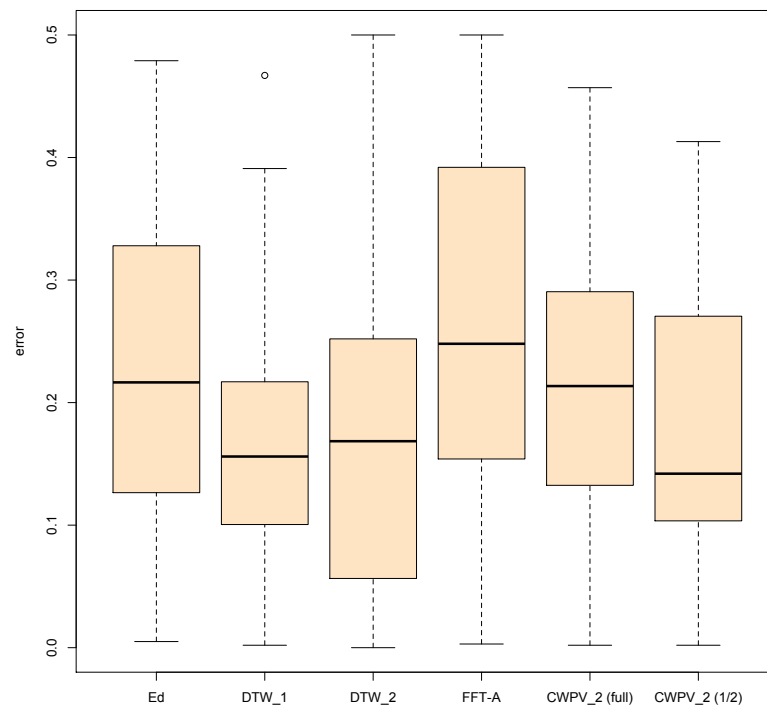


FIGURE 6.2: Box plot comparing techniques from experiment one presented in Table 6.3 (p. 108). The box plot shows the range, median and 25th and 75th percentiles for the errors from all classification problems in experiment one. Ed stands for Euclidean distance, and FFT-A is the Euclidean distance of the FFT amplitude coefficients. DTW\_1 stands for dynamic time warping, DTW\_2 stands for dynamic time warping with the best warping window, and CWPV<sub>2</sub> (full) and CWPV<sub>2</sub> ( $\frac{1}{2}$ ) are two variations of the CWPV term.

TABLE 6.4: CWPV variations comparison.  $CWPV_1$  (full) is the simple sum of the phase variance vector.  $CWPV_2$  (full) and  $CWPV_2 (\frac{1}{2})$  are both multiplied by the Euclidean distance of FFT amplitudes during classification, and FFT-A is simply the Euclidean distance of all FFT amplitude coefficients. Bold values represent the best error rate.

Problem	$CWPV_1$ (full)	$CWPV_2$ (full)	$CWPV_2 (\frac{1}{2})$	FFT-A
Synthetic Control	0.347	0.150	<b>0.100</b>	0.397
Gun-Point	0.093	<b>0.013</b>	0.027	0.027
CBF	0.402	0.266	<b>0.148</b>	0.387
Face (all)	0.256	0.243	<b>0.228</b>	0.257
OSU Leaf	0.583	0.442	<b>0.413</b>	0.430
Swedish Leaf	0.333	<b>0.123</b>	0.144	0.147
50words	0.525	<b>0.371</b>	<b>0.341</b>	0.411
Trace	0.400	0.140	<b>0.120</b>	0.140
Two Patterns	0.497	0.457	<b>0.280</b>	0.496
Wafer	0.005	<b>0.002</b>	<b>0.002</b>	0.003
Face (four)	0.080	0.125	<b>0.068</b>	0.239
Lightning-2	0.377	0.213	0.230	<b>0.148</b>
Lightning-7	0.616	0.315	<b>0.301</b>	<b>0.301</b>
ECG	0.140	0.110	<b>0.100</b>	0.160
Adiac	0.524	0.263	<b>0.261</b>	0.263
Yoga	0.191	0.147	<b>0.140</b>	0.160
Fish	0.217	0.154	<b>0.131</b>	0.229
Beef	<b>0.067</b>	0.433	0.367	0.500
Coffee	<b>0.071</b>	0.214	0.107	0.357
OliveOil	0.433	0.233	<b>0.133</b>	0.200

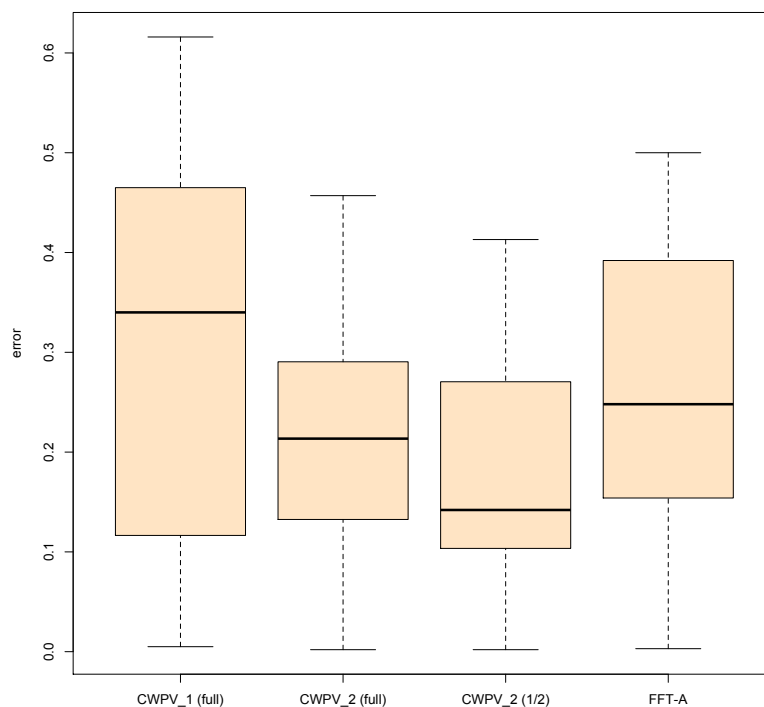


FIGURE 6.3: Box plot comparing CWPV variation results presented in Table 6.4 (p. 110). The box plot shows the range, median and 25th and 75th percentiles for the errors from all classification problems in experiment one. CWPV<sub>1</sub> (full) is the simple sum of the phase variance vector. CWPV<sub>2</sub> (full) and CWPV<sub>2</sub> ( $\frac{1}{2}$ ) are both multiplied by the Euclidean distance of FFT amplitudes during classification, and FFT-A is simply the Euclidean distance of all FFT amplitude coefficients.

### 6.3.4 Analysis and discussion

The first set of analyses were arbitrarily performed on the Coffee, Lightning 2, and Lightning 7 classification problems to see why the CWPV variations returned different errors for Coffee, but performed roughly the same for the Lightning 2 and 7 problems. In this analysis, scale ranges representing frequencies bands from high and low were isolated. Here, only the CWPV<sub>1</sub> variation was re-run on each of these scale ranges. The breakdown is presented in Figure 6.4 (p. 112), which presents the results as a ‘heat map’ representing class specific classification skill. In Figure 6.4 (p. 112) a zero error rate is represented by black and a 100% error rate as white. The scale range is presented as ‘1st quarter’ (high frequencies) down to ‘4th quarter’ (low frequencies) as sections of the variance vector. Although there is some overlap between frequency ranges because of

this breakdown, the relative range yielding the best error rate provides good insight into which frequencies best characterise the classification experiment in terms of the CWPV approach.

The Coffee dataset comprises two classes, such that if the relevant scales (frequency range) are pre-selected (using a minimum to maximum scale range), the accuracy of classification would be a 100%. In the case of Lightning 2 it would not matter which scales are selected as the  $CWPV_1$  variation cannot correctly classify the second class. The accuracy of classification on this problem therefore is a function of 100% correct classification for class 1 combined with some error for class 2. Similarly, for Lightning 7 the  $CWPV_1$  variation would only be able to correctly classify (within a pre-selected high frequency range) three of the seven classes.

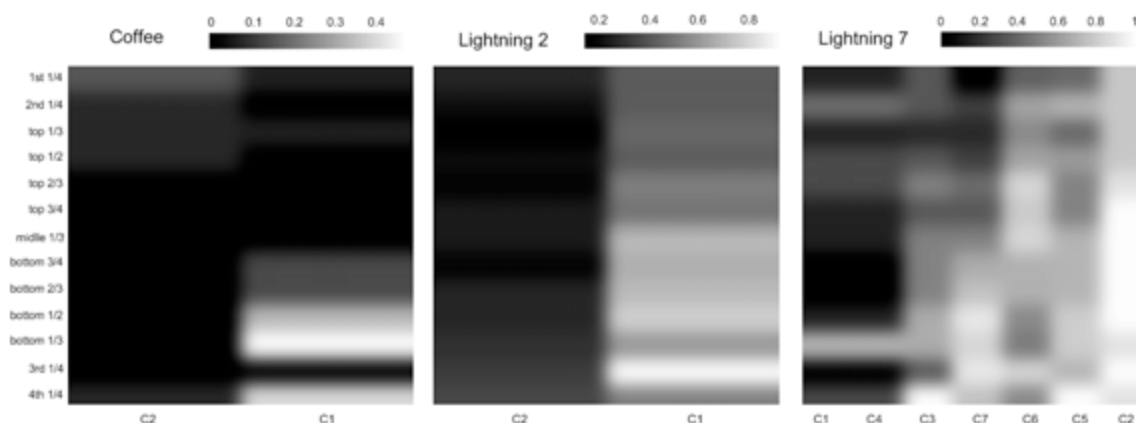


FIGURE 6.4: Analysis of Coffee, Lightning 2, and Lightning 7 classification problems. These results are run using the  $CWPV_1$  variation. The error is from zero error (black) to 100% error (white).

The analysis in Figure 6.4 (p. 112) suggests that the Coffee classification problem is most likely a FM problem defined by variation within a narrow mid-frequency range. To further expand, consider the four arbitrary time series presented in Figure 6.5 (p. 113) extracted from the Coffee dataset representing two time series from each class (coffee arabica and robusta [235]). A cross wavelet analysis shown in Figure 6.6 (p. 114) shows an almost identical power relationship (the domain of Euclidean distance), an indication that a pure AM similarity measure would not perform as well on this problem. Variance of phase, however, highlights slight discrepancies at particular wavelengths, and it is likely that the

summed variance of phase on these discrete scales would reflect either the similar or the dissimilar relationships of the dataset despite a virtually zero amplitude correlation.

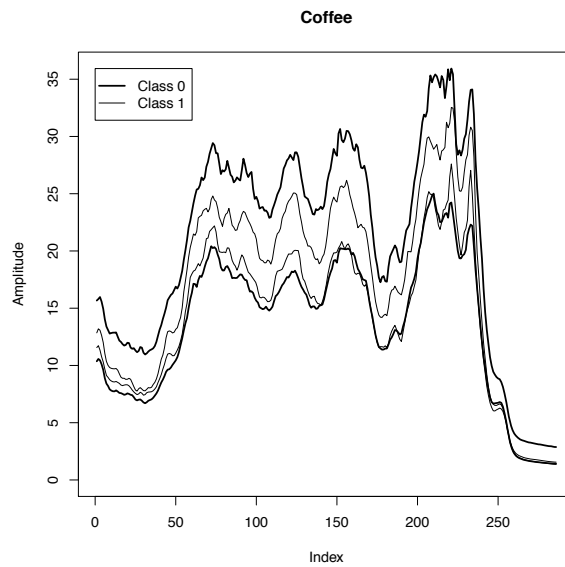


FIGURE 6.5: Coffee database classes. The above figure shows two classes, represented by four arbitrarily extracted time series from the Coffee dataset of the UCR time series classification database [4].

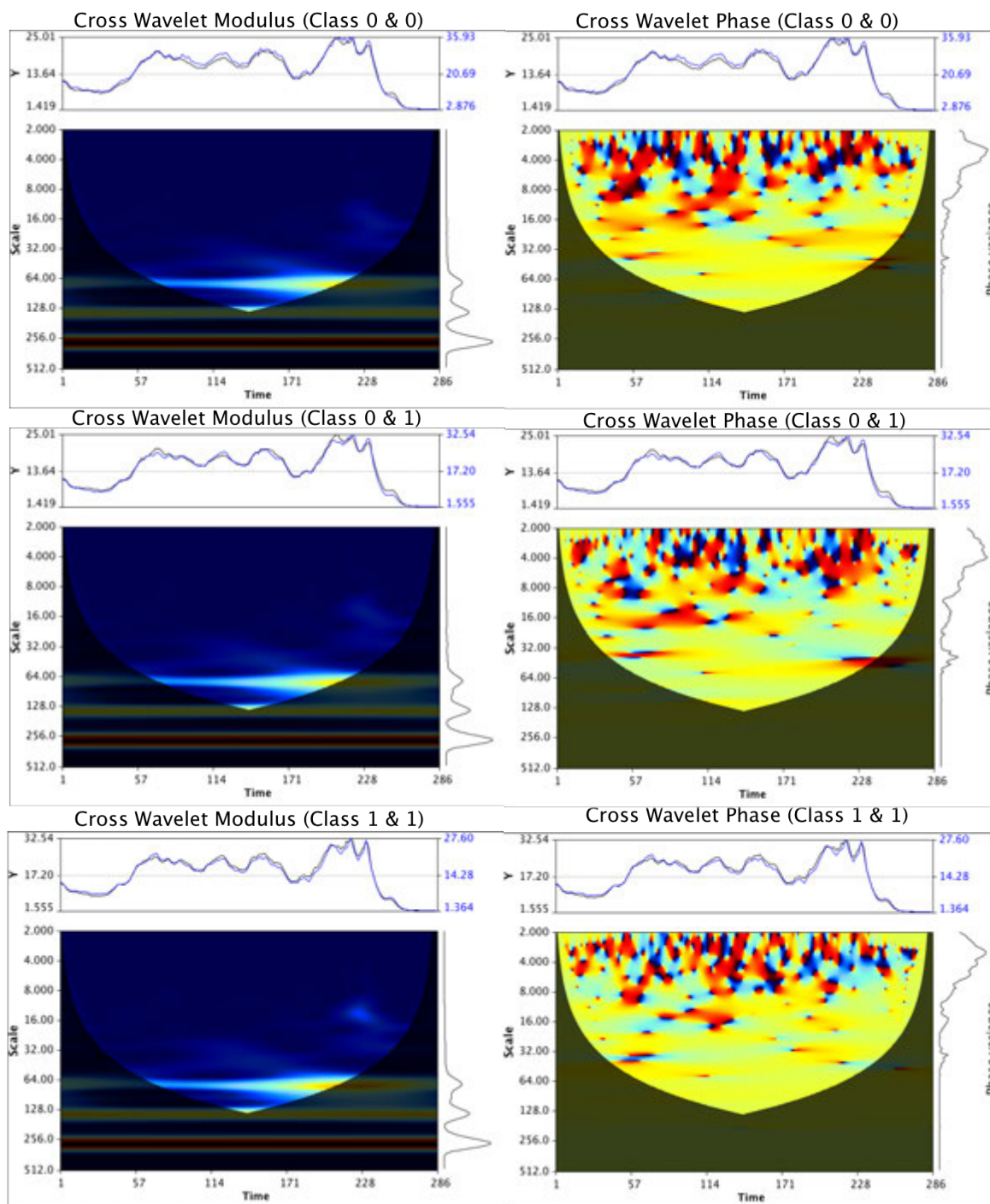


FIGURE 6.6: Cross wavelet modulus and CWPV of time series extracted from the Coffee database. Cross wavelet analysis (left) of the time series presented in Figure 6.5 indicates a similar power relationship, making it very difficult to separate the classes from each other. The phase variance vector (right) on the other hand, reveals discrepancies between the two classes, most pronounced between scales 8 to 64 (shown as a vector on the right hand side of the graphs). By using these features to describe the problem, the sum of the variance at those scales would provide a better similarity measure as opposed to focusing on the whole range of wavelengths, which would measure both the similar and the dissimilar components together.



It would seem likely, based on the results presented in Table 6.4 (p. 110) that Beef is also a FM problem characterised by a selected set of scales. Assuming that the CWPV<sub>1</sub> (full) is predominantly matching similarities in FM over a broad range of scales, the CWPV, CWED, and CWPV<sub>2</sub> terms were calculated for a series of discrete scale ranges to test how well the CWPV outperformed results obtained from the other two over the same scale range. The analysis was performed using a Morlet wavelet with  $\omega_0 = 2\pi$ .

The results are presented in Figure 6.7 (p. 116) as all possible ranges of scales between a minimum and maximum  $s$  (conceptually outlined in Figure 5.3 (p. 89)) and with all three terms returning results from these combinations (i.e. all methods used the same minimum to maximum ranges). This analysis was done using two voices per octave to reduce computation time. This is equivalent to 16 scales (8 octaves with 2 voices each) in total for both Beef and Coffee, which amounts to a permutation of 136 classifications per method per classification problem, giving a total of 816 analyses. It is clear that both Beef and Coffee are potentially characterised by FM for a specific frequency range (denoted in Figure 6.7 by  $S_{min}$  and  $S_{max}$ ) according to this methodology. In the Beef example, it seems that a pure AM approach is not suited at any scale and explains why all the other techniques in Table 6.3 (p. 108), which are amplitude based, perform so badly on this problem.

The second set of analysis in this experiment has an almost identical structure to the methodology presented in Chapter 5, and is largely responsible for the formulation of this methodology. In the second experiment, the approach is adopted to provide a comparison between AM and FM over different subsets of scales for all the classification problems.

## 6.4 Experiment two

In this experiment, empirical results are presented using the methodology described in Chapter 5, which takes into account the CWS and both the CWPV and CWED results. The experiment is performed on the newer version of the UCR time series classification data. The CWPV and CWED results are presented for comparative purposes. The basis function is the Morlet wavelet. Parameterisation during model training (sensitivity

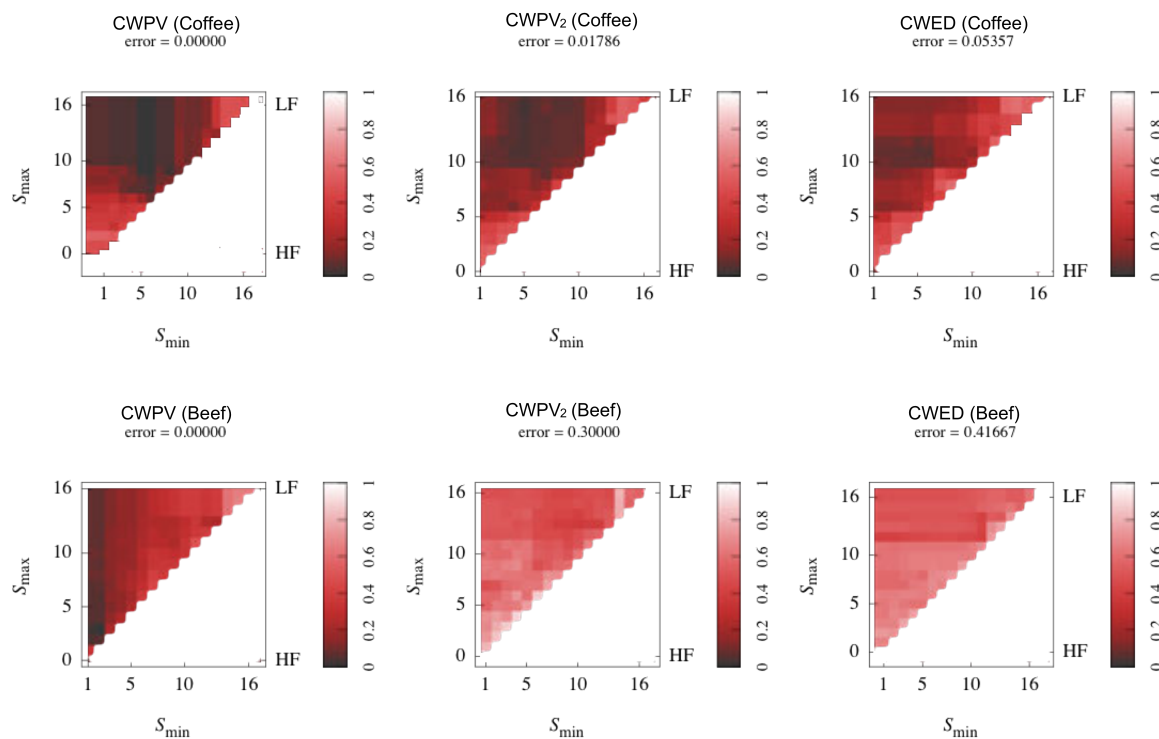


FIGURE 6.7: Detailed analysis of the Coffee and Beef classification problems. These results present all possible linear combinations of scales ranging between a minimum and maximum for the Coffee and Beef datasets. All three experiments used a Morlet wavelet with a central frequency  $\omega_0=2\pi$  and two voices per octave. The error in the above figure represents the best error rate. HF and LF denote "High frequency" and "Low frequency" ranges associated with the combinations of  $s_{min}$  and  $s_{max}$ . All three techniques do well for Coffee, with a zero error rate for the CWPV. Results for Beef show that this problem is characterised mainly by FM in the small wavelength range, as apposed to AM or a combination of FM and AM.

testing) was done using 10-fold cross-validation. The parameters included three central frequency variations ( $1\pi$ ,  $2\pi$ , and  $3\pi$ ) and seven voice resolutions (which ranged between 1 and 7) for each classification problem. Computation time starts to become a problem when using a higher number of scales with this approach, so voice resolution was used to test whether a small number of scales (by using fewer voices) would yield the same result. The features (wavelet scale ranges) that describe the AM and FM similarities were taken as the dominant scale set cluster for the CWPV and CWED terms as described in the methodology chapter.

### 6.4.1 Aim

The aim of this experiment was to empirically investigate if the classification results obtained could be improved through optimised parameterisation, and statistically test this using the error estimates derived from 10-fold cross-validation. The experiment is based on the methodology presented in Chapter 5. The approach takes a similar form to the final analysis performed in experiment one. Another objective of this experiment was to test whether the full characterisation of the classification problem could be achieved during the classification experiment.

### 6.4.2 Method

The classification error rate in this experiment is taken as the miscalculation rate between the training and test sets from the updated UCR database. The classification algorithm used is the  $k$ -NN algorithm. The method is exactly that described in Chapter 5 and code listings for this experiment are given in Appendix D (p. 249), which can be used to reproduce the experiment. The assumption is that previously un-normalised data should not have any meaningful effect on the results from the technique, but could result in different feature sets (CWPV and CWED scale sets) due to amplitude differences. The algorithm returns the best minimum and maximum ranges for  $s$  for both the CWPV and CWED terms. A further assumption is that AM and FM behaviour most often exist at different scales. The CWS results represent the best combination (product) of the CWPV and CWED terms produced during the classification experiment. The data was split into roughly two-thirds training and one-third testing. Stratified 10-fold cross validation was performed on the training data to parameterise the CWS, CWED and CWED terms according to voice resolution and the central frequency parameter.

### 6.4.3 Results

A summary of the training results is shown in Table 6.5 (p. 120) and compares Euclidean distance, DTW, CWS, CWPV and CWED. Figure 6.8 (p. 119) provides a

graphical comparison of the training errors. A more detailed mapping of all the parameters (central frequency and voice resolution combinations) that returned identical results is given in Appendix C (p. 237) for the CWS, CWPV and CWED terms, while the complete breakdown of all the parameters and training results for all the problems can be found in Appendix B (p. 156).

Table C.1 in Appendix C (p. 239) is structured to show a summary of all the parameters that yielded the best results for each problem. There are three parameter columns per technique which total nine parameter columns (CWS  $1\pi$ , CWS  $2\pi$ , CWS  $3\pi$ , CWPV  $1\pi$ , CWPV  $2\pi$ , CWPV  $3\pi$ , CWED  $1\pi$ , CWED  $2\pi$  and CWED  $3\pi$ ). In instances where more than one voice parameter returned the same train error – the value, voice number and scale ranges are given. Table C.1 (p. 239) provides a crucial lookup to select the parameters (central frequency, voice number and scale ranges) to use for model testing. As it was not possible to discriminate between identical train results, a detailed summary of the test results is also provided in the same format in Appendix C (p. 244) for comparative purposes. For both model training and testing 10-fold cross-validation was used.

The summary of the training results in Table 6.5 (p. 120) clearly show that the optimised CWS performs very well, and in some of the problems a minimum error is achieved using fewer voices (by decreasing scales over which to evaluate the classification, a decrease in the computation time also occurs).

In Table 6.6 (p. 121) with accompanying Figures (6.9–6.13) (p. 122–126), however, there is a decrease in the performance of the model possibly due to an over-fitting of the parameters during training. Due to multiple parameter ties during training the test results are summarised according to the min, 1st and 3rd quantiles, mean and max results obtained using all parameter ties (see Appendix C (p. 244) for a more complete breakdown). In some instances, where only one set of optimal parameters were returned during training only one test result is returned and the values ranging between min and max would be the same. Figure 6.9 (p. 126) includes this entire range of test results for the CWS, CWPV and CWED techniques.

Despite the reduction in model performance during testing, the results obtained using the CWS approach still seemingly outperform the other techniques over a wide range of

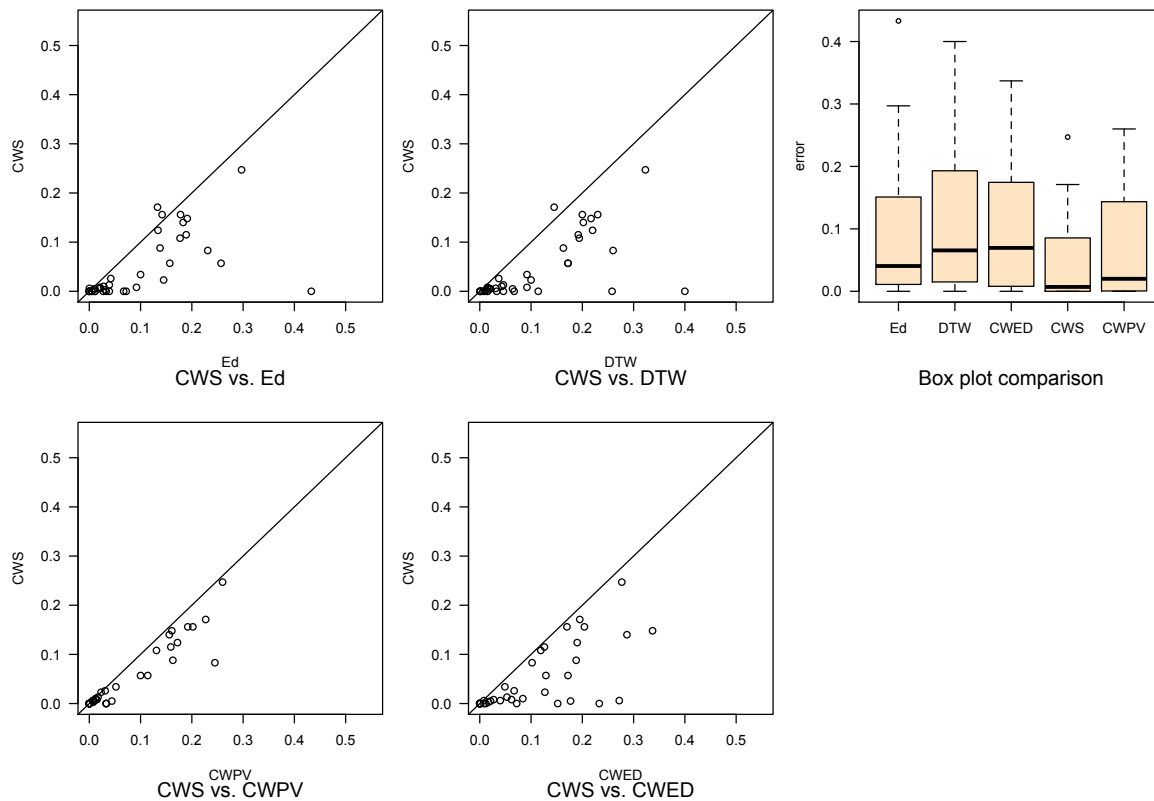


FIGURE 6.8: Box plot of UCR training results for experiment two comparing all techniques. The box plot shows the range, median and 25th and 75th percentiles of the training errors for all classification problems in experiment two. The training errors were calculated using 10-fold cross-validation. The CWS results have a narrower range. Values in the bottom right half for each scatter-plot means that CWS performs better.

time series classification problems. Overall, the CWS method performs the best for both model training and testing. In the next section some analysis regarding prediction versus performance, as well as an overall discussion of the results is provided.

TABLE 6.5: Summary of training results for experiment two. The results are according to the best combination of central frequency parameters ( $1\pi$ ,  $2\pi$ , and  $3\pi$ ) and voice resolutions (between 1–7) for the CWS, CWPV, and CWED techniques. The error rates are calculated as the mean value from 10-fold cross validation. Values in bold are the best error rate for each problem.

Problem	Ed	DTW	CWS	CWPV	CWED
Synthetic Control	0.010	0.064	<b>0.005</b>	0.044	0.177
Gun Point	0.039	0.046	<b>0.000</b>	<b>0.000</b>	0.008
CBF	<b>0.000</b>	0.006	<b>0.000</b>	<b>0.000</b>	0.152
Face (all)	0.039	0.046	<b>0.013</b>	0.017	0.053
OSU Leaf	0.189	0.192	<b>0.115</b>	0.159	0.126
Swedish Leaf	0.100	0.092	<b>0.034</b>	0.052	0.049
50words	0.191	0.217	<b>0.148</b>	0.161	0.337
Trace	<b>0.000</b>	0.258	<b>0.000</b>	0.033	<b>0.000</b>
Two Patterns	<b>0.000</b>	0.015	0.006	0.009	0.272
Wafer	0.011	0.001	<b>0.000</b>	<b>0.000</b>	0.001
Face (four)	0.072	0.114	<b>0.000</b>	<b>0.000</b>	0.072
Lightning2	0.157	0.172	<b>0.057</b>	0.114	0.129
Lightning7	0.138	0.163	<b>0.088</b>	0.163	0.188
ECG200	0.092	0.092	<b>0.008</b>	0.015	0.062
Adiac	0.177	0.194	<b>0.108</b>	0.131	0.119
Yoga	0.042	0.037	<b>0.026</b>	0.031	0.067
Fish	0.145	0.100	<b>0.023</b>	<b>0.023</b>	0.127
Plane	<b>0.000</b>	0.015	<b>0.000</b>	<b>0.000</b>	<b>0.000</b>
Car	0.257	0.172	<b>0.057</b>	0.100	0.172
Beef	0.433	0.400	<b>0.000</b>	0.033	0.233
Coffee	0.033	0.033	<b>0.000</b>	<b>0.000</b>	<b>0.000</b>
OliveOil	0.067	0.067	<b>0.000</b>	0.033	<b>0.000</b>
CinC_ECG_torso	0.011	0.001	<b>0.000</b>	<b>0.000</b>	0.001
ChlorineConcentration	0.019	0.018	<b>0.006</b>	0.007	0.008
DiatomSizeReduction	0.005	<b>0.000</b>	<b>0.000</b>	<b>0.000</b>	<b>0.000</b>
ECGFiveDays	0.005	0.010	<b>0.000</b>	<b>0.000</b>	<b>0.000</b>
FacesUCR	0.021	0.031	<b>0.006</b>	0.007	0.040
Haptics	0.297	0.323	<b>0.247</b>	0.260	0.277
InlineSkate	0.231	0.260	<b>0.083</b>	0.245	0.102
ItalyPowerDemand	0.021	0.015	<b>0.008</b>	0.013	0.027
MedicalImages	<b>0.133</b>	0.145	0.171	0.227	0.195
MoteStrain	0.028	0.043	<b>0.010</b>	0.012	0.084
SonyAIBORobot SurfaceII	0.031	0.012	<b>0.003</b>	0.008	0.017
SonyAIBORobot Surface	0.027	0.015	<b>0.000</b>	<b>0.000</b>	0.012
Symbols	0.011	0.021	<b>0.005</b>	0.008	0.021
TwoLeadECG	<b>0.000</b>	0.001	<b>0.000</b>	0.001	<b>0.000</b>
WordsSynonyms	0.183	0.202	<b>0.140</b>	0.156	0.287
Cricket_X	<b>0.142</b>	0.230	0.156	0.192	0.170
Cricket_Y	0.178	0.200	<b>0.156</b>	0.202	0.204
Cricket_Z	0.134	0.220	<b>0.124</b>	0.172	0.190

TABLE 6.6: Summary of model test results for experiment two. Due to multiple ties during model training, a summary of the results is presented. Mdn stands for median, m stands for mean and (n) is the number of unique results obtained for each experiment. The error rates were calculated using 10-fold cross-validation. Values in bold are the best error rate for each problem.

Problem	Ed	DTW	CWS	CWPV		CWED	
				(Min, 1st Qu., Mdn, m, 3rd Qu., max, (n))	(Min, 1st Qu., Mdn, m, 3rd Qu., max, (n))	(Min, 1st Qu., Mdn, m, 3rd Qu., max, (n))	(Min, 1st Qu., Mdn, m, 3rd Qu., max, (n))
Synthetic Control	0.115	<b>0.000</b>	0.045, 0.046, 0.048, 0.048, 0.049, 0.050 (2)	0.115, 0.119, 0.123, 0.123, 0.126, 0.130 (2)	0.205, 0.209, 0.213, 0.235, 0.239, 0.310 (4)	0.205, 0.209, 0.213, 0.235, 0.239, 0.310 (4)	
Gun Point	0.067	0.067	<b>0.000</b> , 0.013, 0.025, 0.029, 0.042, 0.067 (4)	0.017, 0.021, 0.025, 0.025, 0.029, 0.033 (2)	<b>0.000</b> , 0.017, 0.034, 0.034, 0.050, 0.067 (2)	<b>0.000</b> , 0.017, 0.034, 0.034, 0.050, 0.067 (2)	
CBF	0.003	0.003	<b>0.000</b> , 0.004, 0.008, 0.008, 0.012, 0.016 (6)	<b>0.000</b> , 0.002, 0.003, 0.003, 0.005, 0.006 (3)	0.194, 0.194, 0.194, 0.194, 0.194, 0.194 (1)	0.194, 0.194, 0.194, 0.194, 0.194, 0.194 (1)	
Face (all)	0.047	0.025	<b>0.007</b> , 0.009, 0.010, 0.010, 0.012, 0.013 (3)	0.010, 0.010, 0.010, 0.010, 0.010, 0.010 (1)	0.044, 0.044, 0.044, 0.044, 0.044, 0.044 (1)	0.044, 0.044, 0.044, 0.044, 0.044, 0.044 (1)	
OSU Leaf	0.225	<b>0.175</b>	0.188, 0.188, 0.188, 0.188, 0.188, 0.188 (1)	0.188, 0.194, 0.201, 0.201, 0.207, 0.213 (2)	0.206, 0.206, 0.206, 0.206, 0.206, 0.206 (1)	0.206, 0.206, 0.206, 0.206, 0.206, 0.206 (1)	
Swedish Leaf	0.141	0.121	<b>0.067</b> , <b>0.067</b> , <b>0.067</b> , <b>0.067</b> , <b>0.067</b> , <b>0.067</b> (1)	0.115, 0.117, 0.118, 0.118, 0.120, 0.121 (2)	0.080, 0.083, 0.085, 0.085, 0.088, 0.090 (2)	0.080, 0.083, 0.085, 0.085, 0.088, 0.090 (2)	
50words	0.091	0.137	<b>0.079</b> , <b>0.079</b> , <b>0.079</b> , <b>0.079</b> , <b>0.079</b> , <b>0.079</b> (1)	0.088, 0.088, 0.088, 0.088, 0.088, 0.088 (1)	0.184, 0.184, 0.184, 0.184, 0.184, 0.184 (1)	0.184, 0.184, 0.184, 0.184, 0.184, 0.184 (1)	
Trace	0.172	<b>0.000</b>	<b>0.000</b> , 0.007, 0.014, 0.033, 0.050, 0.086 (3)	0.143, 0.143, 0.143, 0.143, 0.143, 0.143 (1)	<b>0.000</b> , 0.043, 0.086, 0.076, 0.115, 0.143 (3)	<b>0.000</b> , 0.043, 0.086, 0.076, 0.115, 0.143 (3)	
Two Patterns	0.038	<b>0.000</b>	0.018, 0.019, 0.021, 0.021, 0.022, 0.023 (2)	0.020, 0.021, 0.022, 0.022, 0.022, 0.023 (2)	0.300, 0.300, 0.300, 0.300, 0.300, 0.300 (1)	0.300, 0.300, 0.300, 0.300, 0.300, 0.300 (1)	
Wafer	<b>0.000</b>	<b>0.000</b>	<b>0.000</b> , <b>0.000</b> , <b>0.000</b> , <b>0.000</b> , <b>0.000</b> , <b>0.000</b> (1)	<b>0.000</b> , <b>0.000</b> , <b>0.000</b> , <b>0.000</b> , <b>0.000</b> , <b>0.000</b> (1)	<b>0.000</b> , <b>0.000</b> , <b>0.000</b> , <b>0.000</b> , <b>0.000</b> , <b>0.000</b> (1)	<b>0.000</b> , <b>0.000</b> , <b>0.000</b> , <b>0.000</b> , <b>0.000</b> , <b>0.000</b> (1)	
Face (four)	0.100	0.100	<b>0.000</b> , 0.019, 0.038, 0.044, 0.063, 0.100 (4)	<b>0.000</b> , 0.013, 0.025, 0.050, 0.075, 0.125 (3)	0.025, 0.050, 0.075, 0.067, 0.088, 0.100 (3)	0.025, 0.050, 0.075, 0.067, 0.088, 0.100 (3)	
Lightning2	0.225	<b>0.125</b>	0.225, 0.244, 0.263, 0.275, 0.294, 0.350 (4)	0.225, 0.225, 0.225, 0.225, 0.225, 0.225 (1)	0.150, 0.200, 0.225, 0.225, 0.225, 0.250, 0.300 (5)	0.150, 0.200, 0.225, 0.225, 0.225, 0.250, 0.300 (5)	
Lightning7	0.220	<b>0.160</b>	0.240, 0.240, 0.240, 0.240, 0.240, 0.240 (1)	0.200, 0.225, 0.250, 0.250, 0.275, 0.300 (6)	0.320, 0.320, 0.320, 0.320, 0.320, 0.320 (1)	0.320, 0.320, 0.320, 0.320, 0.320, 0.320 (1)	
ECG200	<b>0.017</b>	0.033	<b>0.017</b> , 0.021, 0.025, 0.025, 0.029, 0.033 (2)	<b>0.017</b> , <b>0.017</b> , <b>0.017</b> , <b>0.017</b> , <b>0.017</b> , <b>0.017</b> (1)	0.033, 0.033, 0.033, 0.033, 0.033, 0.033 (1)	0.033, 0.033, 0.033, 0.033, 0.033, 0.033 (1)	
Adiac	0.213	0.213	<b>0.150</b> , 0.151, 0.152, 0.152, 0.152, 0.153 (2)	0.167, 0.168, 0.169, 0.169, 0.169, 0.170 (2)	0.167, 0.167, 0.167, 0.167, 0.167, 0.167 (1)	0.167, 0.167, 0.167, 0.167, 0.167, 0.167 (1)	
Yoga	0.082	0.075	<b>0.056</b> , 0.060, 0.063, 0.061, 0.064, 0.064 (3)	0.065, 0.065, 0.065, 0.065, 0.065 (1)	0.126, 0.126, 0.126, 0.126, 0.126, 0.126 (1)	0.126, 0.126, 0.126, 0.126, 0.126, 0.126 (1)	
Fish	0.100	0.175	<b>0.058</b> , 0.060, 0.063, 0.063, 0.065, 0.067 (2)	<b>0.058</b> , 0.060, 0.063, 0.063, 0.065, 0.067 (2)	0.117, 0.117, 0.117, 0.117, 0.117, 0.117 (1)	0.117, 0.117, 0.117, 0.117, 0.117, 0.117 (1)	
Plane	<b>0.000</b>	<b>0.000</b>	<b>0.000</b> , 0.004, 0.007, 0.007, 0.011, 0.014 (2)	<b>0.000</b> , 0.007, 0.014, 0.014, 0.022, 0.029 (3)	<b>0.000</b> , 0.011, 0.022, 0.029, 0.040, 0.072 (4)	<b>0.000</b> , 0.011, 0.022, 0.029, 0.040, 0.072 (4)	
Car	<b>0.125</b>	0.200	0.150, 0.156, 0.163, 0.163, 0.169, 0.175 (2)	0.150, 0.150, 0.150, 0.150, 0.150, 0.150 (1)	0.250, 0.250, 0.250, 0.250, 0.250, 0.250 (1)	0.250, 0.250, 0.250, 0.250, 0.250, 0.250 (1)	
Beef	0.350	0.350	0.150, 0.150, 0.150, 0.150, 0.150, 0.150 (1)	0.150, 0.163, 0.175, 0.175, 0.188, 0.200 (2)	<b>0.100</b> , 0.250, 0.325, 0.288, 0.363, 0.400 (4)	<b>0.100</b> , 0.250, 0.325, 0.288, 0.363, 0.400 (4)	
Coffee	<b>0.000</b>	0.050	<b>0.000</b> , 0.025, 0.050, 0.067, 0.100, 0.150 (3)	<b>0.000</b> , 0.025, 0.050, 0.067, 0.100, 0.150 (3)	0.150, 0.175, 0.200, 0.200, 0.225, 0.250 (3)	0.150, 0.175, 0.200, 0.200, 0.225, 0.250 (3)	
OliveOil	<b>0.100</b>	0.150	<b>0.100</b> , 0.138, 0.175, 0.188, 0.225, 0.300 (4)	<b>0.100</b> , 0.125, 0.150, 0.167, 0.200, 0.250 (3)	<b>0.000</b> , <b>0.000</b> , <b>0.000</b> , <b>0.000</b> , <b>0.000</b> , <b>0.000</b> (1)	<b>0.000</b> , <b>0.000</b> , <b>0.000</b> , <b>0.000</b> , <b>0.000</b> , <b>0.000</b> (1)	
Cin_C_ECG_torso	0.006	0.041	<b>0.000</b> , 0.001, 0.002, 0.002, 0.003, 0.004 (3)	<b>0.000</b> , 0.000, <b>0.000</b> , <b>0.000</b> , <b>0.000</b> , <b>0.000</b> (1)	0.031, 0.031, 0.031, 0.031, 0.031, 0.031 (1)	0.031, 0.031, 0.031, 0.031, 0.031, 0.031 (1)	
ChlorineConcentration	<b>0.029</b>	<b>0.029</b>	0.030, 0.030, 0.030, 0.030, 0.030, 0.030 (1)	0.002, 0.002, 0.004, 0.004, 0.006, 0.008 (2)	<b>0.000</b> , <b>0.000</b> , <b>0.000</b> , <b>0.000</b> , <b>0.000</b> , <b>0.000</b> (1)	<b>0.000</b> , <b>0.000</b> , <b>0.000</b> , <b>0.000</b> , <b>0.000</b> , <b>0.000</b> (1)	
DiatomSizeReduction	<b>0.000</b>	<b>0.000</b>	<b>0.000</b> , 0.002, 0.004, 0.004, 0.006, 0.008 (2)	0.007, 0.012, 0.017, 0.017, 0.023, 0.027 (7)	<b>0.000</b> , 0.006, 0.016, 0.015, 0.020, 0.034 (6)	<b>0.000</b> , 0.006, 0.016, 0.015, 0.020, 0.034 (6)	
ECGFiveDays	0.021	0.014	<b>0.000</b> , 0.004, 0.009, 0.009, 0.013, 0.017 (6)	<b>0.010</b> , <b>0.010</b> , <b>0.010</b> , <b>0.010</b> , <b>0.010</b> , <b>0.010</b> (1)	0.037, 0.037, 0.037, 0.037, 0.037, 0.037 (1)	0.037, 0.037, 0.037, 0.037, 0.037, 0.037 (1)	
FacesUCR	0.039	0.025	0.011, 0.011, 0.012, 0.012, 0.012, 0.012 (2)	0.333, 0.333, 0.333, 0.333, 0.333, 0.333 (1)	0.300, 0.320, 0.340, 0.349, 0.374, 0.407 (3)	0.300, 0.320, 0.340, 0.349, 0.374, 0.407 (3)	
Haptics	<b>0.280</b>	0.320	0.300, 0.300, 0.300, 0.300, 0.300, 0.300 (1)	0.296, 0.298, 0.300, 0.302, 0.305, 0.309 (3)	0.155, 0.155, 0.155, 0.155, 0.155, 0.155 (1)	0.155, 0.155, 0.155, 0.155, 0.155, 0.155 (1)	
InlineSkate	0.277	0.286	<b>0.123</b> , <b>0.123</b> , <b>0.123</b> , <b>0.123</b> , <b>0.123</b> , <b>0.123</b> (1)	0.033, 0.040, 0.047, 0.045, 0.052, 0.056 (3)	0.050, 0.052, 0.053, 0.053, 0.055, 0.056 (2)	0.050, 0.052, 0.053, 0.053, 0.055, 0.056 (2)	
ItalyPowerDemand	<b>0.022</b>	0.036	0.036, 0.038, 0.039, 0.039, 0.041, 0.042 (2)	0.083, 0.083, 0.083, 0.083, 0.083, 0.083 (1)	0.076, 0.076, 0.076, 0.076, 0.076, 0.076 (1)	0.076, 0.076, 0.076, 0.076, 0.076, 0.076 (1)	
MedicalImages	0.067	<b>0.060</b>	0.074, 0.074, 0.074, 0.074, 0.074, 0.074 (1)	0.012, 0.013, 0.013, 0.013, 0.014, 0.014 (2)	0.076, 0.076, 0.076, 0.076, 0.076, 0.076 (1)	0.076, 0.076, 0.076, 0.076, 0.076, 0.076 (1)	
MoteStrain	0.045	0.041	<b>0.007</b> , 0.008, 0.010, 0.010, 0.011, 0.012 (2)	0.041, 0.042, 0.043, 0.043, 0.043, 0.044 (2)	0.076, 0.076, 0.076, 0.076, 0.076, 0.076 (1)	0.076, 0.076, 0.076, 0.076, 0.076, 0.076 (1)	
SonyAIBORobot SurfaceII	0.044	0.075	<b>0.038</b> , 0.040, 0.044, 0.046, 0.050, 0.059 (4)	0.015, 0.015, 0.015, 0.015, 0.015, 0.015 (1)	0.053, 0.053, 0.053, 0.053, 0.053, 0.053 (1)	0.053, 0.053, 0.053, 0.053, 0.053, 0.053 (1)	
SonyAIBORobot Surface	0.020	0.040	<b>0.005</b> , 0.010, 0.015, 0.015, 0.020, 0.025 (5)	0.026, 0.026, 0.026, 0.026, 0.026, 0.026 (1)	0.047, 0.048, 0.049, 0.049, 0.049, 0.050 (2)	0.047, 0.048, 0.049, 0.049, 0.049, 0.050 (2)	
Symbols	0.020	<b>0.012</b>	0.029, 0.029, 0.029, 0.029, 0.029, 0.029 (1)	0.008, 0.009, 0.009, 0.009, 0.010, 0.010 (2)	0.015, 0.015, 0.015, 0.015, 0.015, 0.015 (1)	0.015, 0.015, 0.015, 0.015, 0.015, 0.015 (1)	
TwoLeadECG	0.008	<b>0.000</b>	0.003, 0.005, 0.007, 0.007, 0.009, 0.013 (4)	0.008, 0.009, 0.009, 0.009, 0.010, 0.010 (2)	0.015, 0.015, 0.015, 0.015, 0.015, 0.015 (1)	0.015, 0.015, 0.015, 0.015, 0.015, 0.015 (1)	
WordsSynonyms	<b>0.052</b>	0.088	0.055, 0.055, 0.055, 0.055, 0.055, 0.055 (1)	0.057, 0.057, 0.057, 0.057, 0.057, 0.057 (1)	0.164, 0.164, 0.164, 0.164, 0.164, 0.164 (1)	0.164, 0.164, 0.164, 0.164, 0.164, 0.164 (1)	
Cricket_X	0.307	<b>0.152</b>	0.204, 0.207, 0.210, 0.210, 0.212, 0.215 (2)	0.266, 0.266, 0.266, 0.266, 0.266, 0.266 (1)	0.226, 0.226, 0.226, 0.226, 0.226, 0.226 (1)	0.226, 0.226, 0.226, 0.226, 0.226, 0.226 (1)	
Cricket_Y	0.274	<b>0.174</b>	0.207, 0.207, 0.207, 0.207, 0.207, 0.207 (1)	0.281, 0.281, 0.281, 0.281, 0.281, 0.281 (1)	0.222, 0.222, 0.222, 0.222, 0.222, 0.222 (1)	0.222, 0.222, 0.222, 0.222, 0.222, 0.222 (1)	
Cricket_Z	0.237	0.170	<b>0.159</b> , <b>0.159</b> , <b>0.159</b> , <b>0.159</b> , <b>0.159</b> , <b>0.159</b> (1)	0.170, 0.177, 0.183, 0.183, 0.190, 0.196 (2)	0.359, 0.359, 0.359, 0.359, 0.359, 0.359 (1)	0.359, 0.359, 0.359, 0.359, 0.359, 0.359 (1)	

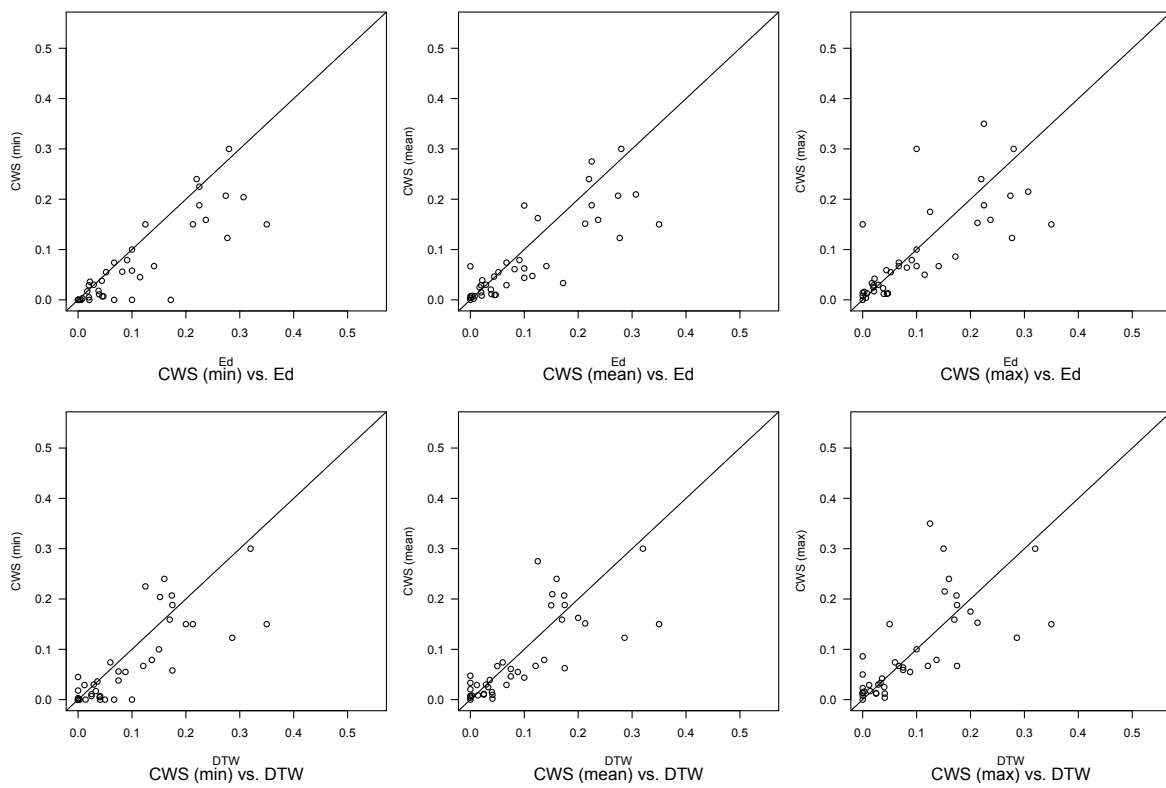


FIGURE 6.9: UCR experiment two model test results comparing CWS against Euclidean distance and DTW. The errors were calculated using 10-fold cross-validation. Values in the bottom right half for each scatter-plot means that CWS performs better. Due to multiple ties during model training the min, mean, and max model results relating to the best set of training parameters are shown.



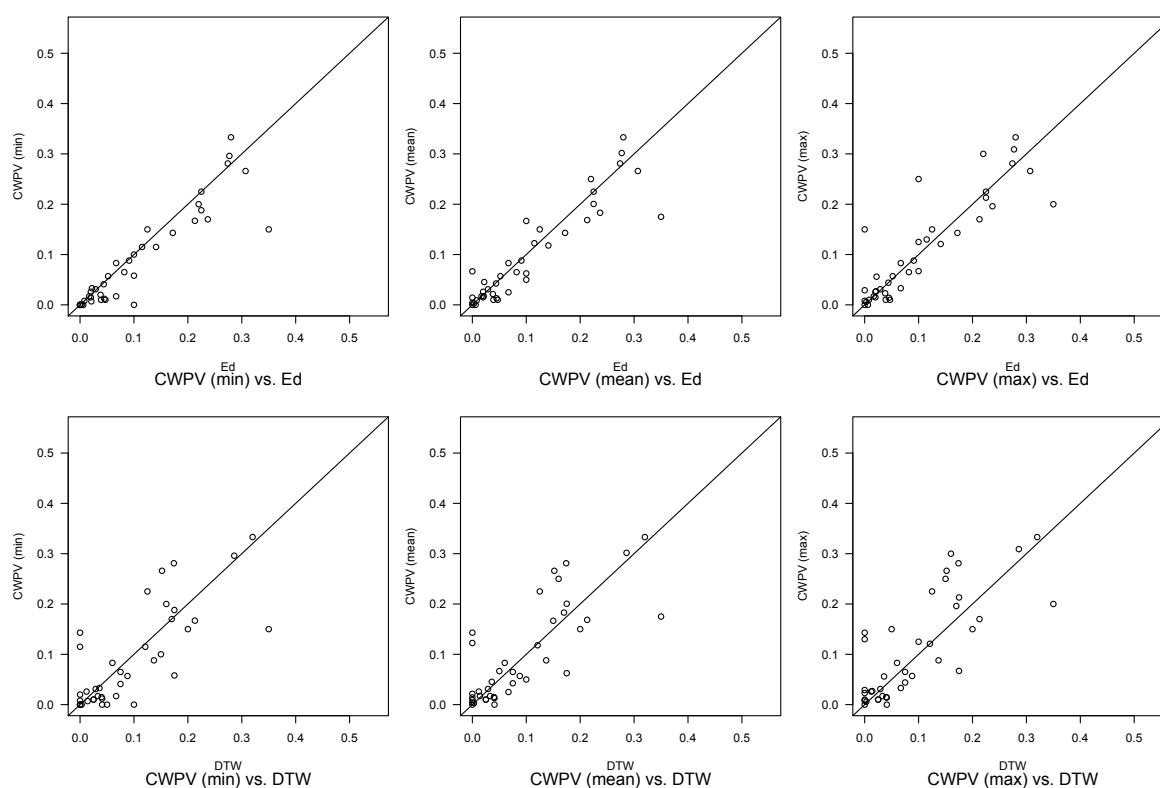


FIGURE 6.10: UCR experiment two model test results comparing CWPV against Euclidean distance and DTW. The errors were calculated using 10-fold cross-validation. Values in the bottom right half for each scatter-plot means that CWPV performs better. Due to multiple ties during model training the min, mean, and max model results relating to the best set of training parameters are shown.

#### 6.4.4 Analysis and discussion

Figure 6.14 (p. 127) shows a comparison between training results and test results for the various techniques, where the variability in test results for the CWS, CWPV and CWED techniques is clear. In general, Euclidean distance had an average of 12% loss in performance, while DTW had a 14% increase in performance. CWS had an average loss in performance that ranged between 36–52%. CPWV had an average loss in performance that ranged between 25–39%, and CWED had an average loss in performance that ranged between 11–31%.

In Figures 6.15–6.17 (p. 128–130) a breakdown analysis comparing of all the train and test results for Wafer, Olive Oil and Lightning 2 problems are shown. These problems represent some of the extremes in model results – Wafer had no variability in test results

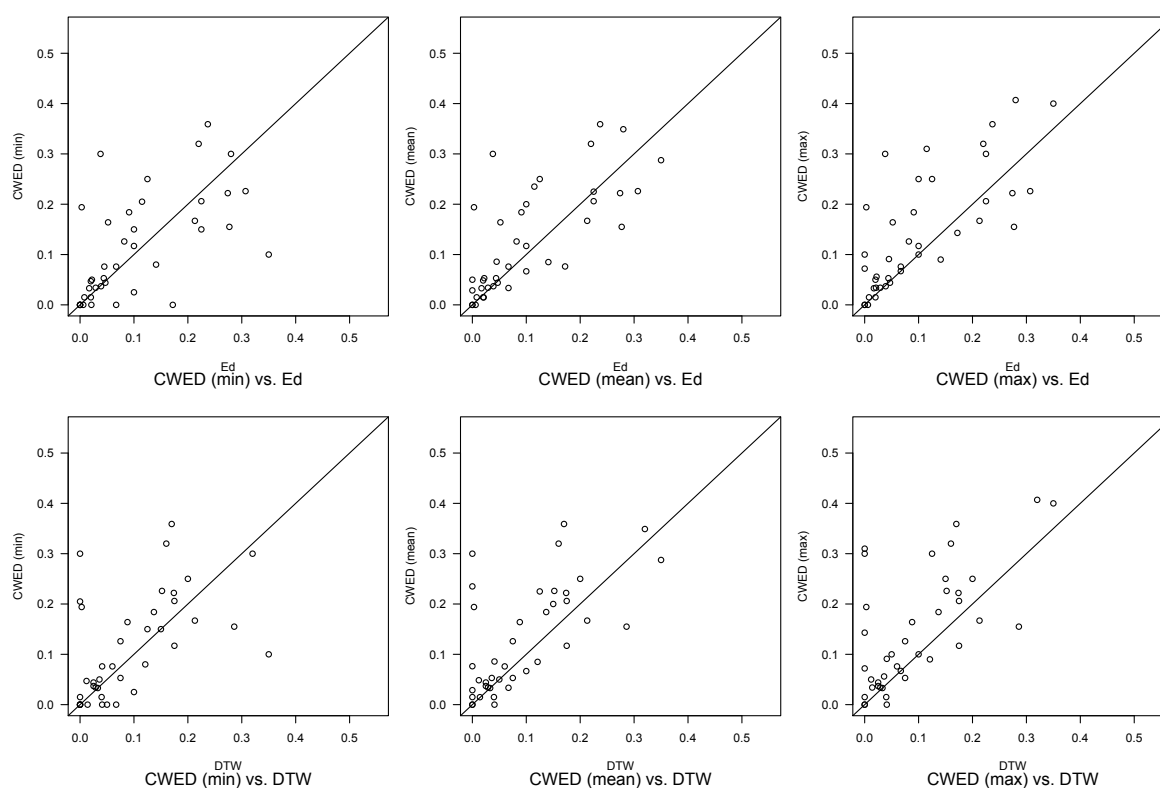


FIGURE 6.11: UCR experiment two model test results comparing CWED against Euclidean distance and DTW. The errors were calculated using 10-fold cross-validation. Values in the bottom right half for each scatter-plot means that CWED performs better. Due to multiple ties during model training the min, mean, and max model results relating to the best set of training parameters are shown.

(all the results were zero) and only slight variability in the train results for the CWED term (or AM features), Olive oil had the most variability in test results (see position 22 in Figure 6.14 (p. 127)), and Lightning 2 had the worst test results (see position 12 in Figure 6.14 (p. 127) for example). While all the train and test results for all the parameter options are shown in these examples, not all of them are valid according to the optimised training parameters. Here, these problems returned a high number of possible test options. In the case of CWS, test options for Wafer were  $1\pi$  [1–7 voices],  $2\pi$  [2–7 voices], and  $3\pi$  [2–7 voices]; for Olive oil the test options were  $1\pi$  [1–7 voices],  $2\pi$  [2–7 voices], and  $3\pi$  [7,6,5,1 voices]; and for Lightning 2 the test options were  $2\pi$  [6–7 voices], and  $3\pi$  [5–7 voices] (see Appendix C (p. 237) for the mapping of the CWPV and CWED terms). In each figure the top three plots represent the training breakdown and the bottom three are the test breakdown.

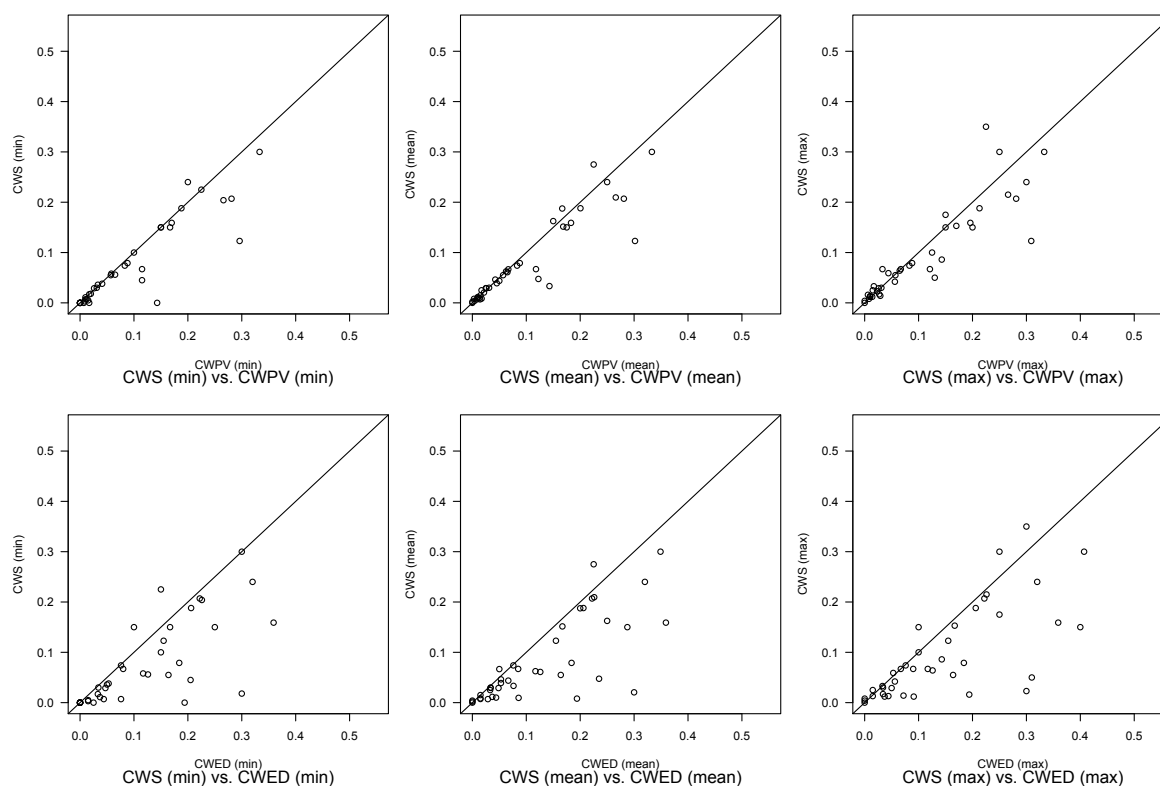


FIGURE 6.12: UCR experiment two model test results comparing CWS, CWPV and CWED. The errors were calculated using 10-fold cross-validation. Values in the bottom right half for each scatter-plot means that CWS performs better. Due to multiple ties during model training the min, mean, and max model results relating to the best set of training parameters are shown.

The Wafer example in Figure 6.15 (p. 128) is fairly easy to interpret – as the central frequency parameter  $\omega_0$  increases, so too does the frequency range (number and position of voices or scales) of the CWED term during training (the top three plots). On the other hand, the entire frequency range was used for the CWPV and CWS techniques. The test results (bottom three plots) are slightly better than the train results when the CWED term is considered in the analysis. Overall, this type of problem seems to have an equal contribution of AM and FM, with a slight bias towards the higher frequency range for the CWED (or AM) scale ranges.

The Olive Oil example in Figure 6.16 (p. 129) is not as easy to interpret. There seems to be an extremely small set of high frequency scales that were used to optimise the CWED term during training (top three plots), which seems to get larger as the central frequency parameter  $\omega_0$  increases. This makes sense, as a higher  $\omega_0$  value means better frequency

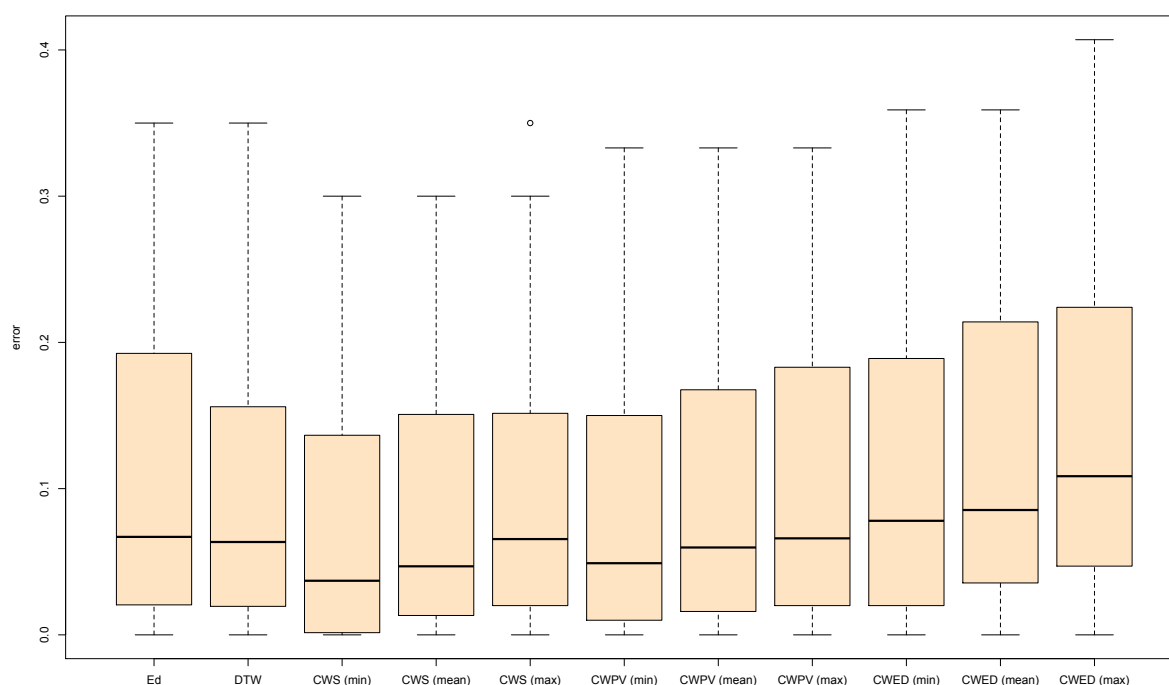


FIGURE 6.13: Box plot of UCR experiment two model test results comparing all techniques. The box plot shows the range, median and 25th and 75th percentiles of the model test errors for all classification problems in experiment two. The errors were calculated using 10-fold cross-validation. The CWS results have a narrower range and smaller median. Due to multiple ties during model training the min, mean, and max model results relating to the best set of training parameters are shown.

localisation and a lower value means better time localisation. This is evident as CWED performs better using  $1\pi$  and worse as  $\omega_0$  increase and *vice versa* for the CWPV technique (This is generally true for most of the problems – see Appendix B (p. 156) for examples). The opposite seems to occur in the test results (the bottom three plots), however, which doesn't make sense and possibly attributable to random test results. Overall, there is a decrease in performance between training and testing and the only realistic conclusion to draw from the analysis of this problem is that the test results are fairly random (this is most likely due to a small number of test samples used in the 10-fold cross-validation during testing). It is unlikely that the method will be able to classify this problem under different circumstances.

The Lightning 2 example in Figure 6.17 (p. 130) is easier to interpret than the Olive Oil problem. In both training and test results the CWS, CWPV and CWED techniques

performed relatively the same, with a slight decrease in performance during testing. The performance difference between training and testing is explicit as detailed analysis was carried out at the end of experiment one. From the analysis in experiment one, It is likely that the optimal parameters were chosen according to those that 'randomly' classified the second class correctly, whereas during testing the method was not able to classify the second class regardless of scale range.

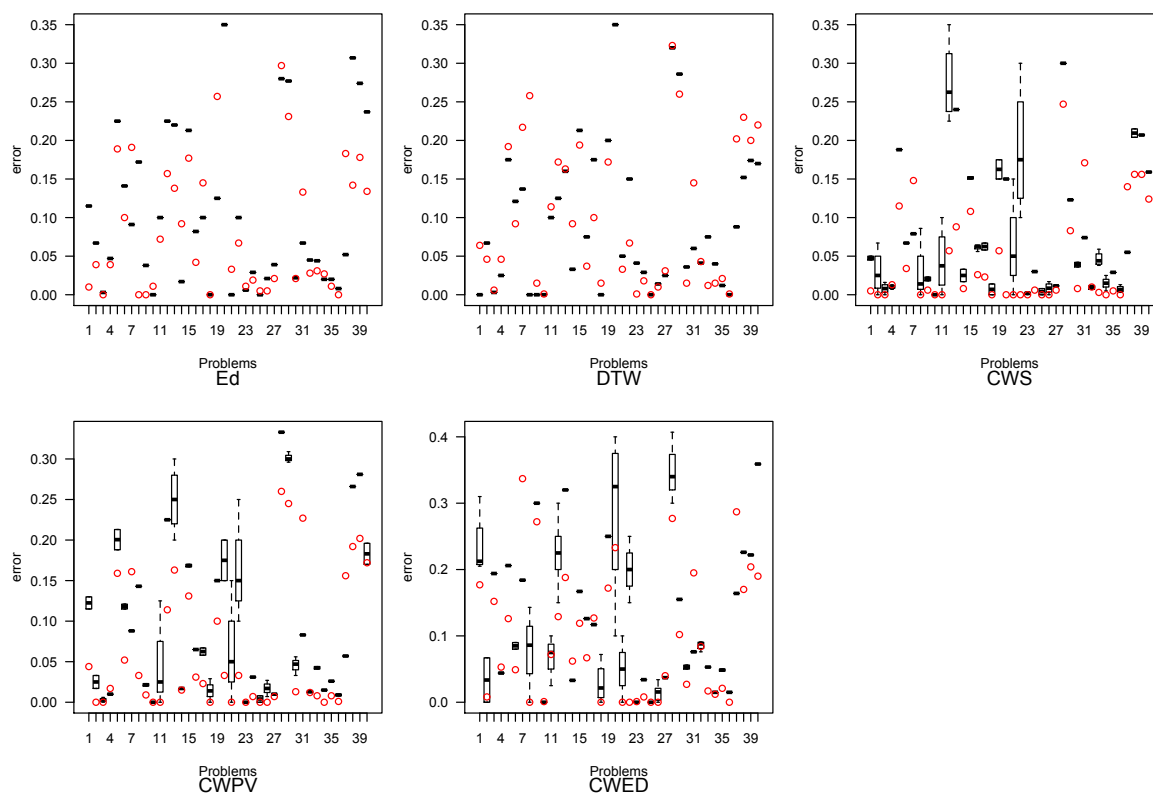


FIGURE 6.14: Comparison of train and test results from experiment two. The red dots are the train results and the others are the test results. The x-axis represents the 40 UCR problems and can be indexed according to their position in Table 6.2 (p. 103).

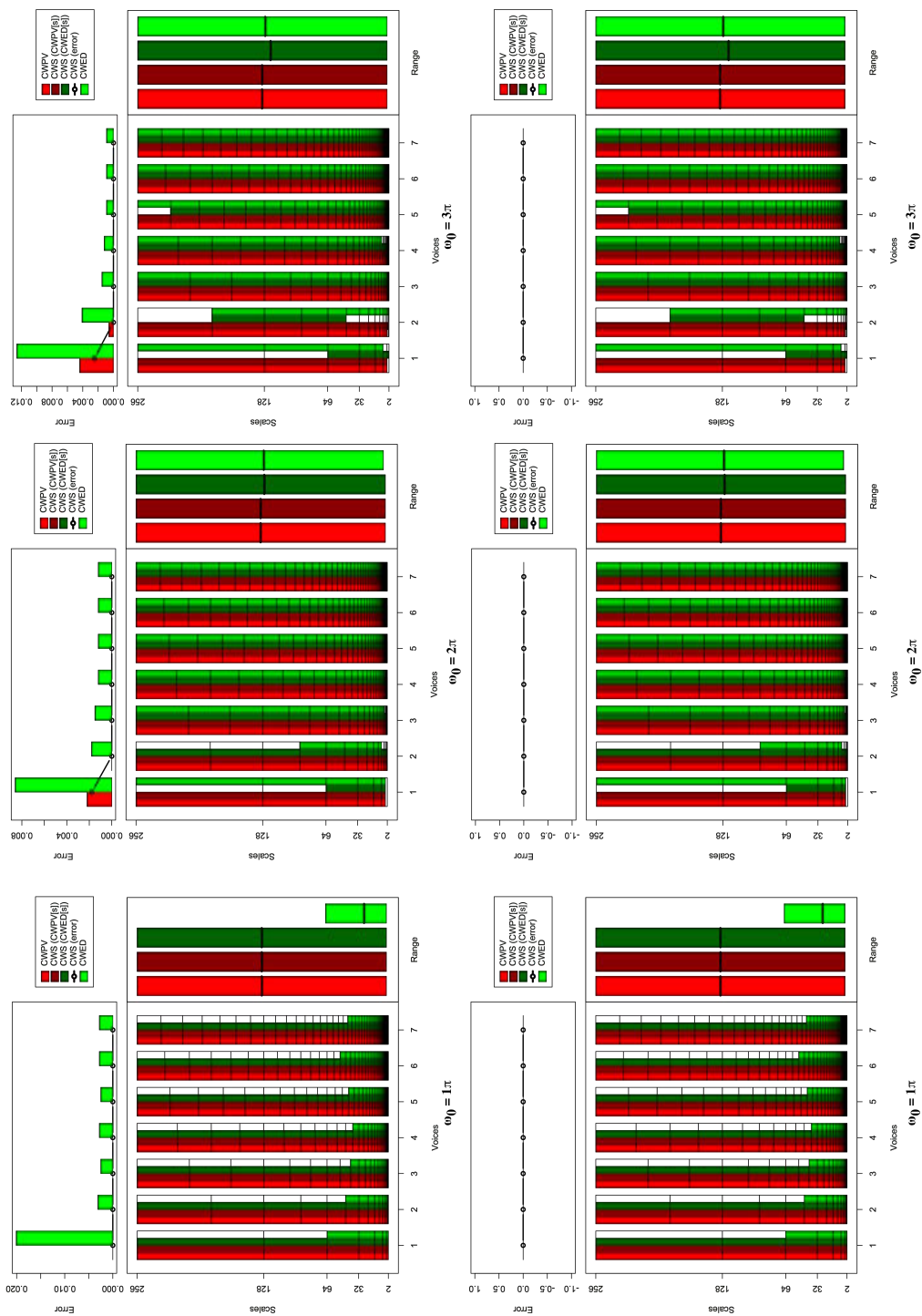


FIGURE 6.15: Summary comparing train and test results for the Wafer classification problem using the CWS, CWPV and CWED techniques with 1-7 voices and three  $\omega_0$  values. A lower CWPV score suggests that the problem is predominantly characterised by FM, whereas a lower CWED implies a predominant AM characteristic. The scale ranges have been translated from scale number to scale value. In the bottom right of each figure the average range of scales for all 7 voices are presented for each technique.

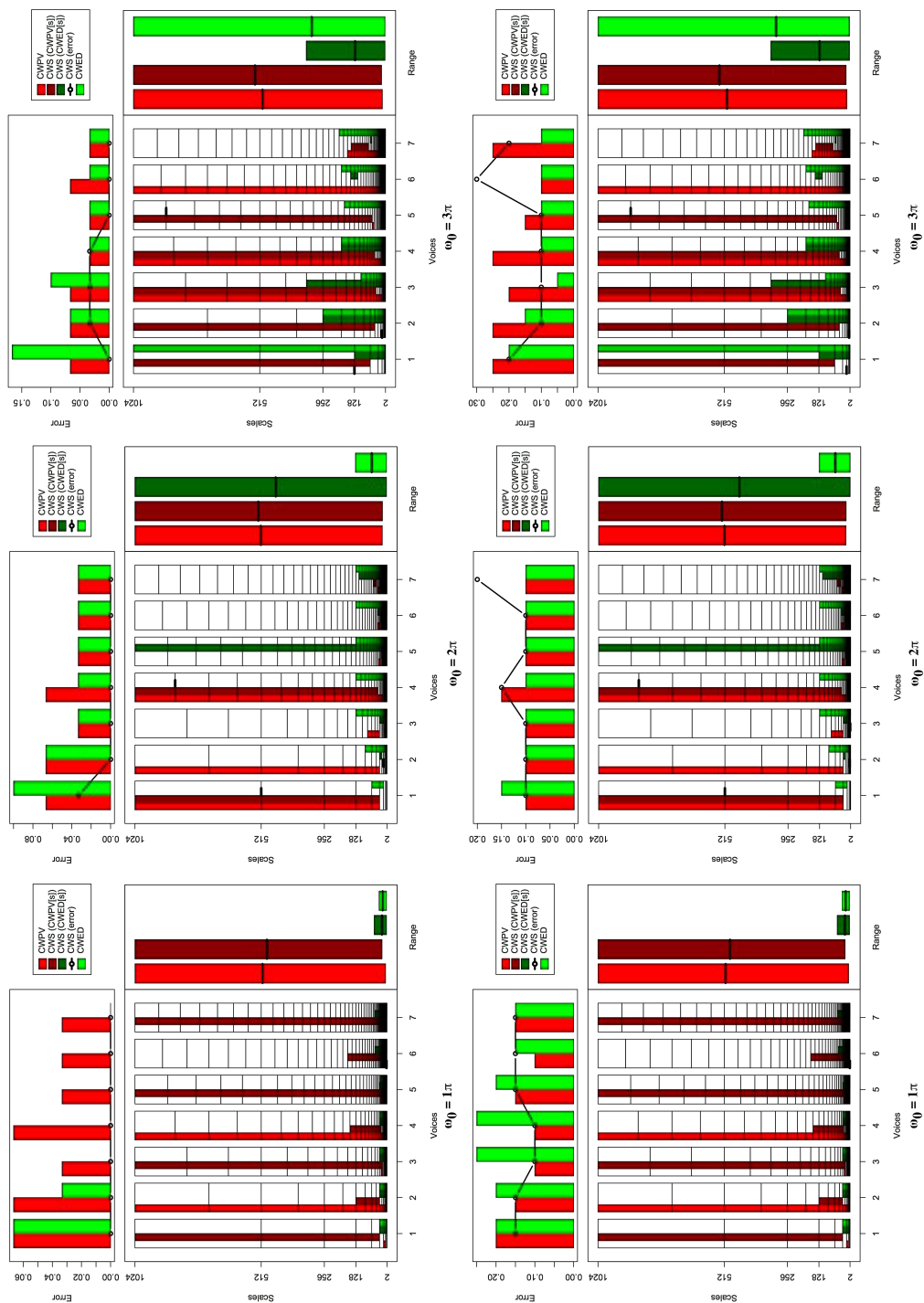


FIGURE 6.16: Summary comparing train and test results for the Olive Oil classification problem using the CWS, CWPV and CWED techniques with 1-7 voices and three  $\omega_0$  values. A lower CWPV score suggests that the problem is predominantly characterised by FM, whereas a lower CWED implies a predominant AM characteristic. The scale ranges have been translated from scale number to scale value. In the bottom right of each figure the average range of scales for all 7 voices are presented for each technique.

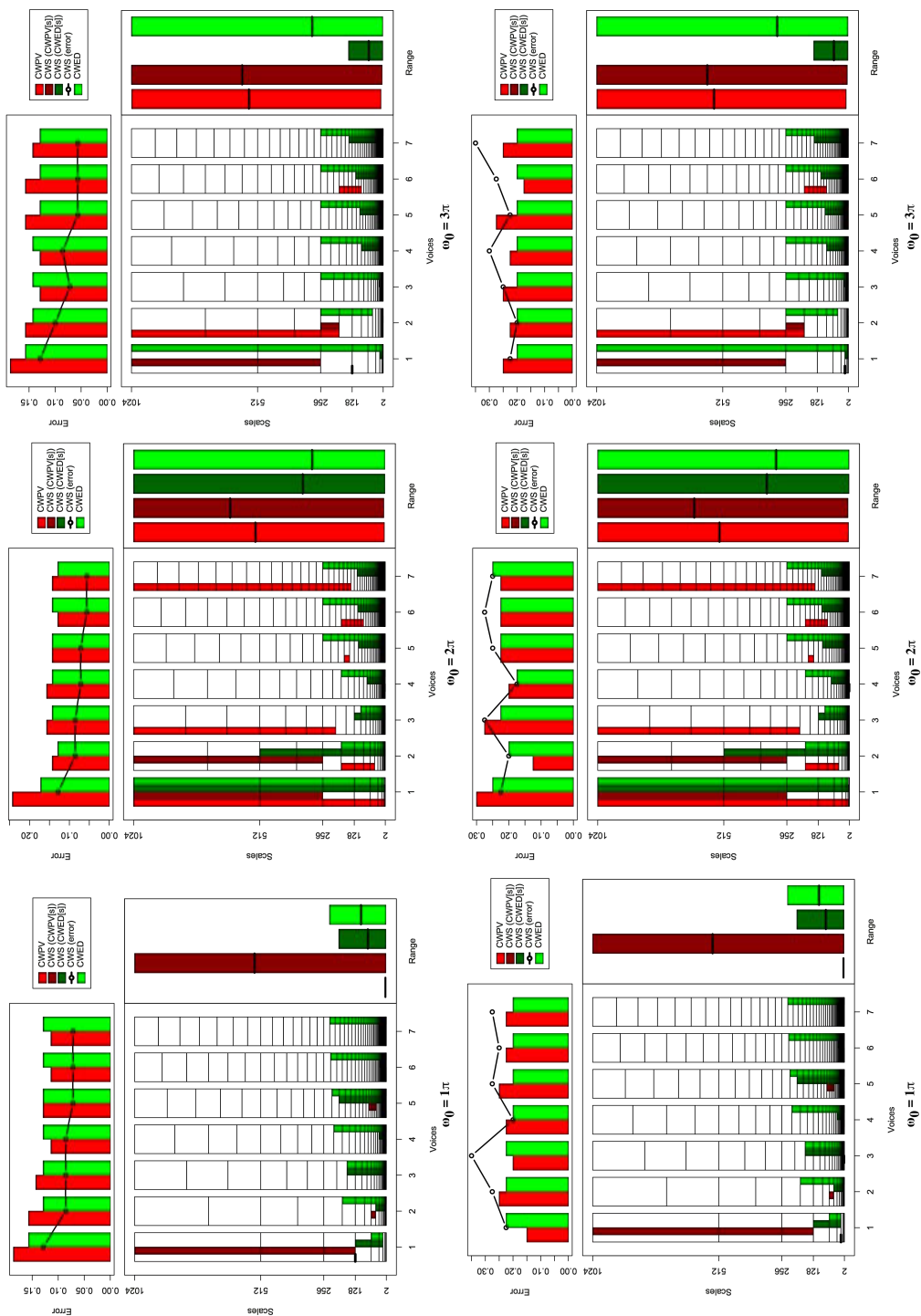


FIGURE 6.17: Summary comparing train and test results for the Lightning 2 classification problem using the CWS, CWPV and CWED techniques with 1-7 voices and three  $\omega_0$  values. A lower CWPV score suggests that the problem is predominantly characterised by FM, whereas a lower CWED implies a predominant AM characteristic. The scale ranges have been translated from scale number to scale value. In the bottom right of each figure the average range of scales for all 7 voices are presented for each technique.



In Table 6.7 (p. 132) a statistical comparison of the results using the Wilcoxon signed rank test is provided. For this comparison only the minimum (best) test results for the CWS method was used. For some of the problems the pairwise difference was zero and it was possible to provide a comparison. To provide an alternative interpretation of test result comparisons it is not always appropriate to compare only the test results. Here, there is typically a decrease in performance between model train results and test results when any form of parameterisation is involved – to provide a simpler solution to the relative performance of a technique a Texas sharpshooter plot [236] may be used. This plot demonstrate the predictability performance of a technique by comparing the expected performance against the actual performance in relation to another technique. Figures 6.18–6.20 (p. 133–133) show a series of Texas sharpshooter plots for the min, mean and max results from the CWS, CWPV and CWED techniques compared to the other techniques. The equation for predicting performance gain is given as

$$gain = \frac{accuracy(technique)}{accuracy(competitor)}, \quad (6.1)$$

were accuracy is obtained by subtracting 1 from the error rate. The gain is calculated for both the train errors (expected gain) and the test error (actual gain), where gain values greater than 1 indicate that the technique performs better than its competitor. The name ‘Texas sharpshooter’ is derived from an anecdotal story of a Texan who shot some bullets into the side of his barn and drew a bullseye around the holes that formed the best cluster [237]. The purpose of these ratio comparison are to demonstrate *a priori* that a given technique does not draw the same conclusion. A simple way to interpret these plots is as follows: All values in the top left quadrant of each plot claimed a decrease in accuracy relative to its comparative technique during training, but ended up having an increase in performance during testing. Values in the top right correctly claimed an increase in performance during both training and testing. Values in the bottom right, however, claimed an increase in accuracy during training, but had a decrease during testing, and finally values in the bottom left claim a decrease during training and had a decrease in performance during testing.

The CWS and CWPV techniques both had very little claims on performing bad, but

TABLE 6.7: Wilcoxon signed-rank test. The medians, W rank statistic, Z-score, p-value, and the effect size r are reported. Significant values are for  $\alpha < 0.05$  (p-values) at the 95% confidence level.

Problem	CWS & Ed				CWS & DTW				DTW & Ed			
	W	Z	p	r	W	Z	p	r	W	Z	p	r
Synthetic Control	0	2.581	0.016	0.577	3.5	-2.469	0.012	0.552	0	2.8	0.004	0.626
Gun Point	0	-2	0.125	0.447	0	-2	0.125	0.447	10.5	0	1	0
CBF	0	-1	1	0.224	0	-1	1	0.224	1.5	0	1	0
Face (all)	1	-1.858	0.062	0.415	0	-2.669	0.008	0.597	6.5	1.798	0.078	0.402
OSU Leaf	15.5	0.258	0.867	0.058	17.5	-1.023	0.338	0.229	4	1.853	0.078	0.414
Swedish Leaf	3	-1.922	0.062	0.43	0	-2.669	0.008	0.597	10	1.44	0.172	0.322
50words	1	-2.703	0.004	0.604	8.5	-1.387	0.18	0.31	0	-2.805	0.002	0.627
Trace	Pairwise differences equal zero											
Two Patterns	0	2.842	0.002	0.636	1.5	-2.311	0.023	0.517	0	2.807	0.002	0.628
Wafer	Pairwise differences equal zero											
Face (four)	0	-2	0.125	0.447	0	-1.727	0.25	0.386	5	0	1	0
Lightning2	0	2	0.125	0.447	1.5	0	1	0	0	2	0.125	0.447
Lightning7	4.5	1.633	0.219	0.365	3	0.175	0.875	0.039	7.5	0.915	0.531	0.205
ECG200	Pairwise differences equal zero											
Adiac	0	-2.669	0.008	0.597	0	-2.814	0.002	0.629	12	-0.052	1	0.012
Yoga	8	-1.736	0.09	0.388	6	-2.191	0.027	0.49	15	0.565	0.617	0.126
Fish	0	-2.765	0.004	0.618	0	-1.725	0.25	0.386	7	-1.951	0.047	0.436
Plane	Pairwise differences equal zero											
Car	2.5	-1	0.625	0.224	0	1	1	0.224	0	-1.732	0.25	0.387
Beef	Pairwise differences equal zero											
Coffee	Pairwise differences equal zero											
OliveOil	Pairwise differences equal zero											
CinC_ECG_torso	0	-2.772	0.004	0.62	0	-1.732	0.25	0.387	0	-2.689	0.008	0.601
ChlorineConcentration	0	1.412	0.5	0.316	0	1	1	0.224	0	1	1	0.224
DiatomSizeReduction	Pairwise differences equal zero											
ECGFiveDays	0	-2	0.125	0.447	0	-2.219	0.062	0.496	10.5	0.532	0.766	0.119
FacesUCR	2.5	-1.976	0.062	0.442	0	-2.671	0.008	0.597	4	1.51	0.172	0.338
Haptics	18	-0.625	0.672	0.14	3	0.233	0.75	0.052	11	-0.932	0.438	0.208
InlineSkate	0	-2.805	0.002	0.627	0	-2.81	0.002	0.628	14	-0.618	0.602	0.138
ItalyPowerDemand	8	1.105	0.375	0.247	5	1.441	0.219	0.322	9.5	-0.941	0.375	0.21
MedicalImages	6.5	1.596	0.141	0.357	5.5	0.956	0.375	0.214	0	1.983	0.125	0.443
MoteStrain	2	-2.032	0.062	0.454	0	-2.687	0.008	0.601	12	0.313	0.797	0.07
SonyAIBORobot SurfaceII	0	-2.204	0.062	0.493	2.5	-1	0.625	0.224	2.5	-1.71	0.156	0.382
SonyAIBORobot Surface	0	-2.21	0.062	0.494	0	-1.412	0.5	0.316	5	-1.443	0.188	0.323
Symbols	1.5	1.808	0.094	0.404	3	1.225	0.25	0.274	0	1.732	0.25	0.387
TwoLeadECG	0	1	1	0.224	0	-1.414	0.5	0.316	0	1.732	0.25	0.387
WordsSynonyms	6.5	-1.591	0.125	0.356	10	0.053	1	0.012	2	-2.259	0.023	0.505
Cricket_X	3	2.278	0.016	0.509	2.5	-2.403	0.016	0.537	0	2.805	0.002	0.627
Cricket_Y	5.5	1.455	0.172	0.325	5	-2.15	0.035	0.481	0	2.675	0.008	0.598
Cricket_Z	9.5	-0.625	0.594	0.14	3	-2.502	0.01	0.559	4	1.745	0.094	0.39

when the entire range is presented, the max test results had a few claims on better performance during training that turned out to be worse performance in testing. Overall the CWS performed better than the CWPV and CWED (which is expected), while the CWED generally claimed bad performance and also had worse performance than some of its claims. It is not clear at all how to discriminate between a range of model results that had identical training performance for multiple parameter sets, which is why the min, mean and max results are given. One of the objectives of this study was to investigate

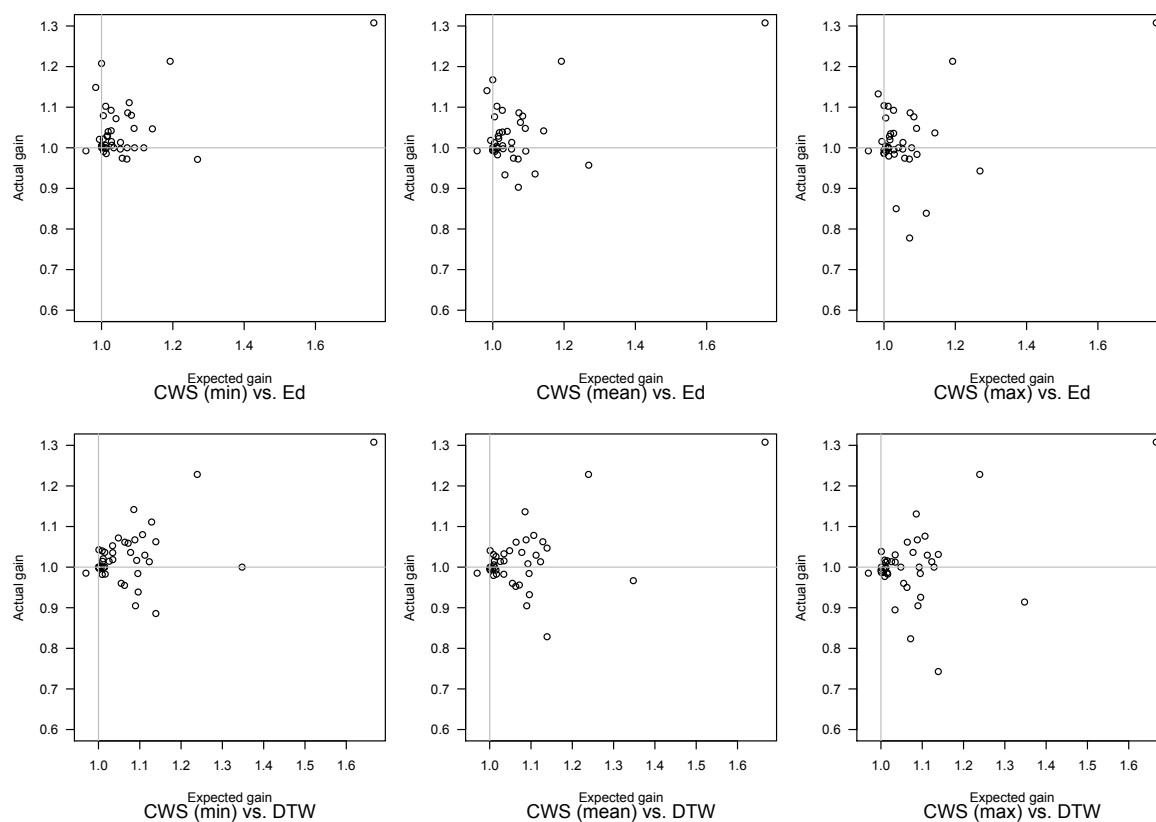


FIGURE 6.18: Texas sharpshooter plot of CWS vs Euclidean distance and DTW. Ed stands for Euclidean distance. All data points (plotted values) represent a claimed performance versus actual performance. Values in the top left quadrant of each plot claimed a decrease in accuracy, but had an increase. Values in the top right correctly claimed an increase in performance. Values in the bottom right claimed an increase in accuracy, but had a decrease, and values in the bottom left claim a decrease and had a decrease in performance.

the characterisation capabilities of the method. It is proposed that this has more value outside of the classification problem when there is variability in test results. Here, the characterisation abilities of the method could provide valuable insight into many large time series databases whose classes are known or pre-determined, and detailed analyses are needed to find similarities in frequency characteristics through automated means. The proposed framework is based on the training procedure and could be used to characterise AM or FM similarities across multiple time series. The following arguments are suggested as an interpretive mechanism for AM and FM characterisation:

- The best error (based on central frequency parameter and voice resolution) used

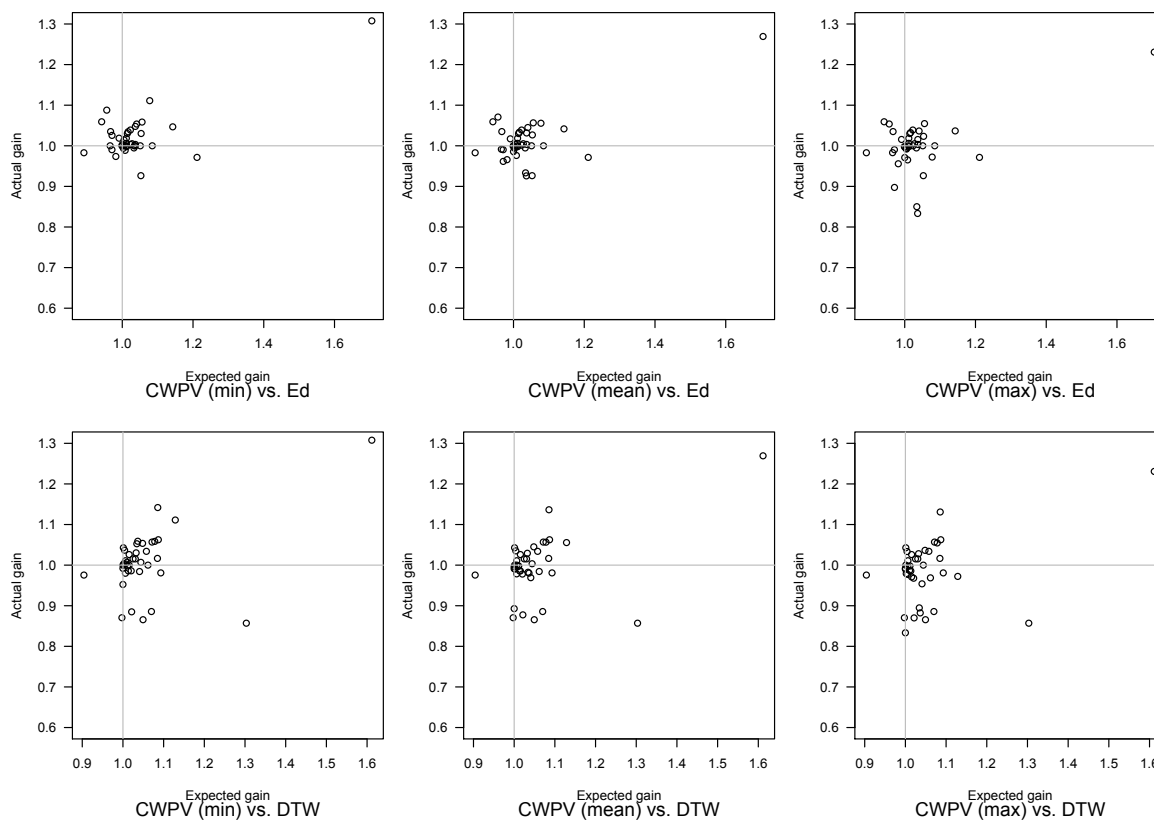


FIGURE 6.19: Texas sharpshooter plot of CWPV vs Euclidean distance and DTW. Ed stands for Euclidean distance. All data points (plotted values) represent a claimed performance versus actual performance. Values in the top left quadrant of each plot claimed a decrease in accuracy, but had an increase. Values in the top right correctly claimed an increase in performance. Values in the bottom right claimed an increase in accuracy, but had a decrease, and values in the bottom left claim a decrease and had a decrease in performance.

to determine the optimum number and position of scales to use, should provide insight into whether the problem is more time or frequency localised in its properties according to the CWPV and CWED error scores.

- The range of scales that reflect the best classification describes the underlying frequency characteristics according to either high, medium or low frequency ranges.
- Where the CWPV errors are consistently lower than the CWED errors, it suggests that the problem is predominantly characterised by FM (or amplitude-invariant problems) and *vice versa*. If the errors vary then the problem is characterised by a mixture of both AM and FM.

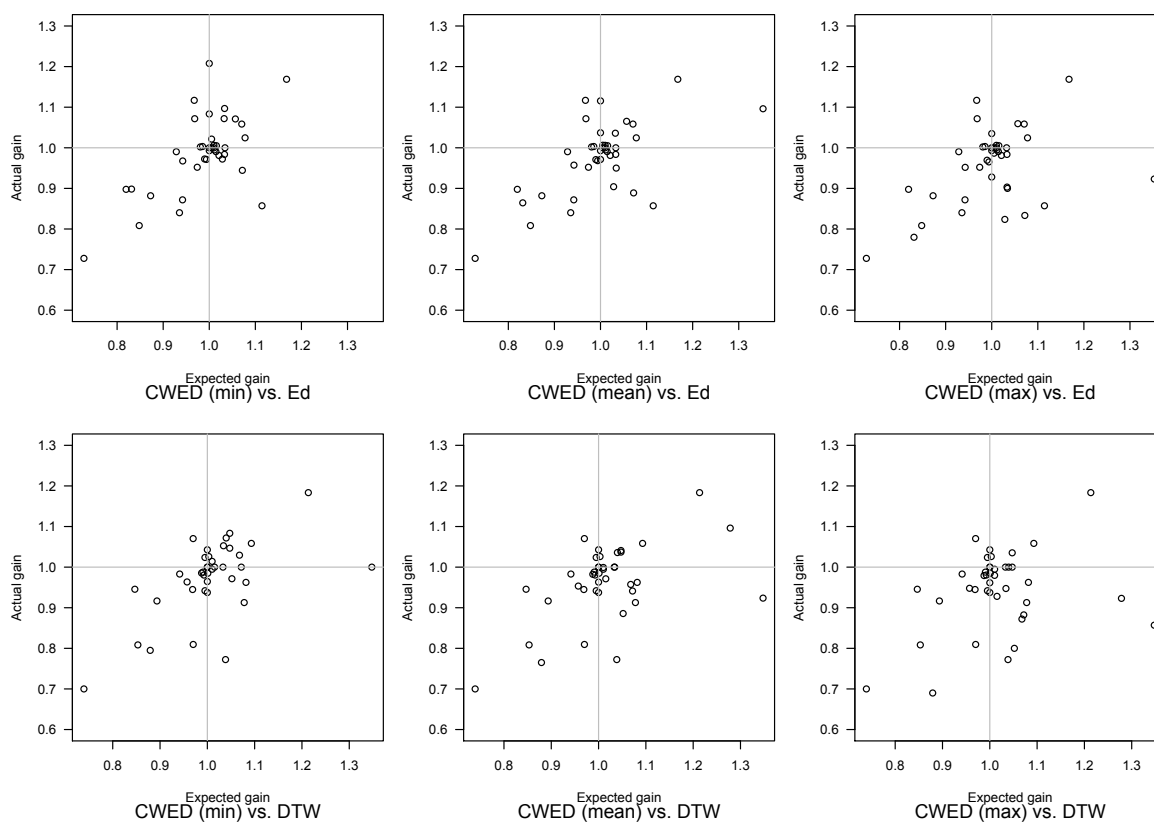


FIGURE 6.20: Texas sharpshooter plot of CWED vs Euclidean distance and DTW. Ed stands for Euclidean distance. All data points (plotted values) represent a claimed performance versus actual performance. Values in the top left quadrant of each plot claimed a decrease in accuracy, but had an increase. Values in the top right correctly claimed an increase in performance. Values in the bottom right claimed an increase in accuracy, but had a decrease, and values in the bottom left claim a decrease and had a decrease in performance.

- If the CWS error rate is roughly the same as either the CWPV or CWED error, then the classification problem can be described as entirely FM or AM accordingly, whereas if the CWS error is lower than either of these, it implies that a combination of AM and FM characterises the problem according to the criteria set out above.
- Generally, the more scales used in the transform (using a higher voice resolution), the better the characterisation potential but also the higher the computation.

Consider the two examples in Figures 6.21 and 6.22 (p. 137–138) reproduced here from Appendix B (p. 156). These are fairly good examples of the framework described above. Figure 6.21 (p. 137) shows a detailed breakdown of the Beef classification problem with

---

an increase in performance in the CPWV (FM) error rate as the central frequency parameter increases. These findings are very similar to the analysis presented in experiment one and provides good examples of the general conclusions made from the extreme case examples in 6.15–6.17 (p. 128–130). The parameterisation for Trace, shown in Figure 6.22 (p. 138) has almost the opposite properties — an increase in performance for the CWED term according to a lower central frequency parameter. This interpretation framework is arguably one of the few (if any) existing ways to simultaneously describe both AM and FM characteristics of time series databases, but there is no doubt much scope for future research both in the interpretation of parameters used during model training and further exploration into the CWS classification and characterisation abilities.

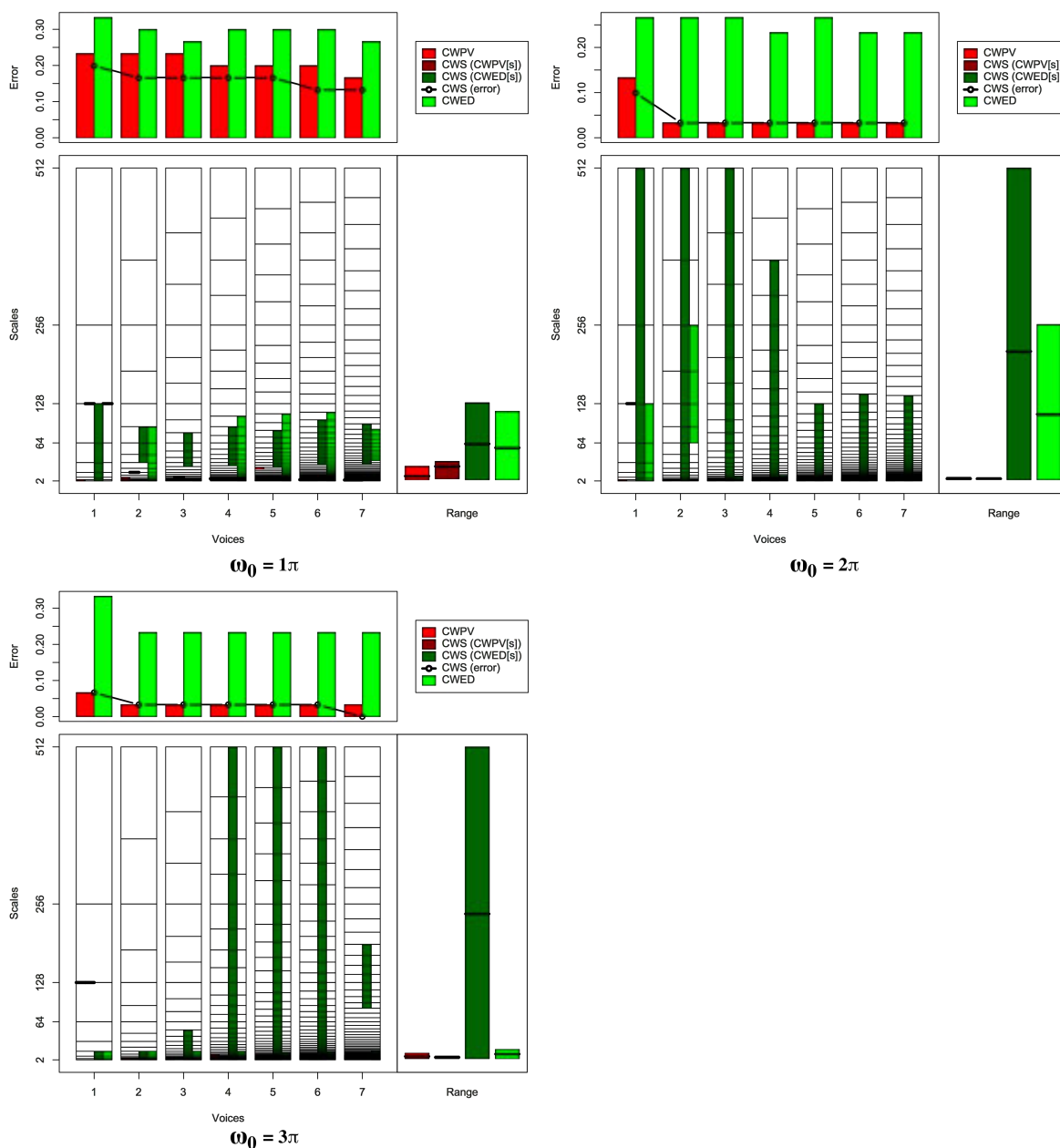


FIGURE 6.21: Summary of results for the Beef classification problem comparing CWS, CWPV and CWED methods using 1-7 voices and three  $\omega_0$  values. A lower CWPV score suggests that the problem is predominantly characterised by FM, whereas a lower CWED implies a predominant AM characteristic. The scale ranges have been translated from scale number to scale value. In the bottom right of each figure the average range of scales for all 7 voices are presented for each technique.

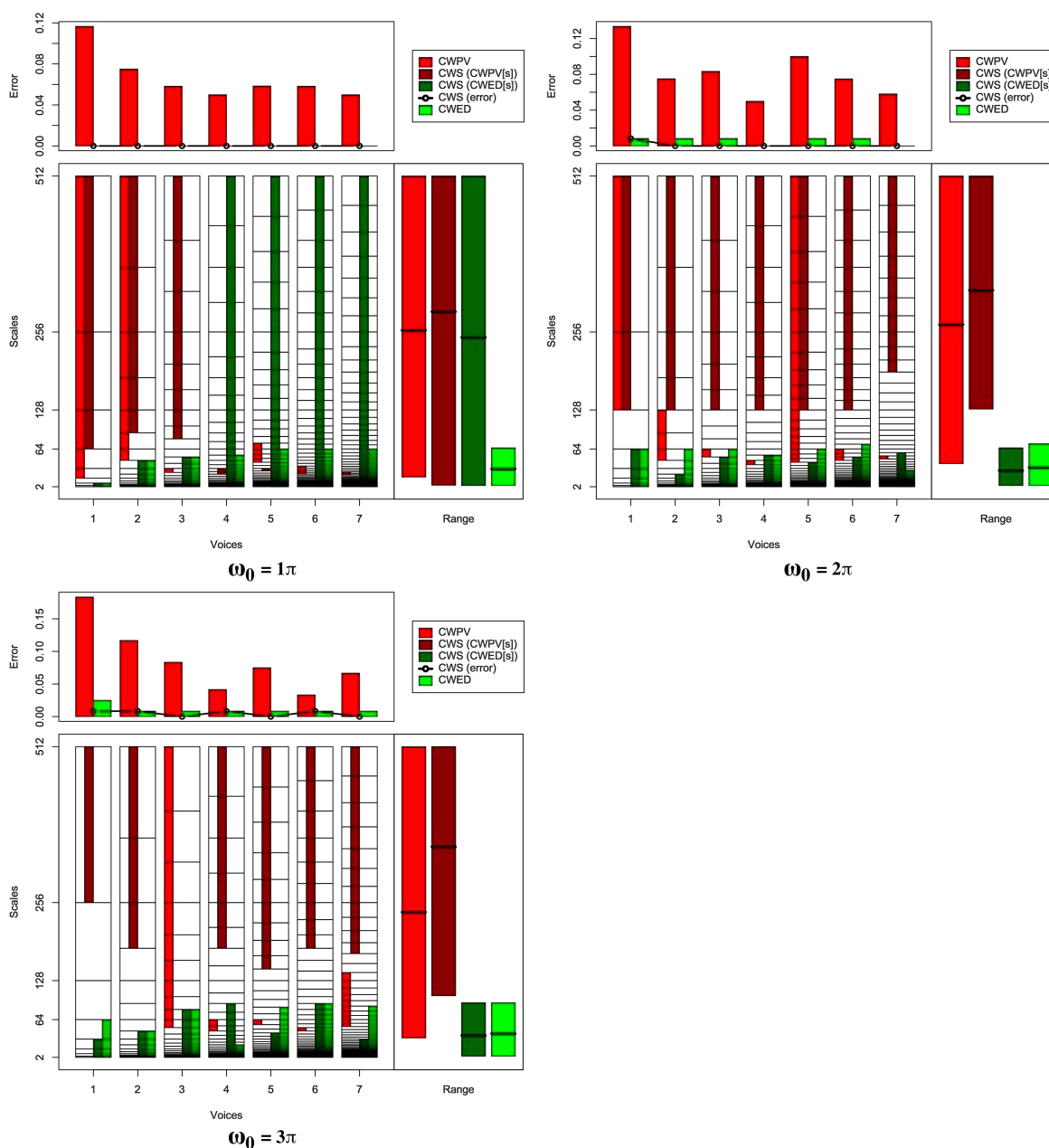


FIGURE 6.22: Summary of results for the Trace classification problem comparing CWS, CWPV and CWED methods using 1-7 voices and three  $\omega_0$  values. A lower CWPV score suggests that the problem is predominantly characterised by FM, whereas a lower CWED implies a predominant AM characteristic. The scale ranges have been translated from scale number to scale value. In the bottom right of each figure the average range of scales for all 7 voices are presented for each technique.



## 6.5 Conclusion

In this chapter two experiments were performed. Each experiment aided in the development or testing of the methodology. In the first experiment, exploration into the classification capability of the CWPV term was done based on the assumption that the least variance in the CWPV coefficients would provide the best descriptors of the problem. This generally did increase classification accuracy, but not to any significant performance levels and it was difficult to provide a characterisation framework using this approach. An analysis of certain problems from experiment one was instrumental in providing a clearer methodology. In experiment two a characterisation of AM and FM was performed using insights gained from experiment one, and an investigation into the best frequency resolution (voice numbers and central frequency parameter) was also explored. Generally, more frequency content used (voice resolution) in the wavelet transform provides better classification results and therefore a better characterisation of AM and FM similarities. There was unfortunately some variability in test results for some of the problems, but despite this the technique still performed relatively well.

To sum up, the approach developed here has good classification skill and potential for further work, but the computational constraint remains fairly large. The characterisation scheme also has potential for many time series databases by exploiting the capabilities of the CWT to provide a distinction between AM and FM features.

*"In literature and in life we ultimately pursue, not conclusions, but beginnings."*

Sam Tanenhaus (AD 1955-)

# 7

## Conclusion

One of the most remarkable insights gained from this study is that, although the continuous wavelet domain is well documented mathematically, large scale applications using this technique have only just begun. In the introduction, I set out to test whether the continuous wavelet transform could be automated to be useful in large time series classification problems.

The results presented in Chapter 6 have met these expectations. Not only does the cross wavelet similarity (CWS) approach to classification developed in this study outperform techniques such as DTW, but the explicit characterisation of underlying amplitude modulated (AM) and frequency modulated (FM) characteristics during the classification experiment is also possible. Recent studies on the performance of DTW [207] argue that

the technique is almost impossible to beat in many classification problems. In this study it is shown that this is not the case. By demonstrating that a combination of AM and FM characteristics (derived from their appropriate frequency ranges (scales)) is needed to optimally classify most time series databases, the underlying characteristics of the time series become explicit using terms (such as AM or FM) that are easy to understand and communicate to the wider scientific audience.

A defining contribution is the development of the cross wavelet phase variance (CWPV) method used to isolate common FM between time series. AM is relatively easy in comparison, and any number of pre-existing techniques could be used to classify such data. The CWS approach developed here explicitly characterises FM and AM behaviour from time series in an automated way.

The following points give a brief overview of this thesis:

- Chapters 2 and 3 provide a detailed background on the events that led to the formation of wavelets, beginning with the ancient Greeks up to the re-introduction of the continuous wavelet transform in the 1970s. These chapters not only provide an interesting story, but also give all the mathematical properties of wavelets and Fourier transforms, describe how these techniques relate to each other, give a detailed account of how they relate to different mathematical eras, and describe how advancements in these fields resulted in functional analysis;
- In Chapter 4, the ‘other’ background is given, where other refers to the broad definition of time series analysis. The focus in this chapter was on time series classification using the measure functions that were compared to the cross wavelet similarity in the results section (Chapter 6).
- Chapter 5 is at the heart of this study. The methodology developed is not only new, but also provides an extremely powerful methodology in which to characterise time series according to their underlying AM or FM behaviour. In Chapter 6 the utility of this approach is presented, and the searching algorithm explicitly extracts common behaviour using an easy to understand analysis framework.

The methodology presented in Chapter 5 and the details of its performance in Chapter 6 are complex and need to be carefully read and understood to fully appreciate their significance. One of the difficulties relates to how the variance of cross wavelet phase is calculated. Arguments were put forth and tested in a machine learning environment, but in order to further test these assumptions it is recommended that a future avenue of research should be based on correlations in natural phenomena. Specifically, remotely-sensed satellite data may provide the necessary information to do this. From a classification view point there are multiple ways to approach the classification of such information, but nearly all earth science applications require some hypothesis on causal agents. The ability to identify AM or FM characteristics, and at which frequencies these occur, provides a powerful avenue to explore these.

In summary, it was the intention of this thesis from the onset to provide a characterisation technique based on wavelet coefficients and test its ability through large scale classification. Benchmark time series provided a sensible database on which to do this, but future research needs to fall back on the properties of cross wavelet phase. It is anticipated that real world phenomena with known underpinnings will hold the answers, and that is the research avenue for another day.

# A

## UCR data summary

### **A.1 UCR data examples**

Examples of the different classes in the UCR database including a brief description of each dataset are provided in Figures A.1 to A.19 (p. 144 to 155) below.

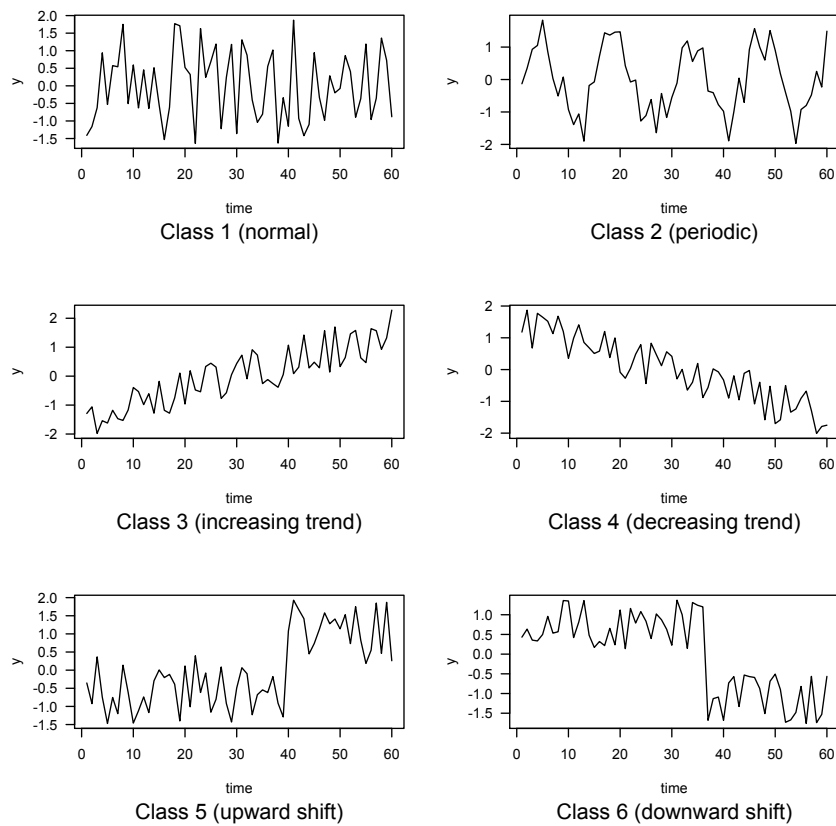


FIGURE A.1: Synthetic control examples. This dataset comprises 6 generated control chart types representing a normal random pattern, an increasing and decreasing trend, upward and downward shifts, and a cyclic pattern [238]. According to [239] it is considered one of the most used datasets among the machine learning community for time series clustering.

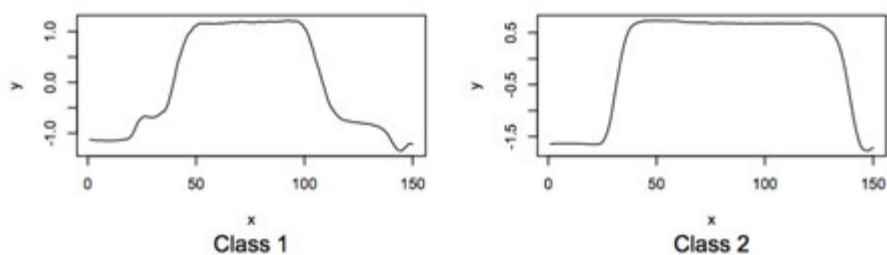


FIGURE A.2: Gun point examples. This dataset comprises 2 classes, made up from actors drawing a gun and pointing and simply pointing an index finger at a specified target within a short time period (approximately one second) [240].

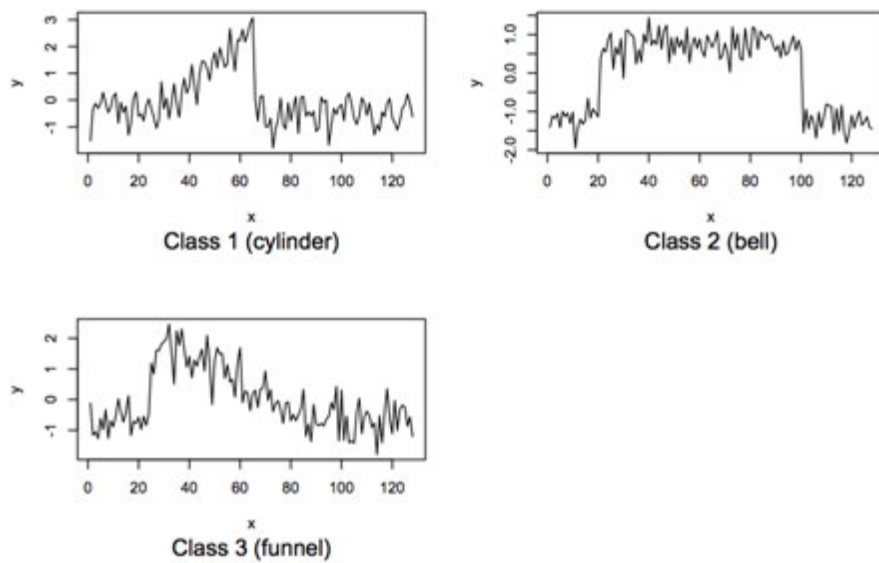


FIGURE A.3: CBF examples. The Cylinder-Bell-Funnel dataset comprises 3 classes of artificially random generated cylinder, bell and funnel patterns [241].

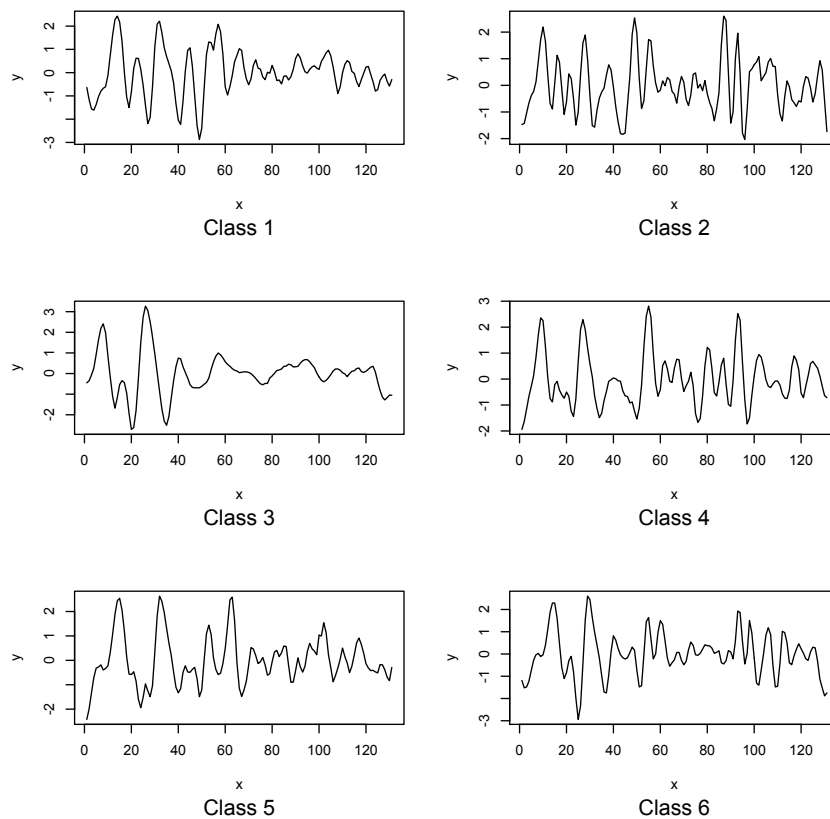


FIGURE A.4: Face (all) examples. This dataset comprises 14 classes of digitised faces whose distance between points on the boundary of the images and the centre make up the time series [242].

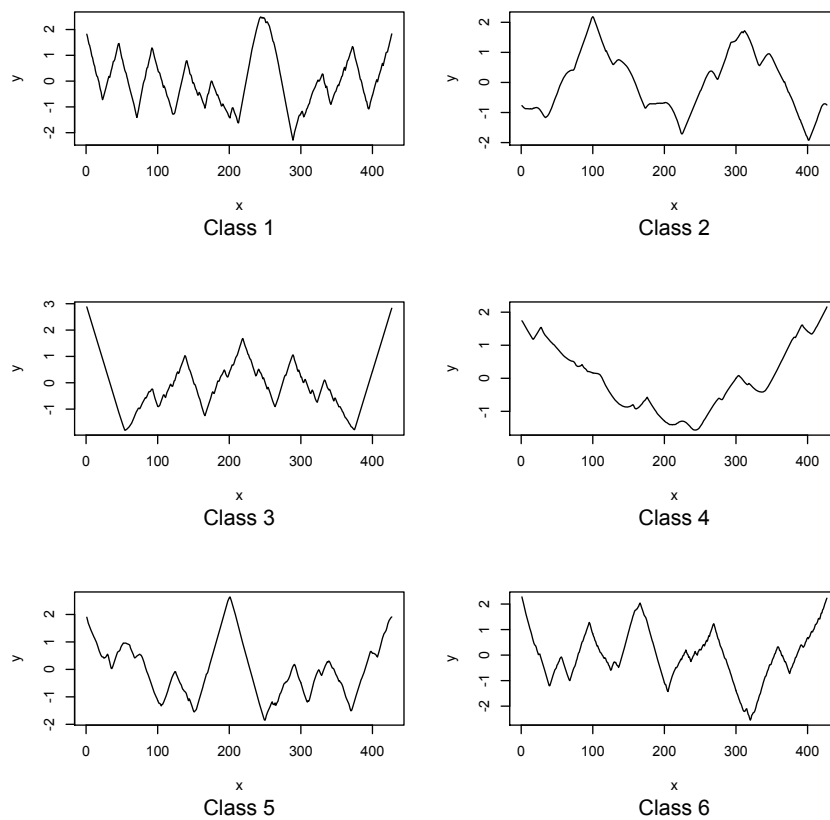


FIGURE A.5: OSU Leaf examples. OSU leaf is made up of 6 classes representing the outer boundary shape of leaves from different plant species. The time series was developed for Masters studies at Oregon State University [243].



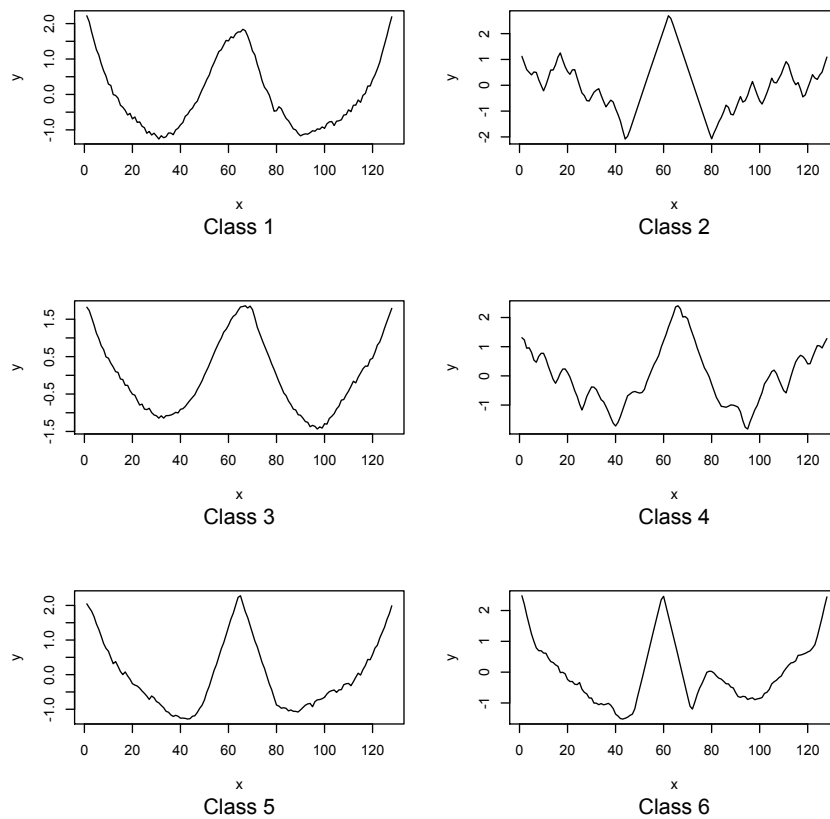


FIGURE A.6: Swedish Leaf examples. The Swedish Leaf dataset is made up of 15 classes (examples of six are shown above), similar to the OSU leaf dataset in Figure A.5 (p. 146), these classes represent the boundary shape of leaves from different tree species in Sweden. The time series was developed for Masters studies at Linköping University in Sweden [244].

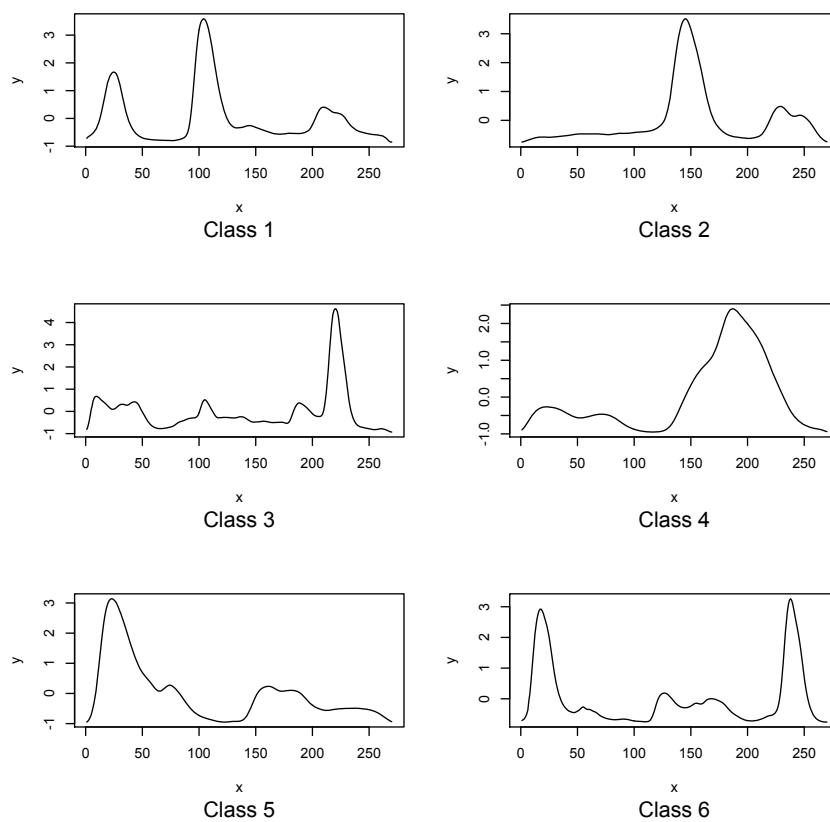


FIGURE A.7: 50words examples. The 50words dataset is made up of 50 classes (examples of six are shown above). These classes represent a collection of handwritten words (taken from a George Washington manuscript) that have been translated into time series by plotting the nearest pixel of a character in a digitised word relative to the word's upper and lower bounding box [202].

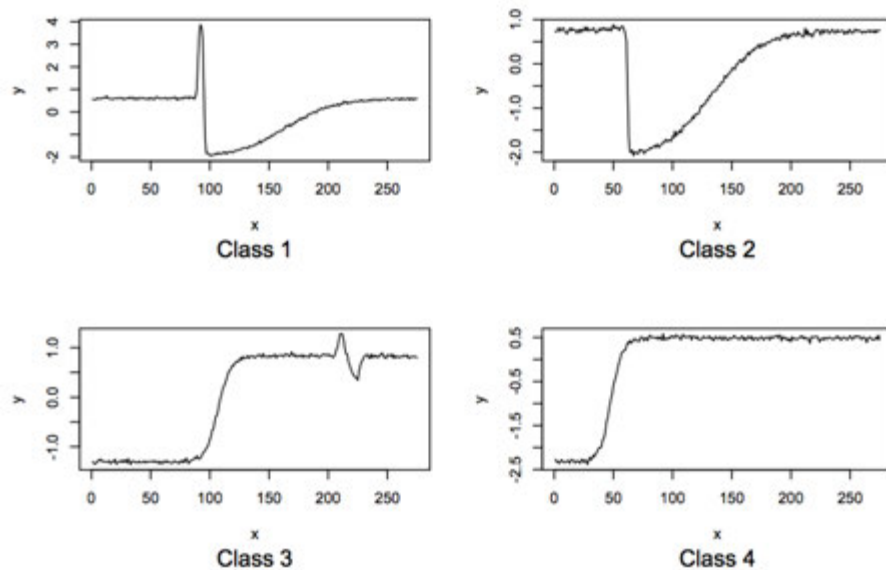


FIGURE A.8: Trace examples. This dataset comprises 4 classes that describe the ‘transient state’ of an industrial plant, based on readings from different sensors. These time series represent a computerised operator support system that uses patterns to identify the general operation of a plant, specifically instrument failures and includes time series translations of readings from different sensors [245].

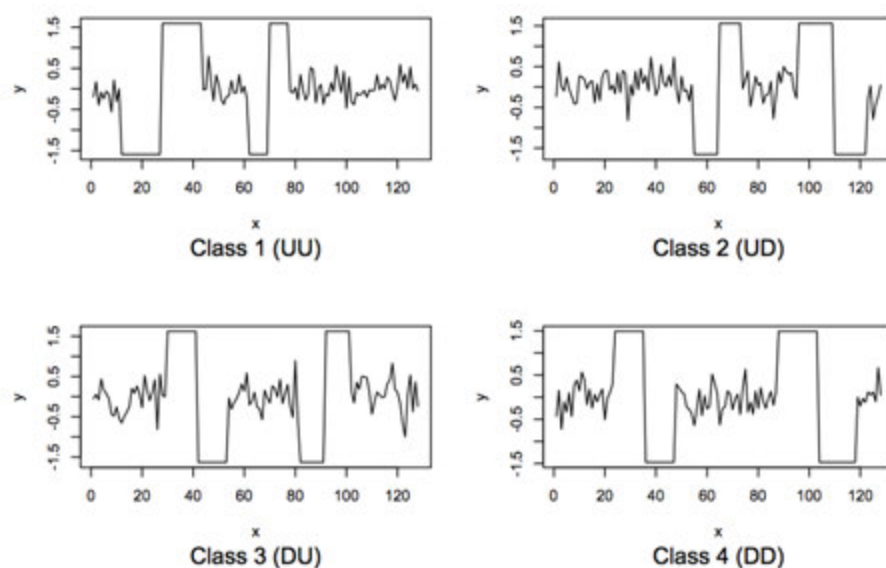


FIGURE A.9: Two patterns examples. This dataset comprises 4 classes characterised by different combinations of an upward step (from -1.5 to 1.5) and a downward step (from 1.5 to -1.5). The first class UU is a succession of two upward steps, the second UD is a succession of an upward step followed by a downward step, the third DU is a succession of a downward step followed by an upward step, and lastly DD is a succession of two downwards steps [246].

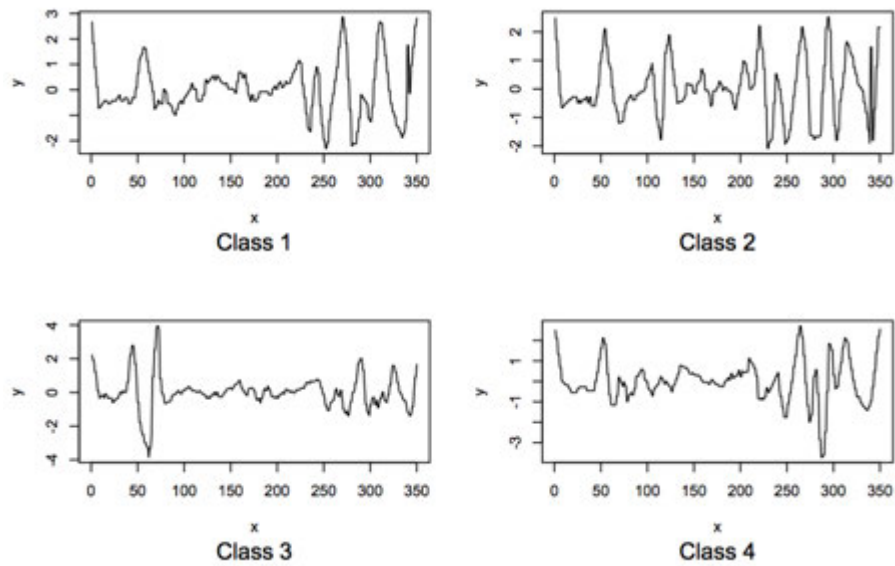


FIGURE A.10: Face (four) examples. This dataset comprises 4 classes representing digitised faces whose distance between points on the boundary of the images and the centre make up the time series [242].

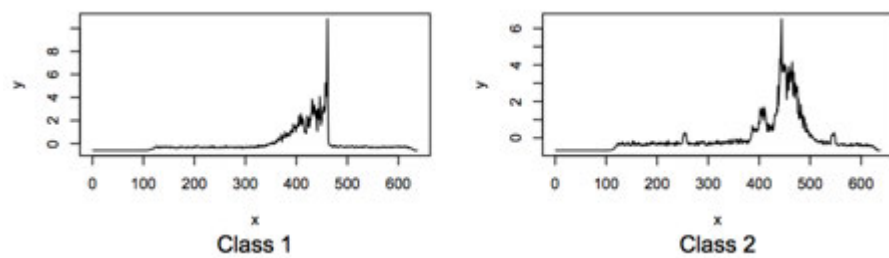


FIGURE A.11: Lightning 2 examples. The dataset comprises 2 classes made up from power density time series acquired by the FORTE satellite, which detects transient electromagnetic events associated with lightning [247].

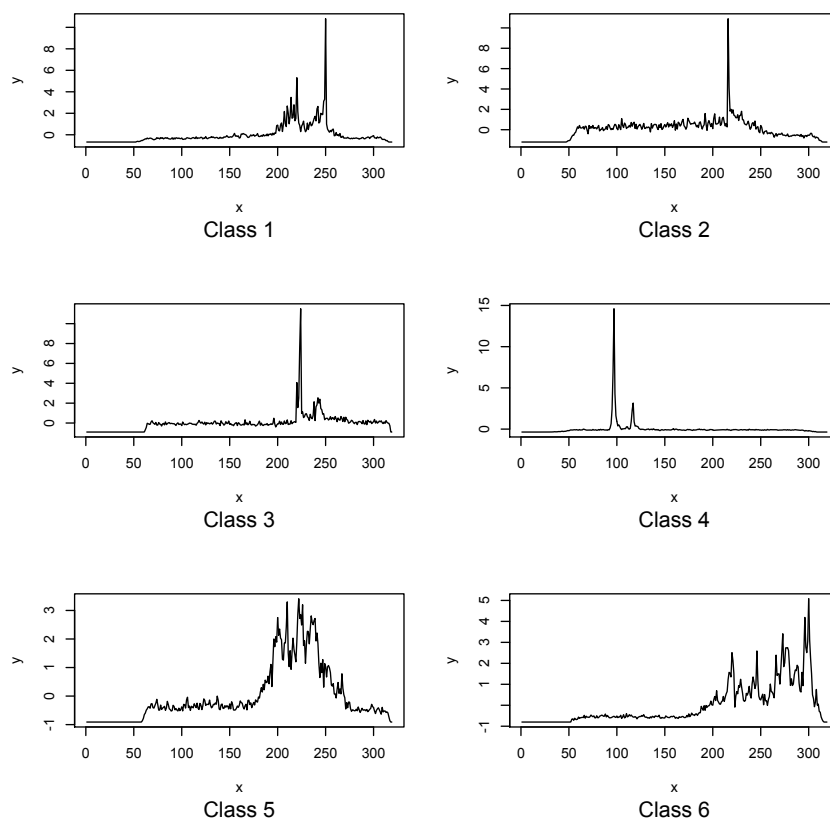


FIGURE A.12: Lightning 7 examples. The dataset comprises 7 classes (samples from six are shown above) made up from power density time series acquired by the FORTE satellite, which detects transient electromagnetic events associated with lightning [247].

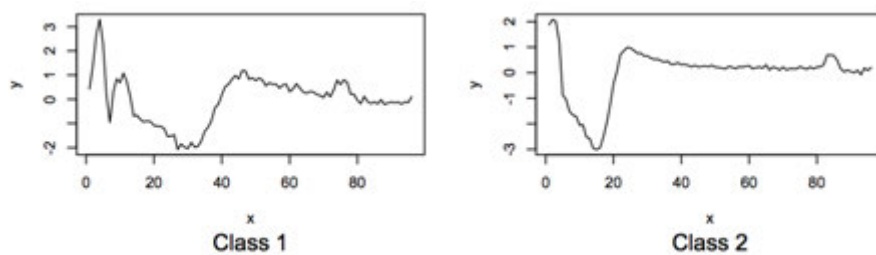


FIGURE A.13: ECG200 examples. This dataset comprises 2 classes representing measurements of heartbeats recorded from an electrode, annotated by cardiologists into normal and abnormal categories [248].

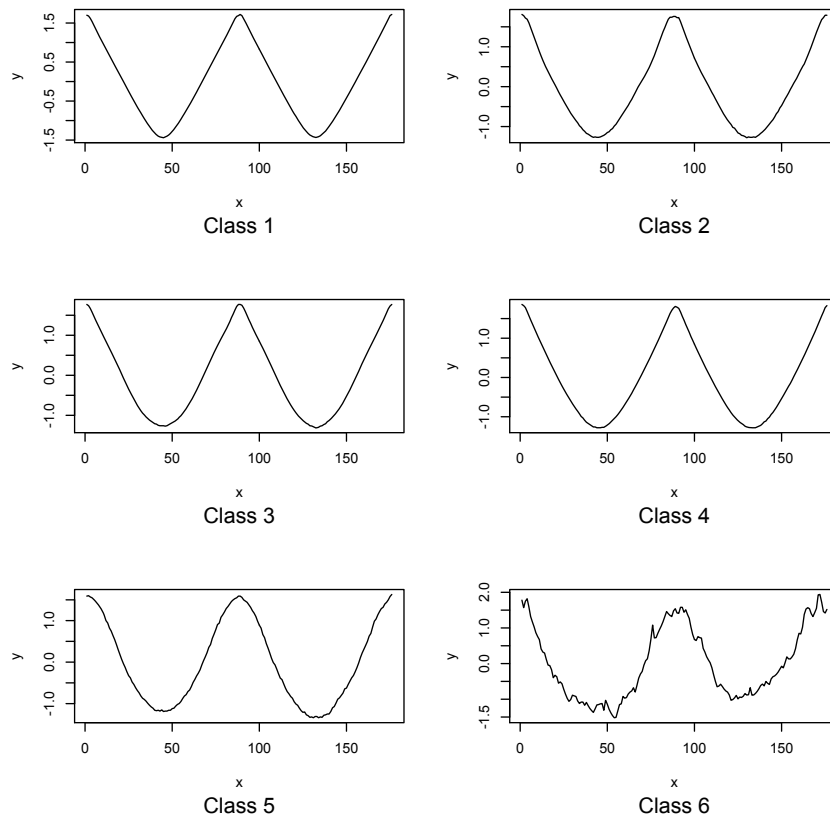


FIGURE A.14: Adiac examples. This dataset comprises 37 classes representing diatom (single-celled algae) shape outlines translated into time series [249].

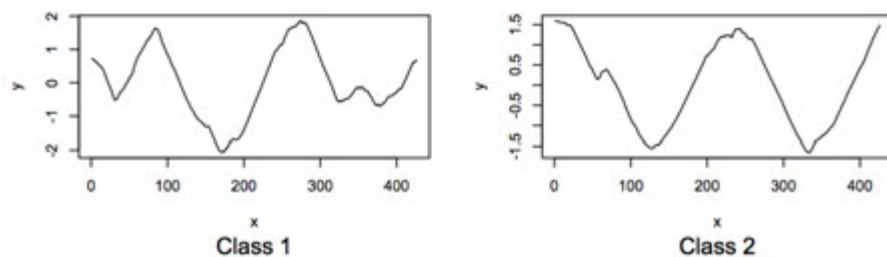


FIGURE A.15: Yoga examples. This dataset comprises 2 classes generated from a male and female model doing various yoga positions in front of a green screen. Here, each position was translated into a time series according to the boundary shape of the actor. The y-axis represents the distance from every point on a model's profile to the centre. The purpose of this dataset is to try distinguish between male and females doing the same yoga routines [250].

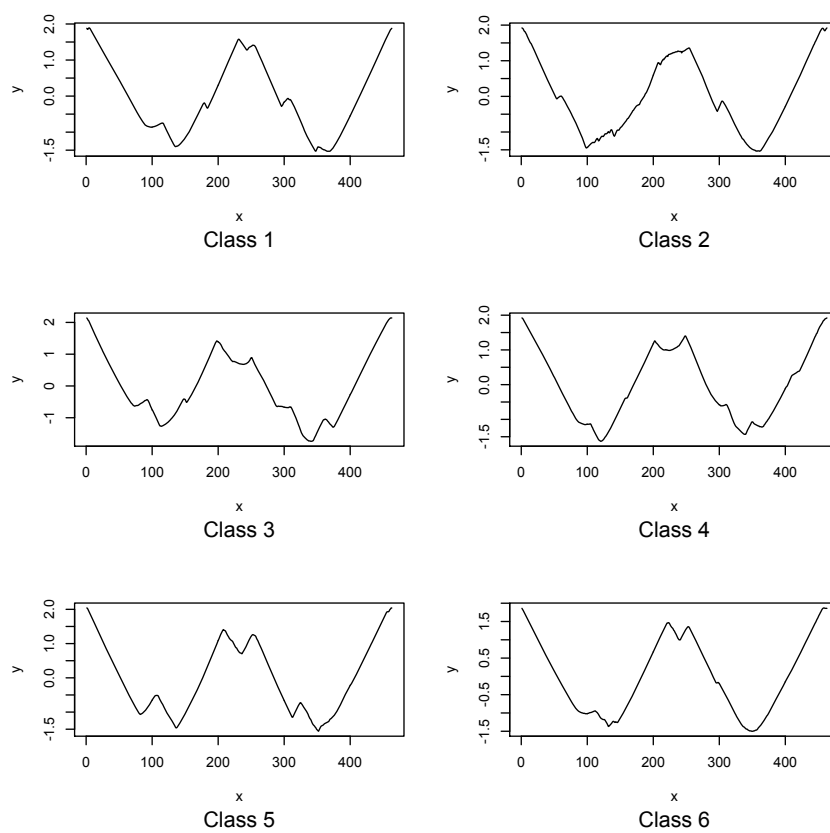


FIGURE A.16: Fish examples. This dataset comprises 7 classes (six samples are displayed above) representing fish shape contours [251].

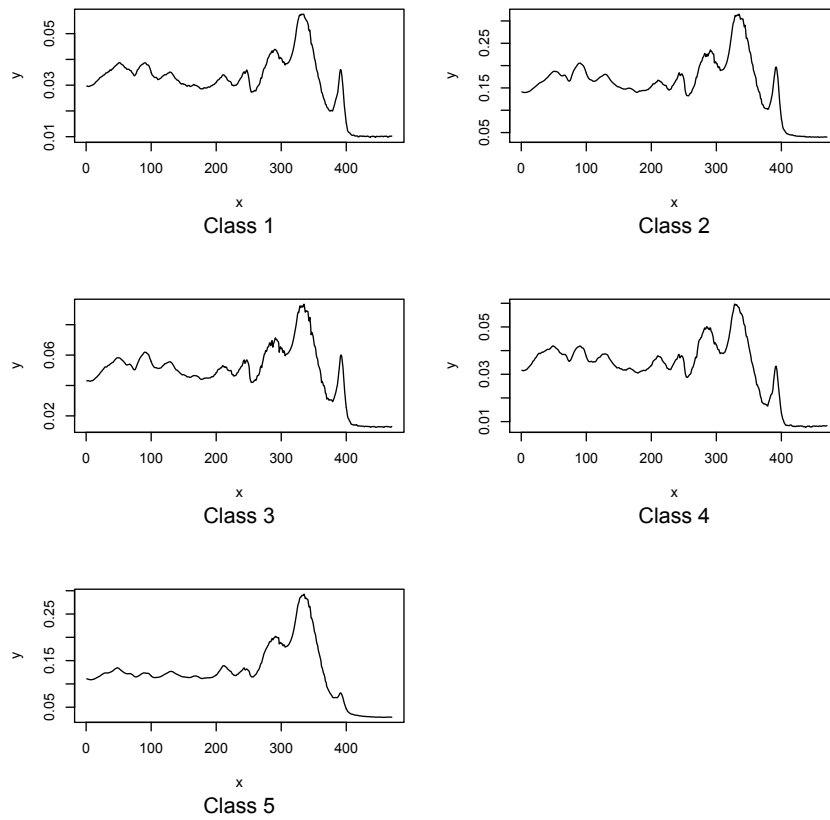


FIGURE A.17: Beef examples. This dataset comprises 5 classes representing spectrograms of beef samples with different degrees of contamination from offal [252].

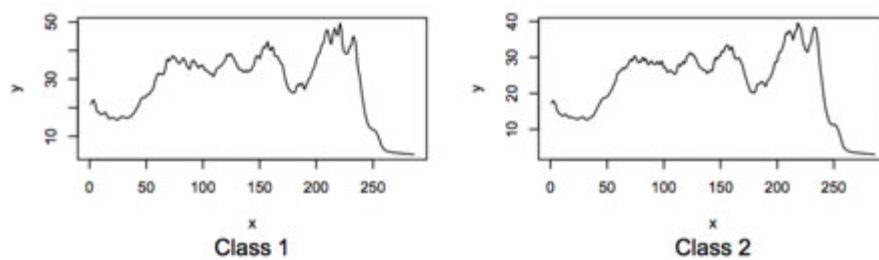


FIGURE A.18: Coffee examples. This dataset comprises 2 classes representing Fourier transform infrared spectroscopy of two variants of coffee (Arabica and Robusta) [235].



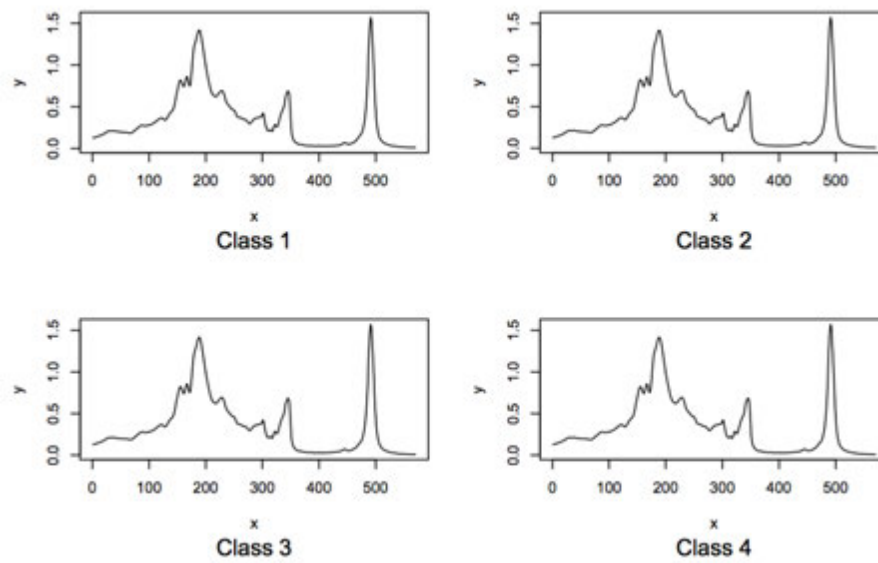


FIGURE A.19: Olive oil examples. This dataset comprises 4 classes representing spectrograms of extra virgin olive oil samples from different countries [235].

# B

## Experiment two summary of parameterisation

### **B.1 Summary of the CWS, CWPV, and CWED parameterisation**

A Summary of the results from experiment two (using 1 - 7 voices and three central frequency parameters) for each classification problem using the CWS, CWPV and CWED methods are presented in Figures B.1–B.22 with corresponding numerical values in Tables B.1–B.22 (p. 158 to 200) below.

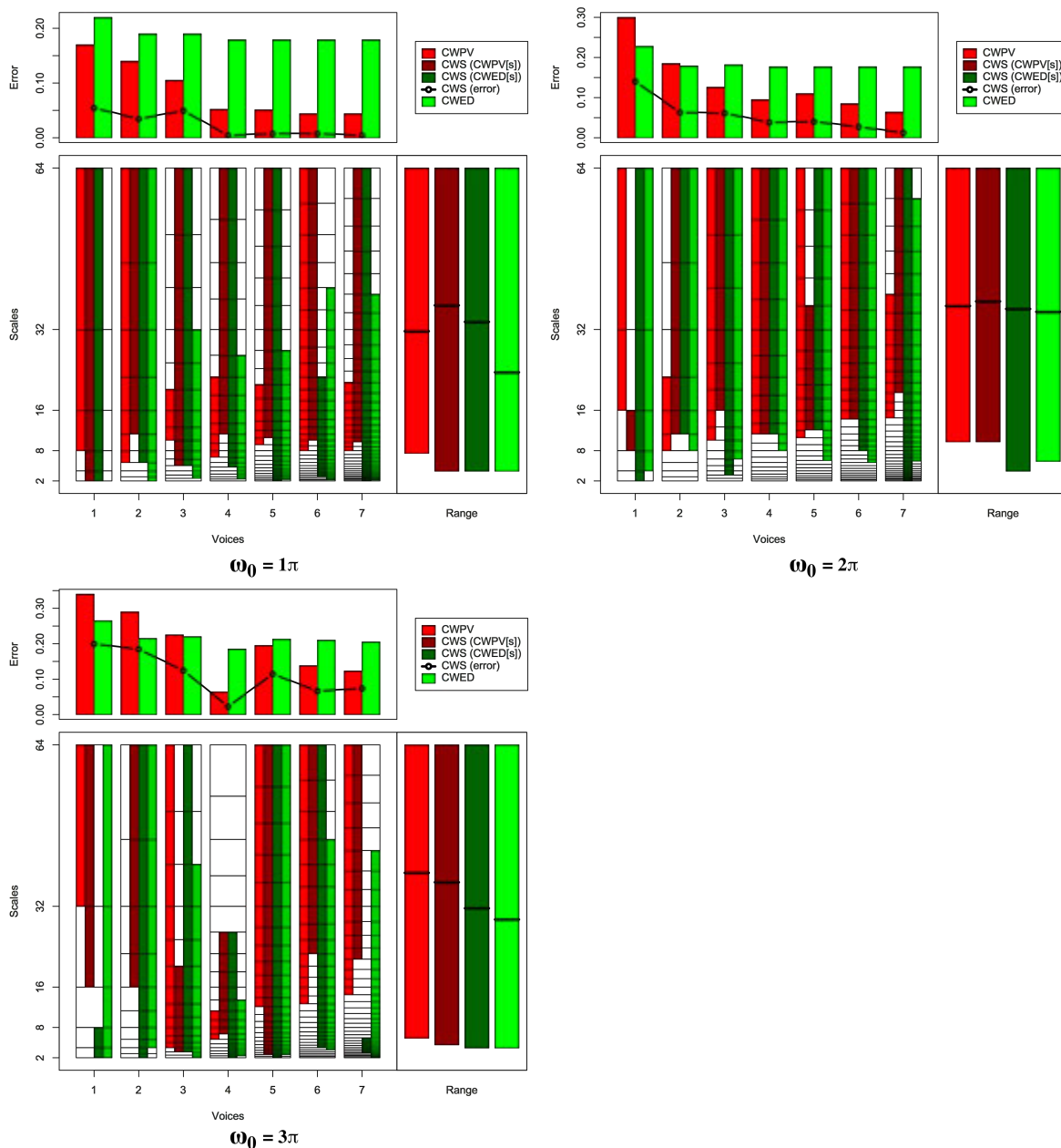


FIGURE B.1: Summary of results for the Synthetic Control classification problem comparing CWS, CWPV, CWED methods using 1-7 voices and three  $\omega_0$  values. A lower CWPV score suggests that the problem is predominantly characterised by FM, whereas a lower CWED implies a predominant AM characteristic. The scale ranges have been translated from scale number to scale value. In the bottom right figure of each figure the average range of scales for all 7 voices are presented for each technique.

TABLE B.1: Summary of results for the Synthetic Control classification problem comparing Ed, DTW, CWS, CWPV, and CWED using 1-7 voices and 3  $\omega_0$  parameters.  $S$  is the scale set(s) associated with the CWS, CWPV and CWED results. The mean values highlighted in bold are the best in model error rate for the problem.

Problem	Technique	Voices	$\omega_0$	$S$	Mean	1	2	3	4	5	6	7	7	9	10
Synthetic Control	Ed				0.064	0.103	0.026	0.128	0.000	0.077	0.026	0.077	0.026	0.179	0.000
Synthetic Control	DTW				0.010	0.000	0.000	0.000	0.026	0.026	0.000	0.051	0.000	0.000	0.000
Synthetic Control	CWS	1	$1\pi$	1:6,1:6	0.055	0.050	0.050	0.050	0.050	0.050	0.100	0.000	0.050	0.100	0.050
Synthetic Control	CWS	1	$2\pi$	3:4,1:6	0.141	0.205	0.077	0.077	0.103	0.205	0.051	0.103	0.154	0.282	0.154
Synthetic Control	CWS	1	$3\pi$	4:6,1:3	0.200	0.200	0.300	0.000	0.200	0.350	0.250	0.150	0.200	0.150	0.200
Synthetic Control	CWS	2	$1\pi$	6:11,4:11	0.035	0.100	0.100	0.050	0.000	0.000	0.050	0.050	0.000	0.000	0.000
Synthetic Control	CWS	2	$2\pi$	6:11,6:11	0.064	0.077	0.051	0.103	0.077	0.026	0.077	0.077	0.051	0.051	0.051
Synthetic Control	CWS	2	$3\pi$	7:11,1:11	0.185	0.150	0.200	0.200	0.150	0.150	0.250	0.050	0.200	0.250	0.250
Synthetic Control	CWS	3	$1\pi$	5:16,5:16	0.050	0.000	0.100	0.000	0.050	0.000	0.050	0.100	0.100	0.050	0.050
Synthetic Control	CWS	3	$2\pi$	10:16,3:16	0.062	0.077	0.128	0.026	0.026	0.051	0.077	0.026	0.103	0.051	0.051
Synthetic Control	CWS	3	$3\pi$	3:11,3:16	0.125	0.100	0.000	0.050	0.100	0.150	0.200	0.150	0.200	0.200	0.100
Synthetic Control	CWS	4	$1\pi$	11:21,6:21	<b>0.005</b>	0.000	0.000	0.000	0.000	0.000	0.000	0.000	0.000	0.026	0.026
Synthetic Control	CWS	4	$2\pi$	11:21,11:21	0.039	0.026	0.026	0.077	0.000	0.026	0.026	0.077	0.026	0.051	0.051
Synthetic Control	CWS	4	$3\pi$	8:16,1:16	0.023	0.000	0.000	0.026	0.000	0.051	0.000	0.026	0.000	0.077	0.051
Synthetic Control	CWS	5	$1\pi$	13:26,1:26	0.008	0.000	0.000	0.026	0.000	0.000	0.000	0.000	0.000	0.026	0.026
Synthetic Control	CWS	5	$2\pi$	14:22,14:26	0.041	0.026	0.051	0.051	0.026	0.103	0.000	0.051	0.051	0.051	0.000
Synthetic Control	CWS	5	$3\pi$	3:26,1:26	0.115	0.154	0.077	0.231	0.103	0.154	0.051	0.179	0.051	0.103	0.051
Synthetic Control	CWS	6	$1\pi$	15:31,4:22	0.008	0.026	0.000	0.000	0.000	0.000	0.000	0.000	0.000	0.051	0.000
Synthetic Control	CWS	6	$2\pi$	18:31,13:31	0.028	0.077	0.026	0.026	0.026	0.051	0.026	0.000	0.000	0.051	0.000
Synthetic Control	CWS	6	$3\pi$	22:31,7:31	0.067	0.026	0.103	0.000	0.077	0.128	0.000	0.026	0.051	0.154	0.103
Synthetic Control	CWS	7	$1\pi$	17:36,1:36	<b>0.005</b>	0.000	0.000	0.000	0.000	0.000	0.000	0.026	0.000	0.026	0.000
Synthetic Control	CWS	7	$2\pi$	24:36,1:36	0.013	0.000	0.051	0.026	0.026	0.000	0.000	0.000	0.000	0.026	0.000
Synthetic Control	CWS	7	$3\pi$	25:36,5:12	0.074	0.026	0.051	0.051	0.051	0.051	0.077	0.051	0.128	0.128	0.128
Synthetic Control	CWPV	1	$1\pi$	3:6	0.170	0.100	0.100	0.200	0.250	0.150	0.150	0.250	0.150	0.150	0.200
Synthetic Control	CWPV	1	$2\pi$	4:6	0.300	0.282	0.256	0.308	0.256	0.359	0.231	0.308	0.385	0.333	0.282
Synthetic Control	CWPV	1	$3\pi$	5:6	0.340	0.400	0.250	0.350	0.400	0.350	0.350	0.350	0.200	0.350	0.400
Synthetic Control	CWPV	2	$1\pi$	4:11	0.140	0.150	0.150	0.050	0.100	0.150	0.100	0.300	0.150	0.150	0.100
Synthetic Control	CWPV	2	$2\pi$	5:8	0.185	0.256	0.077	0.231	0.077	0.256	0.154	0.179	0.154	0.308	0.154
Synthetic Control	CWPV	2	$3\pi$	10:10	0.290	0.200	0.400	0.200	0.300	0.300	0.200	0.250	0.400	0.350	0.300
Synthetic Control	CWPV	3	$1\pi$	8:11	0.105	0.150	0.200	0.050	0.100	0.000	0.100	0.200	0.100	0.050	0.100
Synthetic Control	CWPV	3	$2\pi$	8:16	0.126	0.231	0.026	0.103	0.077	0.205	0.103	0.154	0.154	0.179	0.026
Synthetic Control	CWPV	3	$3\pi$	4:16	0.225	0.150	0.300	0.250	0.250	0.150	0.300	0.200	0.250	0.200	0.200
Synthetic Control	CWPV	4	$1\pi$	8:15	0.052	0.077	0.000	0.103	0.000	0.103	0.000	0.103	0.000	0.103	0.026
Synthetic Control	CWPV	4	$2\pi$	11:21	0.095	0.103	0.026	0.179	0.026	0.128	0.051	0.154	0.051	0.154	0.077
Synthetic Control	CWPV	4	$3\pi$	7:11	0.064	0.051	0.000	0.103	0.000	0.103	0.026	0.154	0.026	0.154	0.026
Synthetic Control	CWPV	5	$1\pi$	12:18	0.051	0.051	0.000	0.051	0.000	0.077	0.000	0.154	0.026	0.103	0.051
Synthetic Control	CWPV	5	$2\pi$	13:26	0.110	0.154	0.000	0.154	0.077	0.179	0.077	0.154	0.077	0.205	0.026
Synthetic Control	CWPV	5	$3\pi$	14:26	0.195	0.256	0.051	0.282	0.103	0.333	0.103	0.256	0.128	0.308	0.128
Synthetic Control	CWPV	6	$1\pi$	13:31	0.044	0.077	0.051	0.051	0.000	0.051	0.026	0.077	0.000	0.077	0.026
Synthetic Control	CWPV	6	$2\pi$	18:31	0.085	0.077	0.026	0.077	0.077	0.205	0.026	0.051	0.077	0.205	0.026
Synthetic Control	CWPV	6	$3\pi$	17:31	0.138	0.179	0.051	0.154	0.103	0.231	0.051	0.282	0.077	0.205	0.051
Synthetic Control	CWPV	7	$1\pi$	15:25	0.044	0.051	0.000	0.051	0.000	0.103	0.026	0.103	0.000	0.077	0.026
Synthetic Control	CWPV	7	$2\pi$	21:31	0.064	0.103	0.000	0.103	0.000	0.103	0.000	0.103	0.000	0.179	0.051
Synthetic Control	CWPV	7	$3\pi$	21:36	0.123	0.179	0.077	0.154	0.077	0.179	0.077	0.154	0.077	0.205	0.051
Synthetic Control	CWED	1	$1\pi$	1:1	0.220	0.250	0.200	0.250	0.100	0.300	0.200	0.150	0.300	0.250	0.200
Synthetic Control	CWED	1	$2\pi$	2:6	0.228	0.179	0.231	0.231	0.205	0.333	0.179	0.179	0.308	0.179	0.256
Synthetic Control	CWED	1	$3\pi$	1:6	0.265	0.250	0.300	0.400	0.200	0.250	0.300	0.250	0.300	0.200	0.200
Synthetic Control	CWED	2	$1\pi$	1:11	0.190	0.100	0.300	0.200	0.100	0.250	0.250	0.150	0.200	0.250	0.100
Synthetic Control	CWED	2	$2\pi$	5:11	0.179	0.231	0.256	0.205	0.128	0.179	0.154	0.128	0.231	0.103	0.179
Synthetic Control	CWED	2	$3\pi$	3:11	0.215	0.200	0.250	0.200	0.300	0.100	0.300	0.250	0.200	0.200	0.150
Synthetic Control	CWED	3	$1\pi$	2:13	0.190	0.100	0.350	0.200	0.150	0.250	0.200	0.150	0.200	0.250	0.050
Synthetic Control	CWED	3	$2\pi$	6:16	0.182	0.256	0.231	0.128	0.128	0.154	0.154	0.205	0.179	0.179	0.205
Synthetic Control	CWED	3	$3\pi$	1:14	0.220	0.200	0.300	0.150	0.250	0.200	0.250	0.250	0.300	0.150	0.150
Synthetic Control	CWED	4	$1\pi$	2:16	0.179	0.205	0.231	0.205	0.205	0.154	0.128	0.179	0.154	0.154	0.179
Synthetic Control	CWED	4	$2\pi$	9:21	0.177	0.205	0.205	0.205	0.154	0.205	0.128	0.077	0.179	0.205	0.205
Synthetic Control	CWED	4	$3\pi$	2:12	0.185	0.231	0.231	0.205	0.205	0.179	0.154	0.179	0.128	0.154	0.179
Synthetic Control	CWED	5	$1\pi$	2:20	0.179	0.205	0.256	0.205	0.205	0.154	0.128	0.154	0.154	0.154	0.179
Synthetic Control	CWED	5	$2\pi$	9:26	0.177	0.231	0.231	0.179	0.128	0.205	0.179	0.128	0.154	0.128	0.205
Synthetic Control	CWED	5	$3\pi$	3:26	0.213	0.231	0.205	0.231	0.154	0.205	0.154	0.179	0.256	0.231	0.282
Synthetic Control	CWED	6	$1\pi$	2:27	0.179	0.205	0.256	0.205	0.179	0.179	0.128	0.154	0.154	0.154	0.179
Synthetic Control	CWED	6	$2\pi$	10:31	0.177	0.231	0.231	0.205	0.103	0.205	0.179	0.128	0.154	0.128	0.205
Synthetic Control	CWED	6	$3\pi$	6:28	0.210	0.256	0.154	0.231	0.128	0.154	0.205	0.179	0.308	0.256	0.231
Synthetic Control	CWED	7	$1\pi$	2:31	0.179	0.205	0.256	0.205	0.179	0.179	0.128	0.154	0.154	0.154	0.179
Synthetic Control	CWED	7	$2\pi$	12:35	0.177	0.231	0.231	0.154	0.128	0.179	0.179	0.128	0.179	0.154	0.205
Synthetic Control	CWED	7	$3\pi$	1:32	0.205	0.231	0.179	0.205	0.154	0.205	0.154	0.179	0.282	0.231	0.231

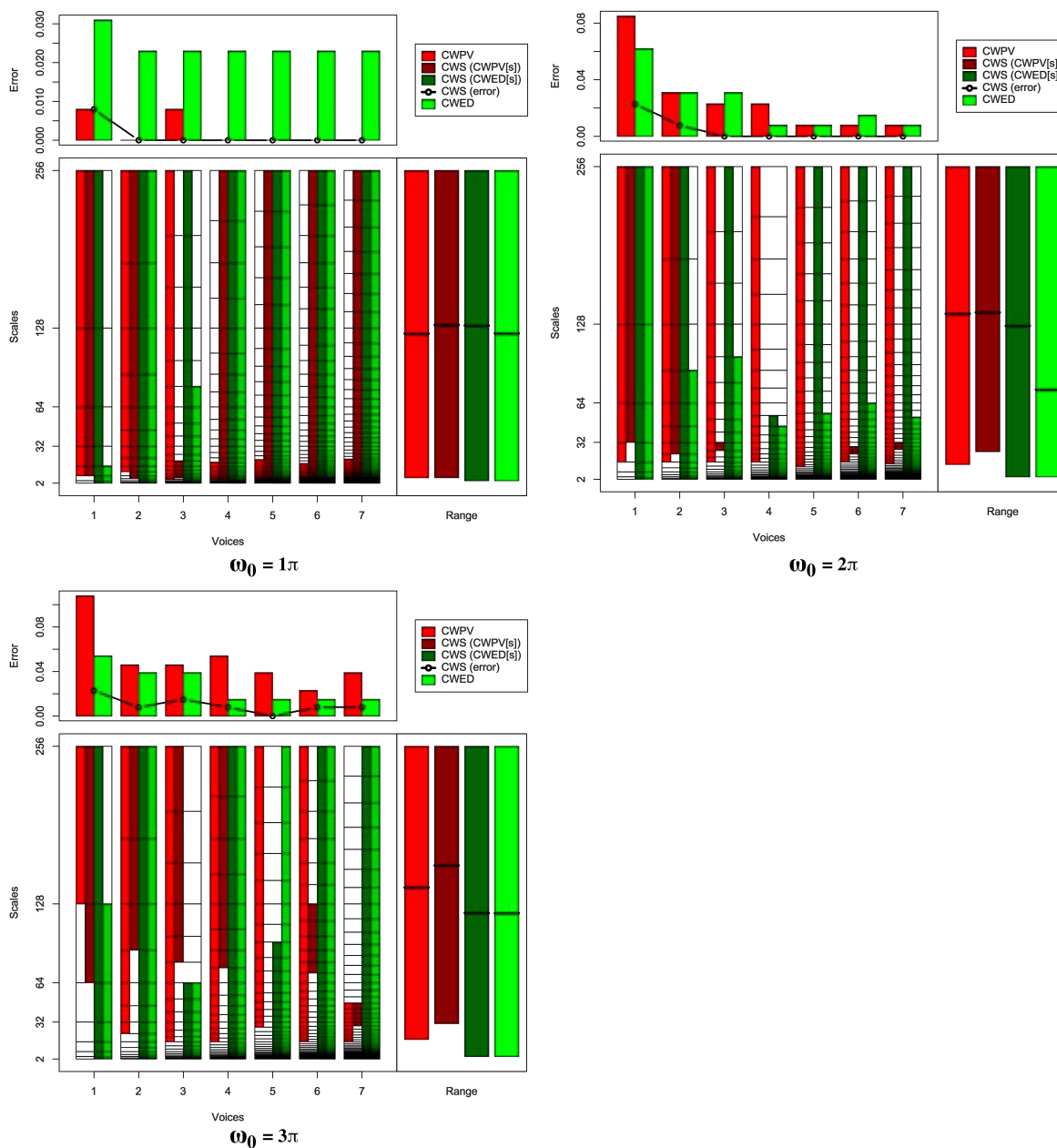


FIGURE B.2: Summary of results for the Gun Point classification problem comparing CWS, CWPV, CWED methods using 1-7 voices and three  $\omega_0$  values. A lower CWPV score suggests that the problem is predominantly characterised by FM, whereas a lower CWED implies a predominant AM characteristic. The scale ranges have been translated from scale number to scale value. In the bottom right figure of each figure the average range of scales for all 7 voices are presented for each technique.

TABLE B.2: Summary of results for the Gun Point classification problem comparing Ed, DTW, CWS, CWPV, and CWED using 1-7 voices and 3  $\omega_0$  parameters.  $S$  is the scale set(s) associated with the CWS, CWPV and CWED results. The mean values highlighted in bold are the best in model error rate for the problem.

Problem	Technique	Voices	$\omega_0$	$S$	Mean	1	2	3	4	5	6	7	7	9	10
Gun Point	Ed				0.046	0.000	0.000	0.000	0.077	0.000	0.154	0.000	0.000	0.154	0.077
Gun Point	DTW				0.039	0.000	0.077	0.077	0.000	0.000	0.077	0.077	0.000	0.077	0.000
Gun Point	CWS	1	$1\pi$	3:8,1:8	0.008	0.000	0.000	0.077	0.000	0.000	0.000	0.000	0.000	0.000	0.000
Gun Point	CWS	1	$2\pi$	5:8,1:8	0.023	0.000	0.000	0.000	0.000	0.000	0.000	0.000	0.077	0.154	0.000
Gun Point	CWS	1	$3\pi$	6:8,1:8	0.023	0.000	0.154	0.000	0.000	0.077	0.000	0.000	0.000	0.000	0.000
Gun Point	CWS	2	$1\pi$	4:15,1:15	<b>0.000</b>	0.000	0.000	0.000	0.000	0.000	0.000	0.000	0.000	0.000	0.000
Gun Point	CWS	2	$2\pi$	8:15,1:15	0.008	0.000	0.000	0.000	0.000	0.000	0.000	0.000	0.077	0.000	0.000
Gun Point	CWS	2	$3\pi$	12:15,1:15	0.008	0.000	0.000	0.000	0.000	0.000	0.000	0.000	0.000	0.000	0.077
Gun Point	CWS	3	$1\pi$	6:11,1:22	<b>0.000</b>	0.000	0.000	0.000	0.000	0.000	0.000	0.000	0.000	0.000	0.000
Gun Point	CWS	3	$2\pi$	12:13,1:22	<b>0.000</b>	0.000	0.000	0.000	0.000	0.000	0.000	0.000	0.000	0.000	0.000
Gun Point	CWS	3	$3\pi$	17:22,1:16	0.015	0.077	0.000	0.000	0.000	0.000	0.000	0.000	0.000	0.000	0.077
Gun Point	CWS	4	$1\pi$	6:29,1:29	<b>0.000</b>	0.000	0.000	0.000	0.000	0.000	0.000	0.000	0.000	0.000	0.000
Gun Point	CWS	4	$2\pi$	19:19,1:20	<b>0.000</b>	0.000	0.000	0.000	0.000	0.000	0.000	0.000	0.000	0.000	0.000
Gun Point	CWS	4	$3\pi$	22:29,1:29	0.008	0.000	0.000	0.000	0.000	0.077	0.000	0.000	0.000	0.000	0.000
Gun Point	CWS	5	$1\pi$	8:36,1:36	<b>0.000</b>	0.000	0.000	0.000	0.000	0.000	0.000	0.000	0.000	0.000	0.000
Gun Point	CWS	5	$2\pi$	19:19,1:36	<b>0.000</b>	0.000	0.000	0.000	0.000	0.000	0.000	0.000	0.000	0.000	0.000
Gun Point	CWS	5	$3\pi$	22:22,1:29	<b>0.000</b>	0.000	0.000	0.000	0.000	0.000	0.000	0.000	0.000	0.000	0.000
Gun Point	CWS	6	$1\pi$	8:43,1:43	<b>0.000</b>	0.000	0.000	0.000	0.000	0.000	0.000	0.000	0.000	0.000	0.000
Gun Point	CWS	6	$2\pi$	22:24,1:43	<b>0.000</b>	0.000	0.000	0.000	0.000	0.000	0.000	0.000	0.000	0.000	0.000
Gun Point	CWS	6	$3\pi$	32:37,1:43	0.008	0.000	0.000	0.000	0.000	0.000	0.000	0.077	0.000	0.000	0.000
Gun Point	CWS	7	$1\pi$	10:50,1:50	<b>0.000</b>	0.000	0.000	0.000	0.000	0.000	0.000	0.000	0.000	0.000	0.000
Gun Point	CWS	7	$2\pi$	27:29,1:50	<b>0.000</b>	0.000	0.000	0.000	0.000	0.000	0.000	0.000	0.000	0.000	0.000
Gun Point	CWS	7	$3\pi$	28:33,1:50	0.008	0.000	0.000	0.000	0.000	0.000	0.000	0.000	0.077	0.000	0.000
Gun Point	CWPV	1	$1\pi$	3:8	0.008	0.000	0.000	0.077	0.000	0.000	0.000	0.000	0.000	0.000	0.000
Gun Point	CWPV	1	$2\pi$	4:8	0.085	0.000	0.154	0.231	0.154	0.000	0.077	0.000	0.077	0.000	0.154
Gun Point	CWPV	1	$3\pi$	7:8	0.108	0.077	0.000	0.077	0.077	0.154	0.000	0.077	0.154	0.308	0.154
Gun Point	CWPV	2	$1\pi$	6:15	<b>0.000</b>	0.000	0.000	0.000	0.000	0.000	0.000	0.000	0.000	0.000	0.000
Gun Point	CWPV	2	$2\pi$	7:15	0.031	0.000	0.000	0.077	0.000	0.000	0.077	0.000	0.077	0.000	0.077
Gun Point	CWPV	2	$3\pi$	8:15	0.046	0.000	0.000	0.077	0.000	0.154	0.077	0.077	0.077	0.000	0.000
Gun Point	CWPV	3	$1\pi$	5:22	0.008	0.000	0.000	0.000	0.000	0.000	0.077	0.000	0.000	0.000	0.000
Gun Point	CWPV	3	$2\pi$	10:22	0.023	0.000	0.000	0.154	0.000	0.000	0.077	0.000	0.000	0.000	0.000
Gun Point	CWPV	3	$3\pi$	10:22	0.046	0.154	0.077	0.077	0.000	0.000	0.000	0.000	0.154	0.000	0.000
Gun Point	CWPV	4	$1\pi$	6:14	<b>0.000</b>	0.000	0.000	0.000	0.000	0.000	0.000	0.000	0.000	0.000	0.000
Gun Point	CWPV	4	$2\pi$	13:29	0.023	0.000	0.000	0.077	0.000	0.000	0.000	0.000	0.077	0.000	0.077
Gun Point	CWPV	4	$3\pi$	13:29	0.054	0.000	0.077	0.231	0.000	0.077	0.000	0.000	0.077	0.077	0.000
Gun Point	CWPV	5	$1\pi$	7:18	<b>0.000</b>	0.000	0.000	0.000	0.000	0.000	0.000	0.000	0.000	0.000	0.000
Gun Point	CWPV	5	$2\pi$	14:36	0.008	0.000	0.000	0.077	0.000	0.000	0.000	0.000	0.000	0.000	0.000
Gun Point	CWPV	5	$3\pi$	20:36	0.039	0.000	0.000	0.077	0.000	0.000	0.077	0.000	0.077	0.077	0.077
Gun Point	CWPV	6	$1\pi$	9:20	<b>0.000</b>	0.000	0.000	0.000	0.000	0.000	0.000	0.000	0.000	0.000	0.000
Gun Point	CWPV	6	$2\pi$	19:43	0.008	0.000	0.000	0.077	0.000	0.000	0.000	0.000	0.000	0.000	0.000
Gun Point	CWPV	6	$3\pi$	19:43	0.023	0.000	0.000	0.077	0.000	0.000	0.077	0.000	0.077	0.000	0.000
Gun Point	CWPV	7	$1\pi$	9:25	<b>0.000</b>	0.000	0.000	0.000	0.000	0.000	0.000	0.000	0.000	0.000	0.000
Gun Point	CWPV	7	$2\pi$	21:50	0.008	0.000	0.000	0.077	0.000	0.000	0.000	0.000	0.000	0.000	0.000
Gun Point	CWPV	7	$3\pi$	22:33	0.039	0.000	0.000	0.077	0.000	0.000	0.077	0.000	0.077	0.077	0.077
Gun Point	CWED	1	$1\pi$	1:4	0.031	0.077	0.000	0.077	0.077	0.077	0.000	0.000	0.000	0.000	0.000
Gun Point	CWED	1	$2\pi$	1:8	0.062	0.000	0.000	0.000	0.077	0.077	0.077	0.077	0.077	0.077	0.154
Gun Point	CWED	1	$3\pi$	1:7	0.054	0.000	0.077	0.000	0.000	0.077	0.000	0.077	0.154	0.077	0.077
Gun Point	CWED	2	$1\pi$	1:15	0.023	0.000	0.000	0.000	0.000	0.000	0.000	0.077	0.000	0.154	0.000
Gun Point	CWED	2	$2\pi$	1:12	0.031	0.000	0.077	0.000	0.000	0.077	0.000	0.077	0.000	0.077	0.000
Gun Point	CWED	2	$3\pi$	1:15	0.039	0.000	0.077	0.000	0.000	0.000	0.077	0.077	0.077	0.000	0.077
Gun Point	CWED	3	$1\pi$	1:17	0.023	0.000	0.000	0.000	0.000	0.000	0.000	0.077	0.000	0.154	0.000
Gun Point	CWED	3	$2\pi$	1:18	0.031	0.000	0.154	0.000	0.000	0.077	0.000	0.000	0.077	0.000	0.000
Gun Point	CWED	3	$3\pi$	1:16	0.039	0.154	0.077	0.000	0.077	0.000	0.000	0.000	0.000	0.000	0.077
Gun Point	CWED	4	$1\pi$	1:29	0.023	0.000	0.077	0.000	0.000	0.077	0.000	0.077	0.000	0.000	0.000
Gun Point	CWED	4	$2\pi$	1:19	0.008	0.000	0.077	0.000	0.000	0.000	0.000	0.000	0.000	0.000	0.000
Gun Point	CWED	4	$3\pi$	1:29	0.015	0.000	0.077	0.000	0.000	0.077	0.000	0.000	0.000	0.000	0.000
Gun Point	CWED	5	$1\pi$	1:36	0.023	0.000	0.077	0.000	0.000	0.077	0.000	0.077	0.000	0.000	0.000
Gun Point	CWED	5	$2\pi$	1:25	0.008	0.000	0.077	0.000	0.000	0.000	0.000	0.000	0.000	0.000	0.000
Gun Point	CWED	5	$3\pi$	1:36	0.015	0.000	0.077	0.000	0.000	0.077	0.000	0.000	0.000	0.000	0.000
Gun Point	CWED	6	$1\pi$	1:43	0.023	0.000	0.077	0.000	0.000	0.077	0.000	0.077	0.000	0.000	0.000
Gun Point	CWED	6	$2\pi$	1:31	0.015	0.000	0.077	0.000	0.000	0.000	0.000	0.000	0.000	0.000	0.077
Gun Point	CWED	6	$3\pi$	1:43	0.015	0.000	0.077	0.000	0.000	0.077	0.000	0.000	0.000	0.000	0.000
Gun Point	CWED	7	$1\pi$	1:50	0.023	0.000	0.077	0.000	0.000	0.077	0.000	0.077	0.000	0.000	0.000
Gun Point	CWED	7	$2\pi$	1:34	0.008	0.000	0.077	0.000	0.000	0.000	0.000	0.000	0.000	0.000	0.000
Gun Point	CWED	7	$3\pi$	1:50	0.015	0.000	0.077	0.000	0.000	0.077	0.000	0.000	0.000	0.000	0.000

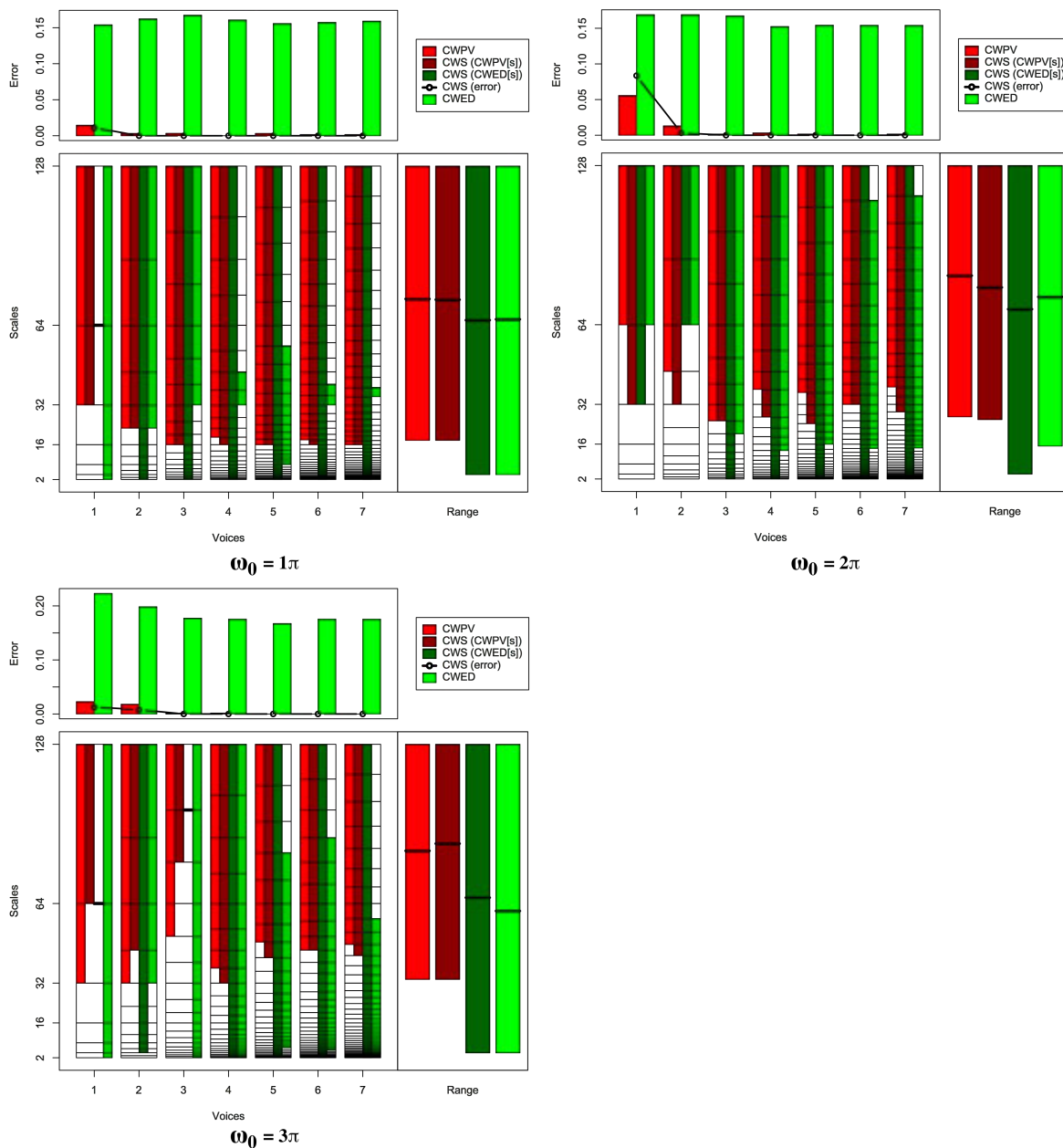


FIGURE B.3: Summary of results for the CBF classification problem comparing CWS, CWPV, CWED methods using 1-7 voices and three  $\omega_0$  values. A lower CWPV score suggests that the problem is predominantly characterised by FM, whereas a lower CWED implies a predominant AM characteristic. The scale ranges have been translated from scale number to scale value. In the bottom right figure of each figure the average range of scales for all 7 voices are presented for each technique.

TABLE B.3: Summary of results for the CBF classification problem comparing Ed, DTW, CWS, CWPV, and CWED using 1-7 voices and 3  $\omega_0$  parameters.  $S$  is the scale set(s) associated with the CWS, CWPV and CWED results. The mean values highlighted in bold are the best in model error rate for the problem.

Problem	Technique	Voices	$\omega_0$	$S$	Mean	1	2	3	4	5	6	7	7	9	10
CBF	Ed				0.006	0.000	0.016	0.000	0.000	0.016	0.016	0.000	0.000	0.016	0.000
CBF	DTW				<b>0.000</b>	0.000	0.000	0.000	0.000	0.000	0.000	0.000	0.000	0.000	0.000
CBF	CWS	1	$1\pi$	5:7,7:7	0.011	0.016	0.016	0.016	0.033	0.016	0.000	0.000	0.000	0.000	0.016
CBF	CWS	1	$2\pi$	5:7,5:7	0.084	0.115	0.098	0.066	0.131	0.049	0.049	0.066	0.098	0.098	0.066
CBF	CWS	1	$3\pi$	6:7,7:7	0.013	0.016	0.000	0.000	0.049	0.016	0.000	0.016	0.016	0.000	0.016
CBF	CWS	2	$1\pi$	8:13,1:13	<b>0.000</b>	0.000	0.000	0.000	0.000	0.000	0.000	0.000	0.000	0.000	0.000
CBF	CWS	2	$2\pi$	9:13,11:13	0.003	0.000	0.000	0.000	0.000	0.033	0.000	0.000	0.000	0.000	0.000
CBF	CWS	2	$3\pi$	10:13,3:13	0.008	0.000	0.000	0.016	0.016	0.000	0.000	0.016	0.016	0.016	0.000
CBF	CWS	3	$1\pi$	10:19,1:19	<b>0.000</b>	0.000	0.000	0.000	0.000	0.000	0.000	0.000	0.000	0.000	0.000
CBF	CWS	3	$2\pi$	12:19,1:19	<b>0.000</b>	0.000	0.000	0.000	0.000	0.000	0.000	0.000	0.000	0.000	0.000
CBF	CWS	3	$3\pi$	17:19,19:19	<b>0.000</b>	0.000	0.000	0.000	0.000	0.000	0.000	0.000	0.000	0.000	0.000
CBF	CWS	4	$1\pi$	13:25,1:25	<b>0.000</b>	0.000	0.000	0.000	0.000	0.000	0.000	0.000	0.000	0.000	0.000
CBF	CWS	4	$2\pi$	16:25,1:25	<b>0.000</b>	0.000	0.000	0.000	0.000	0.000	0.000	0.000	0.000	0.000	0.000
CBF	CWS	4	$3\pi$	17:25,1:25	<b>0.000</b>	0.000	0.000	0.000	0.000	0.000	0.000	0.000	0.000	0.000	0.000
CBF	CWS	5	$1\pi$	16:31,1:31	<b>0.000</b>	0.000	0.000	0.000	0.000	0.000	0.000	0.000	0.000	0.000	0.000
CBF	CWS	5	$2\pi$	19:31,1:31	<b>0.000</b>	0.000	0.000	0.000	0.000	0.000	0.000	0.000	0.000	0.000	0.000
CBF	CWS	5	$3\pi$	23:31,1:31	<b>0.000</b>	0.000	0.000	0.000	0.000	0.000	0.000	0.000	0.000	0.000	0.000
CBF	CWS	6	$1\pi$	19:37,1:37	<b>0.000</b>	0.000	0.000	0.000	0.000	0.000	0.000	0.000	0.000	0.000	0.000
CBF	CWS	6	$2\pi$	25:37,1:37	<b>0.000</b>	0.000	0.000	0.000	0.000	0.000	0.000	0.000	0.000	0.000	0.000
CBF	CWS	6	$3\pi$	28:37,1:37	<b>0.000</b>	0.000	0.000	0.000	0.000	0.000	0.000	0.000	0.000	0.000	0.000
CBF	CWS	7	$1\pi$	22:43,1:43	<b>0.000</b>	0.000	0.000	0.000	0.000	0.000	0.000	0.000	0.000	0.000	0.000
CBF	CWS	7	$2\pi$	28:43,1:43	<b>0.000</b>	0.000	0.000	0.000	0.000	0.000	0.000	0.000	0.000	0.000	0.000
CBF	CWS	7	$3\pi$	32:43,1:43	<b>0.000</b>	0.000	0.000	0.000	0.000	0.000	0.000	0.000	0.000	0.000	0.000
CBF	CWPV	1	$1\pi$	5:7	0.015	0.016	0.016	0.016	0.033	0.016	0.000	0.000	0.000	0.016	0.033
CBF	CWPV	1	$2\pi$	6:7	0.056	0.049	0.016	0.049	0.131	0.066	0.016	0.066	0.049	0.066	0.049
CBF	CWPV	1	$3\pi$	5:7	0.023	0.016	0.000	0.016	0.049	0.033	0.016	0.016	0.033	0.049	0.000
CBF	CWPV	2	$1\pi$	8:13	0.003	0.000	0.000	0.000	0.016	0.016	0.000	0.000	0.000	0.000	0.000
CBF	CWPV	2	$2\pi$	10:13	0.013	0.016	0.000	0.000	0.033	0.066	0.000	0.000	0.000	0.016	0.000
CBF	CWPV	2	$3\pi$	9:13	0.018	0.016	0.000	0.016	0.033	0.033	0.000	0.033	0.016	0.033	0.000
CBF	CWPV	3	$1\pi$	10:19	0.003	0.000	0.000	0.033	0.000	0.000	0.000	0.000	0.000	0.000	0.000
CBF	CWPV	3	$2\pi$	12:19	0.002	0.000	0.000	0.000	0.000	0.000	0.016	0.000	0.000	0.000	0.000
CBF	CWPV	3	$3\pi$	15:19	0.002	0.000	0.000	0.000	0.016	0.000	0.000	0.000	0.000	0.000	0.000
CBF	CWPV	4	$1\pi$	14:25	<b>0.000</b>	0.000	0.000	0.000	0.000	0.000	0.000	0.000	0.000	0.000	0.000
CBF	CWPV	4	$2\pi$	18:25	0.003	0.000	0.000	0.000	0.016	0.000	0.016	0.000	0.000	0.000	0.000
CBF	CWPV	4	$3\pi$	18:25	0.002	0.000	0.000	0.000	0.000	0.000	0.016	0.000	0.000	0.000	0.000
CBF	CWPV	5	$1\pi$	16:31	0.003	0.000	0.016	0.000	0.000	0.000	0.000	0.000	0.016	0.000	0.000
CBF	CWPV	5	$2\pi$	22:31	0.002	0.000	0.000	0.000	0.000	0.000	0.000	0.000	0.000	0.000	0.016
CBF	CWPV	5	$3\pi$	24:31	<b>0.000</b>	0.000	0.000	0.000	0.000	0.000	0.000	0.000	0.000	0.000	0.000
CBF	CWPV	6	$1\pi$	20:37	0.002	0.000	0.000	0.000	0.000	0.016	0.000	0.000	0.000	0.000	0.000
CBF	CWPV	6	$2\pi$	25:37	<b>0.000</b>	0.000	0.000	0.000	0.000	0.000	0.000	0.000	0.000	0.000	0.000
CBF	CWPV	6	$3\pi$	28:37	<b>0.000</b>	0.000	0.000	0.000	0.000	0.000	0.000	0.000	0.000	0.000	0.000
CBF	CWPV	7	$1\pi$	22:43	0.002	0.000	0.016	0.000	0.000	0.000	0.000	0.000	0.000	0.000	0.000
CBF	CWPV	7	$2\pi$	31:43	0.002	0.000	0.000	0.000	0.000	0.016	0.000	0.000	0.000	0.000	0.000
CBF	CWPV	7	$3\pi$	33:43	<b>0.000</b>	0.000	0.000	0.000	0.000	0.000	0.000	0.000	0.000	0.000	0.000
CBF	CWED	1	$1\pi$	1:7	0.154	0.164	0.180	0.180	0.164	0.164	0.164	0.082	0.098	0.180	0.164
CBF	CWED	1	$2\pi$	6:7	0.169	0.115	0.148	0.230	0.197	0.115	0.230	0.180	0.148	0.164	0.164
CBF	CWED	1	$3\pi$	1:7	0.223	0.230	0.197	0.230	0.164	0.262	0.262	0.197	0.197	0.279	0.213
CBF	CWED	2	$1\pi$	8:13	0.162	0.213	0.180	0.180	0.197	0.115	0.164	0.098	0.230	0.115	0.131
CBF	CWED	2	$2\pi$	11:13	0.169	0.115	0.148	0.230	0.197	0.115	0.230	0.180	0.148	0.164	0.164
CBF	CWED	2	$3\pi$	9:13	0.198	0.164	0.213	0.213	0.131	0.230	0.180	0.213	0.197	0.246	0.197
CBF	CWED	3	$1\pi$	13:19	0.167	0.148	0.115	0.230	0.197	0.180	0.213	0.148	0.164	0.164	0.115
CBF	CWED	3	$2\pi$	11:19	0.167	0.148	0.230	0.164	0.082	0.197	0.115	0.180	0.197	0.230	0.131
CBF	CWED	3	$3\pi$	1:19	0.177	0.180	0.213	0.131	0.148	0.230	0.148	0.148	0.246	0.180	0.148
CBF	CWED	4	$1\pi$	17:19	0.161	0.164	0.115	0.197	0.197	0.164	0.213	0.115	0.115	0.164	0.164
CBF	CWED	4	$2\pi$	12:25	0.152	0.180	0.180	0.164	0.066	0.180	0.098	0.180	0.082	0.246	0.148
CBF	CWED	4	$3\pi$	1:25	0.176	0.148	0.230	0.115	0.115	0.213	0.164	0.213	0.213	0.180	0.164
CBF	CWED	5	$1\pi$	11:25	0.156	0.164	0.197	0.164	0.164	0.131	0.066	0.164	0.180	0.197	0.131
CBF	CWED	5	$2\pi$	16:31	0.154	0.148	0.180	0.197	0.066	0.197	0.098	0.148	0.131	0.230	0.148
CBF	CWED	5	$3\pi$	9:28	0.167	0.246	0.148	0.180	0.148	0.197	0.197	0.131	0.115	0.131	0.180
CBF	CWED	6	$1\pi$	25:27	0.157	0.197	0.115	0.197	0.180	0.164	0.115	0.164	0.098	0.164	0.180
CBF	CWED	6	$2\pi$	18:36	0.154	0.131	0.197	0.197	0.049	0.180	0.131	0.148	0.115	0.230	0.164
CBF	CWED	6	$3\pi$	9:34	0.176	0.197	0.246	0.197	0.098	0.197	0.164	0.115	0.213	0.164	0.164
CBF	CWED	7	$1\pi$	30:31	0.159	0.180	0.197	0.197	0.180	0.082	0.197	0.148	0.115	0.164	0.131
CBF	CWED	7	$2\pi$	21:42	0.154	0.164	0.180	0.197	0.049	0.180	0.131	0.131	0.115	0.230	0.164
CBF	CWED	7	$3\pi$	6:35	0.175	0.180	0.213	0.131	0.131	0.197	0.246	0.115	0.180	0.148	0.213



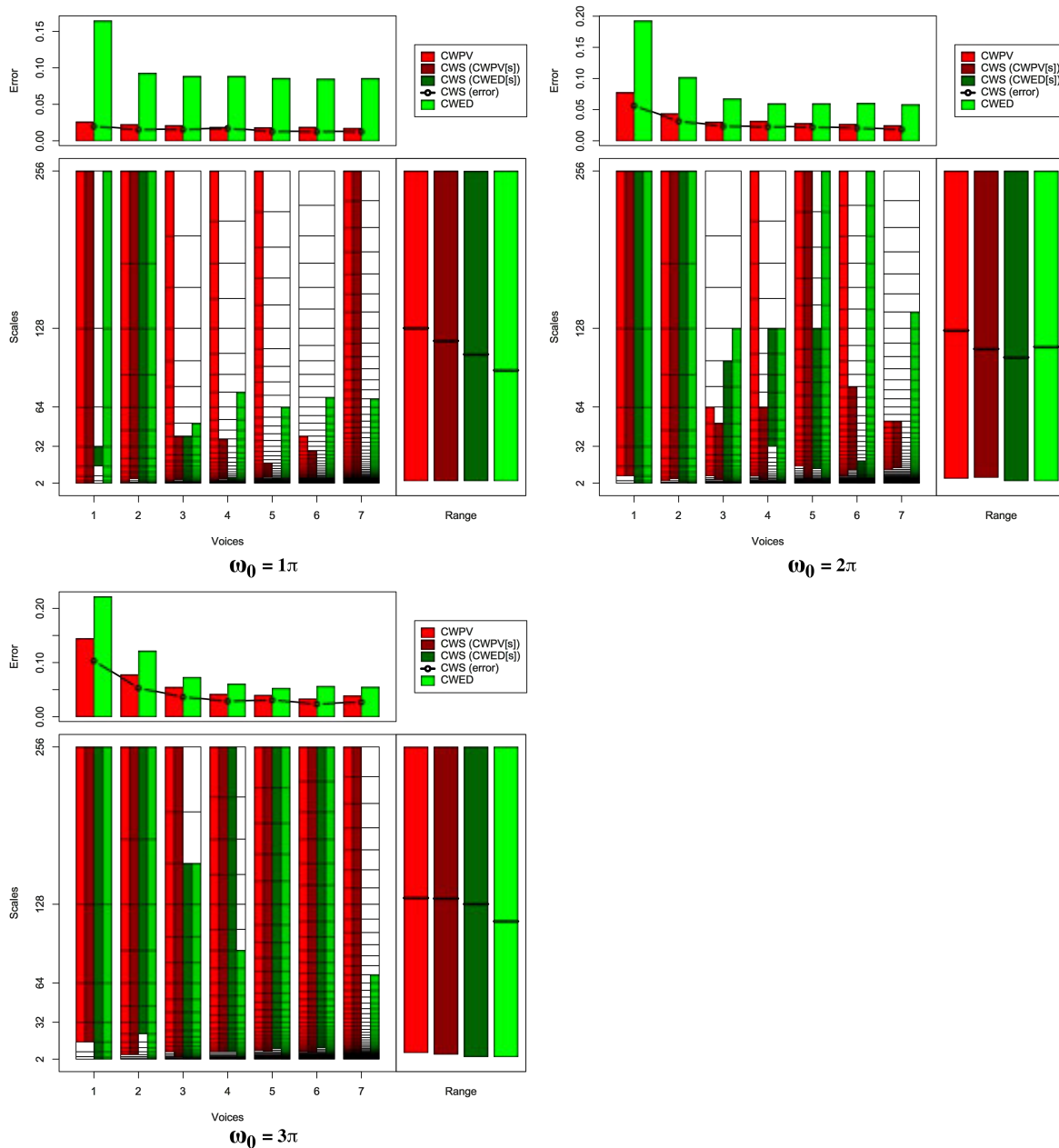


FIGURE B.4: Summary of results for the Face (all) classification problem comparing CWS, CWPV, CWED methods using 1-7 voices and three  $\omega_0$  values. A lower CWPV score suggests that the problem is predominantly characterised by FM, whereas a lower CWED implies a predominant AM characteristic. The scale ranges have been translated from scale number to scale value. In the bottom right figure of each figure the average range of scales for all 7 voices are presented for each technique.

TABLE B.4: Summary of results for the Face (all) classification problem comparing Ed, DTW, CWS, CWPV, and CWED using 1-7 voices and 3  $\omega_0$  parameters.  $S$  is the scale set(s) associated with the CWS, CWPV and CWED results. The mean values highlighted in bold are the best in model error rate for the problem.

Problem	Technique	Voices	$\omega_0$	$S$	Mean	1	2	3	4	5	6	7	7	9	10
Face (All)	Ed				0.046	0.043	0.058	0.022	0.058	0.043	0.036	0.014	0.058	0.058	0.065
Face (All)	DTW				0.039	0.043	0.014	0.029	0.043	0.058	0.014	0.029	0.058	0.043	0.058
Face (All)	CWS	1	$1\pi$	1:8,4:5	0.020	0.022	0.043	0.007	0.022	0.022	0.000	0.000	0.022	0.022	0.043
Face (All)	CWS	1	$2\pi$	3:8,1:8	0.057	0.086	0.065	0.079	0.036	0.094	0.014	0.014	0.079	0.043	0.058
Face (All)	CWS	1	$3\pi$	4:8,1:8	0.104	0.151	0.079	0.151	0.079	0.079	0.079	0.086	0.094	0.158	0.079
Face (All)	CWS	2	$1\pi$	4:15,2:15	0.016	0.014	0.022	0.007	0.029	0.014	0.000	0.007	0.036	0.014	0.014
Face (All)	CWS	2	$2\pi$	4:15,2:15	0.032	0.029	0.036	0.029	0.036	0.058	0.022	0.007	0.029	0.022	0.050
Face (All)	CWS	2	$3\pi$	4:15,8:15	0.053	0.072	0.065	0.043	0.029	0.050	0.050	0.022	0.065	0.058	0.079
Face (All)	CWS	3	$1\pi$	5:14,1:14	0.016	0.029	0.022	0.000	0.036	0.007	0.000	0.000	0.022	0.022	0.022
Face (All)	CWS	3	$2\pi$	5:15,1:18	0.024	0.022	0.029	0.029	0.029	0.029	0.014	0.000	0.029	0.014	0.043
Face (All)	CWS	3	$3\pi$	4:22,1:20	0.037	0.036	0.065	0.022	0.058	0.043	0.022	0.014	0.036	0.036	0.036
Face (All)	CWS	4	$1\pi$	7:18,2:8	0.017	0.029	0.022	0.000	0.029	0.007	0.000	0.000	0.022	0.022	0.043
Face (All)	CWS	4	$2\pi$	6:21,17:25	0.023	0.036	0.029	0.022	0.022	0.029	0.007	0.007	0.022	0.014	0.043
Face (All)	CWS	4	$3\pi$	9:29,9:29	0.029	0.036	0.036	0.022	0.036	0.022	0.022	0.007	0.036	0.022	0.050
Face (All)	CWS	5	$1\pi$	10:17,3:9	0.013	0.022	0.022	0.007	0.022	0.014	0.000	0.000	0.022	0.022	0.000
Face (All)	CWS	5	$2\pi$	8:36,15:31	0.022	0.022	0.036	0.022	0.022	0.022	0.007	0.007	0.014	0.022	0.050
Face (All)	CWS	5	$3\pi$	11:36,13:36	0.031	0.029	0.036	0.022	0.043	0.036	0.014	0.007	0.022	0.043	0.058
Face (All)	CWS	6	$1\pi$	11:24,3:9	0.013	0.022	0.014	0.007	0.022	0.007	0.000	0.007	0.029	0.022	0.000
Face (All)	CWS	6	$2\pi$	17:33,1:21	0.021	0.043	0.022	0.029	0.007	0.022	0.007	0.007	0.022	0.014	0.036
Face (All)	CWS	6	$3\pi$	12:43,16:43	0.024	0.022	0.036	0.022	0.014	0.022	0.014	0.007	0.022	0.029	0.050
Face (All)	CWS	7	$1\pi$	11:50,3:5	<b>0.013</b>	0.022	0.022	0.000	0.029	0.014	0.000	0.000	0.014	0.014	0.014
Face (All)	CWS	7	$2\pi$	21:34,1:11	0.019	0.022	0.007	0.050	0.007	0.022	0.000	0.014	0.036	0.014	0.014
Face (All)	CWS	7	$3\pi$	11:50,3:5	0.027	0.022	0.050	0.036	0.036	0.029	0.000	0.007	0.014	0.029	0.050
Face (All)	CWPV	1	$1\pi$	1:8	0.026	0.029	0.050	0.014	0.036	0.022	0.022	0.000	0.022	0.022	0.043
Face (All)	CWPV	1	$2\pi$	3:8	0.078	0.144	0.065	0.086	0.036	0.144	0.050	0.043	0.094	0.050	0.065
Face (All)	CWPV	1	$3\pi$	4:8	0.144	0.201	0.108	0.194	0.115	0.122	0.122	0.122	0.122	0.216	0.122
Face (All)	CWPV	2	$1\pi$	2:15	0.022	0.014	0.029	0.014	0.022	0.022	0.022	0.007	0.022	0.036	0.036
Face (All)	CWPV	2	$2\pi$	3:15	0.044	0.072	0.058	0.050	0.043	0.043	0.043	0.014	0.014	0.050	0.050
Face (All)	CWPV	2	$3\pi$	4:15	0.078	0.101	0.086	0.072	0.058	0.108	0.079	0.022	0.079	0.086	0.086
Face (All)	CWPV	3	$1\pi$	2:22	0.021	0.022	0.036	0.014	0.022	0.022	0.014	0.007	0.022	0.022	0.029
Face (All)	CWPV	3	$2\pi$	7:16	0.030	0.036	0.036	0.036	0.036	0.050	0.000	0.007	0.029	0.036	0.036
Face (All)	CWPV	3	$3\pi$	7:22	0.055	0.094	0.043	0.050	0.043	0.050	0.043	0.022	0.043	0.086	0.072
Face (All)	CWPV	4	$1\pi$	5:29	0.019	0.014	0.029	0.014	0.022	0.014	0.014	0.007	0.014	0.036	0.022
Face (All)	CWPV	4	$2\pi$	9:29	0.032	0.036	0.036	0.036	0.022	0.050	0.007	0.007	0.029	0.043	0.050
Face (All)	CWPV	4	$3\pi$	9:29	0.042	0.086	0.036	0.043	0.029	0.036	0.043	0.022	0.022	0.050	0.050
Face (All)	CWPV	5	$1\pi$	7:36	0.018	0.022	0.022	0.014	0.022	0.022	0.000	0.007	0.022	0.036	0.014
Face (All)	CWPV	5	$2\pi$	16:36	0.028	0.043	0.022	0.043	0.007	0.036	0.007	0.007	0.043	0.022	0.050
Face (All)	CWPV	5	$3\pi$	12:36	0.040	0.058	0.036	0.043	0.043	0.043	0.022	0.022	0.029	0.036	0.065
Face (All)	CWPV	6	$1\pi$	9:27	0.019	0.029	0.014	0.014	0.029	0.022	0.000	0.007	0.022	0.036	0.014
Face (All)	CWPV	6	$2\pi$	13:43	0.027	0.036	0.043	0.029	0.029	0.029	0.014	0.007	0.014	0.022	0.043
Face (All)	CWPV	6	$3\pi$	13:43	0.033	0.058	0.043	0.014	0.029	0.036	0.014	0.007	0.029	0.050	0.050
Face (All)	CWPV	7	$1\pi$	11:50	0.017	0.029	0.014	0.014	0.036	0.022	0.000	0.007	0.014	0.029	0.007
Face (All)	CWPV	7	$2\pi$	20:34	0.025	0.029	0.022	0.043	0.036	0.029	0.007	0.014	0.029	0.014	0.022
Face (All)	CWPV	7	$3\pi$	11:50	0.039	0.079	0.050	0.036	0.029	0.043	0.000	0.014	0.036	0.043	0.058
Face (All)	CWED	1	$1\pi$	1:8	0.165	0.173	0.173	0.201	0.151	0.165	0.137	0.144	0.165	0.180	0.158
Face (All)	CWED	1	$2\pi$	1:8	0.193	0.223	0.180	0.194	0.187	0.209	0.165	0.180	0.187	0.187	0.216
Face (All)	CWED	1	$3\pi$	1:8	0.222	0.266	0.165	0.252	0.209	0.209	0.252	0.230	0.173	0.281	0.180
Face (All)	CWED	2	$1\pi$	1:15	0.093	0.101	0.058	0.144	0.086	0.122	0.079	0.086	0.086	0.072	0.094
Face (All)	CWED	2	$2\pi$	1:15	0.102	0.115	0.065	0.129	0.086	0.129	0.086	0.115	0.086	0.079	0.129
Face (All)	CWED	2	$3\pi$	1:15	0.122	0.151	0.129	0.158	0.108	0.108	0.122	0.129	0.094	0.122	0.094
Face (All)	CWED	3	$1\pi$	3:15	0.089	0.086	0.065	0.137	0.086	0.122	0.058	0.086	0.094	0.086	0.065
Face (All)	CWED	3	$2\pi$	2:19	0.068	0.079	0.043	0.086	0.086	0.101	0.043	0.079	0.043	0.050	0.065
Face (All)	CWED	3	$3\pi$	1:20	0.073	0.094	0.050	0.115	0.072	0.086	0.043	0.072	0.065	0.072	0.058
Face (All)	CWED	4	$1\pi$	3:22	0.089	0.086	0.065	0.158	0.079	0.115	0.058	0.086	0.086	0.094	0.058
Face (All)	CWED	4	$2\pi$	1:25	0.060	0.072	0.029	0.079	0.065	0.101	0.036	0.050	0.050	0.050	0.065
Face (All)	CWED	4	$3\pi$	1:23	0.061	0.086	0.043	0.065	0.094	0.072	0.043	0.036	0.058	0.058	0.050
Face (All)	CWED	5	$1\pi$	3:26	0.086	0.094	0.065	0.158	0.079	0.122	0.058	0.065	0.079	0.072	0.065
Face (All)	CWED	5	$2\pi$	1:36	0.060	0.072	0.029	0.072	0.072	0.108	0.036	0.050	0.050	0.050	0.058
Face (All)	CWED	5	$3\pi$	1:36	0.053	0.050	0.029	0.072	0.065	0.072	0.036	0.036	0.058	0.050	0.058
Face (All)	CWED	6	$1\pi$	2:32	0.085	0.086	0.065	0.137	0.072	0.115	0.058	0.072	0.079	0.079	0.086
Face (All)	CWED	6	$2\pi$	1:43	0.060	0.079	0.036	0.079	0.072	0.101	0.036	0.050	0.050	0.043	0.058
Face (All)	CWED	6	$3\pi$	5:43	0.056	0.050	0.036	0.108	0.072	0.072	0.029	0.036	0.058	0.043	0.058
Face (All)	CWED	7	$1\pi$	2:37	0.086	0.086	0.072	0.137	0.072	0.122	0.058	0.065	0.079	0.079	0.086
Face (All)	CWED	7	$2\pi$	1:44	0.058	0.072	0.029	0.072	0.072	0.101	0.036	0.050	0.050	0.043	0.058
Face (All)	CWED	7	$3\pi$	2:37	0.055	0.058	0.029	0.094	0.072	0.079	0.036	0.029	0.058	0.036	0.058

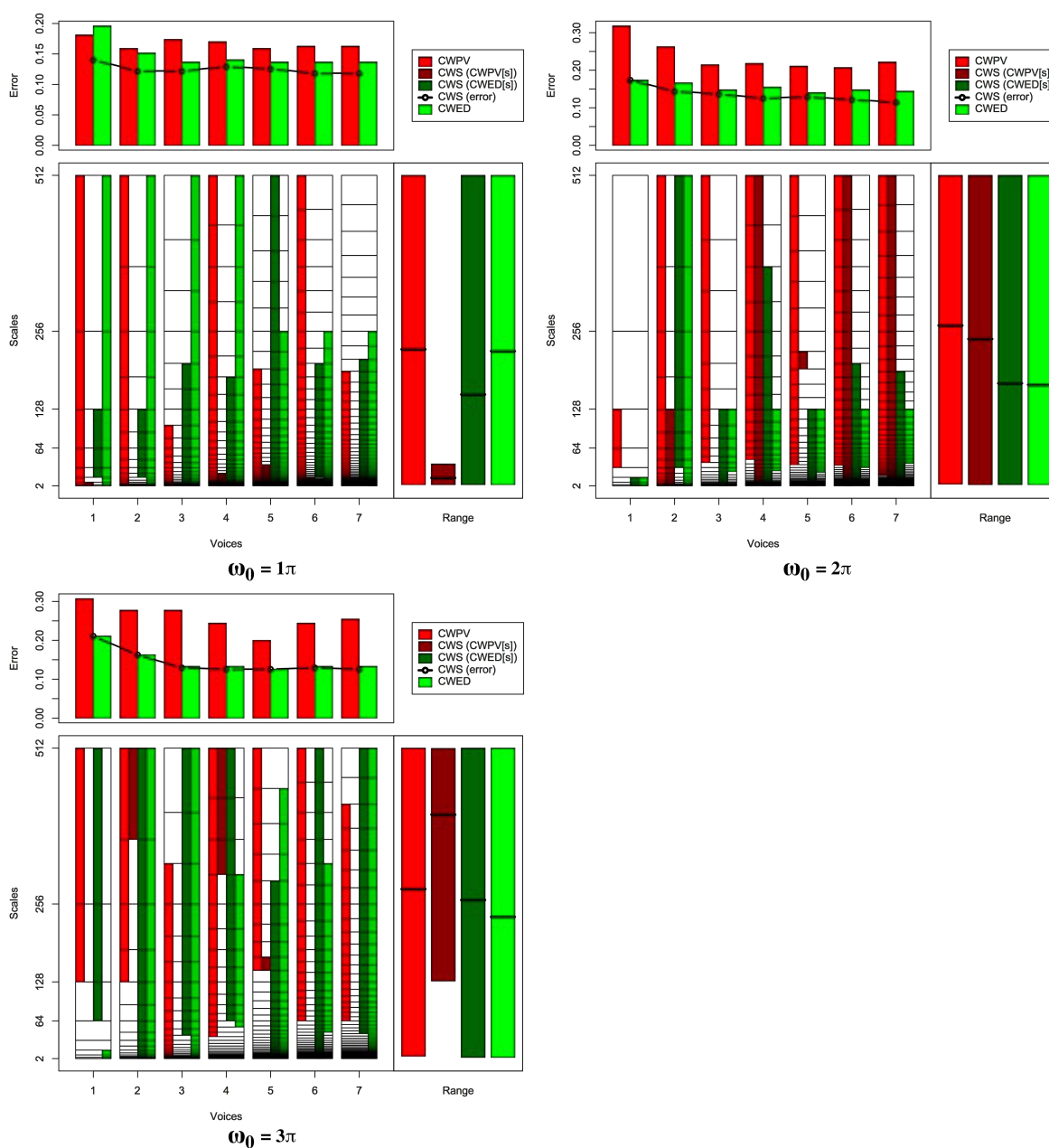


FIGURE B.5: Summary of results for the OSU Leaf classification problem comparing CWS, CWPV, CWED methods using 1-7 voices and three  $\omega_0$  values. A lower CWPV score suggests that the problem is predominantly characterised by FM, whereas a lower CWED implies a predominant AM characteristic. The scale ranges have been translated from scale number to scale value. In the bottom right figure of each figure the average range of scales for all 7 voices are presented for each technique.

TABLE B.5: Summary of results for the OSU Leaf classification problem comparing Ed, DTW, CWS, CWPV, and CWED using 1-7 voices and  $3 \omega_0$  parameters.  $S$  is the scale set(s) associated with the CWS, CWPV and CWED results. The mean values highlighted in bold are the best in model error rate for the problem.

Problem	Technique	Voices	$\omega_0$	$S$	Mean	1	2	3	4	5	6	7	7	9	10
OSU Leaf	Ed				0.192	0.185	0.185	0.111	0.296	0.222	0.148	0.185	0.222	0.111	0.259
OSU Leaf	DTW				0.189	0.074	0.185	0.111	0.296	0.259	0.185	0.185	0.259	0.111	0.222
OSU Leaf	CWS	1	$1\pi$	1:3,4:7	0.141	0.074	0.185	0.074	0.148	0.185	0.185	0.148	0.185	0.111	0.111
OSU Leaf	CWS	1	$2\pi$	9:9,1:4	0.174	0.148	0.185	0.111	0.222	0.333	0.111	0.185	0.148	0.148	0.148
OSU Leaf	CWS	1	$3\pi$	7:7,6:9	0.211	0.148	0.296	0.111	0.333	0.259	0.259	0.111	0.185	0.185	0.222
OSU Leaf	CWS	2	$1\pi$	1:1,7:13	0.122	0.074	0.185	0.074	0.074	0.074	0.148	0.185	0.148	0.111	0.148
OSU Leaf	CWS	2	$2\pi$	2:13,9:17	0.144	0.037	0.111	0.000	0.222	0.222	0.185	0.148	0.222	0.074	0.222
OSU Leaf	CWS	2	$3\pi$	16:17,1:17	0.163	0.111	0.333	0.148	0.074	0.222	0.148	0.185	0.148	0.111	0.148
OSU Leaf	CWS	3	$1\pi$	1:1,1:21	0.122	0.074	0.148	0.074	0.111	0.074	0.148	0.185	0.148	0.074	0.185
OSU Leaf	CWS	3	$2\pi$	22:22,1:19	0.137	0.111	0.222	0.074	0.074	0.148	0.074	0.111	0.222	0.259	0.074
OSU Leaf	CWS	3	$3\pi$	21:21,14:25	0.130	0.148	0.148	0.074	0.037	0.222	0.074	0.148	0.185	0.111	0.148
OSU Leaf	CWS	4	$1\pi$	1:15,1:27	0.130	0.074	0.185	0.074	0.111	0.074	0.148	0.185	0.148	0.111	0.185
OSU Leaf	CWS	4	$2\pi$	2:33,1:31	0.126	0.037	0.111	0.074	0.111	0.148	0.148	0.111	0.222	0.074	0.222
OSU Leaf	CWS	4	$3\pi$	30:33,21:33	0.126	0.074	0.148	0.074	0.111	0.148	0.111	0.037	0.222	0.185	0.148
OSU Leaf	CWS	5	$1\pi$	1:22,1:41	0.126	0.037	0.111	0.074	0.185	0.111	0.148	0.111	0.222	0.074	0.185
OSU Leaf	CWS	5	$2\pi$	34:35,1:31	0.130	0.111	0.111	0.148	0.074	0.185	0.074	0.037	0.259	0.185	0.111
OSU Leaf	CWS	5	$3\pi$	32:33,1:37	0.126	0.148	0.074	0.111	0.037	0.185	0.111	0.148	0.074	0.185	0.185
OSU Leaf	CWS	6	$1\pi$	4:19,19:41	0.118	0.037	0.111	0.074	0.111	0.148	0.222	0.037	0.222	0.074	0.148
OSU Leaf	CWS	6	$2\pi$	1:49,17:41	0.122	0.037	0.074	0.037	0.111	0.148	0.111	0.148	0.259	0.074	0.222
OSU Leaf	CWS	6	$3\pi$	41:41,1:49	0.130	0.148	0.185	0.148	0.037	0.185	0.037	0.074	0.185	0.148	0.148
OSU Leaf	CWS	7	$1\pi$	4:22,14:48	0.118	0.037	0.111	0.074	0.111	0.148	0.185	0.074	0.222	0.074	0.148
OSU Leaf	CWS	7	$2\pi$	7:57,1:47	<b>0.115</b>	0.074	0.111	0.037	0.148	0.148	0.074	0.111	0.148	0.074	0.222
OSU Leaf	CWS	7	$3\pi$	45:45,32:57	0.126	0.148	0.148	0.074	0.037	0.222	0.037	0.148	0.148	0.148	0.148
OSU Leaf	CWPV	1	$1\pi$	1:9	0.181	0.148	0.148	0.074	0.185	0.296	0.259	0.148	0.185	0.111	0.259
OSU Leaf	CWPV	1	$2\pi$	5:7	0.318	0.333	0.370	0.111	0.481	0.259	0.444	0.185	0.481	0.259	0.259
OSU Leaf	CWPV	1	$3\pi$	7:9	0.307	0.370	0.333	0.333	0.259	0.259	0.407	0.259	0.222	0.259	0.370
OSU Leaf	CWPV	2	$1\pi$	1:17	0.159	0.148	0.111	0.111	0.148	0.259	0.185	0.111	0.185	0.148	0.185
OSU Leaf	CWPV	2	$2\pi$	2:17	0.263	0.259	0.370	0.074	0.370	0.259	0.296	0.222	0.370	0.148	0.259
OSU Leaf	CWPV	2	$3\pi$	13:17	0.278	0.259	0.333	0.296	0.259	0.296	0.333	0.296	0.259	0.148	0.296
OSU Leaf	CWPV	3	$1\pi$	3:18	0.174	0.148	0.111	0.111	0.111	0.259	0.296	0.148	0.222	0.111	0.222
OSU Leaf	CWPV	3	$2\pi$	14:25	0.215	0.185	0.333	0.111	0.222	0.259	0.222	0.111	0.296	0.148	0.259
OSU Leaf	CWPV	3	$3\pi$	4:23	0.278	0.333	0.444	0.148	0.370	0.296	0.259	0.185	0.259	0.185	0.296
OSU Leaf	CWPV	4	$1\pi$	3:33	0.170	0.185	0.111	0.074	0.148	0.185	0.259	0.148	0.222	0.111	0.259
OSU Leaf	CWPV	4	$2\pi$	19:33	0.218	0.259	0.259	0.185	0.333	0.222	0.259	0.148	0.222	0.111	0.185
OSU Leaf	CWPV	4	$3\pi$	18:33	0.244	0.185	0.259	0.185	0.407	0.296	0.259	0.148	0.259	0.111	0.333
OSU Leaf	CWPV	5	$1\pi$	4:34	0.159	0.185	0.111	0.074	0.148	0.222	0.259	0.074	0.222	0.074	0.222
OSU Leaf	CWPV	5	$2\pi$	22:41	0.211	0.148	0.296	0.111	0.296	0.259	0.222	0.111	0.296	0.074	0.296
OSU Leaf	CWPV	5	$3\pi$	32:41	0.200	0.333	0.148	0.185	0.185	0.296	0.148	0.222	0.111	0.148	0.222
OSU Leaf	CWPV	6	$1\pi$	7:49	0.163	0.148	0.111	0.074	0.148	0.222	0.259	0.074	0.222	0.111	0.259
OSU Leaf	CWPV	6	$2\pi$	26:49	0.207	0.185	0.296	0.111	0.296	0.222	0.185	0.074	0.296	0.074	0.333
OSU Leaf	CWPV	6	$3\pi$	31:49	0.244	0.222	0.370	0.185	0.370	0.259	0.296	0.185	0.185	0.111	0.259
OSU Leaf	CWPV	7	$1\pi$	4:47	0.163	0.148	0.111	0.074	0.148	0.222	0.259	0.111	0.222	0.074	0.259
OSU Leaf	CWPV	7	$2\pi$	24:57	0.222	0.185	0.407	0.111	0.259	0.259	0.111	0.111	0.296	0.148	0.333
OSU Leaf	CWPV	7	$3\pi$	36:55	0.255	0.259	0.333	0.185	0.333	0.333	0.296	0.148	0.259	0.111	0.290
OSU Leaf	CWED	1	$1\pi$	1:9	0.196	0.074	0.296	0.148	0.222	0.296	0.148	0.148	0.259	0.185	0.185
OSU Leaf	CWED	1	$2\pi$	1:4	0.174	0.148	0.185	0.111	0.222	0.333	0.111	0.185	0.148	0.148	0.148
OSU Leaf	CWED	1	$3\pi$	1:4	0.211	0.111	0.296	0.259	0.148	0.333	0.185	0.259	0.074	0.222	0.222
OSU Leaf	CWED	2	$1\pi$	1:17	0.152	0.111	0.259	0.074	0.111	0.185	0.111	0.185	0.222	0.074	0.185
OSU Leaf	CWED	2	$2\pi$	1:17	0.167	0.148	0.222	0.074	0.111	0.185	0.185	0.185	0.185	0.185	0.185
OSU Leaf	CWED	2	$3\pi$	1:17	0.163	0.111	0.333	0.148	0.074	0.222	0.148	0.185	0.148	0.111	0.148
OSU Leaf	CWED	3	$1\pi$	1:25	0.137	0.074	0.259	0.074	0.148	0.148	0.111	0.148	0.185	0.037	0.185
OSU Leaf	CWED	3	$2\pi$	12:19	0.148	0.111	0.222	0.074	0.074	0.185	0.111	0.148	0.259	0.222	0.074
OSU Leaf	CWED	3	$3\pi$	1:25	0.133	0.148	0.148	0.074	0.037	0.222	0.074	0.185	0.185	0.074	0.185
OSU Leaf	CWED	4	$1\pi$	1:33	0.141	0.074	0.259	0.074	0.148	0.185	0.111	0.148	0.185	0.074	0.148
OSU Leaf	CWED	4	$2\pi$	16:25	0.155	0.111	0.148	0.185	0.111	0.222	0.111	0.074	0.259	0.222	0.111
OSU Leaf	CWED	4	$3\pi$	20:30	0.133	0.185	0.148	0.074	0.037	0.222	0.037	0.148	0.185	0.111	0.185
OSU Leaf	CWED	5	$1\pi$	1:36	0.137	0.074	0.259	0.074	0.111	0.185	0.111	0.148	0.185	0.074	0.148
OSU Leaf	CWED	5	$2\pi$	19:31	0.141	0.111	0.111	0.185	0.074	0.222	0.111	0.037	0.259	0.185	0.111
OSU Leaf	CWED	5	$3\pi$	1:40	0.126	0.148	0.148	0.074	0.037	0.185	0.037	0.148	0.185	0.111	0.185
OSU Leaf	CWED	6	$1\pi$	1:43	0.137	0.074	0.259	0.074	0.111	0.185	0.111	0.148	0.185	0.074	0.148
OSU Leaf	CWED	6	$2\pi$	25:37	0.148	0.111	0.111	0.185	0.111	0.222	0.148	0.037	0.259	0.185	0.111
OSU Leaf	CWED	6	$3\pi$	28:45	0.133	0.148	0.148	0.111	0.037	0.222	0.037	0.148	0.185	0.111	0.185
OSU Leaf	CWED	7	$1\pi$	1:50	0.137	0.074	0.259	0.074	0.111	0.185	0.111	0.148	0.185	0.074	0.148
OSU Leaf	CWED	7	$2\pi$	31:43	0.144	0.111	0.111	0.185	0.111	0.222	0.148	0.037	0.222	0.185	0.111
OSU Leaf	CWED	7	$3\pi$	1:57	0.133	0.148	0.148	0.111	0.037	0.222	0.037	0.148	0.185	0.148	0.148

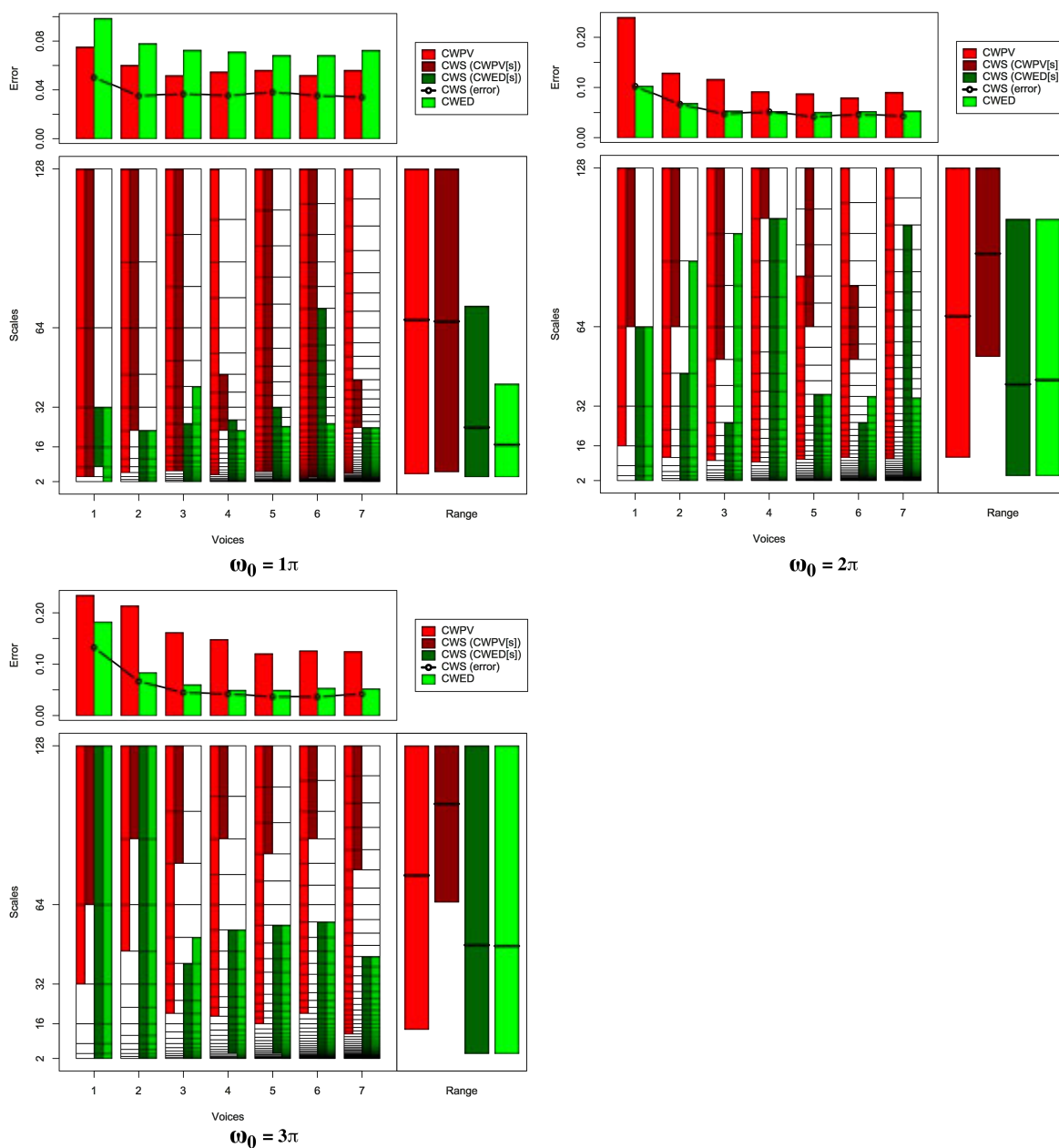


FIGURE B.6: Summary of results for the Swedish Leaf classification problem comparing CWS, CWPV, CWED methods using 1-7 voices and three  $\omega_0$  values. A lower CWPV score suggests that the problem is predominantly characterised by FM, whereas a lower CWED implies a predominant AM characteristic. The scale ranges have been translated from scale number to scale value. In the bottom right figure of each figure the average range of scales for all 7 voices are presented for each technique.

TABLE B.6: Summary of results for the Swedish Leaf classification problem comparing Ed, DTW, CWS, CWPV, and CWED using 1-7 voices and  $3 \omega_0$  parameters.  $S$  is the scale set(s) associated with the CWS, CWPV and CWED results. The mean values highlighted in bold are the best in model error rate for the problem.

Problem	Technique	Voices	$\omega_0$	$S$	Mean	1	2	3	4	5	6	7	7	9	10
Swedish Leaf	Ed				0.092	0.082	0.068	0.096	0.096	0.082	0.110	0.096	0.068	0.164	0.055
Swedish Leaf	DTW				0.100	0.151	0.068	0.137	0.123	0.123	0.082	0.096	0.068	0.068	0.082
Swedish Leaf	CWS	1	$1\pi$	2:7,3:5	0.050	0.027	0.027	0.055	0.068	0.082	0.068	0.068	0.000	0.041	0.068
Swedish Leaf	CWS	1	$2\pi$	6:7,1:6	0.103	0.123	0.082	0.151	0.110	0.096	0.068	0.123	0.068	0.096	0.110
Swedish Leaf	CWS	1	$3\pi$	6:7,1:7	0.133	0.178	0.137	0.110	0.137	0.123	0.110	0.151	0.110	0.151	0.123
Swedish Leaf	CWS	2	$1\pi$	8:13,1:8	0.035	0.068	0.041	0.055	0.027	0.068	0.027	0.041	0.000	0.000	0.027
Swedish Leaf	CWS	2	$2\pi$	11:13,1:10	0.067	0.082	0.055	0.082	0.096	0.041	0.041	0.068	0.014	0.110	0.082
Swedish Leaf	CWS	2	$3\pi$	12:13,1:13	0.067	0.110	0.055	0.082	0.068	0.055	0.027	0.096	0.041	0.055	0.082
Swedish Leaf	CWS	3	$1\pi$	6:19,1:12	0.037	0.027	0.055	0.027	0.027	0.055	0.027	0.082	0.000	0.027	0.041
Swedish Leaf	CWS	3	$2\pi$	15:19,1:12	0.048	0.027	0.041	0.055	0.082	0.068	0.041	0.014	0.068	0.055	0.027
Swedish Leaf	CWS	3	$3\pi$	17:19,1:14	0.045	0.055	0.027	0.027	0.041	0.068	0.055	0.027	0.068	0.055	0.027
Swedish Leaf	CWS	4	$1\pi$	15:19,1:16	0.036	0.068	0.041	0.055	0.027	0.082	0.014	0.055	0.000	0.000	0.014
Swedish Leaf	CWS	4	$2\pi$	24:25,1:24	0.052	0.082	0.041	0.082	0.041	0.082	0.014	0.041	0.041	0.055	0.041
Swedish Leaf	CWS	4	$3\pi$	23:25,5:20	0.042	0.041	0.014	0.027	0.027	0.068	0.041	0.110	0.041	0.014	0.041
Swedish Leaf	CWS	5	$1\pi$	9:31,1:21	0.038	0.014	0.041	0.027	0.027	0.055	0.041	0.096	0.000	0.041	0.041
Swedish Leaf	CWS	5	$2\pi$	26:31,1:22	0.042	0.027	0.027	0.041	0.041	0.041	0.041	0.082	0.027	0.055	0.041
Swedish Leaf	CWS	5	$3\pi$	28:31,6:25	0.037	0.068	0.014	0.027	0.014	0.041	0.027	0.082	0.027	0.014	0.055
Swedish Leaf	CWS	6	$1\pi$	7:37,4:32	0.036	0.014	0.041	0.027	0.055	0.041	0.041	0.068	0.000	0.041	0.027
Swedish Leaf	CWS	6	$2\pi$	29:33,1:23	0.047	0.041	0.041	0.055	0.055	0.055	0.027	0.014	0.068	0.082	0.027
Swedish Leaf	CWS	6	$3\pi$	34:37,1:30	0.037	0.068	0.041	0.027	0.027	0.068	0.027	0.055	0.000	0.014	0.041
Swedish Leaf	CWS	7	$1\pi$	26:32,1:26	<b>0.034</b>	0.055	0.041	0.041	0.027	0.068	0.000	0.068	0.014	0.014	0.014
Swedish Leaf	CWS	7	$2\pi$	39:39,1:41	0.044	0.041	0.041	0.041	0.041	0.082	0.041	0.027	0.041	0.055	0.027
Swedish Leaf	CWS	7	$3\pi$	38:43,1:32	0.042	0.041	0.027	0.027	0.027	0.068	0.055	0.068	0.041	0.027	0.041
Swedish Leaf	CWPV	1	$1\pi$	2:7	0.075	0.041	0.055	0.110	0.096	0.082	0.068	0.096	0.068	0.068	0.068
Swedish Leaf	CWPV	1	$2\pi$	4:7	0.240	0.247	0.219	0.219	0.219	0.233	0.219	0.288	0.233	0.233	0.288
Swedish Leaf	CWPV	1	$3\pi$	5:7	0.234	0.247	0.205	0.219	0.301	0.288	0.274	0.151	0.205	0.219	0.233
Swedish Leaf	CWPV	2	$1\pi$	4:13	0.060	0.041	0.041	0.027	0.082	0.096	0.055	0.123	0.014	0.055	0.068
Swedish Leaf	CWPV	2	$2\pi$	6:13	0.129	0.137	0.096	0.151	0.192	0.096	0.123	0.137	0.123	0.096	0.137
Swedish Leaf	CWPV	2	$3\pi$	10:13	0.214	0.164	0.178	0.151	0.247	0.260	0.233	0.192	0.247	0.247	0.219
Swedish Leaf	CWPV	3	$1\pi$	6:19	0.052	0.041	0.082	0.027	0.027	0.068	0.027	0.123	0.027	0.041	0.055
Swedish Leaf	CWPV	3	$2\pi$	8:19	0.116	0.151	0.082	0.123	0.082	0.082	0.151	0.110	0.178	0.082	0.123
Swedish Leaf	CWPV	3	$3\pi$	11:19	0.162	0.123	0.151	0.205	0.123	0.205	0.205	0.151	0.192	0.151	0.110
Swedish Leaf	CWPV	4	$1\pi$	6:25	0.055	0.055	0.041	0.055	0.068	0.082	0.055	0.110	0.014	0.041	0.027
Swedish Leaf	CWPV	4	$2\pi$	10:25	0.092	0.096	0.068	0.082	0.096	0.068	0.123	0.096	0.110	0.096	0.082
Swedish Leaf	CWPV	4	$3\pi$	14:25	0.148	0.192	0.151	0.123	0.164	0.137	0.178	0.151	0.137	0.137	0.110
Swedish Leaf	CWPV	5	$1\pi$	9:31	0.056	0.068	0.055	0.041	0.055	0.055	0.041	0.110	0.027	0.068	0.041
Swedish Leaf	CWPV	5	$2\pi$	13:28	0.088	0.123	0.096	0.110	0.082	0.082	0.096	0.068	0.110	0.041	0.068
Swedish Leaf	CWPV	5	$3\pi$	16:31	0.121	0.137	0.068	0.164	0.110	0.110	0.137	0.123	0.178	0.096	0.082
Swedish Leaf	CWPV	6	$1\pi$	5:37	0.052	0.027	0.055	0.082	0.068	0.068	0.041	0.096	0.014	0.041	0.027
Swedish Leaf	CWPV	6	$2\pi$	16:37	0.080	0.082	0.110	0.055	0.082	0.055	0.110	0.068	0.096	0.041	0.096
Swedish Leaf	CWPV	6	$3\pi$	21:37	0.126	0.164	0.164	0.137	0.096	0.082	0.137	0.137	0.137	0.110	0.096
Swedish Leaf	CWPV	7	$1\pi$	11:43	0.056	0.055	0.068	0.041	0.055	0.055	0.041	0.123	0.014	0.041	0.068
Swedish Leaf	CWPV	7	$2\pi$	18:43	0.090	0.123	0.123	0.055	0.082	0.055	0.151	0.096	0.096	0.055	0.068
Swedish Leaf	CWPV	7	$3\pi$	19:43	0.125	0.137	0.096	0.096	0.137	0.123	0.137	0.151	0.164	0.110	0.096
Swedish Leaf	CWED	1	$1\pi$	1:5	0.099	0.123	0.027	0.123	0.110	0.096	0.082	0.123	0.082	0.110	0.110
Swedish Leaf	CWED	1	$2\pi$	1:6	0.103	0.123	0.082	0.151	0.110	0.096	0.068	0.123	0.068	0.096	0.110
Swedish Leaf	CWED	1	$3\pi$	1:7	0.182	0.192	0.219	0.164	0.151	0.192	0.164	0.178	0.151	0.192	0.219
Swedish Leaf	CWED	2	$1\pi$	1:8	0.078	0.123	0.082	0.110	0.068	0.068	0.055	0.096	0.055	0.055	0.068
Swedish Leaf	CWED	2	$2\pi$	1:12	0.069	0.123	0.055	0.082	0.055	0.068	0.055	0.096	0.041	0.055	0.055
Swedish Leaf	CWED	2	$3\pi$	1:13	0.084	0.151	0.068	0.110	0.082	0.055	0.041	0.082	0.068	0.055	0.123
Swedish Leaf	CWED	3	$1\pi$	1:14	0.073	0.110	0.068	0.110	0.096	0.068	0.014	0.082	0.055	0.068	0.055
Swedish Leaf	CWED	3	$2\pi$	1:18	0.053	0.082	0.041	0.055	0.041	0.068	0.014	0.068	0.055	0.027	0.082
Swedish Leaf	CWED	3	$3\pi$	1:15	0.060	0.041	0.068	0.055	0.068	0.068	0.055	0.082	0.041	0.055	0.068
Swedish Leaf	CWED	4	$1\pi$	1:15	0.071	0.096	0.068	0.096	0.110	0.055	0.041	0.055	0.041	0.082	0.068
Swedish Leaf	CWED	4	$2\pi$	1:24	0.052	0.082	0.041	0.082	0.041	0.082	0.014	0.041	0.041	0.055	0.041
Swedish Leaf	CWED	4	$3\pi$	1:20	0.049	0.041	0.027	0.041	0.068	0.055	0.055	0.082	0.055	0.014	0.055
Swedish Leaf	CWED	5	$1\pi$	1:19	0.068	0.068	0.068	0.096	0.110	0.041	0.041	0.068	0.055	0.068	0.068
Swedish Leaf	CWED	5	$2\pi$	1:22	0.051	0.041	0.055	0.082	0.041	0.027	0.027	0.082	0.055	0.041	0.055
Swedish Leaf	CWED	5	$3\pi$	1:25	0.049	0.055	0.027	0.041	0.055	0.041	0.027	0.096	0.055	0.014	0.082
Swedish Leaf	CWED	6	$1\pi$	1:23	0.068	0.082	0.068	0.096	0.110	0.027	0.041	0.068	0.055	0.068	0.068
Swedish Leaf	CWED	6	$2\pi$	1:26	0.052	0.041	0.055	0.082	0.041	0.041	0.027	0.068	0.055	0.055	0.055
Swedish Leaf	CWED	6	$3\pi$	1:30	0.053	0.068	0.041	0.096	0.055	0.055	0.027	0.055	0.027	0.014	0.096
Swedish Leaf	CWED	7	$1\pi$	1:26	0.073	0.096	0.068	0.096	0.110	0.055	0.041	0.068	0.055	0.068	0.068
Swedish Leaf	CWED	7	$2\pi$	1:30	0.053	0.041	0.068	0.082	0.041	0.041	0.027	0.068	0.055	0.055	0.055
Swedish Leaf	CWED	7	$3\pi$	1:32	0.052	0.041	0.055	0.041	0.055	0.041	0.055	0.068	0.055	0.068	0.041

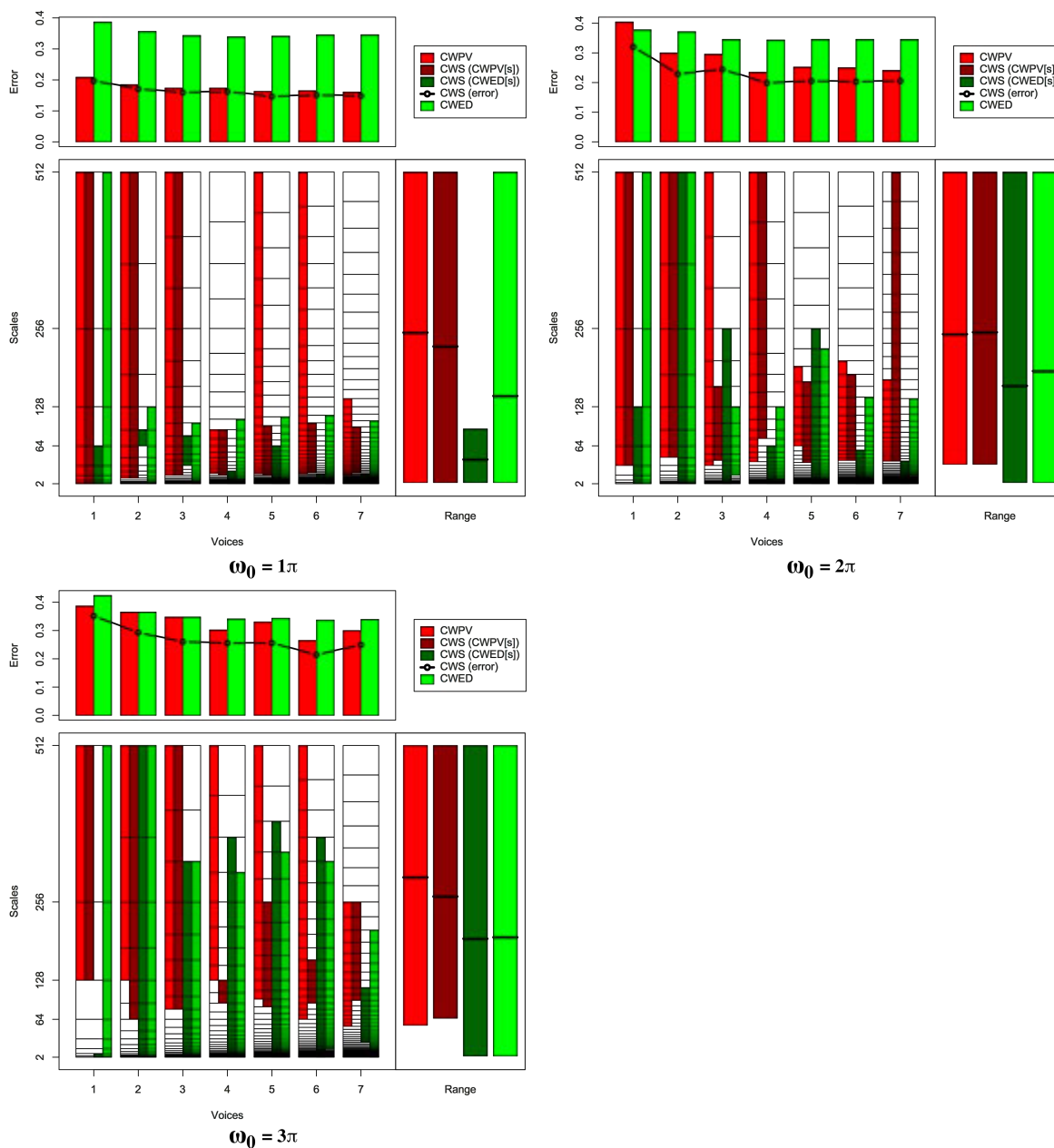


FIGURE B.7: Summary of results for the 50words classification problem comparing CWS, CWPV, CWED methods using 1-7 voices and three  $\omega_0$  values. A lower CWPV score suggests that the problem is predominantly characterised by FM, whereas a lower CWED implies a predominant AM characteristic. The scale ranges have been translated from scale number to scale value. In the bottom right figure of each figure the average range of scales for all 7 voices are presented for each technique.

TABLE B.7: Summary of results for the 50words classification problem comparing Ed, DTW, CWS, CWPV, and CWED using 1-7 voices and 3  $\omega_0$  parameters.  $S$  is the scale set(s) associated with the CWS, CWPV and CWED results. The mean values highlighted in bold are the best in model error rate for the problem.

Problem	Technique	Voices	$\omega_0$	$S$	Mean	1	2	3	4	5	6	7	7	9	10
50words	Ed				0.217	0.304	0.196	0.239	0.196	0.304	0.152	0.196	0.109	0.217	0.261
50words	DTW				0.191	0.196	0.152	0.217	0.130	0.239	0.152	0.152	0.239	0.217	0.217
50words	CWS	1	$1\pi$	1:9,1:6	0.198	0.283	0.196	0.174	0.217	0.196	0.109	0.261	0.152	0.196	0.196
50words	CWS	1	$2\pi$	5:9,1:7	0.322	0.370	0.326	0.391	0.283	0.304	0.348	0.348	0.239	0.261	0.348
50words	CWS	1	$3\pi$	7:9,1:3	0.352	0.326	0.370	0.370	0.348	0.370	0.391	0.326	0.348	0.326	0.348
50words	CWS	2	$1\pi$	6:17,11:12	0.172	0.261	0.174	0.196	0.174	0.217	0.109	0.239	0.065	0.152	0.130
50words	CWS	2	$2\pi$	10:17,1:17	0.230	0.283	0.239	0.239	0.217	0.239	0.239	0.239	0.152	0.196	0.283
50words	CWS	2	$3\pi$	11:17,1:17	0.294	0.391	0.217	0.326	0.239	0.348	0.283	0.304	0.196	0.283	0.348
50words	CWS	3	$1\pi$	10:25,13:17	0.161	0.261	0.152	0.174	0.109	0.174	0.130	0.217	0.065	0.152	0.174
50words	CWS	3	$2\pi$	14:20,1:22	0.246	0.326	0.261	0.261	0.196	0.239	0.239	0.261	0.152	0.217	0.304
50words	CWS	3	$3\pi$	17:25,1:23	0.261	0.370	0.174	0.261	0.283	0.283	0.261	0.261	0.174	0.283	0.261
50words	CWS	4	$1\pi$	13:23,1:15	0.163	0.261	0.174	0.196	0.109	0.196	0.130	0.196	0.087	0.174	0.109
50words	CWS	4	$2\pi$	22:33,1:21	0.200	0.283	0.152	0.261	0.174	0.196	0.174	0.239	0.152	0.217	0.152
50words	CWS	4	$3\pi$	23:25,1:31	0.257	0.304	0.217	0.283	0.261	0.261	0.196	0.261	0.239	0.217	0.326
50words	CWS	5	$1\pi$	16:29,1:26	<b>0.148</b>	0.217	0.152	0.152	0.109	0.174	0.130	0.196	0.065	0.174	0.109
50words	CWS	5	$2\pi$	22:33,1:36	0.207	0.283	0.217	0.239	0.152	0.196	0.174	0.239	0.109	0.196	0.261
50words	CWS	5	$3\pi$	28:36,1:39	0.257	0.326	0.152	0.283	0.283	0.239	0.261	0.239	0.217	0.283	0.283
50words	CWS	6	$1\pi$	21:35,17:20	0.152	0.196	0.130	0.217	0.109	0.130	0.152	0.196	0.087	0.152	0.152
50words	CWS	6	$2\pi$	27:40,1:30	0.204	0.283	0.130	0.196	0.196	0.217	0.239	0.174	0.152	0.174	0.283
50words	CWS	6	$3\pi$	34:39,1:46	0.215	0.239	0.130	0.283	0.217	0.217	0.196	0.239	0.130	0.239	0.261
50words	CWS	7	$1\pi$	24:40,17:23	0.150	0.217	0.174	0.174	0.109	0.130	0.130	0.196	0.065	0.152	0.152
50words	CWS	7	$2\pi$	31:57,1:31	0.207	0.304	0.174	0.239	0.196	0.239	0.196	0.196	0.109	0.174	0.239
50words	CWS	7	$3\pi$	40:50,27:42	0.250	0.326	0.109	0.261	0.239	0.196	0.283	0.304	0.196	0.283	0.304
50words	CWPV	1	$1\pi$	1:9	0.209	0.283	0.174	0.174	0.196	0.196	0.130	0.261	0.174	0.261	0.239
50words	CWPV	1	$2\pi$	5:9	0.404	0.435	0.413	0.348	0.435	0.457	0.391	0.413	0.391	0.391	0.370
50words	CWPV	1	$3\pi$	7:9	0.387	0.391	0.370	0.391	0.435	0.348	0.413	0.348	0.304	0.413	0.457
50words	CWPV	2	$1\pi$	6:17	0.185	0.261	0.196	0.196	0.130	0.217	0.109	0.261	0.109	0.152	0.217
50words	CWPV	2	$2\pi$	10:17	0.300	0.326	0.239	0.283	0.370	0.326	0.326	0.370	0.261	0.152	0.348
50words	CWPV	2	$3\pi$	13:17	0.365	0.348	0.348	0.391	0.413	0.348	0.391	0.326	0.304	0.326	0.457
50words	CWPV	3	$1\pi$	10:25	0.174	0.217	0.152	0.217	0.109	0.152	0.152	0.217	0.109	0.174	0.239
50words	CWPV	3	$2\pi$	13:25	0.296	0.370	0.283	0.261	0.261	0.348	0.326	0.283	0.174	0.304	0.348
50words	CWPV	3	$3\pi$	17:25	0.348	0.413	0.283	0.348	0.370	0.391	0.348	0.326	0.304	0.326	0.370
50words	CWPV	4	$1\pi$	14:23	0.174	0.217	0.174	0.196	0.152	0.217	0.109	0.217	0.087	0.152	0.217
50words	CWPV	4	$2\pi$	18:33	0.235	0.326	0.196	0.261	0.196	0.304	0.174	0.217	0.196	0.196	0.283
50words	CWPV	4	$3\pi$	25:33	0.302	0.348	0.217	0.326	0.261	0.326	0.326	0.283	0.283	0.326	0.326
50words	CWPV	5	$1\pi$	17:41	0.163	0.196	0.109	0.196	0.130	0.174	0.152	0.196	0.065	0.174	0.239
50words	CWPV	5	$2\pi$	26:34	0.252	0.283	0.196	0.283	0.239	0.261	0.261	0.283	0.196	0.283	0.239
50words	CWPV	5	$3\pi$	29:41	0.331	0.326	0.261	0.348	0.348	0.326	0.370	0.304	0.283	0.391	0.348
50words	CWPV	6	$1\pi$	20:49	0.165	0.261	0.152	0.217	0.087	0.174	0.130	0.196	0.065	0.174	0.196
50words	CWPV	6	$2\pi$	27:41	0.250	0.283	0.174	0.283	0.261	0.239	0.304	0.239	0.174	0.196	0.348
50words	CWPV	6	$3\pi$	31:49	0.265	0.348	0.217	0.304	0.239	0.283	0.326	0.261	0.152	0.217	0.304
50words	CWPV	7	$1\pi$	22:44	0.161	0.217	0.152	0.174	0.130	0.174	0.152	0.196	0.065	0.174	0.174
50words	CWPV	7	$2\pi$	31:46	0.241	0.326	0.217	0.217	0.239	0.261	0.239	0.217	0.152	0.196	0.348
50words	CWPV	7	$3\pi$	34:50	0.300	0.391	0.304	0.283	0.217	0.304	0.326	0.326	0.196	0.348	0.304
50words	CWED	1	$1\pi$	1:9	0.387	0.435	0.391	0.457	0.326	0.413	0.435	0.326	0.326	0.370	0.391
50words	CWED	1	$2\pi$	1:9	0.378	0.413	0.304	0.435	0.391	0.391	0.413	0.348	0.348	0.348	0.391
50words	CWED	1	$3\pi$	1:9	0.424	0.435	0.435	0.413	0.435	0.435	0.478	0.413	0.370	0.457	0.370
50words	CWED	2	$1\pi$	1:13	0.357	0.370	0.370	0.413	0.283	0.413	0.370	0.304	0.304	0.326	0.413
50words	CWED	2	$2\pi$	1:17	0.372	0.370	0.348	0.413	0.326	0.391	0.435	0.326	0.326	0.370	0.413
50words	CWED	2	$3\pi$	1:17	0.365	0.413	0.326	0.391	0.348	0.413	0.435	0.304	0.283	0.370	0.370
50words	CWED	3	$1\pi$	1:18	0.344	0.348	0.370	0.413	0.239	0.413	0.326	0.283	0.304	0.348	0.391
50words	CWED	3	$2\pi$	10:19	0.346	0.370	0.304	0.391	0.348	0.457	0.391	0.304	0.261	0.304	0.326
50words	CWED	3	$3\pi$	1:23	0.348	0.370	0.283	0.348	0.370	0.435	0.348	0.304	0.261	0.391	0.370
50words	CWED	4	$1\pi$	1:24	0.339	0.326	0.370	0.391	0.283	0.391	0.326	0.283	0.304	0.348	0.370
50words	CWED	4	$2\pi$	1:25	0.344	0.370	0.304	0.370	0.370	0.457	0.348	0.304	0.239	0.348	0.326
50words	CWED	4	$3\pi$	1:30	0.341	0.348	0.304	0.348	0.391	0.435	0.370	0.304	0.261	0.304	0.348
50words	CWED	5	$1\pi$	1:30	0.341	0.326	0.370	0.391	0.283	0.391	0.348	0.283	0.304	0.348	0.370
50words	CWED	5	$2\pi$	1:35	0.346	0.370	0.304	0.370	0.370	0.457	0.348	0.326	0.261	0.326	0.326
50words	CWED	5	$3\pi$	1:38	0.344	0.348	0.304	0.391	0.391	0.435	0.370	0.283	0.239	0.326	0.348
50words	CWED	6	$1\pi$	1:36	0.346	0.326	0.370	0.391	0.304	0.391	0.348	0.283	0.304	0.348	0.391
50words	CWED	6	$2\pi$	1:38	0.346	0.391	0.304	0.370	0.370	0.457	0.348	0.326	0.239	0.326	0.326
50words	CWED	6	$3\pi$	19:45	0.337	0.348	0.304	0.370	0.370	0.435	0.348	0.283	0.239	0.326	0.348
50words	CWED	7	$1\pi$	1:41	0.346	0.348	0.370	0.391	0.261	0.413	0.326	0.304	0.304	0.370	0.370
50words	CWED	7	$2\pi$	22:44	0.346	0.391	0.304	0.370	0.391	0.391	0.370	0.304	0.283	0.326	0.326
50words	CWED	7	$3\pi$	1:48	0.339	0.370	0.283	0.370	0.391	0.435	0.370	0.283	0.239	0.326	0.326



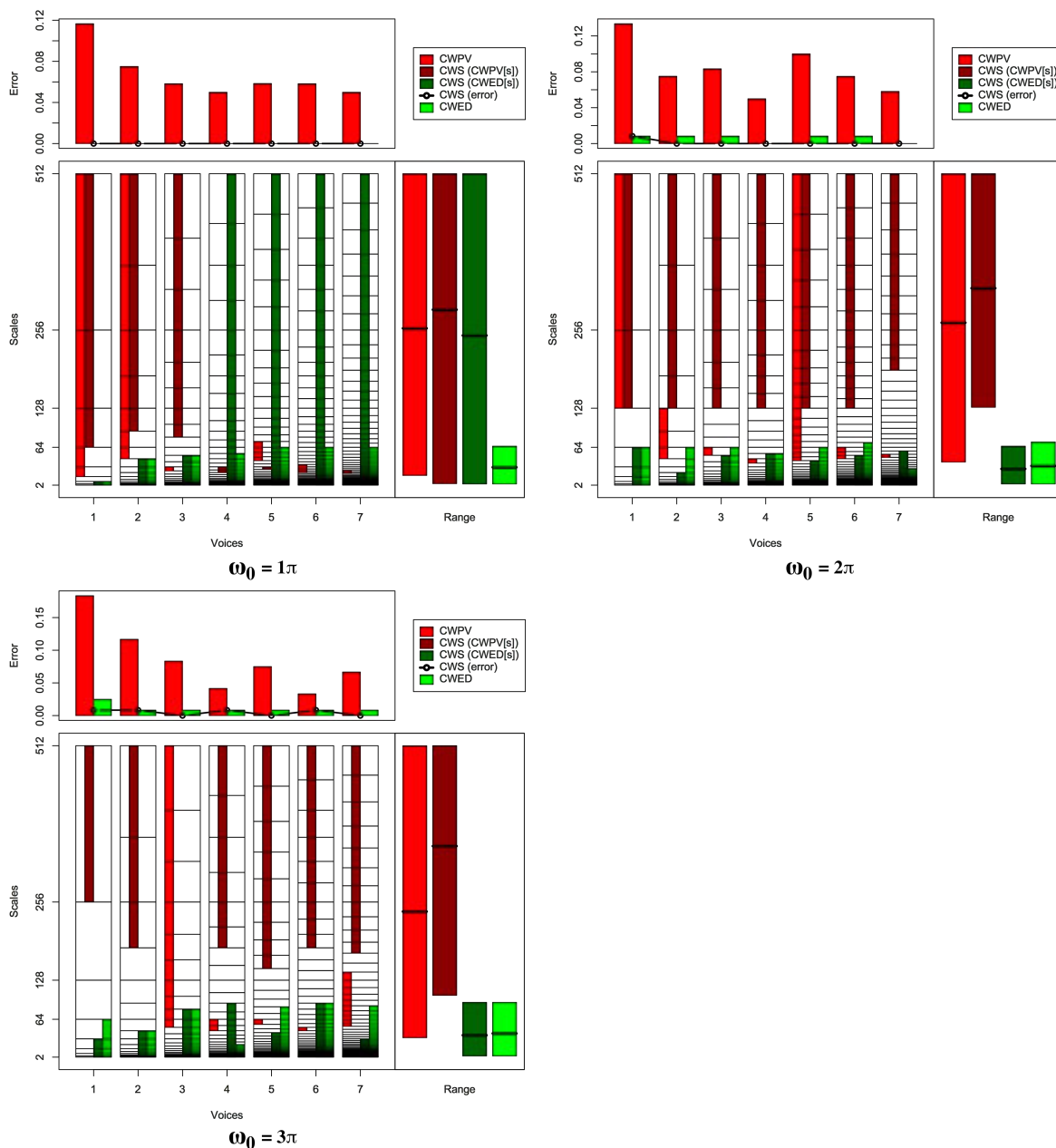


FIGURE B.8: Summary of results for the Trace classification problem comparing CWS, CWPV, CWED methods using 1-7 voices and three  $\omega_0$  values. A lower CWPV score suggests that the problem is predominantly characterised by FM, whereas a lower CWED implies a predominant AM characteristic. The scale ranges have been translated from scale number to scale value. In the bottom right figure of each figure the average range of scales for all 7 voices are presented for each technique.



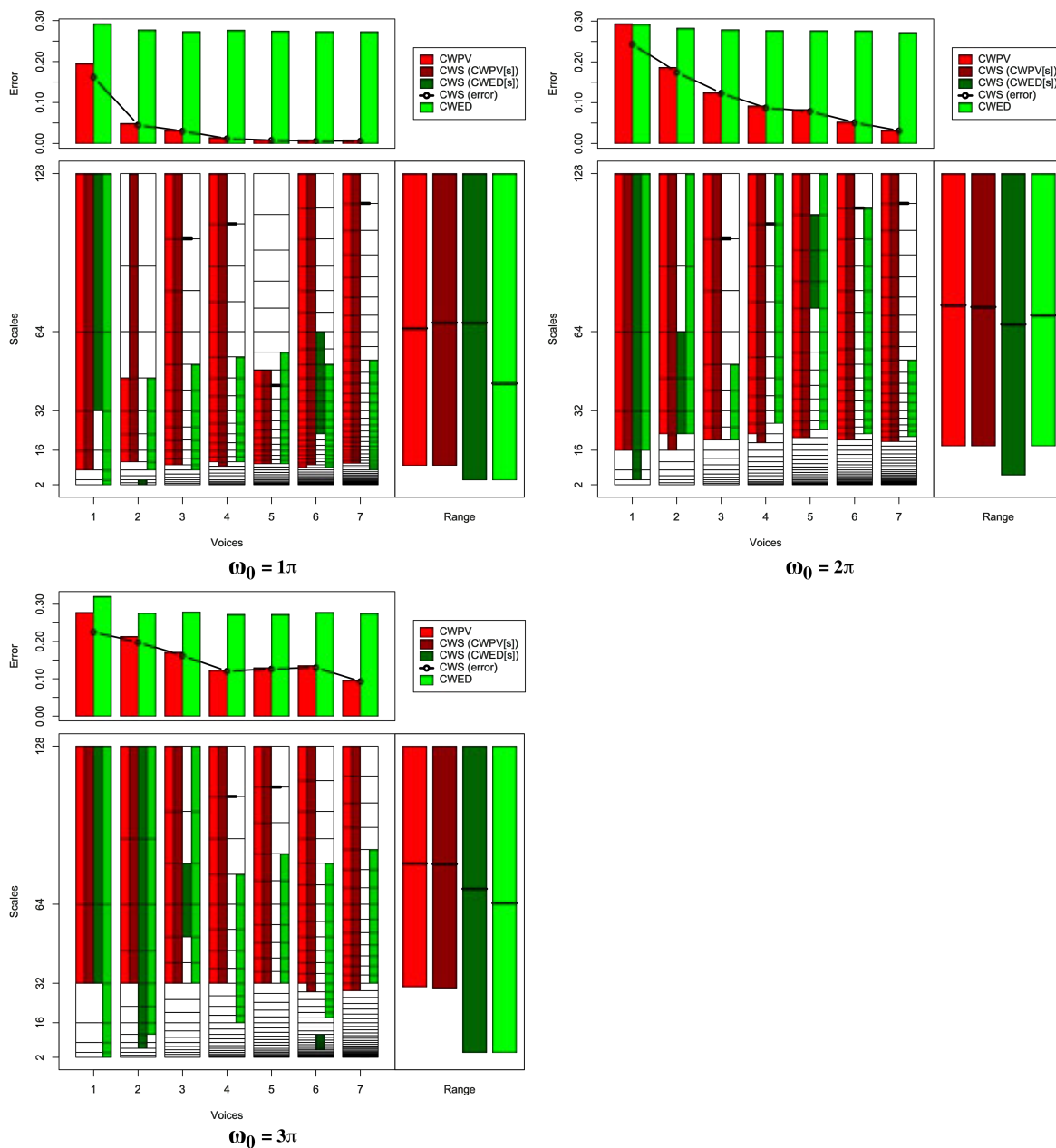


FIGURE B.9: Summary of results for the Two Patterns classification problem comparing CWS, CWPV, CWED methods using 1-7 voices and three  $\omega_0$  values. A lower CWPV score suggests that the problem is predominantly characterised by FM, whereas a lower CWED implies a predominant AM characteristic. The scale ranges have been translated from scale number to scale value. In the bottom right figure of each figure the average range of scales for all 7 voices are presented for each technique.

TABLE B.9: Summary of results for the Two Patterns classification problem comparing Ed, DTW, CWS, CWPV, and CWED using 1-7 voices and 3  $\omega_0$  parameters.  $S$  is the scale set(s) associated with the CWS, CWPV and CWED results. The mean values highlighted in bold are the best in model error rate for the problem.

Problem	Technique	Voices	$\omega_0$	$S$	Mean	1	2	3	4	5	6	7	7	9	10
Two Patterns	Ed				0.015	0.012	0.018	0.012	0.018	0.018	0.012	0.018	0.012	0.015	0.015
Two Patterns	DTW				<b>0.000</b>	0.000	0.000	0.000	0.000	0.000	0.000	0.000	0.000	0.000	0.000
Two Patterns	CWS	1	$1\pi$	3:7,5:7	0.163	0.178	0.160	0.166	0.184	0.172	0.160	0.169	0.148	0.151	0.139
Two Patterns	CWS	1	$2\pi$	4:7,2:7	0.244	0.265	0.199	0.271	0.289	0.238	0.220	0.229	0.241	0.232	0.256
Two Patterns	CWS	1	$3\pi$	5:7,5:7	0.225	0.250	0.226	0.262	0.226	0.220	0.187	0.214	0.220	0.211	0.238
Two Patterns	CWS	2	$1\pi$	6:13,1:3	0.046	0.042	0.045	0.054	0.042	0.072	0.036	0.030	0.042	0.036	0.057
Two Patterns	CWS	2	$2\pi$	7:13,8:11	0.175	0.199	0.157	0.178	0.190	0.172	0.169	0.163	0.166	0.193	0.166
Two Patterns	CWS	2	$3\pi$	9:13,4:13	0.198	0.223	0.217	0.190	0.214	0.178	0.169	0.184	0.193	0.214	0.199
Two Patterns	CWS	3	$1\pi$	8:19,14:14	0.031	0.030	0.027	0.015	0.024	0.045	0.027	0.042	0.024	0.042	0.030
Two Patterns	CWS	3	$2\pi$	11:19,17:17	0.124	0.114	0.114	0.130	0.123	0.130	0.130	0.123	0.111	0.136	0.127
Two Patterns	CWS	3	$3\pi$	13:19,15:17	0.162	0.199	0.190	0.160	0.166	0.145	0.151	0.130	0.151	0.163	0.169
Two Patterns	CWS	4	$1\pi$	10:25,19:19	0.012	0.012	0.003	0.012	0.009	0.024	0.009	0.009	0.015	0.009	0.018
Two Patterns	CWS	4	$2\pi$	14:25,20:20	0.088	0.111	0.087	0.075	0.069	0.102	0.084	0.099	0.105	0.075	0.069
Two Patterns	CWS	4	$3\pi$	17:25,7:7	0.121	0.127	0.127	0.111	0.127	0.117	0.105	0.127	0.136	0.130	0.099
Two Patterns	CWS	5	$1\pi$	13:24,18:18	0.008	0.006	0.009	0.003	0.006	0.018	0.000	0.012	0.003	0.015	0.009
Two Patterns	CWS	5	$2\pi$	18:31,27:30	0.079	0.072	0.096	0.078	0.075	0.096	0.078	0.057	0.081	0.081	0.078
Two Patterns	CWS	5	$3\pi$	21:31,23:23	0.127	0.114	0.136	0.127	0.136	0.117	0.142	0.120	0.108	0.145	0.120
Two Patterns	CWS	6	$1\pi$	15:37,22:31	0.006	0.000	0.003	0.000	0.009	0.018	0.009	0.000	0.006	0.015	0.003
Two Patterns	CWS	6	$2\pi$	21:37,33:33	0.052	0.051	0.069	0.054	0.054	0.066	0.036	0.042	0.039	0.060	0.045
Two Patterns	CWS	6	$3\pi$	24:37,9:16	0.130	0.127	0.148	0.123	0.108	0.120	0.123	0.117	0.127	0.184	0.127
Two Patterns	CWS	7	$1\pi$	18:43,32:32	0.006	0.006	0.012	0.000	0.000	0.015	0.006	0.009	0.000	0.012	0.003
Two Patterns	CWS	7	$2\pi$	24:43,17:17	0.032	0.024	0.030	0.030	0.042	0.036	0.027	0.030	0.015	0.033	0.048
Two Patterns	CWS	7	$3\pi$	28:43,1:4	0.093	0.084	0.087	0.081	0.114	0.105	0.081	0.090	0.096	0.090	0.102
Two Patterns	CWPV	1	$1\pi$	3:7	0.195	0.196	0.211	0.187	0.223	0.193	0.193	0.196	0.184	0.172	0.199
Two Patterns	CWPV	1	$2\pi$	4:7	0.294	0.313	0.274	0.319	0.307	0.289	0.286	0.280	0.304	0.259	0.304
Two Patterns	CWPV	1	$3\pi$	5:7	0.278	0.301	0.250	0.301	0.265	0.265	0.295	0.301	0.283	0.259	0.259
Two Patterns	CWPV	2	$1\pi$	6:10	0.049	0.039	0.039	0.063	0.039	0.078	0.042	0.042	0.042	0.045	0.060
Two Patterns	CWPV	2	$2\pi$	8:13	0.186	0.196	0.196	0.172	0.181	0.217	0.163	0.169	0.187	0.220	0.163
Two Patterns	CWPV	2	$3\pi$	9:13	0.213	0.226	0.217	0.223	0.193	0.226	0.178	0.208	0.214	0.223	0.226
Two Patterns	CWPV	3	$1\pi$	8:19	0.033	0.027	0.033	0.024	0.024	0.045	0.024	0.039	0.027	0.042	0.042
Two Patterns	CWPV	3	$2\pi$	11:19	0.125	0.117	0.123	0.127	0.108	0.133	0.133	0.130	0.114	0.133	0.130
Two Patterns	CWPV	3	$3\pi$	13:19	0.171	0.175	0.160	0.187	0.163	0.166	0.184	0.169	0.172	0.169	0.166
Two Patterns	CWPV	4	$1\pi$	11:25	0.014	0.027	0.009	0.009	0.009	0.024	0.021	0.009	0.015	0.015	0.006
Two Patterns	CWPV	4	$2\pi$	15:25	0.092	0.090	0.108	0.075	0.090	0.108	0.078	0.096	0.099	0.087	0.090
Two Patterns	CWPV	4	$3\pi$	17:25	0.123	0.123	0.120	0.123	0.127	0.142	0.114	0.120	0.127	0.117	0.117
Two Patterns	CWPV	5	$1\pi$	13:24	0.009	0.009	0.009	0.006	0.006	0.015	0.006	0.012	0.006	0.015	0.009
Two Patterns	CWPV	5	$2\pi$	18:31	0.083	0.066	0.087	0.111	0.081	0.108	0.075	0.066	0.060	0.090	0.087
Two Patterns	CWPV	5	$3\pi$	21:31	0.129	0.114	0.133	0.127	0.133	0.117	0.157	0.130	0.117	0.139	0.127
Two Patterns	CWPV	6	$1\pi$	14:37	0.009	0.009	0.003	0.006	0.006	0.018	0.006	0.018	0.009	0.006	0.009
Two Patterns	CWPV	6	$2\pi$	21:37	0.053	0.048	0.069	0.051	0.057	0.069	0.039	0.045	0.045	0.063	0.039
Two Patterns	CWPV	6	$3\pi$	25:37	0.135	0.142	0.142	0.136	0.114	0.136	0.157	0.136	0.114	0.139	0.136
Two Patterns	CWPV	7	$1\pi$	18:43	0.009	0.009	0.012	0.006	0.000	0.018	0.009	0.009	0.006	0.012	0.006
Two Patterns	CWPV	7	$2\pi$	24:43	0.032	0.024	0.033	0.030	0.039	0.030	0.027	0.042	0.018	0.033	0.045
Two Patterns	CWPV	7	$3\pi$	28:43	0.095	0.093	0.087	0.084	0.117	0.108	0.078	0.090	0.102	0.090	0.105
Two Patterns	CWED	1	$1\pi$	1:7	0.292	0.289	0.298	0.292	0.298	0.277	0.304	0.286	0.286	0.289	0.304
Two Patterns	CWED	1	$2\pi$	4:7	0.292	0.268	0.346	0.283	0.262	0.319	0.298	0.274	0.274	0.310	0.289
Two Patterns	CWED	1	$3\pi$	1:7	0.321	0.337	0.328	0.322	0.340	0.325	0.316	0.319	0.304	0.304	0.316
Two Patterns	CWED	2	$1\pi$	5:10	0.277	0.247	0.280	0.310	0.295	0.265	0.250	0.253	0.271	0.304	0.298
Two Patterns	CWED	2	$2\pi$	8:13	0.283	0.271	0.301	0.268	0.319	0.259	0.280	0.259	0.277	0.316	0.277
Two Patterns	CWED	2	$3\pi$	6:13	0.276	0.256	0.280	0.292	0.298	0.268	0.241	0.283	0.310	0.259	0.277
Two Patterns	CWED	3	$1\pi$	7:15	0.273	0.238	0.292	0.301	0.307	0.253	0.262	0.244	0.250	0.301	0.283
Two Patterns	CWED	3	$2\pi$	11:15	0.279	0.313	0.286	0.271	0.298	0.286	0.262	0.283	0.277	0.262	0.250
Two Patterns	CWED	3	$3\pi$	13:19	0.279	0.304	0.271	0.277	0.310	0.262	0.271	0.280	0.271	0.268	0.277
Two Patterns	CWED	4	$1\pi$	11:20	0.277	0.268	0.292	0.274	0.307	0.259	0.265	0.250	0.283	0.304	0.265
Two Patterns	CWED	4	$2\pi$	16:25	0.277	0.262	0.307	0.283	0.313	0.247	0.256	0.265	0.274	0.313	0.247
Two Patterns	CWED	4	$3\pi$	13:22	0.273	0.286	0.247	0.262	0.268	0.280	0.262	0.295	0.304	0.277	0.247
Two Patterns	CWED	5	$1\pi$	13:25	0.274	0.262	0.292	0.283	0.307	0.259	0.271	0.247	0.262	0.304	0.256
Two Patterns	CWED	5	$2\pi$	19:31	0.276	0.280	0.262	0.274	0.289	0.247	0.259	0.274	0.301	0.304	0.274
Two Patterns	CWED	5	$3\pi$	21:28	0.273	0.301	0.265	0.271	0.304	0.265	0.256	0.256	0.274	0.268	0.268
Two Patterns	CWED	6	$1\pi$	14:29	0.273	0.241	0.301	0.298	0.292	0.253	0.271	0.256	0.259	0.301	0.259
Two Patterns	CWED	6	$2\pi$	22:36	0.276	0.280	0.277	0.268	0.298	0.235	0.259	0.274	0.298	0.307	0.265
Two Patterns	CWED	6	$3\pi$	20:33	0.278	0.265	0.277	0.277	0.271	0.286	0.265	0.292	0.307	0.274	0.268
Two Patterns	CWED	7	$1\pi$	15:34	0.273	0.238	0.298	0.304	0.289	0.265	0.265	0.244	0.259	0.295	0.271
Two Patterns	CWED	7	$2\pi$	25:34	0.272	0.301	0.259	0.280	0.277	0.271	0.247	0.283	0.271	0.265	0.265
Two Patterns	CWED	7	$3\pi$	29:39	0.275	0.301	0.256	0.274	0.310	0.265	0.259	0.265	0.274	0.265	0.283

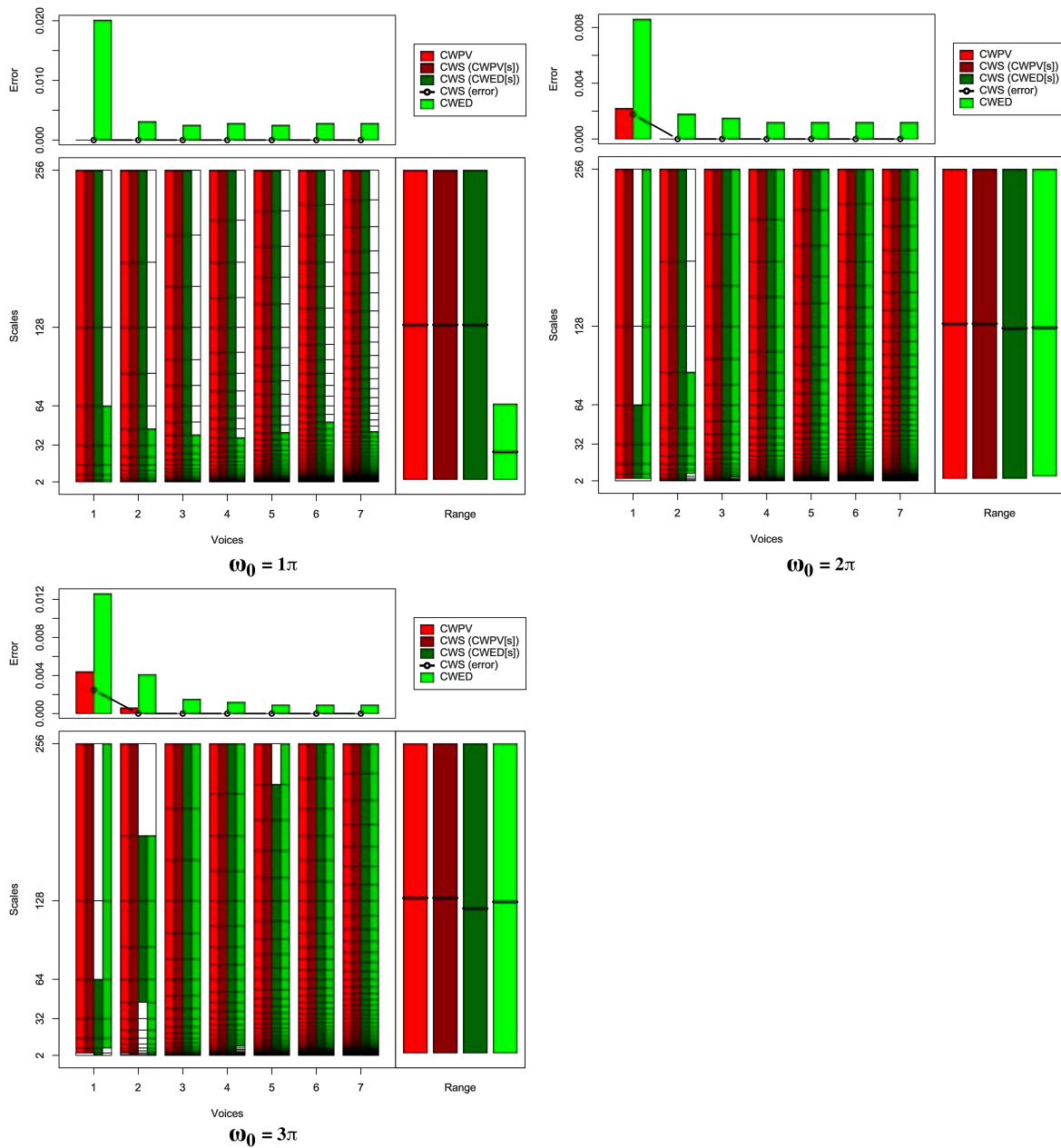


FIGURE B.10: Summary of results for the Wafer classification problem comparing CWS, CWPV, CWED methods using 1-7 voices and three  $\omega_0$  values. A lower CWPV score suggests that the problem is predominantly characterised by FM, whereas a lower CWED implies a predominant AM characteristic. The scale ranges have been translated from scale number to scale value. In the bottom right figure of each figure the average range of scales for all 7 voices are presented for each technique.

TABLE B.10: Summary of results for the Wafer classification problem comparing Ed, DTW, CWS, CWPV, and CWED using 1-7 voices and 3  $\omega_0$  parameters.  $S$  is the scale set(s) associated with the CWS, CWPV and CWED results. The mean values highlighted in bold are the best in model error rate for the problem.

Problem	Technique	Voices	$\omega_0$	$S$	Mean	1	2	3	4	5	6	7	7	9	10
Wafer	Ed				0.001	0.003	0.000	0.000	0.000	0.000	0.000	0.000	0.000	0.000	0.003
Wafer	DTW				0.011	0.019	0.035	0.025	0.006	0.010	0.000	0.006	0.003	0.000	0.003
Wafer	CWS	1	$1\pi$	1:8,1:8	<b>0.000</b>	0.000	0.000	0.000	0.000	0.000	0.000	0.000	0.000	0.000	0.000
Wafer	CWS	1	$2\pi$	2:8,2:6	0.002	0.003	0.006	0.006	0.003	0.000	0.000	0.000	0.000	0.000	0.000
Wafer	CWS	1	$3\pi$	2:8,1:6	0.003	0.010	0.003	0.006	0.006	0.000	0.000	0.000	0.000	0.000	0.000
Wafer	CWS	2	$1\pi$	1:15,1:15	<b>0.000</b>	0.000	0.000	0.000	0.000	0.000	0.000	0.000	0.000	0.000	0.000
Wafer	CWS	2	$2\pi$	1:15,1:15	<b>0.000</b>	0.000	0.000	0.000	0.000	0.000	0.000	0.000	0.000	0.000	0.000
Wafer	CWS	2	$3\pi$	2:15,10:14	<b>0.000</b>	0.000	0.000	0.000	0.000	0.000	0.000	0.000	0.000	0.000	0.000
Wafer	CWS	3	$1\pi$	1:22,1:22	<b>0.000</b>	0.000	0.000	0.000	0.000	0.000	0.000	0.000	0.000	0.000	0.000
Wafer	CWS	3	$2\pi$	1:22,1:22	<b>0.000</b>	0.000	0.000	0.000	0.000	0.000	0.000	0.000	0.000	0.000	0.000
Wafer	CWS	3	$3\pi$	1:22,1:22	<b>0.000</b>	0.000	0.000	0.000	0.000	0.000	0.000	0.000	0.000	0.000	0.000
Wafer	CWS	4	$1\pi$	1:29,1:29	<b>0.000</b>	0.000	0.000	0.000	0.000	0.000	0.000	0.000	0.000	0.000	0.000
Wafer	CWS	4	$2\pi$	1:29,1:29	<b>0.000</b>	0.000	0.000	0.000	0.000	0.000	0.000	0.000	0.000	0.000	0.000
Wafer	CWS	4	$3\pi$	3:29,1:29	<b>0.000</b>	0.000	0.000	0.000	0.000	0.000	0.000	0.000	0.000	0.000	0.000
Wafer	CWS	5	$1\pi$	1:36,1:36	<b>0.000</b>	0.000	0.000	0.000	0.000	0.000	0.000	0.000	0.000	0.000	0.000
Wafer	CWS	5	$2\pi$	1:36,1:36	<b>0.000</b>	0.000	0.000	0.000	0.000	0.000	0.000	0.000	0.000	0.000	0.000
Wafer	CWS	5	$3\pi$	1:36,1:35	<b>0.000</b>	0.000	0.000	0.000	0.000	0.000	0.000	0.000	0.000	0.000	0.000
Wafer	CWS	6	$1\pi$	1:43,1:43	<b>0.000</b>	0.000	0.000	0.000	0.000	0.000	0.000	0.000	0.000	0.000	0.000
Wafer	CWS	6	$2\pi$	1:43,1:43	<b>0.000</b>	0.000	0.000	0.000	0.000	0.000	0.000	0.000	0.000	0.000	0.000
Wafer	CWS	6	$3\pi$	4:43,1:43	<b>0.000</b>	0.000	0.000	0.000	0.000	0.000	0.000	0.000	0.000	0.000	0.000
Wafer	CWS	7	$1\pi$	1:50,1:50	<b>0.000</b>	0.000	0.000	0.000	0.000	0.000	0.000	0.000	0.000	0.000	0.000
Wafer	CWS	7	$2\pi$	1:50,1:50	<b>0.000</b>	0.000	0.000	0.000	0.000	0.000	0.000	0.000	0.000	0.000	0.000
Wafer	CWS	7	$3\pi$	4:50,1:50	<b>0.000</b>	0.000	0.000	0.000	0.000	0.000	0.000	0.000	0.000	0.000	0.000
Wafer	CWPV	1	$1\pi$	1:8	<b>0.000</b>	0.000	0.000	0.000	0.000	0.000	0.000	0.000	0.000	0.000	0.000
Wafer	CWPV	1	$2\pi$	2:8	0.002	0.003	0.013	0.006	0.000	0.000	0.000	0.000	0.000	0.000	0.000
Wafer	CWPV	1	$3\pi$	2:8	0.004	0.016	0.006	0.006	0.010	0.003	0.000	0.000	0.000	0.003	0.000
Wafer	CWPV	2	$1\pi$	1:15	<b>0.000</b>	0.000	0.000	0.000	0.000	0.000	0.000	0.000	0.000	0.000	0.000
Wafer	CWPV	2	$2\pi$	1:15	<b>0.000</b>	0.000	0.000	0.000	0.000	0.000	0.000	0.000	0.000	0.000	0.000
Wafer	CWPV	2	$3\pi$	3:15	0.001	0.000	0.000	0.006	0.000	0.000	0.000	0.000	0.000	0.000	0.000
Wafer	CWPV	3	$1\pi$	1:22	<b>0.000</b>	0.000	0.000	0.000	0.000	0.000	0.000	0.000	0.000	0.000	0.000
Wafer	CWPV	3	$2\pi$	1:22	<b>0.000</b>	0.000	0.000	0.000	0.000	0.000	0.000	0.000	0.000	0.000	0.000
Wafer	CWPV	3	$3\pi$	1:22	<b>0.000</b>	0.000	0.000	0.000	0.000	0.000	0.000	0.000	0.000	0.000	0.000
Wafer	CWPV	4	$1\pi$	1:29	<b>0.000</b>	0.000	0.000	0.000	0.000	0.000	0.000	0.000	0.000	0.000	0.000
Wafer	CWPV	4	$2\pi$	1:29	<b>0.000</b>	0.000	0.000	0.000	0.000	0.000	0.000	0.000	0.000	0.000	0.000
Wafer	CWPV	4	$3\pi$	3:29	<b>0.000</b>	0.000	0.000	0.000	0.000	0.000	0.000	0.000	0.000	0.000	0.000
Wafer	CWPV	5	$1\pi$	1:36	<b>0.000</b>	0.000	0.000	0.000	0.000	0.000	0.000	0.000	0.000	0.000	0.000
Wafer	CWPV	5	$2\pi$	1:36	<b>0.000</b>	0.000	0.000	0.000	0.000	0.000	0.000	0.000	0.000	0.000	0.000
Wafer	CWPV	5	$3\pi$	4:36	<b>0.000</b>	0.000	0.000	0.000	0.000	0.000	0.000	0.000	0.000	0.000	0.000
Wafer	CWPV	6	$1\pi$	1:43	<b>0.000</b>	0.000	0.000	0.000	0.000	0.000	0.000	0.000	0.000	0.000	0.000
Wafer	CWPV	6	$2\pi$	1:43	<b>0.000</b>	0.000	0.000	0.000	0.000	0.000	0.000	0.000	0.000	0.000	0.000
Wafer	CWPV	6	$3\pi$	1:43	<b>0.000</b>	0.000	0.000	0.000	0.000	0.000	0.000	0.000	0.000	0.000	0.000
Wafer	CWPV	7	$1\pi$	1:50	<b>0.000</b>	0.000	0.000	0.000	0.000	0.000	0.000	0.000	0.000	0.000	0.000
Wafer	CWPV	7	$2\pi$	1:50	<b>0.000</b>	0.000	0.000	0.000	0.000	0.000	0.000	0.000	0.000	0.000	0.000
Wafer	CWPV	7	$3\pi$	3:50	<b>0.000</b>	0.000	0.000	0.000	0.000	0.000	0.000	0.000	0.000	0.000	0.000
Wafer	CWED	1	$1\pi$	1:6	0.020	0.048	0.035	0.022	0.051	0.019	0.000	0.013	0.000	0.010	0.003
Wafer	CWED	1	$2\pi$	2:8	0.009	0.022	0.016	0.013	0.010	0.019	0.000	0.003	0.000	0.003	0.000
Wafer	CWED	1	$3\pi$	3:8	0.013	0.029	0.022	0.032	0.003	0.022	0.003	0.003	0.003	0.006	0.003
Wafer	CWED	2	$1\pi$	1:10	0.003	0.000	0.013	0.006	0.006	0.000	0.000	0.000	0.003	0.003	0.000
Wafer	CWED	2	$2\pi$	5:12	0.002	0.000	0.006	0.003	0.006	0.000	0.000	0.000	0.000	0.000	0.003
Wafer	CWED	2	$3\pi$	1:14	0.004	0.010	0.016	0.006	0.003	0.003	0.000	0.003	0.000	0.000	0.000
Wafer	CWED	3	$1\pi$	1:14	0.003	0.006	0.013	0.000	0.006	0.000	0.000	0.000	0.000	0.000	0.000
Wafer	CWED	3	$2\pi$	5:22	0.002	0.000	0.003	0.003	0.003	0.000	0.000	0.006	0.000	0.000	0.000
Wafer	CWED	3	$3\pi$	1:22	0.002	0.000	0.003	0.003	0.006	0.000	0.000	0.003	0.000	0.000	0.000
Wafer	CWED	4	$1\pi$	1:18	0.003	0.006	0.016	0.000	0.006	0.000	0.000	0.000	0.000	0.000	0.000
Wafer	CWED	4	$2\pi$	6:29	0.001	0.000	0.003	0.000	0.003	0.000	0.000	0.006	0.000	0.000	0.000
Wafer	CWED	4	$3\pi$	10:29	0.001	0.000	0.006	0.000	0.003	0.000	0.000	0.003	0.000	0.000	0.000
Wafer	CWED	5	$1\pi$	1:23	0.003	0.006	0.013	0.000	0.006	0.000	0.000	0.000	0.000	0.000	0.000
Wafer	CWED	5	$2\pi$	8:36	0.001	0.000	0.003	0.000	0.003	0.000	0.000	0.006	0.000	0.000	0.000
Wafer	CWED	5	$3\pi$	6:36	0.001	0.000	0.003	0.000	0.003	0.000	0.000	0.003	0.000	0.000	0.000
Wafer	CWED	6	$1\pi$	1:29	0.003	0.003	0.013	0.003	0.006	0.000	0.000	0.003	0.000	0.000	0.000
Wafer	CWED	6	$2\pi$	9:43	0.001	0.000	0.003	0.000	0.003	0.000	0.000	0.006	0.000	0.000	0.000
Wafer	CWED	6	$3\pi$	1:43	0.001	0.000	0.003	0.000	0.003	0.000	0.000	0.003	0.000	0.000	0.000
Wafer	CWED	7	$1\pi$	1:32	0.003	0.006	0.016	0.000	0.006	0.000	0.000	0.000	0.000	0.000	0.000
Wafer	CWED	7	$2\pi$	11:50	0.001	0.000	0.003	0.000	0.003	0.000	0.000	0.006	0.000	0.000	0.000
Wafer	CWED	7	$3\pi$	1:50	0.001	0.000	0.003	0.000	0.003	0.000	0.000	0.003	0.000	0.000	0.000

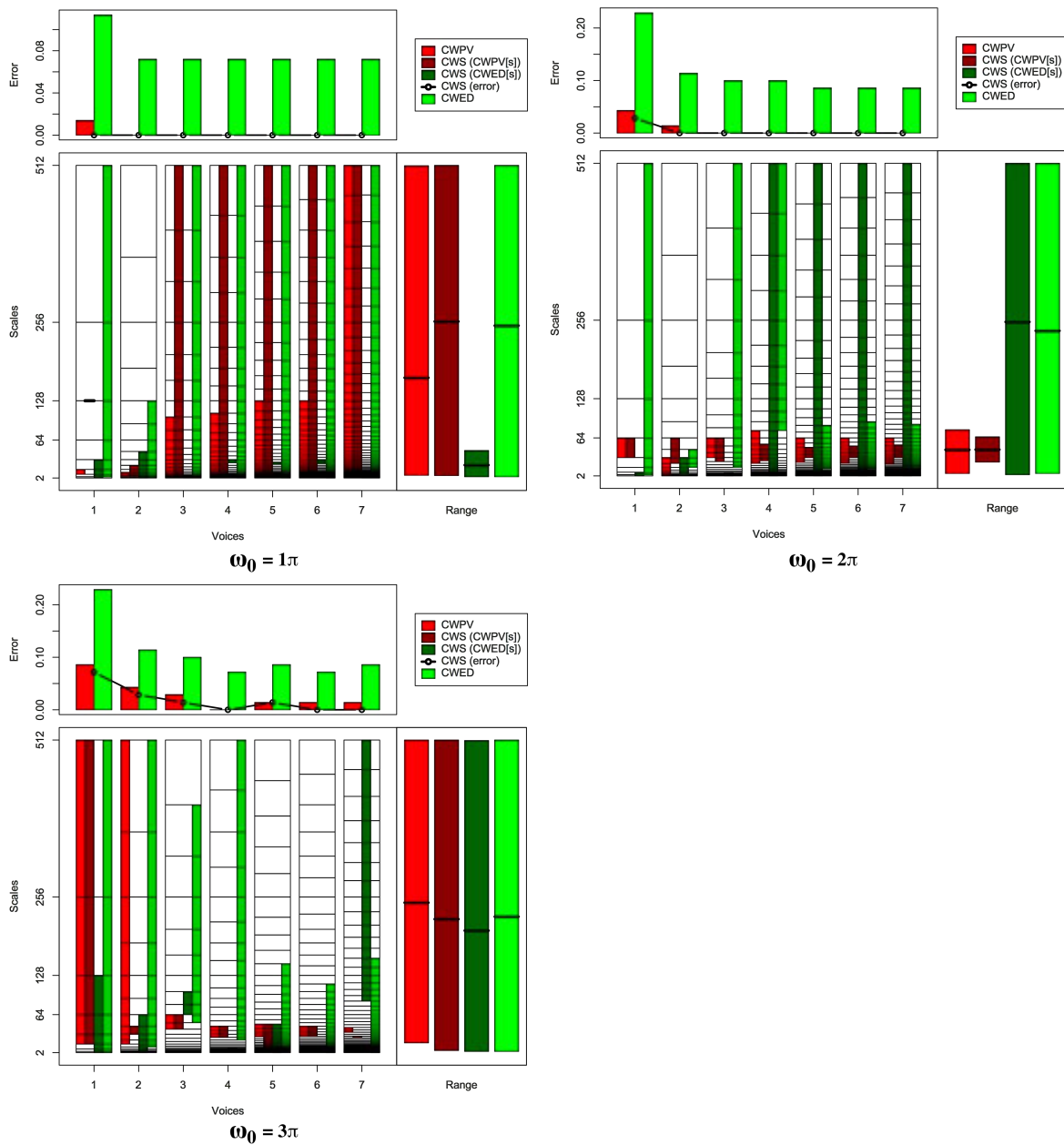


FIGURE B.11: Summary of results for the Face (four) classification problem comparing CWS, CWPV, CWED methods using 1-7 voices and three  $\omega_0$  values. A lower CWPV score suggests that the problem is predominantly characterised by FM, whereas a lower CWED implies a predominant AM characteristic. The scale ranges have been translated from scale number to scale value. In the bottom right figure of each figure the average range of scales for all 7 voices are presented for each technique.

TABLE B.11: Summary of results for the Face (four) classification problem comparing Ed, DTW, CWS, CWPV, and CWED using 1-7 voices and 3  $\omega_0$  parameters.  $S$  is the scale set(s) associated with the CWS, CWPV and CWED results. The mean values highlighted in bold are the best in model error rate for the problem.

Problem	Technique	Voices	$\omega_0$	$S$	Mean	1	2	3	4	5	6	7	7	9	10
Face (four)	Ed				0.114	0.000	0.429	0.000	0.286	0.000	0.143	0.000	0.143	0.143	0.000
Face (four)	DTW				0.072	0.143	0.286	0.000	0.143	0.000	0.143	0.000	0.000	0.000	0.000
Face (four)	CWS	1	$1\pi$	4:4,1:5	<b>0.000</b>	0.000	0.000	0.000	0.000	0.000	0.000	0.000	0.000	0.000	0.000
Face (four)	CWS	1	$2\pi$	5:6,1:3	0.029	0.000	0.286	0.000	0.000	0.000	0.000	0.000	0.000	0.000	0.000
Face (four)	CWS	1	$3\pi$	4:9,1:7	0.072	0.143	0.000	0.000	0.286	0.000	0.143	0.000	0.000	0.143	0.000
Face (four)	CWS	2	$1\pi$	4:8,1:10	<b>0.000</b>	0.000	0.000	0.000	0.000	0.000	0.000	0.000	0.000	0.000	0.000
Face (four)	CWS	2	$2\pi$	8:11,4:9	<b>0.000</b>	0.000	0.000	0.000	0.000	0.000	0.000	0.000	0.000	0.000	0.000
Face (four)	CWS	2	$3\pi$	9:10,1:11	0.029	0.000	0.143	0.000	0.143	0.000	0.000	0.000	0.000	0.000	0.000
Face (four)	CWS	3	$1\pi$	5:25,1:3	<b>0.000</b>	0.000	0.000	0.000	0.000	0.000	0.000	0.000	0.000	0.000	0.000
Face (four)	CWS	3	$2\pi$	12:16,1:7	<b>0.000</b>	0.000	0.000	0.000	0.000	0.000	0.000	0.000	0.000	0.000	0.000
Face (four)	CWS	3	$3\pi$	14:16,16:18	0.014	0.000	0.000	0.000	0.143	0.000	0.000	0.000	0.000	0.000	0.000
Face (four)	CWS	4	$1\pi$	5:33,16:17	<b>0.000</b>	0.000	0.000	0.000	0.000	0.000	0.000	0.000	0.000	0.000	0.000
Face (four)	CWS	4	$2\pi$	16:20,1:33	<b>0.000</b>	0.000	0.000	0.000	0.000	0.000	0.000	0.000	0.000	0.000	0.000
Face (four)	CWS	4	$3\pi$	16:19,4:10	<b>0.000</b>	0.000	0.000	0.000	0.000	0.000	0.000	0.000	0.000	0.000	0.000
Face (four)	CWS	5	$1\pi$	7:41,19:20	<b>0.000</b>	0.000	0.000	0.000	0.000	0.000	0.000	0.000	0.000	0.000	0.000
Face (four)	CWS	5	$2\pi$	21:24,1:41	<b>0.000</b>	0.000	0.000	0.000	0.000	0.000	0.000	0.000	0.000	0.000	0.000
Face (four)	CWS	5	$3\pi$	5:24,1:24	0.014	0.000	0.000	0.000	0.000	0.000	0.000	0.000	0.000	0.143	0.000
Face (four)	CWS	6	$1\pi$	7:49,23:25	<b>0.000</b>	0.000	0.000	0.000	0.000	0.000	0.000	0.000	0.000	0.000	0.000
Face (four)	CWS	6	$2\pi$	25:29,1:49	<b>0.000</b>	0.000	0.000	0.000	0.000	0.000	0.000	0.000	0.000	0.000	0.000
Face (four)	CWS	6	$3\pi$	24:28,8:11	<b>0.000</b>	0.000	0.000	0.000	0.000	0.000	0.000	0.000	0.000	0.000	0.000
Face (four)	CWS	7	$1\pi$	9:57,1:9	<b>0.000</b>	0.000	0.000	0.000	0.000	0.000	0.000	0.000	0.000	0.000	0.000
Face (four)	CWS	7	$2\pi$	29:34,1:57	<b>0.000</b>	0.000	0.000	0.000	0.000	0.000	0.000	0.000	0.000	0.000	0.000
Face (four)	CWS	7	$3\pi$	27:28,39:57	<b>0.000</b>	0.000	0.000	0.000	0.000	0.000	0.000	0.000	0.000	0.000	0.000
Face (four)	CWPV	1	$1\pi$	3:4	0.014	0.000	0.000	0.000	0.143	0.000	0.000	0.000	0.000	0.000	0.000
Face (four)	CWPV	1	$2\pi$	5:6	0.043	0.000	0.286	0.000	0.000	0.000	0.000	0.000	0.000	0.143	0.000
Face (four)	CWPV	1	$3\pi$	4:9	0.086	0.143	0.000	0.000	0.286	0.000	0.000	0.143	0.000	0.143	0.143
Face (four)	CWPV	2	$1\pi$	4:6	<b>0.000</b>	0.000	0.000	0.000	0.000	0.000	0.000	0.000	0.000	0.000	0.000
Face (four)	CWPV	2	$2\pi$	3:9	0.014	0.000	0.000	0.000	0.000	0.000	0.000	0.000	0.000	0.143	0.000
Face (four)	CWPV	2	$3\pi$	7:17	0.043	0.000	0.000	0.000	0.286	0.000	0.000	0.000	0.000	0.000	0.143
Face (four)	CWPV	3	$1\pi$	6:18	<b>0.000</b>	0.000	0.000	0.000	0.000	0.000	0.000	0.000	0.000	0.000	0.000
Face (four)	CWPV	3	$2\pi$	13:16	<b>0.000</b>	0.000	0.000	0.000	0.000	0.000	0.000	0.000	0.000	0.000	0.000
Face (four)	CWPV	3	$3\pi$	14:16	0.029	0.000	0.000	0.000	0.143	0.000	0.000	0.000	0.143	0.000	0.000
Face (four)	CWPV	4	$1\pi$	9:24	<b>0.000</b>	0.000	0.000	0.000	0.000	0.000	0.000	0.000	0.000	0.000	0.000
Face (four)	CWPV	4	$2\pi$	15:22	<b>0.000</b>	0.000	0.000	0.000	0.000	0.000	0.000	0.000	0.000	0.000	0.000
Face (four)	CWPV	4	$3\pi$	16:19	<b>0.000</b>	0.000	0.000	0.000	0.000	0.000	0.000	0.000	0.000	0.000	0.000
Face (four)	CWPV	5	$1\pi$	8:31	<b>0.000</b>	0.000	0.000	0.000	0.000	0.000	0.000	0.000	0.000	0.000	0.000
Face (four)	CWPV	5	$2\pi$	19:26	<b>0.000</b>	0.000	0.000	0.000	0.000	0.000	0.000	0.000	0.000	0.000	0.000
Face (four)	CWPV	5	$3\pi$	20:24	0.014	0.000	0.000	0.000	0.000	0.000	0.000	0.000	0.000	0.000	0.143
Face (four)	CWPV	6	$1\pi$	10:37	<b>0.000</b>	0.000	0.000	0.000	0.000	0.000	0.000	0.000	0.000	0.000	0.000
Face (four)	CWPV	6	$2\pi$	22:31	<b>0.000</b>	0.000	0.000	0.000	0.000	0.000	0.000	0.000	0.000	0.000	0.000
Face (four)	CWPV	6	$3\pi$	24:28	0.014	0.000	0.000	0.000	0.143	0.000	0.000	0.000	0.000	0.000	0.000
Face (four)	CWPV	7	$1\pi$	9:57	<b>0.000</b>	0.000	0.000	0.000	0.000	0.000	0.000	0.000	0.000	0.000	0.000
Face (four)	CWPV	7	$2\pi$	25:36	<b>0.000</b>	0.000	0.000	0.000	0.000	0.000	0.000	0.000	0.000	0.000	0.000
Face (four)	CWPV	7	$3\pi$	30:32	0.014	0.000	0.143	0.000	0.000	0.000	0.000	0.000	0.000	0.000	0.000
Face (four)	CWED	1	$1\pi$	2:9	0.114	0.000	0.286	0.143	0.143	0.000	0.286	0.000	0.000	0.143	0.143
Face (four)	CWED	1	$2\pi$	2:9	0.229	0.286	0.429	0.000	0.286	0.143	0.429	0.143	0.429	0.143	0.000
Face (four)	CWED	1	$3\pi$	1:9	0.229	0.143	0.571	0.143	0.143	0.000	0.286	0.000	0.286	0.286	0.429
Face (four)	CWED	2	$1\pi$	2:13	0.072	0.000	0.429	0.000	0.143	0.000	0.143	0.000	0.000	0.000	0.000
Face (four)	CWED	2	$2\pi$	7:10	0.114	0.000	0.429	0.000	0.286	0.000	0.143	0.000	0.143	0.000	0.143
Face (four)	CWED	2	$3\pi$	6:17	0.114	0.000	0.286	0.000	0.143	0.000	0.286	0.000	0.143	0.000	0.286
Face (four)	CWED	3	$1\pi$	1:25	0.072	0.000	0.429	0.000	0.143	0.000	0.143	0.000	0.000	0.000	0.000
Face (four)	CWED	3	$2\pi$	10:25	0.100	0.000	0.429	0.000	0.286	0.000	0.143	0.000	0.143	0.000	0.000
Face (four)	CWED	3	$3\pi$	15:24	0.100	0.143	0.286	0.000	0.143	0.000	0.143	0.000	0.143	0.000	0.143
Face (four)	CWED	4	$1\pi$	1:33	0.072	0.000	0.429	0.000	0.143	0.000	0.143	0.000	0.000	0.000	0.000
Face (four)	CWED	4	$2\pi$	22:33	0.100	0.000	0.286	0.000	0.000	0.000	0.143	0.000	0.286	0.286	0.000
Face (four)	CWED	4	$3\pi$	15:33	0.072	0.000	0.286	0.000	0.286	0.000	0.143	0.000	0.000	0.000	0.000
Face (four)	CWED	5	$1\pi$	1:41	0.072	0.000	0.429	0.000	0.143	0.000	0.143	0.000	0.000	0.000	0.000
Face (four)	CWED	5	$2\pi$	15:28	0.086	0.000	0.429	0.000	0.286	0.000	0.143	0.000	0.000	0.000	0.000
Face (four)	CWED	5	$3\pi$	13:32	0.086	0.000	0.429	0.000	0.286	0.000	0.143	0.000	0.000	0.000	0.000
Face (four)	CWED	6	$1\pi$	1:49	0.072	0.000	0.429	0.000	0.143	0.000	0.143	0.000	0.000	0.000	0.000
Face (four)	CWED	6	$2\pi$	18:34	0.086	0.000	0.429	0.000	0.286	0.000	0.143	0.000	0.000	0.000	0.000
Face (four)	CWED	6	$3\pi$	1:36	0.072	0.000	0.286	0.000	0.286	0.143	0.000	0.000	0.000	0.000	0.000
Face (four)	CWED	7	$1\pi$	1:57	0.072	0.000	0.429	0.000	0.143	0.000	0.143	0.000	0.000	0.000	0.000
Face (four)	CWED	7	$2\pi$	20:39	0.086	0.000	0.429	0.000	0.286	0.000	0.143	0.000	0.000	0.000	0.000
Face (four)	CWED	7	$3\pi$	1:45	0.086	0.000	0.286	0.000	0.286	0.143	0.143	0.000	0.000	0.000	0.000



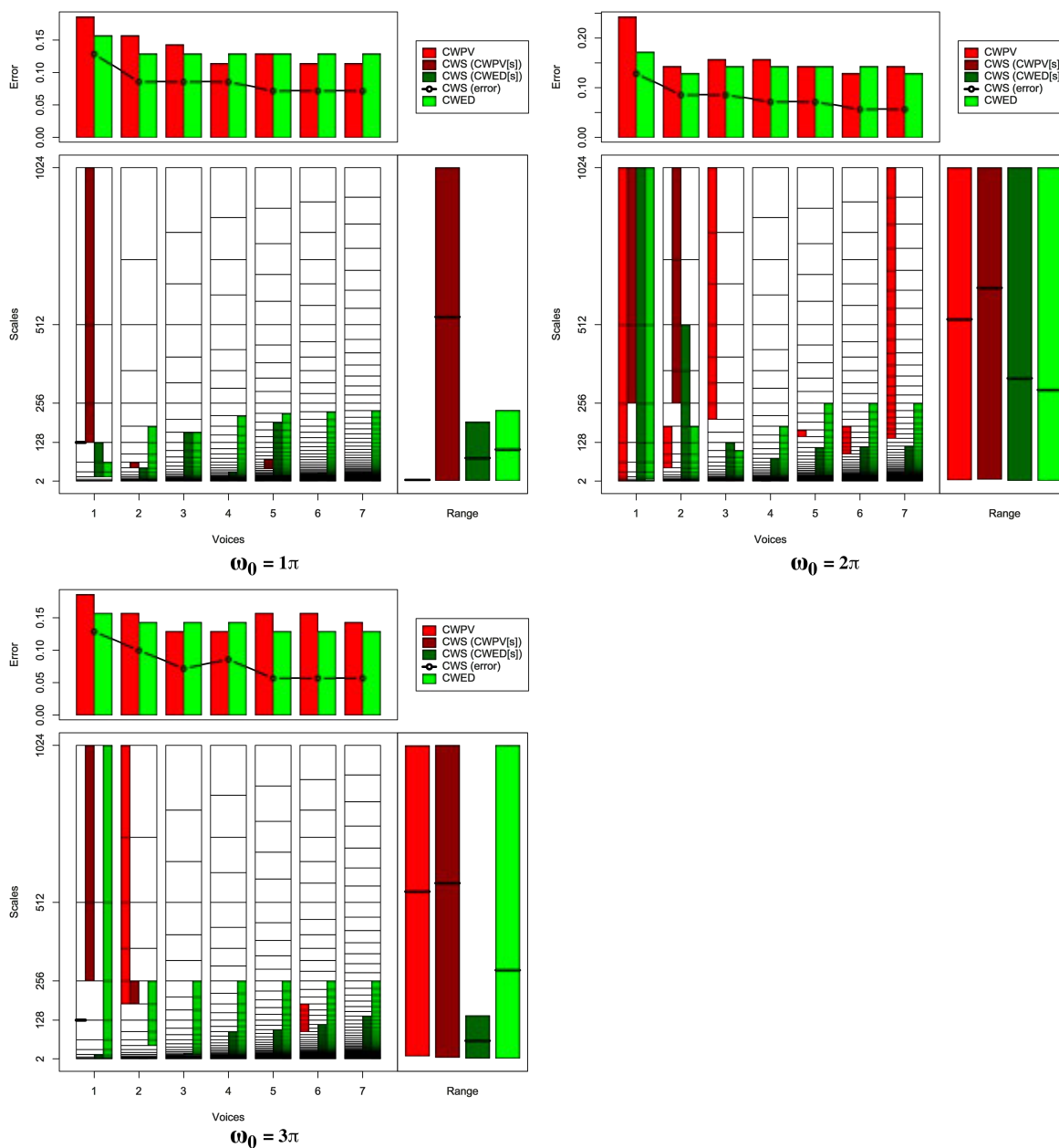


FIGURE B.12: Summary of results for the Lightning2 classification problem comparing CWS, CWPV, CWED methods using 1-7 voices and three  $\omega_0$  values. A lower CWPV score suggests that the problem is predominantly characterised by FM, whereas a lower CWED implies a predominant AM characteristic. The scale ranges have been translated from scale number to scale value. In the bottom right figure of each figure the average range of scales for all 7 voices are presented for each technique.

TABLE B.12: Summary of results for the Lightning2 classification problem comparing Ed, DTW, CWS, CWPV, and CWED using 1-7 voices and 3  $\omega_0$  parameters.  $S$  is the scale set(s) associated with the CWS, CWPV and CWED results. The mean values highlighted in bold are the best in model error rate for the problem.

Problem	Technique	Voices	$\omega_0$	$S$	Mean	1	2	3	4	5	6	7	7	9	10
Lightning2	Ed				0.172	0.000	0.143	0.143	0.143	0.143	0.286	0.143	0.286	0.286	0.143
Lightning2	DTW				0.157	0.286	0.143	0.000	0.143	0.429	0.000	0.286	0.143	0.143	0.000
Lightning2	CWS	1	$1\pi$	7:10,4:7	0.129	0.000	0.143	0.143	0.143	0.143	0.000	0.286	0.286	0.143	0.000
Lightning2	CWS	1	$2\pi$	8:10,1:10	0.129	0.000	0.143	0.286	0.143	0.143	0.000	0.143	0.286	0.000	0.143
Lightning2	CWS	1	$3\pi$	8:10,1:4	0.129	0.143	0.000	0.143	0.143	0.143	0.286	0.000	0.143	0.286	0.000
Lightning2	CWS	2	$1\pi$	10:11,4:10	0.086	0.000	0.000	0.000	0.143	0.286	0.000	0.143	0.143	0.143	0.000
Lightning2	CWS	2	$2\pi$	15:19,1:17	0.086	0.000	0.143	0.000	0.000	0.143	0.143	0.000	0.286	0.000	0.143
Lightning2	CWS	2	$3\pi$	14:15,1:5	0.100	0.000	0.143	0.143	0.000	0.000	0.143	0.143	0.000	0.143	0.286
Lightning2	CWS	3	$1\pi$	2:2,1:20	0.086	0.000	0.286	0.143	0.143	0.143	0.000	0.000	0.000	0.143	0.000
Lightning2	CWS	3	$2\pi$	7:8,1:19	0.086	0.000	0.000	0.000	0.000	0.000	0.143	0.000	0.143	0.143	0.429
Lightning2	CWS	3	$3\pi$	8:9,10:11	0.072	0.000	0.000	0.000	0.000	0.000	0.000	0.143	0.429	0.000	0.143
Lightning2	CWS	4	$1\pi$	1:10,10:17	0.086	0.143	0.143	0.000	0.000	0.000	0.143	0.143	0.286	0.000	0.000
Lightning2	CWS	4	$2\pi$	27:27,10:22	0.072	0.000	0.000	0.000	0.143	0.143	0.143	0.143	0.143	0.000	0.000
Lightning2	CWS	4	$3\pi$	8:12,7:23	0.086	0.143	0.000	0.286	0.000	0.000	0.000	0.143	0.286	0.000	0.000
Lightning2	CWS	5	$1\pi$	23:27,8:34	0.072	0.000	0.286	0.000	0.000	0.000	0.000	0.143	0.143	0.000	0.143
Lightning2	CWS	5	$2\pi$	9:14,10:30	0.072	0.000	0.000	0.143	0.000	0.143	0.000	0.143	0.143	0.143	0.000
Lightning2	CWS	5	$3\pi$	7:16,17:29	<b>0.057</b>	0.000	0.000	0.000	0.000	0.143	0.000	0.143	0.143	0.000	0.143
Lightning2	CWS	6	$1\pi$	1:12,17:24	0.072	0.000	0.143	0.000	0.000	0.143	0.000	0.143	0.143	0.000	0.143
Lightning2	CWS	6	$2\pi$	12:16,15:36	<b>0.057</b>	0.000	0.000	0.000	0.000	0.000	0.143	0.143	0.143	0.000	0.143
Lightning2	CWS	6	$3\pi$	12:16,15:36	<b>0.057</b>	0.000	0.000	0.429	0.000	0.000	0.000	0.000	0.000	0.000	0.143
Lightning2	CWS	7	$1\pi$	2:14,19:28	0.072	0.000	0.143	0.000	0.000	0.143	0.000	0.143	0.143	0.000	0.143
Lightning2	CWS	7	$2\pi$	13:19,17:42	0.057	0.000	0.000	0.143	0.000	0.000	0.000	0.143	0.143	0.000	0.143
Lightning2	CWS	7	$3\pi$	12:25,16:44	0.057	0.000	0.143	0.286	0.000	0.000	0.000	0.143	0.000	0.000	0.000
Lightning2	CWPV	1	$1\pi$	2:2	0.186	0.143	0.286	0.286	0.143	0.143	0.143	0.286	0.143	0.000	0.286
Lightning2	CWPV	1	$2\pi$	2:10	0.243	0.286	0.429	0.286	0.429	0.429	0.000	0.000	0.429	0.000	0.143
Lightning2	CWPV	1	$3\pi$	4:4	0.186	0.143	0.000	0.286	0.143	0.000	0.143	0.286	0.286	0.429	0.143
Lightning2	CWPV	2	$1\pi$	2:4	0.157	0.000	0.286	0.286	0.286	0.000	0.143	0.286	0.000	0.143	0.143
Lightning2	CWPV	2	$2\pi$	10:14	0.143	0.000	0.000	0.143	0.143	0.286	0.143	0.143	0.143	0.143	0.286
Lightning2	CWPV	2	$3\pi$	14:19	0.157	0.000	0.143	0.143	0.000	0.000	0.143	0.286	0.286	0.286	0.286
Lightning2	CWPV	3	$1\pi$	2:5	0.143	0.000	0.286	0.143	0.143	0.143	0.286	0.143	0.000	0.000	0.286
Lightning2	CWPV	3	$2\pi$	21:28	0.157	0.000	0.143	0.143	0.143	0.143	0.286	0.143	0.286	0.286	0.000
Lightning2	CWPV	3	$3\pi$	8:9	0.129	0.143	0.143	0.000	0.000	0.000	0.286	0.143	0.429	0.000	0.143
Lightning2	CWPV	4	$1\pi$	2:7	0.114	0.000	0.286	0.143	0.143	0.000	0.143	0.143	0.000	0.143	0.143
Lightning2	CWPV	4	$2\pi$	8:10	0.157	0.000	0.000	0.143	0.143	0.000	0.000	0.143	0.429	0.286	0.429
Lightning2	CWPV	4	$3\pi$	10:12	0.129	0.000	0.143	0.143	0.000	0.143	0.000	0.286	0.143	0.286	0.143
Lightning2	CWPV	5	$1\pi$	1:9	0.129	0.000	0.143	0.286	0.143	0.143	0.143	0.143	0.000	0.143	0.143
Lightning2	CWPV	5	$2\pi$	32:33	0.143	0.000	0.286	0.143	0.143	0.000	0.143	0.000	0.286	0.286	0.143
Lightning2	CWPV	5	$3\pi$	12:15	0.157	0.000	0.000	0.143	0.143	0.143	0.143	0.143	0.286	0.143	0.429
Lightning2	CWPV	6	$1\pi$	1:10	0.114	0.000	0.143	0.143	0.143	0.000	0.143	0.143	0.000	0.143	0.286
Lightning2	CWPV	6	$2\pi$	34:40	0.129	0.000	0.143	0.000	0.143	0.143	0.143	0.143	0.286	0.143	0.143
Lightning2	CWPV	6	$3\pi$	34:40	0.157	0.143	0.143	0.000	0.143	0.000	0.000	0.143	0.286	0.286	0.429
Lightning2	CWPV	7	$1\pi$	2:12	0.114	0.000	0.286	0.143	0.143	0.000	0.143	0.143	0.000	0.143	0.143
Lightning2	CWPV	7	$2\pi$	44:64	0.143	0.000	0.143	0.000	0.143	0.000	0.000	0.143	0.429	0.286	0.286
Lightning2	CWPV	7	$3\pi$	17:21	0.143	0.000	0.143	0.000	0.143	0.143	0.000	0.143	0.286	0.143	0.429
Lightning2	CWED	1	$1\pi$	4:6	0.157	0.000	0.143	0.286	0.143	0.000	0.143	0.429	0.429	0.000	0.000
Lightning2	CWED	1	$2\pi$	3:10	0.172	0.143	0.143	0.429	0.143	0.143	0.000	0.143	0.286	0.143	0.143
Lightning2	CWED	1	$3\pi$	1:10	0.157	0.143	0.143	0.000	0.286	0.143	0.000	0.286	0.286	0.143	0.143
Lightning2	CWED	2	$1\pi$	1:14	0.129	0.000	0.143	0.143	0.286	0.143	0.000	0.000	0.286	0.143	0.143
Lightning2	CWED	2	$2\pi$	5:14	0.129	0.143	0.143	0.143	0.286	0.143	0.000	0.000	0.429	0.000	0.000
Lightning2	CWED	2	$3\pi$	10:15	0.143	0.143	0.143	0.143	0.143	0.000	0.000	0.286	0.286	0.286	0.000
Lightning2	CWED	3	$1\pi$	1:20	0.129	0.000	0.143	0.143	0.286	0.143	0.000	0.000	0.286	0.143	0.143
Lightning2	CWED	3	$2\pi$	9:18	0.143	0.143	0.143	0.143	0.000	0.143	0.000	0.143	0.429	0.143	0.143
Lightning2	CWED	3	$3\pi$	10:22	0.143	0.000	0.143	0.000	0.143	0.143	0.000	0.429	0.429	0.143	0.000
Lightning2	CWED	4	$1\pi$	1:28	0.129	0.000	0.143	0.000	0.286	0.143	0.143	0.143	0.429	0.000	0.000
Lightning2	CWED	4	$2\pi$	1:27	0.143	0.000	0.143	0.000	0.286	0.143	0.000	0.286	0.429	0.143	0.000
Lightning2	CWED	4	$3\pi$	7:29	0.143	0.000	0.143	0.000	0.143	0.143	0.000	0.429	0.429	0.143	0.000
Lightning2	CWED	5	$1\pi$	1:35	0.129	0.000	0.143	0.143	0.143	0.143	0.000	0.143	0.286	0.143	0.143
Lightning2	CWED	5	$2\pi$	2:36	0.143	0.000	0.143	0.143	0.286	0.143	0.000	0.143	0.429	0.143	0.000
Lightning2	CWED	5	$3\pi$	1:36	0.129	0.000	0.143	0.000	0.143	0.143	0.000	0.286	0.429	0.143	0.000
Lightning2	CWED	6	$1\pi$	1:42	0.129	0.143	0.000	0.286	0.143	0.143	0.143	0.429	0.000	0.000	0.000
Lightning2	CWED	6	$2\pi$	2:43	0.143	0.000	0.143	0.143	0.286	0.143	0.000	0.143	0.429	0.143	0.000
Lightning2	CWED	6	$3\pi$	2:43	0.129	0.000	0.143	0.000	0.143	0.143	0.000	0.286	0.429	0.143	0.000
Lightning2	CWED	7	$1\pi$	1:49	0.129	0.000	0.143	0.000	0.286	0.143	0.143	0.143	0.429	0.000	0.000
Lightning2	CWED	7	$2\pi$	12:50	0.129	0.000	0.143	0.143	0.286	0.143	0.000	0.143	0.429	0.000	0.000
Lightning2	CWED	7	$3\pi$	1:50	0.129	0.000	0.143	0.000	0.143	0.143	0.000	0.286	0.429	0.143	0.000

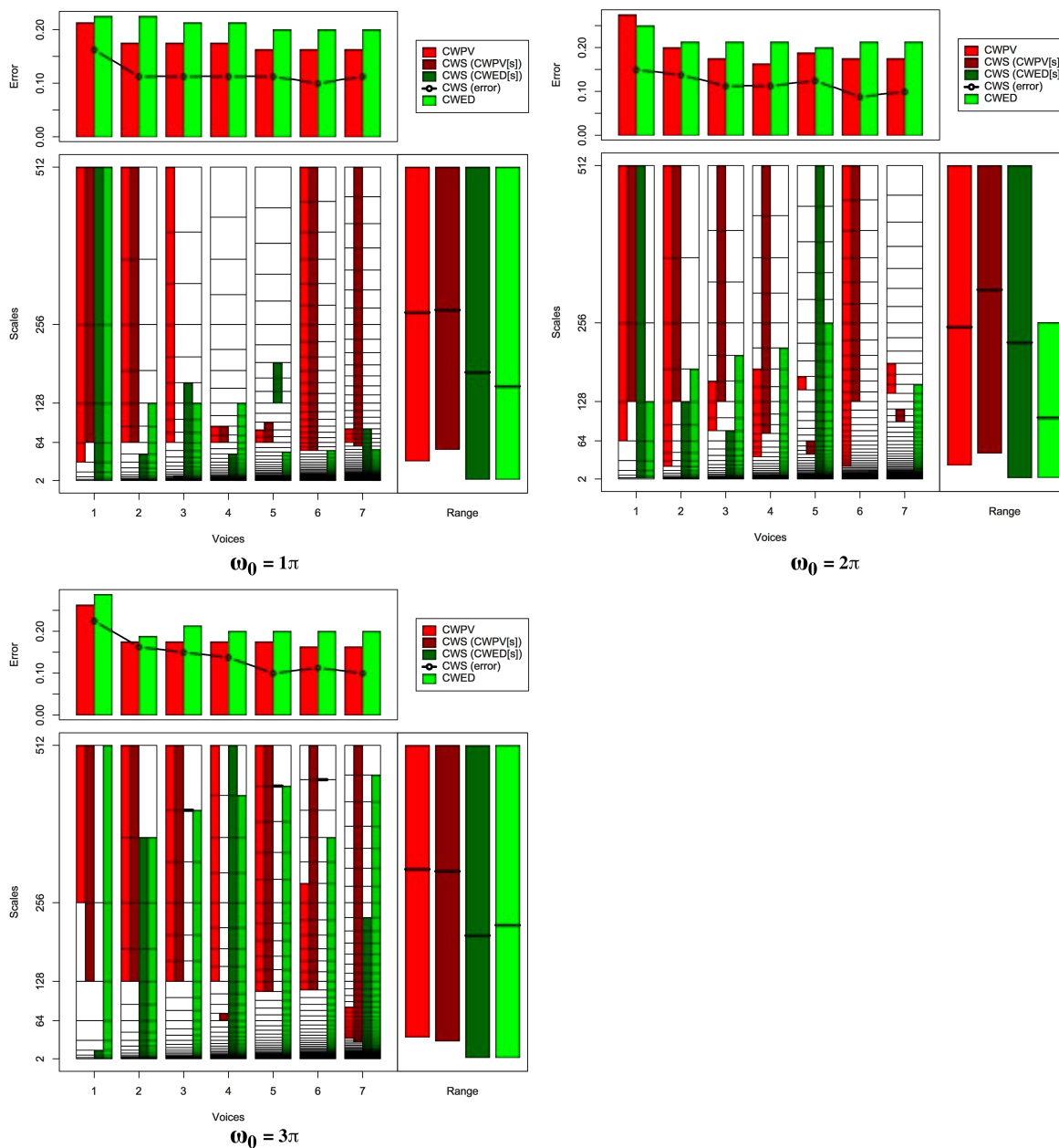


FIGURE B.13: Summary of results for the Lightning7 classification problem comparing CWS, CWPV, CWED methods using 1-7 voices and three  $\omega_0$  values. A lower CWPV score suggests that the problem is predominantly characterised by FM, whereas a lower CWED implies a predominant AM characteristic. The scale ranges have been translated from scale number to scale value. In the bottom right figure of each figure the average range of scales for all 7 voices are presented for each technique.

TABLE B.13: Summary of results for the Lightning7 classification problem comparing Ed, DTW, CWS, CWPV, and CWED using 1-7 voices and 3  $\omega_0$  parameters.  $S$  is the scale set(s) associated with the CWS, CWPV and CWED results. The mean values highlighted in bold are the best in model error rate for the problem.

Problem	Technique	Voices	$\omega_0$	$S$	Mean	1	2	3	4	5	6	7	7	9	10
Lightning7	Ed				0.163	0.125	0.250	0.125	0.125	0.250	0.125	0.250	0.125	0.250	0.000
Lightning7	DTW				0.138	0.000	0.250	0.000	0.250	0.000	0.000	0.250	0.125	0.250	0.250
Lightning7	CWS	1	$1\pi$	6:9,1:9	0.163	0.000	0.250	0.125	0.250	0.125	0.125	0.125	0.125	0.250	0.250
Lightning7	CWS	1	$2\pi$	7:9,2:9	0.150	0.125	0.250	0.125	0.125	0.125	0.125	0.125	0.250	0.125	0.125
Lightning7	CWS	1	$3\pi$	7:9,1:4	0.225	0.125	0.250	0.125	0.250	0.000	0.250	0.125	0.500	0.250	0.375
Lightning7	CWS	2	$1\pi$	11:17,2:10	0.113	0.000	0.125	0.250	0.125	0.125	0.000	0.125	0.125	0.125	0.125
Lightning7	CWS	2	$2\pi$	13:17,3:13	0.138	0.125	0.250	0.250	0.125	0.125	0.000	0.125	0.125	0.125	0.125
Lightning7	CWS	2	$3\pi$	13:17,1:16	0.163	0.125	0.250	0.125	0.125	0.250	0.000	0.125	0.125	0.250	0.250
Lightning7	CWS	3	$1\pi$	15:15,1:20	0.113	0.000	0.250	0.125	0.125	0.125	0.000	0.000	0.125	0.125	0.250
Lightning7	CWS	3	$2\pi$	19:25,4:17	0.113	0.000	0.250	0.000	0.125	0.125	0.125	0.125	0.125	0.125	0.125
Lightning7	CWS	3	$3\pi$	19:25,6:6	0.150	0.125	0.125	0.125	0.250	0.000	0.125	0.125	0.125	0.250	0.250
Lightning7	CWS	4	$1\pi$	21:23,2:19	0.113	0.000	0.125	0.125	0.125	0.125	0.000	0.125	0.250	0.125	0.125
Lightning7	CWS	4	$2\pi$	22:33,5:10	0.113	0.000	0.250	0.000	0.125	0.250	0.000	0.125	0.125	0.000	0.250
Lightning7	CWS	4	$3\pi$	21:22,6:33	0.138	0.125	0.250	0.000	0.125	0.125	0.250	0.125	0.125	0.250	0.000
Lightning7	CWS	5	$1\pi$	26:29,31:34	0.113	0.000	0.250	0.125	0.125	0.125	0.000	0.125	0.125	0.125	0.125
Lightning7	CWS	5	$2\pi$	23:26,1:41	0.125	0.250	0.250	0.125	0.125	0.125	0.125	0.000	0.000	0.125	0.125
Lightning7	CWS	5	$3\pi$	30:41,14:14	0.100	0.000	0.125	0.000	0.000	0.250	0.000	0.125	0.125	0.125	0.250
Lightning7	CWS	6	$1\pi$	29:49,2:12	0.100	0.000	0.125	0.125	0.000	0.125	0.125	0.125	0.125	0.000	0.250
Lightning7	CWS	6	$2\pi$	37:49,13:14	<b>0.088</b>	0.000	0.000	0.125	0.000	0.125	0.000	0.125	0.125	0.125	0.250
Lightning7	CWS	6	$3\pi$	36:49,17:17	0.113	0.125	0.125	0.125	0.125	0.125	0.000	0.000	0.125	0.125	0.250
Lightning7	CWS	7	$1\pi$	35:57,12:39	0.113	0.000	0.125	0.125	0.125	0.125	0.125	0.125	0.125	0.125	0.125
Lightning7	CWS	7	$2\pi$	40:42,15:16	0.100	0.125	0.250	0.125	0.125	0.125	0.000	0.000	0.000	0.000	0.250
Lightning7	CWS	7	$3\pi$	28:57,13:49	0.100	0.000	0.375	0.000	0.000	0.000	0.125	0.125	0.125	0.250	0.000
Lightning7	CWPV	1	$1\pi$	5:9	0.213	0.250	0.375	0.125	0.125	0.250	0.250	0.250	0.125	0.250	0.125
Lightning7	CWPV	1	$2\pi$	6:9	0.275	0.375	0.500	0.125	0.250	0.250	0.250	0.250	0.125	0.250	0.375
Lightning7	CWPV	1	$3\pi$	8:9	0.263	0.125	0.125	0.250	0.375	0.250	0.250	0.125	0.500	0.250	0.375
Lightning7	CWPV	2	$1\pi$	11:17	0.175	0.125	0.125	0.125	0.000	0.250	0.125	0.250	0.250	0.250	0.250
Lightning7	CWPV	2	$2\pi$	8:17	0.200	0.000	0.375	0.000	0.375	0.250	0.125	0.125	0.125	0.250	0.375
Lightning7	CWPV	2	$3\pi$	13:17	0.175	0.000	0.125	0.125	0.250	0.250	0.125	0.250	0.125	0.125	0.375
Lightning7	CWPV	3	$1\pi$	16:25	0.175	0.125	0.125	0.250	0.000	0.250	0.125	0.125	0.250	0.250	0.250
Lightning7	CWPV	3	$2\pi$	17:20	0.175	0.000	0.125	0.125	0.125	0.250	0.250	0.250	0.125	0.125	0.375
Lightning7	CWPV	3	$3\pi$	19:25	0.175	0.000	0.125	0.250	0.125	0.250	0.125	0.125	0.250	0.125	0.375
Lightning7	CWPV	4	$1\pi$	21:23	0.175	0.000	0.125	0.125	0.000	0.250	0.125	0.250	0.375	0.250	0.250
Lightning7	CWPV	4	$2\pi$	18:27	0.163	0.125	0.375	0.000	0.125	0.250	0.125	0.250	0.125	0.125	0.125
Lightning7	CWPV	4	$3\pi$	25:33	0.175	0.000	0.125	0.125	0.250	0.250	0.125	0.250	0.125	0.250	0.250
Lightning7	CWPV	5	$1\pi$	26:28	0.163	0.000	0.125	0.125	0.000	0.250	0.125	0.250	0.250	0.125	0.375
Lightning7	CWPV	5	$2\pi$	32:33	0.188	0.000	0.125	0.125	0.125	0.250	0.125	0.250	0.250	0.250	0.375
Lightning7	CWPV	5	$3\pi$	30:41	0.175	0.000	0.375	0.125	0.125	0.250	0.125	0.250	0.125	0.125	0.250
Lightning7	CWPV	6	$1\pi$	29:49	0.163	0.125	0.125	0.125	0.000	0.250	0.125	0.250	0.125	0.125	0.375
Lightning7	CWPV	6	$2\pi$	22:49	0.175	0.250	0.375	0.000	0.250	0.125	0.125	0.250	0.125	0.250	0.000
Lightning7	CWPV	6	$3\pi$	36:44	0.163	0.000	0.250	0.125	0.125	0.250	0.125	0.250	0.125	0.125	0.250
Lightning7	CWPV	7	$1\pi$	36:39	0.163	0.000	0.125	0.125	0.000	0.250	0.125	0.250	0.250	0.125	0.375
Lightning7	CWPV	7	$2\pi$	44:47	0.175	0.000	0.125	0.250	0.000	0.250	0.125	0.250	0.250	0.250	0.250
Lightning7	CWPV	7	$3\pi$	30:39	0.163	0.125	0.500	0.000	0.250	0.000	0.125	0.375	0.000	0.250	0.000
Lightning7	CWED	1	$1\pi$	1:9	0.225	0.125	0.250	0.250	0.250	0.125	0.125	0.250	0.250	0.375	0.250
Lightning7	CWED	1	$2\pi$	2:7	0.250	0.125	0.375	0.250	0.250	0.250	0.000	0.250	0.500	0.375	0.125
Lightning7	CWED	1	$3\pi$	1:9	0.288	0.125	0.375	0.250	0.375	0.125	0.125	0.375	0.250	0.500	0.375
Lightning7	CWED	2	$1\pi$	1:13	0.225	0.125	0.250	0.250	0.375	0.125	0.000	0.250	0.250	0.250	0.375
Lightning7	CWED	2	$2\pi$	3:14	0.213	0.125	0.250	0.250	0.250	0.250	0.000	0.250	0.500	0.125	0.125
Lightning7	CWED	2	$3\pi$	1:16	0.188	0.125	0.375	0.250	0.125	0.125	0.000	0.125	0.375	0.250	0.125
Lightning7	CWED	3	$1\pi$	1:19	0.213	0.125	0.250	0.250	0.250	0.125	0.000	0.250	0.250	0.250	0.375
Lightning7	CWED	3	$2\pi$	3:21	0.213	0.125	0.250	0.250	0.125	0.125	0.000	0.250	0.500	0.125	0.375
Lightning7	CWED	3	$3\pi$	5:24	0.213	0.250	0.250	0.250	0.125	0.125	0.000	0.125	0.500	0.125	0.375
Lightning7	CWED	4	$1\pi$	1:25	0.213	0.125	0.250	0.250	0.250	0.125	0.000	0.250	0.250	0.250	0.375
Lightning7	CWED	4	$2\pi$	2:28	0.213	0.125	0.250	0.250	0.125	0.125	0.000	0.250	0.500	0.125	0.375
Lightning7	CWED	4	$3\pi$	7:32	0.200	0.250	0.250	0.250	0.250	0.125	0.000	0.125	0.250	0.125	0.375
Lightning7	CWED	5	$1\pi$	1:24	0.200	0.125	0.125	0.250	0.250	0.125	0.125	0.125	0.375	0.250	0.250
Lightning7	CWED	5	$2\pi$	7:36	0.200	0.250	0.250	0.250	0.125	0.125	0.000	0.250	0.250	0.125	0.375
Lightning7	CWED	5	$3\pi$	7:40	0.200	0.250	0.250	0.250	0.250	0.125	0.000	0.125	0.250	0.125	0.375
Lightning7	CWED	6	$1\pi$	1:29	0.200	0.125	0.125	0.250	0.250	0.125	0.125	0.125	0.375	0.250	0.250
Lightning7	CWED	6	$2\pi$	11:19	0.213	0.000	0.125	0.250	0.000	0.250	0.125	0.125	0.375	0.500	0.375
Lightning7	CWED	6	$3\pi$	14:46	0.200	0.250	0.375	0.250	0.125	0.125	0.000	0.125	0.375	0.125	0.250
Lightning7	CWED	7	$1\pi$	1:34	0.200	0.125	0.125	0.250	0.250	0.125	0.125	0.125	0.375	0.250	0.250
Lightning7	CWED	7	$2\pi$	8:45	0.213	0.250	0.250	0.250	0.125	0.125	0.000	0.250	0.500	0.125	0.250
Lightning7	CWED	7	$3\pi$	9:56	0.200	0.250	0.250	0.250	0.250	0.125	0.000	0.125	0.250	0.125	0.375

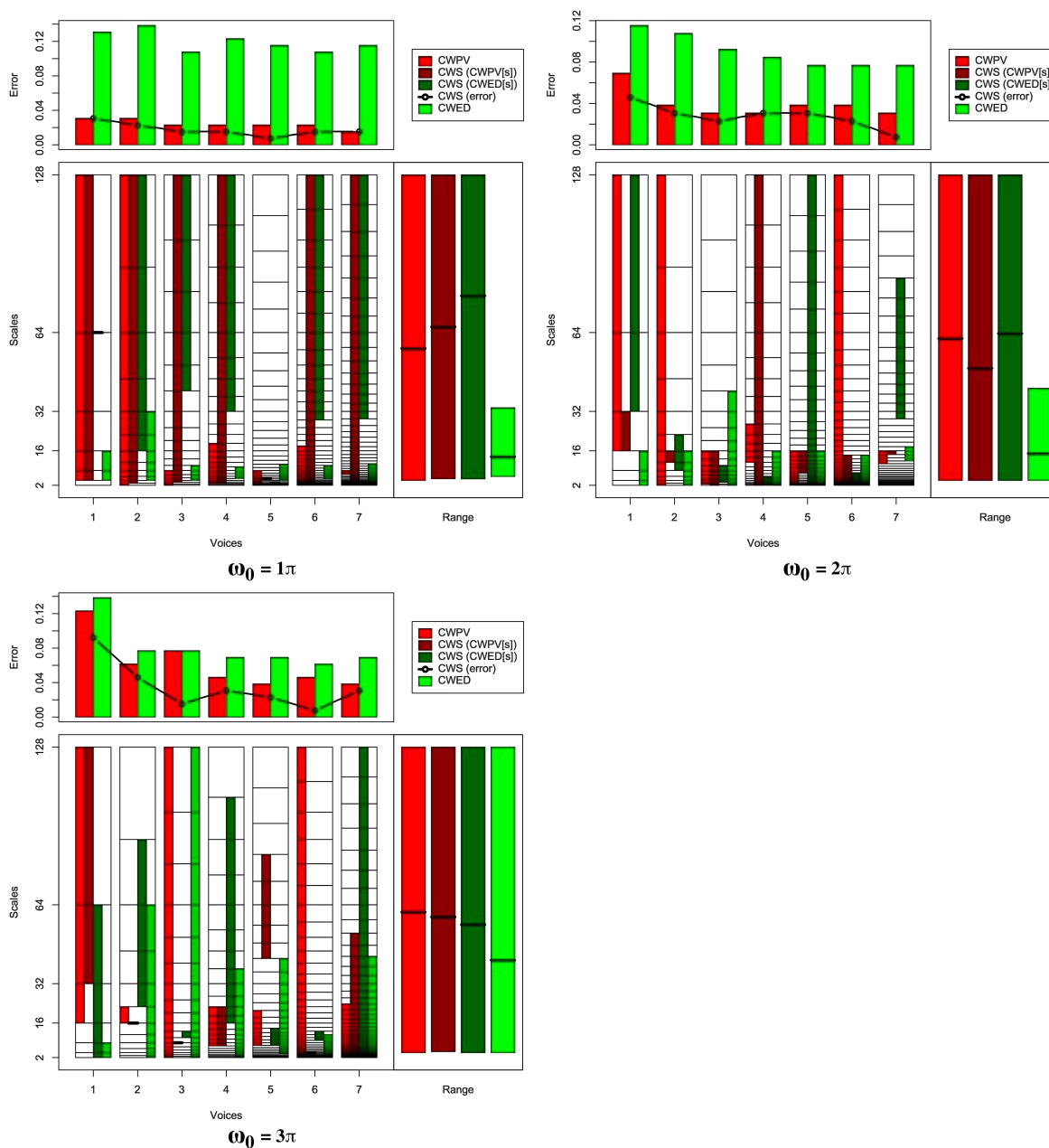


FIGURE B.14: Summary of results for the ECG200 classification problem comparing CWS, CWPV, CWED methods using 1-7 voices and three  $\omega_0$  values. A lower CWPV score suggests that the problem is predominantly characterised by FM, whereas a lower CWED implies a predominant AM characteristic. The scale ranges have been translated from scale number to scale value. In the bottom right figure of each figure the average range of scales for all 7 voices are presented for each technique.

TABLE B.14: Summary of results for the ECG200 classification problem comparing Ed, DTW, CWS, CWPV, and CWED using 1-7 voices and 3  $\omega_0$  parameters.  $S$  is the scale set(s) associated with the CWS, CWPV and CWED results. The mean values highlighted in bold are the best in model error rate for the problem.

Problem	Technique	Voices	$\omega_0$	$S$	Mean	1	2	3	4	5	6	7	7	9	10
ECG200	Ed				0.092	0.154	0.077	0.077	0.000	0.154	0.077	0.154	0.000	0.154	0.077
ECG200	DTW				0.092	0.077	0.154	0.000	0.154	0.154	0.154	0.077	0.000	0.077	0.077
ECG200	CWS	1	$1\pi$	2:7,7:7	0.031	0.077	0.000	0.000	0.000	0.077	0.000	0.077	0.000	0.077	0.000
ECG200	CWS	1	$2\pi$	4:5,5:7	0.046	0.077	0.077	0.000	0.000	0.000	0.000	0.154	0.000	0.000	0.154
ECG200	CWS	1	$3\pi$	5:7,1:6	0.092	0.000	0.077	0.000	0.077	0.154	0.077	0.231	0.077	0.154	0.077
ECG200	CWS	2	$1\pi$	2:13,7:13	0.023	0.077	0.000	0.000	0.000	0.077	0.000	0.077	0.000	0.000	0.000
ECG200	CWS	2	$2\pi$	6:7,5:8	0.031	0.000	0.077	0.000	0.000	0.154	0.000	0.077	0.000	0.000	0.000
ECG200	CWS	2	$3\pi$	8:8,8:12	0.046	0.077	0.077	0.077	0.000	0.000	0.077	0.000	0.000	0.154	0.000
ECG200	CWS	3	$1\pi$	3:19,14:19	0.015	0.000	0.000	0.000	0.000	0.077	0.000	0.077	0.000	0.000	0.000
ECG200	CWS	3	$2\pi$	1:10,3:8	0.023	0.000	0.000	0.000	0.000	0.077	0.077	0.077	0.000	0.000	0.000
ECG200	CWS	3	$3\pi$	11:11,8:9	0.015	0.000	0.000	0.000	0.000	0.077	0.000	0.000	0.000	0.077	0.000
ECG200	CWS	4	$1\pi$	3:25,17:25	0.015	0.000	0.000	0.000	0.000	0.077	0.000	0.077	0.000	0.000	0.000
ECG200	CWS	4	$2\pi$	1:25,2:7	0.031	0.000	0.000	0.000	0.000	0.077	0.077	0.077	0.000	0.077	0.000
ECG200	CWS	4	$3\pi$	8:15,13:24	0.031	0.000	0.077	0.000	0.000	0.077	0.000	0.077	0.000	0.077	0.000
ECG200	CWS	5	$1\pi$	10:10,3:5	<b>0.008</b>	0.000	0.000	0.000	0.000	0.077	0.000	0.000	0.000	0.000	0.000
ECG200	CWS	5	$2\pi$	10:16,1:31	0.031	0.000	0.000	0.000	0.000	0.077	0.077	0.077	0.000	0.077	0.000
ECG200	CWS	5	$3\pi$	23:28,10:15	0.023	0.000	0.077	0.000	0.077	0.000	0.000	0.077	0.000	0.000	0.000
ECG200	CWS	6	$1\pi$	4:37,24:37	0.015	0.000	0.000	0.000	0.000	0.077	0.000	0.077	0.000	0.000	0.000
ECG200	CWS	6	$2\pi$	1:18,1:12	0.023	0.000	0.000	0.000	0.000	0.077	0.077	0.000	0.000	0.077	0.000
ECG200	CWS	6	$3\pi$	21:21,14:17	<b>0.008</b>	0.000	0.000	0.000	0.000	0.000	0.000	0.000	0.000	0.077	0.000
ECG200	CWS	7	$1\pi$	4:43,28:43	0.015	0.000	0.000	0.000	0.000	0.077	0.000	0.077	0.000	0.000	0.000
ECG200	CWS	7	$2\pi$	21:22,28:39	<b>0.008</b>	0.000	0.000	0.000	0.000	0.000	0.000	0.000	0.000	0.000	0.077
ECG200	CWS	7	$3\pi$	3:34,1:43	0.031	0.000	0.000	0.000	0.000	0.077	0.077	0.077	0.000	0.000	0.077
ECG200	CWPV	1	$1\pi$	2:7	0.031	0.077	0.000	0.000	0.000	0.077	0.000	0.077	0.000	0.077	0.000
ECG200	CWPV	1	$2\pi$	4:7	0.069	0.077	0.154	0.000	0.000	0.077	0.000	0.308	0.000	0.000	0.077
ECG200	CWPV	1	$3\pi$	4:7	0.123	0.077	0.077	0.077	0.154	0.154	0.077	0.231	0.000	0.231	0.154
ECG200	CWPV	2	$1\pi$	1:13	0.031	0.077	0.077	0.000	0.000	0.077	0.000	0.077	0.000	0.000	0.000
ECG200	CWPV	2	$2\pi$	1:13	0.039	0.000	0.000	0.000	0.000	0.154	0.077	0.077	0.077	0.000	0.000
ECG200	CWPV	2	$3\pi$	7:8	0.062	0.077	0.077	0.000	0.077	0.077	0.000	0.077	0.077	0.077	0.077
ECG200	CWPV	3	$1\pi$	1:7	0.023	0.077	0.000	0.000	0.000	0.077	0.000	0.077	0.000	0.000	0.000
ECG200	CWPV	3	$2\pi$	2:10	0.031	0.000	0.000	0.000	0.000	0.077	0.077	0.154	0.000	0.000	0.000
ECG200	CWPV	3	$3\pi$	1:19	0.077	0.077	0.077	0.000	0.077	0.154	0.077	0.231	0.077	0.000	0.000
ECG200	CWPV	4	$1\pi$	3:14	0.023	0.077	0.000	0.000	0.000	0.077	0.000	0.077	0.000	0.000	0.000
ECG200	CWPV	4	$2\pi$	11:16	0.031	0.000	0.077	0.000	0.000	0.154	0.000	0.077	0.000	0.000	0.000
ECG200	CWPV	4	$3\pi$	8:15	0.046	0.000	0.077	0.000	0.000	0.154	0.077	0.077	0.000	0.077	0.000
ECG200	CWPV	5	$1\pi$	1:11	0.023	0.077	0.000	0.000	0.000	0.077	0.000	0.077	0.000	0.000	0.000
ECG200	CWPV	5	$2\pi$	2:16	0.039	0.000	0.077	0.000	0.000	0.077	0.077	0.077	0.000	0.077	0.000
ECG200	CWPV	5	$3\pi$	10:18	0.039	0.000	0.000	0.000	0.000	0.077	0.000	0.154	0.000	0.077	0.077
ECG200	CWPV	6	$1\pi$	5:20	0.023	0.077	0.000	0.000	0.000	0.077	0.000	0.077	0.000	0.000	0.000
ECG200	CWPV	6	$2\pi$	2:37	0.039	0.000	0.000	0.000	0.077	0.077	0.077	0.077	0.000	0.077	0.000
ECG200	CWPV	6	$3\pi$	4:37	0.046	0.000	0.000	0.000	0.077	0.154	0.077	0.154	0.000	0.000	0.000
ECG200	CWPV	7	$1\pi$	13:15	0.015	0.000	0.000	0.000	0.000	0.077	0.000	0.077	0.000	0.000	0.000
ECG200	CWPV	7	$2\pi$	18:22	0.031	0.000	0.077	0.000	0.000	0.154	0.000	0.077	0.000	0.000	0.000
ECG200	CWPV	7	$3\pi$	6:26	0.039	0.000	0.154	0.000	0.000	0.077	0.077	0.077	0.000	0.000	0.000
ECG200	CWED	1	$1\pi$	2:4	0.131	0.308	0.154	0.077	0.077	0.231	0.000	0.077	0.154	0.154	0.077
ECG200	CWED	1	$2\pi$	1:4	0.116	0.154	0.000	0.154	0.154	0.077	0.077	0.231	0.077	0.077	0.154
ECG200	CWED	1	$3\pi$	1:3	0.139	0.231	0.077	0.154	0.231	0.077	0.077	0.077	0.154	0.154	0.154
ECG200	CWED	2	$1\pi$	3:9	0.139	0.077	0.154	0.077	0.154	0.231	0.000	0.308	0.077	0.231	0.077
ECG200	CWED	2	$2\pi$	1:7	0.108	0.000	0.231	0.154	0.077	0.000	0.077	0.231	0.077	0.231	0.000
ECG200	CWED	2	$3\pi$	1:11	0.077	0.000	0.077	0.000	0.077	0.077	0.000	0.077	0.000	0.231	0.231
ECG200	CWED	3	$1\pi$	4:8	0.108	0.077	0.077	0.231	0.154	0.077	0.000	0.077	0.077	0.231	0.077
ECG200	CWED	3	$2\pi$	1:14	0.092	0.077	0.154	0.000	0.077	0.077	0.000	0.154	0.000	0.231	0.154
ECG200	CWED	3	$3\pi$	1:19	0.077	0.077	0.077	0.000	0.154	0.154	0.000	0.154	0.000	0.077	0.077
ECG200	CWED	4	$1\pi$	6:10	0.123	0.154	0.077	0.231	0.154	0.000	0.000	0.077	0.077	0.308	0.154
ECG200	CWED	4	$2\pi$	1:13	0.085	0.000	0.231	0.077	0.000	0.077	0.077	0.154	0.000	0.154	0.077
ECG200	CWED	4	$3\pi$	1:18	0.069	0.000	0.154	0.000	0.077	0.154	0.000	0.077	0.000	0.154	0.077
ECG200	CWED	5	$1\pi$	6:13	0.116	0.077	0.077	0.231	0.077	0.077	0.077	0.154	0.077	0.231	0.077
ECG200	CWED	5	$2\pi$	1:16	0.077	0.000	0.154	0.077	0.000	0.077	0.077	0.154	0.000	0.154	0.077
ECG200	CWED	5	$3\pi$	5:23	0.069	0.077	0.154	0.000	0.077	0.077	0.000	0.154	0.000	0.077	0.077
ECG200	CWED	6	$1\pi$	8:15	0.108	0.154	0.077	0.231	0.077	0.000	0.000	0.077	0.077	0.308	0.077
ECG200	CWED	6	$2\pi$	1:18	0.077	0.000	0.154	0.077	0.000	0.154	0.077	0.077	0.077	0.154	0.000
ECG200	CWED	6	$3\pi$	5:16	0.062	0.000	0.077	0.000	0.077	0.077	0.077	0.077	0.077	0.154	0.000
ECG200	CWED	7	$1\pi$	7:18	0.116	0.077	0.077	0.231	0.154	0.077	0.000	0.154	0.077	0.231	0.077
ECG200	CWED	7	$2\pi$	19:23	0.077	0.000	0.077	0.077	0.077	0.077	0.000	0.154	0.154	0.077	0.077
ECG200	CWED	7	$3\pi$	1:32	0.069	0.077	0.154	0.000	0.077	0.077	0.000	0.077	0.000	0.154	0.077

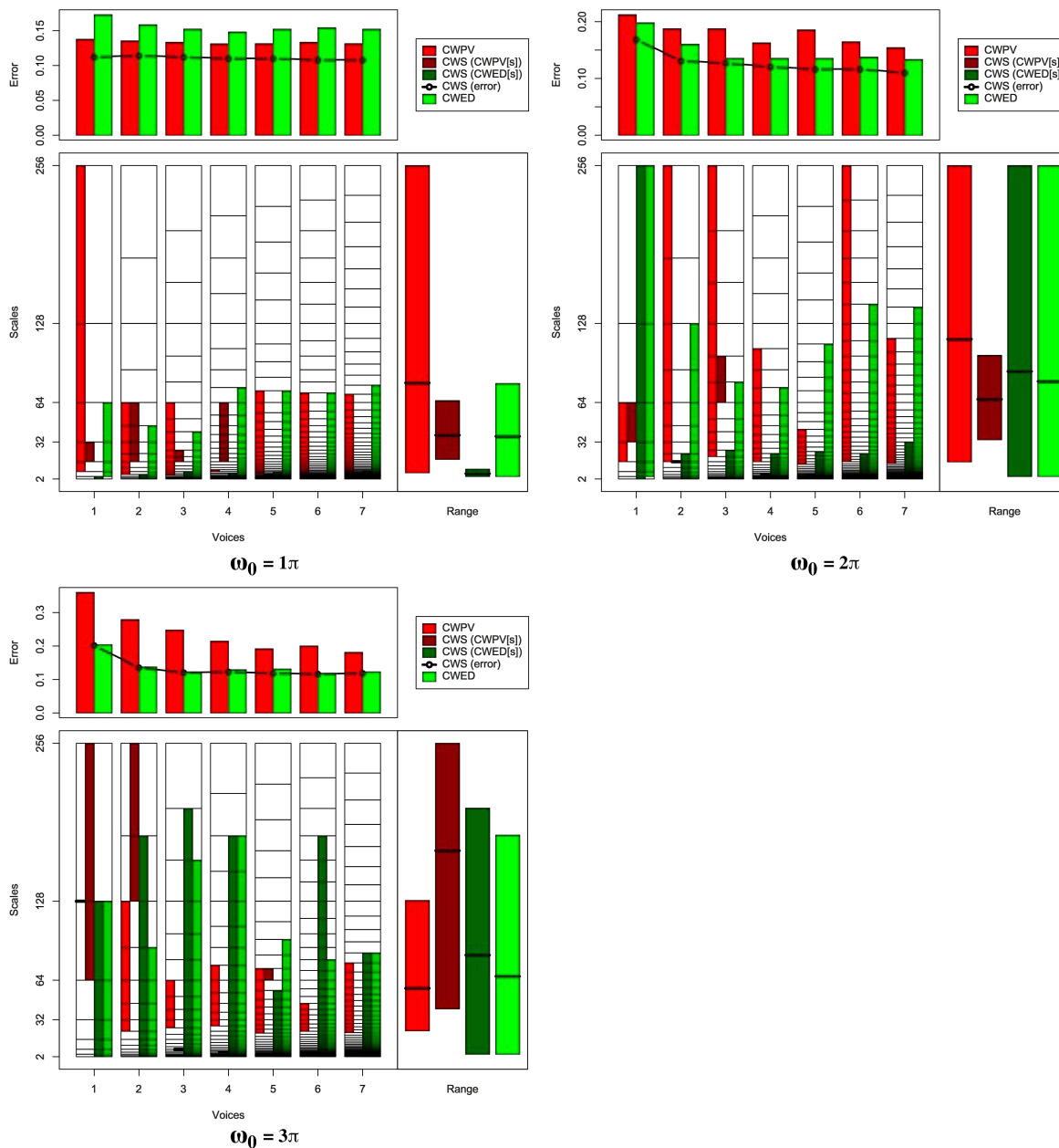


FIGURE B.15: Summary of results for the Adiac classification problem comparing CWS, CWPV, CWED methods using 1-7 voices and three  $\omega_0$  values. A lower CWPV score suggests that the problem is predominantly characterised by FM, whereas a lower CWED implies a predominant AM characteristic. The scale ranges have been translated from scale number to scale value. In the bottom right figure of each figure the average range of scales for all 7 voices are presented for each technique.

TABLE B.15: Summary of results for the Adiac classification problem comparing Ed, DTW, CWS, CWPV, and CWED using 1-7 voices and 3  $\omega_0$  parameters.  $S$  is the scale set(s) associated with the CWS, CWPV and CWED results. The mean values highlighted in bold are the best in model error rate for the problem.

Problem	Technique	Voices	$\omega_0$	$S$	Mean	1	2	3	4	5	6	7	7	9	10
Adiac	Ed				0.194	0.208	0.146	0.188	0.271	0.229	0.208	0.146	0.250	0.125	0.167
Adiac	DTW				0.177	0.208	0.167	0.125	0.229	0.167	0.188	0.167	0.208	0.167	0.146
Adiac	CWS	1	$1\pi$	4:5,1:2	0.112	0.083	0.125	0.146	0.146	0.167	0.125	0.083	0.083	0.062	0.104
Adiac	CWS	1	$2\pi$	5:6,1:8	0.169	0.188	0.146	0.208	0.188	0.208	0.188	0.146	0.146	0.125	0.146
Adiac	CWS	1	$3\pi$	6:8,1:7	0.202	0.188	0.208	0.208	0.146	0.208	0.250	0.208	0.208	0.188	0.208
Adiac	CWS	2	$1\pi$	7:11,1:4	0.115	0.104	0.125	0.104	0.125	0.167	0.146	0.083	0.125	0.062	0.104
Adiac	CWS	2	$2\pi$	10:10,1:8	0.131	0.146	0.083	0.125	0.146	0.167	0.229	0.104	0.125	0.146	0.042
Adiac	CWS	2	$3\pi$	13:15,1:14	0.136	0.125	0.125	0.146	0.146	0.167	0.167	0.125	0.146	0.062	0.146
Adiac	CWS	3	$1\pi$	10:12,1:7	0.112	0.104	0.125	0.083	0.125	0.188	0.146	0.083	0.083	0.083	0.104
Adiac	CWS	3	$2\pi$	16:18,1:12	0.127	0.125	0.125	0.167	0.167	0.188	0.188	0.021	0.188	0.042	0.062
Adiac	CWS	3	$3\pi$	14:14,1:21	0.121	0.083	0.083	0.146	0.125	0.125	0.125	0.146	0.146	0.104	0.125
Adiac	CWS	4	$1\pi$	13:21,1:8	0.110	0.104	0.125	0.083	0.146	0.167	0.146	0.083	0.083	0.062	0.104
Adiac	CWS	4	$2\pi$	19:19,1:15	0.121	0.125	0.125	0.104	0.146	0.146	0.146	0.125	0.104	0.104	0.083
Adiac	CWS	4	$3\pi$	19:19,1:27	0.123	0.125	0.125	0.125	0.125	0.125	0.146	0.146	0.125	0.083	0.104
Adiac	CWS	5	$1\pi$	16:16,5:11	0.110	0.104	0.146	0.083	0.104	0.167	0.146	0.083	0.083	0.083	0.104
Adiac	CWS	5	$2\pi$	24:24,1:19	0.117	0.125	0.104	0.104	0.125	0.125	0.188	0.083	0.125	0.125	0.062
Adiac	CWS	5	$3\pi$	26:27,1:25	0.119	0.146	0.083	0.188	0.104	0.146	0.146	0.104	0.104	0.083	0.083
Adiac	CWS	6	$1\pi$	19:19,1:10	<b>0.108</b>	0.104	0.125	0.104	0.125	0.167	0.146	0.062	0.083	0.062	0.104
Adiac	CWS	6	$2\pi$	28:28,1:22	0.117	0.104	0.083	0.104	0.146	0.146	0.188	0.104	0.104	0.125	0.062
Adiac	CWS	6	$3\pi$	32:32,1:40	0.117	0.125	0.125	0.104	0.104	0.125	0.104	0.146	0.104	0.125	0.104
Adiac	CWS	7	$1\pi$	22:22,1:16	<b>0.108</b>	0.104	0.146	0.083	0.104	0.167	0.146	0.083	0.083	0.083	0.083
Adiac	CWS	7	$2\pi$	33:33,1:29	0.110	0.104	0.104	0.104	0.167	0.104	0.167	0.104	0.125	0.083	0.042
Adiac	CWS	7	$3\pi$	31:31,1:39	0.119	0.083	0.104	0.146	0.083	0.125	0.104	0.167	0.125	0.104	0.146
Adiac	CWPV	1	$1\pi$	3:8	0.138	0.167	0.104	0.125	0.188	0.167	0.125	0.167	0.125	0.042	0.167
Adiac	CWPV	1	$2\pi$	4:6	0.212	0.208	0.208	0.167	0.271	0.208	0.208	0.229	0.229	0.229	0.167
Adiac	CWPV	1	$3\pi$	5:5	0.360	0.354	0.417	0.438	0.354	0.333	0.375	0.333	0.396	0.312	0.292
Adiac	CWPV	2	$1\pi$	4:11	0.135	0.146	0.125	0.125	0.208	0.167	0.125	0.125	0.125	0.062	0.146
Adiac	CWPV	2	$2\pi$	7:15	0.188	0.146	0.208	0.167	0.188	0.167	0.229	0.229	0.146	0.167	0.229
Adiac	CWPV	2	$3\pi$	8:13	0.279	0.312	0.292	0.229	0.312	0.292	0.292	0.229	0.312	0.271	0.250
Adiac	CWPV	3	$1\pi$	5:16	0.133	0.125	0.104	0.146	0.188	0.167	0.125	0.125	0.125	0.062	0.167
Adiac	CWPV	3	$2\pi$	11:22	0.188	0.188	0.146	0.208	0.146	0.250	0.250	0.229	0.146	0.146	0.167
Adiac	CWPV	3	$3\pi$	12:16	0.248	0.250	0.271	0.208	0.208	0.292	0.250	0.208	0.312	0.250	0.229
Adiac	CWPV	4	$1\pi$	9:10	0.131	0.125	0.125	0.125	0.208	0.146	0.104	0.167	0.104	0.062	0.146
Adiac	CWPV	4	$2\pi$	13:24	0.163	0.146	0.167	0.167	0.146	0.188	0.229	0.146	0.167	0.167	0.104
Adiac	CWPV	4	$3\pi$	16:22	0.215	0.250	0.229	0.167	0.250	0.271	0.229	0.208	0.208	0.167	0.167
Adiac	CWPV	5	$1\pi$	9:27	0.131	0.146	0.125	0.104	0.188	0.167	0.125	0.146	0.125	0.042	0.146
Adiac	CWPV	5	$2\pi$	15:23	0.186	0.188	0.208	0.125	0.188	0.167	0.229	0.271	0.188	0.125	0.167
Adiac	CWPV	5	$3\pi$	18:27	0.192	0.146	0.188	0.104	0.271	0.208	0.229	0.188	0.250	0.167	0.167
Adiac	CWPV	6	$1\pi$	10:32	0.133	0.146	0.104	0.146	0.188	0.167	0.125	0.125	0.125	0.062	0.146
Adiac	CWPV	6	$2\pi$	19:43	0.165	0.125	0.146	0.188	0.167	0.208	0.208	0.188	0.083	0.125	0.208
Adiac	CWPV	6	$3\pi$	22:28	0.200	0.167	0.188	0.229	0.271	0.146	0.208	0.229	0.167	0.167	0.229
Adiac	CWPV	7	$1\pi$	12:37	0.131	0.125	0.125	0.125	0.188	0.167	0.125	0.146	0.125	0.042	0.146
Adiac	CWPV	7	$2\pi$	21:42	0.154	0.125	0.167	0.125	0.146	0.167	0.208	0.167	0.167	0.125	0.146
Adiac	CWPV	7	$3\pi$	25:38	0.181	0.167	0.167	0.104	0.208	0.208	0.250	0.167	0.208	0.208	0.125
Adiac	CWED	1	$1\pi$	2:6	0.173	0.125	0.167	0.208	0.188	0.208	0.208	0.188	0.146	0.146	0.146
Adiac	CWED	1	$2\pi$	2:8	0.198	0.146	0.188	0.188	0.229	0.250	0.208	0.229	0.188	0.167	0.188
Adiac	CWED	1	$3\pi$	1:7	0.204	0.188	0.208	0.208	0.146	0.208	0.250	0.229	0.208	0.188	0.208
Adiac	CWED	2	$1\pi$	1:10	0.159	0.188	0.167	0.146	0.208	0.167	0.188	0.167	0.167	0.104	0.083
Adiac	CWED	2	$2\pi$	1:13	0.160	0.146	0.167	0.146	0.125	0.208	0.208	0.208	0.167	0.083	0.146
Adiac	CWED	2	$3\pi$	1:12	0.138	0.104	0.146	0.167	0.146	0.125	0.167	0.125	0.125	0.104	0.167
Adiac	CWED	3	$1\pi$	2:14	0.152	0.167	0.167	0.167	0.188	0.167	0.188	0.167	0.167	0.083	0.062
Adiac	CWED	3	$2\pi$	1:17	0.136	0.146	0.125	0.146	0.083	0.188	0.167	0.167	0.146	0.083	0.104
Adiac	CWED	3	$3\pi$	1:20	0.123	0.104	0.146	0.125	0.083	0.125	0.167	0.125	0.104	0.104	0.146
Adiac	CWED	4	$1\pi$	1:22	0.148	0.188	0.167	0.188	0.167	0.125	0.167	0.167	0.125	0.104	0.083
Adiac	CWED	4	$2\pi$	1:22	0.136	0.104	0.125	0.125	0.083	0.188	0.167	0.167	0.146	0.083	0.167
Adiac	CWED	4	$3\pi$	1:27	0.129	0.125	0.125	0.146	0.146	0.125	0.167	0.146	0.104	0.083	0.125
Adiac	CWED	5	$1\pi$	1:27	0.152	0.167	0.146	0.167	0.208	0.167	0.167	0.167	0.167	0.083	0.083
Adiac	CWED	5	$2\pi$	1:30	0.136	0.125	0.125	0.125	0.083	0.188	0.167	0.146	0.146	0.083	0.167
Adiac	CWED	5	$3\pi$	1:29	0.131	0.125	0.125	0.125	0.125	0.146	0.125	0.146	0.167	0.104	0.125
Adiac	CWED	6	$1\pi$	2:32	0.154	0.167	0.146	0.146	0.208	0.167	0.167	0.188	0.167	0.104	0.083
Adiac	CWED	6	$2\pi$	1:38	0.138	0.146	0.125	0.125	0.083	0.188	0.167	0.146	0.146	0.083	0.167
Adiac	CWED	6	$3\pi$	1:33	0.119	0.104	0.125	0.146	0.083	0.125	0.167	0.146	0.104	0.062	0.125
Adiac	CWED	7	$1\pi$	1:38	0.152	0.208	0.167	0.188	0.188	0.125	0.167	0.167	0.125	0.104	0.083
Adiac	CWED	7	$2\pi$	1:44	0.133	0.125	0.125	0.167	0.104	0.125	0.188	0.125	0.125	0.104	0.146
Adiac	CWED	7	$3\pi$	1:39	0.123	0.125	0.125	0.146	0.104	0.125	0.125	0.146	0.125	0.083	0.125



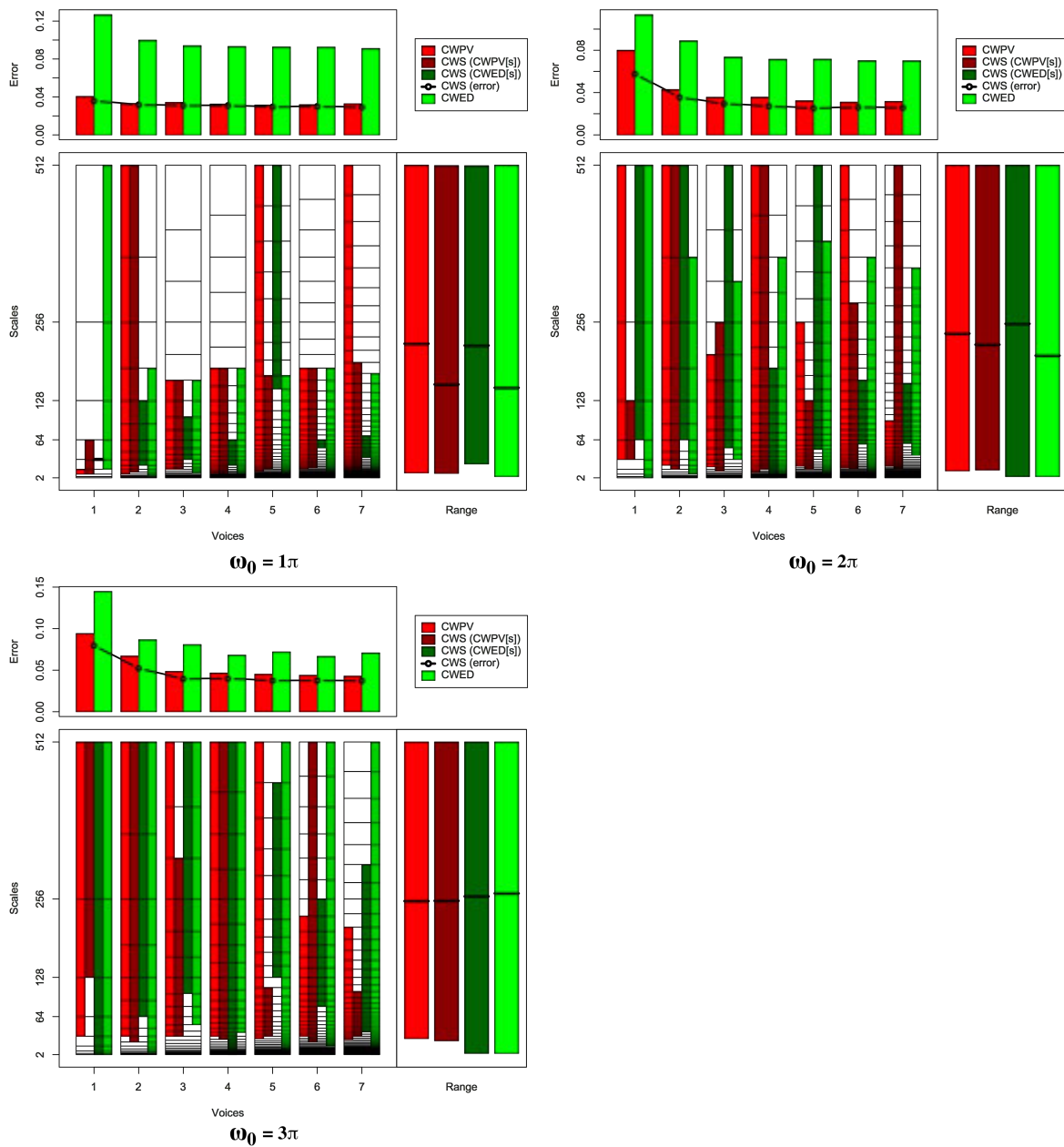


FIGURE B.16: Summary of results for the Yoga classification problem comparing CWS, CWPV, CWED methods using 1-7 voices and three  $\omega_0$  values. A lower CWPV score suggests that the problem is predominantly characterised by FM, whereas a lower CWED implies a predominant AM characteristic. The scale ranges have been translated from scale number to scale value. In the bottom right figure of each figure the average range of scales for all 7 voices are presented for each technique.

TABLE B.16: Summary of results for the Yoga classification problem comparing Ed, DTW, CWS, CWPV, and CWED using 1-7 voices and 3  $\omega_0$  parameters.  $S$  is the scale set(s) associated with the CWS, CWPV and CWED results. The mean values highlighted in bold are the best in model error rate for the problem.

Problem	Technique	Voices	$\omega_0$	$S$	Mean	1	2	3	4	5	6	7	7	9	10
Yoga	Ed				0.037	0.041	0.027	0.046	0.041	0.064	0.037	0.041	0.014	0.023	0.032
Yoga	DTW				0.042	0.037	0.037	0.046	0.059	0.073	0.023	0.041	0.018	0.037	0.050
Yoga	CWS	1	1 $\pi$	3:6,7:7	0.036	0.027	0.023	0.041	0.023	0.064	0.027	0.046	0.037	0.046	0.027
Yoga	CWS	1	2 $\pi$	5:7,6:9	0.058	0.082	0.041	0.050	0.078	0.078	0.041	0.055	0.027	0.068	0.059
Yoga	CWS	1	3 $\pi$	7:9,1:9	0.080	0.082	0.050	0.073	0.114	0.110	0.059	0.078	0.078	0.064	0.091
Yoga	CWS	2	1 $\pi$	6:17,8:13	0.032	0.023	0.032	0.027	0.023	0.046	0.018	0.046	0.027	0.046	0.032
Yoga	CWS	2	2 $\pi$	7:17,11:17	0.036	0.037	0.014	0.046	0.032	0.037	0.037	0.059	0.027	0.037	0.032
Yoga	CWS	2	3 $\pi$	8:17,11:17	0.052	0.055	0.041	0.046	0.087	0.068	0.032	0.059	0.050	0.059	0.027
Yoga	CWS	3	1 $\pi$	10:20,13:18	0.031	0.023	0.014	0.046	0.032	0.050	0.018	0.037	0.023	0.046	0.023
Yoga	CWS	3	2 $\pi$	9:22,15:25	0.030	0.037	0.009	0.027	0.027	0.041	0.023	0.037	0.032	0.041	0.023
Yoga	CWS	3	3 $\pi$	13:23,18:25	0.040	0.046	0.032	0.046	0.032	0.037	0.041	0.073	0.032	0.059	0.000
Yoga	CWS	4	1 $\pi$	9:27,15:21	0.031	0.027	0.014	0.032	0.014	0.073	0.014	0.055	0.014	0.037	0.032
Yoga	CWS	4	2 $\pi$	13:33,1:27	0.027	0.027	0.018	0.023	0.023	0.032	0.023	0.050	0.014	0.046	0.018
Yoga	CWS	4	3 $\pi$	16:33,1:33	0.040	0.037	0.018	0.041	0.046	0.050	0.018	0.055	0.046	0.064	0.027
Yoga	CWS	5	1 $\pi$	16:33,32:41	0.030	0.027	0.009	0.032	0.023	0.055	0.023	0.032	0.023	0.041	0.032
Yoga	CWS	5	2 $\pi$	16:31,24:41	<b>0.026</b>	0.027	0.014	0.027	0.023	0.032	0.018	0.041	0.014	0.041	0.018
Yoga	CWS	5	3 $\pi$	21:30,31:40	0.038	0.037	0.014	0.046	0.018	0.032	0.032	0.064	0.037	0.064	0.032
Yoga	CWS	6	1 $\pi$	20:40,29:31	0.030	0.023	0.014	0.041	0.023	0.037	0.023	0.046	0.023	0.050	0.023
Yoga	CWS	6	2 $\pi$	19:44,30:39	0.026	0.027	0.018	0.027	0.018	0.027	0.023	0.037	0.014	0.050	0.023
Yoga	CWS	6	3 $\pi$	22:49,33:43	0.038	0.050	0.018	0.027	0.027	0.041	0.032	0.064	0.032	0.064	0.023
Yoga	CWS	7	1 $\pi$	14:47,30:37	0.029	0.027	0.014	0.037	0.018	0.059	0.014	0.046	0.009	0.037	0.032
Yoga	CWS	7	2 $\pi$	22:57,35:45	0.026	0.027	0.023	0.032	0.027	0.023	0.009	0.037	0.018	0.050	0.014
Yoga	CWS	7	3 $\pi$	29:41,31:52	0.037	0.055	0.027	0.032	0.032	0.041	0.027	0.064	0.014	0.059	0.023
Yoga	CWPV	1	1 $\pi$	3:4	0.041	0.046	0.027	0.046	0.023	0.073	0.023	0.059	0.023	0.059	0.027
Yoga	CWPV	1	2 $\pi$	5:9	0.080	0.114	0.087	0.082	0.110	0.114	0.055	0.064	0.037	0.078	0.059
Yoga	CWPV	1	3 $\pi$	5:9	0.094	0.087	0.091	0.078	0.110	0.123	0.087	0.078	0.114	0.091	0.082
Yoga	CWPV	2	1 $\pi$	5:17	0.033	0.023	0.027	0.027	0.018	0.073	0.018	0.046	0.027	0.041	0.032
Yoga	CWPV	2	2 $\pi$	8:17	0.043	0.041	0.032	0.050	0.046	0.041	0.046	0.064	0.027	0.041	0.041
Yoga	CWPV	2	3 $\pi$	9:17	0.067	0.068	0.059	0.055	0.091	0.073	0.041	0.096	0.064	0.078	0.046
Yoga	CWPV	3	1 $\pi$	10:20	0.034	0.032	0.014	0.046	0.027	0.059	0.023	0.041	0.023	0.046	0.032
Yoga	CWPV	3	2 $\pi$	11:21	0.036	0.023	0.027	0.046	0.041	0.050	0.027	0.046	0.027	0.046	0.023
Yoga	CWPV	3	3 $\pi$	13:25	0.049	0.055	0.050	0.050	0.055	0.037	0.050	0.078	0.032	0.064	0.014
Yoga	CWPV	4	1 $\pi$	10:27	0.033	0.023	0.023	0.037	0.014	0.068	0.023	0.046	0.023	0.041	0.027
Yoga	CWPV	4	2 $\pi$	11:33	0.036	0.037	0.023	0.032	0.032	0.046	0.037	0.050	0.027	0.041	0.032
Yoga	CWPV	4	3 $\pi$	17:33	0.047	0.041	0.032	0.037	0.037	0.073	0.027	0.073	0.055	0.064	0.027
Yoga	CWPV	5	1 $\pi$	14:41	0.032	0.018	0.023	0.037	0.018	0.064	0.027	0.037	0.018	0.046	0.027
Yoga	CWPV	5	2 $\pi$	18:36	0.032	0.027	0.009	0.041	0.018	0.041	0.032	0.050	0.018	0.050	0.037
Yoga	CWPV	5	3 $\pi$	20:41	0.045	0.046	0.018	0.059	0.046	0.050	0.037	0.068	0.037	0.059	0.032
Yoga	CWPV	6	1 $\pi$	19:40	0.032	0.023	0.018	0.041	0.027	0.046	0.023	0.050	0.023	0.041	0.027
Yoga	CWPV	6	2 $\pi$	20:49	0.031	0.023	0.009	0.041	0.027	0.032	0.041	0.041	0.018	0.055	0.023
Yoga	CWPV	6	3 $\pi$	25:42	0.044	0.046	0.046	0.037	0.027	0.055	0.027	0.064	0.041	0.059	0.037
Yoga	CWPV	7	1 $\pi$	19:57	0.033	0.027	0.014	0.041	0.018	0.055	0.027	0.041	0.027	0.046	0.032
Yoga	CWPV	7	2 $\pi$	25:40	0.032	0.032	0.014	0.037	0.027	0.046	0.027	0.046	0.023	0.027	0.037
Yoga	CWPV	7	3 $\pi$	27:48	0.043	0.050	0.027	0.046	0.041	0.055	0.037	0.059	0.027	0.055	0.032
Yoga	CWED	1	1 $\pi$	4:9	0.127	0.160	0.132	0.123	0.132	0.142	0.091	0.123	0.119	0.100	0.146
Yoga	CWED	1	2 $\pi$	1:9	0.114	0.137	0.096	0.105	0.132	0.110	0.119	0.091	0.128	0.091	0.128
Yoga	CWED	1	3 $\pi$	1:9	0.145	0.169	0.146	0.128	0.155	0.169	0.142	0.123	0.160	0.110	0.146
Yoga	CWED	2	1 $\pi$	4:14	0.100	0.137	0.100	0.082	0.110	0.128	0.068	0.105	0.087	0.091	0.091
Yoga	CWED	2	2 $\pi$	5:16	0.089	0.096	0.078	0.068	0.110	0.105	0.082	0.082	0.091	0.064	0.114
Yoga	CWED	2	3 $\pi$	4:17	0.087	0.119	0.073	0.082	0.105	0.114	0.064	0.078	0.091	0.059	0.082
Yoga	CWED	3	1 $\pi$	8:20	0.094	0.100	0.096	0.087	0.100	0.114	0.073	0.078	0.110	0.078	0.105
Yoga	CWED	3	2 $\pi$	13:23	0.074	0.096	0.059	0.064	0.087	0.078	0.064	0.055	0.096	0.055	0.082
Yoga	CWED	3	3 $\pi$	15:25	0.081	0.119	0.064	0.059	0.096	0.096	0.046	0.073	0.100	0.068	0.087
Yoga	CWED	4	1 $\pi$	6:27	0.093	0.110	0.096	0.078	0.105	0.114	0.064	0.096	0.100	0.087	0.082
Yoga	CWED	4	2 $\pi$	3:31	0.072	0.100	0.055	0.073	0.100	0.073	0.059	0.059	0.078	0.050	0.068
Yoga	CWED	4	3 $\pi$	18:33	0.068	0.091	0.064	0.055	0.078	0.082	0.055	0.064	0.087	0.046	0.059
Yoga	CWED	5	1 $\pi$	13:33	0.093	0.105	0.087	0.091	0.110	0.119	0.073	0.082	0.096	0.068	0.096
Yoga	CWED	5	2 $\pi$	9:39	0.072	0.110	0.059	0.068	0.096	0.059	0.059	0.064	0.068	0.055	0.078
Yoga	CWED	5	3 $\pi$	6:41	0.072	0.105	0.055	0.068	0.078	0.082	0.059	0.068	0.091	0.050	0.064
Yoga	CWED	6	1 $\pi$	9:40	0.093	0.110	0.096	0.064	0.110	0.114	0.068	0.100	0.100	0.082	0.082
Yoga	CWED	6	2 $\pi$	1:46	0.070	0.091	0.055	0.073	0.100	0.068	0.064	0.059	0.078	0.046	0.068
Yoga	CWED	6	3 $\pi$	19:49	0.067	0.091	0.055	0.059	0.078	0.073	0.055	0.073	0.082	0.037	0.064
Yoga	CWED	7	1 $\pi$	1:46	0.091	0.110	0.100	0.082	0.091	0.123	0.068	0.082	0.091	0.068	0.096
Yoga	CWED	7	2 $\pi$	31:53	0.070	0.091	0.050	0.078	0.096	0.068	0.059	0.059	0.091	0.041	0.068
Yoga	CWED	7	3 $\pi$	1:57	0.071	0.100	0.064	0.059	0.078	0.082	0.055	0.078	0.087	0.046	0.059

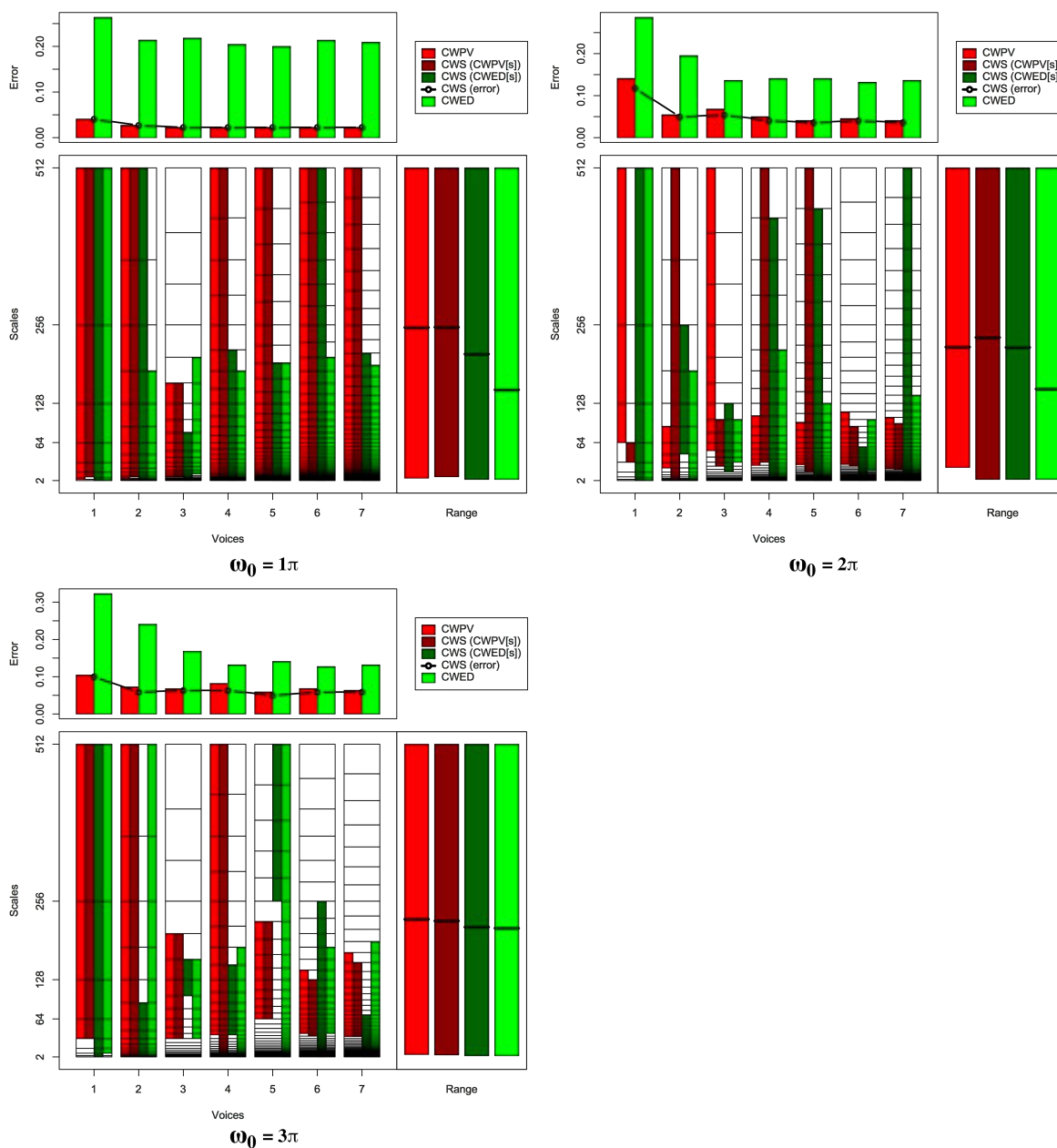


FIGURE B.17: Summary of results for the Fish classification problem comparing CWS, CWPV, CWED methods using 1-7 voices and three  $\omega_0$  values. A lower CWPV score suggests that the problem is predominantly characterised by FM, whereas a lower CWED implies a predominant AM characteristic. The scale ranges have been translated from scale number to scale value. In the bottom right figure of each figure the average range of scales for all 7 voices are presented for each technique.

TABLE B.17: Summary of results for the Fish classification problem comparing Ed, DTW, CWS, CWPV, and CWED using 1-7 voices and 3  $\omega_0$  parameters.  $S$  is the scale set(s) associated with the CWS, CWPV and CWED results. The mean values highlighted in bold are the best in model error rate for the problem.

Problem	Technique	Voices	$\omega_0$	$S$	Mean	1	2	3	4	5	6	7	7	9	10
Fish	Ed				0.100	0.136	0.045	0.091	0.136	0.091	0.091	0.045	0.136	0.136	0.091
Fish	DTW				0.145	0.227	0.091	0.136	0.182	0.136	0.227	0.227	0.091	0.091	0.045
Fish	CWS	1	$1\pi$	3:9,1:9	0.041	0.091	0.045	0.000	0.000	0.045	0.045	0.045	0.091	0.045	0.000
Fish	CWS	1	$2\pi$	5:6,1:9	0.118	0.136	0.182	0.000	0.182	0.045	0.136	0.136	0.091	0.136	0.136
Fish	CWS	1	$3\pi$	5:9,1:9	0.100	0.136	0.182	0.000	0.091	0.091	0.091	0.091	0.091	0.136	0.091
Fish	CWS	2	$1\pi$	5:17,1:17	0.027	0.045	0.000	0.000	0.000	0.045	0.000	0.045	0.091	0.045	0.000
Fish	CWS	2	$2\pi$	1:17,10:15	0.050	0.136	0.000	0.000	0.045	0.091	0.045	0.045	0.000	0.091	0.045
Fish	CWS	2	$3\pi$	3:17,1:12	0.059	0.091	0.045	0.000	0.045	0.000	0.091	0.091	0.045	0.091	0.091
Fish	CWS	3	$1\pi$	7:20,1:17	<b>0.023</b>	0.045	0.000	0.000	0.000	0.000	0.000	0.045	0.091	0.045	0.000
Fish	CWS	3	$2\pi$	12:18,10:19	0.054	0.136	0.045	0.000	0.091	0.000	0.045	0.045	0.091	0.091	0.000
Fish	CWS	3	$3\pi$	13:21,18:20	0.063	0.136	0.000	0.045	0.136	0.045	0.091	0.045	0.045	0.045	0.045
Fish	CWS	4	$1\pi$	9:33,1:28	<b>0.023</b>	0.045	0.000	0.000	0.000	0.000	0.000	0.045	0.091	0.045	0.000
Fish	CWS	4	$2\pi$	17:33,1:32	0.041	0.091	0.045	0.000	0.091	0.000	0.000	0.045	0.045	0.091	0.000
Fish	CWS	4	$3\pi$	4:33,18:26	0.063	0.182	0.045	0.000	0.000	0.045	0.136	0.045	0.045	0.045	0.091
Fish	CWS	5	$1\pi$	10:41,1:34	<b>0.023</b>	0.045	0.000	0.000	0.000	0.000	0.000	0.045	0.091	0.045	0.000
Fish	CWS	5	$2\pi$	16:41,1:40	0.036	0.045	0.045	0.000	0.000	0.045	0.045	0.045	0.091	0.045	0.000
Fish	CWS	5	$3\pi$	26:35,36:41	0.050	0.091	0.045	0.000	0.045	0.000	0.091	0.091	0.091	0.045	0.000
Fish	CWS	6	$1\pi$	11:49,1:49	<b>0.023</b>	0.045	0.000	0.000	0.000	0.000	0.000	0.045	0.091	0.045	0.000
Fish	CWS	6	$2\pi$	23:34,1:30	0.041	0.136	0.045	0.000	0.045	0.000	0.000	0.045	0.045	0.091	0.000
Fish	CWS	6	$3\pi$	26:37,1:43	0.059	0.136	0.045	0.000	0.045	0.000	0.136	0.045	0.091	0.045	0.045
Fish	CWS	7	$1\pi$	13:57,1:48	<b>0.023</b>	0.045	0.000	0.000	0.000	0.000	0.000	0.045	0.091	0.045	0.000
Fish	CWS	7	$2\pi$	24:40,1:57	0.036	0.136	0.000	0.000	0.000	0.045	0.000	0.045	0.045	0.091	0.000
Fish	CWS	7	$3\pi$	30:45,1:37	0.059	0.091	0.045	0.000	0.091	0.000	0.136	0.045	0.045	0.091	0.045
Fish	CWPV	1	$1\pi$	2:9	0.041	0.045	0.045	0.091	0.000	0.045	0.000	0.045	0.091	0.045	0.000
Fish	CWPV	1	$2\pi$	6:9	0.141	0.182	0.136	0.045	0.227	0.091	0.182	0.182	0.091	0.182	0.091
Fish	CWPV	1	$3\pi$	5:9	0.105	0.136	0.182	0.000	0.091	0.091	0.091	0.091	0.136	0.136	0.091
Fish	CWPV	2	$1\pi$	4:17	0.027	0.045	0.000	0.000	0.000	0.045	0.000	0.045	0.091	0.045	0.000
Fish	CWPV	2	$2\pi$	8:12	0.054	0.182	0.000	0.000	0.091	0.000	0.045	0.045	0.045	0.136	0.000
Fish	CWPV	2	$3\pi$	3:17	0.073	0.136	0.091	0.000	0.045	0.000	0.091	0.136	0.045	0.091	0.091
Fish	CWPV	3	$1\pi$	7:20	<b>0.023</b>	0.045	0.000	0.000	0.000	0.000	0.000	0.045	0.091	0.045	0.000
Fish	CWPV	3	$2\pi$	15:25	0.068	0.136	0.182	0.045	0.182	0.000	0.045	0.045	0.000	0.045	0.000
Fish	CWPV	3	$3\pi$	13:21	0.068	0.136	0.045	0.045	0.091	0.045	0.136	0.045	0.045	0.045	0.045
Fish	CWPV	4	$1\pi$	9:33	<b>0.023</b>	0.045	0.000	0.000	0.000	0.000	0.000	0.045	0.091	0.045	0.000
Fish	CWPV	4	$2\pi$	16:24	0.050	0.136	0.045	0.045	0.091	0.000	0.000	0.045	0.045	0.091	0.000
Fish	CWPV	4	$3\pi$	18:33	0.082	0.136	0.091	0.000	0.091	0.000	0.182	0.091	0.091	0.091	0.045
Fish	CWPV	5	$1\pi$	10:41	<b>0.023</b>	0.045	0.000	0.000	0.000	0.000	0.000	0.045	0.091	0.045	0.000
Fish	CWPV	5	$2\pi$	20:29	0.041	0.136	0.000	0.000	0.045	0.000	0.045	0.045	0.091	0.045	0.000
Fish	CWPV	5	$3\pi$	26:35	0.059	0.091	0.045	0.000	0.091	0.000	0.091	0.136	0.091	0.045	0.000
Fish	CWPV	6	$1\pi$	12:49	<b>0.023</b>	0.045	0.000	0.000	0.000	0.000	0.000	0.045	0.091	0.045	0.000
Fish	CWPV	6	$2\pi$	24:36	0.045	0.091	0.045	0.000	0.091	0.000	0.045	0.045	0.091	0.045	0.000
Fish	CWPV	6	$3\pi$	27:38	0.068	0.136	0.091	0.000	0.091	0.000	0.136	0.045	0.091	0.045	0.045
Fish	CWPV	7	$1\pi$	14:57	<b>0.023</b>	0.045	0.000	0.000	0.000	0.000	0.000	0.045	0.091	0.045	0.000
Fish	CWPV	7	$2\pi$	25:41	0.041	0.136	0.000	0.000	0.045	0.000	0.045	0.045	0.045	0.091	0.000
Fish	CWPV	7	$3\pi$	30:46	0.064	0.091	0.091	0.000	0.091	0.000	0.136	0.045	0.045	0.091	0.045
Fish	CWED	1	$1\pi$	1:9	0.264	0.182	0.318	0.318	0.273	0.182	0.273	0.273	0.227	0.318	0.273
Fish	CWED	1	$2\pi$	1:9	0.286	0.318	0.273	0.318	0.273	0.318	0.318	0.318	0.273	0.273	0.182
Fish	CWED	1	$3\pi$	3:9	0.323	0.273	0.409	0.318	0.409	0.182	0.273	0.409	0.364	0.318	0.273
Fish	CWED	2	$1\pi$	1:14	0.214	0.182	0.318	0.182	0.318	0.182	0.318	0.091	0.182	0.182	0.182
Fish	CWED	2	$2\pi$	1:14	0.195	0.182	0.409	0.136	0.227	0.136	0.227	0.227	0.182	0.136	0.091
Fish	CWED	2	$3\pi$	1:17	0.241	0.227	0.409	0.182	0.136	0.273	0.182	0.273	0.182	0.318	0.227
Fish	CWED	3	$1\pi$	9:21	0.218	0.182	0.273	0.227	0.364	0.136	0.227	0.091	0.136	0.318	0.227
Fish	CWED	3	$2\pi$	13:18	0.136	0.091	0.136	0.227	0.227	0.045	0.227	0.136	0.182	0.045	0.045
Fish	CWED	3	$3\pi$	13:20	0.168	0.136	0.273	0.227	0.364	0.091	0.136	0.182	0.091	0.136	0.045
Fish	CWED	4	$1\pi$	10:27	0.205	0.227	0.273	0.182	0.318	0.136	0.364	0.091	0.182	0.136	0.136
Fish	CWED	4	$2\pi$	1:28	0.141	0.091	0.227	0.136	0.318	0.045	0.182	0.136	0.091	0.136	0.045
Fish	CWED	4	$3\pi$	1:27	0.132	0.136	0.136	0.136	0.227	0.045	0.182	0.091	0.091	0.182	0.091
Fish	CWED	5	$1\pi$	1:34	0.200	0.136	0.273	0.182	0.364	0.136	0.273	0.091	0.182	0.227	0.136
Fish	CWED	5	$2\pi$	1:31	0.141	0.091	0.227	0.182	0.318	0.045	0.136	0.136	0.091	0.136	0.045
Fish	CWED	5	$3\pi$	1:41	0.141	0.227	0.273	0.091	0.227	0.091	0.136	0.045	0.091	0.182	0.045
Fish	CWED	6	$1\pi$	15:41	0.214	0.136	0.318	0.182	0.364	0.136	0.227	0.091	0.136	0.318	0.227
Fish	CWED	6	$2\pi$	20:35	0.132	0.091	0.182	0.182	0.227	0.045	0.182	0.136	0.091	0.136	0.045
Fish	CWED	6	$3\pi$	27:40	0.127	0.182	0.136	0.182	0.227	0.045	0.136	0.136	0.091	0.045	0.091
Fish	CWED	7	$1\pi$	1:47	0.209	0.227	0.273	0.182	0.318	0.136	0.318	0.091	0.182	0.182	0.182
Fish	CWED	7	$2\pi$	1:44	0.136	0.136	0.227	0.182	0.318	0.045	0.136	0.091	0.091	0.091	0.045
Fish	CWED	7	$3\pi$	1:47	0.132	0.136	0.227	0.136	0.273	0.045	0.136	0.136	0.091	0.091	0.045

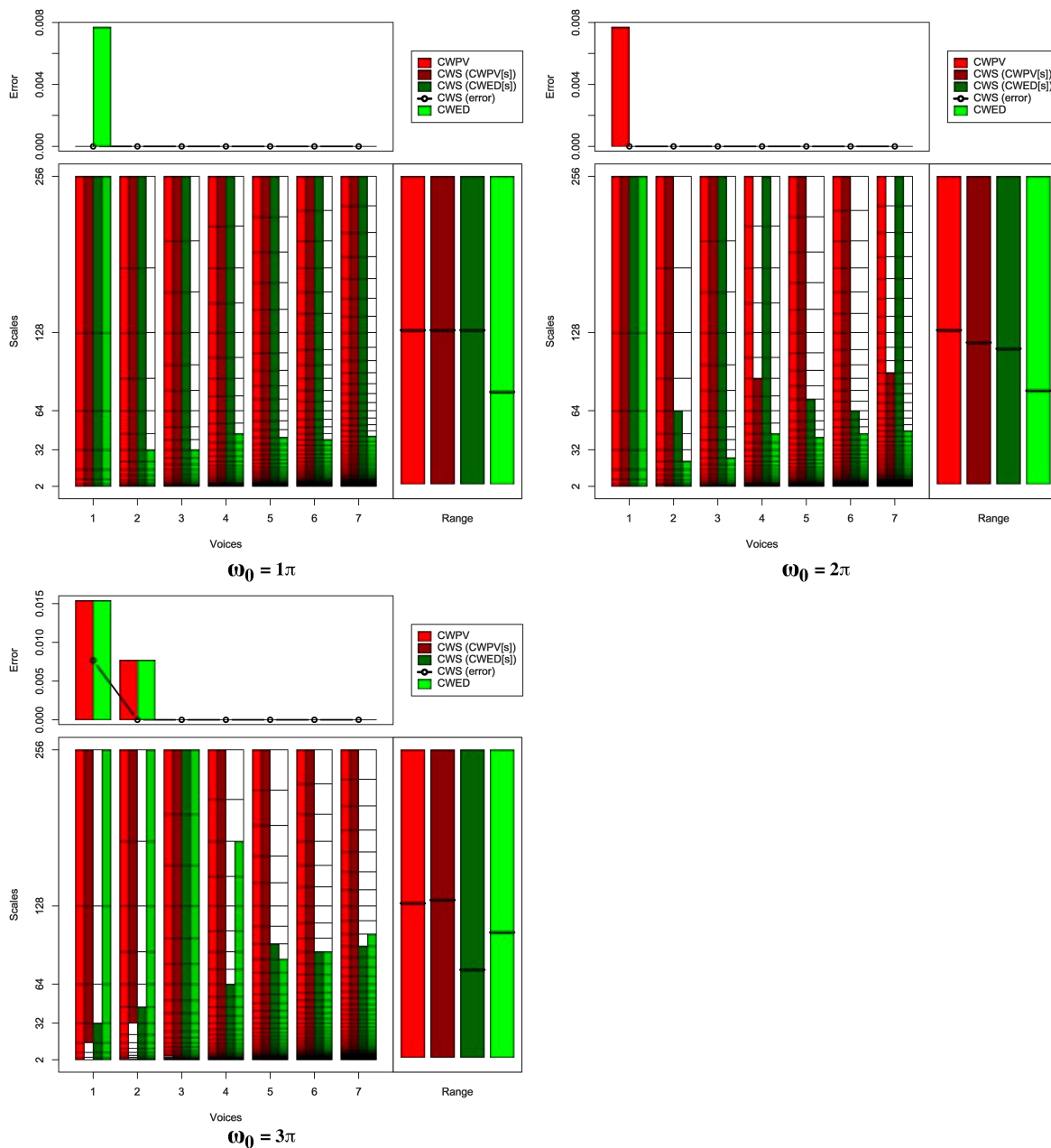


FIGURE B.18: Summary of results for the Plane classification problem comparing CWS, CWPV, CWED methods using 1-7 voices and three  $\omega_0$  values. A lower CWPV score suggests that the problem is predominantly characterised by FM, whereas a lower CWED implies a predominant AM characteristic. The scale ranges have been translated from scale number to scale value. In the bottom right figure of each figure the average range of scales for all 7 voices are presented for each technique.



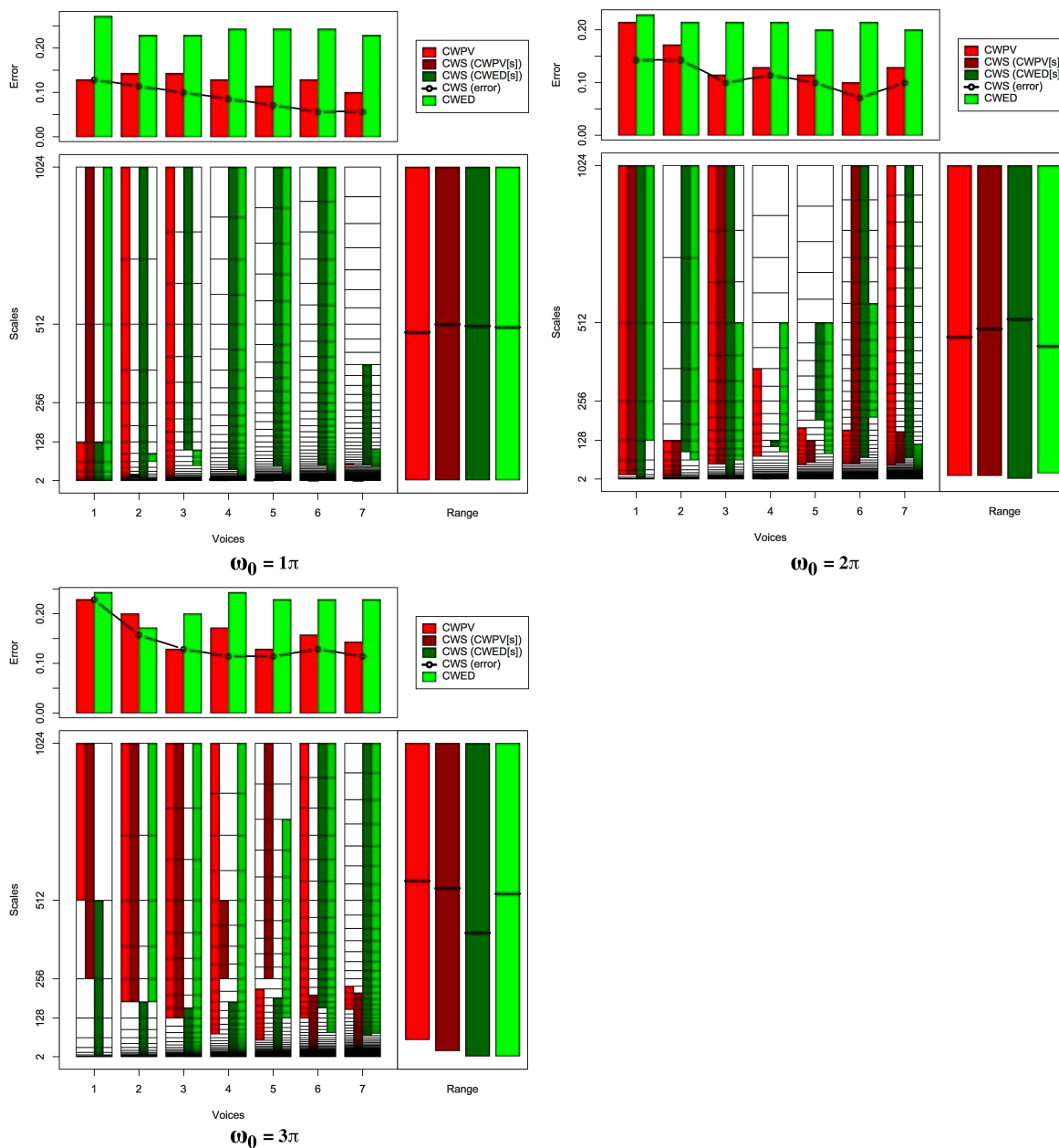


FIGURE B.19: Summary of results for the Car classification problem comparing CWS, CWPV, CWED methods using 1-7 voices and three  $\omega_0$  values. A lower CWPV score suggests that the problem is predominantly characterised by FM, whereas a lower CWED implies a predominant AM characteristic. The scale ranges have been translated from scale number to scale value. In the bottom right figure of each figure the average range of scales for all 7 voices are presented for each technique.

TABLE B.19: Summary of results for the Car classification problem comparing Ed, DTW, CWS, CWPV, and CWED using 1-7 voices and 3  $\omega_0$  parameters.  $S$  is the scale set(s) associated with the CWS, CWPV and CWED results. The mean values highlighted in bold are the best in model error rate for the problem.

Problem	Technique	Voices	$\omega_0$	$S$	Mean	1	2	3	4	5	6	7	7	9	10
Car	Ed				0.172	0.000	0.143	0.143	0.143	0.000	0.143	0.429	0.286	0.143	0.286
Car	DTW				0.257	0.286	0.143	0.000	0.286	0.286	0.143	0.571	0.429	0.143	0.286
Car	CWS	1	$1\pi$	1:10,1:7	0.129	0.000	0.286	0.000	0.143	0.000	0.143	0.143	0.286	0.000	0.286
Car	CWS	1	$2\pi$	4:10,1:10	0.143	0.143	0.143	0.000	0.143	0.143	0.143	0.143	0.286	0.143	0.143
Car	CWS	1	$3\pi$	8:10,1:9	0.229	0.286	0.286	0.000	0.571	0.143	0.286	0.286	0.286	0.143	0.000
Car	CWS	2	$1\pi$	4:4,1:19	0.114	0.143	0.286	0.143	0.000	0.000	0.143	0.143	0.143	0.000	0.143
Car	CWS	2	$2\pi$	6:13,12:19	0.143	0.000	0.143	0.000	0.286	0.143	0.143	0.143	0.286	0.143	0.143
Car	CWS	2	$3\pi$	14:19,1:14	0.157	0.143	0.143	0.000	0.143	0.143	0.143	0.143	0.286	0.143	0.286
Car	CWS	3	$1\pi$	15:15,18:28	0.100	0.000	0.143	0.000	0.000	0.000	0.143	0.143	0.286	0.286	0.000
Car	CWS	3	$2\pi$	15:28,1:28	0.100	0.000	0.143	0.000	0.143	0.143	0.143	0.000	0.286	0.143	0.000
Car	CWS	3	$3\pi$	19:28,1:20	0.129	0.000	0.143	0.000	0.143	0.143	0.143	0.000	0.286	0.143	0.286
Car	CWS	4	$1\pi$	8:8,18:37	0.086	0.286	0.143	0.143	0.000	0.000	0.143	0.000	0.143	0.000	0.000
Car	CWS	4	$2\pi$	26:26,24:25	0.114	0.143	0.143	0.143	0.000	0.143	0.000	0.143	0.286	0.143	0.000
Car	CWS	4	$3\pi$	29:33,1:27	0.114	0.000	0.143	0.000	0.000	0.000	0.000	0.286	0.286	0.143	0.286
Car	CWS	5	$1\pi$	10:10,24:46	0.072	0.143	0.143	0.143	0.000	0.000	0.143	0.000	0.143	0.000	0.000
Car	CWS	5	$2\pi$	25:31,34:41	0.100	0.000	0.143	0.000	0.143	0.143	0.143	0.000	0.286	0.143	0.000
Car	CWS	5	$3\pi$	36:46,1:34	0.114	0.000	0.143	0.000	0.000	0.000	0.143	0.286	0.143	0.143	0.286
Car	CWS	6	$1\pi$	12:12,29:55	<b>0.057</b>	0.143	0.143	0.000	0.000	0.000	0.143	0.000	0.143	0.000	0.000
Car	CWS	6	$2\pi$	29:55,32:55	0.072	0.000	0.000	0.000	0.143	0.000	0.143	0.000	0.286	0.143	0.000
Car	CWS	6	$3\pi$	22:41,39:55	0.129	0.000	0.143	0.000	0.286	0.143	0.143	0.286	0.143	0.143	0.000
Car	CWS	7	$1\pi$	14:14,34:54	<b>0.057</b>	0.143	0.143	0.000	0.000	0.000	0.143	0.000	0.143	0.000	0.000
Car	CWS	7	$2\pi$	34:45,37:64	0.100	0.000	0.143	0.000	0.143	0.143	0.143	0.000	0.286	0.143	0.000
Car	CWS	7	$3\pi$	24:48,37:64	0.114	0.143	0.143	0.000	0.286	0.000	0.143	0.143	0.143	0.143	0.000
Car	CWPV	1	$1\pi$	1:7	0.129	0.000	0.286	0.000	0.286	0.000	0.143	0.000	0.286	0.000	0.286
Car	CWPV	1	$2\pi$	4:10	0.215	0.429	0.143	0.143	0.143	0.143	0.143	0.143	0.286	0.143	0.429
Car	CWPV	1	$3\pi$	9:10	0.229	0.143	0.143	0.143	0.286	0.429	0.143	0.429	0.143	0.429	0.000
Car	CWPV	2	$1\pi$	1:19	0.143	0.000	0.286	0.000	0.143	0.143	0.143	0.143	0.286	0.000	0.286
Car	CWPV	2	$2\pi$	6:13	0.172	0.000	0.286	0.143	0.286	0.143	0.143	0.143	0.286	0.143	0.143
Car	CWPV	2	$3\pi$	14:19	0.200	0.143	0.143	0.143	0.143	0.286	0.143	0.143	0.429	0.286	0.143
Car	CWPV	3	$1\pi$	1:28	0.143	0.000	0.286	0.000	0.143	0.143	0.143	0.143	0.286	0.000	0.286
Car	CWPV	3	$2\pi$	15:28	0.114	0.000	0.143	0.000	0.143	0.143	0.143	0.143	0.286	0.143	0.000
Car	CWPV	3	$3\pi$	19:28	0.129	0.000	0.143	0.000	0.143	0.143	0.143	0.000	0.286	0.143	0.286
Car	CWPV	4	$1\pi$	20:20	0.129	0.000	0.143	0.000	0.286	0.000	0.143	0.143	0.286	0.143	0.143
Car	CWPV	4	$2\pi$	22:31	0.129	0.000	0.286	0.000	0.286	0.000	0.143	0.000	0.286	0.143	0.143
Car	CWPV	4	$3\pi$	22:37	0.172	0.143	0.143	0.143	0.143	0.000	0.143	0.286	0.429	0.143	0.143
Car	CWPV	5	$1\pi$	25:25	0.114	0.000	0.143	0.000	0.143	0.000	0.143	0.143	0.286	0.143	0.143
Car	CWPV	5	$2\pi$	24:33	0.114	0.000	0.143	0.000	0.143	0.143	0.143	0.000	0.286	0.143	0.143
Car	CWPV	5	$3\pi$	25:35	0.129	0.143	0.000	0.000	0.286	0.000	0.143	0.143	0.286	0.143	0.143
Car	CWPV	6	$1\pi$	8:14	0.129	0.143	0.286	0.000	0.143	0.000	0.143	0.143	0.143	0.000	0.286
Car	CWPV	6	$2\pi$	29:39	0.100	0.000	0.000	0.000	0.143	0.143	0.143	0.000	0.286	0.143	0.143
Car	CWPV	6	$3\pi$	37:55	0.157	0.143	0.143	0.000	0.143	0.143	0.143	0.143	0.286	0.143	0.286
Car	CWPV	7	$1\pi$	34:35	0.100	0.000	0.000	0.000	0.286	0.000	0.143	0.143	0.286	0.143	0.000
Car	CWPV	7	$2\pi$	33:64	0.129	0.000	0.286	0.000	0.143	0.143	0.143	0.000	0.286	0.143	0.143
Car	CWPV	7	$3\pi$	45:49	0.143	0.143	0.143	0.143	0.143	0.143	0.143	0.000	0.286	0.143	0.143
Car	CWED	1	$1\pi$	1:10	0.272	0.286	0.286	0.286	0.429	0.286	0.000	0.429	0.143	0.429	0.143
Car	CWED	1	$2\pi$	7:10	0.229	0.000	0.286	0.286	0.286	0.286	0.000	0.286	0.143	0.429	0.286
Car	CWED	1	$3\pi$	1:3	0.243	0.286	0.286	0.286	0.286	0.286	0.000	0.429	0.286	0.143	0.143
Car	CWED	2	$1\pi$	11:12	0.229	0.286	0.143	0.000	0.429	0.286	0.286	0.286	0.143	0.143	0.286
Car	CWED	2	$2\pi$	11:19	0.215	0.143	0.143	0.143	0.286	0.286	0.143	0.286	0.143	0.286	0.286
Car	CWED	2	$3\pi$	14:19	0.172	0.143	0.143	0.000	0.143	0.286	0.286	0.286	0.000	0.286	0.143
Car	CWED	3	$1\pi$	15:18	0.229	0.286	0.286	0.000	0.429	0.286	0.143	0.286	0.143	0.143	0.286
Car	CWED	3	$2\pi$	16:25	0.215	0.000	0.286	0.143	0.286	0.286	0.143	0.286	0.143	0.286	0.286
Car	CWED	3	$3\pi$	1:28	0.200	0.143	0.143	0.143	0.286	0.143	0.143	0.286	0.000	0.429	0.286
Car	CWED	4	$1\pi$	9:37	0.243	0.286	0.286	0.286	0.286	0.143	0.000	0.429	0.143	0.429	0.143
Car	CWED	4	$2\pi$	23:33	0.215	0.143	0.143	0.143	0.286	0.286	0.143	0.286	0.143	0.286	0.286
Car	CWED	4	$3\pi$	1:37	0.243	0.429	0.143	0.143	0.286	0.000	0.143	0.286	0.143	0.571	0.286
Car	CWED	5	$1\pi$	11:46	0.243	0.286	0.286	0.286	0.286	0.143	0.000	0.429	0.143	0.429	0.143
Car	CWED	5	$2\pi$	28:41	0.200	0.143	0.143	0.143	0.286	0.143	0.143	0.286	0.143	0.286	0.286
Car	CWED	5	$3\pi$	31:44	0.229	0.286	0.143	0.143	0.286	0.000	0.286	0.286	0.143	0.429	0.286
Car	CWED	6	$1\pi$	12:55	0.243	0.286	0.286	0.286	0.286	0.143	0.000	0.429	0.143	0.429	0.143
Car	CWED	6	$2\pi$	41:50	0.215	0.286	0.143	0.286	0.286	0.143	0.143	0.286	0.143	0.286	0.143
Car	CWED	6	$3\pi$	33:55	0.229	0.286	0.143	0.143	0.286	0.000	0.143	0.286	0.143	0.571	0.286
Car	CWED	7	$1\pi$	33:41	0.229	0.286	0.286	0.000	0.429	0.286	0.143	0.286	0.143	0.143	0.286
Car	CWED	7	$2\pi$	24:42	0.200	0.286	0.286	0.000	0.143	0.143	0.000	0.286	0.286	0.143	0.429
Car	CWED	7	$3\pi$	38:64	0.229	0.286	0.143	0.143	0.286	0.000	0.143	0.286	0.143	0.571	0.286



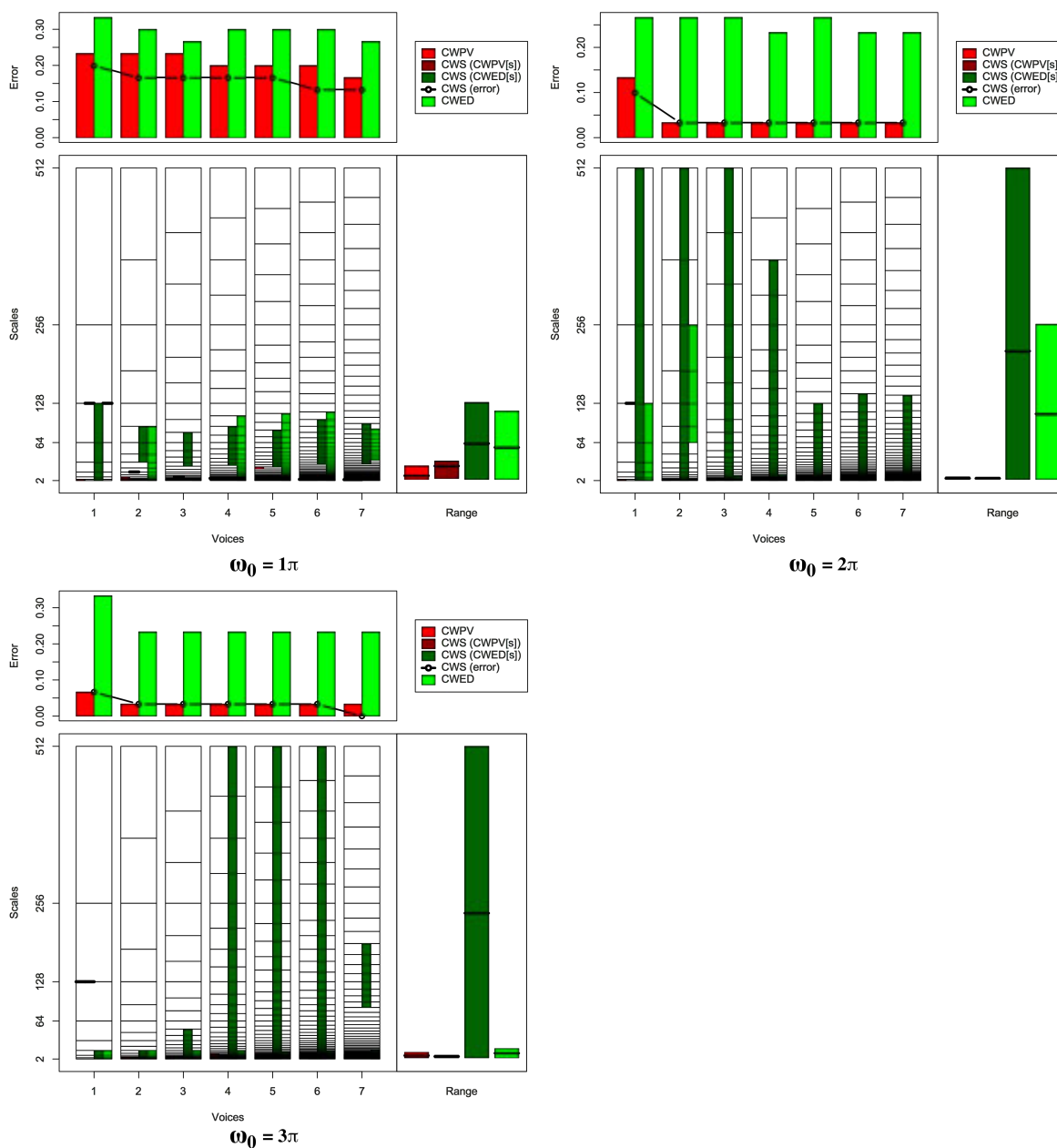


FIGURE B.20: Summary of results for the Beef classification problem comparing CWS, CWPV, CWED methods using 1-7 voices and three  $\omega_0$  values. A lower CWPV score suggests that the problem is predominantly characterised by FM, whereas a lower CWED implies a predominant AM characteristic. The scale ranges have been translated from scale number to scale value. In the bottom right figure of each figure the average range of scales for all 7 voices are presented for each technique.

TABLE B.20: Summary of results for the Beef classification problem comparing Ed, DTW, CWS, CWPV, and CWED using 1-7 voices and 3  $\omega_0$  parameters.  $S$  is the scale set(s) associated with the CWS, CWPV and CWED results. The mean values highlighted in bold are the best in model error rate for the problem.

Problem	Technique	Voices	$\omega_0$	$S$	Mean	1	2	3	4	5	6	7	7	9	10
Beef	Ed				0.400	0.667	0.333	0.333	0.333	0.333	0.333	0.000	0.667	0.333	0.667
Beef	DTW				0.433	0.667	0.333	0.333	0.333	0.667	0.333	0.000	0.667	0.333	0.667
Beef	CWS	1	$1\pi$	5:5,1:7	0.200	0.333	0.000	0.333	0.000	0.667	0.000	0.333	0.000	0.333	0.000
Beef	CWS	1	$2\pi$	2:2,1:9	0.100	0.000	0.000	0.000	0.000	0.333	0.000	0.000	0.000	0.000	0.667
Beef	CWS	1	$3\pi$	2:2,1:4	0.067	0.000	0.333	0.000	0.000	0.000	0.000	0.000	0.333	0.000	0.000
Beef	CWS	2	$1\pi$	9:9,9:12	0.167	0.333	0.000	0.333	0.000	0.667	0.000	0.000	0.000	0.333	0.000
Beef	CWS	2	$2\pi$	2:3,1:17	0.033	0.000	0.000	0.000	0.000	0.000	0.000	0.000	0.000	0.000	0.333
Beef	CWS	2	$3\pi$	3:4,1:7	0.033	0.000	0.000	0.000	0.000	0.000	0.000	0.000	0.000	0.000	0.333
Beef	CWS	3	$1\pi$	13:13,12:17	0.167	0.333	0.000	0.333	0.000	0.667	0.000	0.000	0.000	0.333	0.000
Beef	CWS	3	$2\pi$	2:6,1:25	0.033	0.000	0.000	0.000	0.000	0.000	0.000	0.000	0.000	0.000	0.333
Beef	CWS	3	$3\pi$	3:6,1:15	0.033	0.000	0.000	0.000	0.000	0.000	0.000	0.000	0.000	0.000	0.333
Beef	CWS	4	$1\pi$	17:17,16:23	0.167	0.333	0.000	0.333	0.000	0.667	0.000	0.000	0.000	0.333	0.000
Beef	CWS	4	$2\pi$	3:6,1:31	0.033	0.000	0.000	0.000	0.000	0.000	0.000	0.000	0.000	0.000	0.333
Beef	CWS	4	$3\pi$	5:8,1:33	0.033	0.000	0.000	0.000	0.000	0.000	0.000	0.000	0.000	0.000	0.333
Beef	CWS	5	$1\pi$	21:21,19:28	0.167	0.333	0.000	0.333	0.000	0.667	0.000	0.000	0.000	0.333	0.000
Beef	CWS	5	$2\pi$	3:7,1:31	0.033	0.000	0.000	0.000	0.000	0.000	0.000	0.000	0.000	0.000	0.333
Beef	CWS	5	$3\pi$	1:8,1:41	0.033	0.000	0.000	0.000	0.000	0.000	0.000	0.000	0.000	0.000	0.333
Beef	CWS	6	$1\pi$	6:6,24:35	0.133	0.333	0.000	0.333	0.000	0.333	0.000	0.000	0.000	0.000	0.333
Beef	CWS	6	$2\pi$	4:8,1:38	0.033	0.000	0.000	0.000	0.000	0.000	0.000	0.000	0.000	0.000	0.333
Beef	CWS	6	$3\pi$	1:9,1:49	0.033	0.000	0.000	0.000	0.000	0.000	0.000	0.000	0.000	0.000	0.333
Beef	CWS	7	$1\pi$	7:7,28:40	0.133	0.333	0.000	0.333	0.000	0.333	0.000	0.000	0.000	0.000	0.333
Beef	CWS	7	$2\pi$	4:8,1:44	0.033	0.000	0.000	0.000	0.000	0.000	0.000	0.000	0.000	0.000	0.333
Beef	CWS	7	$3\pi$	7:8,39:47	<b>0.000</b>	0.000	0.000	0.000	0.000	0.000	0.000	0.000	0.000	0.000	0.000
Beef	CWPV	1	$1\pi$	1:2	0.233	0.333	0.000	0.333	0.333	0.000	0.000	0.333	0.333	0.000	0.667
Beef	CWPV	1	$2\pi$	1:2	0.133	0.000	0.000	0.000	0.000	0.333	0.000	0.333	0.000	0.000	0.667
Beef	CWPV	1	$3\pi$	2:2	0.067	0.000	0.333	0.000	0.000	0.000	0.000	0.000	0.333	0.000	0.000
Beef	CWPV	2	$1\pi$	1:5	0.233	0.333	0.000	0.333	0.333	0.000	0.000	0.333	0.333	0.000	0.667
Beef	CWPV	2	$2\pi$	1:3	0.033	0.000	0.000	0.000	0.000	0.000	0.000	0.000	0.000	0.000	0.333
Beef	CWPV	2	$3\pi$	3:4	0.033	0.000	0.000	0.000	0.000	0.000	0.000	0.000	0.000	0.000	0.333
Beef	CWPV	3	$1\pi$	2:4	0.233	0.333	0.000	0.333	0.000	0.333	0.000	0.333	0.333	0.000	0.667
Beef	CWPV	3	$2\pi$	1:6	0.033	0.000	0.000	0.000	0.000	0.000	0.000	0.000	0.000	0.000	0.333
Beef	CWPV	3	$3\pi$	1:6	0.033	0.000	0.000	0.000	0.000	0.000	0.000	0.000	0.000	0.000	0.333
Beef	CWPV	4	$1\pi$	4:4	0.200	0.333	0.000	0.333	0.000	0.333	0.000	0.000	0.333	0.000	0.667
Beef	CWPV	4	$2\pi$	1:7	0.033	0.000	0.000	0.000	0.000	0.000	0.000	0.000	0.000	0.000	0.333
Beef	CWPV	4	$3\pi$	3:11	0.033	0.000	0.000	0.000	0.000	0.000	0.000	0.000	0.000	0.000	0.333
Beef	CWPV	5	$1\pi$	18:19	0.200	0.333	0.000	0.333	0.000	0.333	0.000	0.333	0.000	0.333	0.333
Beef	CWPV	5	$2\pi$	1:9	0.033	0.000	0.000	0.000	0.000	0.000	0.000	0.000	0.000	0.000	0.333
Beef	CWPV	5	$3\pi$	1:7	0.033	0.000	0.000	0.000	0.000	0.000	0.000	0.000	0.000	0.000	0.333
Beef	CWPV	6	$1\pi$	6:6	0.200	0.333	0.000	0.333	0.000	0.333	0.000	0.000	0.333	0.000	0.667
Beef	CWPV	6	$2\pi$	1:11	0.033	0.000	0.000	0.000	0.000	0.000	0.000	0.000	0.000	0.000	0.333
Beef	CWPV	6	$3\pi$	6:14	0.033	0.000	0.000	0.000	0.000	0.000	0.000	0.000	0.000	0.000	0.333
Beef	CWPV	7	$1\pi$	7:7	0.167	0.333	0.000	0.000	0.000	0.333	0.000	0.000	0.333	0.000	0.667
Beef	CWPV	7	$2\pi$	1:12	0.033	0.000	0.000	0.000	0.000	0.000	0.000	0.000	0.000	0.000	0.333
Beef	CWPV	7	$3\pi$	7:17	0.033	0.000	0.000	0.000	0.000	0.000	0.000	0.000	0.000	0.000	0.333
Beef	CWED	1	$1\pi$	1:1	0.333	0.667	0.333	0.333	0.333	0.333	0.000	0.333	0.333	0.333	0.333
Beef	CWED	1	$2\pi$	1:7	0.267	0.000	0.333	0.333	0.000	0.333	0.000	0.333	0.667	0.333	0.333
Beef	CWED	1	$3\pi$	1:4	0.333	0.333	0.000	0.333	0.000	0.667	0.000	0.333	0.333	0.667	0.667
Beef	CWED	2	$1\pi$	1:12	0.300	0.667	0.333	0.333	0.000	0.667	0.000	0.000	0.333	0.333	0.333
Beef	CWED	2	$2\pi$	11:15	0.267	0.333	0.333	0.333	0.000	0.667	0.000	0.000	0.333	0.333	0.333
Beef	CWED	2	$3\pi$	1:7	0.233	0.000	0.000	0.333	0.000	0.667	0.000	0.000	0.333	0.667	0.333
Beef	CWED	3	$1\pi$	1:5	0.267	0.333	0.000	0.333	0.000	0.667	0.000	0.333	0.333	0.333	0.333
Beef	CWED	3	$2\pi$	4:8	0.267	0.333	0.000	0.333	0.000	0.667	0.000	0.000	0.333	0.667	0.333
Beef	CWED	3	$3\pi$	1:10	0.233	0.000	0.000	0.333	0.000	0.667	0.000	0.000	0.333	0.667	0.333
Beef	CWED	4	$1\pi$	1:24	0.300	0.333	0.000	0.333	0.000	0.667	0.000	0.333	0.333	0.333	0.667
Beef	CWED	4	$2\pi$	4:11	0.233	0.333	0.000	0.333	0.000	0.667	0.000	0.000	0.333	0.333	0.333
Beef	CWED	4	$3\pi$	6:13	0.233	0.000	0.000	0.333	0.000	0.667	0.000	0.000	0.333	0.667	0.333
Beef	CWED	5	$1\pi$	1:30	0.300	0.667	0.333	0.333	0.000	0.333	0.000	0.333	0.333	0.333	0.333
Beef	CWED	5	$2\pi$	5:13	0.267	0.333	0.000	0.333	0.000	0.667	0.000	0.000	0.333	0.667	0.333
Beef	CWED	5	$3\pi$	10:15	0.233	0.333	0.000	0.333	0.000	0.667	0.000	0.000	0.333	0.333	0.333
Beef	CWED	6	$1\pi$	1:36	0.300	0.667	0.333	0.333	0.000	0.667	0.000	0.000	0.333	0.333	0.333
Beef	CWED	6	$2\pi$	5:16	0.233	0.333	0.000	0.333	0.000	0.667	0.000	0.000	0.333	0.333	0.333
Beef	CWED	6	$3\pi$	8:19	0.233	0.000	0.000	0.333	0.000	0.667	0.000	0.000	0.333	0.667	0.333
Beef	CWED	7	$1\pi$	30:39	0.267	0.667	0.333	0.333	0.000	0.667	0.333	0.000	0.333	0.000	0.000
Beef	CWED	7	$2\pi$	5:19	0.233	0.333	0.000	0.333	0.000	0.667	0.000	0.000	0.333	0.333	0.333
Beef	CWED	7	$3\pi$	1:23	0.233	0.333	0.000	0.333	0.000	0.667	0.000	0.000	0.333	0.333	0.333

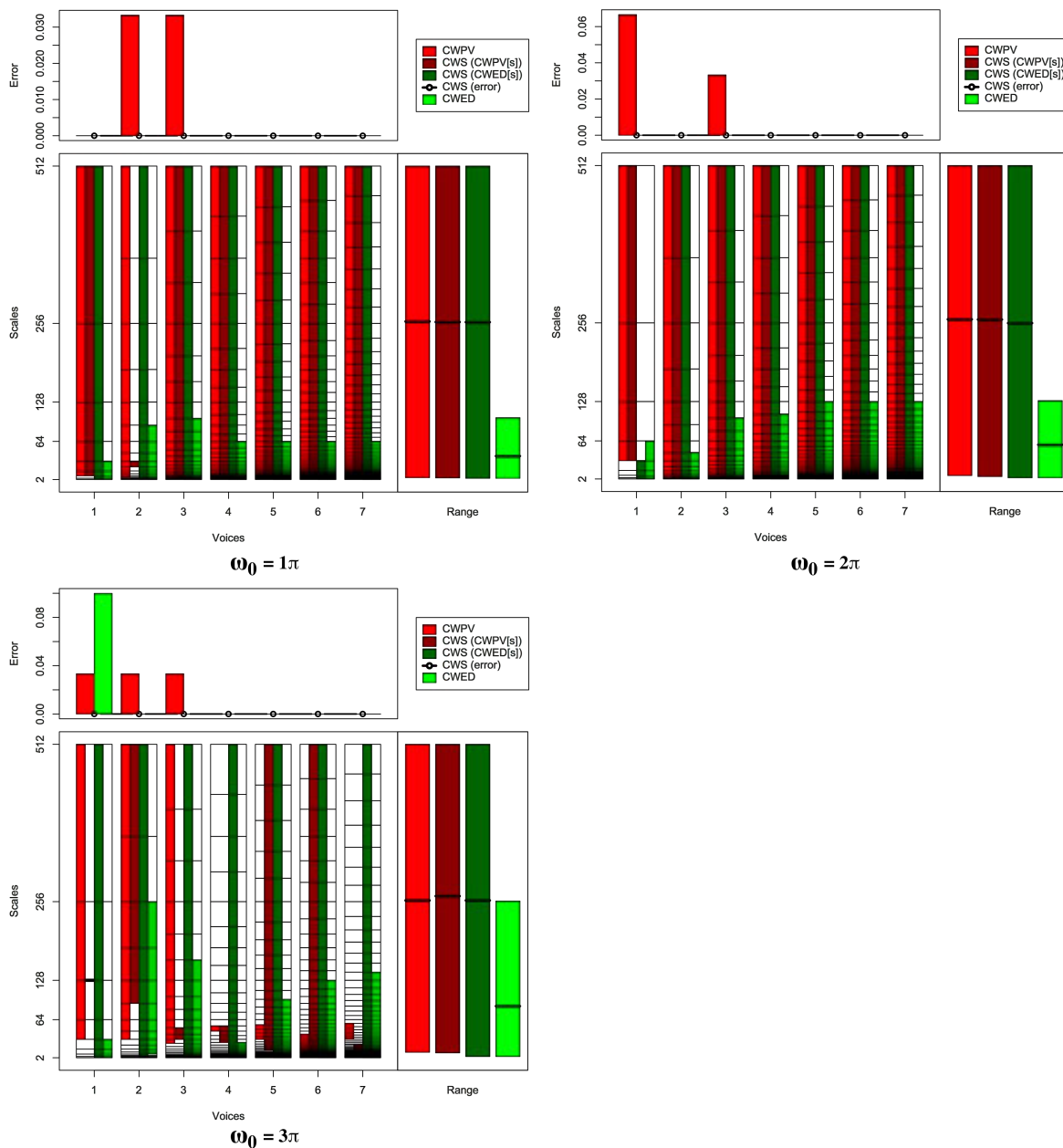


FIGURE B.21: Summary of results for the Coffee classification problem comparing CWS, CWPV, CWED methods using 1-7 voices and three  $\omega_0$  values. A lower CWPV score suggests that the problem is predominantly characterised by FM, whereas a lower CWED implies a predominant AM characteristic. The scale ranges have been translated from scale number to scale value. In the bottom right figure of each figure the average range of scales for all 7 voices are presented for each technique.



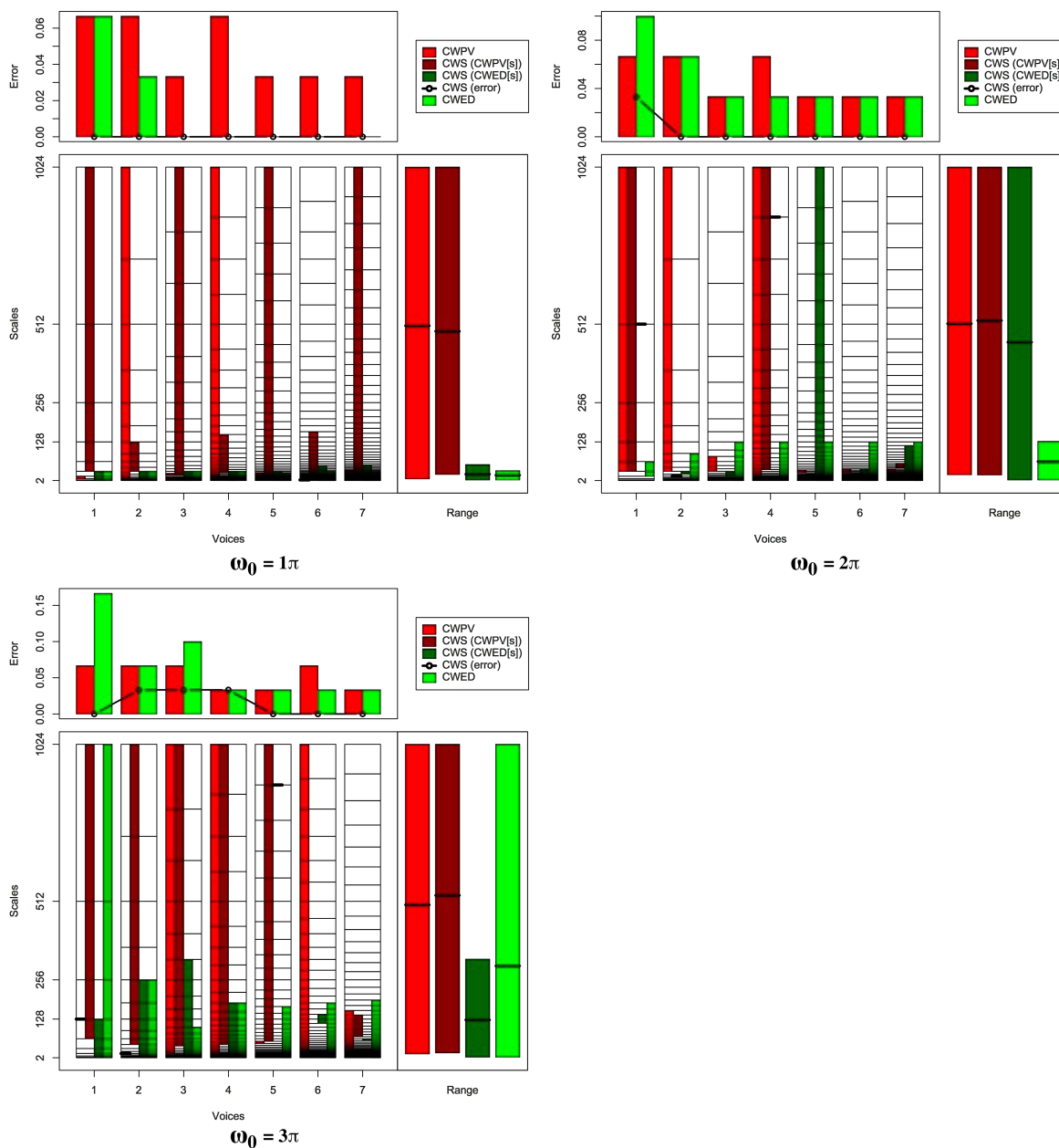


FIGURE B.22: Summary of results for the Olive Oil classification problem comparing CWS, CWPV, CWED methods using 1-7 voices and three  $\omega_0$  values. A lower CWPV score suggests that the problem is predominantly characterised by FM, whereas a lower CWED implies a predominant AM characteristic. The scale ranges have been translated from scale number to scale value. In the bottom right figure of each figure the average range of scales for all 7 voices are presented for each technique.

TABLE B.22: Summary of results for the Olive Oil classification problem comparing Ed, DTW, CWS, CWPV, and CWED using 1-7 voices and 3  $\omega_0$  parameters.  $S$  is the scale set(s) associated with the CWS, CWPV and CWED results. The mean values highlighted in bold are the best in model error rate for the problem.

Problem	Technique	Voices	$\omega_0$	$S$	Mean	1	2	3	4	5	6	7	7	9	10
Olive Oil	Ed				0.067	0.000	0.000	0.000	0.000	0.000	0.000	0.333	0.000	0.333	0.000
Olive Oil	DTW				0.067	0.000	0.000	0.000	0.000	0.000	0.000	0.333	0.000	0.333	0.000
Olive Oil	CWS	1	1 $\pi$	5:10,1:5	<b>0.000</b>	0.000	0.000	0.000	0.000	0.000	0.000	0.000	0.000	0.000	0.000
Olive Oil	CWS	1	2 $\pi$	5:10,1:1	0.033	0.000	0.000	0.000	0.000	0.000	0.000	0.000	0.000	0.333	0.000
Olive Oil	CWS	1	3 $\pi$	6:10,1:7	<b>0.000</b>	0.000	0.000	0.000	0.000	0.000	0.000	0.000	0.000	0.000	0.000
Olive Oil	CWS	2	1 $\pi$	9:13,1:9	<b>0.000</b>	0.000	0.000	0.000	0.000	0.000	0.000	0.000	0.000	0.000	0.000
Olive Oil	CWS	2	2 $\pi$	8:8,8:9	<b>0.000</b>	0.000	0.000	0.000	0.000	0.000	0.000	0.000	0.000	0.000	0.000
Olive Oil	CWS	2	3 $\pi$	10:19,1:15	0.033	0.000	0.000	0.000	0.000	0.000	0.000	0.333	0.000	0.000	0.000
Olive Oil	CWS	3	1 $\pi$	11:28,1:13	<b>0.000</b>	0.000	0.000	0.000	0.000	0.000	0.000	0.000	0.000	0.000	0.000
Olive Oil	CWS	3	2 $\pi$	12:12,10:13	<b>0.000</b>	0.000	0.000	0.000	0.000	0.000	0.000	0.000	0.000	0.000	0.000
Olive Oil	CWS	3	3 $\pi$	14:28,1:23	0.033	0.000	0.000	0.000	0.000	0.000	0.000	0.000	0.000	0.333	0.000
Olive Oil	CWS	4	1 $\pi$	16:26,1:17	<b>0.000</b>	0.000	0.000	0.000	0.000	0.000	0.000	0.000	0.000	0.000	0.000
Olive Oil	CWS	4	2 $\pi$	18:37,18:18	<b>0.000</b>	0.000	0.000	0.000	0.000	0.000	0.000	0.000	0.000	0.000	0.000
Olive Oil	CWS	4	3 $\pi$	19:37,1:27	0.033	0.000	0.000	0.000	0.000	0.000	0.000	0.333	0.000	0.000	0.000
Olive Oil	CWS	5	1 $\pi$	18:46,1:21	<b>0.000</b>	0.000	0.000	0.000	0.000	0.000	0.000	0.000	0.000	0.000	0.000
Olive Oil	CWS	5	2 $\pi$	17:19,1:46	<b>0.000</b>	0.000	0.000	0.000	0.000	0.000	0.000	0.000	0.000	0.000	0.000
Olive Oil	CWS	5	3 $\pi$	25:46,21:21	<b>0.000</b>	0.000	0.000	0.000	0.000	0.000	0.000	0.000	0.000	0.000	0.000
Olive Oil	CWS	6	1 $\pi$	23:39,1:29	<b>0.000</b>	0.000	0.000	0.000	0.000	0.000	0.000	0.000	0.000	0.000	0.000
Olive Oil	CWS	6	2 $\pi$	22:23,1:27	<b>0.000</b>	0.000	0.000	0.000	0.000	0.000	0.000	0.000	0.000	0.000	0.000
Olive Oil	CWS	6	3 $\pi$	19:20,36:38	<b>0.000</b>	0.000	0.000	0.000	0.000	0.000	0.000	0.000	0.000	0.000	0.000
Olive Oil	CWS	7	1 $\pi$	25:64,1:34	<b>0.000</b>	0.000	0.000	0.000	0.000	0.000	0.000	0.000	0.000	0.000	0.000
Olive Oil	CWS	7	2 $\pi$	32:35,28:42	<b>0.000</b>	0.000	0.000	0.000	0.000	0.000	0.000	0.000	0.000	0.000	0.000
Olive Oil	CWS	7	3 $\pi$	37:44,35:36	<b>0.000</b>	0.000	0.000	0.000	0.000	0.000	0.000	0.000	0.000	0.000	0.000
Olive Oil	CWPV	1	1 $\pi$	3:4	0.067	0.000	0.000	0.000	0.000	0.000	0.000	0.000	0.000	0.333	0.333
Olive Oil	CWPV	1	2 $\pi$	5:10	0.067	0.000	0.000	0.000	0.000	0.000	0.000	0.000	0.000	0.333	0.333
Olive Oil	CWPV	1	3 $\pi$	7:7	0.067	0.000	0.000	0.000	0.000	0.000	0.000	0.333	0.000	0.333	0.000
Olive Oil	CWPV	2	1 $\pi$	4:19	0.067	0.000	0.000	0.000	0.000	0.000	0.000	0.000	0.000	0.333	0.333
Olive Oil	CWPV	2	2 $\pi$	9:19	0.067	0.000	0.000	0.000	0.000	0.000	0.000	0.000	0.000	0.333	0.333
Olive Oil	CWPV	2	3 $\pi$	13:13	0.067	0.000	0.000	0.000	0.000	0.000	0.000	0.333	0.000	0.333	0.000
Olive Oil	CWPV	3	1 $\pi$	11:12	0.033	0.000	0.000	0.000	0.000	0.000	0.000	0.000	0.000	0.333	0.000
Olive Oil	CWPV	3	2 $\pi$	13:17	0.033	0.000	0.000	0.000	0.000	0.000	0.000	0.000	0.000	0.333	0.000
Olive Oil	CWPV	3	3 $\pi$	10:28	0.067	0.000	0.000	0.000	0.000	0.000	0.000	0.000	0.000	0.333	0.333
Olive Oil	CWPV	4	1 $\pi$	8:37	0.067	0.000	0.000	0.000	0.000	0.000	0.000	0.000	0.000	0.333	0.333
Olive Oil	CWPV	4	2 $\pi$	14:37	0.067	0.000	0.000	0.000	0.000	0.000	0.000	0.000	0.000	0.333	0.333
Olive Oil	CWPV	4	3 $\pi$	13:37	0.033	0.000	0.000	0.000	0.000	0.000	0.000	0.000	0.000	0.333	0.000
Olive Oil	CWPV	5	1 $\pi$	18:20	0.033	0.000	0.000	0.000	0.000	0.000	0.000	0.000	0.000	0.333	0.000
Olive Oil	CWPV	5	2 $\pi$	20:22	0.033	0.000	0.000	0.000	0.000	0.000	0.000	0.000	0.000	0.333	0.000
Olive Oil	CWPV	5	3 $\pi$	24:25	0.033	0.000	0.000	0.000	0.000	0.000	0.000	0.000	0.000	0.333	0.000
Olive Oil	CWPV	6	1 $\pi$	21:21	0.033	0.000	0.000	0.000	0.000	0.000	0.000	0.000	0.000	0.333	0.000
Olive Oil	CWPV	6	2 $\pi$	24:27	0.033	0.000	0.000	0.000	0.000	0.000	0.000	0.000	0.000	0.333	0.000
Olive Oil	CWPV	6	3 $\pi$	17:55	0.067	0.000	0.000	0.000	0.000	0.000	0.000	0.000	0.000	0.333	0.333
Olive Oil	CWPV	7	1 $\pi$	24:30	0.033	0.000	0.000	0.000	0.000	0.000	0.000	0.000	0.000	0.333	0.000
Olive Oil	CWPV	7	2 $\pi$	27:31	0.033	0.000	0.000	0.000	0.000	0.000	0.000	0.000	0.000	0.333	0.000
Olive Oil	CWPV	7	3 $\pi$	25:45	0.033	0.000	0.000	0.000	0.000	0.000	0.000	0.000	0.000	0.333	0.000
Olive Oil	CWED	1	1 $\pi$	1:5	0.067	0.000	0.333	0.000	0.000	0.000	0.000	0.000	0.000	0.000	0.333
Olive Oil	CWED	1	2 $\pi$	4:6	0.100	0.000	0.333	0.000	0.000	0.333	0.000	0.333	0.000	0.000	0.000
Olive Oil	CWED	1	3 $\pi$	1:10	0.167	0.333	0.000	0.333	0.000	0.333	0.000	0.333	0.000	0.000	0.333
Olive Oil	CWED	2	1 $\pi$	1:9	0.033	0.000	0.000	0.000	0.000	0.000	0.000	0.000	0.000	0.000	0.333
Olive Oil	CWED	2	2 $\pi$	1:12	0.067	0.000	0.000	0.000	0.000	0.000	0.000	0.333	0.000	0.000	0.333
Olive Oil	CWED	2	3 $\pi$	1:15	0.067	0.000	0.000	0.000	0.000	0.333	0.000	0.333	0.000	0.000	0.000
Olive Oil	CWED	3	1 $\pi$	9:13	<b>0.000</b>	0.000	0.000	0.000	0.000	0.000	0.000	0.000	0.000	0.000	0.000
Olive Oil	CWED	3	2 $\pi$	1:19	0.033	0.000	0.000	0.000	0.000	0.000	0.000	0.333	0.000	0.000	0.000
Olive Oil	CWED	3	3 $\pi$	1:18	0.100	0.000	0.000	0.000	0.000	0.333	0.000	0.333	0.000	0.000	0.333
Olive Oil	CWED	4	1 $\pi$	10:17	<b>0.000</b>	0.000	0.000	0.000	0.000	0.000	0.000	0.000	0.000	0.000	0.000
Olive Oil	CWED	4	2 $\pi$	13:25	0.033	0.000	0.000	0.000	0.000	0.000	0.000	0.333	0.000	0.000	0.000
Olive Oil	CWED	4	3 $\pi$	1:27	0.033	0.000	0.000	0.000	0.000	0.000	0.000	0.333	0.000	0.000	0.000
Olive Oil	CWED	5	1 $\pi$	1:20	<b>0.000</b>	0.000	0.000	0.000	0.000	0.000	0.000	0.000	0.000	0.000	0.000
Olive Oil	CWED	5	2 $\pi$	1:31	0.033	0.000	0.000	0.000	0.000	0.000	0.000	0.333	0.000	0.000	0.000
Olive Oil	CWED	5	3 $\pi$	1:33	0.033	0.000	0.000	0.000	0.000	0.000	0.000	0.333	0.000	0.000	0.000
Olive Oil	CWED	6	1 $\pi$	1:25	<b>0.000</b>	0.000	0.000	0.000	0.000	0.000	0.000	0.000	0.000	0.000	0.000
Olive Oil	CWED	6	2 $\pi$	1:37	0.033	0.000	0.000	0.000	0.000	0.000	0.000	0.333	0.000	0.000	0.000
Olive Oil	CWED	6	3 $\pi$	1:40	0.033	0.000	0.000	0.000	0.000	0.000	0.000	0.333	0.000	0.000	0.000
Olive Oil	CWED	7	1 $\pi$	1:29	<b>0.000</b>	0.000	0.000	0.000	0.000	0.000	0.000	0.000	0.000	0.000	0.000
Olive Oil	CWED	7	2 $\pi$	1:43	0.033	0.000	0.000	0.000	0.000	0.000	0.000	0.333	0.000	0.000	0.000
Olive Oil	CWED	7	3 $\pi$	1:47	0.033	0.000	0.000	0.000	0.000	0.000	0.000	0.333	0.000	0.000	0.000

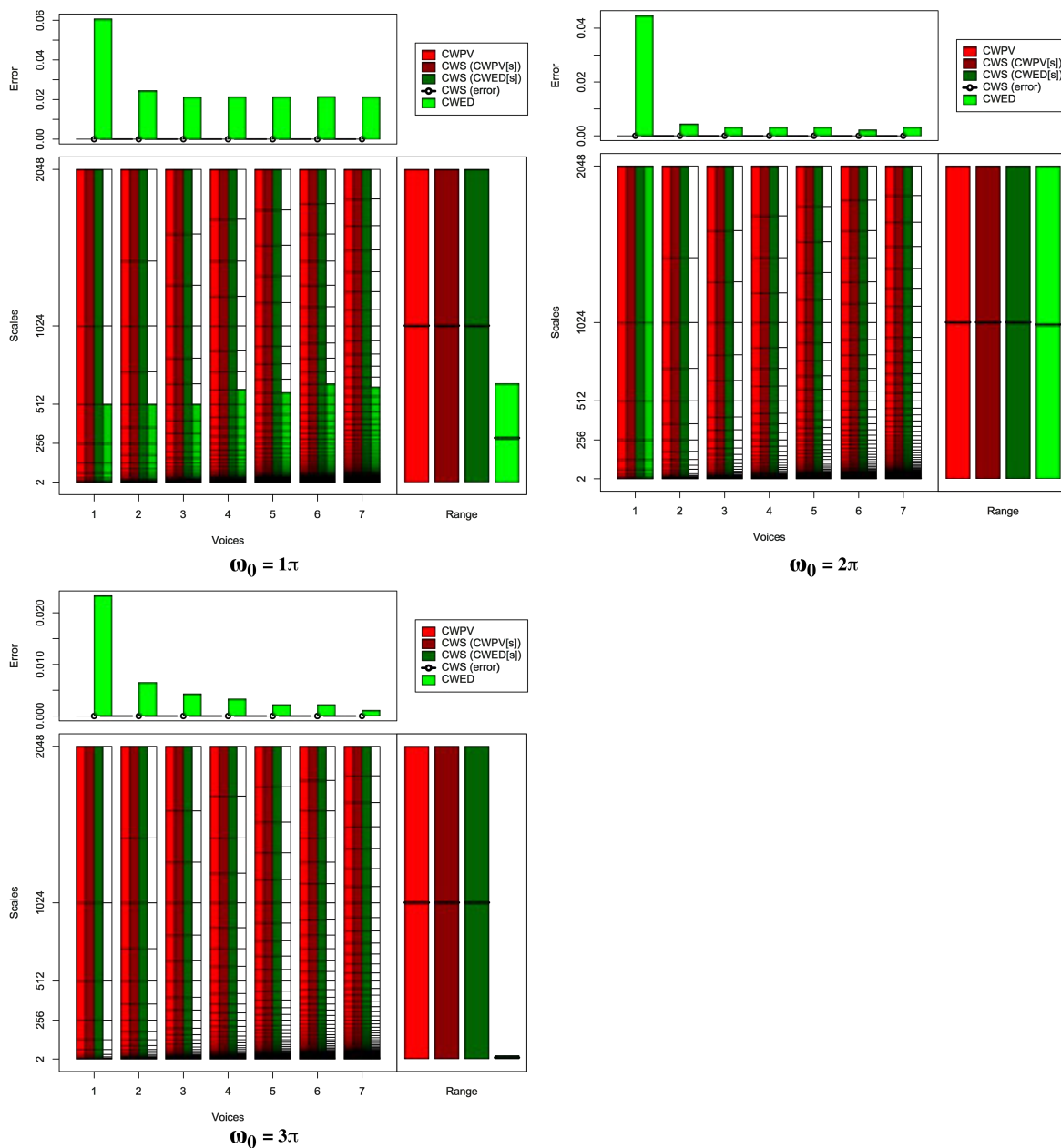


FIGURE B.23: Summary of results for the CinC\_ECG\_Torso classification problem comparing CWS, CWPV, CWED methods using 1-7 voices and three  $\omega_0$  values. A lower CWPV score suggests that the problem is predominantly characterised by FM, whereas a lower CWED implies a predominant AM characteristic. The scale ranges have been translated from scale number to scale value. In the bottom right figure of each figure the average range of scales for all 7 voices are presented for each technique.

TABLE B.23: Summary of results for the CinC\_ECG\_torso classification problem comparing Ed, DTW, CWS, CWPV, and CWED using 1-7 voices and 3  $\omega_0$  parameters.  $S$  is the scale set(s) associated with the CWS, CWPV and CWED results. The mean values highlighted in bold are the best in model error rate for the problem.

Problem	Technique	Voices	$\omega_0$	$S$	Mean	1	2	3	4	5	6	7	7	9	10
CinC_ECG_torso	Ed				0.001	0.000	0.000	0.011	0.000	0.000	0.000	0.000	0.000	0.000	0.000
CinC_ECG_torso	DTW				0.010	0.011	0.000	0.021	0.011	0.000	0.000	0.021	0.011	0.011	0.011
CinC_ECG_torso	CWS	1	$1\pi$	1:11,1:11	<b>0.000</b>	0.000	0.000	0.000	0.000	0.000	0.000	0.000	0.000	0.000	0.000
CinC_ECG_torso	CWS	1	$2\pi$	1:11,1:11	<b>0.000</b>	0.000	0.000	0.000	0.000	0.000	0.000	0.000	0.000	0.000	0.000
CinC_ECG_torso	CWS	1	$3\pi$	1:11,1:11	<b>0.000</b>	0.000	0.000	0.000	0.000	0.000	0.000	0.000	0.000	0.000	0.000
CinC_ECG_torso	CWS	2	$1\pi$	1:21,1:21	<b>0.000</b>	0.000	0.000	0.000	0.000	0.000	0.000	0.000	0.000	0.000	0.000
CinC_ECG_torso	CWS	2	$2\pi$	1:21,1:21	<b>0.000</b>	0.000	0.000	0.000	0.000	0.000	0.000	0.000	0.000	0.000	0.000
CinC_ECG_torso	CWS	2	$3\pi$	1:21,1:21	<b>0.000</b>	0.000	0.000	0.000	0.000	0.000	0.000	0.000	0.000	0.000	0.000
CinC_ECG_torso	CWS	3	$1\pi$	1:31,1:31	<b>0.000</b>	0.000	0.000	0.000	0.000	0.000	0.000	0.000	0.000	0.000	0.000
CinC_ECG_torso	CWS	3	$2\pi$	1:31,1:31	<b>0.000</b>	0.000	0.000	0.000	0.000	0.000	0.000	0.000	0.000	0.000	0.000
CinC_ECG_torso	CWS	3	$3\pi$	1:31,1:31	<b>0.000</b>	0.000	0.000	0.000	0.000	0.000	0.000	0.000	0.000	0.000	0.000
CinC_ECG_torso	CWS	4	$1\pi$	1:41,1:41	<b>0.000</b>	0.000	0.000	0.000	0.000	0.000	0.000	0.000	0.000	0.000	0.000
CinC_ECG_torso	CWS	4	$2\pi$	1:41,1:41	<b>0.000</b>	0.000	0.000	0.000	0.000	0.000	0.000	0.000	0.000	0.000	0.000
CinC_ECG_torso	CWS	4	$3\pi$	1:41,1:41	<b>0.000</b>	0.000	0.000	0.000	0.000	0.000	0.000	0.000	0.000	0.000	0.000
CinC_ECG_torso	CWS	5	$1\pi$	1:51,1:51	<b>0.000</b>	0.000	0.000	0.000	0.000	0.000	0.000	0.000	0.000	0.000	0.000
CinC_ECG_torso	CWS	5	$2\pi$	1:51,1:51	<b>0.000</b>	0.000	0.000	0.000	0.000	0.000	0.000	0.000	0.000	0.000	0.000
CinC_ECG_torso	CWS	5	$3\pi$	1:51,1:51	<b>0.000</b>	0.000	0.000	0.000	0.000	0.000	0.000	0.000	0.000	0.000	0.000
CinC_ECG_torso	CWS	6	$1\pi$	1:61,1:61	<b>0.000</b>	0.000	0.000	0.000	0.000	0.000	0.000	0.000	0.000	0.000	0.000
CinC_ECG_torso	CWS	6	$2\pi$	1:61,1:61	<b>0.000</b>	0.000	0.000	0.000	0.000	0.000	0.000	0.000	0.000	0.000	0.000
CinC_ECG_torso	CWS	6	$3\pi$	1:61,1:61	<b>0.000</b>	0.000	0.000	0.000	0.000	0.000	0.000	0.000	0.000	0.000	0.000
CinC_ECG_torso	CWS	7	$1\pi$	1:71,1:71	<b>0.000</b>	0.000	0.000	0.000	0.000	0.000	0.000	0.000	0.000	0.000	0.000
CinC_ECG_torso	CWS	7	$2\pi$	1:71,1:71	<b>0.000</b>	0.000	0.000	0.000	0.000	0.000	0.000	0.000	0.000	0.000	0.000
CinC_ECG_torso	CWS	7	$3\pi$	1:71,1:71	<b>0.000</b>	0.000	0.000	0.000	0.000	0.000	0.000	0.000	0.000	0.000	0.000
CinC_ECG_torso	CWPV	1	$1\pi$	1:11	<b>0.000</b>	0.000	0.000	0.000	0.000	0.000	0.000	0.000	0.000	0.000	0.000
CinC_ECG_torso	CWPV	1	$2\pi$	1:11	<b>0.000</b>	0.000	0.000	0.000	0.000	0.000	0.000	0.000	0.000	0.000	0.000
CinC_ECG_torso	CWPV	1	$3\pi$	1:11	<b>0.000</b>	0.000	0.000	0.000	0.000	0.000	0.000	0.000	0.000	0.000	0.000
CinC_ECG_torso	CWPV	2	$1\pi$	1:21	<b>0.000</b>	0.000	0.000	0.000	0.000	0.000	0.000	0.000	0.000	0.000	0.000
CinC_ECG_torso	CWPV	2	$2\pi$	1:21	<b>0.000</b>	0.000	0.000	0.000	0.000	0.000	0.000	0.000	0.000	0.000	0.000
CinC_ECG_torso	CWPV	2	$3\pi$	1:21	<b>0.000</b>	0.000	0.000	0.000	0.000	0.000	0.000	0.000	0.000	0.000	0.000
CinC_ECG_torso	CWPV	3	$1\pi$	1:31	<b>0.000</b>	0.000	0.000	0.000	0.000	0.000	0.000	0.000	0.000	0.000	0.000
CinC_ECG_torso	CWPV	3	$2\pi$	1:31	<b>0.000</b>	0.000	0.000	0.000	0.000	0.000	0.000	0.000	0.000	0.000	0.000
CinC_ECG_torso	CWPV	3	$3\pi$	1:31	<b>0.000</b>	0.000	0.000	0.000	0.000	0.000	0.000	0.000	0.000	0.000	0.000
CinC_ECG_torso	CWPV	4	$1\pi$	1:41	<b>0.000</b>	0.000	0.000	0.000	0.000	0.000	0.000	0.000	0.000	0.000	0.000
CinC_ECG_torso	CWPV	4	$2\pi$	1:41	<b>0.000</b>	0.000	0.000	0.000	0.000	0.000	0.000	0.000	0.000	0.000	0.000
CinC_ECG_torso	CWPV	4	$3\pi$	1:41	<b>0.000</b>	0.000	0.000	0.000	0.000	0.000	0.000	0.000	0.000	0.000	0.000
CinC_ECG_torso	CWPV	5	$1\pi$	1:51	<b>0.000</b>	0.000	0.000	0.000	0.000	0.000	0.000	0.000	0.000	0.000	0.000
CinC_ECG_torso	CWPV	5	$2\pi$	1:51	<b>0.000</b>	0.000	0.000	0.000	0.000	0.000	0.000	0.000	0.000	0.000	0.000
CinC_ECG_torso	CWPV	5	$3\pi$	1:51	<b>0.000</b>	0.000	0.000	0.000	0.000	0.000	0.000	0.000	0.000	0.000	0.000
CinC_ECG_torso	CWPV	6	$1\pi$	1:61	<b>0.000</b>	0.000	0.000	0.000	0.000	0.000	0.000	0.000	0.000	0.000	0.000
CinC_ECG_torso	CWPV	6	$2\pi$	1:61	<b>0.000</b>	0.000	0.000	0.000	0.000	0.000	0.000	0.000	0.000	0.000	0.000
CinC_ECG_torso	CWPV	6	$3\pi$	1:61	<b>0.000</b>	0.000	0.000	0.000	0.000	0.000	0.000	0.000	0.000	0.000	0.000
CinC_ECG_torso	CWPV	7	$1\pi$	1:71	<b>0.000</b>	0.000	0.000	0.000	0.000	0.000	0.000	0.000	0.000	0.000	0.000
CinC_ECG_torso	CWPV	7	$2\pi$	1:71	<b>0.000</b>	0.000	0.000	0.000	0.000	0.000	0.000	0.000	0.000	0.000	0.000
CinC_ECG_torso	CWPV	7	$3\pi$	1:71	<b>0.000</b>	0.000	0.000	0.000	0.000	0.000	0.000	0.000	0.000	0.000	0.000
CinC_ECG_torso	CWED	1	$1\pi$	1:9	0.061	0.043	0.043	0.085	0.064	0.074	0.064	0.032	0.117	0.064	0.021
CinC_ECG_torso	CWED	1	$2\pi$	1:11	0.045	0.021	0.032	0.064	0.043	0.053	0.043	0.053	0.074	0.032	0.032
CinC_ECG_torso	CWED	1	$3\pi$	1:3	0.023	0.032	0.032	0.021	0.032	0.000	0.021	0.021	0.021	0.032	0.021
CinC_ECG_torso	CWED	2	$1\pi$	5:17	0.025	0.021	0.011	0.032	0.021	0.021	0.032	0.011	0.064	0.021	0.011
CinC_ECG_torso	CWED	2	$2\pi$	1:4	0.004	0.000	0.000	0.011	0.000	0.000	0.011	0.011	0.000	0.000	0.011
CinC_ECG_torso	CWED	2	$3\pi$	1:5	0.007	0.000	0.011	0.011	0.011	0.000	0.000	0.000	0.000	0.032	0.000
CinC_ECG_torso	CWED	3	$1\pi$	1:25	0.021	0.021	0.011	0.032	0.021	0.000	0.032	0.011	0.053	0.021	0.011
CinC_ECG_torso	CWED	3	$2\pi$	1:6	0.003	0.000	0.000	0.011	0.000	0.000	0.011	0.011	0.000	0.000	0.000
CinC_ECG_torso	CWED	3	$3\pi$	1:11	0.004	0.000	0.000	0.011	0.011	0.000	0.021	0.000	0.000	0.000	0.000
CinC_ECG_torso	CWED	4	$1\pi$	1:34	0.021	0.021	0.000	0.043	0.011	0.011	0.032	0.011	0.043	0.021	0.021
CinC_ECG_torso	CWED	4	$2\pi$	1:7	0.003	0.000	0.000	0.011	0.000	0.000	0.011	0.011	0.000	0.000	0.000
CinC_ECG_torso	CWED	4	$3\pi$	1:15	0.003	0.000	0.011	0.011	0.000	0.011	0.000	0.000	0.000	0.000	0.000
CinC_ECG_torso	CWED	5	$1\pi$	1:42	0.021	0.021	0.000	0.043	0.011	0.011	0.032	0.011	0.053	0.021	0.011
CinC_ECG_torso	CWED	5	$2\pi$	1:10	0.003	0.000	0.011	0.011	0.000	0.000	0.000	0.011	0.000	0.000	0.000
CinC_ECG_torso	CWED	5	$3\pi$	1:18	0.002	0.000	0.000	0.000	0.000	0.000	0.011	0.011	0.000	0.000	0.000
CinC_ECG_torso	CWED	6	$1\pi$	1:51	0.022	0.011	0.011	0.043	0.011	0.011	0.032	0.011	0.053	0.011	0.021
CinC_ECG_torso	CWED	6	$2\pi$	1:10	0.002	0.000	0.000	0.011	0.000	0.000	0.000	0.011	0.000	0.000	0.000
CinC_ECG_torso	CWED	6	$3\pi$	1:17	0.002	0.000	0.000	0.000	0.000	0.000	0.011	0.011	0.000	0.000	0.000
CinC_ECG_torso	CWED	7	$1\pi$	1:59	0.021	0.021	0.000	0.043	0.011	0.011	0.032	0.011	0.043	0.021	0.021
CinC_ECG_torso	CWED	7	$2\pi$	1:15	0.003	0.000	0.011	0.011	0.000	0.000	0.000	0.011	0.000	0.000	0.000
CinC_ECG_torso	CWED	7	$3\pi$	1:20	0.001	0.000	0.000	0.000	0.000	0.000	0.000	0.011	0.000	0.000	0.000



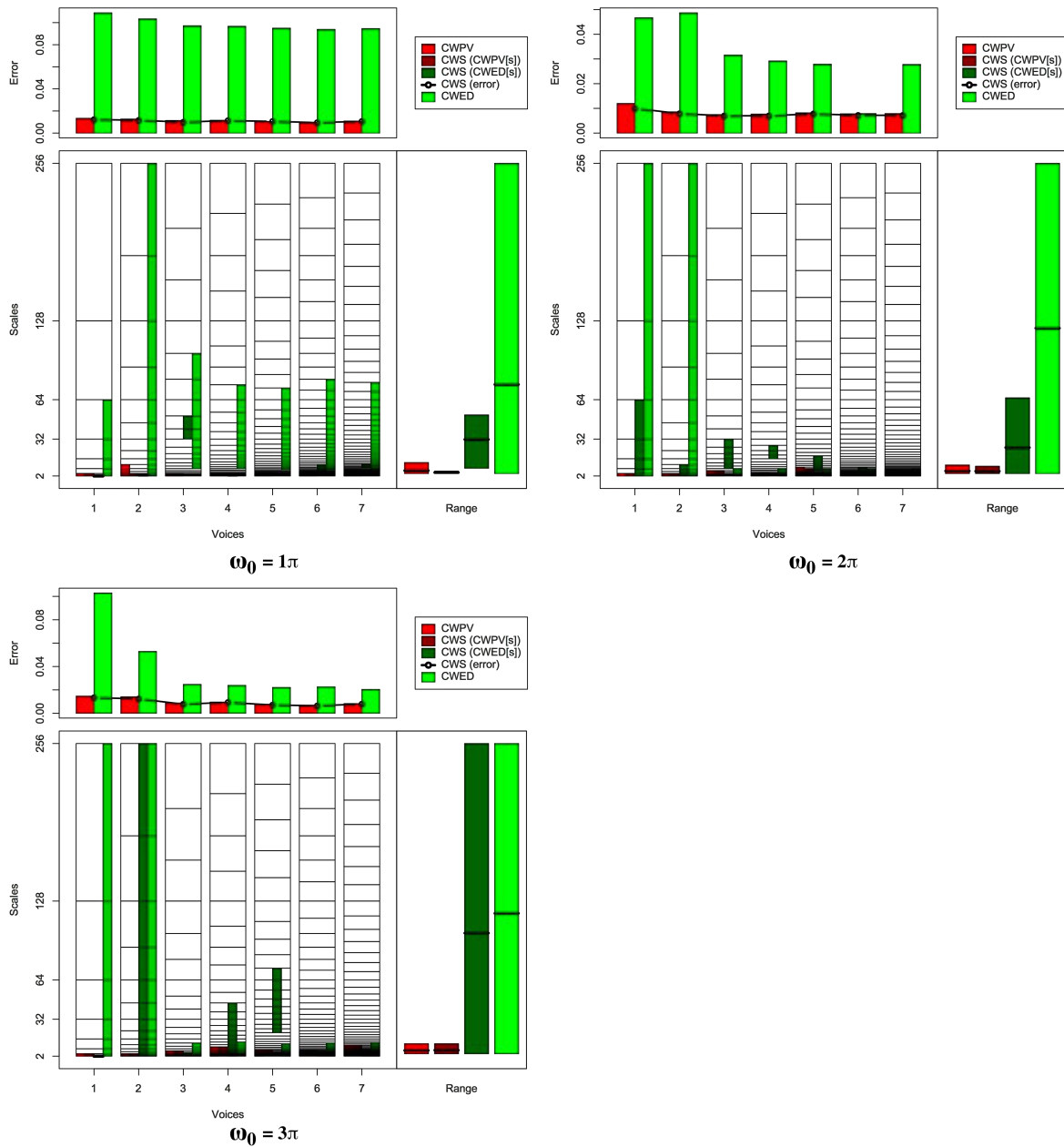


FIGURE B.24: Summary of results for the Chlorine Concentration classification problem comparing CWS, CWPV, CWED methods using 1-7 voices and three  $\omega_0$  values. A lower CWPV score suggests that the problem is predominantly characterised by FM, whereas a lower CWED implies a predominant AM characteristic. The scale ranges have been translated from scale number to scale value. In the bottom right figure of each figure the average range of scales for all 7 voices are presented for each technique.

TABLE B.24: Summary of results for the Chlorine Concentration classification problem comparing Ed, DTW, CWS, CWPV, and CWED using 1-7 voices and 3  $\omega_0$  parameters.  $S$  is the scale set(s) associated with the CWS, CWPV and CWED results. The mean values highlighted in bold are the best in model error rate for the problem.

Problem	Technique	Voices	$\omega_0$	$S$	Mean	1	2	3	4	5	6	7	7	9	10
Chlorine Concentration	Ed				0.018	0.017	0.014	0.007	0.014	0.017	0.024	0.031	0.010	0.035	0.014
Chlorine Concentration	DTW				0.019	0.014	0.014	0.014	0.010	0.021	0.017	0.031	0.014	0.035	0.017
Chlorine Concentration	CWS	1	$1\pi$	1:2,5:5	0.012	0.010	0.007	0.010	0.017	0.014	0.003	0.021	0.007	0.017	0.017
Chlorine Concentration	CWS	1	$2\pi$	1:2,1:6	0.010	0.007	0.007	0.000	0.007	0.014	0.010	0.017	0.007	0.024	0.007
Chlorine Concentration	CWS	1	$3\pi$	1:2,7:7	0.013	0.007	0.014	0.014	0.010	0.024	0.010	0.021	0.007	0.017	0.010
Chlorine Concentration	CWS	2	$1\pi$	1:3,10:10	0.012	0.010	0.014	0.003	0.014	0.017	0.003	0.014	0.007	0.017	0.017
Chlorine Concentration	CWS	2	$2\pi$	1:3,1:6	0.008	0.007	0.007	0.000	0.010	0.007	0.007	0.010	0.003	0.021	0.007
Chlorine Concentration	CWS	2	$3\pi$	1:3,1:15	0.012	0.007	0.007	0.003	0.010	0.017	0.017	0.017	0.007	0.028	0.010
Chlorine Concentration	CWS	3	$1\pi$	1:4,13:15	0.010	0.010	0.007	0.007	0.007	0.017	0.003	0.010	0.003	0.021	0.014
Chlorine Concentration	CWS	3	$2\pi$	1:6,7:13	0.007	0.003	0.003	0.000	0.003	0.010	0.007	0.010	0.003	0.024	0.007
Chlorine Concentration	CWS	3	$3\pi$	2:6,1:5	0.008	0.010	0.003	0.000	0.007	0.010	0.003	0.014	0.007	0.017	0.007
Chlorine Concentration	CWS	4	$1\pi$	1:4,10:10	0.011	0.017	0.014	0.007	0.010	0.017	0.000	0.010	0.007	0.017	0.014
Chlorine Concentration	CWS	4	$2\pi$	1:6,13:16	0.007	0.003	0.003	0.000	0.007	0.010	0.003	0.014	0.003	0.017	0.010
Chlorine Concentration	CWS	4	$3\pi$	2:10,1:19	0.009	0.007	0.003	0.000	0.014	0.014	0.000	0.021	0.003	0.021	0.010
Chlorine Concentration	CWS	5	$1\pi$	1:6,12:12	0.011	0.014	0.003	0.010	0.010	0.014	0.003	0.007	0.007	0.024	0.014
Chlorine Concentration	CWS	5	$2\pi$	1:11,9:17	0.008	0.000	0.010	0.003	0.003	0.014	0.007	0.010	0.003	0.021	0.007
Chlorine Concentration	CWS	5	$3\pi$	2:10,18:27	0.007	0.003	0.003	0.000	0.007	0.017	0.000	0.007	0.003	0.021	0.010
Chlorine Concentration	CWS	6	$1\pi$	1:6,11:16	0.010	0.007	0.010	0.007	0.010	0.017	0.000	0.010	0.003	0.017	0.014
Chlorine Concentration	CWS	6	$2\pi$	1:5,1:14	0.007	0.003	0.007	0.000	0.007	0.014	0.000	0.010	0.003	0.021	0.007
Chlorine Concentration	CWS	6	$3\pi$	5:11,1:6	<b>0.006</b>	0.010	0.003	0.000	0.007	0.010	0.000	0.007	0.003	0.017	0.007
Chlorine Concentration	CWS	7	$1\pi$	1:6,16:19	0.011	0.017	0.010	0.007	0.007	0.007	0.003	0.017	0.007	0.017	0.014
Chlorine Concentration	CWS	7	$2\pi$	1:14,1:10	0.007	0.000	0.007	0.000	0.007	0.010	0.003	0.014	0.003	0.021	0.007
Chlorine Concentration	CWS	7	$3\pi$	2:18,1:11	0.008	0.007	0.000	0.000	0.014	0.007	0.000	0.017	0.003	0.021	0.010
Chlorine Concentration	CWPV	1	$1\pi$	1:2	0.013	0.010	0.010	0.014	0.014	0.021	0.003	0.017	0.007	0.021	0.017
Chlorine Concentration	CWPV	1	$2\pi$	1:2	0.012	0.003	0.010	0.003	0.007	0.021	0.010	0.021	0.017	0.021	0.007
Chlorine Concentration	CWPV	1	$3\pi$	1:2	0.015	0.007	0.017	0.010	0.017	0.021	0.010	0.024	0.010	0.021	0.010
Chlorine Concentration	CWPV	2	$1\pi$	1:6	0.013	0.017	0.010	0.007	0.014	0.017	0.010	0.014	0.003	0.021	0.014
Chlorine Concentration	CWPV	2	$2\pi$	1:3	0.009	0.007	0.007	0.000	0.010	0.010	0.007	0.014	0.003	0.021	0.007
Chlorine Concentration	CWPV	2	$3\pi$	1:3	0.014	0.003	0.010	0.010	0.014	0.021	0.014	0.024	0.007	0.024	0.014
Chlorine Concentration	CWPV	3	$1\pi$	1:4	0.011	0.014	0.007	0.007	0.007	0.024	0.003	0.010	0.007	0.021	0.014
Chlorine Concentration	CWPV	3	$2\pi$	1:6	0.008	0.003	0.003	0.000	0.000	0.014	0.007	0.014	0.003	0.024	0.007
Chlorine Concentration	CWPV	3	$3\pi$	2:6	0.009	0.010	0.003	0.007	0.007	0.010	0.003	0.017	0.007	0.017	0.007
Chlorine Concentration	CWPV	4	$1\pi$	1:2	0.012	0.017	0.007	0.010	0.010	0.010	0.003	0.014	0.007	0.024	0.014
Chlorine Concentration	CWPV	4	$2\pi$	1:5	0.008	0.003	0.007	0.000	0.010	0.010	0.003	0.014	0.003	0.017	0.010
Chlorine Concentration	CWPV	4	$3\pi$	1:10	0.010	0.007	0.003	0.000	0.017	0.014	0.000	0.021	0.003	0.021	0.010
Chlorine Concentration	CWPV	5	$1\pi$	1:2	0.011	0.014	0.003	0.007	0.010	0.014	0.003	0.010	0.007	0.024	0.014
Chlorine Concentration	CWPV	5	$2\pi$	1:12	0.008	0.003	0.007	0.000	0.003	0.014	0.007	0.014	0.003	0.024	0.007
Chlorine Concentration	CWPV	5	$3\pi$	1:10	0.008	0.003	0.003	0.000	0.014	0.017	0.000	0.007	0.003	0.021	0.010
Chlorine Concentration	CWPV	6	$1\pi$	1:10	0.010	0.010	0.003	0.007	0.021	0.003	0.010	0.003	0.021	0.014	0.007
Chlorine Concentration	CWPV	6	$2\pi$	1:6	0.008	0.003	0.010	0.000	0.007	0.014	0.003	0.010	0.003	0.021	0.007
Chlorine Concentration	CWPV	6	$3\pi$	3:11	0.007	0.010	0.003	0.000	0.007	0.010	0.003	0.010	0.003	0.017	0.007
Chlorine Concentration	CWPV	7	$1\pi$	1:5	0.011	0.010	0.014	0.003	0.010	0.014	0.003	0.014	0.007	0.024	0.010
Chlorine Concentration	CWPV	7	$2\pi$	1:14	0.008	0.000	0.007	0.000	0.003	0.014	0.003	0.021	0.003	0.021	0.007
Chlorine Concentration	CWPV	7	$3\pi$	2:18	0.008	0.007	0.000	0.000	0.014	0.007	0.000	0.021	0.003	0.021	0.010
Chlorine Concentration	CWED	1	$1\pi$	1:6	0.109	0.112	0.105	0.115	0.105	0.101	0.101	0.108	0.122	0.115	0.105
Chlorine Concentration	CWED	1	$2\pi$	1:8	0.047	0.056	0.049	0.031	0.035	0.063	0.042	0.063	0.045	0.052	0.031
Chlorine Concentration	CWED	1	$3\pi$	1:8	0.103	0.108	0.094	0.105	0.091	0.108	0.108	0.101	0.115	0.094	0.105
Chlorine Concentration	CWED	2	$1\pi$	1:15	0.103	0.112	0.094	0.108	0.080	0.105	0.108	0.105	0.126	0.105	0.091
Chlorine Concentration	CWED	2	$2\pi$	1:15	0.049	0.049	0.038	0.045	0.045	0.049	0.035	0.066	0.056	0.059	0.045
Chlorine Concentration	CWED	2	$3\pi$	1:15	0.053	0.052	0.035	0.056	0.042	0.052	0.059	0.059	0.052	0.070	0.052
Chlorine Concentration	CWED	3	$1\pi$	7:18	0.097	0.101	0.101	0.066	0.115	0.094	0.101	0.084	0.122	0.108	0.080
Chlorine Concentration	CWED	3	$2\pi$	1:7	0.032	0.024	0.028	0.038	0.038	0.035	0.035	0.031	0.024	0.035	0.028
Chlorine Concentration	CWED	3	$3\pi$	1:9	0.025	0.021	0.024	0.028	0.035	0.024	0.014	0.031	0.021	0.035	0.014
Chlorine Concentration	CWED	4	$1\pi$	9:22	0.097	0.101	0.094	0.070	0.126	0.098	0.112	0.087	0.115	0.101	0.063
Chlorine Concentration	CWED	4	$2\pi$	1:9	0.029	0.024	0.028	0.028	0.038	0.028	0.031	0.028	0.021	0.038	0.028
Chlorine Concentration	CWED	4	$3\pi$	4:12	0.024	0.010	0.021	0.024	0.038	0.021	0.028	0.035	0.017	0.028	0.017
Chlorine Concentration	CWED	5	$1\pi$	10:27	0.095	0.108	0.087	0.066	0.119	0.105	0.105	0.077	0.122	0.098	0.063
Chlorine Concentration	CWED	5	$2\pi$	1:11	0.028	0.014	0.028	0.028	0.035	0.028	0.031	0.028	0.021	0.038	0.028
Chlorine Concentration	CWED	5	$3\pi$	1:14	0.022	0.014	0.017	0.028	0.021	0.021	0.017	0.038	0.010	0.031	0.024
Chlorine Concentration	CWED	6	$1\pi$	12:33	0.094	0.112	0.091	0.070	0.112	0.094	0.094	0.087	0.119	0.101	0.059
Chlorine Concentration	CWED	6	$2\pi$	1:13	0.008	0.003	0.007	0.000	0.007	0.014	0.000	0.017	0.003	0.021	0.007
Chlorine Concentration	CWED	6	$3\pi$	1:17	0.023	0.010	0.021	0.031	0.028	0.017	0.021	0.035	0.014	0.028	0.021
Chlorine Concentration	CWED	7	$1\pi$	14:38	0.095	0.101	0.091	0.070	0.115	0.098	0.101	0.087	0.119	0.101	0.063
Chlorine Concentration	CWED	7	$2\pi$	1:15	0.028	0.017	0.021	0.035	0.035	0.024	0.031	0.028	0.024	0.035	0.028
Chlorine Concentration	CWED	7	$3\pi$	1:20	0.020	0.010	0.021	0.028	0.024	0.017	0.014	0.035	0.010	0.028	0.017

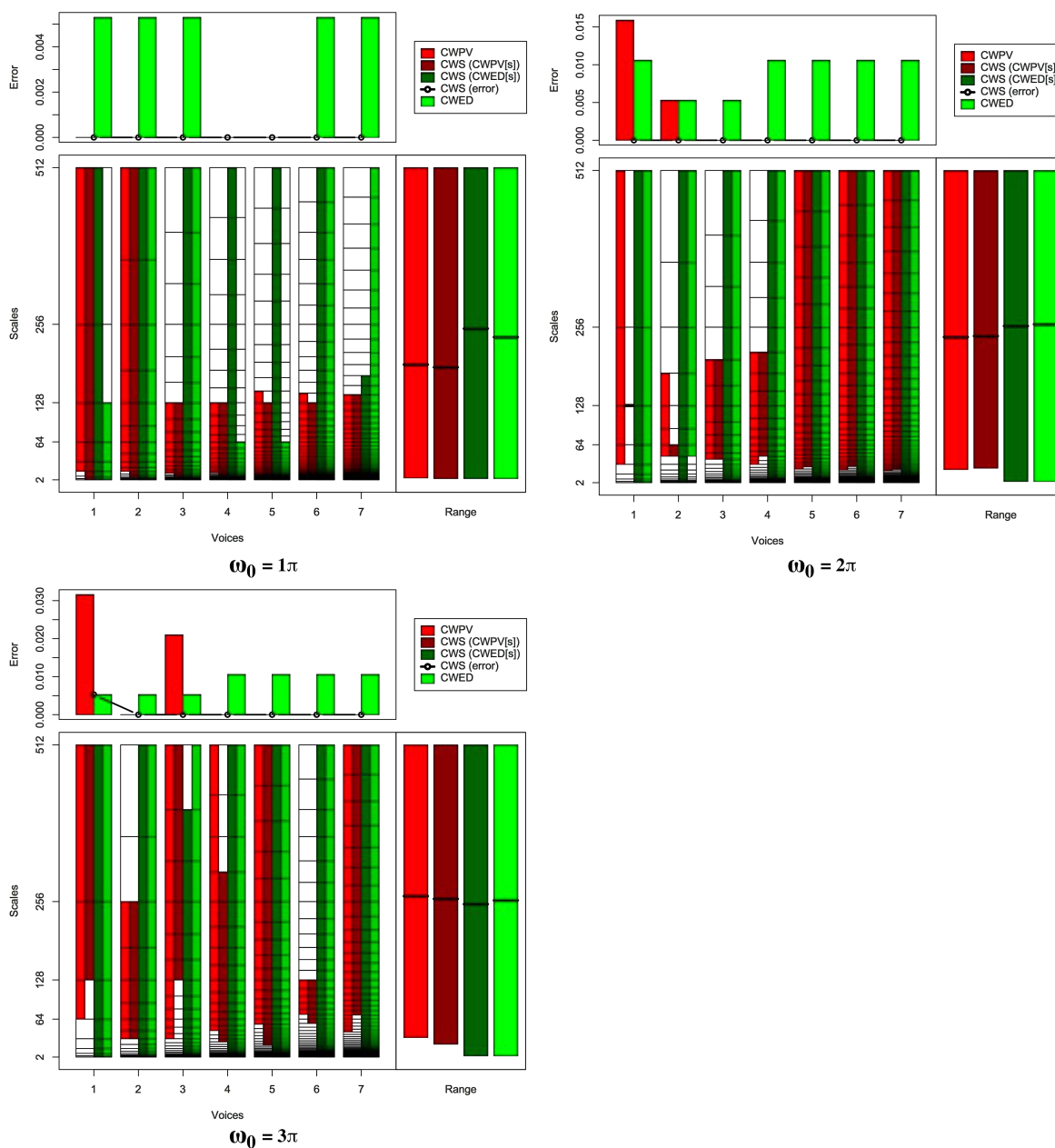


FIGURE B.25: Summary of results for the Diatom Size Reduction classification problem comparing CWS, CWPV, CWED methods using 1-7 voices and three  $\omega_0$  values. A lower CWPV score suggests that the problem is predominantly characterised by FM, whereas a lower CWED implies a predominant AM characteristic. The scale ranges have been translated from scale number to scale value. In the bottom right figure of each figure the average range of scales for all 7 voices are presented for each technique.

TABLE B.25: Summary of results for the Diatom Size Reduction classification problem comparing Ed, DTW, CWS, CWPV, and CWED using 1-7 voices and 3  $\omega_0$  parameters.  $S$  is the scale set(s) associated with the CWS, CWPV and CWED results. The mean values highlighted in bold are the best in model error rate for the problem.

Problem	Technique	Voices	$\omega_0$	$S$	Mean	1	2	3	4	5	6	7	7	9	10
Diatom Size Reduction	Ed				<b>0.000</b>	0.000	0.000	0.000	0.000	0.000	0.000	0.000	0.000	0.000	0.000
Diatom Size Reduction	DTW				0.005	0.000	0.000	0.000	0.000	0.053	0.000	0.000	0.000	0.000	0.000
Diatom Size Reduction	CWS	1	$1\pi$	1:9,1:9	<b>0.000</b>	0.000	0.000	0.000	0.000	0.000	0.000	0.000	0.000	0.000	0.000
Diatom Size Reduction	CWS	1	$2\pi$	7:7,1:9	<b>0.000</b>	0.000	0.000	0.000	0.000	0.000	0.000	0.000	0.000	0.000	0.000
Diatom Size Reduction	CWS	1	$3\pi$	7:9,1:9	0.005	0.000	0.000	0.000	0.000	0.053	0.000	0.000	0.000	0.000	0.000
Diatom Size Reduction	CWS	2	$1\pi$	4:17,1:17	<b>0.000</b>	0.000	0.000	0.000	0.000	0.000	0.000	0.000	0.000	0.000	0.000
Diatom Size Reduction	CWS	2	$2\pi$	10:11,1:17	<b>0.000</b>	0.000	0.000	0.000	0.000	0.000	0.000	0.000	0.000	0.000	0.000
Diatom Size Reduction	CWS	2	$3\pi$	9:15,1:17	<b>0.000</b>	0.000	0.000	0.000	0.000	0.000	0.000	0.000	0.000	0.000	0.000
Diatom Size Reduction	CWS	3	$1\pi$	4:19,1:25	<b>0.000</b>	0.000	0.000	0.000	0.000	0.000	0.000	0.000	0.000	0.000	0.000
Diatom Size Reduction	CWS	3	$2\pi$	14:21,1:25	<b>0.000</b>	0.000	0.000	0.000	0.000	0.000	0.000	0.000	0.000	0.000	0.000
Diatom Size Reduction	CWS	3	$3\pi$	19:25,1:24	<b>0.000</b>	0.000	0.000	0.000	0.000	0.000	0.000	0.000	0.000	0.000	0.000
Diatom Size Reduction	CWS	4	$1\pi$	5:25,1:33	<b>0.000</b>	0.000	0.000	0.000	0.000	0.000	0.000	0.000	0.000	0.000	0.000
Diatom Size Reduction	CWS	4	$2\pi$	19:28,1:33	<b>0.000</b>	0.000	0.000	0.000	0.000	0.000	0.000	0.000	0.000	0.000	0.000
Diatom Size Reduction	CWS	4	$3\pi$	16:30,1:33	<b>0.000</b>	0.000	0.000	0.000	0.000	0.000	0.000	0.000	0.000	0.000	0.000
Diatom Size Reduction	CWS	5	$1\pi$	8:31,1:41	<b>0.000</b>	0.000	0.000	0.000	0.000	0.000	0.000	0.000	0.000	0.000	0.000
Diatom Size Reduction	CWS	5	$2\pi$	20:41,1:41	<b>0.000</b>	0.000	0.000	0.000	0.000	0.000	0.000	0.000	0.000	0.000	0.000
Diatom Size Reduction	CWS	5	$3\pi$	18:41,1:41	<b>0.000</b>	0.000	0.000	0.000	0.000	0.000	0.000	0.000	0.000	0.000	0.000
Diatom Size Reduction	CWS	6	$1\pi$	10:37,1:49	<b>0.000</b>	0.000	0.000	0.000	0.000	0.000	0.000	0.000	0.000	0.000	0.000
Diatom Size Reduction	CWS	6	$2\pi$	24:49,1:49	<b>0.000</b>	0.000	0.000	0.000	0.000	0.000	0.000	0.000	0.000	0.000	0.000
Diatom Size Reduction	CWS	6	$3\pi$	30:37,1:49	<b>0.000</b>	0.000	0.000	0.000	0.000	0.000	0.000	0.000	0.000	0.000	0.000
Diatom Size Reduction	CWS	7	$1\pi$	1:44,1:46	<b>0.000</b>	0.000	0.000	0.000	0.000	0.000	0.000	0.000	0.000	0.000	0.000
Diatom Size Reduction	CWS	7	$2\pi$	26:57,1:57	<b>0.000</b>	0.000	0.000	0.000	0.000	0.000	0.000	0.000	0.000	0.000	0.000
Diatom Size Reduction	CWS	7	$3\pi$	37:57,1:57	<b>0.000</b>	0.000	0.000	0.000	0.000	0.000	0.000	0.000	0.000	0.000	0.000
Diatom Size Reduction	CWPV	1	$1\pi$	4:9	<b>0.000</b>	0.000	0.000	0.000	0.000	0.000	0.000	0.000	0.000	0.000	0.000
Diatom Size Reduction	CWPV	1	$2\pi$	5:9	0.016	0.053	0.000	0.053	0.000	0.053	0.000	0.000	0.000	0.000	0.000
Diatom Size Reduction	CWPV	1	$3\pi$	6:9	0.032	0.158	0.000	0.000	0.000	0.105	0.000	0.053	0.000	0.000	0.000
Diatom Size Reduction	CWPV	2	$1\pi$	7:17	<b>0.000</b>	0.000	0.000	0.000	0.000	0.000	0.000	0.000	0.000	0.000	0.000
Diatom Size Reduction	CWPV	2	$2\pi$	10:14	0.005	0.000	0.000	0.000	0.000	0.053	0.000	0.000	0.000	0.000	0.000
Diatom Size Reduction	CWPV	2	$3\pi$	9:15	<b>0.000</b>	0.000	0.000	0.000	0.000	0.000	0.000	0.000	0.000	0.000	0.000
Diatom Size Reduction	CWPV	3	$1\pi$	9:19	<b>0.000</b>	0.000	0.000	0.000	0.000	0.000	0.000	0.000	0.000	0.000	0.000
Diatom Size Reduction	CWPV	3	$2\pi$	14:21	<b>0.000</b>	0.000	0.000	0.000	0.000	0.000	0.000	0.000	0.000	0.000	0.000
Diatom Size Reduction	CWPV	3	$3\pi$	13:25	0.021	0.000	0.000	0.105	0.000	0.105	0.000	0.000	0.000	0.000	0.000
Diatom Size Reduction	CWPV	4	$1\pi$	12:25	<b>0.000</b>	0.000	0.000	0.000	0.000	0.000	0.000	0.000	0.000	0.000	0.000
Diatom Size Reduction	CWPV	4	$2\pi$	17:28	<b>0.000</b>	0.000	0.000	0.000	0.000	0.000	0.000	0.000	0.000	0.000	0.000
Diatom Size Reduction	CWPV	4	$3\pi$	19:33	<b>0.000</b>	0.000	0.000	0.000	0.000	0.000	0.000	0.000	0.000	0.000	0.000
Diatom Size Reduction	CWPV	5	$1\pi$	13:32	<b>0.000</b>	0.000	0.000	0.000	0.000	0.000	0.000	0.000	0.000	0.000	0.000
Diatom Size Reduction	CWPV	5	$2\pi$	19:41	<b>0.000</b>	0.000	0.000	0.000	0.000	0.000	0.000	0.000	0.000	0.000	0.000
Diatom Size Reduction	CWPV	5	$3\pi$	25:41	<b>0.000</b>	0.000	0.000	0.000	0.000	0.000	0.000	0.000	0.000	0.000	0.000
Diatom Size Reduction	CWPV	6	$1\pi$	5:38	<b>0.000</b>	0.000	0.000	0.000	0.000	0.000	0.000	0.000	0.000	0.000	0.000
Diatom Size Reduction	CWPV	6	$2\pi$	22:49	<b>0.000</b>	0.000	0.000	0.000	0.000	0.000	0.000	0.000	0.000	0.000	0.000
Diatom Size Reduction	CWPV	6	$3\pi$	32:37	<b>0.000</b>	0.000	0.000	0.000	0.000	0.000	0.000	0.000	0.000	0.000	0.000
Diatom Size Reduction	CWPV	7	$1\pi$	13:44	<b>0.000</b>	0.000	0.000	0.000	0.000	0.000	0.000	0.000	0.000	0.000	0.000
Diatom Size Reduction	CWPV	7	$2\pi$	25:57	<b>0.000</b>	0.000	0.000	0.000	0.000	0.000	0.000	0.000	0.000	0.000	0.000
Diatom Size Reduction	CWPV	7	$3\pi$	32:57	<b>0.000</b>	0.000	0.000	0.000	0.000	0.000	0.000	0.000	0.000	0.000	0.000
Diatom Size Reduction	CWED	1	$1\pi$	1:7	0.005	0.000	0.000	0.000	0.000	0.053	0.000	0.000	0.000	0.000	0.000
Diatom Size Reduction	CWED	1	$2\pi$	1:9	0.011	0.000	0.000	0.053	0.000	0.053	0.000	0.000	0.000	0.000	0.000
Diatom Size Reduction	CWED	1	$3\pi$	1:9	0.005	0.000	0.000	0.000	0.000	0.053	0.000	0.000	0.000	0.000	0.000
Diatom Size Reduction	CWED	2	$1\pi$	1:17	0.005	0.000	0.000	0.000	0.000	0.053	0.000	0.000	0.000	0.000	0.000
Diatom Size Reduction	CWED	2	$2\pi$	10:17	0.005	0.000	0.000	0.000	0.000	0.053	0.000	0.000	0.000	0.000	0.000
Diatom Size Reduction	CWED	2	$3\pi$	1:17	0.005	0.000	0.000	0.000	0.000	0.053	0.000	0.000	0.000	0.000	0.000
Diatom Size Reduction	CWED	3	$1\pi$	1:25	0.005	0.000	0.000	0.000	0.000	0.053	0.000	0.000	0.000	0.000	0.000
Diatom Size Reduction	CWED	3	$2\pi$	1:25	0.005	0.000	0.000	0.000	0.000	0.053	0.000	0.000	0.000	0.000	0.000
Diatom Size Reduction	CWED	3	$3\pi$	1:25	0.005	0.000	0.000	0.000	0.000	0.053	0.000	0.000	0.000	0.000	0.000
Diatom Size Reduction	CWED	4	$1\pi$	1:21	<b>0.000</b>	0.000	0.000	0.000	0.000	0.000	0.000	0.000	0.000	0.000	0.000
Diatom Size Reduction	CWED	4	$2\pi$	1:33	0.011	0.000	0.000	0.053	0.000	0.053	0.000	0.000	0.000	0.000	0.000
Diatom Size Reduction	CWED	4	$3\pi$	1:33	0.011	0.000	0.000	0.053	0.000	0.053	0.000	0.000	0.000	0.000	0.000
Diatom Size Reduction	CWED	5	$1\pi$	1:26	<b>0.000</b>	0.000	0.000	0.000	0.000	0.000	0.000	0.000	0.000	0.000	0.000
Diatom Size Reduction	CWED	5	$2\pi$	1:41	0.011	0.000	0.000	0.053	0.000	0.053	0.000	0.000	0.000	0.000	0.000
Diatom Size Reduction	CWED	5	$3\pi$	1:41	0.011	0.000	0.000	0.053	0.000	0.053	0.000	0.000	0.000	0.000	0.000
Diatom Size Reduction	CWED	6	$1\pi$	1:49	0.005	0.000	0.000	0.000	0.000	0.053	0.000	0.000	0.000	0.000	0.000
Diatom Size Reduction	CWED	6	$2\pi$	1:49	0.011	0.000	0.000	0.053	0.000	0.053	0.000	0.000	0.000	0.000	0.000
Diatom Size Reduction	CWED	6	$3\pi$	1:49	0.011	0.000	0.000	0.053	0.000	0.053	0.000	0.000	0.000	0.000	0.000
Diatom Size Reduction	CWED	7	$1\pi$	1:57	0.005	0.000	0.000	0.000	0.000	0.053	0.000	0.000	0.000	0.000	0.000
Diatom Size Reduction	CWED	7	$2\pi$	1:57	0.011	0.000	0.000	0.053	0.000	0.053	0.000	0.000	0.000	0.000	0.000
Diatom Size Reduction	CWED	7	$3\pi$	1:57	0.011	0.000	0.000	0.053	0.000	0.053	0.000	0.000	0.000	0.000	0.000

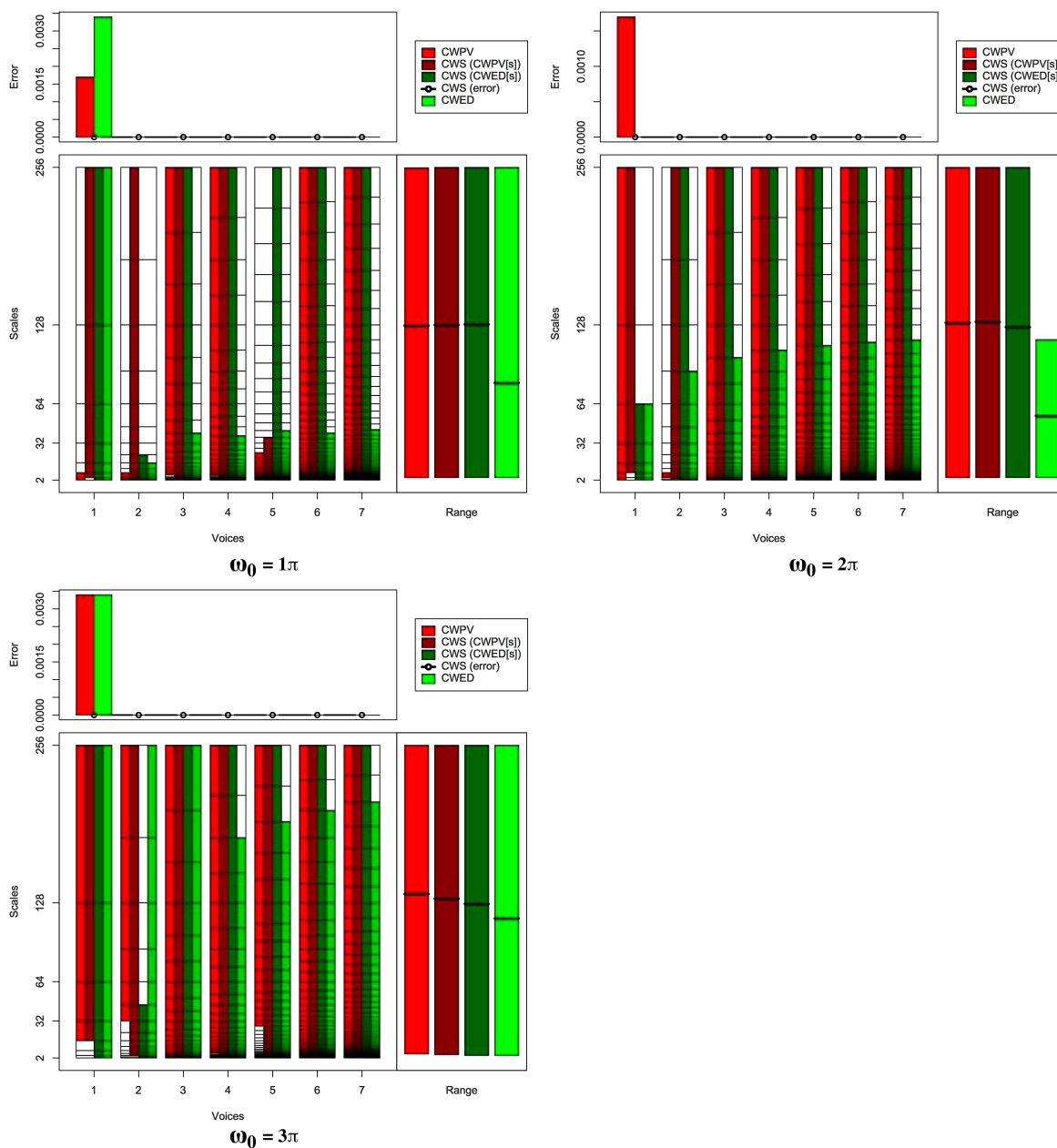


FIGURE B.26: Summary of results for the ECG Five Days classification problem comparing CWS, CWPV, CWED methods using 1-7 voices and three  $\omega_0$  values. A lower CWPV score suggests that the problem is predominantly characterised by FM, whereas a lower CWED implies a predominant AM characteristic. The scale ranges have been translated from scale number to scale value. In the bottom right figure of each figure the average range of scales for all 7 voices are presented for each technique.



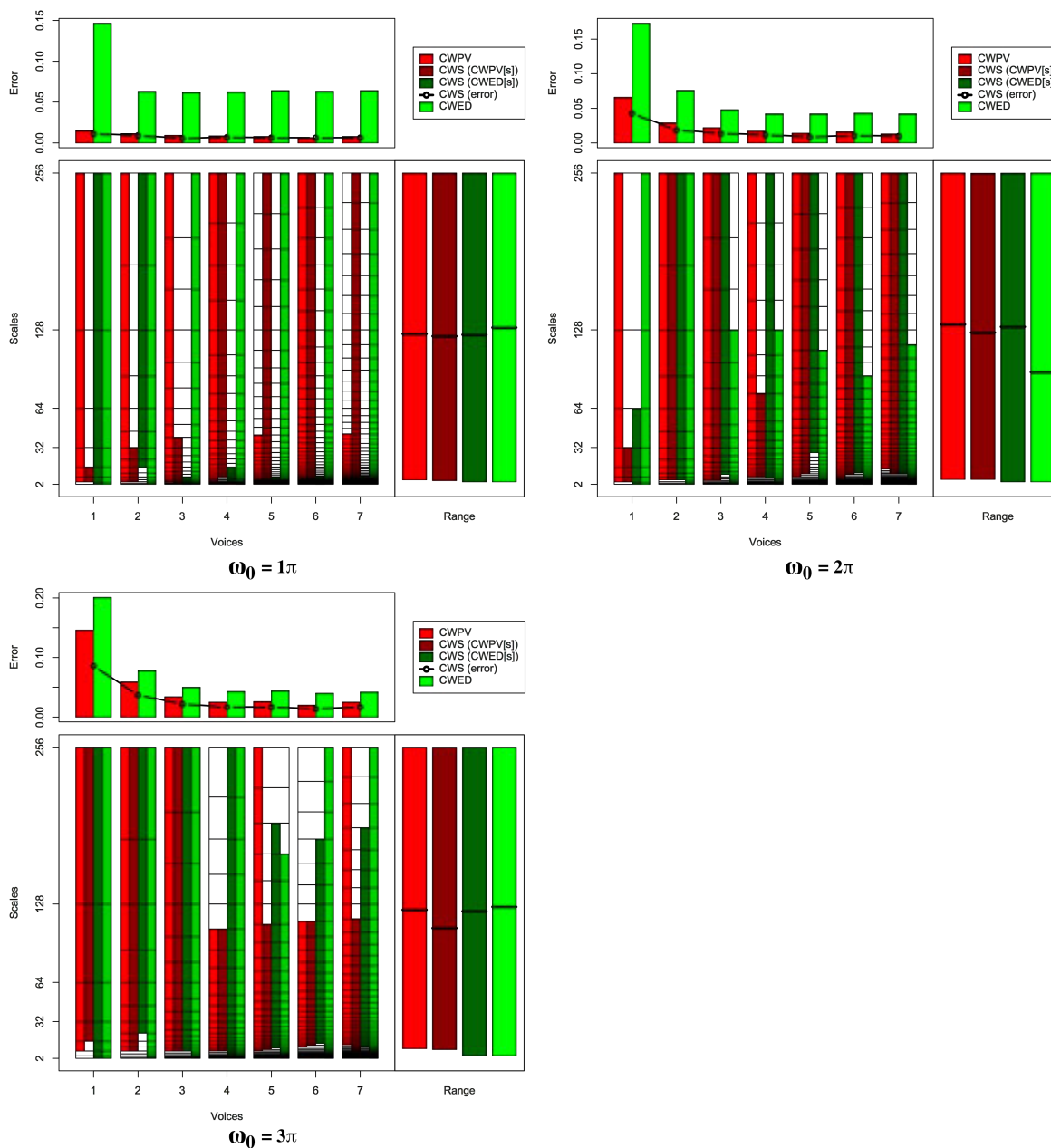


FIGURE B.27: Summary of results for the Faces UCR classification problem comparing CWS, CWPV, CWED methods using 1-7 voices and three  $\omega_0$  values. A lower CWPV score suggests that the problem is predominantly characterised by FM, whereas a lower CWED implies a predominant AM characteristic. The scale ranges have been translated from scale number to scale value. In the bottom right figure of each figure the average range of scales for all 7 voices are presented for each technique.

TABLE B.27: Summary of results for the Faces UCR classification problem comparing Ed, DTW, CWS, CWPV, and CWED using 1-7 voices and 3  $\omega_0$  parameters.  $S$  is the scale set(s) associated with the CWS, CWPV and CWED results. The mean values highlighted in bold are the best in model error rate for the problem.

Problem	Technique	Voices	$\omega_0$	$S$	Mean	1	2	3	4	5	6	7	7	9	10
Faces UCR	Ed				0.031	0.043	0.029	0.036	0.036	0.022	0.043	0.029	0.036	0.007	0.029
Faces UCR	DTW				0.021	0.058	0.007	0.036	0.022	0.014	0.007	0.014	0.007	0.036	0.007
Faces UCR	CWS	1	$1\pi$	2:4,1:8	0.011	0.029	0.000	0.014	0.029	0.007	0.014	0.007	0.000	0.007	0.007
Faces UCR	CWS	1	$2\pi$	2:5,1:6	0.043	0.058	0.065	0.050	0.029	0.029	0.036	0.050	0.029	0.029	0.050
Faces UCR	CWS	1	$3\pi$	4:8,1:8	0.086	0.144	0.086	0.101	0.079	0.086	0.122	0.065	0.072	0.065	0.043
Faces UCR	CWS	2	$1\pi$	3:9,7:15	0.009	0.022	0.000	0.007	0.022	0.007	0.007	0.007	0.007	0.007	0.007
Faces UCR	CWS	2	$2\pi$	4:15,4:15	0.019	0.036	0.029	0.036	0.029	0.007	0.014	0.007	0.014	0.014	0.007
Faces UCR	CWS	2	$3\pi$	5:15,8:15	0.037	0.058	0.043	0.072	0.043	0.036	0.043	0.014	0.029	0.007	0.029
Faces UCR	CWS	3	$1\pi$	3:14,1:7	<b>0.006</b>	0.029	0.000	0.000	0.014	0.000	0.000	0.007	0.000	0.007	0.000
Faces UCR	CWS	3	$2\pi$	5:22,8:22	0.014	0.022	0.014	0.014	0.029	0.007	0.014	0.007	0.014	0.007	0.007
Faces UCR	CWS	3	$3\pi$	7:22,7:22	0.022	0.043	0.036	0.036	0.036	0.007	0.014	0.022	0.014	0.007	0.007
Faces UCR	CWS	4	$1\pi$	9:29,4:13	0.007	0.014	0.000	0.014	0.022	0.000	0.007	0.007	0.000	0.007	0.000
Faces UCR	CWS	4	$2\pi$	9:22,8:29	0.012	0.029	0.000	0.014	0.029	0.014	0.014	0.007	0.007	0.007	0.000
Faces UCR	CWS	4	$3\pi$	9:24,1:29	0.017	0.043	0.014	0.022	0.022	0.007	0.022	0.014	0.014	0.007	0.007
Faces UCR	CWS	5	$1\pi$	5:36,2:11	0.007	0.029	0.000	0.000	0.022	0.000	0.000	0.007	0.000	0.007	0.000
Faces UCR	CWS	5	$2\pi$	13:36,20:36	0.009	0.022	0.007	0.000	0.022	0.000	0.014	0.014	0.014	0.000	0.000
Faces UCR	CWS	5	$3\pi$	12:30,13:34	0.017	0.036	0.014	0.022	0.022	0.007	0.022	0.007	0.014	0.014	0.007
Faces UCR	CWS	6	$1\pi$	5:43,1:14	0.006	0.029	0.000	0.000	0.014	0.000	0.000	0.007	0.000	0.007	0.007
Faces UCR	CWS	6	$2\pi$	15:43,16:43	0.011	0.029	0.000	0.007	0.029	0.007	0.014	0.014	0.007	0.000	0.000
Faces UCR	CWS	6	$3\pi$	17:36,18:40	0.014	0.029	0.014	0.036	0.014	0.022	0.014	0.007	0.007	0.000	0.000
Faces UCR	CWS	7	$1\pi$	5:50,2:16	0.007	0.029	0.000	0.000	0.022	0.000	0.000	0.007	0.000	0.007	0.000
Faces UCR	CWS	7	$2\pi$	18:50,18:50	0.010	0.022	0.000	0.014	0.022	0.007	0.014	0.014	0.000	0.007	0.000
Faces UCR	CWS	7	$3\pi$	14:42,19:47	0.017	0.036	0.014	0.014	0.022	0.022	0.022	0.014	0.022	0.007	0.000
Faces UCR	CWPV	1	$1\pi$	2:8	0.015	0.029	0.022	0.014	0.036	0.007	0.007	0.014	0.007	0.007	0.007
Faces UCR	CWPV	1	$2\pi$	2:8	0.066	0.072	0.086	0.058	0.072	0.058	0.086	0.058	0.050	0.050	0.065
Faces UCR	CWPV	1	$3\pi$	3:8	0.146	0.187	0.165	0.187	0.108	0.180	0.144	0.144	0.079	0.165	0.101
Faces UCR	CWPV	2	$1\pi$	3:15	0.011	0.029	0.007	0.007	0.022	0.007	0.007	0.007	0.014	0.007	0.007
Faces UCR	CWPV	2	$2\pi$	4:15	0.029	0.065	0.036	0.043	0.036	0.036	0.014	0.022	0.022	0.007	0.007
Faces UCR	CWPV	2	$3\pi$	5:15	0.059	0.065	0.072	0.086	0.065	0.072	0.094	0.036	0.043	0.036	0.022
Faces UCR	CWPV	3	$1\pi$	4:22	0.009	0.029	0.000	0.000	0.022	0.014	0.014	0.007	0.007	0.000	0.000
Faces UCR	CWPV	3	$2\pi$	5:22	0.022	0.022	0.029	0.029	0.029	0.007	0.043	0.014	0.022	0.014	0.014
Faces UCR	CWPV	3	$3\pi$	7:22	0.034	0.050	0.058	0.050	0.036	0.029	0.029	0.022	0.022	0.029	0.014
Faces UCR	CWPV	4	$1\pi$	5:29	0.009	0.022	0.007	0.000	0.022	0.007	0.007	0.007	0.007	0.000	0.007
Faces UCR	CWPV	4	$2\pi$	9:29	0.017	0.043	0.014	0.022	0.029	0.022	0.014	0.007	0.007	0.007	0.007
Faces UCR	CWPV	4	$3\pi$	9:24	0.025	0.050	0.029	0.043	0.022	0.022	0.029	0.014	0.014	0.007	0.022
Faces UCR	CWPV	5	$1\pi$	6:23	0.008	0.022	0.007	0.000	0.022	0.000	0.007	0.014	0.007	0.000	0.000
Faces UCR	CWPV	5	$2\pi$	11:36	0.014	0.022	0.014	0.022	0.029	0.014	0.014	0.014	0.007	0.000	0.007
Faces UCR	CWPV	5	$3\pi$	11:36	0.026	0.036	0.022	0.043	0.029	0.029	0.029	0.014	0.029	0.029	0.000
Faces UCR	CWPV	6	$1\pi$	7:43	0.007	0.022	0.000	0.000	0.022	0.000	0.007	0.007	0.007	0.000	0.000
Faces UCR	CWPV	6	$2\pi$	10:43	0.016	0.022	0.029	0.014	0.029	0.014	0.014	0.000	0.022	0.000	0.014
Faces UCR	CWPV	6	$3\pi$	16:36	0.020	0.036	0.022	0.043	0.022	0.022	0.022	0.007	0.022	0.000	0.000
Faces UCR	CWPV	7	$1\pi$	7:32	0.008	0.022	0.007	0.000	0.022	0.007	0.007	0.007	0.007	0.000	0.000
Faces UCR	CWPV	7	$2\pi$	21:50	0.013	0.043	0.007	0.014	0.029	0.014	0.007	0.000	0.007	0.000	0.007
Faces UCR	CWPV	7	$3\pi$	20:50	0.025	0.043	0.029	0.043	0.029	0.022	0.022	0.014	0.014	0.022	0.007
Faces UCR	CWED	1	$1\pi$	1:8	0.147	0.201	0.173	0.122	0.129	0.144	0.158	0.122	0.122	0.144	0.151
Faces UCR	CWED	1	$2\pi$	1:8	0.173	0.194	0.187	0.187	0.158	0.137	0.180	0.173	0.158	0.194	0.165
Faces UCR	CWED	1	$3\pi$	1:8	0.201	0.209	0.237	0.223	0.173	0.201	0.230	0.180	0.173	0.230	0.158
Faces UCR	CWED	2	$1\pi$	1:15	0.063	0.108	0.079	0.079	0.043	0.058	0.050	0.050	0.050	0.065	0.050
Faces UCR	CWED	2	$2\pi$	1:15	0.076	0.079	0.086	0.115	0.065	0.108	0.072	0.072	0.072	0.050	0.043
Faces UCR	CWED	2	$3\pi$	1:15	0.078	0.094	0.072	0.079	0.065	0.043	0.079	0.086	0.094	0.086	0.086
Faces UCR	CWED	3	$1\pi$	2:22	0.062	0.108	0.072	0.079	0.043	0.065	0.050	0.058	0.058	0.043	0.043
Faces UCR	CWED	3	$2\pi$	2:19	0.048	0.072	0.050	0.065	0.058	0.072	0.050	0.029	0.029	0.022	0.029
Faces UCR	CWED	3	$3\pi$	1:22	0.050	0.072	0.079	0.072	0.050	0.043	0.043	0.036	0.029	0.043	0.036
Faces UCR	CWED	4	$1\pi$	1:29	0.063	0.115	0.072	0.079	0.036	0.058	0.050	0.058	0.058	0.050	0.050
Faces UCR	CWED	4	$2\pi$	1:25	0.042	0.050	0.050	0.043	0.058	0.058	0.050	0.022	0.036	0.029	0.022
Faces UCR	CWED	4	$3\pi$	1:29	0.043	0.058	0.043	0.065	0.058	0.043	0.043	0.036	0.022	0.022	0.043
Faces UCR	CWED	5	$1\pi$	2:36	0.064	0.108	0.065	0.079	0.050	0.065	0.058	0.058	0.058	0.050	0.050
Faces UCR	CWED	5	$2\pi$	1:30	0.042	0.050	0.050	0.050	0.050	0.050	0.050	0.029	0.036	0.029	0.022
Faces UCR	CWED	5	$3\pi$	1:33	0.044	0.058	0.058	0.050	0.065	0.050	0.050	0.029	0.029	0.022	0.029
Faces UCR	CWED	6	$1\pi$	2:43	0.063	0.108	0.065	0.079	0.050	0.065	0.050	0.058	0.058	0.050	0.050
Faces UCR	CWED	6	$2\pi$	1:34	0.043	0.058	0.058	0.058	0.058	0.043	0.050	0.029	0.036	0.014	0.022
Faces UCR	CWED	6	$3\pi$	1:43	0.040	0.050	0.050	0.050	0.058	0.050	0.036	0.029	0.022	0.022	0.029
Faces UCR	CWED	7	$1\pi$	2:50	0.064	0.108	0.065	0.079	0.050	0.065	0.058	0.058	0.058	0.050	0.050
Faces UCR	CWED	7	$2\pi$	1:42	0.042	0.058	0.050	0.050	0.050	0.050	0.050	0.029	0.036	0.022	0.022
Faces UCR	CWED	7	$3\pi$	1:50	0.042	0.050	0.058	0.050	0.058	0.050	0.043	0.029	0.022	0.022	0.036



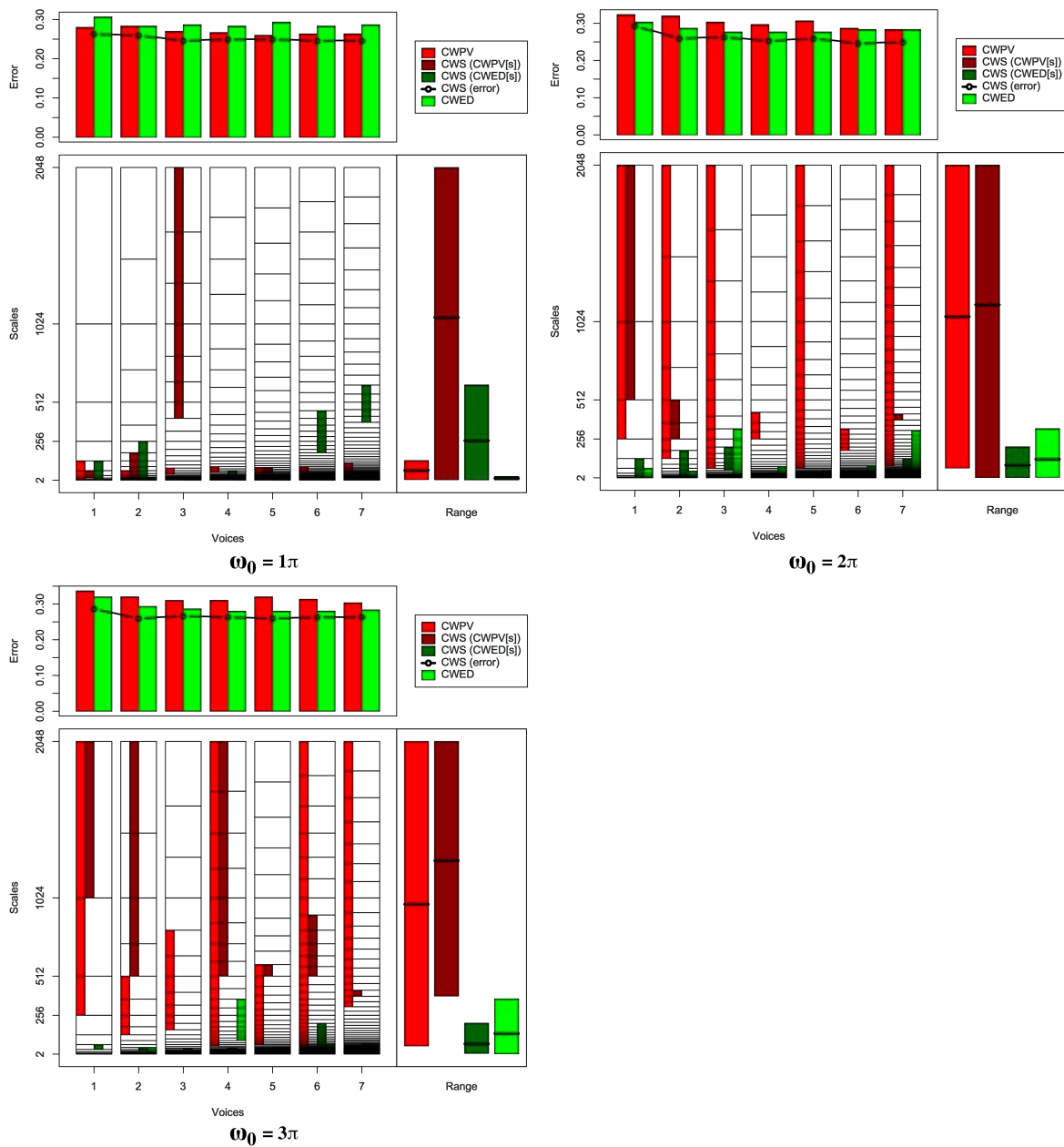


FIGURE B.28: Summary of results for the Haptics classification problem comparing CWS, CWPV, CWED methods using 1-7 voices and three  $\omega_0$  values. A lower CWPV score suggests that the problem is predominantly characterised by FM, whereas a lower CWED implies a predominant AM characteristic. The scale ranges have been translated from scale number to scale value. In the bottom right figure of each figure the average range of scales for all 7 voices are presented for each technique.

TABLE B.28: Summary of results for the Haptics classification problem comparing Ed, DTW, CWS, CWPV, and CWED using 1-7 voices and 3  $\omega_0$  parameters.  $S$  is the scale set(s) associated with the CWS, CWPV and CWED results. The mean values highlighted in bold are the best in model error rate for the problem.

Problem	Technique	Voices	$\omega_0$	$S$	Mean	1	2	3	4	5	6	7	7	9	10
Haptics	Ed				0.323	0.400	0.233	0.333	0.400	0.233	0.267	0.367	0.300	0.367	0.333
Haptics	DTW				0.297	0.333	0.367	0.233	0.300	0.233	0.267	0.367	0.300	0.367	0.200
Haptics	CWS	1	$1\pi$	4:6,3:7	0.263	0.300	0.200	0.300	0.367	0.233	0.133	0.367	0.200	0.267	0.267
Haptics	CWS	1	$2\pi$	9:11,1:7	0.293	0.300	0.267	0.333	0.400	0.200	0.300	0.267	0.267	0.300	0.300
Haptics	CWS	1	$3\pi$	10:11,5:6	0.287	0.300	0.267	0.233	0.300	0.300	0.200	0.267	0.400	0.333	0.267
Haptics	CWS	2	$1\pi$	2:14,1:15	0.260	0.233	0.300	0.233	0.367	0.233	0.100	0.367	0.233	0.233	0.300
Haptics	CWS	2	$2\pi$	15:17,6:14	0.260	0.300	0.267	0.133	0.267	0.200	0.267	0.367	0.233	0.233	0.333
Haptics	CWS	2	$3\pi$	17:21,8:10	0.260	0.333	0.267	0.267	0.333	0.200	0.200	0.300	0.300	0.233	0.167
Haptics	CWS	3	$1\pi$	24:31,1:11	<b>0.247</b>	0.233	0.167	0.200	0.300	0.233	0.233	0.267	0.333	0.300	0.200
Haptics	CWS	3	$2\pi$	1:1,15:21	0.263	0.267	0.333	0.233	0.233	0.233	0.267	0.300	0.233	0.267	0.267
Haptics	CWS	3	$3\pi$	25:25,7:14	0.267	0.300	0.167	0.300	0.333	0.167	0.300	0.267	0.300	0.300	0.233
Haptics	CWS	4	$1\pi$	24:24,4:21	0.250	0.233	0.267	0.267	0.267	0.233	0.233	0.333	0.200	0.233	0.233
Haptics	CWS	4	$2\pi$	34:34,14:18	0.253	0.333	0.267	0.267	0.200	0.267	0.267	0.233	0.300	0.233	0.167
Haptics	CWS	4	$3\pi$	33:41,14:19	0.263	0.233	0.333	0.300	0.300	0.167	0.200	0.367	0.333	0.233	0.167
Haptics	CWS	5	$1\pi$	24:28,1:8	0.250	0.300	0.233	0.233	0.300	0.200	0.167	0.333	0.200	0.233	0.300
Haptics	CWS	5	$2\pi$	41:41,1:20	0.260	0.267	0.233	0.267	0.233	0.200	0.233	0.233	0.333	0.367	0.233
Haptics	CWS	5	$3\pi$	41:42,10:23	0.260	0.333	0.200	0.267	0.300	0.133	0.267	0.233	0.300	0.367	0.200
Haptics	CWS	6	$1\pi$	28:28,40:48	<b>0.247</b>	0.200	0.233	0.333	0.333	0.167	0.233	0.267	0.233	0.233	0.233
Haptics	CWS	6	$2\pi$	49:49,2:24	<b>0.247</b>	0.267	0.233	0.267	0.233	0.200	0.167	0.233	0.300	0.333	0.233
Haptics	CWS	6	$3\pi$	49:54,11:41	0.263	0.333	0.267	0.333	0.267	0.200	0.233	0.300	0.267	0.300	0.133
Haptics	CWS	7	$1\pi$	34:34,54:59	<b>0.247</b>	0.233	0.267	0.267	0.167	0.233	0.267	0.333	0.200	0.267	0.233
Haptics	CWS	7	$2\pi$	54:55,11:43	0.250	0.300	0.300	0.167	0.267	0.267	0.167	0.233	0.300	0.333	0.167
Haptics	CWS	7	$3\pi$	54:55,10:37	0.264	0.367	0.167	0.267	0.367	0.267	0.167	0.300	0.300	0.233	0.200
Haptics	CWPV	1	$1\pi$	2:7	0.280	0.267	0.300	0.267	0.333	0.167	0.233	0.367	0.333	0.267	0.267
Haptics	CWPV	1	$2\pi$	8:11	0.323	0.367	0.400	0.300	0.300	0.233	0.267	0.367	0.300	0.400	0.300
Haptics	CWPV	1	$3\pi$	8:11	0.337	0.400	0.300	0.300	0.300	0.267	0.333	0.367	0.400	0.333	0.367
Haptics	CWPV	2	$1\pi$	3:11	0.283	0.333	0.300	0.300	0.367	0.233	0.200	0.333	0.267	0.233	0.267
Haptics	CWPV	2	$2\pi$	13:21	0.320	0.333	0.333	0.300	0.200	0.300	0.367	0.400	0.400	0.233	0.333
Haptics	CWPV	2	$3\pi$	13:17	0.320	0.300	0.300	0.333	0.400	0.233	0.367	0.367	0.300	0.333	0.267
Haptics	CWPV	3	$1\pi$	14:17	0.270	0.333	0.267	0.267	0.333	0.200	0.200	0.300	0.233	0.233	0.333
Haptics	CWPV	3	$2\pi$	16:31	0.303	0.233	0.333	0.333	0.400	0.300	0.267	0.267	0.267	0.333	0.300
Haptics	CWPV	3	$3\pi$	20:27	0.310	0.300	0.300	0.333	0.300	0.200	0.367	0.367	0.233	0.400	0.300
Haptics	CWPV	4	$1\pi$	20:23	0.267	0.367	0.267	0.267	0.267	0.167	0.167	0.300	0.233	0.267	0.367
Haptics	CWPV	4	$2\pi$	29:32	0.297	0.367	0.333	0.333	0.267	0.300	0.233	0.400	0.300	0.200	0.233
Haptics	CWPV	4	$3\pi$	20:41	0.310	0.333	0.267	0.367	0.367	0.267	0.200	0.367	0.267	0.400	0.267
Haptics	CWPV	5	$1\pi$	24:28	0.260	0.333	0.233	0.233	0.333	0.200	0.167	0.333	0.200	0.233	0.333
Haptics	CWPV	5	$2\pi$	26:51	0.307	0.300	0.233	0.333	0.433	0.267	0.300	0.333	0.233	0.300	0.333
Haptics	CWPV	5	$3\pi$	26:42	0.320	0.333	0.333	0.333	0.400	0.267	0.333	0.300	0.267	0.300	0.333
Haptics	CWPV	6	$1\pi$	29:34	0.263	0.367	0.233	0.200	0.300	0.233	0.167	0.333	0.200	0.267	0.333
Haptics	CWPV	6	$2\pi$	40:45	0.287	0.367	0.300	0.167	0.300	0.200	0.233	0.300	0.333	0.300	0.367
Haptics	CWPV	6	$3\pi$	30:61	0.313	0.300	0.233	0.333	0.367	0.267	0.333	0.333	0.367	0.333	0.267
Haptics	CWPV	7	$1\pi$	34:42	0.263	0.367	0.233	0.200	0.300	0.233	0.167	0.300	0.200	0.267	0.367
Haptics	CWPV	7	$2\pi$	38:71	0.283	0.300	0.300	0.267	0.333	0.200	0.267	0.300	0.267	0.300	0.300
Haptics	CWPV	7	$3\pi$	52:71	0.303	0.333	0.400	0.200	0.300	0.400	0.267	0.400	0.300	0.233	0.200
Haptics	CWED	1	$1\pi$	1:3	0.307	0.333	0.300	0.400	0.300	0.300	0.233	0.333	0.300	0.300	0.267
Haptics	CWED	1	$2\pi$	2:6	0.303	0.200	0.333	0.367	0.367	0.300	0.233	0.400	0.333	0.300	0.200
Haptics	CWED	1	$3\pi$	1:2	0.320	0.333	0.367	0.333	0.300	0.400	0.333	0.300	0.333	0.333	0.167
Haptics	CWED	2	$1\pi$	1:8	0.283	0.300	0.300	0.300	0.367	0.200	0.233	0.333	0.300	0.367	0.133
Haptics	CWED	2	$2\pi$	3:10	0.287	0.333	0.267	0.300	0.400	0.300	0.300	0.300	0.267	0.300	0.100
Haptics	CWED	2	$3\pi$	3:10	0.293	0.333	0.333	0.233	0.300	0.200	0.300	0.367	0.333	0.300	0.233
Haptics	CWED	3	$1\pi$	1:11	0.287	0.267	0.267	0.333	0.367	0.233	0.233	0.300	0.333	0.367	0.167
Haptics	CWED	3	$2\pi$	10:23	0.277	0.300	0.267	0.333	0.233	0.267	0.233	0.267	0.267	0.333	0.267
Haptics	CWED	3	$3\pi$	5:13	0.287	0.333	0.233	0.300	0.333	0.233	0.267	0.267	0.333	0.333	0.233
Haptics	CWED	4	$1\pi$	1:15	0.283	0.300	0.300	0.300	0.367	0.200	0.233	0.333	0.300	0.367	0.133
Haptics	CWED	4	$2\pi$	3:22	0.277	0.267	0.200	0.333	0.300	0.300	0.200	0.267	0.267	0.333	0.300
Haptics	CWED	4	$3\pi$	23:31	0.280	0.367	0.400	0.333	0.200	0.233	0.233	0.333	0.300	0.233	0.167
Haptics	CWED	5	$1\pi$	1:19	0.293	0.267	0.267	0.333	0.300	0.300	0.200	0.333	0.367	0.367	0.200
Haptics	CWED	5	$2\pi$	13:24	0.277	0.367	0.267	0.200	0.267	0.300	0.233	0.333	0.267	0.300	0.233
Haptics	CWED	5	$3\pi$	7:23	0.280	0.333	0.267	0.233	0.267	0.233	0.233	0.267	0.333	0.400	0.233
Haptics	CWED	6	$1\pi$	1:22	0.283	0.267	0.300	0.333	0.367	0.200	0.233	0.333	0.300	0.367	0.133
Haptics	CWED	6	$2\pi$	6:33	0.283	0.267	0.267	0.267	0.300	0.300	0.200	0.300	0.267	0.333	0.333
Haptics	CWED	6	$3\pi$	10:32	0.280	0.400	0.267	0.300	0.400	0.267	0.233	0.300	0.267	0.267	0.100
Haptics	CWED	7	$1\pi$	6:25	0.287	0.300	0.233	0.233	0.400	0.267	0.200	0.367	0.333	0.333	0.200
Haptics	CWED	7	$2\pi$	5:52	0.283	0.267	0.233	0.333	0.300	0.333	0.200	0.267	0.267	0.333	0.300
Haptics	CWED	7	$3\pi$	14:37	0.283	0.367	0.267	0.233	0.400	0.267	0.267	0.333	0.300	0.267	0.133

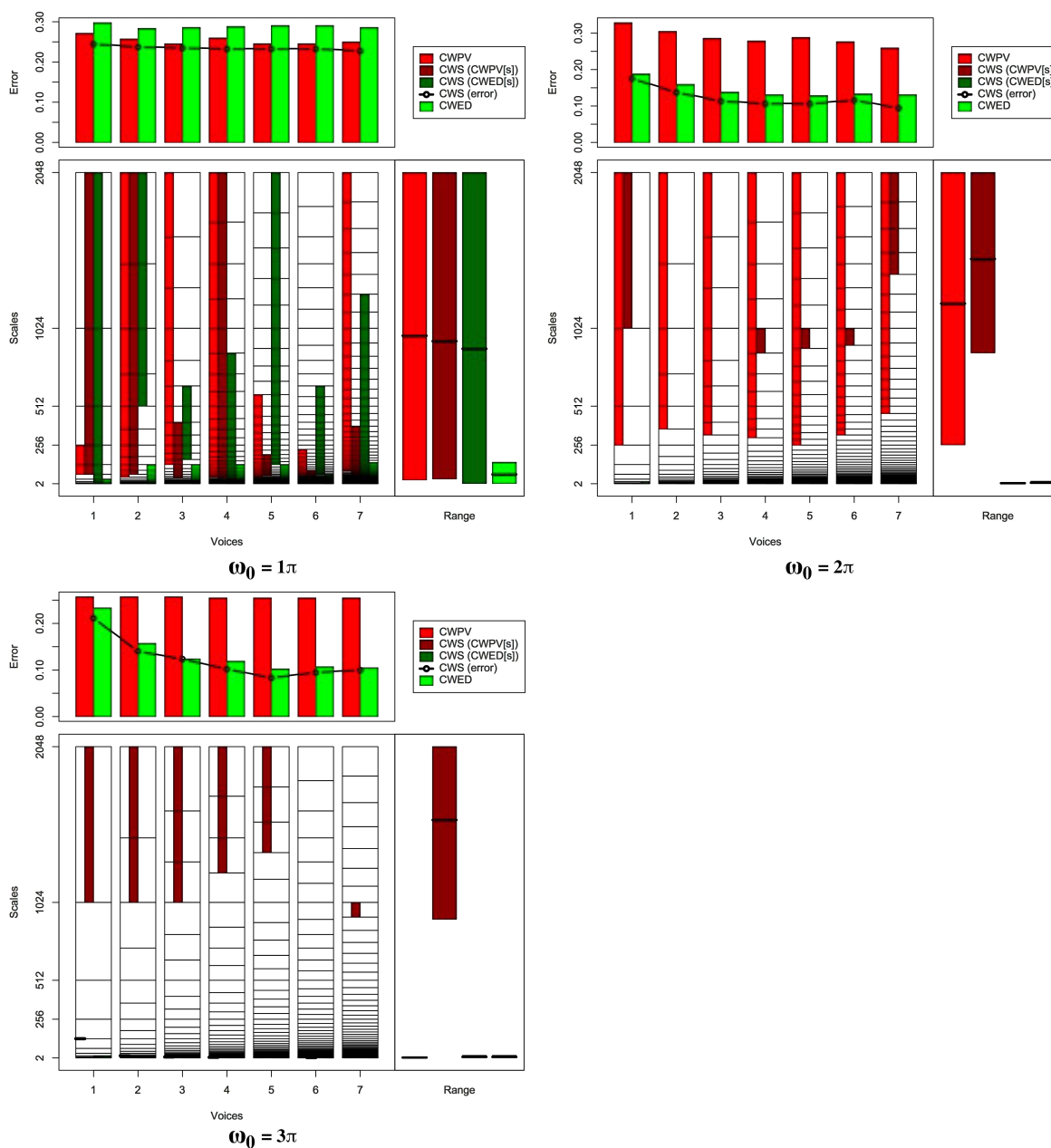


FIGURE B.29: Summary of results for the Inline Skate classification problem comparing CWS, CWPV, CWED methods using 1-7 voices and three  $\omega_0$  values. A lower CWPV score suggests that the problem is predominantly characterised by FM, whereas a lower CWED implies a predominant AM characteristic. The scale ranges have been translated from scale number to scale value. In the bottom right figure of each figure the average range of scales for all 7 voices are presented for each technique.

TABLE B.29: Summary of results for the Inline Skate classification problem comparing Ed, DTW, CWS, CWPV, and CWED using 1-7 voices and 3  $\omega_0$  parameters.  $S$  is the scale set(s) associated with the CWS, CWPV and CWED results. The mean values highlighted in bold are the best in model error rate for the problem.

Problem	Technique	Voices	$\omega_0$	$S$	Mean	1	2	3	4	5	6	7	7	9	10
Inline Skate	Ed				0.260	0.238	0.262	0.238	0.286	0.238	0.238	0.286	0.286	0.190	0.333
Inline Skate	DTW				0.231	0.333	0.167	0.310	0.214	0.143	0.190	0.167	0.214	0.262	0.310
Inline Skate	CWS	1	1 $\pi$	6:11,1:11	0.245	0.310	0.214	0.238	0.214	0.262	0.167	0.190	0.310	0.262	0.286
Inline Skate	CWS	1	2 $\pi$	10:11,1:2	0.176	0.214	0.190	0.214	0.143	0.214	0.214	0.143	0.167	0.119	0.143
Inline Skate	CWS	1	3 $\pi$	10:11,1:4	0.212	0.238	0.214	0.286	0.143	0.190	0.238	0.214	0.190	0.190	0.214
Inline Skate	CWS	2	1 $\pi$	11:21,17:21	0.238	0.286	0.214	0.190	0.238	0.286	0.190	0.214	0.286	0.238	0.238
Inline Skate	CWS	2	2 $\pi$	19:19,1:5	0.138	0.119	0.095	0.143	0.095	0.143	0.167	0.119	0.167	0.143	0.190
Inline Skate	CWS	2	3 $\pi$	19:21,1:5	0.141	0.143	0.167	0.167	0.071	0.119	0.143	0.119	0.119	0.190	0.167
Inline Skate	CWS	3	1 $\pi$	14:24,20:26	0.236	0.310	0.190	0.214	0.190	0.262	0.190	0.262	0.262	0.214	0.262
Inline Skate	CWS	3	2 $\pi$	28:28,1:3	0.114	0.143	0.119	0.119	0.119	0.143	0.095	0.071	0.095	0.071	0.167
Inline Skate	CWS	3	3 $\pi$	28:31,1:5	0.124	0.071	0.119	0.238	0.071	0.095	0.119	0.095	0.095	0.119	0.214
Inline Skate	CWS	4	1 $\pi$	18:41,1:36	0.233	0.310	0.214	0.238	0.190	0.262	0.190	0.238	0.190	0.214	0.286
Inline Skate	CWS	4	2 $\pi$	36:37,1:3	0.107	0.143	0.095	0.167	0.119	0.048	0.095	0.095	0.119	0.071	0.119
Inline Skate	CWS	4	3 $\pi$	38:41,1:6	0.102	0.119	0.095	0.190	0.071	0.119	0.095	0.095	0.071	0.048	0.119
Inline Skate	CWS	5	1 $\pi$	25:34,31:51	0.233	0.262	0.214	0.190	0.214	0.310	0.190	0.190	0.262	0.238	0.262
Inline Skate	CWS	5	2 $\pi$	45:46,1:4	0.107	0.119	0.095	0.190	0.071	0.119	0.095	0.071	0.095	0.071	0.143
Inline Skate	CWS	5	3 $\pi$	48:51,1:7	<b>0.083</b>	0.143	0.095	0.143	0.048	0.071	0.048	0.000	0.048	0.048	0.190
Inline Skate	CWS	6	1 $\pi$	25:34,31:51	0.233	0.262	0.214	0.190	0.214	0.310	0.190	0.190	0.262	0.238	0.262
Inline Skate	CWS	6	2 $\pi$	54:55,1:5	0.117	0.095	0.167	0.167	0.143	0.143	0.095	0.071	0.095	0.071	0.119
Inline Skate	CWS	6	3 $\pi$	54:54,4:8	0.095	0.119	0.071	0.167	0.095	0.143	0.048	0.095	0.071	0.024	0.119
Inline Skate	CWS	7	1 $\pi$	31:54,1:66	0.228	0.286	0.214	0.214	0.190	0.262	0.190	0.238	0.190	0.238	0.262
Inline Skate	CWS	7	2 $\pi$	67:71,1:5	0.095	0.119	0.048	0.143	0.071	0.143	0.119	0.071	0.071	0.048	0.119
Inline Skate	CWS	7	3 $\pi$	63:64,5:10	0.100	0.071	0.095	0.238	0.048	0.119	0.071	0.048	0.095	0.048	0.167
Inline Skate	CWPV	1	1 $\pi$	6:8	0.271	0.357	0.262	0.214	0.214	0.333	0.190	0.238	0.310	0.310	0.286
Inline Skate	CWPV	1	2 $\pi$	8:11	0.329	0.333	0.357	0.310	0.310	0.381	0.286	0.310	0.286	0.357	0.357
Inline Skate	CWPV	1	3 $\pi$	1:1	0.257	0.333	0.262	0.286	0.214	0.310	0.214	0.214	0.190	0.238	0.310
Inline Skate	CWPV	2	1 $\pi$	10:21	0.257	0.310	0.214	0.214	0.190	0.310	0.262	0.238	0.310	0.214	0.310
Inline Skate	CWPV	2	2 $\pi$	16:21	0.305	0.286	0.262	0.333	0.214	0.357	0.286	0.333	0.310	0.310	0.357
Inline Skate	CWPV	2	3 $\pi$	1:1	0.257	0.333	0.262	0.286	0.214	0.310	0.214	0.214	0.190	0.238	0.310
Inline Skate	CWPV	3	1 $\pi$	19:31	0.245	0.286	0.238	0.238	0.190	0.262	0.262	0.262	0.262	0.214	0.238
Inline Skate	CWPV	3	2 $\pi$	23:31	0.286	0.262	0.238	0.310	0.262	0.333	0.262	0.357	0.262	0.262	0.310
Inline Skate	CWPV	3	3 $\pi$	1:1	0.257	0.333	0.262	0.286	0.214	0.310	0.214	0.214	0.190	0.238	0.310
Inline Skate	CWPV	4	1 $\pi$	19:41	0.260	0.310	0.214	0.214	0.167	0.310	0.286	0.238	0.310	0.238	0.310
Inline Skate	CWPV	4	2 $\pi$	30:41	0.279	0.286	0.262	0.333	0.238	0.333	0.286	0.310	0.238	0.238	0.262
Inline Skate	CWPV	4	3 $\pi$	2:2	0.255	0.310	0.262	0.262	0.214	0.310	0.214	0.190	0.214	0.286	0.286
Inline Skate	CWPV	5	1 $\pi$	23:42	0.245	0.286	0.167	0.238	0.143	0.286	0.238	0.238	0.310	0.238	0.310
Inline Skate	CWPV	5	2 $\pi$	36:51	0.288	0.238	0.286	0.286	0.238	0.357	0.286	0.310	0.238	0.310	0.333
Inline Skate	CWPV	5	3 $\pi$	1:3	0.255	0.333	0.262	0.262	0.167	0.310	0.214	0.214	0.238	0.238	0.310
Inline Skate	CWPV	6	1 $\pi$	23:42	0.245	0.286	0.167	0.238	0.143	0.286	0.238	0.238	0.310	0.238	0.310
Inline Skate	CWPV	6	2 $\pi$	45:61	0.276	0.262	0.286	0.286	0.167	0.262	0.310	0.310	0.333	0.238	0.310
Inline Skate	CWPV	6	3 $\pi$	2:3	0.255	0.310	0.262	0.262	0.214	0.310	0.214	0.190	0.214	0.286	0.286
Inline Skate	CWPV	7	1 $\pi$	39:71	0.250	0.286	0.190	0.286	0.214	0.262	0.238	0.262	0.286	0.238	0.238
Inline Skate	CWPV	7	2 $\pi$	56:71	0.259	0.286	0.214	0.357	0.238	0.214	0.262	0.190	0.238	0.214	0.381
Inline Skate	CWPV	7	3 $\pi$	2:3	0.255	0.310	0.262	0.262	0.214	0.310	0.214	0.190	0.214	0.286	0.286
Inline Skate	CWED	1	1 $\pi$	1:5	0.298	0.262	0.262	0.333	0.262	0.310	0.310	0.357	0.381	0.286	0.214
Inline Skate	CWED	1	2 $\pi$	1:4	0.188	0.238	0.238	0.238	0.214	0.214	0.167	0.143	0.167	0.119	0.143
Inline Skate	CWED	1	3 $\pi$	1:4	0.233	0.238	0.238	0.262	0.190	0.262	0.262	0.262	0.167	0.190	0.262
Inline Skate	CWED	2	1 $\pi$	1:13	0.284	0.310	0.286	0.381	0.238	0.310	0.310	0.214	0.262	0.238	0.286
Inline Skate	CWED	2	2 $\pi$	1:4	0.159	0.190	0.143	0.167	0.143	0.095	0.167	0.119	0.190	0.190	0.190
Inline Skate	CWED	2	3 $\pi$	1:4	0.157	0.167	0.167	0.238	0.095	0.143	0.143	0.143	0.143	0.190	0.143
Inline Skate	CWED	3	1 $\pi$	1:19	0.286	0.286	0.286	0.381	0.214	0.310	0.310	0.238	0.238	0.262	0.333
Inline Skate	CWED	3	2 $\pi$	1:3	0.138	0.190	0.095	0.167	0.143	0.143	0.167	0.071	0.119	0.119	0.167
Inline Skate	CWED	3	3 $\pi$	1:8	0.124	0.119	0.119	0.190	0.119	0.119	0.167	0.119	0.095	0.071	0.119
Inline Skate	CWED	4	1 $\pi$	1:25	0.288	0.310	0.286	0.357	0.214	0.310	0.310	0.238	0.286	0.286	0.286
Inline Skate	CWED	4	2 $\pi$	1:3	0.131	0.095	0.119	0.190	0.167	0.143	0.143	0.119	0.119	0.095	0.119
Inline Skate	CWED	4	3 $\pi$	1:6	0.119	0.143	0.143	0.167	0.143	0.119	0.119	0.095	0.095	0.071	0.095
Inline Skate	CWED	5	1 $\pi$	1:31	0.291	0.310	0.286	0.357	0.214	0.310	0.333	0.238	0.262	0.286	0.310
Inline Skate	CWED	5	2 $\pi$	1:4	0.129	0.119	0.095	0.190	0.143	0.143	0.143	0.095	0.119	0.119	0.119
Inline Skate	CWED	5	3 $\pi$	1:8	0.102	0.143	0.071	0.143	0.167	0.119	0.071	0.095	0.071	0.048	0.095
Inline Skate	CWED	6	1 $\pi$	1:31	0.291	0.310	0.286	0.357	0.214	0.310	0.333	0.238	0.262	0.286	0.310
Inline Skate	CWED	6	2 $\pi$	1:4	0.133	0.071	0.167	0.214	0.143	0.143	0.143	0.119	0.119	0.095	0.119
Inline Skate	CWED	6	3 $\pi$	1:8	0.107	0.119	0.071	0.190	0.119	0.167	0.071	0.095	0.071	0.048	0.119
Inline Skate	CWED	7	1 $\pi$	1:44	0.286	0.310	0.357	0.310	0.238	0.333	0.310	0.214	0.262	0.238	0.286
Inline Skate	CWED	7	2 $\pi$	1:5	0.131	0.071	0.095	0.190	0.167	0.143	0.143	0.119	0.119	0.119	0.143
Inline Skate	CWED	7	3 $\pi$	1:11	0.105	0.143	0.119	0.119	0.095	0.119	0.095	0.095	0.071	0.048	0.143

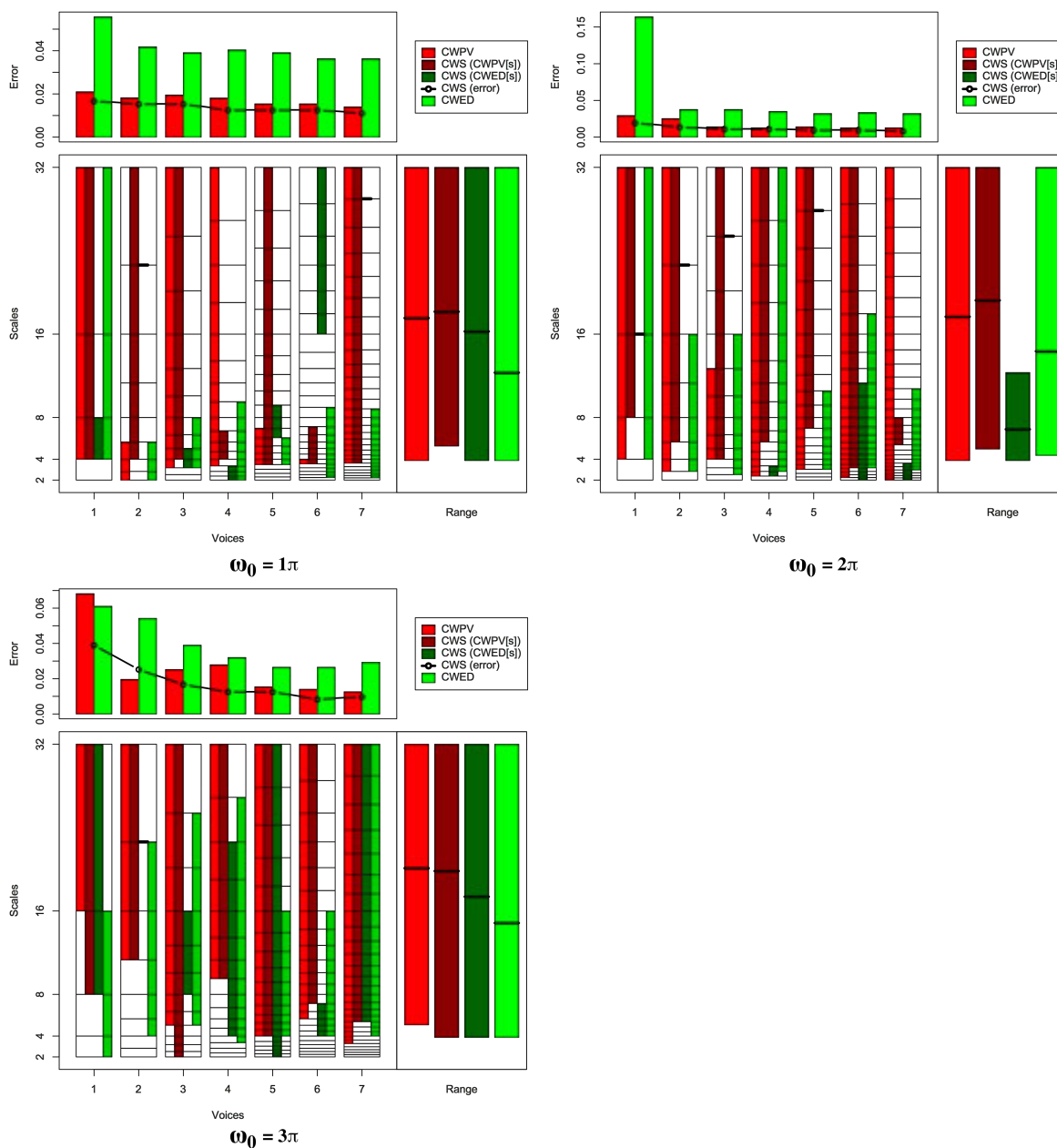


FIGURE B.30: Summary of results for the Italy Power Demand classification problem comparing CWS, CWPV, CWED methods using 1-7 voices and three  $\omega_0$  values. A lower CWPV score suggests that the problem is predominantly characterised by FM, whereas a lower CWED implies a predominant AM characteristic. The scale ranges have been translated from scale number to scale value. In the bottom right figure of each figure the average range of scales for all 7 voices are presented for each technique.

TABLE B.30: Summary of results for the Italy Power Demand classification problem comparing Ed, DTW, CWS, CWPV, and CWED using 1-7 voices and 3  $\omega_0$  parameters.  $S$  is the scale set(s) associated with the CWS, CWPV and CWED results. The mean values highlighted in bold are the best in model error rate for the problem.

Problem	Technique	Voices	$\omega_0$	$S$	Mean	1	2	3	4	5	6	7	7	9	10
Italy Power Demand	Ed				0.015	0.028	0.014	0.014	0.000	0.014	0.042	0.000	0.028	0.000	0.014
Italy Power Demand	DTW				0.021	0.028	0.042	0.042	0.000	0.028	0.014	0.000	0.028	0.028	0.000
Italy Power Demand	CWS	1	$1\pi$	2:5,2:3	0.017	0.028	0.000	0.014	0.014	0.014	0.042	0.000	0.014	0.028	0.014
Italy Power Demand	CWS	1	$2\pi$	3:5,2:2	0.020	0.014	0.014	0.014	0.000	0.014	0.056	0.014	0.028	0.042	0.000
Italy Power Demand	CWS	1	$3\pi$	3:5,3:5	0.039	0.056	0.042	0.042	0.028	0.014	0.083	0.014	0.056	0.028	0.028
Italy Power Demand	CWS	2	$1\pi$	3:9,2:2	0.015	0.028	0.000	0.014	0.014	0.028	0.042	0.000	0.014	0.014	0.000
Italy Power Demand	CWS	2	$2\pi$	4:9,1:1	0.014	0.000	0.000	0.028	0.014	0.000	0.042	0.000	0.014	0.028	0.014
Italy Power Demand	CWS	2	$3\pi$	6:9,1:1	0.025	0.014	0.000	0.014	0.042	0.042	0.028	0.042	0.028	0.014	0.014
Italy Power Demand	CWS	3	$1\pi$	4:13,3:5	0.015	0.028	0.000	0.014	0.014	0.014	0.042	0.000	0.014	0.028	0.000
Italy Power Demand	CWS	3	$2\pi$	4:13,7:7	0.011	0.014	0.000	0.014	0.014	0.000	0.028	0.000	0.014	0.028	0.000
Italy Power Demand	CWS	3	$3\pi$	1:13,7:10	0.017	0.014	0.000	0.028	0.000	0.042	0.042	0.014	0.028	0.000	0.000
Italy Power Demand	CWS	4	$1\pi$	5:8,1:4	0.013	0.028	0.000	0.014	0.000	0.014	0.042	0.000	0.014	0.014	0.000
Italy Power Demand	CWS	4	$2\pi$	7:17,2:4	0.011	0.000	0.000	0.028	0.000	0.014	0.042	0.000	0.000	0.014	0.014
Italy Power Demand	CWS	4	$3\pi$	10:17,5:15	0.013	0.028	0.014	0.028	0.000	0.000	0.042	0.000	0.014	0.000	0.000
Italy Power Demand	CWS	5	$1\pi$	5:21,9:12	0.013	0.028	0.000	0.000	0.014	0.014	0.028	0.000	0.014	0.028	0.000
Italy Power Demand	CWS	5	$2\pi$	10:21,1:1	0.010	0.014	0.000	0.014	0.000	0.014	0.042	0.000	0.000	0.000	0.014
Italy Power Demand	CWS	5	$3\pi$	6:21,1:21	0.013	0.014	0.000	0.028	0.000	0.014	0.028	0.014	0.028	0.000	0.000
Italy Power Demand	CWS	6	$1\pi$	6:12,19:25	0.013	0.028	0.000	0.014	0.000	0.014	0.042	0.000	0.014	0.014	0.000
Italy Power Demand	CWS	6	$2\pi$	5:25,1:16	0.010	0.028	0.000	0.014	0.014	0.000	0.028	0.000	0.014	0.000	0.000
Italy Power Demand	CWS	6	$3\pi$	12:25,7:12	<b>0.008</b>	0.014	0.000	0.000	0.014	0.014	0.028	0.000	0.014	0.000	0.000
Italy Power Demand	CWS	7	$1\pi$	7:29,6:6	0.011	0.028	0.000	0.014	0.000	0.028	0.028	0.000	0.014	0.000	0.000
Italy Power Demand	CWS	7	$2\pi$	11:15,1:7	<b>0.008</b>	0.000	0.000	0.014	0.000	0.000	0.042	0.000	0.014	0.000	0.014
Italy Power Demand	CWS	7	$3\pi$	11:29,11:29	0.010	0.028	0.000	0.000	0.000	0.000	0.028	0.000	0.028	0.000	0.014
Italy Power Demand	CWPV	1	$1\pi$	2:5	0.021	0.028	0.000	0.014	0.014	0.028	0.056	0.014	0.028	0.028	0.000
Italy Power Demand	CWPV	1	$2\pi$	2:5	0.029	0.014	0.028	0.056	0.042	0.028	0.056	0.014	0.028	0.014	0.014
Italy Power Demand	CWPV	1	$3\pi$	4:5	0.068	0.056	0.056	0.042	0.056	0.083	0.097	0.056	0.097	0.111	0.028
Italy Power Demand	CWPV	2	$1\pi$	1:4	0.018	0.028	0.000	0.014	0.000	0.028	0.042	0.014	0.042	0.014	0.000
Italy Power Demand	CWPV	2	$2\pi$	2:9	0.025	0.028	0.028	0.042	0.000	0.056	0.042	0.000	0.042	0.014	0.000
Italy Power Demand	CWPV	2	$3\pi$	6:9	0.020	0.014	0.014	0.028	0.014	0.014	0.042	0.000	0.056	0.014	0.000
Italy Power Demand	CWPV	3	$1\pi$	3:13	0.020	0.028	0.000	0.014	0.014	0.028	0.069	0.014	0.014	0.014	0.000
Italy Power Demand	CWPV	3	$2\pi$	4:9	0.014	0.014	0.000	0.028	0.028	0.000	0.028	0.000	0.028	0.014	0.000
Italy Power Demand	CWPV	3	$3\pi$	5:13	0.025	0.028	0.056	0.028	0.056	0.014	0.056	0.000	0.014	0.000	0.000
Italy Power Demand	CWPV	4	$1\pi$	4:17	0.018	0.028	0.000	0.014	0.014	0.028	0.069	0.000	0.014	0.014	0.000
Italy Power Demand	CWPV	4	$2\pi$	2:17	0.013	0.028	0.000	0.028	0.014	0.014	0.028	0.000	0.014	0.000	0.000
Italy Power Demand	CWPV	4	$3\pi$	10:17	0.028	0.014	0.000	0.014	0.042	0.028	0.069	0.014	0.056	0.028	0.014
Italy Power Demand	CWPV	5	$1\pi$	5:10	0.015	0.028	0.000	0.000	0.014	0.028	0.056	0.000	0.014	0.014	0.000
Italy Power Demand	CWPV	5	$2\pi$	4:21	0.014	0.028	0.014	0.028	0.014	0.000	0.042	0.000	0.014	0.000	0.000
Italy Power Demand	CWPV	5	$3\pi$	6:21	0.015	0.014	0.014	0.042	0.014	0.000	0.028	0.014	0.028	0.000	0.000
Italy Power Demand	CWPV	6	$1\pi$	6:7	0.015	0.028	0.000	0.000	0.000	0.014	0.056	0.014	0.014	0.028	0.000
Italy Power Demand	CWPV	6	$2\pi$	2:25	0.013	0.028	0.000	0.014	0.014	0.014	0.042	0.000	0.014	0.000	0.000
Italy Power Demand	CWPV	6	$3\pi$	10:25	0.014	0.028	0.000	0.014	0.028	0.000	0.042	0.000	0.014	0.014	0.000
Italy Power Demand	CWPV	7	$1\pi$	7:29	0.014	0.028	0.000	0.014	0.000	0.028	0.028	0.014	0.014	0.014	0.000
Italy Power Demand	CWPV	7	$2\pi$	1:29	0.013	0.028	0.000	0.014	0.000	0.028	0.042	0.000	0.014	0.000	0.000
Italy Power Demand	CWPV	7	$3\pi$	6:29	0.013	0.028	0.000	0.000	0.014	0.028	0.028	0.014	0.014	0.000	0.000
Italy Power Demand	CWED	1	$1\pi$	2:5	0.056	0.042	0.083	0.069	0.056	0.056	0.083	0.042	0.056	0.028	0.042
Italy Power Demand	CWED	1	$2\pi$	2:5	0.164	0.167	0.208	0.222	0.153	0.139	0.139	0.125	0.194	0.167	0.125
Italy Power Demand	CWED	1	$3\pi$	1:4	0.061	0.028	0.069	0.056	0.097	0.069	0.097	0.069	0.056	0.028	0.042
Italy Power Demand	CWED	2	$1\pi$	1:4	0.042	0.069	0.028	0.028	0.056	0.042	0.069	0.028	0.042	0.028	0.028
Italy Power Demand	CWED	2	$2\pi$	2:7	0.038	0.042	0.097	0.056	0.014	0.014	0.042	0.014	0.069	0.028	0.000
Italy Power Demand	CWED	2	$3\pi$	3:8	0.054	0.028	0.056	0.111	0.069	0.042	0.097	0.028	0.069	0.028	0.014
Italy Power Demand	CWED	3	$1\pi$	3:7	0.039	0.014	0.042	0.056	0.056	0.042	0.069	0.042	0.042	0.014	0.014
Italy Power Demand	CWED	3	$2\pi$	2:10	0.038	0.042	0.042	0.056	0.014	0.028	0.069	0.014	0.069	0.042	0.000
Italy Power Demand	CWED	3	$3\pi$	5:12	0.039	0.042	0.042	0.097	0.014	0.014	0.042	0.028	0.083	0.028	0.000
Italy Power Demand	CWED	4	$1\pi$	1:10	0.040	0.069	0.028	0.014	0.056	0.028	0.083	0.056	0.014	0.028	0.028
Italy Power Demand	CWED	4	$2\pi$	3:17	0.035	0.042	0.056	0.056	0.000	0.028	0.069	0.014	0.056	0.028	0.000
Italy Power Demand	CWED	4	$3\pi$	4:16	0.032	0.028	0.069	0.042	0.014	0.014	0.056	0.014	0.069	0.014	0.000
Italy Power Demand	CWED	5	$1\pi$	5:9	0.039	0.014	0.042	0.056	0.028	0.028	0.083	0.028	0.056	0.028	0.028
Italy Power Demand	CWED	5	$2\pi$	4:13	0.032	0.042	0.042	0.028	0.000	0.028	0.083	0.014	0.056	0.028	0.000
Italy Power Demand	CWED	5	$3\pi$	6:16	0.027	0.028	0.056	0.028	0.014	0.000	0.069	0.014	0.028	0.028	0.000
Italy Power Demand	CWED	6	$1\pi$	2:14	0.036	0.056	0.028	0.014	0.042	0.042	0.083	0.042	0.028	0.014	0.014
Italy Power Demand	CWED	6	$2\pi$	5:20	0.034	0.042	0.042	0.056	0.000	0.028	0.069	0.014	0.056	0.028	0.000
Italy Power Demand	CWED	6	$3\pi$	7:19	0.027	0.028	0.069	0.042	0.014	0.000	0.056	0.014	0.028	0.014	0.000
Italy Power Demand	CWED	7	$1\pi$	2:16	0.036	0.056	0.028	0.014	0.042	0.042	0.083	0.042	0.028	0.014	0.014
Italy Power Demand	CWED	7	$2\pi$	5:18	0.032	0.042	0.042	0.042	0.000	0.014	0.083	0.014	0.056	0.028	0.000
Italy Power Demand	CWED	7	$3\pi$	8:29	0.029	0.028	0.056	0.042	0.000	0.000	0.069	0.000	0.056	0.028	0.014

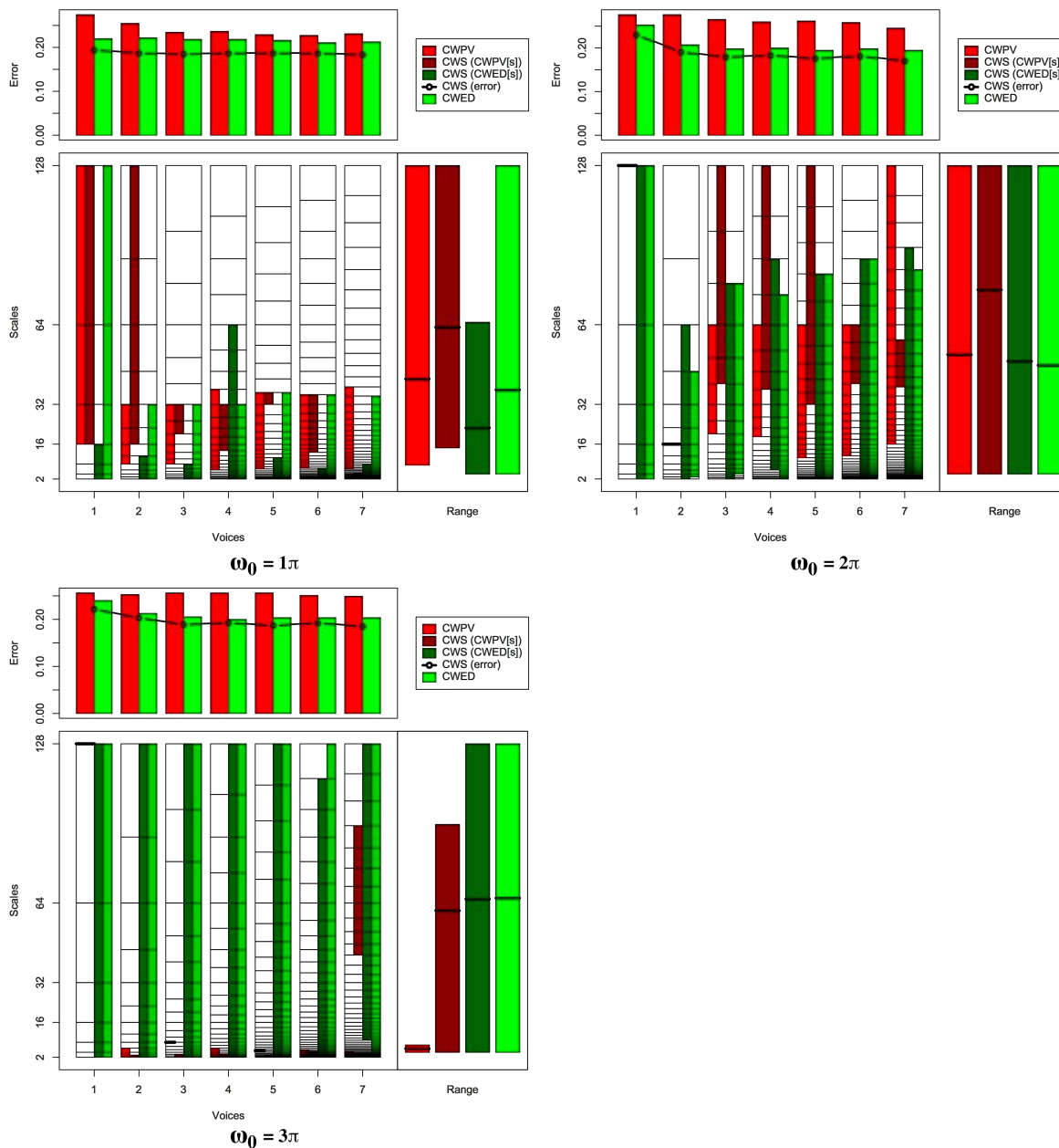


FIGURE B.31: Summary of results for the Medical Images classification problem comparing CWS, CWPV, CWED methods using 1-7 voices and three  $\omega_0$  values. A lower CWPV score suggests that the problem is predominantly characterised by FM, whereas a lower CWED implies a predominant AM characteristic. The scale ranges have been translated from scale number to scale value. In the bottom right figure of each figure the average range of scales for all 7 voices are presented for each technique.

TABLE B.31: Summary of results for the Medical Images classification problem comparing Ed, DTW, CWS, CWPV, and CWED using 1-7 voices and 3  $\omega_0$  parameters.  $S$  is the scale set(s) associated with the CWS, CWPV and CWED results. The mean values highlighted in bold are the best in model error rate for the problem.

Problem	Technique	Voices	$\omega_0$	$S$	Mean	1	2	3	4	5	6	7	7	9	10
Medical Images	Ed				<b>0.145</b>	0.145	0.091	0.127	0.164	0.091	0.109	0.164	0.145	0.200	0.218
Medical Images	DTW				<b>0.133</b>	0.109	0.145	0.073	0.164	0.073	0.127	0.182	0.127	0.127	0.200
Medical Images	CWS	1	$1\pi$	4:7,1:4	0.195	0.218	0.200	0.200	0.218	0.109	0.309	0.200	0.200	0.164	0.127
Medical Images	CWS	1	$2\pi$	1:1,1:7	0.231	0.218	0.236	0.291	0.218	0.164	0.327	0.236	0.182	0.200	0.236
Medical Images	CWS	1	$3\pi$	5:5,1:7	0.222	0.218	0.218	0.273	0.182	0.236	0.309	0.218	0.218	0.182	0.164
Medical Images	CWS	2	$1\pi$	7:13,1:6	0.187	0.200	0.164	0.182	0.218	0.109	0.291	0.218	0.182	0.182	0.127
Medical Images	CWS	2	$2\pi$	1:1,1:11	0.191	0.218	0.164	0.164	0.164	0.109	0.255	0.255	0.164	0.182	0.236
Medical Images	CWS	2	$3\pi$	1:2,1:13	0.204	0.182	0.236	0.218	0.145	0.109	0.327	0.182	0.218	0.200	0.218
Medical Images	CWS	3	$1\pi$	11:13,1:7	0.186	0.182	0.127	0.255	0.255	0.109	0.236	0.182	0.182	0.200	0.127
Medical Images	CWS	3	$2\pi$	14:19,1:17	0.180	0.164	0.145	0.164	0.200	0.109	0.200	0.236	0.164	0.236	0.182
Medical Images	CWS	3	$3\pi$	1:3,1:19	0.189	0.182	0.218	0.182	0.127	0.091	0.291	0.200	0.164	0.182	0.255
Medical Images	CWS	4	$1\pi$	12:17,1:21	0.187	0.236	0.182	0.127	0.218	0.127	0.236	0.255	0.200	0.164	0.127
Medical Images	CWS	4	$2\pi$	18:25,7:23	0.184	0.200	0.145	0.182	0.164	0.145	0.236	0.218	0.164	0.236	0.145
Medical Images	CWS	4	$3\pi$	1:4,1:25	0.193	0.182	0.182	0.200	0.164	0.091	0.255	0.236	0.164	0.200	0.255
Medical Images	CWS	5	$1\pi$	21:22,1:13	0.187	0.091	0.164	0.255	0.218	0.164	0.273	0.200	0.200	0.145	0.164
Medical Images	CWS	5	$2\pi$	21:31,1:28	0.176	0.182	0.182	0.164	0.127	0.127	0.182	0.218	0.145	0.255	0.182
Medical Images	CWS	5	$3\pi$	1:4,1:31	0.187	0.182	0.200	0.182	0.127	0.091	0.291	0.218	0.164	0.200	0.218
Medical Images	CWS	6	$1\pi$	17:26,1:11	0.187	0.182	0.218	0.145	0.218	0.145	0.218	0.218	0.218	0.200	0.109
Medical Images	CWS	6	$2\pi$	27:31,1:34	0.182	0.127	0.200	0.164	0.182	0.127	0.200	0.236	0.164	0.236	0.182
Medical Images	CWS	6	$3\pi$	6:6,1:36	0.193	0.218	0.200	0.218	0.145	0.109	0.236	0.218	0.145	0.182	0.255
Medical Images	CWS	7	$1\pi$	29:29,1:15	0.184	0.109	0.164	0.236	0.200	0.127	0.255	0.255	0.164	0.164	0.164
Medical Images	CWS	7	$2\pi$	31:35,1:40	0.171	0.200	0.164	0.182	0.182	0.109	0.164	0.236	0.145	0.164	0.164
Medical Images	CWS	7	$3\pi$	32:40,16:43	0.185	0.236	0.218	0.145	0.145	0.127	0.200	0.218	0.182	0.182	0.200
Medical Images	CWPV	1	$1\pi$	4:7	0.275	0.273	0.273	0.309	0.273	0.200	0.382	0.327	0.291	0.218	0.200
Medical Images	CWPV	1	$2\pi$	1:1	0.276	0.345	0.218	0.291	0.164	0.200	0.309	0.255	0.327	0.382	0.273
Medical Images	CWPV	1	$3\pi$	2:2	0.256	0.291	0.200	0.236	0.291	0.236	0.255	0.182	0.291	0.236	0.345
Medical Images	CWPV	2	$1\pi$	5:9	0.255	0.255	0.273	0.309	0.273	0.182	0.309	0.255	0.291	0.255	0.145
Medical Images	CWPV	2	$2\pi$	1:1	0.276	0.345	0.218	0.291	0.164	0.200	0.309	0.255	0.327	0.382	0.273
Medical Images	CWPV	2	$3\pi$	1:4	0.253	0.327	0.236	0.255	0.273	0.109	0.218	0.218	0.291	0.291	0.309
Medical Images	CWPV	3	$1\pi$	7:13	0.234	0.218	0.236	0.236	0.218	0.218	0.327	0.255	0.236	0.218	0.182
Medical Images	CWPV	3	$2\pi$	11:16	0.265	0.345	0.255	0.364	0.218	0.182	0.327	0.255	0.327	0.236	0.145
Medical Images	CWPV	3	$3\pi$	4:4	0.256	0.291	0.200	0.236	0.291	0.236	0.255	0.182	0.291	0.236	0.345
Medical Images	CWPV	4	$1\pi$	7:18	0.237	0.255	0.255	0.291	0.255	0.182	0.291	0.200	0.200	0.255	0.182
Medical Images	CWPV	4	$2\pi$	14:21	0.260	0.273	0.291	0.327	0.218	0.218	0.345	0.236	0.273	0.236	0.182
Medical Images	CWPV	4	$3\pi$	1:7	0.256	0.327	0.200	0.218	0.236	0.145	0.273	0.218	0.291	0.327	0.327
Medical Images	CWPV	5	$1\pi$	9:22	0.229	0.236	0.255	0.291	0.236	0.182	0.291	0.200	0.218	0.218	0.164
Medical Images	CWPV	5	$2\pi$	13:26	0.262	0.255	0.218	0.327	0.291	0.145	0.345	0.327	0.273	0.273	0.164
Medical Images	CWPV	5	$3\pi$	6:6	0.256	0.291	0.200	0.236	0.291	0.236	0.255	0.182	0.291	0.236	0.345
Medical Images	CWPV	6	$1\pi$	11:26	0.227	0.236	0.273	0.255	0.236	0.164	0.273	0.200	0.236	0.236	0.164
Medical Images	CWPV	6	$2\pi$	16:31	0.258	0.273	0.255	0.345	0.255	0.164	0.364	0.291	0.218	0.255	0.164
Medical Images	CWPV	6	$3\pi$	1:9	0.251	0.327	0.236	0.200	0.291	0.182	0.255	0.200	0.236	0.291	0.291
Medical Images	CWPV	7	$1\pi$	12:31	0.231	0.236	0.291	0.255	0.273	0.182	0.291	0.182	0.200	0.218	0.182
Medical Images	CWPV	7	$2\pi$	22:43	0.246	0.291	0.255	0.273	0.255	0.236	0.327	0.273	0.218	0.200	0.127
Medical Images	CWPV	7	$3\pi$	1:9	0.249	0.327	0.218	0.164	0.236	0.200	0.273	0.182	0.309	0.273	0.309
Medical Images	CWED	1	$1\pi$	1:7	0.220	0.200	0.164	0.345	0.218	0.145	0.255	0.255	0.218	0.236	0.164
Medical Images	CWED	1	$2\pi$	1:7	0.253	0.255	0.218	0.309	0.273	0.273	0.218	0.255	0.236	0.273	0.218
Medical Images	CWED	1	$3\pi$	1:7	0.240	0.236	0.218	0.345	0.164	0.236	0.273	0.255	0.218	0.255	0.200
Medical Images	CWED	2	$1\pi$	1:9	0.222	0.236	0.200	0.273	0.164	0.145	0.255	0.255	0.255	0.236	0.200
Medical Images	CWED	2	$2\pi$	2:10	0.207	0.200	0.200	0.164	0.182	0.164	0.236	0.218	0.200	0.291	0.218
Medical Images	CWED	2	$3\pi$	1:13	0.213	0.200	0.182	0.255	0.200	0.127	0.327	0.218	0.236	0.182	0.200
Medical Images	CWED	3	$1\pi$	1:13	0.218	0.255	0.182	0.255	0.145	0.127	0.273	0.255	0.273	0.218	0.200
Medical Images	CWED	3	$2\pi$	4:17	0.198	0.164	0.182	0.236	0.182	0.145	0.273	0.236	0.182	0.200	0.182
Medical Images	CWED	3	$3\pi$	1:19	0.205	0.218	0.182	0.218	0.145	0.145	0.273	0.218	0.200	0.236	0.218
Medical Images	CWED	4	$1\pi$	1:17	0.218	0.255	0.182	0.273	0.127	0.127	0.273	0.255	0.273	0.218	0.200
Medical Images	CWED	4	$2\pi$	1:22	0.200	0.200	0.164	0.218	0.182	0.164	0.255	0.218	0.200	0.218	0.182
Medical Images	CWED	4	$3\pi$	1:25	0.200	0.182	0.182	0.218	0.182	0.127	0.255	0.236	0.182	0.218	0.218
Medical Images	CWED	5	$1\pi$	1:22	0.216	0.236	0.218	0.291	0.145	0.145	0.255	0.236	0.200	0.236	0.200
Medical Images	CWED	5	$2\pi$	1:28	0.195	0.182	0.182	0.236	0.164	0.145	0.236	0.236	0.182	0.182	0.200
Medical Images	CWED	5	$3\pi$	1:31	0.204	0.182	0.182	0.200	0.200	0.145	0.255	0.255	0.182	0.236	0.200
Medical Images	CWED	6	$1\pi$	1:26	0.211	0.236	0.200	0.273	0.145	0.127	0.255	0.218	0.236	0.218	0.200
Medical Images	CWED	6	$2\pi$	5:34	0.198	0.182	0.182	0.236	0.164	0.164	0.255	0.236	0.182	0.182	0.200
Medical Images	CWED	6	$3\pi$	1:37	0.204	0.182	0.182	0.200	0.182	0.145	0.255	0.255	0.182	0.236	0.218
Medical Images	CWED	7	$1\pi$	1:30	0.213	0.236	0.200	0.255	0.145	0.127	0.255	0.236	0.255	0.218	0.200
Medical Images	CWED	7	$2\pi$	1:39	0.195	0.182	0.182	0.236	0.164	0.164	0.236	0.236	0.182	0.182	0.182
Medical Images	CWED	7	$3\pi$	1:43	0.204	0.182	0.182	0.200	0.182	0.145	0.255	0.255	0.182	0.236	0.218



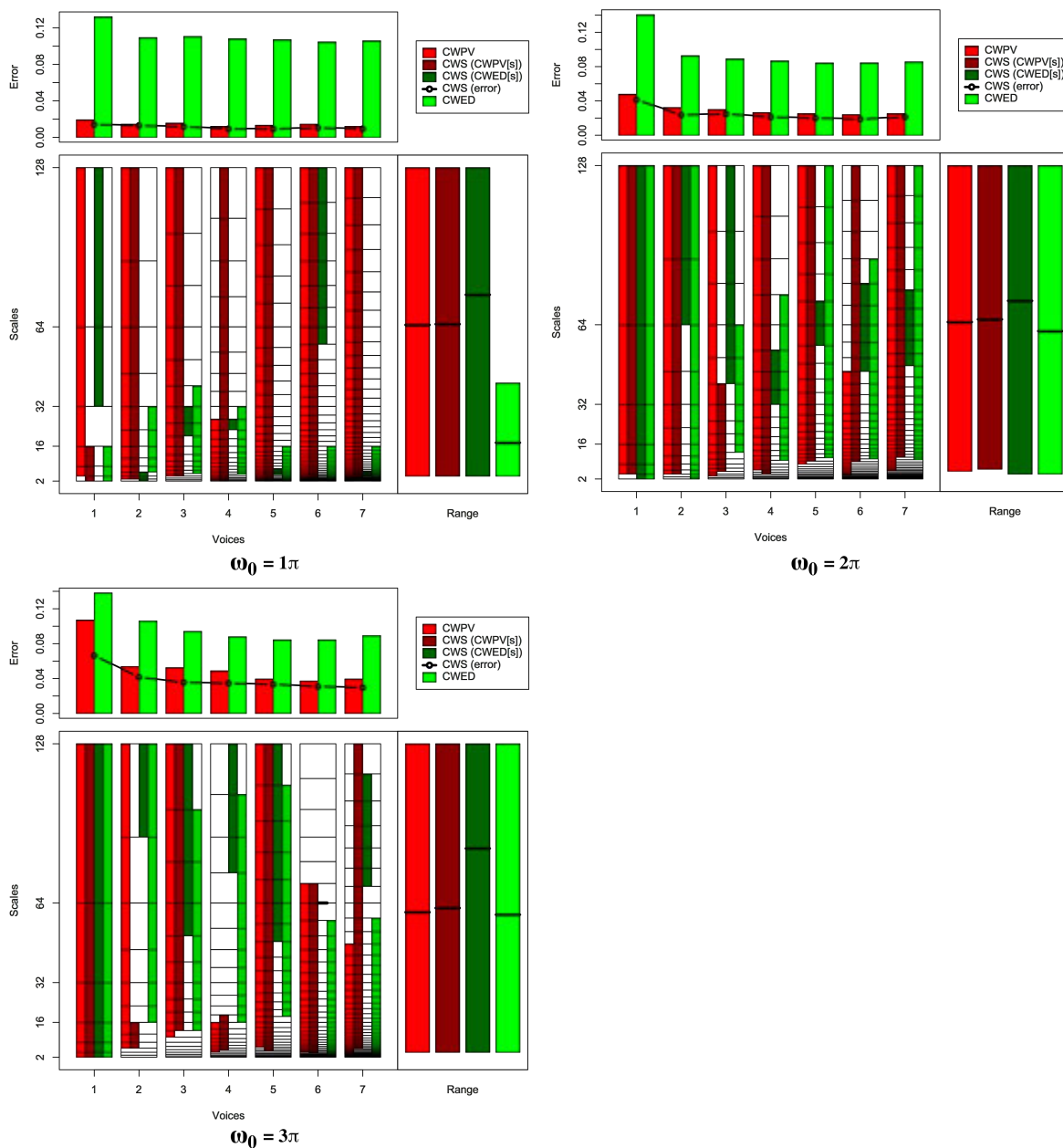


FIGURE B.32: Summary of results for the Mote Strain classification problem comparing CWS, CWPV, CWED methods using 1-7 voices and three  $\omega_0$  values. A lower CWPV score suggests that the problem is predominantly characterised by FM, whereas a lower CWED implies a predominant AM characteristic. The scale ranges have been translated from scale number to scale value. In the bottom right figure of each figure the average range of scales for all 7 voices are presented for each technique.

TABLE B.32: Summary of results for the Mote Strain classification problem comparing Ed, DTW, CWS, CWPV, and CWED using 1-7 voices and 3  $\omega_0$  parameters.  $S$  is the scale set(s) associated with the CWS, CWPV and CWED results. The mean values highlighted in bold are the best in model error rate for the problem.

Problem	Technique	Voices	$\omega_0$	$S$	Mean	1	2	3	4	5	6	7	7	9	10
Mote Strain	Ed				0.043	0.060	0.036	0.048	0.060	0.024	0.036	0.036	0.060	0.036	0.036
Mote Strain	DTW				0.028	0.036	0.012	0.036	0.024	0.000	0.024	0.012	0.024	0.048	0.060
Mote Strain	CWS	1	1 $\pi$	1:4,5:7	0.014	0.048	0.000	0.000	0.024	0.024	0.000	0.024	0.012	0.012	0.000
Mote Strain	CWS	1	2 $\pi$	2:7,1:7	0.042	0.095	0.036	0.024	0.071	0.060	0.024	0.036	0.036	0.000	0.036
Mote Strain	CWS	1	3 $\pi$	1:7,1:7	0.067	0.071	0.048	0.048	0.107	0.071	0.024	0.036	0.095	0.071	0.095
Mote Strain	CWS	2	1 $\pi$	2:13,1:4	0.013	0.036	0.012	0.000	0.024	0.012	0.012	0.024	0.000	0.012	0.000
Mote Strain	CWS	2	2 $\pi$	3:13,11:13	0.024	0.060	0.024	0.012	0.048	0.000	0.048	0.024	0.000	0.024	0.000
Mote Strain	CWS	2	3 $\pi$	4:7,12:13	0.042	0.119	0.024	0.000	0.036	0.071	0.024	0.036	0.024	0.024	0.060
Mote Strain	CWS	3	1 $\pi$	4:19,11:13	0.012	0.024	0.012	0.000	0.024	0.012	0.012	0.024	0.000	0.000	0.012
Mote Strain	CWS	3	2 $\pi$	5:14,14:19	0.025	0.060	0.000	0.000	0.048	0.036	0.012	0.036	0.024	0.012	0.024
Mote Strain	CWS	3	3 $\pi$	9:19,15:19	0.036	0.107	0.012	0.000	0.083	0.012	0.024	0.024	0.024	0.036	0.036
Mote Strain	CWS	4	1 $\pi$	1:25,15:16	0.010	0.036	0.000	0.000	0.012	0.000	0.012	0.024	0.000	0.012	0.000
Mote Strain	CWS	4	2 $\pi$	5:25,17:20	0.022	0.048	0.012	0.012	0.024	0.036	0.012	0.024	0.012	0.024	0.012
Mote Strain	CWS	4	3 $\pi$	6:14,22:25	0.035	0.060	0.012	0.024	0.024	0.036	0.048	0.060	0.024	0.012	0.048
Mote Strain	CWS	5	1 $\pi$	1:31,7:10	<b>0.010</b>	0.024	0.000	0.000	0.012	0.012	0.000	0.024	0.012	0.012	0.000
Mote Strain	CWS	5	2 $\pi$	12:31,25:27	0.020	0.036	0.024	0.012	0.060	0.012	0.012	0.048	0.000	0.000	0.000
Mote Strain	CWS	5	3 $\pi$	7:31,24:31	0.034	0.060	0.012	0.012	0.048	0.036	0.048	0.024	0.024	0.048	0.024
Mote Strain	CWS	6	1 $\pi$	1:37,30:37	0.011	0.036	0.012	0.000	0.024	0.000	0.000	0.024	0.000	0.012	0.000
Mote Strain	CWS	6	2 $\pi$	14:37,28:33	0.019	0.048	0.012	0.000	0.036	0.024	0.024	0.036	0.000	0.012	0.000
Mote Strain	CWS	6	3 $\pi$	6:32,18:18	0.031	0.048	0.012	0.036	0.012	0.012	0.012	0.036	0.060	0.048	0.036
Mote Strain	CWS	7	1 $\pi$	2:43,8:12	<b>0.010</b>	0.036	0.000	0.000	0.012	0.012	0.000	0.024	0.000	0.012	0.000
Mote Strain	CWS	7	2 $\pi$	18:43,33:38	0.022	0.024	0.024	0.012	0.048	0.000	0.036	0.048	0.000	0.024	0.000
Mote Strain	CWS	7	3 $\pi$	11:43,37:42	0.030	0.071	0.012	0.012	0.012	0.048	0.024	0.024	0.036	0.024	0.036
Mote Strain	CWPV	1	1 $\pi$	2:7	0.019	0.060	0.000	0.000	0.036	0.024	0.012	0.012	0.012	0.012	0.024
Mote Strain	CWPV	1	2 $\pi$	2:7	0.048	0.107	0.036	0.024	0.071	0.060	0.024	0.048	0.024	0.024	0.060
Mote Strain	CWPV	1	3 $\pi$	1:7	0.107	0.131	0.119	0.071	0.179	0.071	0.107	0.060	0.131	0.071	0.131
Mote Strain	CWPV	2	1 $\pi$	2:13	0.014	0.060	0.000	0.000	0.024	0.024	0.000	0.024	0.000	0.012	0.000
Mote Strain	CWPV	2	2 $\pi$	3:13	0.032	0.071	0.012	0.012	0.048	0.024	0.048	0.036	0.024	0.024	0.024
Mote Strain	CWPV	2	3 $\pi$	4:13	0.054	0.095	0.095	0.012	0.036	0.060	0.036	0.048	0.060	0.048	0.048
Mote Strain	CWPV	3	1 $\pi$	4:19	0.016	0.048	0.012	0.000	0.024	0.012	0.012	0.024	0.000	0.012	0.012
Mote Strain	CWPV	3	2 $\pi$	3:19	0.030	0.060	0.000	0.012	0.048	0.036	0.048	0.036	0.012	0.024	0.024
Mote Strain	CWPV	3	3 $\pi$	8:19	0.053	0.071	0.024	0.036	0.083	0.024	0.048	0.083	0.048	0.048	0.060
Mote Strain	CWPV	4	1 $\pi$	2:16	0.012	0.036	0.012	0.000	0.024	0.012	0.000	0.024	0.000	0.012	0.000
Mote Strain	CWPV	4	2 $\pi$	7:25	0.026	0.060	0.024	0.012	0.024	0.024	0.024	0.024	0.024	0.024	0.024
Mote Strain	CWPV	4	3 $\pi$	5:13	0.049	0.083	0.012	0.012	0.048	0.071	0.048	0.071	0.048	0.036	0.060
Mote Strain	CWPV	5	1 $\pi$	3:31	0.013	0.036	0.012	0.000	0.024	0.012	0.012	0.024	0.000	0.012	0.000
Mote Strain	CWPV	5	2 $\pi$	11:31	0.025	0.036	0.024	0.000	0.048	0.036	0.000	0.024	0.000	0.048	0.036
Mote Strain	CWPV	5	3 $\pi$	9:31	0.040	0.071	0.012	0.024	0.060	0.048	0.036	0.024	0.060	0.024	0.036
Mote Strain	CWPV	6	1 $\pi$	1:37	0.014	0.036	0.000	0.000	0.024	0.012	0.012	0.024	0.012	0.024	0.000
Mote Strain	CWPV	6	2 $\pi$	6:28	0.024	0.060	0.000	0.012	0.012	0.036	0.012	0.024	0.036	0.024	0.024
Mote Strain	CWPV	6	3 $\pi$	7:32	0.037	0.060	0.012	0.036	0.012	0.036	0.036	0.036	0.060	0.036	0.048
Mote Strain	CWPV	7	1 $\pi$	1:43	0.012	0.036	0.000	0.000	0.024	0.012	0.012	0.024	0.000	0.012	0.000
Mote Strain	CWPV	7	2 $\pi$	11:43	0.025	0.060	0.000	0.012	0.024	0.036	0.000	0.036	0.024	0.024	0.036
Mote Strain	CWPV	7	3 $\pi$	6:33	0.040	0.095	0.012	0.024	0.036	0.024	0.048	0.036	0.060	0.024	0.036
Mote Strain	CWED	1	1 $\pi$	1:4	0.132	0.155	0.107	0.060	0.167	0.155	0.131	0.131	0.167	0.071	0.179
Mote Strain	CWED	1	2 $\pi$	1:7	0.141	0.167	0.131	0.155	0.155	0.119	0.119	0.131	0.131	0.131	0.167
Mote Strain	CWED	1	3 $\pi$	1:7	0.138	0.179	0.107	0.119	0.131	0.107	0.167	0.179	0.131	0.107	0.155
Mote Strain	CWED	2	1 $\pi$	4:9	0.109	0.083	0.107	0.131	0.107	0.119	0.107	0.119	0.131	0.083	0.107
Mote Strain	CWED	2	2 $\pi$	1:13	0.093	0.095	0.071	0.107	0.155	0.131	0.095	0.071	0.048	0.060	0.095
Mote Strain	CWED	2	3 $\pi$	7:13	0.106	0.107	0.083	0.060	0.143	0.119	0.095	0.155	0.107	0.048	0.143
Mote Strain	CWED	3	1 $\pi$	5:14	0.111	0.060	0.107	0.107	0.095	0.107	0.119	0.131	0.155	0.095	0.131
Mote Strain	CWED	3	2 $\pi$	9:16	0.089	0.071	0.071	0.119	0.095	0.083	0.095	0.143	0.095	0.036	0.083
Mote Strain	CWED	3	3 $\pi$	9:18	0.094	0.119	0.060	0.107	0.119	0.107	0.071	0.119	0.131	0.048	0.060
Mote Strain	CWED	4	1 $\pi$	6:17	0.108	0.095	0.107	0.119	0.119	0.107	0.095	0.107	0.131	0.071	0.131
Mote Strain	CWED	4	2 $\pi$	10:22	0.087	0.071	0.071	0.083	0.095	0.107	0.119	0.119	0.095	0.036	0.071
Mote Strain	CWED	4	3 $\pi$	13:24	0.088	0.131	0.071	0.071	0.083	0.083	0.083	0.143	0.095	0.048	0.071
Mote Strain	CWED	5	1 $\pi$	1:16	0.107	0.131	0.095	0.119	0.107	0.167	0.095	0.083	0.095	0.060	0.119
Mote Strain	CWED	5	2 $\pi$	13:31	0.084	0.083	0.071	0.083	0.095	0.119	0.083	0.107	0.071	0.036	0.095
Mote Strain	CWED	5	3 $\pi$	17:30	0.084	0.095	0.060	0.083	0.083	0.107	0.071	0.131	0.095	0.036	0.083
Mote Strain	CWED	6	1 $\pi$	1:19	0.105	0.119	0.095	0.119	0.095	0.167	0.095	0.083	0.095	0.060	0.119
Mote Strain	CWED	6	2 $\pi$	15:34	0.084	0.060	0.083	0.083	0.095	0.119	0.095	0.107	0.071	0.036	0.095
Mote Strain	CWED	6	3 $\pi$	1:30	0.084	0.107	0.083	0.107	0.095	0.095	0.060	0.095	0.095	0.024	0.083
Mote Strain	CWED	7	1 $\pi$	1:22	0.106	0.131	0.095	0.119	0.095	0.167	0.095	0.083	0.095	0.060	0.119
Mote Strain	CWED	7	2 $\pi$	17:43	0.086	0.060	0.083	0.083	0.095	0.119	0.095	0.119	0.071	0.036	0.095
Mote Strain	CWED	7	3 $\pi$	1:35	0.089	0.119	0.083	0.107	0.095	0.131	0.060	0.107	0.083	0.024	0.083

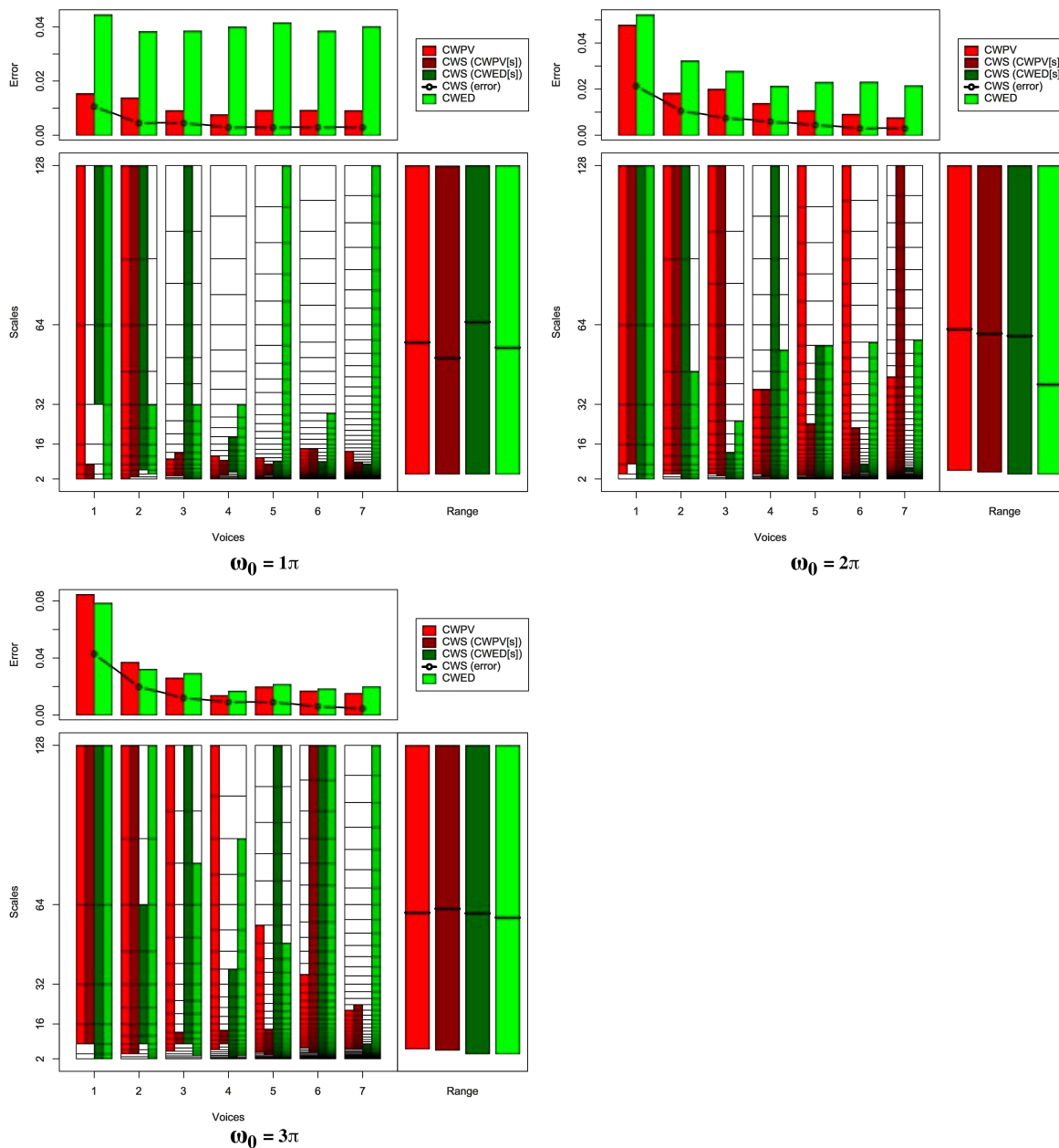


FIGURE B.33: Summary of results for the SonyAIBORobot SurfaceII classification problem comparing CWS, CWPV, CWED methods using 1-7 voices and three  $\omega_0$  values. A lower CWPV score suggests that the problem is predominantly characterised by FM, whereas a lower CWED implies a predominant AM characteristic. The scale ranges have been translated from scale number to scale value. In the bottom right figure of each figure the average range of scales for all 7 voices are presented for each technique.

TABLE B.33: Summary of results for the SonyAIBORobot SurfaceII classification problem comparing Ed, DTW, CWS, CWPV, and CWED using 1-7 voices and 3  $\omega_0$  parameters.  $S$  is the scale set(s) associated with the CWS, CWPV and CWED results. The mean values highlighted in bold are the best in model error rate for the problem.

Problem	Technique	Voices	$\omega_0$	$S$	Mean	1	2	3	4	5	6	7	7	9	10
SonyAIBORobot SurfaceII	Ed				0.012	0.015	0.000	0.000	0.000	0.062	0.000	0.000	0.031	0.015	0.000
SonyAIBORobot SurfaceII	DTW				0.031	0.031	0.015	0.062	0.000	0.077	0.000	0.031	0.015	0.077	0.000
SonyAIBORobot SurfaceII	CWS	1	$1\pi$	1:3,5:7	0.011	0.000	0.000	0.015	0.000	0.046	0.000	0.000	0.031	0.000	0.015
SonyAIBORobot SurfaceII	CWS	1	$2\pi$	3:7,1:7	0.022	0.000	0.031	0.015	0.000	0.031	0.015	0.031	0.015	0.031	0.015
SonyAIBORobot SurfaceII	CWS	1	$3\pi$	3:7,1:7	0.043	0.046	0.046	0.077	0.046	0.046	0.015	0.031	0.046	0.062	0.015
SonyAIBORobot SurfaceII	CWS	2	$1\pi$	2:13,4:13	0.005	0.000	0.000	0.000	0.000	0.000	0.000	0.000	0.031	0.000	0.015
SonyAIBORobot SurfaceII	CWS	2	$2\pi$	3:13,1:13	0.011	0.000	0.046	0.000	0.000	0.015	0.000	0.000	0.031	0.000	0.015
SonyAIBORobot SurfaceII	CWS	2	$3\pi$	3:13,5:11	0.020	0.000	0.046	0.031	0.000	0.031	0.015	0.015	0.031	0.015	0.015
SonyAIBORobot SurfaceII	CWS	3	$1\pi$	3:9,1:19	0.005	0.000	0.000	0.000	0.000	0.000	0.000	0.000	0.031	0.015	0.000
SonyAIBORobot SurfaceII	CWS	3	$2\pi$	3:19,1:9	0.008	0.000	0.000	0.000	0.000	0.015	0.015	0.000	0.031	0.000	0.015
SonyAIBORobot SurfaceII	CWS	3	$3\pi$	7:9,7:19	0.012	0.000	0.015	0.015	0.015	0.000	0.000	0.015	0.031	0.015	0.015
SonyAIBORobot SurfaceII	CWS	4	$1\pi$	4:10,6:14	<b>0.003</b>	0.000	0.000	0.000	0.000	0.000	0.000	0.000	0.015	0.015	0.000
SonyAIBORobot SurfaceII	CWS	4	$2\pi$	3:18,1:25	0.006	0.000	0.015	0.000	0.000	0.015	0.000	0.000	0.015	0.015	0.000
SonyAIBORobot SurfaceII	CWS	4	$3\pi$	9:12,1:18	0.009	0.015	0.031	0.015	0.000	0.000	0.000	0.000	0.031	0.000	0.000
SonyAIBORobot SurfaceII	CWS	5	$1\pi$	5:11,1:12	<b>0.003</b>	0.000	0.000	0.000	0.000	0.015	0.000	0.000	0.000	0.015	0.000
SonyAIBORobot SurfaceII	CWS	5	$2\pi$	4:19,1:25	0.005	0.000	0.000	0.000	0.000	0.000	0.000	0.000	0.031	0.015	0.000
SonyAIBORobot SurfaceII	CWS	5	$3\pi$	5:15,1:31	0.009	0.000	0.015	0.015	0.000	0.000	0.015	0.000	0.031	0.015	0.000
SonyAIBORobot SurfaceII	CWS	6	$1\pi$	5:18,5:14	<b>0.003</b>	0.000	0.000	0.000	0.000	0.000	0.000	0.000	0.015	0.015	0.000
SonyAIBORobot SurfaceII	CWS	6	$2\pi$	5:22,8:13	<b>0.003</b>	0.000	0.000	0.000	0.000	0.000	0.000	0.000	0.031	0.000	0.000
SonyAIBORobot SurfaceII	CWS	6	$3\pi$	8:37,1:37	0.006	0.000	0.000	0.000	0.015	0.000	0.015	0.000	0.031	0.000	0.000
SonyAIBORobot SurfaceII	CWS	7	$1\pi$	5:16,4:15	<b>0.003</b>	0.000	0.000	0.000	0.000	0.000	0.000	0.000	0.015	0.015	0.000
SonyAIBORobot SurfaceII	CWS	7	$2\pi$	5:43,10:13	<b>0.003</b>	0.000	0.000	0.000	0.000	0.000	0.000	0.000	0.031	0.000	0.000
SonyAIBORobot SurfaceII	CWS	7	$3\pi$	12:26,1:15	0.005	0.000	0.000	0.000	0.000	0.000	0.000	0.000	0.031	0.000	0.015
SonyAIBORobot SurfaceII	CWPV	1	$1\pi$	1:7	0.015	0.000	0.031	0.015	0.000	0.031	0.000	0.000	0.031	0.031	0.015
SonyAIBORobot SurfaceII	CWPV	1	$2\pi$	2:7	0.048	0.000	0.046	0.062	0.015	0.062	0.062	0.015	0.031	0.077	0.108
SonyAIBORobot SurfaceII	CWPV	1	$3\pi$	3:7	0.085	0.046	0.092	0.077	0.092	0.108	0.046	0.077	0.123	0.108	0.077
SonyAIBORobot SurfaceII	CWPV	2	$1\pi$	1:13	0.014	0.015	0.031	0.000	0.000	0.031	0.000	0.000	0.031	0.015	0.015
SonyAIBORobot SurfaceII	CWPV	2	$2\pi$	3:13	0.018	0.015	0.031	0.015	0.000	0.031	0.015	0.000	0.046	0.015	0.015
SonyAIBORobot SurfaceII	CWPV	2	$3\pi$	3:13	0.037	0.000	0.031	0.062	0.015	0.046	0.031	0.015	0.062	0.031	0.077
SonyAIBORobot SurfaceII	CWPV	3	$1\pi$	3:8	0.009	0.015	0.000	0.000	0.000	0.015	0.000	0.000	0.046	0.015	0.000
SonyAIBORobot SurfaceII	CWPV	3	$2\pi$	4:19	0.020	0.000	0.031	0.015	0.000	0.046	0.031	0.000	0.031	0.015	0.031
SonyAIBORobot SurfaceII	CWPV	3	$3\pi$	5:19	0.026	0.046	0.015	0.015	0.015	0.015	0.031	0.000	0.046	0.015	0.062
SonyAIBORobot SurfaceII	CWPV	4	$1\pi$	2:11	0.008	0.000	0.015	0.000	0.000	0.015	0.000	0.000	0.031	0.015	0.000
SonyAIBORobot SurfaceII	CWPV	4	$2\pi$	5:18	0.014	0.000	0.015	0.000	0.000	0.031	0.000	0.000	0.046	0.015	0.031
SonyAIBORobot SurfaceII	CWPV	4	$3\pi$	7:25	0.014	0.000	0.015	0.015	0.000	0.015	0.015	0.000	0.046	0.000	0.031
SonyAIBORobot SurfaceII	CWPV	5	$1\pi$	1:13	0.009	0.000	0.015	0.000	0.000	0.031	0.000	0.000	0.031	0.015	0.000
SonyAIBORobot SurfaceII	CWPV	5	$2\pi$	5:31	0.011	0.000	0.015	0.015	0.000	0.000	0.000	0.000	0.046	0.000	0.031
SonyAIBORobot SurfaceII	CWPV	5	$3\pi$	7:25	0.020	0.031	0.015	0.015	0.015	0.015	0.000	0.000	0.046	0.046	0.015
SonyAIBORobot SurfaceII	CWPV	6	$1\pi$	5:18	0.009	0.015	0.000	0.000	0.000	0.031	0.000	0.000	0.031	0.015	0.000
SonyAIBORobot SurfaceII	CWPV	6	$2\pi$	7:37	0.009	0.000	0.015	0.000	0.000	0.000	0.015	0.000	0.046	0.000	0.015
SonyAIBORobot SurfaceII	CWPV	6	$3\pi$	11:26	0.017	0.031	0.000	0.000	0.015	0.000	0.031	0.000	0.046	0.000	0.046
SonyAIBORobot SurfaceII	CWPV	7	$1\pi$	3:20	0.009	0.000	0.015	0.000	0.000	0.015	0.000	0.000	0.046	0.015	0.000
SonyAIBORobot SurfaceII	CWPV	7	$2\pi$	7:32	0.008	0.000	0.015	0.000	0.000	0.015	0.000	0.000	0.031	0.000	0.015
SonyAIBORobot SurfaceII	CWPV	7	$3\pi$	12:25	0.015	0.000	0.015	0.015	0.015	0.015	0.000	0.000	0.062	0.015	0.015
SonyAIBORobot SurfaceII	CWED	1	$1\pi$	1:7	0.045	0.062	0.015	0.015	0.092	0.046	0.046	0.046	0.046	0.062	0.015
SonyAIBORobot SurfaceII	CWED	1	$2\pi$	1:7	0.052	0.062	0.015	0.062	0.092	0.031	0.077	0.046	0.092	0.031	0.015
SonyAIBORobot SurfaceII	CWED	1	$3\pi$	1:7	0.079	0.062	0.062	0.092	0.108	0.077	0.062	0.062	0.077	0.092	0.092
SonyAIBORobot SurfaceII	CWED	2	$1\pi$	3:9	0.038	0.015	0.031	0.015	0.092	0.062	0.046	0.046	0.046	0.015	0.015
SonyAIBORobot SurfaceII	CWED	2	$2\pi$	1:10	0.032	0.046	0.000	0.031	0.077	0.031	0.015	0.062	0.031	0.015	0.015
SonyAIBORobot SurfaceII	CWED	2	$3\pi$	1:13	0.032	0.015	0.015	0.015	0.077	0.046	0.015	0.077	0.031	0.015	0.015
SonyAIBORobot SurfaceII	CWED	3	$1\pi$	1:13	0.039	0.031	0.015	0.015	0.046	0.031	0.062	0.077	0.062	0.031	0.015
SonyAIBORobot SurfaceII	CWED	3	$2\pi$	1:12	0.028	0.031	0.015	0.031	0.031	0.031	0.000	0.031	0.046	0.031	0.031
SonyAIBORobot SurfaceII	CWED	3	$3\pi$	3:17	0.029	0.031	0.015	0.015	0.062	0.062	0.000	0.031	0.015	0.015	0.046
SonyAIBORobot SurfaceII	CWED	4	$1\pi$	1:17	0.040	0.031	0.015	0.015	0.046	0.031	0.062	0.077	0.077	0.031	0.015
SonyAIBORobot SurfaceII	CWED	4	$2\pi$	2:20	0.021	0.015	0.015	0.015	0.031	0.046	0.015	0.015	0.046	0.000	0.015
SonyAIBORobot SurfaceII	CWED	4	$3\pi$	4:23	0.017	0.015	0.015	0.000	0.062	0.046	0.000	0.015	0.015	0.000	0.000
SonyAIBORobot SurfaceII	CWED	5	$1\pi$	1:31	0.042	0.031	0.015	0.015	0.046	0.046	0.062	0.077	0.077	0.031	0.015
SonyAIBORobot SurfaceII	CWED	5	$2\pi$	2:25	0.023	0.015	0.015	0.000	0.031	0.031	0.031	0.046	0.046	0.000	0.015
SonyAIBORobot SurfaceII	CWED	5	$3\pi$	1:24	0.022	0.031	0.015	0.031	0.031	0.046	0.000	0.015	0.031	0.000	0.015
SonyAIBORobot SurfaceII	CWED	6	$1\pi$	6:24	0.039	0.031	0.015	0.000	0.077	0.062	0.062	0.062	0.046	0.015	0.015
SonyAIBORobot SurfaceII	CWED	6	$2\pi$	3:30	0.023	0.031	0.015	0.000	0.031	0.031	0.031	0.046	0.031	0.000	0.015
SonyAIBORobot SurfaceII	CWED	6	$3\pi$	1:37	0.018	0.031	0.015	0.031	0.046	0.046	0.000	0.000	0.015	0.000	0.000
SonyAIBORobot SurfaceII	CWED	7	$1\pi$	2:43	0.040	0.031	0.015	0.015	0.062	0.046	0.062	0.062	0.077	0.031	0.000
SonyAIBORobot SurfaceII	CWED	7	$2\pi$	5:35	0.022	0.015	0.015	0.000	0.046	0.031	0.031	0.031	0.031	0.000	0.015
SonyAIBORobot SurfaceII	CWED	7	$3\pi$	1:43	0.020	0.031	0.015	0.031	0.046	0.046	0.000	0.000	0.015	0.000	0.015

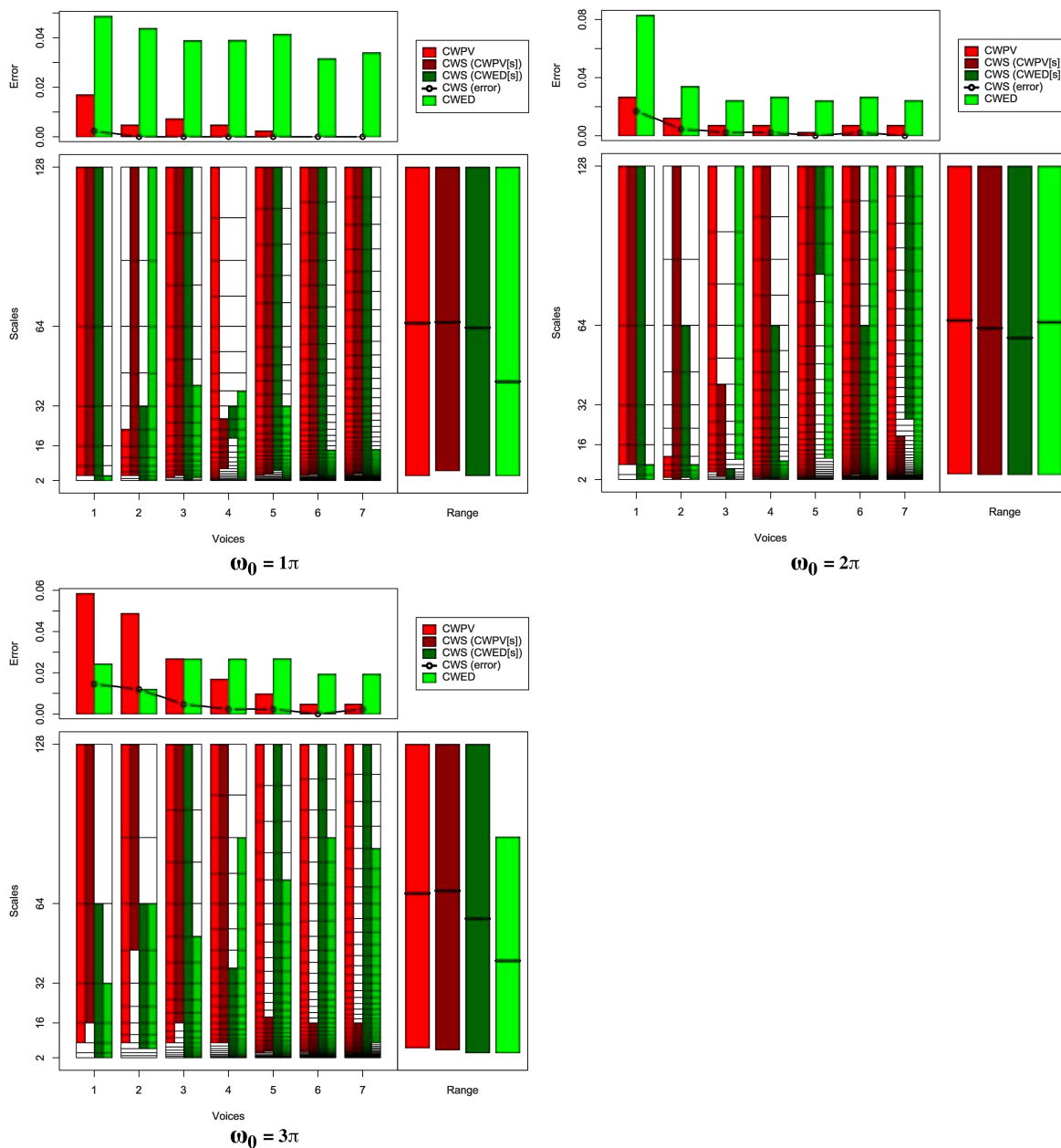


FIGURE B.34: Summary of results for the SonyAIBORobot Surface classification problem comparing CWS, CWPV, CWED methods using 1-7 voices and three  $\omega_0$  values. A lower CWPV score suggests that the problem is predominantly characterised by FM, whereas a lower CWED implies a predominant AM characteristic. The scale ranges have been translated from scale number to scale value. In the bottom right figure of each figure the average range of scales for all 7 voices are presented for each technique.

TABLE B.34: Summary of results for the SonyAIBORobot Surface classification problem comparing Ed, DTW, CWS, CWPV, and CWED using 1-7 voices and 3  $\omega_0$  parameters.  $S$  is the scale set(s) associated with the CWS, CWPV and CWED results. The mean values highlighted in bold are the best in model error rate for the problem.

Problem	Technique	Voices	$\omega_0$	$S$	Mean	1	2	3	4	5	6	7	7	9	10
SonyAIBORobot Surface	Ed				0.015	0.024	0.000	0.000	0.000	0.049	0.000	0.024	0.000	0.049	0.000
SonyAIBORobot Surface	DTW				0.027	0.073	0.000	0.024	0.000	0.024	0.000	0.073	0.000	0.073	0.000
SonyAIBORobot Surface	CWS	1	$1\pi$	2:7,1:7	0.002	0.000	0.000	0.000	0.000	0.000	0.000	0.000	0.000	0.024	0.000
SonyAIBORobot Surface	CWS	1	$2\pi$	3:7,1:7	0.017	0.000	0.000	0.049	0.000	0.073	0.000	0.049	0.000	0.000	0.000
SonyAIBORobot Surface	CWS	1	$3\pi$	4:7,1:6	0.015	0.049	0.024	0.000	0.000	0.073	0.000	0.000	0.000	0.000	0.000
SonyAIBORobot Surface	CWS	2	$1\pi$	3:13,1:9	<b>0.000</b>	0.000	0.000	0.000	0.000	0.000	0.000	0.000	0.000	0.000	0.000
SonyAIBORobot Surface	CWS	2	$2\pi$	1:13,2:11	0.005	0.000	0.000	0.000	0.000	0.024	0.024	0.000	0.000	0.000	0.000
SonyAIBORobot Surface	CWS	2	$3\pi$	10:13,4:11	0.012	0.024	0.000	0.024	0.000	0.024	0.000	0.024	0.024	0.000	0.000
SonyAIBORobot Surface	CWS	3	$1\pi$	4:19,1:19	<b>0.000</b>	0.000	0.000	0.000	0.000	0.000	0.000	0.000	0.000	0.000	0.000
SonyAIBORobot Surface	CWS	3	$2\pi$	3:14,1:6	0.002	0.000	0.000	0.000	0.000	0.024	0.000	0.000	0.000	0.000	0.000
SonyAIBORobot Surface	CWS	3	$3\pi$	10:19,1:19	0.005	0.024	0.000	0.000	0.000	0.000	0.000	0.000	0.000	0.024	0.000
SonyAIBORobot Surface	CWS	4	$1\pi$	8:16,14:17	<b>0.000</b>	0.000	0.000	0.000	0.000	0.000	0.000	0.000	0.000	0.000	0.000
SonyAIBORobot Surface	CWS	4	$2\pi$	2:25,1:21	0.002	0.000	0.000	0.000	0.000	0.000	0.024	0.000	0.000	0.000	0.000
SonyAIBORobot Surface	CWS	4	$3\pi$	9:25,1:18	0.002	0.024	0.000	0.000	0.000	0.000	0.000	0.000	0.000	0.000	0.000
SonyAIBORobot Surface	CWS	5	$1\pi$	7:31,9:31	<b>0.000</b>	0.000	0.000	0.000	0.000	0.000	0.000	0.000	0.000	0.000	0.000
SonyAIBORobot Surface	CWS	5	$2\pi$	3:31,28:31	<b>0.000</b>	0.000	0.000	0.000	0.000	0.000	0.000	0.000	0.000	0.000	0.000
SonyAIBORobot Surface	CWS	5	$3\pi$	7:17,1:31	0.002	0.000	0.000	0.000	0.000	0.024	0.000	0.000	0.000	0.000	0.000
SonyAIBORobot Surface	CWS	6	$1\pi$	8:37,1:37	<b>0.000</b>	0.000	0.000	0.000	0.000	0.000	0.000	0.000	0.000	0.000	0.000
SonyAIBORobot Surface	CWS	6	$2\pi$	7:37,1:31	0.002	0.000	0.024	0.000	0.000	0.000	0.000	0.000	0.000	0.000	0.000
SonyAIBORobot Surface	CWS	6	$3\pi$	5:19,1:37	<b>0.000</b>	0.000	0.000	0.000	0.000	0.000	0.000	0.000	0.000	0.000	0.000
SonyAIBORobot Surface	CWS	7	$1\pi$	10:43,7:43	<b>0.000</b>	0.000	0.000	0.000	0.000	0.000	0.000	0.000	0.000	0.000	0.000
SonyAIBORobot Surface	CWS	7	$2\pi$	1:24,27:43	<b>0.000</b>	0.000	0.000	0.000	0.000	0.000	0.000	0.000	0.000	0.000	0.000
SonyAIBORobot Surface	CWS	7	$3\pi$	6:22,1:43	0.002	0.000	0.000	0.000	0.000	0.000	0.000	0.000	0.000	0.024	0.000
SonyAIBORobot Surface	CWPV	1	$1\pi$	2:7	0.017	0.024	0.000	0.000	0.000	0.049	0.000	0.024	0.000	0.073	0.000
SonyAIBORobot Surface	CWPV	1	$2\pi$	3:7	0.027	0.049	0.049	0.000	0.024	0.024	0.024	0.049	0.024	0.024	0.000
SonyAIBORobot Surface	CWPV	1	$3\pi$	3:7	0.059	0.122	0.049	0.098	0.024	0.073	0.049	0.049	0.024	0.073	0.024
SonyAIBORobot Surface	CWPV	2	$1\pi$	3:8	0.005	0.000	0.000	0.000	0.000	0.024	0.000	0.024	0.000	0.000	0.000
SonyAIBORobot Surface	CWPV	2	$2\pi$	2:6	0.012	0.000	0.024	0.000	0.000	0.000	0.000	0.049	0.000	0.049	0.000
SonyAIBORobot Surface	CWPV	2	$3\pi$	5:13	0.049	0.122	0.024	0.098	0.000	0.073	0.049	0.049	0.024	0.049	0.000
SonyAIBORobot Surface	CWPV	3	$1\pi$	3:19	0.007	0.000	0.000	0.000	0.000	0.024	0.000	0.049	0.000	0.000	0.000
SonyAIBORobot Surface	CWPV	3	$2\pi$	5:19	0.007	0.000	0.000	0.024	0.000	0.000	0.024	0.024	0.000	0.000	0.000
SonyAIBORobot Surface	CWPV	3	$3\pi$	7:19	0.027	0.049	0.024	0.024	0.000	0.049	0.000	0.049	0.000	0.073	0.000
SonyAIBORobot Surface	CWPV	4	$1\pi$	1:25	0.005	0.024	0.000	0.000	0.000	0.024	0.000	0.000	0.000	0.000	0.000
SonyAIBORobot Surface	CWPV	4	$2\pi$	3:25	0.007	0.024	0.024	0.000	0.000	0.000	0.000	0.000	0.000	0.024	0.000
SonyAIBORobot Surface	CWPV	4	$3\pi$	9:25	0.017	0.024	0.000	0.024	0.024	0.049	0.024	0.000	0.000	0.024	0.000
SonyAIBORobot Surface	CWPV	5	$1\pi$	6:31	0.002	0.000	0.000	0.000	0.000	0.024	0.000	0.000	0.000	0.000	0.000
SonyAIBORobot Surface	CWPV	5	$2\pi$	2:31	0.002	0.024	0.000	0.000	0.000	0.000	0.000	0.000	0.000	0.000	0.000
SonyAIBORobot Surface	CWPV	5	$3\pi$	6:31	0.010	0.049	0.000	0.000	0.000	0.000	0.000	0.000	0.000	0.049	0.000
SonyAIBORobot Surface	CWPV	6	$1\pi$	7:37	<b>0.000</b>	0.000	0.000	0.000	0.000	0.000	0.000	0.000	0.000	0.000	0.000
SonyAIBORobot Surface	CWPV	6	$2\pi$	5:37	0.007	0.024	0.024	0.000	0.000	0.000	0.000	0.000	0.000	0.024	0.000
SonyAIBORobot Surface	CWPV	6	$3\pi$	8:37	0.005	0.024	0.000	0.000	0.000	0.000	0.000	0.000	0.000	0.024	0.000
SonyAIBORobot Surface	CWPV	7	$1\pi$	8:43	<b>0.000</b>	0.000	0.000	0.000	0.000	0.000	0.000	0.000	0.000	0.000	0.000
SonyAIBORobot Surface	CWPV	7	$2\pi$	4:43	0.007	0.024	0.024	0.000	0.000	0.000	0.024	0.000	0.000	0.000	0.000
SonyAIBORobot Surface	CWPV	7	$3\pi$	8:43	0.005	0.000	0.024	0.000	0.000	0.000	0.000	0.000	0.000	0.024	0.000
SonyAIBORobot Surface	CWED	1	$1\pi$	1:2	0.049	0.024	0.000	0.073	0.000	0.122	0.049	0.049	0.073	0.073	0.024
SonyAIBORobot Surface	CWED	1	$2\pi$	1:3	0.083	0.098	0.122	0.122	0.000	0.146	0.049	0.049	0.122	0.049	0.073
SonyAIBORobot Surface	CWED	1	$3\pi$	1:5	0.024	0.049	0.073	0.024	0.000	0.073	0.024	0.000	0.000	0.000	0.000
SonyAIBORobot Surface	CWED	2	$1\pi$	1:13	0.044	0.049	0.073	0.073	0.000	0.073	0.000	0.049	0.073	0.024	0.024
SonyAIBORobot Surface	CWED	2	$2\pi$	1:5	0.034	0.049	0.024	0.024	0.073	0.024	0.024	0.000	0.049	0.049	0.024
SonyAIBORobot Surface	CWED	2	$3\pi$	4:11	0.012	0.024	0.000	0.024	0.000	0.024	0.000	0.024	0.024	0.000	0.000
SonyAIBORobot Surface	CWED	3	$1\pi$	3:14	0.039	0.024	0.073	0.073	0.000	0.049	0.000	0.024	0.073	0.049	0.024
SonyAIBORobot Surface	CWED	3	$2\pi$	8:19	0.024	0.073	0.024	0.049	0.000	0.049	0.000	0.000	0.024	0.024	0.000
SonyAIBORobot Surface	CWED	3	$3\pi$	1:15	0.027	0.049	0.000	0.024	0.024	0.073	0.024	0.049	0.000	0.024	0.000
SonyAIBORobot Surface	CWED	4	$1\pi$	3:18	0.039	0.049	0.073	0.049	0.000	0.049	0.000	0.024	0.073	0.049	0.024
SonyAIBORobot Surface	CWED	4	$2\pi$	3:10	0.027	0.049	0.000	0.073	0.024	0.024	0.000	0.000	0.049	0.024	0.024
SonyAIBORobot Surface	CWED	4	$3\pi$	1:23	0.027	0.073	0.000	0.024	0.000	0.073	0.000	0.049	0.000	0.024	0.024
SonyAIBORobot Surface	CWED	5	$1\pi$	1:21	0.041	0.073	0.024	0.049	0.024	0.098	0.000	0.049	0.024	0.049	0.024
SonyAIBORobot Surface	CWED	5	$2\pi$	13:31	0.024	0.073	0.024	0.024	0.000	0.049	0.000	0.024	0.024	0.024	0.000
SonyAIBORobot Surface	CWED	5	$3\pi$	4:27	0.027	0.073	0.000	0.049	0.000	0.073	0.000	0.049	0.000	0.024	0.000
SonyAIBORobot Surface	CWED	6	$1\pi$	1:18	0.032	0.000	0.024	0.073	0.000	0.098	0.000	0.049	0.024	0.024	0.024
SonyAIBORobot Surface	CWED	6	$2\pi$	1:37	0.027	0.073	0.000	0.024	0.000	0.049	0.000	0.024	0.024	0.049	0.024
SonyAIBORobot Surface	CWED	6	$3\pi$	5:34	0.019	0.049	0.000	0.024	0.000	0.073	0.000	0.024	0.000	0.024	0.000
SonyAIBORobot Surface	CWED	7	$1\pi$	1:21	0.034	0.024	0.024	0.073	0.000	0.098	0.000	0.049	0.024	0.024	0.024
SonyAIBORobot Surface	CWED	7	$2\pi$	4:43	0.024	0.024	0.000	0.049	0.024	0.024	0.000	0.000	0.049	0.049	0.024
SonyAIBORobot Surface	CWED	7	$3\pi$	15:39	0.019	0.073	0.000	0.000	0.000	0.073	0.000	0.024	0.000	0.000	0.024

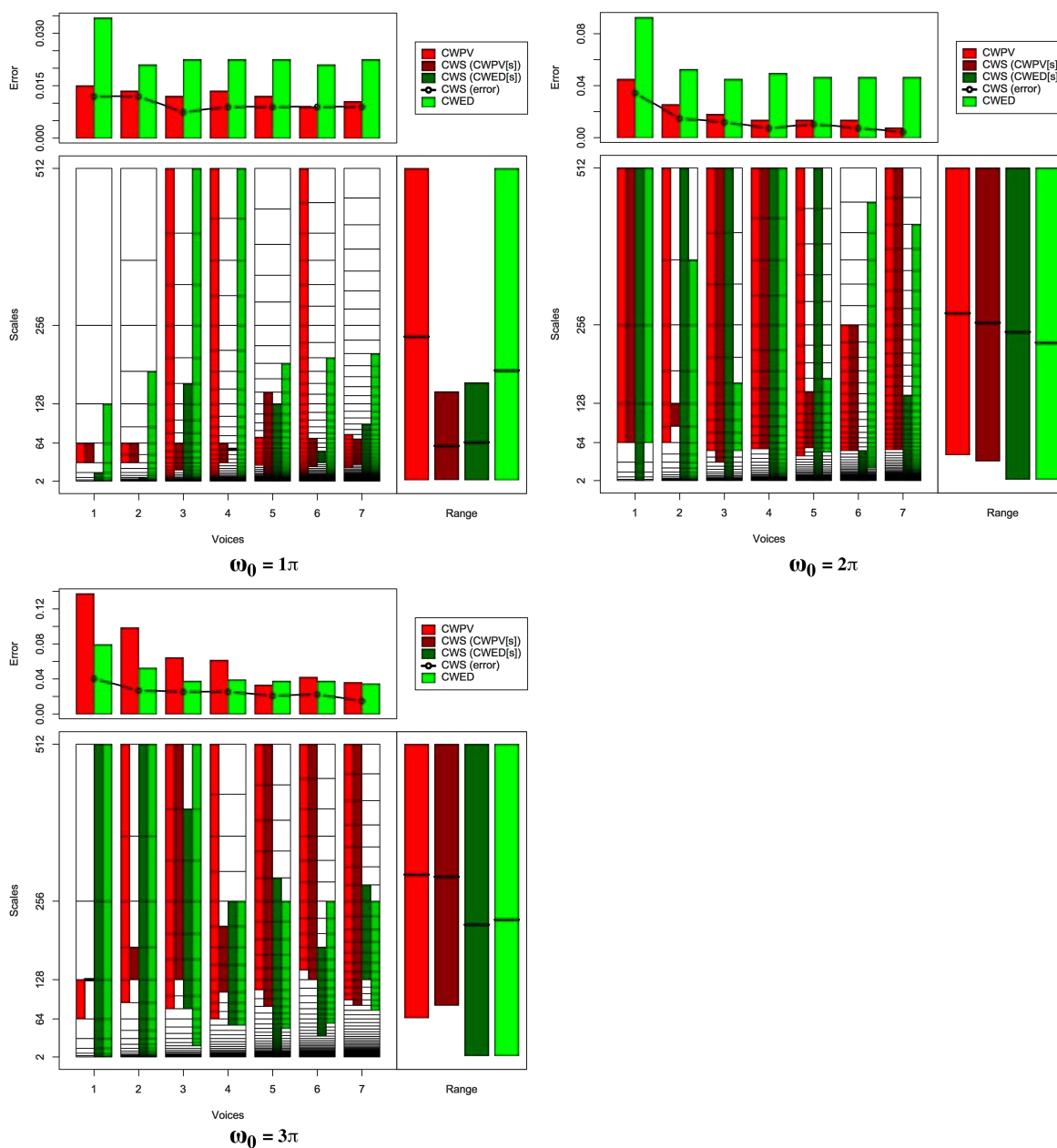


FIGURE B.35: Summary of results for the Symbols classification problem comparing CWS, CWPV, CWED methods using 1-7 voices and three  $\omega_0$  values. A lower CWPV score suggests that the problem is predominantly characterised by FM, whereas a lower CWED implies a predominant AM characteristic. The scale ranges have been translated from scale number to scale value. In the bottom right figure of each figure the average range of scales for all 7 voices are presented for each technique.

TABLE B.35: Summary of results for the Symbols classification problem comparing Ed, DTW, CWS, CWPV, and CWED using 1-7 voices and 3  $\omega_0$  parameters.  $S$  is the scale set(s) associated with the CWS, CWPV and CWED results. The mean values highlighted in bold are the best in model error rate for the problem.

Problem	Technique	Voices	$\omega_0$	$S$	Mean	1	2	3	4	5	6	7	7	9	10
Symbols	Ed				0.021	0.000	0.075	0.015	0.015	0.000	0.030	0.015	0.015	0.030	0.015
Symbols	DTW				0.011	0.015	0.030	0.000	0.000	0.000	0.000	0.015	0.015	0.030	0.000
Symbols	CWS	1	$1\pi$	5:6,1:4	0.012	0.000	0.045	0.015	0.015	0.000	0.015	0.015	0.015	0.000	0.000
Symbols	CWS	1	$2\pi$	6:9,1:9	0.035	0.045	0.015	0.000	0.045	0.015	0.015	0.030	0.075	0.045	0.060
Symbols	CWS	1	$3\pi$	7:7,1:9	0.041	0.045	0.060	0.030	0.000	0.000	0.045	0.015	0.075	0.090	0.045
Symbols	CWS	2	$1\pi$	9:11,1:5	0.012	0.015	0.045	0.000	0.000	0.015	0.015	0.015	0.015	0.000	0.000
Symbols	CWS	2	$2\pi$	12:13,1:17	0.015	0.015	0.045	0.015	0.000	0.000	0.000	0.030	0.015	0.000	0.030
Symbols	CWS	2	$3\pi$	13:14,1:17	0.027	0.015	0.045	0.000	0.030	0.030	0.015	0.015	0.030	0.060	0.030
Symbols	CWS	3	$1\pi$	11:16,1:20	0.008	0.000	0.030	0.000	0.000	0.000	0.000	0.015	0.015	0.015	0.000
Symbols	CWS	3	$2\pi$	13:25,1:25	0.012	0.030	0.030	0.015	0.000	0.000	0.000	0.030	0.000	0.000	0.015
Symbols	CWS	3	$3\pi$	19:25,17:24	0.026	0.000	0.045	0.000	0.030	0.015	0.030	0.030	0.045	0.030	0.030
Symbols	CWS	4	$1\pi$	17:21,18:18	0.009	0.015	0.030	0.000	0.000	0.000	0.015	0.015	0.015	0.000	0.000
Symbols	CWS	4	$2\pi$	20:33,1:33	0.008	0.000	0.030	0.000	0.000	0.000	0.000	0.015	0.015	0.000	0.015
Symbols	CWS	4	$3\pi$	24:28,20:29	0.026	0.030	0.045	0.015	0.015	0.015	0.045	0.015	0.015	0.045	0.015
Symbols	CWS	5	$1\pi$	2:32,1:31	0.009	0.000	0.015	0.015	0.000	0.000	0.015	0.015	0.015	0.015	0.000
Symbols	CWS	5	$2\pi$	25:32,1:41	0.011	0.015	0.030	0.000	0.000	0.000	0.030	0.015	0.015	0.000	0.000
Symbols	CWS	5	$3\pi$	28:41,1:37	0.021	0.045	0.075	0.000	0.000	0.015	0.000	0.030	0.030	0.000	0.015
Symbols	CWS	6	$1\pi$	23:32,25:29	0.009	0.000	0.045	0.000	0.000	0.000	0.015	0.015	0.015	0.000	0.000
Symbols	CWS	6	$2\pi$	29:43,1:29	0.008	0.000	0.030	0.000	0.015	0.000	0.000	0.015	0.015	0.000	0.000
Symbols	CWS	6	$3\pi$	37:49,26:40	0.023	0.000	0.060	0.000	0.015	0.015	0.015	0.030	0.045	0.030	0.015
Symbols	CWS	7	$1\pi$	28:37,1:40	0.009	0.000	0.045	0.000	0.000	0.000	0.015	0.000	0.015	0.000	0.015
Symbols	CWS	7	$2\pi$	34:57,1:44	<b>0.005</b>	0.000	0.030	0.000	0.000	0.000	0.000	0.015	0.000	0.000	0.000
Symbols	CWS	7	$3\pi$	39:57,43:51	0.015	0.015	0.045	0.000	0.000	0.015	0.015	0.030	0.030	0.000	0.000
Symbols	CWPV	1	$1\pi$	5:6	0.015	0.000	0.045	0.030	0.015	0.015	0.015	0.000	0.015	0.015	0.000
Symbols	CWPV	1	$2\pi$	6:9	0.045	0.045	0.045	0.015	0.060	0.045	0.045	0.045	0.075	0.045	0.030
Symbols	CWPV	1	$3\pi$	6:7	0.137	0.090	0.224	0.075	0.134	0.075	0.164	0.090	0.179	0.194	0.149
Symbols	CWPV	2	$1\pi$	9:11	0.014	0.015	0.045	0.000	0.000	0.015	0.015	0.015	0.015	0.015	0.000
Symbols	CWPV	2	$2\pi$	11:17	0.026	0.030	0.030	0.000	0.015	0.015	0.030	0.030	0.075	0.015	0.015
Symbols	CWPV	2	$3\pi$	12:17	0.099	0.075	0.209	0.030	0.075	0.045	0.134	0.104	0.119	0.104	0.090
Symbols	CWPV	3	$1\pi$	1:25	0.012	0.000	0.045	0.030	0.000	0.000	0.015	0.015	0.015	0.000	0.000
Symbols	CWPV	3	$2\pi$	15:25	0.018	0.000	0.060	0.000	0.030	0.000	0.000	0.030	0.060	0.000	0.000
Symbols	CWPV	3	$3\pi$	17:25	0.064	0.045	0.164	0.015	0.045	0.045	0.060	0.060	0.119	0.030	0.060
Symbols	CWPV	4	$1\pi$	1:33	0.014	0.000	0.030	0.030	0.000	0.000	0.015	0.030	0.015	0.015	0.000
Symbols	CWPV	4	$2\pi$	20:33	0.014	0.015	0.045	0.000	0.000	0.015	0.000	0.015	0.015	0.015	0.015
Symbols	CWPV	4	$3\pi$	21:33	0.061	0.075	0.149	0.000	0.045	0.030	0.060	0.030	0.090	0.075	0.060
Symbols	CWPV	5	$1\pi$	20:27	0.012	0.015	0.045	0.000	0.015	0.000	0.015	0.015	0.015	0.000	0.000
Symbols	CWPV	5	$2\pi$	23:41	0.014	0.015	0.045	0.000	0.000	0.000	0.000	0.030	0.030	0.015	0.000
Symbols	CWPV	5	$3\pi$	30:41	0.033	0.030	0.060	0.045	0.015	0.000	0.015	0.045	0.045	0.030	0.045
Symbols	CWPV	6	$1\pi$	2:49	0.009	0.000	0.015	0.015	0.000	0.000	0.015	0.015	0.015	0.015	0.000
Symbols	CWPV	6	$2\pi$	29:43	0.014	0.015	0.030	0.000	0.015	0.000	0.000	0.045	0.015	0.000	0.015
Symbols	CWPV	6	$3\pi$	38:49	0.042	0.015	0.090	0.045	0.045	0.015	0.060	0.045	0.060	0.030	0.015
Symbols	CWPV	7	$1\pi$	26:38	0.011	0.000	0.045	0.000	0.000	0.000	0.015	0.030	0.015	0.000	0.000
Symbols	CWPV	7	$2\pi$	34:57	0.008	0.000	0.045	0.000	0.000	0.000	0.015	0.015	0.000	0.000	0.000
Symbols	CWPV	7	$3\pi$	40:57	0.036	0.045	0.060	0.015	0.000	0.000	0.060	0.030	0.075	0.000	0.075
Symbols	CWED	1	$1\pi$	1:7	0.034	0.000	0.045	0.030	0.045	0.015	0.000	0.030	0.045	0.104	0.030
Symbols	CWED	1	$2\pi$	6:9	0.093	0.075	0.075	0.090	0.075	0.090	0.104	0.104	0.090	0.104	0.119
Symbols	CWED	1	$3\pi$	1:9	0.079	0.104	0.090	0.060	0.075	0.090	0.045	0.090	0.090	0.119	0.030
Symbols	CWED	2	$1\pi$	3:14	0.021	0.000	0.045	0.000	0.015	0.000	0.030	0.015	0.030	0.060	0.015
Symbols	CWED	2	$2\pi$	1:16	0.053	0.060	0.030	0.075	0.030	0.015	0.045	0.090	0.075	0.060	0.045
Symbols	CWED	2	$3\pi$	1:17	0.053	0.030	0.045	0.045	0.030	0.060	0.030	0.075	0.060	0.090	0.060
Symbols	CWED	3	$1\pi$	1:25	0.023	0.000	0.030	0.015	0.000	0.000	0.030	0.030	0.030	0.075	0.015
Symbols	CWED	3	$2\pi$	15:20	0.045	0.060	0.045	0.060	0.030	0.045	0.030	0.075	0.015	0.045	0.045
Symbols	CWED	3	$3\pi$	11:25	0.038	0.015	0.030	0.060	0.030	0.030	0.045	0.060	0.015	0.045	0.045
Symbols	CWED	4	$1\pi$	1:33	0.023	0.000	0.030	0.015	0.000	0.000	0.030	0.030	0.030	0.075	0.015
Symbols	CWED	4	$2\pi$	1:33	0.050	0.030	0.045	0.060	0.060	0.015	0.060	0.090	0.030	0.060	0.045
Symbols	CWED	4	$3\pi$	20:29	0.039	0.045	0.045	0.030	0.045	0.060	0.030	0.030	0.015	0.045	0.045
Symbols	CWED	5	$1\pi$	10:34	0.023	0.000	0.045	0.015	0.000	0.000	0.030	0.015	0.030	0.075	0.015
Symbols	CWED	5	$2\pi$	24:33	0.047	0.045	0.045	0.045	0.075	0.045	0.030	0.060	0.015	0.060	0.045
Symbols	CWED	5	$3\pi$	24:36	0.038	0.045	0.045	0.030	0.045	0.045	0.030	0.030	0.015	0.045	0.045
Symbols	CWED	6	$1\pi$	1:41	0.021	0.000	0.045	0.000	0.000	0.000	0.030	0.015	0.030	0.075	0.015
Symbols	CWED	6	$2\pi$	22:48	0.047	0.045	0.030	0.045	0.045	0.015	0.060	0.090	0.030	0.060	0.045
Symbols	CWED	6	$3\pi$	30:43	0.038	0.030	0.045	0.045	0.045	0.045	0.030	0.030	0.015	0.045	0.045
Symbols	CWED	7	$1\pi$	1:48	0.023	0.000	0.045	0.000	0.000	0.000	0.030	0.030	0.030	0.075	0.015
Symbols	CWED	7	$2\pi$	1:55	0.047	0.045	0.030	0.045	0.045	0.015	0.060	0.090	0.030	0.060	0.045
Symbols	CWED	7	$3\pi$	38:50	0.035	0.045	0.045	0.045	0.045	0.015	0.030	0.030	0.015	0.045	0.030



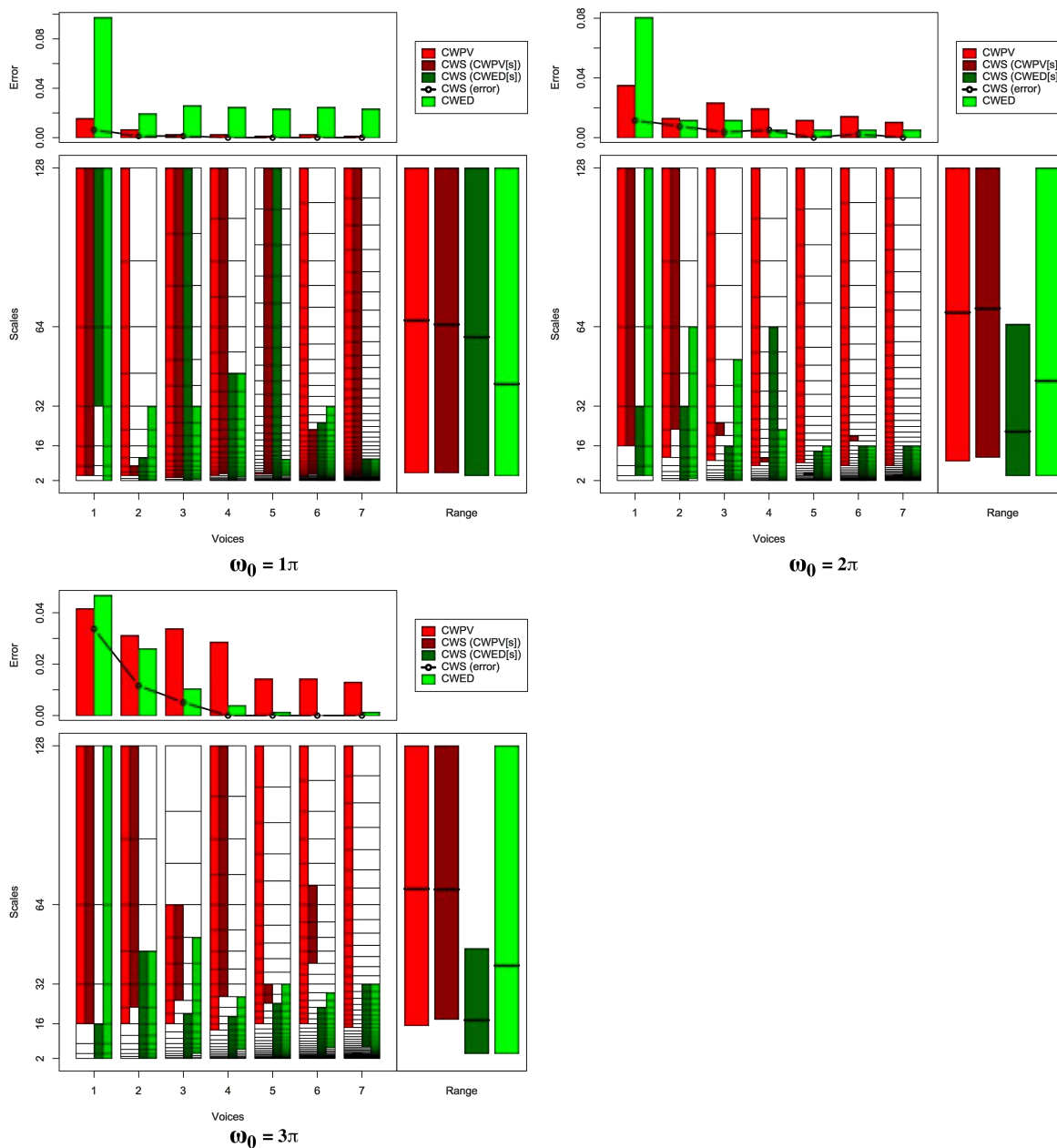


FIGURE B.36: Summary of results for the Two Lead ECG classification problem comparing CWS, CWPV, CWED methods using 1-7 voices and three  $\omega_0$  values. A lower CWPV score suggests that the problem is predominantly characterised by FM, whereas a lower CWED implies a predominant AM characteristic. The scale ranges have been translated from scale number to scale value. In the bottom right figure of each figure the average range of scales for all 7 voices are presented for each technique.



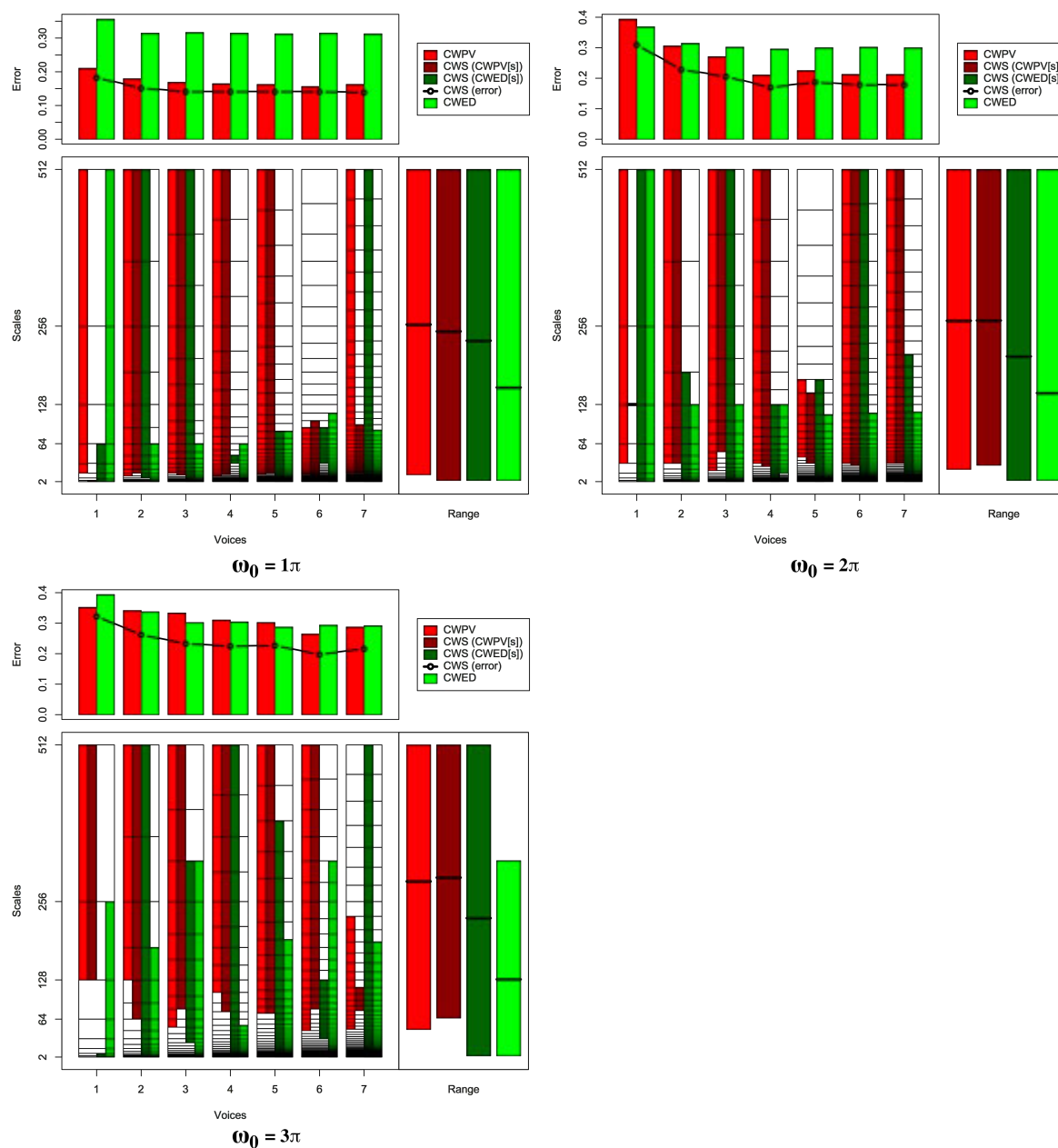


FIGURE B.37: Summary of results for the Word Synonyms classification problem comparing CWS, CWPV, CWED methods using 1-7 voices and three  $\omega_0$  values. A lower CWPV score suggests that the problem is predominantly characterised by FM, whereas a lower CWED implies a predominant AM characteristic. The scale ranges have been translated from scale number to scale value. In the bottom right figure of each figure the average range of scales for all 7 voices are presented for each technique.

TABLE B.37: Summary of results for the Word Synonyms classification problem comparing Ed, DTW, CWS, CWPV, and CWED using 1-7 voices and 3  $\omega_0$  parameters.  $S$  is the scale set(s) associated with the CWS, CWPV and CWED results. The mean values highlighted in bold are the best in model error rate for the problem.

Problem	Technique	Voices	$\omega_0$	$S$	Mean	1	2	3	4	5	6	7	7	9	10
Word Synonyms	Ed				0.202	0.146	0.292	0.208	0.208	0.188	0.146	0.229	0.188	0.229	0.188
Word Synonyms	DTW				0.183	0.188	0.208	0.229	0.146	0.208	0.167	0.188	0.125	0.125	0.250
Word Synonyms	CWS	1	$1\pi$	1:2,1:6	0.183	0.208	0.271	0.188	0.167	0.146	0.167	0.229	0.062	0.146	0.250
Word Synonyms	CWS	1	$2\pi$	6:6,1:9	0.310	0.292	0.354	0.333	0.292	0.271	0.333	0.333	0.271	0.354	0.271
Word Synonyms	CWS	1	$3\pi$	7:9,1:3	0.323	0.312	0.333	0.333	0.417	0.292	0.354	0.333	0.271	0.271	0.312
Word Synonyms	CWS	2	$1\pi$	7:17,5:17	0.152	0.229	0.250	0.146	0.125	0.083	0.146	0.167	0.104	0.125	0.146
Word Synonyms	CWS	2	$2\pi$	9:17,1:14	0.229	0.292	0.333	0.292	0.250	0.188	0.146	0.229	0.229	0.188	0.146
Word Synonyms	CWS	2	$3\pi$	11:17,1:17	0.263	0.271	0.333	0.292	0.271	0.229	0.250	0.208	0.229	0.271	0.271
Word Synonyms	CWS	3	$1\pi$	9:25,1:25	0.142	0.188	0.250	0.167	0.104	0.125	0.083	0.188	0.062	0.125	0.125
Word Synonyms	CWS	3	$2\pi$	15:25,1:25	0.206	0.229	0.250	0.271	0.188	0.188	0.208	0.229	0.125	0.208	0.167
Word Synonyms	CWS	3	$3\pi$	17:25,12:23	0.233	0.250	0.292	0.250	0.292	0.167	0.208	0.271	0.208	0.208	0.188
Word Synonyms	CWS	4	$1\pi$	12:33,17:19	0.142	0.208	0.229	0.146	0.125	0.125	0.104	0.188	0.083	0.125	0.083
Word Synonyms	CWS	4	$2\pi$	16:33,1:25	0.171	0.188	0.292	0.188	0.188	0.104	0.125	0.229	0.104	0.146	0.146
Word Synonyms	CWS	4	$3\pi$	22:33,1:33	0.225	0.208	0.292	0.229	0.208	0.146	0.229	0.188	0.250	0.250	0.250
Word Synonyms	CWS	5	$1\pi$	16:41,1:28	0.142	0.188	0.229	0.125	0.125	0.125	0.104	0.167	0.083	0.125	0.146
Word Synonyms	CWS	5	$2\pi$	21:32,1:33	0.188	0.250	0.292	0.188	0.167	0.125	0.125	0.208	0.146	0.167	0.208
Word Synonyms	CWS	5	$3\pi$	27:41,1:39	0.227	0.250	0.312	0.208	0.250	0.167	0.208	0.229	0.208	0.188	0.250
Word Synonyms	CWS	6	$1\pi$	16:35,25:34	0.142	0.208	0.208	0.167	0.125	0.146	0.083	0.188	0.062	0.104	0.125
Word Synonyms	CWS	6	$2\pi$	24:49,1:49	0.179	0.229	0.292	0.208	0.167	0.125	0.104	0.229	0.104	0.167	0.167
Word Synonyms	CWS	6	$3\pi$	33:49,25:37	0.198	0.229	0.250	0.208	0.208	0.146	0.167	0.167	0.146	0.250	0.208
Word Synonyms	CWS	7	$1\pi$	22:40,1:57	<b>0.140</b>	0.208	0.250	0.125	0.104	0.083	0.125	0.167	0.083	0.104	0.146
Word Synonyms	CWS	7	$2\pi$	29:57,1:48	0.179	0.208	0.271	0.188	0.188	0.125	0.083	0.229	0.167	0.167	0.167
Word Synonyms	CWS	7	$3\pi$	38:42,1:57	0.217	0.229	0.250	0.229	0.208	0.208	0.229	0.208	0.188	0.229	0.188
Word Synonyms	CWPV	1	$1\pi$	4:9	0.211	0.250	0.292	0.229	0.208	0.167	0.188	0.250	0.125	0.146	0.250
Word Synonyms	CWPV	1	$2\pi$	5:9	0.394	0.417	0.458	0.375	0.438	0.417	0.375	0.354	0.333	0.354	0.417
Word Synonyms	CWPV	1	$3\pi$	7:9	0.352	0.375	0.312	0.354	0.375	0.333	0.333	0.375	0.333	0.354	0.375
Word Synonyms	CWPV	2	$1\pi$	6:17	0.179	0.208	0.250	0.167	0.188	0.146	0.188	0.229	0.125	0.146	0.146
Word Synonyms	CWPV	2	$2\pi$	9:17	0.306	0.354	0.333	0.312	0.312	0.292	0.208	0.312	0.333	0.271	0.333
Word Synonyms	CWPV	2	$3\pi$	13:17	0.342	0.375	0.292	0.333	0.333	0.354	0.333	0.354	0.333	0.354	0.354
Word Synonyms	CWPV	3	$1\pi$	10:25	0.169	0.250	0.229	0.146	0.208	0.125	0.125	0.188	0.104	0.167	0.146
Word Synonyms	CWPV	3	$2\pi$	11:25	0.271	0.292	0.354	0.271	0.208	0.208	0.208	0.312	0.271	0.271	0.312
Word Synonyms	CWPV	3	$3\pi$	15:25	0.333	0.417	0.458	0.333	0.375	0.271	0.250	0.312	0.250	0.312	0.354
Word Synonyms	CWPV	4	$1\pi$	11:33	0.165	0.208	0.229	0.167	0.167	0.146	0.146	0.229	0.083	0.146	0.125
Word Synonyms	CWPV	4	$2\pi$	17:33	0.211	0.229	0.271	0.229	0.188	0.167	0.188	0.250	0.167	0.167	0.250
Word Synonyms	CWPV	4	$3\pi$	24:33	0.310	0.292	0.417	0.250	0.354	0.312	0.312	0.333	0.208	0.292	0.333
Word Synonyms	CWPV	5	$1\pi$	15:41	0.163	0.229	0.250	0.146	0.167	0.146	0.104	0.229	0.104	0.125	0.125
Word Synonyms	CWPV	5	$2\pi$	23:33	0.225	0.208	0.333	0.229	0.229	0.146	0.167	0.271	0.146	0.229	0.292
Word Synonyms	CWPV	5	$3\pi$	27:41	0.302	0.292	0.354	0.292	0.354	0.271	0.271	0.250	0.292	0.333	0.312
Word Synonyms	CWPV	6	$1\pi$	18:34	0.156	0.208	0.250	0.125	0.146	0.146	0.125	0.188	0.104	0.146	0.125
Word Synonyms	CWPV	6	$2\pi$	25:49	0.213	0.229	0.292	0.208	0.229	0.188	0.146	0.250	0.146	0.167	0.271
Word Synonyms	CWPV	6	$3\pi$	28:49	0.265	0.312	0.333	0.292	0.250	0.229	0.229	0.292	0.229	0.208	0.271
Word Synonyms	CWPV	7	$1\pi$	22:57	0.163	0.250	0.229	0.167	0.167	0.146	0.104	0.188	0.104	0.146	0.125
Word Synonyms	CWPV	7	$2\pi$	29:57	0.213	0.229	0.271	0.208	0.188	0.146	0.125	0.250	0.208	0.208	0.292
Word Synonyms	CWPV	7	$3\pi$	33:49	0.287	0.354	0.396	0.271	0.312	0.271	0.208	0.292	0.229	0.208	0.333
Word Synonyms	CWED	1	$1\pi$	1:9	0.356	0.375	0.312	0.375	0.312	0.375	0.375	0.375	0.333	0.375	0.354
Word Synonyms	CWED	1	$2\pi$	1:9	0.369	0.354	0.333	0.417	0.333	0.375	0.396	0.396	0.354	0.312	0.417
Word Synonyms	CWED	1	$3\pi$	1:8	0.394	0.438	0.396	0.438	0.458	0.417	0.354	0.312	0.375	0.354	0.396
Word Synonyms	CWED	2	$1\pi$	1:11	0.314	0.333	0.354	0.333	0.229	0.312	0.333	0.333	0.292	0.354	0.271
Word Synonyms	CWED	2	$2\pi$	1:13	0.315	0.292	0.354	0.312	0.292	0.292	0.396	0.312	0.354	0.292	0.250
Word Synonyms	CWED	2	$3\pi$	1:14	0.337	0.354	0.396	0.312	0.312	0.375	0.333	0.292	0.312	0.333	0.354
Word Synonyms	CWED	3	$1\pi$	1:16	0.317	0.312	0.354	0.292	0.292	0.312	0.354	0.333	0.292	0.333	0.292
Word Synonyms	CWED	3	$2\pi$	1:19	0.302	0.271	0.354	0.292	0.271	0.292	0.312	0.312	0.271	0.312	0.333
Word Synonyms	CWED	3	$3\pi$	1:23	0.302	0.271	0.375	0.333	0.333	0.250	0.312	0.250	0.292	0.312	0.292
Word Synonyms	CWED	4	$1\pi$	1:21	0.315	0.312	0.354	0.292	0.271	0.312	0.354	0.333	0.292	0.333	0.292
Word Synonyms	CWED	4	$2\pi$	13:25	0.296	0.292	0.333	0.312	0.250	0.271	0.292	0.333	0.292	0.271	0.312
Word Synonyms	CWED	4	$3\pi$	19:3	0.304	0.354	0.375	0.292	0.271	0.292	0.312	0.333	0.292	0.292	0.229
Word Synonyms	CWED	5	$1\pi$	1:28	0.313	0.333	0.375	0.271	0.292	0.292	0.312	0.333	0.292	0.375	0.250
Word Synonyms	CWED	5	$2\pi$	13:30	0.300	0.333	0.354	0.333	0.250	0.312	0.292	0.312	0.292	0.229	0.292
Word Synonyms	CWED	5	$3\pi$	1:34	0.287	0.271	0.354	0.312	0.271	0.312	0.292	0.312	0.229	0.250	0.271
Word Synonyms	CWED	6	$1\pi$	1:36	0.315	0.292	0.354	0.271	0.312	0.292	0.292	0.354	0.333	0.375	0.271
Word Synonyms	CWED	6	$2\pi$	1:36	0.302	0.375	0.354	0.333	0.250	0.312	0.292	0.312	0.292	0.229	0.271
Word Synonyms	CWED	6	$3\pi$	1:45	0.294	0.271	0.354	0.333	0.292	0.271	0.292	0.312	0.271	0.271	0.271
Word Synonyms	CWED	7	$1\pi$	1:39	0.313	0.333	0.375	0.271	0.292	0.292	0.312	0.333	0.292	0.375	0.250
Word Synonyms	CWED	7	$2\pi$	1:42	0.300	0.354	0.354	0.333	0.229	0.312	0.292	0.312	0.292	0.229	0.292
Word Synonyms	CWED	7	$3\pi$	1:47	0.292	0.292	0.354	0.312	0.271	0.312	0.292	0.333	0.250	0.250	0.250

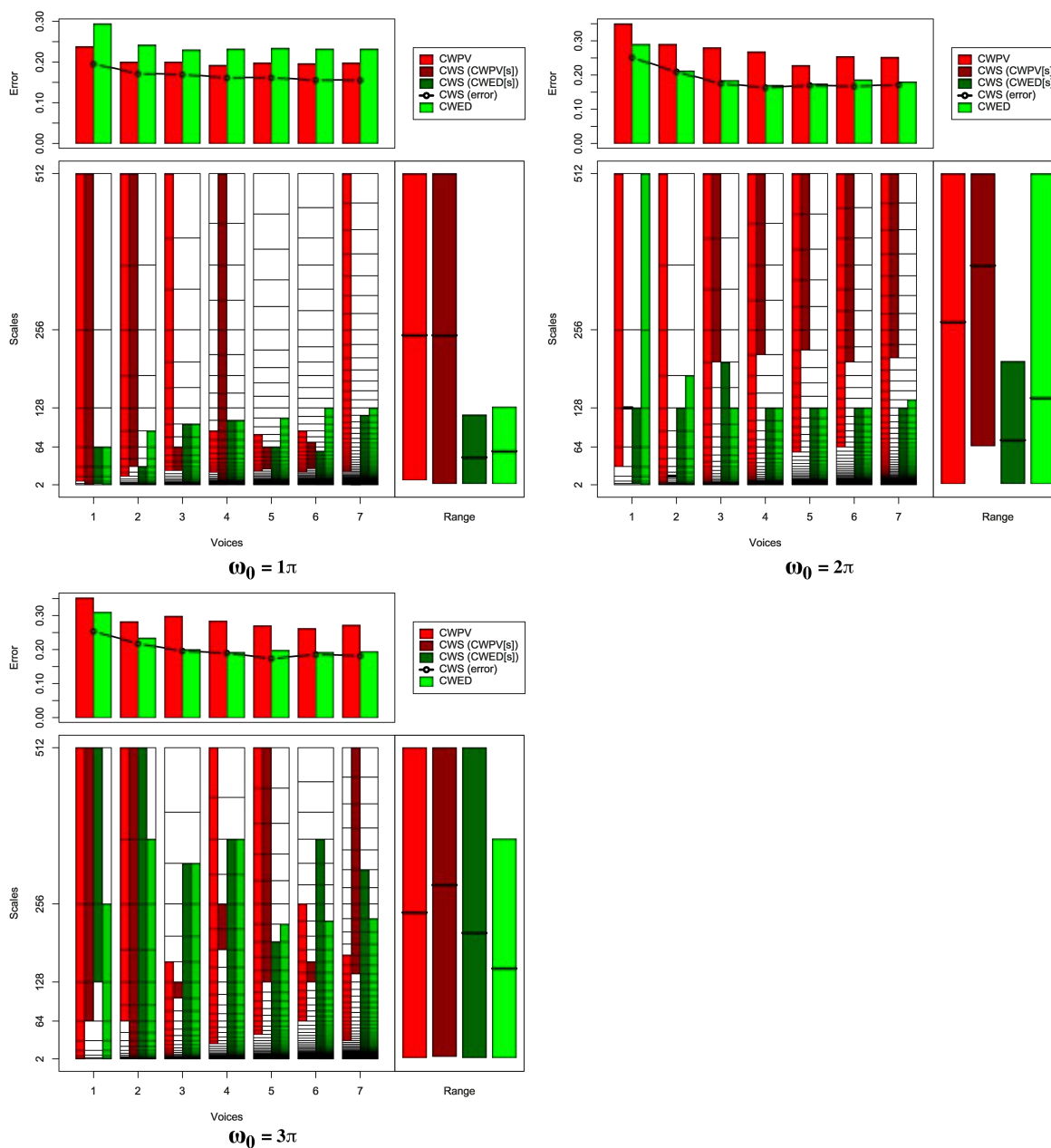


FIGURE B.38: Summary of results for the Cricket\_X classification problem comparing CWS, CWPV, CWED methods using 1-7 voices and three  $\omega_0$  values. A lower CWPV score suggests that the problem is predominantly characterised by FM, whereas a lower CWED implies a predominant AM characteristic. The scale ranges have been translated from scale number to scale value. In the bottom right figure of each figure the average range of scales for all 7 voices are presented for each technique.

TABLE B.38: Summary of results for the Cricket\_X classification problem comparing Ed, DTW, CWS, CWPV, and CWED using 1-7 voices and 3  $\omega_0$  parameters.  $S$  is the scale set(s) associated with the CWS, CWPV and CWED results. The mean values highlighted in bold are the best in model error rate for the problem.

Problem	Technique	Voices	$\omega_0$	$S$	Mean	1	2	3	4	5	6	7	7	9	10
Cricket_X	Ed				0.230	0.160	0.200	0.180	0.240	0.200	0.240	0.260	0.300	0.260	0.260
Cricket_X	DTW				<b>0.142</b>	0.160	0.140	0.160	0.140	0.200	0.160	0.120	0.160	0.080	0.100
Cricket_X	CWS	1	$1\pi$	1:9,2:6	0.196	0.120	0.220	0.200	0.180	0.160	0.240	0.280	0.220	0.200	0.140
Cricket_X	CWS	1	$2\pi$	6:6,2:7	0.252	0.240	0.240	0.240	0.260	0.220	0.340	0.280	0.260	0.220	0.220
Cricket_X	CWS	1	$3\pi$	6:9,7:9	0.254	0.140	0.220	0.260	0.280	0.220	0.300	0.300	0.260	0.280	0.280
Cricket_X	CWS	2	$1\pi$	9:17,1:9	0.172	0.140	0.160	0.160	0.220	0.120	0.160	0.220	0.180	0.180	0.180
Cricket_X	CWS	2	$2\pi$	12:12,3:13	0.210	0.220	0.180	0.120	0.240	0.240	0.200	0.280	0.220	0.200	0.200
Cricket_X	CWS	2	$3\pi$	3:17,1:17	0.218	0.160	0.200	0.240	0.180	0.320	0.240	0.180	0.180	0.240	0.240
Cricket_X	CWS	3	$1\pi$	12:16,1:18	0.170	0.140	0.120	0.140	0.200	0.180	0.160	0.200	0.220	0.160	0.180
Cricket_X	CWS	3	$2\pi$	21:25,1:21	0.176	0.200	0.220	0.160	0.220	0.120	0.160	0.180	0.140	0.160	0.200
Cricket_X	CWS	3	$3\pi$	18:19,1:23	0.196	0.120	0.140	0.180	0.260	0.180	0.200	0.260	0.260	0.200	0.160
Cricket_X	CWS	4	$1\pi$	1:33,3:24	0.162	0.100	0.160	0.200	0.140	0.160	0.200	0.220	0.180	0.160	0.100
Cricket_X	CWS	4	$2\pi$	28:33,1:25	0.164	0.180	0.180	0.160	0.160	0.120	0.140	0.200	0.120	0.240	0.140
Cricket_X	CWS	4	$3\pi$	27:29,1:31	0.190	0.200	0.220	0.160	0.240	0.080	0.180	0.320	0.160	0.160	0.180
Cricket_X	CWS	5	$1\pi$	20:26,4:26	0.162	0.120	0.120	0.100	0.200	0.140	0.180	0.180	0.200	0.220	0.160
Cricket_X	CWS	5	$2\pi$	35:41,2:31	0.170	0.180	0.160	0.160	0.160	0.140	0.160	0.200	0.140	0.280	0.120
Cricket_X	CWS	5	$3\pi$	31:41,1:34	0.174	0.120	0.140	0.200	0.240	0.100	0.240	0.240	0.200	0.140	0.120
Cricket_X	CWS	6	$1\pi$	24:32,1:30	0.156	0.120	0.120	0.120	0.220	0.120	0.200	0.180	0.160	0.160	0.160
Cricket_X	CWS	6	$2\pi$	41:49,8:37	0.168	0.160	0.200	0.140	0.220	0.140	0.180	0.180	0.120	0.200	0.140
Cricket_X	CWS	6	$3\pi$	37:39,1:46	0.186	0.140	0.180	0.200	0.220	0.100	0.180	0.280	0.200	0.200	0.160
Cricket_X	CWS	7	$1\pi$	33:33,1:42	0.156	0.200	0.200	0.140	0.160	0.120	0.160	0.140	0.140	0.120	0.180
Cricket_X	CWS	7	$2\pi$	48:57,5:43	0.172	0.200	0.180	0.160	0.180	0.160	0.160	0.220	0.120	0.220	0.120
Cricket_X	CWS	7	$3\pi$	44:57,7:52	0.182	0.200	0.220	0.180	0.220	0.160	0.200	0.260	0.180	0.120	0.080
Cricket_X	CWPV	1	$1\pi$	3:9	0.238	0.180	0.220	0.260	0.200	0.180	0.320	0.260	0.240	0.300	0.220
Cricket_X	CWPV	1	$2\pi$	5:9	0.350	0.320	0.320	0.300	0.320	0.340	0.420	0.400	0.400	0.320	0.360
Cricket_X	CWPV	1	$3\pi$	1:9	0.352	0.340	0.440	0.360	0.360	0.320	0.320	0.360	0.400	0.320	0.300
Cricket_X	CWPV	2	$1\pi$	7:17	0.200	0.160	0.180	0.160	0.180	0.200	0.220	0.240	0.240	0.220	0.200
Cricket_X	CWPV	2	$2\pi$	4:17	0.290	0.260	0.280	0.300	0.240	0.340	0.320	0.360	0.320	0.180	0.300
Cricket_X	CWPV	2	$3\pi$	11:17	0.282	0.240	0.300	0.240	0.280	0.280	0.300	0.320	0.300	0.300	0.260
Cricket_X	CWPV	3	$1\pi$	12:25	0.200	0.140	0.140	0.240	0.220	0.200	0.180	0.220	0.260	0.220	0.180
Cricket_X	CWPV	3	$2\pi$	4:25	0.280	0.240	0.300	0.280	0.320	0.320	0.280	0.320	0.280	0.180	0.280
Cricket_X	CWPV	3	$3\pi$	3:20	0.298	0.280	0.400	0.260	0.280	0.320	0.260	0.300	0.300	0.280	0.300
Cricket_X	CWPV	4	$1\pi$	15:23	0.192	0.160	0.160	0.180	0.200	0.180	0.180	0.180	0.260	0.240	0.180
Cricket_X	CWPV	4	$2\pi$	1:33	0.268	0.260	0.300	0.280	0.240	0.300	0.280	0.300	0.240	0.180	0.300
Cricket_X	CWPV	4	$3\pi$	16:33	0.284	0.280	0.260	0.260	0.240	0.260	0.280	0.320	0.300	0.320	0.320
Cricket_X	CWPV	5	$1\pi$	19:28	0.198	0.180	0.160	0.200	0.200	0.180	0.220	0.180	0.240	0.240	0.180
Cricket_X	CWPV	5	$2\pi$	25:41	0.228	0.140	0.180	0.280	0.300	0.240	0.280	0.240	0.220	0.200	0.200
Cricket_X	CWPV	5	$3\pi$	23:41	0.270	0.280	0.220	0.300	0.320	0.200	0.320	0.280	0.280	0.300	0.200
Cricket_X	CWPV	6	$1\pi$	22:34	0.196	0.180	0.160	0.180	0.200	0.180	0.220	0.200	0.220	0.240	0.180
Cricket_X	CWPV	6	$2\pi$	31:49	0.254	0.120	0.300	0.300	0.220	0.320	0.300	0.300	0.240	0.240	0.200
Cricket_X	CWPV	6	$3\pi$	31:43	0.262	0.240	0.280	0.220	0.240	0.260	0.300	0.280	0.300	0.260	0.240
Cricket_X	CWPV	7	$1\pi$	26:57	0.198	0.160	0.180	0.220	0.180	0.200	0.160	0.200	0.260	0.240	0.180
Cricket_X	CWPV	7	$2\pi$	17:57	0.252	0.220	0.220	0.260	0.240	0.240	0.260	0.260	0.320	0.220	0.280
Cricket_X	CWPV	7	$3\pi$	29:46	0.272	0.180	0.300	0.260	0.320	0.220	0.280	0.320	0.280	0.320	0.240
Cricket_X	CWED	1	$1\pi$	1:6	0.294	0.320	0.300	0.320	0.240	0.300	0.200	0.300	0.320	0.300	0.340
Cricket_X	CWED	1	$2\pi$	1:9	0.290	0.260	0.280	0.280	0.260	0.320	0.300	0.260	0.360	0.260	0.320
Cricket_X	CWED	1	$3\pi$	1:8	0.310	0.240	0.320	0.240	0.340	0.320	0.300	0.340	0.240	0.340	0.420
Cricket_X	CWED	2	$1\pi$	1:12	0.242	0.240	0.280	0.260	0.200	0.280	0.220	0.260	0.200	0.260	0.220
Cricket_X	CWED	2	$2\pi$	1:14	0.212	0.260	0.160	0.180	0.220	0.260	0.240	0.260	0.160	0.180	0.200
Cricket_X	CWED	2	$3\pi$	1:16	0.234	0.200	0.260	0.200	0.200	0.260	0.220	0.300	0.180	0.340	0.180
Cricket_X	CWED	3	$1\pi$	1:18	0.230	0.240	0.240	0.240	0.200	0.220	0.200	0.280	0.200	0.260	0.220
Cricket_X	CWED	3	$2\pi$	1:19	0.184	0.240	0.160	0.200	0.180	0.160	0.140	0.200	0.160	0.260	0.140
Cricket_X	CWED	3	$3\pi$	1:23	0.200	0.220	0.180	0.180	0.220	0.160	0.140	0.260	0.180	0.240	0.220
Cricket_X	CWED	4	$1\pi$	1:24	0.232	0.220	0.240	0.240	0.220	0.220	0.200	0.280	0.200	0.260	0.240
Cricket_X	CWED	4	$2\pi$	1:25	0.170	0.180	0.160	0.160	0.160	0.140	0.160	0.220	0.140	0.240	0.140
Cricket_X	CWED	4	$3\pi$	1:31	0.192	0.200	0.200	0.140	0.220	0.180	0.180	0.220	0.180	0.220	0.180
Cricket_X	CWED	5	$1\pi$	1:30	0.234	0.240	0.240	0.240	0.220	0.220	0.200	0.280	0.200	0.260	0.240
Cricket_X	CWED	5	$2\pi$	2:31	0.174	0.180	0.160	0.160	0.160	0.140	0.160	0.220	0.140	0.300	0.120
Cricket_X	CWED	5	$3\pi$	1:35	0.198	0.240	0.220	0.120	0.220	0.140	0.180	0.220	0.200	0.240	0.200
Cricket_X	CWED	6	$1\pi$	1:37	0.232	0.220	0.200	0.260	0.220	0.260	0.200	0.260	0.200	0.280	0.220
Cricket_X	CWED	6	$2\pi$	5:37	0.186	0.180	0.180	0.160	0.180	0.180	0.160	0.260	0.160	0.260	0.140
Cricket_X	CWED	6	$3\pi$	1:42	0.192	0.220	0.220	0.120	0.220	0.100	0.180	0.240	0.180	0.240	0.200
Cricket_X	CWED	7	$1\pi$	1:43	0.232	0.240	0.240	0.260	0.220	0.220	0.180	0.240	0.200	0.280	0.240
Cricket_X	CWED	7	$2\pi$	2:44	0.180	0.180	0.200	0.160	0.220	0.120	0.180	0.220	0.160	0.220	0.140
Cricket_X	CWED	7	$3\pi$	1:49	0.194	0.240	0.220	0.120	0.220	0.100	0.180	0.240	0.180	0.240	0.200

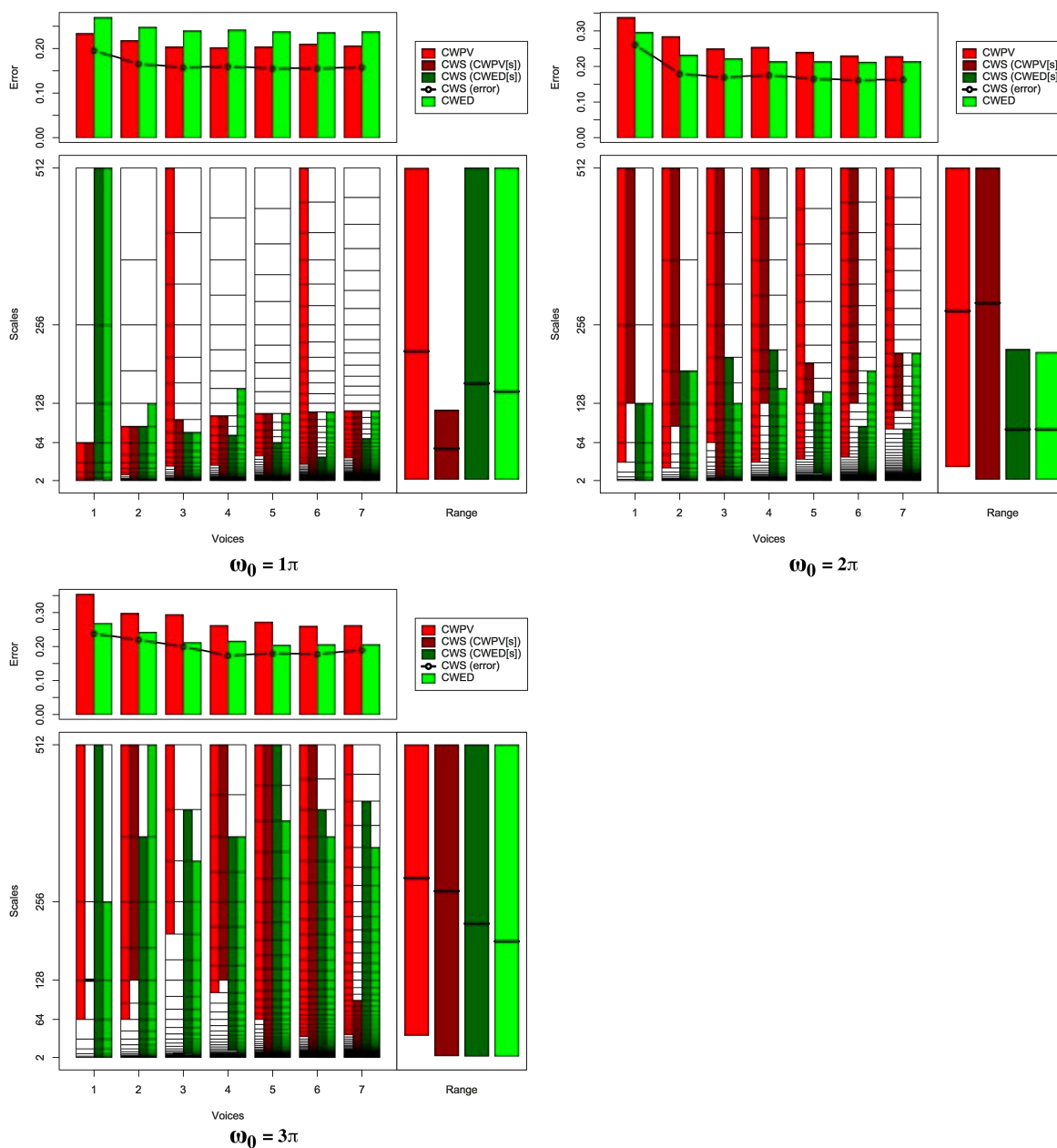


FIGURE B.39: Summary of results for the Cricket\_Y classification problem comparing CWS, CWPV, CWED methods using 1-7 voices and three  $\omega_0$  values. A lower CWPV score suggests that the problem is predominantly characterised by FM, whereas a lower CWED implies a predominant AM characteristic. The scale ranges have been translated from scale number to scale value. In the bottom right figure of each figure the average range of scales for all 7 voices are presented for each technique.

TABLE B.39: Summary of results for the Cricket\_Y classification problem comparing Ed, DTW, CWS, CWPV, and CWED using 1-7 voices and 3  $\omega_0$  parameters.  $S$  is the scale set(s) associated with the CWS, CWPV and CWED results. The mean values highlighted in bold are the best in model error rate for the problem.

Problem	Technique	Voices	$\omega_0$	$S$	Mean	1	2	3	4	5	6	7	7	9	10
Cricket_Y	Ed				0.200	0.120	0.220	0.200	0.200	0.160	0.220	0.200	0.220	0.200	0.260
Cricket_Y	DTW				0.178	0.220	0.160	0.240	0.160	0.160	0.160	0.180	0.180	0.140	0.180
Cricket_Y	CWS	1	$1\pi$	1:6,2:9	0.196	0.140	0.200	0.260	0.160	0.100	0.240	0.180	0.180	0.220	0.280
Cricket_Y	CWS	1	$2\pi$	7:9,1:7	0.262	0.240	0.280	0.340	0.200	0.360	0.200	0.240	0.220	0.260	0.280
Cricket_Y	CWS	1	$3\pi$	6:6,1:9	0.238	0.280	0.260	0.240	0.220	0.260	0.300	0.200	0.180	0.160	0.280
Cricket_Y	CWS	2	$1\pi$	2:12,1:12	0.166	0.120	0.180	0.160	0.120	0.080	0.240	0.140	0.140	0.220	0.260
Cricket_Y	CWS	2	$2\pi$	12:17,1:14	0.180	0.180	0.160	0.200	0.180	0.180	0.200	0.160	0.160	0.140	0.240
Cricket_Y	CWS	2	$3\pi$	13:17,1:16	0.220	0.180	0.220	0.220	0.180	0.260	0.240	0.220	0.240	0.180	0.260
Cricket_Y	CWS	3	$1\pi$	1:18,1:17	0.158	0.100	0.180	0.160	0.100	0.120	0.240	0.140	0.100	0.180	0.260
Cricket_Y	CWS	3	$2\pi$	1:25,4:21	0.170	0.160	0.200	0.140	0.180	0.160	0.180	0.140	0.120	0.200	0.220
Cricket_Y	CWS	3	$3\pi$	16:16,7:24	0.200	0.200	0.180	0.200	0.180	0.220	0.240	0.200	0.200	0.120	0.260
Cricket_Y	CWS	4	$1\pi$	1:24,1:22	0.160	0.140	0.200	0.160	0.100	0.080	0.240	0.140	0.100	0.180	0.260
Cricket_Y	CWS	4	$2\pi$	25:33,1:28	0.176	0.180	0.220	0.200	0.140	0.220	0.140	0.140	0.140	0.160	0.220
Cricket_Y	CWS	4	$3\pi$	25:33,12:31	0.174	0.100	0.220	0.200	0.160	0.160	0.180	0.200	0.160	0.180	0.180
Cricket_Y	CWS	5	$1\pi$	2:30,1:26	<b>0.156</b>	0.100	0.200	0.160	0.100	0.080	0.220	0.120	0.100	0.200	0.280
Cricket_Y	CWS	5	$2\pi$	31:34,15:31	0.166	0.180	0.160	0.200	0.160	0.160	0.160	0.160	0.120	0.140	0.220
Cricket_Y	CWS	5	$3\pi$	3:41,1:41	0.180	0.140	0.200	0.160	0.180	0.200	0.240	0.120	0.140	0.180	0.240
Cricket_Y	CWS	6	$1\pi$	2:36,1:27	<b>0.156</b>	0.120	0.200	0.140	0.100	0.120	0.200	0.160	0.100	0.200	0.220
Cricket_Y	CWS	6	$2\pi$	37:49,2:34	0.162	0.140	0.140	0.240	0.120	0.180	0.160	0.140	0.120	0.160	0.220
Cricket_Y	CWS	6	$3\pi$	4:49,1:47	0.178	0.160	0.200	0.180	0.180	0.160	0.220	0.160	0.120	0.160	0.240
Cricket_Y	CWS	7	$1\pi$	3:42,1:37	0.158	0.100	0.200	0.160	0.100	0.080	0.240	0.120	0.100	0.200	0.280
Cricket_Y	CWS	7	$2\pi$	42:48,4:39	0.164	0.120	0.180	0.200	0.200	0.160	0.140	0.160	0.100	0.200	0.180
Cricket_Y	CWS	7	$3\pi$	5:40,1:55	0.190	0.200	0.220	0.160	0.200	0.180	0.260	0.160	0.140	0.140	0.240
Cricket_Y	CWPV	1	$1\pi$	1:6	0.234	0.220	0.280	0.200	0.240	0.140	0.220	0.260	0.240	0.240	0.300
Cricket_Y	CWPV	1	$2\pi$	5:9	0.338	0.280	0.380	0.340	0.320	0.300	0.340	0.360	0.380	0.380	0.300
Cricket_Y	CWPV	1	$3\pi$	6:9	0.354	0.320	0.400	0.320	0.380	0.360	0.340	0.320	0.360	0.340	0.400
Cricket_Y	CWPV	2	$1\pi$	6:12	0.218	0.180	0.200	0.240	0.260	0.140	0.260	0.160	0.260	0.200	0.280
Cricket_Y	CWPV	2	$2\pi$	8:17	0.284	0.220	0.300	0.240	0.280	0.240	0.380	0.240	0.260	0.360	0.320
Cricket_Y	CWPV	2	$3\pi$	11:17	0.298	0.240	0.380	0.260	0.280	0.260	0.300	0.300	0.340	0.280	0.340
Cricket_Y	CWPV	3	$1\pi$	12:25	0.204	0.160	0.220	0.220	0.180	0.140	0.260	0.180	0.220	0.220	0.240
Cricket_Y	CWPV	3	$2\pi$	16:25	0.250	0.180	0.260	0.240	0.260	0.200	0.280	0.300	0.180	0.340	0.260
Cricket_Y	CWPV	3	$3\pi$	21:25	0.294	0.280	0.260	0.220	0.340	0.240	0.320	0.340	0.300	0.340	0.300
Cricket_Y	CWPV	4	$1\pi$	16:24	0.202	0.140	0.260	0.120	0.220	0.160	0.280	0.160	0.240	0.240	0.200
Cricket_Y	CWPV	4	$2\pi$	17:33	0.254	0.260	0.280	0.240	0.280	0.220	0.260	0.220	0.220	0.280	0.280
Cricket_Y	CWPV	4	$3\pi$	24:33	0.262	0.220	0.280	0.260	0.280	0.200	0.280	0.220	0.260	0.360	0.260
Cricket_Y	CWPV	5	$1\pi$	23:30	0.204	0.260	0.220	0.160	0.220	0.200	0.260	0.160	0.160	0.200	0.200
Cricket_Y	CWPV	5	$2\pi$	22:41	0.240	0.220	0.340	0.240	0.260	0.240	0.260	0.180	0.200	0.180	0.280
Cricket_Y	CWPV	5	$3\pi$	26:41	0.272	0.240	0.340	0.260	0.300	0.340	0.280	0.280	0.220	0.160	0.300
Cricket_Y	CWPV	6	$1\pi$	24:49	0.210	0.180	0.240	0.200	0.240	0.160	0.220	0.160	0.240	0.260	0.200
Cricket_Y	CWPV	6	$2\pi$	27:49	0.230	0.160	0.260	0.280	0.220	0.260	0.200	0.220	0.260	0.200	0.240
Cricket_Y	CWPV	6	$3\pi$	26:49	0.260	0.180	0.320	0.280	0.300	0.220	0.300	0.180	0.260	0.280	0.280
Cricket_Y	CWPV	7	$1\pi$	31:42	0.206	0.220	0.220	0.180	0.240	0.160	0.240	0.200	0.160	0.220	0.220
Cricket_Y	CWPV	7	$2\pi$	39:57	0.228	0.180	0.340	0.180	0.220	0.200	0.240	0.240	0.180	0.200	0.300
Cricket_Y	CWPV	7	$3\pi$	31:57	0.262	0.200	0.340	0.220	0.280	0.200	0.320	0.300	0.280	0.240	0.240
Cricket_Y	CWED	1	$1\pi$	1:9	0.270	0.260	0.300	0.320	0.260	0.260	0.320	0.220	0.280	0.200	0.280
Cricket_Y	CWED	1	$2\pi$	1:7	0.296	0.300	0.260	0.380	0.240	0.400	0.300	0.220	0.300	0.240	0.320
Cricket_Y	CWED	1	$3\pi$	1:8	0.268	0.320	0.280	0.200	0.240	0.320	0.300	0.200	0.260	0.280	0.280
Cricket_Y	CWED	2	$1\pi$	1:13	0.248	0.240	0.260	0.300	0.200	0.180	0.340	0.240	0.280	0.200	0.240
Cricket_Y	CWED	2	$2\pi$	1:14	0.232	0.200	0.240	0.280	0.200	0.240	0.260	0.240	0.220	0.180	0.260
Cricket_Y	CWED	2	$3\pi$	1:17	0.242	0.200	0.320	0.260	0.160	0.320	0.240	0.240	0.220	0.180	0.280
Cricket_Y	CWED	3	$1\pi$	6:17	0.240	0.180	0.240	0.260	0.160	0.200	0.320	0.240	0.220	0.240	0.340
Cricket_Y	CWED	3	$2\pi$	1:19	0.222	0.160	0.220	0.260	0.100	0.280	0.300	0.200	0.220	0.180	0.300
Cricket_Y	CWED	3	$3\pi$	1:23	0.212	0.200	0.200	0.240	0.200	0.200	0.260	0.140	0.220	0.220	0.240
Cricket_Y	CWED	4	$1\pi$	1:26	0.242	0.240	0.220	0.300	0.200	0.200	0.340	0.220	0.260	0.200	0.240
Cricket_Y	CWED	4	$2\pi$	1:26	0.214	0.200	0.240	0.260	0.120	0.240	0.240	0.180	0.200	0.180	0.280
Cricket_Y	CWED	4	$3\pi$	1:31	0.216	0.220	0.220	0.240	0.160	0.320	0.260	0.160	0.200	0.140	0.240
Cricket_Y	CWED	5	$1\pi$	8:30	0.238	0.180	0.260	0.280	0.160	0.200	0.380	0.200	0.220	0.180	0.320
Cricket_Y	CWED	5	$2\pi$	1:32	0.214	0.200	0.240	0.260	0.120	0.240	0.240	0.200	0.180	0.160	0.300
Cricket_Y	CWED	5	$3\pi$	1:39	0.204	0.180	0.200	0.240	0.160	0.260	0.220	0.180	0.180	0.160	0.260
Cricket_Y	CWED	6	$1\pi$	9:36	0.236	0.180	0.240	0.280	0.160	0.200	0.380	0.200	0.220	0.180	0.320
Cricket_Y	CWED	6	$2\pi$	1:40	0.212	0.180	0.240	0.260	0.120	0.240	0.240	0.200	0.180	0.160	0.300
Cricket_Y	CWED	6	$3\pi$	1:46	0.206	0.180	0.220	0.260	0.160	0.280	0.240	0.160	0.200	0.120	0.240
Cricket_Y	CWED	7	$1\pi$	10:42	0.238	0.180	0.240	0.280	0.160	0.200	0.380	0.200	0.240	0.180	0.320
Cricket_Y	CWED	7	$2\pi$	1:48	0.214	0.200	0.240	0.260	0.120	0.240	0.240	0.180	0.200	0.160	0.300
Cricket_Y	CWED	7	$3\pi$	1:53	0.206	0.180	0.200	0.260	0.160	0.280	0.240	0.200	0.180	0.120	0.240



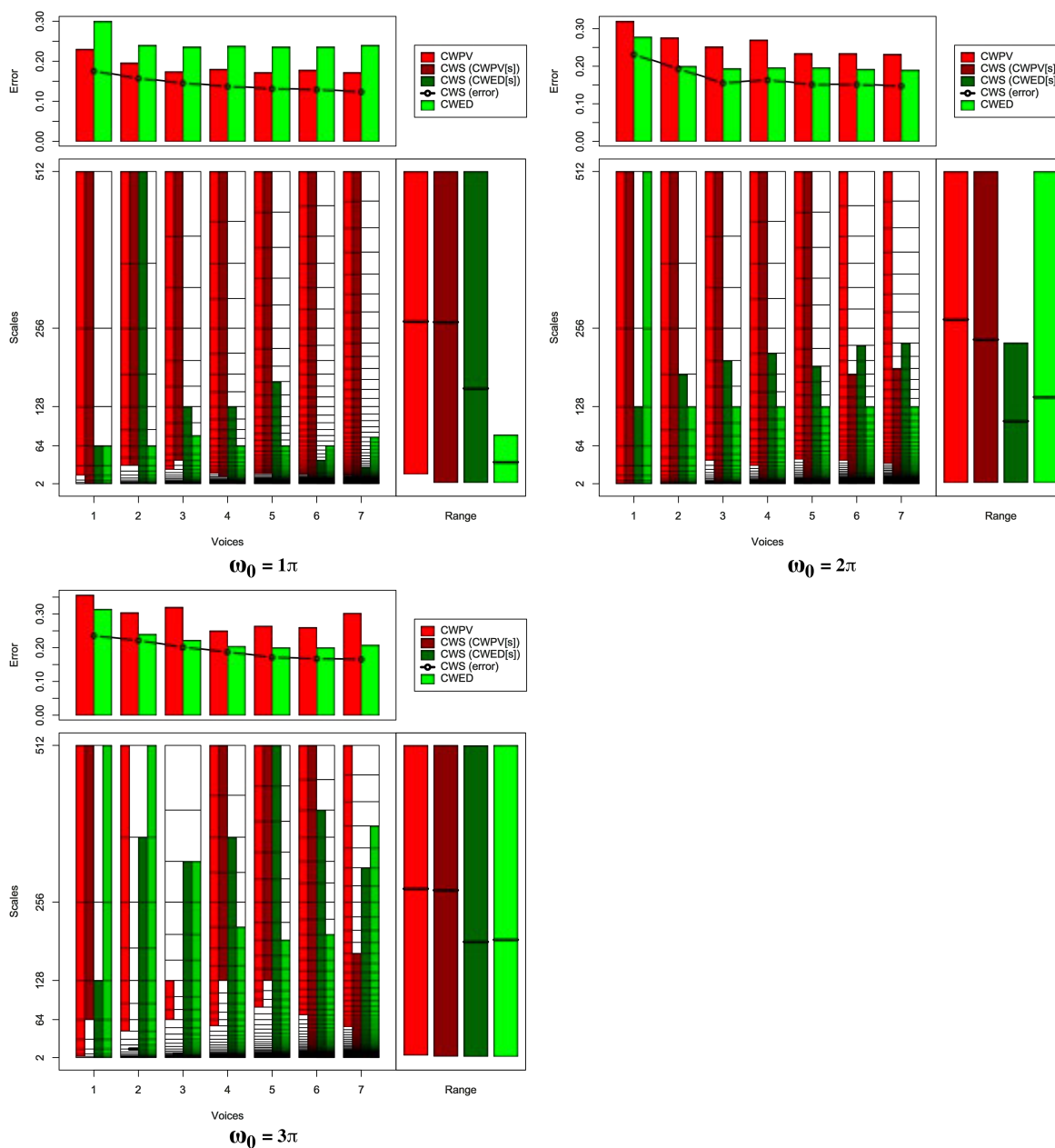


FIGURE B.40: Summary of results for the Cricket\_Z classification problem comparing CWS, CWPV, CWED methods using 1-7 voices and three  $\omega_0$  values. A lower CWPV score suggests that the problem is predominantly characterised by FM, whereas a lower CWED implies a predominant AM characteristic. The scale ranges have been translated from scale number to scale value. In the bottom right figure of each figure the average range of scales for all 7 voices are presented for each technique.

TABLE B.40: Summary of results for the Cricket\_Z classification problem comparing Ed, DTW, CWS, CWPV, and CWED using 1-7 voices and 3  $\omega_0$  parameters.  $S$  is the scale set(s) associated with the CWS, CWPV and CWED results. The mean values highlighted in bold are the best in model error rate for the problem.

Problem	Technique	Voices	$\omega_0$	$S$	Mean	1	2	3	4	5	6	7	7	9	10
Cricket_Z	Ed				0.220	0.220	0.240	0.220	0.200	0.320	0.200	0.260	0.160	0.200	0.180
Cricket_Z	DTW				0.134	0.140	0.200	0.120	0.120	0.200	0.160	0.080	0.120	0.100	0.100
Cricket_Z	CWS	1	$1\pi$	1:9,1:6	0.176	0.200	0.200	0.180	0.160	0.200	0.180	0.140	0.180	0.180	0.140
Cricket_Z	CWS	1	$2\pi$	1:9,1:7	0.232	0.280	0.260	0.140	0.260	0.220	0.280	0.240	0.160	0.280	0.200
Cricket_Z	CWS	1	$3\pi$	6:9,1:7	0.236	0.240	0.260	0.200	0.200	0.280	0.280	0.220	0.300	0.260	0.120
Cricket_Z	CWS	2	$1\pi$	9:17,3:17	0.158	0.220	0.180	0.200	0.100	0.220	0.120	0.100	0.160	0.180	0.100
Cricket_Z	CWS	2	$2\pi$	1:17,1:14	0.194	0.180	0.200	0.160	0.200	0.200	0.260	0.200	0.180	0.200	0.160
Cricket_Z	CWS	2	$3\pi$	13:13,1:16	0.222	0.180	0.220	0.200	0.240	0.240	0.260	0.160	0.260	0.280	0.180
Cricket_Z	CWS	3	$1\pi$	14:25,1:19	0.146	0.180	0.240	0.120	0.140	0.160	0.140	0.120	0.120	0.140	0.100
Cricket_Z	CWS	3	$2\pi$	1:25,4:21	0.156	0.140	0.200	0.160	0.160	0.180	0.180	0.140	0.120	0.140	0.140
Cricket_Z	CWS	3	$3\pi$	19:19,1:23	0.202	0.160	0.180	0.180	0.200	0.260	0.260	0.120	0.240	0.320	0.100
Cricket_Z	CWS	4	$1\pi$	12:33,3:25	0.138	0.120	0.180	0.100	0.180	0.160	0.160	0.080	0.160	0.100	0.140
Cricket_Z	CWS	4	$2\pi$	1:33,1:28	0.164	0.160	0.200	0.160	0.100	0.200	0.200	0.160	0.160	0.180	0.120
Cricket_Z	CWS	4	$3\pi$	25:33,1:31	0.188	0.200	0.280	0.220	0.180	0.240	0.220	0.100	0.140	0.200	0.100
Cricket_Z	CWS	5	$1\pi$	17:41,1:33	0.132	0.100	0.180	0.060	0.140	0.200	0.180	0.080	0.120	0.120	0.140
Cricket_Z	CWS	5	$2\pi$	1:41,7:34	0.152	0.140	0.180	0.160	0.100	0.200	0.180	0.160	0.120	0.140	0.140
Cricket_Z	CWS	5	$3\pi$	31:41,5:41	0.172	0.200	0.160	0.200	0.180	0.220	0.140	0.120	0.180	0.220	0.100
Cricket_Z	CWS	6	$1\pi$	17:49,1:27	0.130	0.120	0.180	0.060	0.180	0.180	0.160	0.100	0.140	0.100	0.080
Cricket_Z	CWS	6	$2\pi$	1:40,5:42	0.152	0.140	0.160	0.160	0.100	0.200	0.160	0.140	0.160	0.160	0.140
Cricket_Z	CWS	6	$3\pi$	3:49,1:47	0.168	0.160	0.200	0.160	0.140	0.200	0.200	0.140	0.160	0.160	0.160
Cricket_Z	CWS	7	$1\pi$	20:57,1:28	<b>0.124</b>	0.120	0.160	0.060	0.140	0.180	0.160	0.080	0.120	0.120	0.100
Cricket_Z	CWS	7	$2\pi$	1:47,1:49	0.148	0.140	0.160	0.160	0.100	0.200	0.160	0.160	0.140	0.120	0.140
Cricket_Z	CWS	7	$3\pi$	2:46,9:52	0.166	0.120	0.240	0.160	0.180	0.200	0.180	0.120	0.120	0.220	0.120
Cricket_Z	CWPV	1	$1\pi$	4:9	0.230	0.240	0.240	0.200	0.200	0.240	0.240	0.200	0.240	0.300	0.200
Cricket_Z	CWPV	1	$2\pi$	1:9	0.320	0.340	0.360	0.300	0.300	0.300	0.340	0.340	0.280	0.380	0.260
Cricket_Z	CWPV	1	$3\pi$	2:9	0.356	0.440	0.460	0.340	0.420	0.320	0.320	0.300	0.320	0.360	0.280
Cricket_Z	CWPV	2	$1\pi$	9:17	0.196	0.240	0.200	0.180	0.180	0.280	0.200	0.140	0.200	0.220	0.120
Cricket_Z	CWPV	2	$2\pi$	1:17	0.276	0.300	0.280	0.220	0.300	0.260	0.300	0.260	0.280	0.320	0.240
Cricket_Z	CWPV	2	$3\pi$	10:17	0.304	0.360	0.260	0.340	0.280	0.320	0.280	0.280	0.340	0.360	0.220
Cricket_Z	CWPV	3	$1\pi$	12:25	0.174	0.180	0.220	0.060	0.200	0.240	0.180	0.140	0.180	0.220	0.120
Cricket_Z	CWPV	3	$2\pi$	14:25	0.252	0.260	0.180	0.220	0.280	0.340	0.220	0.200	0.220	0.340	0.260
Cricket_Z	CWPV	3	$3\pi$	16:19	0.320	0.300	0.280	0.300	0.360	0.320	0.360	0.300	0.280	0.380	0.320
Cricket_Z	CWPV	4	$1\pi$	14:33	0.180	0.200	0.240	0.060	0.220	0.200	0.200	0.120	0.200	0.200	0.160
Cricket_Z	CWPV	4	$2\pi$	17:33	0.270	0.220	0.280	0.280	0.280	0.300	0.280	0.260	0.260	0.320	0.220
Cricket_Z	CWPV	4	$3\pi$	20:33	0.250	0.260	0.260	0.200	0.300	0.280	0.280	0.200	0.300	0.260	0.160
Cricket_Z	CWPV	5	$1\pi$	17:41	0.172	0.200	0.240	0.060	0.200	0.200	0.180	0.160	0.180	0.180	0.120
Cricket_Z	CWPV	5	$2\pi$	23:41	0.234	0.200	0.240	0.200	0.260	0.300	0.260	0.180	0.240	0.280	0.180
Cricket_Z	CWPV	5	$3\pi$	28:41	0.264	0.340	0.260	0.260	0.240	0.280	0.240	0.280	0.220	0.280	0.240
Cricket_Z	CWPV	6	$1\pi$	20:49	0.178	0.220	0.240	0.060	0.200	0.200	0.200	0.160	0.180	0.180	0.140
Cricket_Z	CWPV	6	$2\pi$	27:49	0.234	0.200	0.220	0.200	0.240	0.260	0.300	0.180	0.300	0.280	0.160
Cricket_Z	CWPV	6	$3\pi$	32:49	0.260	0.180	0.260	0.220	0.260	0.340	0.320	0.220	0.240	0.340	0.220
Cricket_Z	CWPV	7	$1\pi$	22:57	0.172	0.200	0.200	0.040	0.220	0.200	0.200	0.140	0.180	0.220	0.120
Cricket_Z	CWPV	7	$2\pi$	30:57	0.232	0.200	0.220	0.220	0.280	0.240	0.260	0.140	0.280	0.300	0.180
Cricket_Z	CWPV	7	$3\pi$	34:57	0.302	0.240	0.280	0.300	0.380	0.340	0.340	0.220	0.320	0.360	0.240
Cricket_Z	CWED	1	$1\pi$	1:6	0.300	0.320	0.300	0.280	0.320	0.240	0.340	0.240	0.360	0.380	0.220
Cricket_Z	CWED	1	$2\pi$	1:9	0.278	0.240	0.260	0.200	0.300	0.320	0.280	0.260	0.280	0.340	0.300
Cricket_Z	CWED	1	$3\pi$	1:9	0.314	0.180	0.400	0.360	0.340	0.300	0.320	0.260	0.400	0.320	0.260
Cricket_Z	CWED	2	$1\pi$	1:11	0.240	0.200	0.280	0.200	0.260	0.300	0.260	0.180	0.280	0.260	0.180
Cricket_Z	CWED	2	$2\pi$	1:13	0.200	0.160	0.220	0.140	0.260	0.240	0.300	0.140	0.160	0.200	0.180
Cricket_Z	CWED	2	$3\pi$	3:17	0.240	0.180	0.240	0.200	0.300	0.240	0.280	0.260	0.260	0.220	0.220
Cricket_Z	CWED	3	$1\pi$	1:17	0.236	0.220	0.260	0.180	0.260	0.300	0.240	0.200	0.240	0.280	0.180
Cricket_Z	CWED	3	$2\pi$	1:19	0.194	0.200	0.220	0.120	0.220	0.280	0.220	0.140	0.180	0.180	0.180
Cricket_Z	CWED	3	$3\pi$	1:23	0.222	0.220	0.260	0.160	0.260	0.280	0.260	0.160	0.200	0.260	0.160
Cricket_Z	CWED	4	$1\pi$	1:21	0.238	0.240	0.280	0.200	0.240	0.300	0.240	0.200	0.240	0.260	0.180
Cricket_Z	CWED	4	$2\pi$	1:25	0.196	0.200	0.220	0.140	0.220	0.280	0.220	0.180	0.140	0.160	0.200
Cricket_Z	CWED	4	$3\pi$	1:28	0.204	0.180	0.200	0.140	0.220	0.280	0.240	0.140	0.220	0.240	0.180
Cricket_Z	CWED	5	$1\pi$	1:26	0.236	0.240	0.280	0.200	0.240	0.280	0.240	0.200	0.240	0.260	0.180
Cricket_Z	CWED	5	$2\pi$	1:31	0.196	0.200	0.220	0.140	0.220	0.280	0.200	0.180	0.160	0.160	0.200
Cricket_Z	CWED	5	$3\pi$	4:34	0.200	0.200	0.180	0.120	0.220	0.260	0.260	0.140	0.200	0.220	0.200
Cricket_Z	CWED	6	$1\pi$	1:31	0.236	0.240	0.280	0.200	0.240	0.280	0.240	0.200	0.240	0.260	0.180
Cricket_Z	CWED	6	$2\pi$	3:37	0.192	0.200	0.200	0.140	0.220	0.260	0.200	0.160	0.180	0.160	0.200
Cricket_Z	CWED	6	$3\pi$	1:41	0.200	0.180	0.220	0.120	0.200	0.280	0.240	0.140	0.200	0.240	0.180
Cricket_Z	CWED	7	$1\pi$	2:38	0.240	0.240	0.280	0.200	0.240	0.300	0.260	0.200	0.240	0.260	0.180
Cricket_Z	CWED	7	$2\pi$	1:43	0.190	0.200	0.200	0.140	0.240	0.260	0.200	0.160	0.160	0.160	0.180
Cricket_Z	CWED	7	$3\pi$	1:54	0.208	0.180	0.180	0.180	0.240	0.280	0.220	0.180	0.180	0.240	0.200



## Experiment two summary of the training and test results

### **C.1 Summary of the CWS, CWPV, and CWED training and test results**

A Summary of the results for training and testing from experiment two (using 1 - 7 voices and three central frequency parameters) for each classification problem using the CWS, CWPV and CWED methods are presented in Tables C.1–C.2 (p. 239 to 244) below. The tables are structured to show a summary of all the parameters that yielded the best results for each problem. There are three parameter columns per technique which total

nine parameter columns (CWS  $1\pi$ , CWS  $2\pi$ , CWS  $3\pi$ , CWPV  $1\pi$ , CWPV  $2\pi$ , CWPV  $3\pi$ , CWED  $1\pi$ , CWED  $2\pi$  and CWED  $3\pi$ ). In instances where more than one voice parameter returned the same train error – the value, voice number and scale ranges are given. Table C.1 provides a crucial lookup to select the parameters (central frequency, voice number and scale ranges) to use for model testing. As it was not possible to discriminate between identical train results, a detailed summary of the test results is also provided in the same format. For both model training and testing 10-fold cross-validation was used.

TABLE C.1: Summary of parameters according to the results presented in Table 6.5 (p. 120) according to different central frequency parameters ( $1\pi$ ,  $2\pi$ , and  $3\pi$ ) and different voice resolutions (1–7) for the CWS, CWPV, and CWED techniques. The parameters are given as the voice resolution followed by the scale ranges for each technique in brackets.

Problem	CWS $1\pi$	CWS $2\pi$	CWS $3\pi$	CWPV $1\pi$	CWPV $2\pi$	CWPV $3\pi$	CWED $1\pi$	CWED $2\pi$	CWED $3\pi$
Synthetic Control	0.005 [7](17:36,1:36)			0.044 [7](15:25)				0.300 [7](12:35)	
Synthetic Control	0.005 [4](11:21,6:21)			0.044 [6](13:31)				0.177 [6](10:31)	
Synthetic Control								0.177 [5](9:26)	
Synthetic Control								0.177 [4](9:21)	
Gun Point	0.000 [7](10:50,1:50)	0.000 [7](27:29,1:50)	0.000 [5](22:22,1:29)	0.000 [7](9:25)				0.085 [7](1:34)	
Gun Point	0.000 [6](8:43,1:43)	0.000 [6](22:24,1:43)		0.000 [6](9:20)				0.008 [5](1:25)	
Gun Point	0.000 [5](8:36,1:36)	0.000 [5](19:19,1:36)		0.000 [5](7:18)				0.008 [4](1:19)	
Gun Point	0.000 [4](6:29,1:29)	0.000 [4](19:19,1:20)		0.000 [4](6:14)					
Gun Point	0.000 [3](6:11,1:22)	0.000 [3](12:13,1:22)		0.000 [2](6:15)					
Gun Point	0.000 [2](4:15,1:15)								
CBF	0.000 [7](22:43,1:43)	0.000 [7](28:43,1:43)	0.000 [7](32:43,1:43)	0.000 [4](14:25)	0.000 [6](25:37)	0.000 [7](33:43)		0.152 [4](12:25)	
CBF	0.000 [6](19:37,1:37)	0.000 [6](25:37,1:37)	0.000 [6](28:37,1:37)			0.000 [6](28:37)			
CBF	0.000 [5](16:31,1:31)	0.000 [5](19:31,1:31)	0.000 [5](23:31,1:31)			0.000 [5](24:31)			
CBF	0.000 [4](13:25,1:25)	0.000 [4](16:25,1:25)	0.000 [4](17:25,1:25)						
CBF	0.000 [3](10:19,1:19)	0.000 [3](12:19,1:19)	0.000 [3](17:19,1:19)						
CBF	0.000 [2](8:13,1:13)			0.017 [7](11:50)					0.053 [5](1:36)
Face (all)	0.013 [7](11:50,3:5)								
Face (all)	0.013 [6](11:24,3:9)								
Face (all)	0.013 [5](10:17,3:9)								
OSU Leaf									
OSU Leaf		0.115 [7](7:57,1:47)		0.159 [5](4:34)					0.126 [5](1:40)
Swedish Leaf	0.034 [7](26:32,1:26)			0.159 [2](1:17)					
Swedish Leaf				0.052 [6](5:37)					0.049 [5](1:25)
50words				0.052 [3](6:19)					0.049 [4](1:20)
Trace	0.148 [5](16:29,1:26)			0.161 [7](22:44)					0.337 [6](19:45)
Trace	0.000 [7](4:17,1:57)	0.000 [7](47:57,1:35)	0.000 [7](46:57,1:29)			0.033 [6](28:29)	0.117 [7](1:36)	0.134 [7](1:28)	
Trace	0.000 [6](3:15,1:49)	0.000 [6](37:49,1:29)	0.000 [5](32:41,1:23)				0.000 [6](1:31)	0.000 [4](1:20)	
Trace	0.000 [5](20:21,1:41)	0.000 [5](31:41,1:23)	0.000 [3](18:18,6:17)				0.000 [5](1:26)		
Trace	0.000 [4](15:17,1:33)	0.000 [4](25:33,1:20)					0.000 [4](1:20)		
Trace	0.000 [3](17:25,1:15)	0.000 [3](19:25,1:15)					0.000 [3](1:15)		
Trace	0.000 [2](12:17,1:10)	0.000 [2](13:17,1:8)					0.000 [2](1:10)		
Trace	0.000 [1](6:9,1:3)						0.000 [1](1:3)		
Two Patterns	0.006 [7](18:43,32:32)			0.009 [7](18:43)				0.294 [7](25:34)	
Two Patterns	0.006 [6](15:37,22:31)			0.009 [6](14:37)					
Two Patterns				0.009 [5](13:24)					
Wafer	0.000 [7](1:50,1:50)	0.000 [7](1:50,1:50)	0.000 [7](4:50,1:50)	0.000 [7](1:50)	0.000 [7](1:50)	0.000 [7](3:50)		0.002 [7](11:50)	0.004 [7](1:50)
Wafer	0.000 [6](1:43,1:43)	0.000 [6](1:43,1:43)	0.000 [6](4:43,1:43)	0.000 [6](1:43)	0.000 [6](1:43)	0.000 [6](1:43)		0.001 [6](9:43)	0.001 [6](1:43)

Continued on next page

Table C.1 – continued from previous page

Problem	CWS 1 $\pi$	CWS 2 $\pi$	CWS 3 $\pi$	CWVPV 1 $\pi$	CWVPV 2 $\pi$	CWVPV 3 $\pi$	CWED 1 $\pi$	CWED 2 $\pi$	CWED 3 $\pi$
Wafer	0.000 [5](1:36,1:36)	0.000 [5](1:36,1:36)	0.000 [5](1:36,1:35)	0.000 [5](1:36)	0.000 [5](1:36)	0.000 [5](4:36)		0.001 [5](8:36)	0.001 [5](6:36)
Wafer	0.000 [4](1:29,1:29)	0.000 [4](1:29,1:29)	0.000 [4](3:29,1:29)	0.000 [4](1:29)	0.000 [4](1:29)	0.000 [4](3:29)		0.001 [4](6:29)	0.001 [4](10:29)
Wafer	0.000 [3](1:22,1:22)	0.000 [3](1:22,1:22)	0.000 [3](1:22,1:22)	0.000 [3](1:22)	0.000 [3](1:22)	0.000 [3](1:22)			
Wafer	0.000 [2](1:15,1:15)	0.000 [2](1:15,1:15)	0.000 [2](2:15,10:14)	0.000 [2](1:15)	0.000 [2](1:15)				
Wafer	0.000 [1](1:8,1:8)			0.000 [1](1:8)					
Face (four)	0.000 [7](9:57,1:9)	0.000 [7](29:34,1:57)	0.000 [7](27:28,39:57)	0.000 [7](9:57)	0.000 [7](25:36)	0.000 [4](16:19)	0.014 [7](1:57)		0.072 [6](1:36)
Face (four)	0.000 [6](7:49,23:25)	0.000 [6](25:29,1:49)	0.000 [6](24:28,8:11)	0.000 [6](10:37)	0.000 [6](22:31)		0.072 [6](1:49)		0.072 [4](15:33)
Face (four)	0.000 [5](7:41,19:20)	0.000 [5](21:24,1:41)	0.000 [4](16:19,4:10)	0.000 [5](8:31)	0.000 [5](19:26)		0.072 [5](1:41)		
Face (four)	0.000 [4](5:33,16:17)	0.000 [4](16:20,1:33)		0.000 [4](9:24)	0.000 [4](15:22)		0.072 [4](1:33)		
Face (four)	0.000 [3](5:25,1:3)	0.000 [3](12:16,1:7)		0.000 [3](6:18)	0.000 [3](13:16)		0.072 [3](1:25)		
Face (four)	0.000 [2](4:8,1:10)	0.000 [2](8:11,4:9)		0.000 [2](4:6)			0.072 [2](2:13)		
Face (four)	0.000 [1](4:4,1:5)								
Lightning2		0.057 [7](13:19,17:42)	0.057 [7](12:25,16:44)	0.114 [7](2:12)			0.186 [7](1:49)	0.243 [7](12:50)	0.186 [7](1:50)
Lightning2		0.057 [6](12:16,15:36)	0.057 [6](12:16,15:36)	0.114 [6](1:10)			0.129 [6](1:42)	0.129 [2](5:14)	0.129 [6](2:43)
Lightning2			0.057 [5](7:16,17:29)	0.114 [4](2:7)			0.129 [5](1:35)		0.129 [5](1:36)
Lightning2							0.129 [4](1:28)		
Lightning2							0.129 [3](1:20)		
Lightning2							0.129 [2](1:14)		
Lightning7		0.088 [6](37:49,13:14)		0.163 [7](36:39)	0.163 [4](18:27)	0.163 [7](30:39)			0.188 [2](1:16)
Lightning7				0.163 [6](29:49)		0.163 [6](36:44)			
Lightning7				0.163 [5](26:28)					
ECG200	0.008 [5](10:10,3:5)	0.008 [7](21:22,28:39)	0.008 [6](21:21,14:17)	0.015 [7](13:15)					0.062 [6](5:16)
Adiac	0.108 [7](22:22,1:16)			0.131 [7](12:37)					0.119 [6](1:33)
Adiac	0.108 [6](19:19,1:10)			0.131 [5](9:27)					
Adiac				0.131 [4](9:10)		0.031 [6](20:49)			0.067 [6](19:49)
Yoga		0.026 [7](22:57,35:45)							
Yoga		0.026 [6](19:44,30:39)							
Yoga		0.026 [5](16:31,24:41)							
Fish	0.023 [7](13:57,1:48)			0.023 [7](14:57)					0.127 [6](27:40)
Fish	0.023 [6](11:49,1:49)			0.023 [6](12:49)					
Fish	0.023 [5](10:41,1:34)			0.023 [5](10:41)					
Fish	0.023 [4](9:33,1:28)			0.023 [4](9:33)					
Fish	0.023 [3](7:20,1:17)			0.023 [3](7:20)					
Plane	0.000 [7](1:50,1:50)	0.000 [7](1:40,1:50)	0.000 [7](1:50,1:40)	0.000 [7](1:50)	0.000 [7](1:50)	0.000 [7](1:50)	0.000 [7](1:32)	0.008 [7](1:33)	0.015 [7](1:41)
Plane	0.000 [6](1:43,1:43)	0.000 [6](1:43,1:31)	0.000 [6](1:43,1:34)	0.000 [6](1:43)	0.000 [6](1:43)	0.000 [6](1:43)	0.000 [6](1:27)	0.000 [6](1:28)	0.000 [6](1:34)
Plane	0.000 [5](1:36,1:36)	0.000 [5](1:36,1:27)	0.000 [5](1:36,1:29)	0.000 [5](1:36)	0.000 [5](1:36)	0.000 [5](2:36)	0.000 [5](1:23)	0.000 [5](1:23)	0.000 [5](1:28)
Plane	0.000 [4](1:29,1:29)	0.000 [4](1:23,1:29)	0.000 [4](1:29,1:21)	0.000 [4](1:29)	0.000 [4](1:29)	0.000 [4](1:29)	0.000 [4](1:19)	0.000 [4](1:19)	0.000 [4](1:27)
Plane	0.000 [3](1:22,1:22)	0.000 [3](1:22,1:22)	0.000 [3](1:22,1:22)	0.000 [3](1:22)	0.000 [3](1:22)	0.000 [3](1:22)	0.000 [3](1:13)	0.000 [3](1:12)	0.000 [3](1:22)
Plane	0.000 [2](1:15,1:15)	0.000 [2](1:15,1:11)	0.000 [2](9:15,1:10)	0.000 [2](1:15)	0.000 [2](1:15)	0.000 [2](2:15)	0.000 [2](1:9)	0.000 [2](1:8)	
Plane	0.000 [1](1:8,1:8)	0.000 [1](1:8,1:8)		0.000 [1](1:8)				0.000 [1](1:8)	

Continued on next page

Table C.1 – continued from previous page

Problem	CWS 1 $\pi$	CWS 2 $\pi$	CWS 3 $\pi$	CWVPV 1 $\pi$	CWVPV 2 $\pi$	CWVPV 3 $\pi$	CWED 1 $\pi$	CWED 2 $\pi$	CWED 3 $\pi$
Car	0.057 [7](14:14,34:54)			0.100 [7](34:35)	0.100 [6](29:39)				0.172 [2](14:19)
Car	0.057 [6](12:12,29:55)								
Beef			0.000 [7](7:8,39:47)		0.033 [7](1:12)	0.033 [7](7:17)		0.133 [7](5:19)	0.067 [7](1:23)
Beef					0.033 [6](1:11)	0.033 [6](6:14)		0.233 [6](5:16)	0.233 [6](8:19)
Beef					0.033 [5](1:9)	0.033 [5](1:7)		0.233 [4](4:11)	0.233 [5](10:15)
Beef					0.033 [4](1:7)	0.033 [4](3:11)			0.233 [4](6:13)
Beef					0.033 [3](1:6)	0.033 [3](1:6)			0.233 [3](1:10)
Beef					0.033 [2](1:3)	0.033 [2](3:4)			0.233 [2](1:7)
Coffee	0.000 [7](5:57,1:57)	0.000 [7](11:57,1:57)	0.000 [7](21:26,1:57)	0.000 [7](6:57)	0.000 [7](13:57)	0.000 [7](29:35)	0.000 [7](1:36)	0.067 [7](1:43)	0.033 [7](1:44)
Coffee	0.000 [6](5:49,1:49)	0.000 [6](10:49,1:49)	0.000 [6](13:49,1:49)	0.000 [6](6:49)	0.000 [6](11:49)	0.000 [6](14:27)	0.000 [6](1:31)	0.000 [6](1:37)	0.000 [6](1:37)
Coffee	0.000 [5](3:41,1:41)	0.000 [5](9:41,1:41)	0.000 [5](15:41,1:41)	0.000 [5](4:41)	0.000 [5](10:41)	0.000 [5](21:25)	0.000 [5](1:26)	0.000 [5](1:31)	0.000 [5](1:29)
Coffee	0.000 [4](3:33,1:33)	0.000 [4](8:33,1:33)	0.000 [4](16:20,1:33)	0.000 [4](4:33)	0.000 [4](8:33)	0.000 [4](19:20)	0.000 [4](1:21)	0.000 [4](1:24)	0.000 [4](1:16)
Coffee	0.000 [3](6:25,1:25)	0.000 [3](6:25,1:25)	0.000 [3](13:15,1:25)	0.000 [1](3:9)	0.000 [2](4:17)		0.000 [3](1:18)	0.000 [3](1:18)	0.000 [3](1:20)
Coffee	0.000 [2](8:9,1:17)	0.000 [2](3:17,1:17)	0.000 [2](12:17,1:17)				0.000 [2](1:12)	0.000 [2](1:10)	0.000 [2](5:15)
Coffee	0.000 [1](3:9,1:9)	0.000 [1](5:9,1:5)	0.000 [1](5:5,1:9)				0.000 [1](1:5)	0.000 [1](1:6)	
OliveOil	0.000 [7](25:64,1:34)	0.000 [7](32:35,28:42)	0.000 [7](37:44,35:36)	0.033 [7](24:30)	0.033 [7](27:31)	0.033 [7](25:45)	0.067 [7](1:29)		
OliveOil	0.000 [6](23:39,1:29)	0.000 [6](22:23,1:27)	0.000 [6](19:20,36:38)	0.033 [6](21:21)	0.033 [6](24:27)	0.033 [5](24:25)	0.000 [6](1:25)		
OliveOil	0.000 [5](18:46,1:21)	0.000 [5](17:19,1:46)	0.000 [5](25:46,21:21)	0.033 [5](18:20)	0.033 [5](20:22)	0.033 [4](13:37)	0.000 [5](1:20)		
OliveOil	0.000 [4](16:26,1:17)	0.000 [4](18:37,18:18)	0.000 [1](6:10,1:7)	0.033 [3](11:12)	0.033 [3](13:17)		0.000 [4](10:17)		
OliveOil	0.000 [3](11:28,1:13)	0.000 [3](12:12,10:13)					0.000 [3](9:13)		
OliveOil	0.000 [2](9:13,1:9)	0.000 [2](8:8,8:9)							
OliveOil	0.000 [1](5:10,1:5)								
CinC_ECG_torso	0.000 [7](1:71,1:71)	0.000 [7](1:71,1:71)	0.000 [7](1:71,1:71)	0.000 [7](1:71)	0.000 [7](1:71)	0.000 [7](1:71)			0.000 [7](1:20)
CinC_ECG_torso	0.000 [6](1:61,1:61)	0.000 [6](1:61,1:61)	0.000 [6](1:61,1:61)	0.000 [6](1:61)	0.000 [6](1:61)	0.000 [6](1:61)			
CinC_ECG_torso	0.000 [5](1:51,1:51)	0.000 [5](1:51,1:51)	0.000 [5](1:51,1:51)	0.000 [5](1:51)	0.000 [5](1:51)	0.000 [5](1:51)			
CinC_ECG_torso	0.000 [4](1:41,1:41)	0.000 [4](1:41,1:41)	0.000 [4](1:41,1:41)	0.000 [4](1:41)	0.000 [4](1:41)	0.000 [4](1:41)			
CinC_ECG_torso	0.000 [3](1:31,1:31)	0.000 [3](1:31,1:31)	0.000 [3](1:31,1:31)	0.000 [3](1:31)	0.000 [3](1:31)	0.000 [3](1:31)			
CinC_ECG_torso	0.000 [2](1:21,1:21)	0.000 [2](1:21,1:21)	0.000 [2](1:21,1:21)	0.000 [2](1:21)	0.000 [2](1:21)	0.000 [2](1:21)			
CinC_ECG_torso	0.000 [1](1:11,1:11)	0.000 [1](1:11,1:11)	0.000 [1](1:11,1:11)	0.000 [1](1:11)	0.000 [1](1:11)	0.000 [1](1:11)			
ChlorineConcentration			0.006 [6](5:11,1:6)			0.007 [6](3:11)		0.008 [6](1:13)	
DiatomSizeReduction	0.000 [7](1:44,1:46)	0.000 [7](26:57,1:57)	0.000 [7](37:57,1:57)	0.000 [7](13:44)	0.000 [7](25:57)	0.000 [7](32:57)	0.000 [5](1:26)		
DiatomSizeReduction	0.000 [6](10:37,1:49)	0.000 [6](24:49,1:49)	0.000 [6](30:37,1:49)	0.000 [6](5:38)	0.000 [6](22:49)	0.000 [6](32:37)	0.000 [4](1:21)		
DiatomSizeReduction	0.000 [5](8:31,1:41)	0.000 [5](20:41,1:41)	0.000 [5](18:41,1:41)	0.000 [5](13:32)	0.000 [5](19:41)	0.000 [5](25:41)			
DiatomSizeReduction	0.000 [4](5:25,1:33)	0.000 [4](19:28,1:33)	0.000 [4](16:30,1:33)	0.000 [4](12:25)	0.000 [4](17:28)	0.000 [4](19:33)			
DiatomSizeReduction	0.000 [3](4:19,1:25)	0.000 [3](14:21,1:25)	0.000 [3](19:25,1:24)	0.000 [3](9:19)	0.000 [3](14:21)	0.000 [2](9:15)			
DiatomSizeReduction	0.000 [2](4:17,1:17)	0.000 [2](10:11,1:17)	0.000 [2](9:15,1:17)	0.000 [2](7:17)					
DiatomSizeReduction	0.000 [1](1:9,1:9)	0.000 [1](7:7,1:9)		0.000 [1](4:9)					
ECGFiveDays	0.000 [7](7:50,1:50)	0.000 [7](1:50,1:50)	0.000 [7](4:50,1:50)	0.000 [7](11:50)	0.000 [7](4:50)	0.000 [7](6:50)	0.002 [7](1:32)	0.002 [7](1:42)	0.003 [7](1:48)
ECGFiveDays	0.000 [6](7:43,1:43)	0.000 [6](1:43,1:43)	0.000 [6](5:43,1:43)	0.000 [6](10:43)	0.000 [6](4:43)	0.000 [6](8:43)	0.000 [6](1:27)	0.000 [6](1:36)	0.000 [6](1:41)
ECGFiveDays	0.000 [5](1:22,1:36)	0.000 [5](1:36,1:36)	0.000 [5](5:36,1:36)	0.000 [5](3:19)	0.000 [5](2:36)	0.000 [5](20:36)	0.000 [5](1:23)	0.000 [5](1:30)	0.000 [5](1:34)

Continued on next page

Table C.1 – continued from previous page

Problem	CWS 1 $\pi$	CWS 2 $\pi$	CWS 3 $\pi$	CWPV 1 $\pi$	CWPV 2 $\pi$	CWPV 3 $\pi$	CWED 1 $\pi$	CWED 2 $\pi$	CWED 3 $\pi$
ECGFiveDays	0.000 [4](1:29,1:29)	0.000 [4](2:29,1:29)	0.000 [4](4:29,1:29)	0.000 [4](7:29)	0.000 [4](3:29)	0.000 [4](7:29)	0.000 [4](1:18)	0.000 [4](1:24)	0.000 [4](1:27)
ECGFiveDays	0.000 [3](2:22,1:22)	0.000 [3](2:22,1:22)	0.000 [3](3:22,1:22)	0.000 [3](6:22)	0.000 [3](3:22)	0.000 [3](4:22)	0.000 [3](1:14)	0.000 [3](1:18)	0.000 [3](1:22)
ECGFiveDays	0.000 [2](1:15,1:8)	0.000 [2](2:15,1:15)	0.000 [2](3:15,1:10)	0.000 [2](1:5)	0.000 [2](3:5)	0.000 [2](9:15)	0.000 [2](1:7)	0.000 [2](1:12)	0.000 [2](1:15)
ECGFiveDays	0.000 [1](2:8,1:8)	0.000 [1](3:8,1:6)	0.000 [1](4:8,1:8)					0.000 [1](1:6)	
FacesUCR	0.007 [7](5:50,2:16)			0.007 [6](7:43)					0.040 [6](1:43)
FacesUCR	0.006 [6](5:43,1:14)								
FacesUCR	0.007 [5](5:36,2:11)								
FacesUCR	0.006 [3](3:14,1:7)								
Haptics	0.247 [6](28:28,40:48)			0.260 [5](24:28)				0.277 [5](13:24)	
Haptics								0.277 [4](3:22)	
Haptics								0.277 [3](10:23)	
InlineSkate			0.083 [5](48:51,1:7)	0.245 [6](23:42)					0.102 [5](1:8)
InlineSkate				0.245 [5](23:42)					
InlineSkate				0.245 [3](19:31)					
ItalyPowerDemand									
ItalyPowerDemand						0.013 [7](1:29)			0.027 [6](7:19)
ItalyPowerDemand						0.013 [6](2:25)			0.027 [5](6:16)
MedicalImages						0.013 [4](2:17)			
MoteStrain	0.010 [7](2:43,8:12)								
MoteStrain	0.010 [5](1:31,7:10)								
MoteStrain	0.010 [4](1:25,15:16)								
SonyAIBORobot SurfaceII	0.003 [7](5:16,4:15)								
SonyAIBORobot SurfaceII	0.003 [6](5:18,5:14)								0.084 [6](15:34)
SonyAIBORobot SurfaceII	0.003 [5](5:11,1:12)								0.084 [5](17:30)
SonyAIBORobot SurfaceII	0.003 [4](4:10,6:14)								
SonyAIBORobot Surface	0.000 [7](10:43,7:43)								
SonyAIBORobot Surface	0.000 [6](8:37,1:37)								0.012 [2](4:11)
SonyAIBORobot Surface	0.000 [5](7:31,9:31)								
SonyAIBORobot Surface	0.000 [4](8:16,14:17)								
SonyAIBORobot Surface	0.000 [3](4:19,1:19)								
SonyAIBORobot Surface	0.000 [2](3:13,1:9)								
Symbols									
Symbols									
TwoLeadECG	0.000 [7](8:43,1:18)								
TwoLeadECG	0.000 [6](8:22,1:23)								
TwoLeadECG	0.000 [5](7:31,1:31)								
TwoLeadECG	0.000 [4](6:25,1:19)								
WordsSynonyms	0.140 [7](22:40,1:57)								
Cricket_X	0.156 [7](33:33,1:42)								
Cricket_X	0.156 [6](24:32,1:30)								
								0.021 [6](1:41)	
								0.021 [2](3:14)	
									0.000 [6](11:24)
									0.287 [5](1:34)
								0.170 [4](1:25)	

Continued on next page



Table C.1 – continued from previous page

Problem	CWS $1\pi$	CWS $2\pi$	CWS $3\pi$	CWPV $1\pi$	CWPV $2\pi$	CWPV $3\pi$	CWED $1\pi$	CWED $2\pi$	CWED $3\pi$
Cricket_Y	0.156 [6] (2:36, 1:27)			0.202 [4] (16:24)					0.204 [5] (1:39)
Cricket_Y	0.156 [5] (2:30, 1:26)								
Cricket_Z	0.124 [7] (20:57, 1:28)			0.172 [7] (22:57)				0.320 [7] (1:43)	
Cricket_Z				0.172 [5] (17:41)					

TABLE C.2: Summary of model test results and parameters according to the same mapping presented in Table 6.5 (p. 120) according to different central frequency parameters ( $1\pi$ ,  $2\pi$ , and  $3\pi$ ) and different voice resolutions (1-7) for the CWS, CWPV, and CWED techniques. The parameters are given as the voice resolution followed by the scale ranges for each technique in brackets.

Problem	CWS $1\pi$	CWS $2\pi$	CWS $3\pi$	CWPV $1\pi$	CWPV $2\pi$	CWPV $3\pi$	CWED $1\pi$	CWED $2\pi$	CWED $3\pi$
Synthetic Control	0.050 [7](17:36,1:36)			0.115 [7](15:25)				0.310 [7](12:35)	
Synthetic Control	0.045 [4](11:21,6:21)			0.130 [6](13:31)				0.210 [6](10:31)	
Synthetic Control								0.205 [5](9:26)	
Synthetic Control								0.215 [4](9:21)	
Gun Point	0.017 [7](10:50,1:50)	0.067 [7](27:29,1:50)	0.017 [5](22:22,1:29)	0.017 [7](9:25)				0.067 [7](1:34)	
Gun Point	0.017 [6](8:43,1:43)	0.017 [6](22:24,1:43)		0.017 [6](9:20)				0.000 [5](1:25)	
Gun Point	0.017 [5](8:36,1:36)	0.033 [5](19:19,1:36)		0.017 [5](7:18)				0.067 [4](1:19)	
Gun Point	0.017 [4](6:29,1:29)	0.000 [4](19:19,1:20)		0.017 [4](6:14)					
Gun Point	0.017 [3](6:11,1:22)	0.067 [3](12:13,1:22)		0.033 [2](6:15)					
Gun Point	0.000 [2](4:15,1:15)								
CBF	0.006 [7](22:43,1:43)	0.000 [7](28:43,1:43)	0.003 [7](32:43,1:43)	0.006 [4](14:25)	0.003 [6](25:37)	0.006 [7](33:43)		0.194 [4](12:25)	
CBF	0.010 [6](19:37,1:37)	0.000 [6](25:37,1:37)	0.000 [6](28:37,1:37)			0.000 [6](28:37)			
CBF	0.010 [5](16:31,1:31)	0.000 [5](19:31,1:31)	0.003 [5](23:31,1:31)			0.003 [5](24:31)			
CBF	0.010 [4](13:25,1:25)	0.003 [4](16:25,1:25)	0.006 [4](17:25,1:25)						
CBF	0.016 [3](10:19,1:19)	0.003 [3](12:19,1:19)	0.000 [3](17:19,1:19)						
CBF	0.013 [2](8:13,1:13)			0.010 [7](11:50)					0.044 [5](1:36)
Face (all)	0.013 [7](11:50,3:5)								
Face (all)	0.007 [6](11:24,3:9)								
Face (all)	0.010 [5](10:17,3:9)								
OSU Leaf									
OSU Leaf		0.188 [7](7:57,1:47)		0.213 [5](4:34)					0.206 [5](1:40)
OSU Leaf				0.188 [2](1:17)					
OSU Leaf				0.121 [6](5:37)					0.080 [5](1:25)
OSU Leaf				0.115 [3](6:19)					0.090 [4](1:20)
OSU Leaf				0.088 [7](22:44)					0.184 [6](19:45)
Swedish Leaf									
Swedish Leaf									
Swedish Leaf									
Swedish Leaf									
Swedish Leaf									
50words									
Trace	0.079 [5](16:29,1:26)								
Trace	0.086 [7](4:17,1:57)	0.000 [7](47:57,1:35)	0.000 [7](46:57,1:29)			0.143 [6](28:29)		0.143 [7](1:28)	
Trace	0.086 [6](3:15,1:49)	0.000 [6](37:49,1:29)	0.000 [5](32:41,1:23)					0.000 [4](1:20)	
Trace	0.000 [5](20:21,1:41)	0.000 [5](31:41,1:23)	0.014 [3](18:18,6:17)					0.000 [6](1:31)	
Trace	0.014 [4](15:17,1:33)	0.000 [4](25:33,1:20)						0.000 [5](1:26)	
Trace	0.014 [3](17:25,1:15)	0.000 [3](19:25,1:15)						0.000 [4](1:20)	
Trace	0.000 [2](12:17,1:10)	0.000 [2](13:17,1:8)						0.000 [3](1:15)	
Trace	0.000 [1](6:9,1:3)							0.000 [2](1:10)	
Trace	0.018 [7](18:43,32:32)			0.020 [7](18:43)				0.086 [7](1:36)	
Trace	0.023 [6](15:37,22:31)			0.023 [6](14:37)				0.000 [6](1:31)	
Two Patterns				0.023 [5](13:24)				0.000 [5](1:26)	
Two Patterns				0.000 [7](1:50)				0.000 [4](1:20)	
Two Patterns				0.000 [7](1:50)				0.000 [3](1:15)	
Wafer				0.000 [6](1:43)				0.000 [2](1:10)	
Wafer				0.000 [7](18:43)				0.086 [1](1:3)	
Wafer				0.023 [6](14:37)				0.300 [7](25:34)	
Wafer				0.023 [5](13:24)					
Wafer				0.000 [7](1:50)					
Wafer				0.000 [7](3:50)				0.000 [7](11:50)	0.000 [7](1:50)
Wafer				0.000 [6](1:43)				0.000 [6](9:43)	0.000 [6](1:43)

Continued on next page

Table C.2 – continued from previous page

Problem	CWS 1 $\pi$	CWS 2 $\pi$	CWS 3 $\pi$	CWPV 1 $\pi$	CWPV 2 $\pi$	CWPV 3 $\pi$	CWED 1 $\pi$	CWED 2 $\pi$	CWED 3 $\pi$
Wafer	0.000 [5](1:36,1:36)	0.000 [5](1:36,1:36)	0.000 [5](1:36,1:35)	0.000 [5](1:36)	0.000 [5](1:36)	0.000 [5](4:36)		0.000 [5](8:36)	0.000 [5](6:36)
Wafer	0.000 [4](1:29,1:29)	0.000 [4](1:29,1:29)	0.000 [4](3:29,1:29)	0.000 [4](1:29)	0.000 [4](1:29)	0.000 [4](3:29)		0.000 [4](6:29)	0.000 [4](10:29)
Wafer	0.000 [3](1:22,1:22)	0.000 [3](1:22,1:22)	0.000 [3](1:22,1:22)	0.000 [3](1:22)	0.000 [3](1:22)	0.000 [3](1:22)			
Wafer	0.000 [2](1:15,1:15)	0.000 [2](1:15,1:15)	0.000 [2](2:15,10:14)	0.000 [2](1:15)	0.000 [2](1:15)				
Wafer	0.000 [1](1:8,1:8)			0.000 [1](1:8)					
Face (four)	0.025 [7](9:57,1:9)	0.025 [7](29:34,1:57)	0.100 [7](27:28,39:57)	0.025 [7](9:57)	0.025 [7](25:36)	0.000 [4](16:19)	0.025 [7](1:57)		0.100 [6](1:36)
Face (four)	0.050 [6](7:49,23:25)	0.025 [6](25:29,1:49)	0.100 [6](24:28,8:11)	0.025 [6](10:37)	0.025 [6](22:31)		0.075 [6](1:49)		0.075 [4](15:33)
Face (four)	0.025 [5](7:41,19:20)	0.025 [5](21:24,1:41)	0.000 [4](16:19,4:10)	0.025 [5](8:31)	0.025 [5](19:26)		0.075 [5](1:41)		
Face (four)	0.050 [4](5:33,16:17)	0.025 [4](16:20,1:33)		0.025 [4](9:24)	0.025 [4](15:22)		0.075 [4](1:33)		
Face (four)	0.025 [3](5:25,1:3)	0.025 [3](12:16,1:7)		0.000 [3](6:18)	0.025 [3](13:16)		0.075 [3](1:25)		
Face (four)	0.025 [2](4:8,1:10)	0.025 [2](8:11,4:9)		0.125 [2](4:6)			0.075 [2](2:13)		
Face (four)	0.025 [1](4:4,1:5)								
Lightning2		0.250 [7](13:19,17:42)	0.350 [7](12:25,16:44)	0.225 [7](2:12)			0.150 [7](1:49)	0.300 [7](12:50)	0.250 [7](1:50)
Lightning2		0.275 [6](12:16,15:36)	0.275 [6](12:16,15:36)	0.225 [6](1:10)			0.200 [6](1:42)	0.200 [2](5:14)	0.200 [6](2:43)
Lightning2			0.225 [5](7:16,17:29)	0.225 [4](2:7)			0.200 [5](1:35)		0.200 [5](1:36)
Lightning2							0.200 [4](1:28)		
Lightning2							0.225 [3](1:20)		
Lightning2							0.225 [2](1:14)		
Lightning7		0.240 [6](37:49,13:14)		0.220 [7](36:39)	0.260 [4](18:27)	0.280 [7](30:39)			0.320 [2](1:16)
Lightning7				0.200 [6](29:49)		0.300 [6](36:44)			
Lightning7				0.240 [5](26:28)					
ECG200	0.017 [5](10:10,3:5)	0.033 [7](21:22,28:39)	0.017 [6](21:21,14:17)	0.017 [7](13:15)					0.033 [6](5:16)
Adiac	0.150 [7](22:22,1:16)			0.167 [7](12:37)					0.167 [6](1:33)
Adiac	0.153 [6](19:19,1:10)			0.167 [5](9:27)					
Adiac				0.170 [4](9:10)		0.065 [6](20:49)			0.126 [6](19:49)
Yoga		0.064 [7](22:57,35:45)							
Yoga		0.056 [6](19:44,30:39)							
Yoga		0.063 [5](16:31,24:41)							0.117 [6](27:40)
Fish	0.067 [7](13:57,1:48)			0.058 [7](14:57)					
Fish	0.058 [6](11:49,1:49)			0.067 [6](12:49)					
Fish	0.058 [5](10:41,1:34)			0.058 [5](10:41)					
Fish	0.058 [4](9:33,1:28)			0.058 [4](9:33)					
Fish	0.067 [3](7:20,1:17)			0.067 [3](7:20)					
Plane	0.000 [7](1:50,1:50)	0.000 [7](1:40,1:50)	0.014 [7](1:50,1:40)	0.000 [7](1:50)	0.014 [7](1:50)	0.014 [7](6:50)	0.000 [7](1:32)	0.014 [7](1:33)	0.072 [7](1:41)
Plane	0.000 [6](1:43,1:43)	0.000 [6](1:43,1:31)	0.014 [6](1:43,1:34)	0.000 [6](1:43)	0.014 [6](1:43)	0.014 [6](1:43)	0.000 [6](1:27)	0.000 [6](1:28)	0.000 [6](1:34)
Plane	0.000 [5](1:36,1:36)	0.000 [5](1:36,1:27)	0.014 [5](1:36,1:29)	0.000 [5](1:36)	0.014 [5](1:36)	0.014 [5](2:36)	0.000 [5](1:23)	0.000 [5](1:23)	0.000 [5](1:28)
Plane	0.000 [4](1:29,1:29)	0.000 [4](1:23,1:29)	0.014 [4](1:29,1:21)	0.000 [4](1:29)	0.014 [4](1:29)	0.029 [4](1:29)	0.000 [4](1:19)	0.000 [4](1:19)	0.000 [4](1:27)
Plane	0.000 [3](1:22,1:22)	0.000 [3](1:22,1:22)	0.014 [3](1:22,1:22)	0.000 [3](1:22)	0.014 [3](1:22)	0.014 [3](5:22)	0.000 [3](1:13)	0.000 [3](1:12)	0.000 [3](1:22)
Plane	0.000 [2](1:15,1:15)	0.014 [2](1:15,1:11)	0.014 [2](9:15,1:10)	0.000 [2](1:15)	0.014 [2](2:15)		0.000 [2](1:9)	0.029 [2](1:8)	
Plane	0.000 [1](1:8,1:8)	0.014 [1](1:8,1:8)		0.000 [1](1:8)					

Continued on next page

Table C.2 – continued from previous page

Problem	CWS 1 $\pi$	CWS 2 $\pi$	CWS 3 $\pi$	CWVPV 1 $\pi$	CWVPV 2 $\pi$	CWVPV 3 $\pi$	CWED 1 $\pi$	CWED 2 $\pi$	CWED 3 $\pi$
Car	0.175 [7](14:14,34:54)			0.150 [7](34:35)	0.150 [6](29:39)				0.250 [2](14:19)
Car	0.150 [6](12:12,29:55)								
Beef			0.150 [7](7:8,39:47)		0.150 [7](1:12)	0.150 [7](7:17)		0.300 [7](5:19)	0.100 [7](1:23)
Beef					0.150 [6](1:11)	0.200 [6](6:14)		0.400 [6](5:16)	0.350 [6](8:19)
Beef					0.150 [5](1:9)	0.150 [5](1:7)		0.400 [4](4:11)	0.400 [5](10:15)
Beef					0.150 [4](1:7)	0.150 [4](3:11)			0.350 [4](6:13)
Beef					0.200 [3](1:6)	0.150 [3](1:6)			0.400 [3](1:10)
Beef					0.150 [2](1:3)	0.150 [2](3:4)			0.400 [2](1:7)
Coffee	0.050 [7](5:57,1:57)	0.050 [7](11:57,1:57)	0.050 [7](21:26,1:57)	0.050 [7](6:57)	0.050 [7](13:57)	0.050 [7](29:35)	0.050 [7](1:36)	0.100 [7](1:43)	0.000 [7](1:44)
Coffee	0.000 [6](5:49,1:49)	0.050 [6](10:49,1:49)	0.150 [6](13:49,1:49)	0.050 [6](6:49)	0.050 [6](11:49)	0.150 [6](14:27)	0.000 [6](1:31)	0.050 [6](1:37)	0.050 [6](1:37)
Coffee	0.000 [5](3:41,1:41)	0.050 [5](9:41,1:41)	0.050 [5](15:41,1:41)	0.050 [5](4:41)	0.050 [5](10:41)	0.050 [5](21:25)	0.000 [5](1:26)	0.050 [5](1:31)	0.050 [5](1:29)
Coffee	0.050 [4](3:33,1:33)	0.050 [4](8:33,1:33)	0.000 [4](16:20,1:33)	0.050 [4](4:33)	0.050 [4](8:33)	0.000 [4](19:20)	0.000 [4](1:21)	0.050 [4](1:24)	0.000 [4](1:16)
Coffee	0.000 [3](6:25,1:25)	0.050 [3](6:25,1:25)	0.000 [3](13:15,1:25)	0.050 [1](3:9)	0.000 [2](4:17)		0.000 [3](1:18)	0.050 [3](1:18)	0.050 [3](1:20)
Coffee	0.000 [2](8:9,1:17)	0.000 [2](3:17,1:17)	0.050 [2](12:17,1:17)				0.050 [2](1:12)	0.050 [2](1:10)	0.050 [2](5:15)
Coffee	0.050 [1](3:9,1:9)	0.050 [1](5:9,1:5)	0.050 [1](5:5,1:9)				0.000 [1](1:5)	0.050 [1](1:6)	
OliveOil	0.150 [7](25:64,1:34)	0.200 [7](32:35,28:42)	0.200 [7](37:44,35:36)	0.150 [7](24:30)	0.100 [7](27:31)	0.250 [7](25:45)	0.200 [7](1:29)		
OliveOil	0.150 [6](23:39,1:29)	0.100 [6](22:23,1:27)	0.300 [6](19:20,36:38)	0.100 [6](21:21)	0.100 [6](24:27)	0.150 [5](24:25)	0.150 [6](1:25)		
OliveOil	0.150 [5](18:46,1:21)	0.100 [5](17:19,1:46)	0.100 [5](25:46,21:21)	0.150 [5](18:20)	0.100 [5](20:22)	0.250 [4](13:37)	0.200 [5](1:20)		
OliveOil	0.100 [4](16:26,1:17)	0.150 [4](18:37,18:18)	0.200 [1](6:10,1:7)	0.100 [3](11:12)	0.100 [3](13:17)		0.250 [4](10:17)		
OliveOil	0.100 [3](11:28,1:13)	0.100 [3](12:12,10:13)					0.250 [3](9:13)		
OliveOil	0.150 [2](9:13,1:9)	0.100 [2](8:8,8:9)							
OliveOil	0.150 [1](5:10,1:5)								
CinC_ECG_torso	0.000 [7](1:71,1:71)	0.002 [7](1:71,1:71)	0.000 [7](1:71,1:71)	0.000 [7](1:71)	0.000 [7](1:71)	0.000 [7](1:71)	0.000 [7](1:71)		0.000 [7](1:20)
CinC_ECG_torso	0.000 [6](1:61,1:61)	0.002 [6](1:61,1:61)	0.000 [6](1:61,1:61)	0.000 [6](1:61)	0.000 [6](1:61)	0.000 [6](1:61)	0.000 [6](1:61)		
CinC_ECG_torso	0.000 [5](1:51,1:51)	0.002 [5](1:51,1:51)	0.000 [5](1:51,1:51)	0.000 [5](1:51)	0.000 [5](1:51)	0.000 [5](1:51)	0.000 [5](1:51)		
CinC_ECG_torso	0.000 [4](1:41,1:41)	0.002 [4](1:41,1:41)	0.000 [4](1:41,1:41)	0.000 [4](1:41)	0.000 [4](1:41)	0.000 [4](1:41)	0.000 [4](1:41)		
CinC_ECG_torso	0.000 [3](1:31,1:31)	0.000 [3](1:31,1:31)	0.002 [3](1:31,1:31)	0.000 [3](1:31)	0.000 [3](1:31)	0.000 [3](1:31)	0.000 [3](1:31)		
CinC_ECG_torso	0.000 [2](1:21,1:21)	0.000 [2](1:21,1:21)	0.000 [2](1:21,1:21)	0.000 [2](1:21)	0.000 [2](1:21)	0.000 [2](1:21)	0.000 [2](1:21)		
CinC_ECG_torso	0.000 [1](1:11,1:11)	0.000 [1](1:11,1:11)	0.004 [1](1:11,1:11)	0.000 [1](1:11)	0.000 [1](1:11)	0.000 [1](1:11)	0.000 [1](1:11)		
ChlorineConcentration			0.030 [6](5:11,1:6)			0.031 [6](3:11)		0.034 [6](1:13)	
DiatomSizeReduction	0.000 [7](1:44,1:46)	0.000 [7](26:57,1:57)	0.000 [7](37:57,1:57)	0.000 [7](13:44)	0.000 [7](25:57)	0.000 [7](32:57)	0.000 [5](1:26)		
DiatomSizeReduction	0.000 [6](10:37,1:49)	0.000 [6](24:49,1:49)	0.000 [6](30:37,1:49)	0.000 [6](5:38)	0.000 [6](22:49)	0.008 [6](32:37)	0.000 [4](1:21)		
DiatomSizeReduction	0.000 [5](8:31,1:41)	0.000 [5](20:41,1:41)	0.000 [5](18:41,1:41)	0.000 [5](13:32)	0.000 [5](19:41)	0.000 [5](25:41)			
DiatomSizeReduction	0.000 [4](5:25,1:33)	0.000 [4](19:28,1:33)	0.000 [4](16:30,1:33)	0.000 [4](12:25)	0.000 [4](17:28)	0.000 [4](19:33)			
DiatomSizeReduction	0.000 [3](4:19,1:25)	0.000 [3](14:21,1:25)	0.008 [3](19:25,1:24)	0.000 [3](9:19)	0.000 [3](14:21)	0.000 [2](9:15)			
DiatomSizeReduction	0.000 [2](4:17,1:17)	0.000 [2](10:11,1:17)	0.000 [2](9:15,1:17)	0.000 [2](7:17)					
DiatomSizeReduction	0.000 [1](1:9,1:9)	0.000 [1](7:7,1:9)		0.000 [1](4:9)					
ECGFiveDays	0.003 [7](7:50,1:50)	0.003 [7](1:50,1:50)	0.007 [7](4:50,1:50)	0.007 [7](11:50)	0.014 [7](4:50)	0.021 [7](6:50)	0.014 [7](1:32)	0.021 [7](1:42)	0.034 [7](1:48)
ECGFiveDays	0.010 [6](7:43,1:43)	0.003 [6](1:43,1:43)	0.007 [6](5:43,1:43)	0.017 [6](10:43)	0.014 [6](4:43)	0.024 [6](8:43)	0.003 [6](1:27)	0.000 [6](1:36)	0.000 [6](1:41)
ECGFiveDays	0.003 [5](1:22,1:36)	0.003 [5](1:36,1:36)	0.003 [5](5:36,1:36)	0.007 [5](3:19)	0.014 [5](2:36)	0.024 [5](20:36)	0.003 [5](1:23)	0.000 [5](1:30)	0.000 [5](1:34)

Continued on next page

Table C.2 – continued from previous page

Problem	CWS 1 $\pi$	CWS 2 $\pi$	CWS 3 $\pi$	CWPV 1 $\pi$	CWPV 2 $\pi$	CWPV 3 $\pi$	CWED 1 $\pi$	CWED 2 $\pi$	CWED 3 $\pi$
ECGFiveDays	0.000 [4](1:29,1:29)	0.003 [4](2:29,1:29)	0.000 [4](4:29,1:29)	0.010 [4](7:29)	0.014 [4](3:29)	0.021 [4](7:29)	0.003 [4](1:18)	0.000 [4](1:24)	0.000 [4](1:27)
ECGFiveDays	0.000 [3](2:22,1:22)	0.007 [3](2:22,1:22)	0.014 [3](3:22,1:22)	0.014 [3](6:22)	0.010 [3](3:22)	0.024 [3](4:22)	0.003 [3](1:14)	0.000 [3](1:18)	0.000 [3](1:22)
ECGFiveDays	0.000 [2](1:15,1:8)	0.000 [2](2:15,1:15)	0.017 [2](3:15,1:10)	0.017 [2](1:5)	0.027 [2](3:5)	0.024 [2](9:15)	0.017 [2](1:7)	0.000 [2](1:12)	0.000 [2](1:15)
ECGFiveDays	0.003 [1](2:8,1:8)	0.003 [1](3:8,1:6)	0.000 [1](4:8,1:8)					0.000 [1](1:6)	
FacesUCR	0.012 [7](5:50,2:16)			0.010 [6](7:43)					0.037 [6](1:43)
FacesUCR	0.011 [6](5:43,1:14)								
FacesUCR	0.011 [5](5:36,2:11)								
FacesUCR	0.012 [3](3:14,1:7)								
Haptics	0.300 [6](28:28,40:48)			0.333 [5](24:28)				0.407 [5](13:24)	
Haptics								0.340 [4](3:22)	
Haptics								0.300 [3](10:23)	
InlineSkate			0.123 [5](48:51,1:7)	0.300 [6](23:42)					0.155 [5](1:8)
InlineSkate				0.296 [5](23:42)					
InlineSkate				0.309 [3](19:31)					
ItalyPowerDemand									
ItalyPowerDemand			0.042 [6](12:25,7:12)			0.056 [7](6:29)			0.056 [6](7:19)
ItalyPowerDemand						0.047 [7](1:29)			0.050 [5](6:16)
MedicalImages						0.047 [6](2:25)			
MedicalImages						0.033 [4](2:17)			
MotorStrain	0.007 [7](2:43,8:12)	0.074 [7](31:35,1:40)		0.083 [6](11:26)				0.076 [5](1:28)	
MotorStrain	0.007 [5](1:31,7:10)			0.012 [7](1:43)				0.091 [6](15:34)	0.086 [6](1:30)
MotorStrain	0.012 [4](1:25,15:16)			0.014 [4](2:16)				0.076 [5](13:31)	0.090 [5](17:30)
SonyAIBORobot SurfaceII	0.038 [7](5:16,4:15)	0.047 [7](5:43,10:13)		0.041 [4](2:11)		0.044 [7](7:32)			0.053 [4](4:23)
SonyAIBORobot SurfaceII	0.041 [6](5:18,5:14)	0.059 [6](5:22,8:13)							
SonyAIBORobot SurfaceII	0.041 [5](5:11,1:12)								
SonyAIBORobot SurfaceII	0.038 [4](4:10,6:14)								
SonyAIBORobot Surface	0.010 [7](10:43,7:43)	0.020 [7](1:24,27:43)	0.020 [6](5:19,1:37)	0.015 [7](8:43)					0.015 [2](4:11)
SonyAIBORobot Surface	0.010 [6](8:37,1:37)	0.010 [5](3:31,28:31)		0.015 [6](7:37)					
SonyAIBORobot Surface	0.005 [5](7:31,9:31)								
SonyAIBORobot Surface	0.015 [4](8:16,14:17)								
SonyAIBORobot Surface	0.020 [3](4:19,1:19)								
SonyAIBORobot Surface	0.025 [2](3:13,1:9)								
Symbols		0.029 [7](34:57,1:44)						0.026 [7](34:57)	
Symbols							0.050 [6](1:41)		
TwoLeadECG	0.008 [7](8:43,1:18)	0.008 [7](25:25,1:22)	0.013 [7](26:26,13:29)	0.008 [7](7:43)			0.047 [2](3:14)		0.015 [6](11:24)
TwoLeadECG	0.005 [6](8:22,1:23)	0.008 [5](18:18,1:15)	0.008 [6](27:32,1:22)	0.010 [5](7:8)					
TwoLeadECG	0.003 [5](7:31,1:31)		0.008 [5](19:21,1:19)						
TwoLeadECG	0.005 [4](6:25,1:19)		0.008 [4](16:25,1:14)						
WordsSynonyms	0.055 [7](22:40,1:57)			0.057 [6](18:34)					0.164 [5](1:34)
Cricket_X	0.215 [7](33:33,1:42)			0.266 [4](15:23)				0.226 [4](1:25)	
Cricket_X	0.204 [6](24:32,1:30)								

Continued on next page

Table C.2 – continued from previous page

Problem	CWS $1\pi$	CWS $2\pi$	CWS $3\pi$	CWVPV $1\pi$	CWVPV $2\pi$	CWVPV $3\pi$	CWED $1\pi$	CWED $2\pi$	CWED $3\pi$
Cricket_Y	0.207 [6](2:36,1:27)			0.281 [4](16:24)					0.222 [5](1:39)
Cricket_Y	0.207 [5](2:30,1:26)								
Cricket_Z	0.159 [7](20:57,1:28)			0.196 [7](22:57)				0.359 [7](1:43)	
Cricket_Z				0.170 [5](17:41)					

# D

## Source code listings

The code and figures used in this thesis were generated using a variety of software products and packages which include: R (<http://www.r-project.org>); Mathematica 8 [73]; and Java – coded using the Netbeans IDE (<http://netbeans.org/>). The FFT implementation of the continuous wavelet transform (CWT) is adapted from a Matlab package written by Christopher Torrence and Gilbert P. Compo [3] available at : <http://atoc.colorado.edu/research/wavelets/> for which the disclaimer is shown below:

---

Copyright (C) 1995-2004, Christopher Torrence and Gilbert P. Compo

This software may be used, copied, or redistributed as long as it is not

sold and this copyright notice is reproduced on each copy made. This routine is provided as is without any express or implied warranties whatsoever.

Notice: Please acknowledge the use of the above software in any publications:

```
``Wavelet software was provided by C. Torrence and G. Compo,  
and is available at URL: http://paos.colorado.edu/research/wavelets/''.
```

Reference: Torrence, C. and G. P. Compo, 1998: A Practical Guide to Wavelet Analysis. *Bull. Amer. Meteor. Soc.*, 79, 61-78.

Please send a copy of such publications to either C. Torrence or G. Compo:

Dr. Christopher Torrence	Dr. Gilbert P. Compo
Research Systems, Inc.	Climate Diagnostics Center
4990 Pearl East Circle	325 Broadway R/CDC1
Boulder, CO 80301, USA	Boulder, CO 80305-3328, USA
E-mail: <a href="mailto:chris@rsinc.com">chris[AT]rsinc[DOT]com</a>	E-mail: <a href="mailto:compo@colorado.edu">compo[AT]colorado[DOT]edu</a>

---

## D.1 Code examples

All source code in this thesis is performed in java and tested using the Netbeans IDE . The Java FFT algorithm is accredited to Bruce Miller at the National Institute of Standards and Technology (NIST) ([bruce.miller@nist.gov](mailto:bruce.miller@nist.gov)), using routines derived from Brian Gough available in the Gnu Scientific Library (GSL).

LISTING D.1: Main class

```
1 package cws;  
2  
3 import java.io.IOException;  
4 /**  
5  * This is the main class used to run the classification experiment.  
6  * @author Marc Pienaar  
7  * @version 1.0 */
```



```

8  */
9  public class CWS {
10     static NN_evaluate nn = new NN_evaluate();
11     public static void main(String[] args) throws IOException {
12         String class_train = args[0]; // e.g. "-path/CBF_TRAIN";
13         String class_test = args[1]; // e.g. "-path/CBF_TEST";
14         String voices = args[2]; // e.g. 7
15         nn.main(class_train, class_test, voices);
16     }
17 }

```

LISTING D.2: K-NN evaluate

```

1  package cws;
2
3  import java.io.IOException;
4  import java.text.DecimalFormat;
5  import java.util.ArrayList;
6  import java.util.List;
7
8  /**
9   * This class performs the NN classification using a leave one out approach.
10  * author Marc Pienaar
11  *
12  * @version 1.0 *
13  */
14  public class NN_evaluate {
15
16     double[][] all;
17     int[] all_labels;
18     int voices;
19     double[] scale;
20     private static long t1;
21     private static long t2;
22     double w0;
23     int acc;
24     int acc2;
25     String[] rnames;
26
27     public void main(final String train, final String test, final String voice) {
28         w0 = 2 * Math.PI;
29         double[] scalee;
30         try {
31             String class_train = train; //train
32             String class_test = test; //test
33             Dataset datatest = new Dataset(class_test);
34             Dataset datatrain = new Dataset(class_train);
35             List dd = new ArrayList();

```

```

36     ArrayList<Integer> dl = new ArrayList<Integer>();
37     for (int i = 0; i < datatest.size(); i++) {
38         dd.add(datatest.dataAt(i));
39         dl.add(datatest.labelAt(i));
40     }
41     for (int i = 0; i < datatrain.size(); i++) {
42         dd.add(datatrain.dataAt(i));
43         dl.add(datatrain.labelAt(i));
44     }
45     all = new double[dd.size()][datatest.dataAt(0).length];
46     all_labels = new int[dd.size()];
47     for (int i = 0; i < dd.size(); i++) {
48         all[i] = (double[]) dd.get(i);
49         all_labels[i] = dl.get(i);
50     }
51     double oct = Math.ceil(Math.log((double) datatest.dataAt(0).length) / Math.log(2.));
52     double last = oct, first = 1.;
53     voices = Integer.parseInt(voice);
54     double length = (((last - 1) * voices) - (((first - 1) * voices))) + 1.;
55     ArrayList<Double> scaleeee = new ArrayList<Double>();
56     for (int i = (int) ((first - 1) * voices); i < (int) ((last - 1) * voices) + 1; i++) {
57         scaleeee.add(2. * Math.pow(2., (i * (1. / voices))));
58     }
59     scalee = new double[scaleeee.size()];
60     for (int i = 0; i < scalee.length; i++) {
61         scalee[i] = scaleeee.get(i);
62     }
63     scale = scalee;
64     acc = 0;
65     for (int i = 0; i < scale.length; i++) {
66         for (int j = i; j < scale.length; j++) {
67             acc++;
68         }
69     }
70     rnames = new String[acc];
71     acc2 = 0;
72     for (int i = 0; i < scale.length; i++) {
73         for (int j = i; j < scale.length; j++) {
74             int ii = i + 1;
75             int jj = j + 1;
76             rnames[acc2] = (ii + "_" + jj);
77             acc2++;
78         }
79     }
80     try {
81         NN_evaluate_All(all, all_labels, voices);
82     } catch (Exception ex) {
83     }

```

```

84     System.exit(0);
85 } catch (IOException ex) {
86     System.out.println(ex);
87 }
88 }
89
90 private void NN_evaluate_All(final double[][] all, final int[] all_labels, int voices) {
91     t1 = System.currentTimeMillis();//get current time
92     final int[][] cor = new int[acc + 2][acc];
93     for (int i = 0; i < all.length; ++i) {
94         int[] train_labels = gettrlab(all_labels, i);
95         int test_labels = gettelab(all_labels, i);
96         double[][] train = gettrain(all, i);
97         double[] test = gettest(all, i);
98         int[][] predicted_label = classify_All(train, test, train_labels);
99         for (int j = 0; j < predicted_label.length; j++) {
100             for (int k = 0; k < predicted_label[0].length; k++) {
101                 if (predicted_label[j][k] == test_labels) {
102                     cor[j][k] = cor[j][k] + 1;
103                 } else {
104                     cor[j][k] = cor[j][k] + 0;
105                 }
106             }
107         }
108         System.out.println(i + " of " + all.length + " complete.");
109     }
110     int[][] correct = new int[acc][acc];
111     for (int i = 0; i < correct.length; i++) {
112         for (int j = 0; j < correct[0].length; j++) {
113             correct[i][j] = cor[i][j];
114         }
115     }
116     String[] outputp = new String[4];
117     DecimalFormat threeDForm = new DecimalFormat("0.000");
118     t2 = System.currentTimeMillis();
119     double val = ((t2 - t1) / 1000.), val3 = ((val));
120     System.out.println("Time taken" + ": " + threeDForm.format(val3) + " seconds");
121     System.out.println("Function" + ", " + "Error" + ", " + " s_min:s_max");
122     double absminn = Double.MAX_VALUE;
123     for (int i = 2; i < correct.length - 2; i++) {
124         for (int j = 0; j < correct[0].length; j++) {
125             double answer = ((double) all_labels.length - (double) correct[i][j])
126                 / (double) all_labels.length;
127             absminn = Math.min(answer, absminn);
128         }
129     }
130     ArrayList vecvecCWPV1 = null, vecvecCWPV2 = null, vecvecCWED1 = null, vecvecCWED2 = new ArrayList
    ();

```

```

131     for (int i = 2; i < correct.length; i++) {
132         for (int j = 0; j < correct[0].length; j++) {
133             double answer = ((double) all_labels.length - (double) correct[i][j])
134                 / (double) all_labels.length;
135             if (answer == absminn) {
136                 String[] g = rnames[i - 2].split("_");
137                 vecvecCWPV1.add(Integer.parseInt(g[0]));
138                 vecvecCWPV2.add(Integer.parseInt(g[1]));
139                 String[] g2 = rnames[j].split("_");
140                 vecvecCWED1.add(Integer.parseInt(g2[0]));
141                 vecvecCWED2.add(Integer.parseInt(g2[1]));
142             }
143         }
144     }
145     double maxxxx = -1, maxxxx2 = -1, Mmaxxxx = -1, Mmaxxxx2 = -1;
146     for (int i = 0; i < vecvecCWPV1.size(); i++) {
147         int h = (int) vecvecCWPV2.get(i) - (int) vecvecCWPV1.get(i);
148         int h2 = (int) vecvecCWED2.get(i) - (int) vecvecCWED1.get(i);
149         maxxxx = h + h2;
150         if (maxxxx > maxxxx2) {
151             System.out.println("Both, " + threeDForm.format(absminn) + " , " + vecvecCWPV1.get(i) + "_"
+ vecvecCWPV2.get(i) + " , " + vecvecCWED1.get(i) + "_" + vecvecCWED2.get(i) + " , " + maxxxx);
152             Mmaxxxx2 = Mmaxxxx;
153             outputp[0] = vecvecCWPV1.get(i) + "_" + vecvecCWPV2.get(i);
154             outputp[1] = vecvecCWED1.get(i) + "_" + vecvecCWED2.get(i);
155             maxxxx2 = maxxxx;
156         }
157     }
158     ArrayList vecCWPV1 = null, vecCWPV2 = null, vecCWED1 = null, vecCWED2 = new ArrayList();
159     absminn = Double.MAX_VALUE;
160     for (int i = 0; i < correct[0].length; i++) {
161         double answer = ((double) all_labels.length - (double) correct[0][i])
162             / (double) all_labels.length;
163         absminn = Math.min(answer, absminn);
164     }
165     for (int i = 0; i < correct[0].length; i++) {
166         double answer = ((double) all_labels.length - (double) correct[0][i])
167             / (double) all_labels.length;
168         if (answer == absminn) {
169             String[] g = rnames[i].split("_");
170             vecCWPV1.add(Integer.parseInt(g[0]));
171             vecCWPV2.add(Integer.parseInt(g[1]));
172         }
173     }
174     System.out.println();
175     maxxxx2 = -1;
176     for (int i = 0; i < vecCWPV1.size(); i++) {
177         int h = (int) vecCWPV2.get(i) - (int) vecCWPV1.get(i);

```

```

178         maxxxx = h;
179         if (maxxxx > maxxxx2) {
180             System.out.println("CWPV," + threeDForm.format(absminn) + "," + vecCWPV1.get(i) + "_" +
vecCWPV2.get(i));
181             maxxxx2 = maxxxx;
182             outputp[2] = vecCWPV1.get(i) + "_" + vecCWPV2.get(i);
183         }
184     }
185     absminn = Double.MAX_VALUE;
186     for (int i = 0; i < correct[0].length; i++) {
187         double answer2 = ((double) all_labels.length - (double) correct[1][i])
188             / (double) all_labels.length;
189         absminn = Math.min(answer2, absminn);
190     }
191     System.out.println();
192     for (int i = 0; i < correct[0].length; i++) {
193         double answer2 = ((double) all_labels.length - (double) correct[1][i])
194             / (double) all_labels.length;
195         if (answer2 == absminn) {
196             String[] g = rnames[i].split("_");
197             vecCWED1.add(Integer.parseInt(g[0]));
198             vecCWED2.add(Integer.parseInt(g[1]));
199         }
200     }
201     maxxxx2 = -1;
202     for (int i = 0; i < vecCWED1.size(); i++) {
203         int h = (int) vecCWED2.get(i) - (int) vecCWED1.get(i);
204         maxxxx = h;
205         if (maxxxx > maxxxx2) {
206             System.out.println("CWED," + threeDForm.format(absminn) + "," + vecCWED1.get(i) + "_" +
vecCWED2.get(i));
207             maxxxx2 = maxxxx;
208             outputp[3] = vecCWED1.get(i) + "_" + vecCWED2.get(i);
209         }
210     }
211     System.out.println();
212     for (int i = 0; i < outputp.length; i++) {
213         System.out.print(outputp[i] + "_");
214     }
215 }
216
217 private int[][] classify_All(double[][] train, double[] test, int[] train_labels) {
218     int[][] predicted_class = new int[acc + 2][acc];
219     double[][] best_so_far = new double[acc + 2][acc];
220     for (int i = 0; i < predicted_class.length; i++) {
221         for (int j = 0; j < predicted_class[0].length; j++) {
222             predicted_class[i][j] = -1;
223             best_so_far[i][j] = Double.MAX_VALUE;

```

```
224     }
225 }
226 double[][] distance2 = null;
227 CWS_method pv = new CWS_method();
228 for (int i = 0; i < train.length; i++) {
229     distance2 = pv.distance(train[i], test, scale, w0, voices);
230     for (int j = 0; j < distance2.length; j++) {
231         for (int k = 0; k < distance2[0].length; k++) {
232             if (distance2[j][k] < best_so_far[j][k]) {
233                 predicted_class[j][k] = train_labels[i];
234                 best_so_far[j][k] = distance2[j][k];
235             }
236         }
237     }
238 }
239 return predicted_class;
240 }
241
242 private int[] gettrlab(int[] all_labels, int val) {
243     ArrayList<Integer> f = new ArrayList<Integer>();
244     int[] retlab = new int[all_labels.length - 1];
245     for (int i = 0; i < all_labels.length; i++) {
246         f.add(all_labels[i]);
247     }
248     f.remove(val);
249     for (int i = 0; i < f.size(); i++) {
250         retlab[i] = f.get(i);
251     }
252     return (retlab);
253 }
254
255 private int gettelab(int[] all_labels, int val) {
256     ArrayList<Integer> temp = new ArrayList<Integer>();
257     for (int i = 0; i < all_labels.length; i++) {
258         temp.add(all_labels[i]);
259     }
260     return (temp.get(val));
261 }
262
263 private double[][] gettrain(double[][] all_vals, int val) {
264     double[][] all2 = new double[all_vals.length - 1][all_vals[0].length];
265     List valls = new ArrayList();
266     for (int i = 0; i < all_vals.length; i++) {
267         valls.add(all_vals[i]);
268     }
269     valls.remove(val);
270     for (int i = 0; i < valls.size(); i++) {
271         all2[i] = (double[]) valls.get(i);
```

```
272     }
273     return (all12);
274 }
275
276 private double[] gettest(double[][] all_vals, int val) {
277     double[] all12 = new double[1];
278     List vall1 = new ArrayList();
279     for (int i = 0; i < all_vals.length; i++) {
280         vall1.add(all_vals[i]);
281     }
282     all12 = (double[]) vall1.get(val);
283     return (all12);
284 }
285 }
```

LISTING D.3: Load dataset

```
1 package cws;
2
3 import java.io.BufferedReader;
4 import java.io.FileNotFoundException;
5 import java.io.FileReader;
6 import java.io.IOException;
7 import java.util.NoSuchElementException;
8 import java.util.StringTokenizer;
9 import java.util.Vector;
10 /**
11  * This class reads in a dataset.
12  * @author Marc Pienaar
13  * @version 1.0 *
14  */
15 class Dataset extends CWS{
16     private Vector<double[]> data=new Vector<double[]>(1);
17     private Vector<Integer> labels=new Vector<Integer>(1);
18     private int dim=0;
19     public Dataset(String fname) throws FileNotFoundException,IOException
20     {
21         BufferedReader br=new BufferedReader(new FileReader(fname));
22         String line=br.readLine();
23         StringTokenizer st=new StringTokenizer(line);
24         dim=st.countTokens()-1;
25         try
26         {
27             while(line!=null)
28             {
29                 st=new StringTokenizer(line);
30                 data.add(new double[dim]);
31                 labels.add((int)Double.parseDouble(st.nextToken()));
```

```

32         try
33         {
34             for(int i=0;i<dim;i++)
35             {
36                 data.lastElement()[i]=Double.parseDouble(st.nextToken());
37             }
38         }
39         catch(NoSuchElementException e)
40         {
41             System.out.println("Input file "+fname+" corrupted?");
42             System.out.println(e);
43         }
44         line=br.readLine();
45     }
46 }
47 catch(IOException e){System.out.println(e);}
48 }
49 double[] dataAt(int i){return data.elementAt(i);} //Returns an element from a dataset.
50 public int labelAt(int i){return labels.elementAt(i);} //Returns the class label.
51 public int size(){return data.size();} //Returns the number of elements in a dataset.
52 }

```

LISTING D.4: CWS method

```

1 package cws;
2
3 import java.util.ArrayList;
4 import java.util.Arrays;
5 import java.util.List;
6 /**
7  * This class performs the CWS method.
8  * @author Marc Pienaar
9  * @version 1.0 *
10 */
11 class CWS_method {
12
13     public double [][] distance(double[] a,double[] b,double[] scale2,double w0,int voices)
14     {
15         int sampleCount=a.length;
16         double data11[]=new double[sampleCount*2];
17         double data21[]=new double[sampleCount*2];
18         int DT=1;
19         int n=sampleCount;
20         int halfSampleCount=sampleCount/2;
21         double kk[]=new double[halfSampleCount];double k[]=new double[sampleCount];
22         ArrayList<Double> temp=new ArrayList<Double>(),kke=new ArrayList<Double>();
23         k[0]=0;
24         for(int i=1;i<halfSampleCount+1;i++){kk[i-1]=i;kk[i-1]=kk[i-1]*((2*Math.PI)/n*DT);}

```



```

25     for(int i=halfSampleCount-2;i>=0;i--){temp.add(-kk[i]);}
26     for(int i=0;i<kk.length;i++){kke.add(kk[i]);}
27     for(int i=0;i<temp.size();i++){kke.add(temp.get(i));}
28     for(int i=0;i<kke.size();i++){k[i+1]=kke.get(i);}
29     morlet_base base=new morlet_base();
30     double func1[],func2[];
31     func1=new double[sampleCount+1];
32     func2=new double[sampleCount+1];
33     double scale[]=scale2;
34     for(int i=0;i<sampleCount;i++){data11[i*2]=a[i];data21[i*2]=b[i];}
35     ComplexDoubleFFT_Mixed fft_mixed=new ComplexDoubleFFT_Mixed(sampleCount);
36     ComplexDoubleFFT_Mixed fft_mixed2=new ComplexDoubleFFT_Mixed(sampleCount);
37     n=k.length;
38     fft_mixed.transform(data11);fft_mixed2.transform(data21);
39     double[][] wave1=new double[2][scale.length][n];
40     double[][] wave2=new double[2][scale.length][n];
41     for(int i=0;i<scale.length;i++)
42     {
43         double[] daughter=base.wave_bases(k,scale,sampleCount,w0,i);
44         double[] prod1=new double[data11.length];
45         double[] prod2=new double[data11.length];
46         for(int j=0;j<2*n;j++)
47         {
48             prod1[j]=(data11[j]*daughter[j/2]);prod2[j]=(data21[j]*daughter[j/2]);
49         }
50         fft_mixed.inverse(prod1);fft_mixed2.inverse(prod2);
51         for(int j=0;j<n;j++)
52         {
53             wave1[0][i][j]=prod1[j*2];wave1[1][i][j]=prod1[j*2+1];
54             wave2[0][i][j]=prod2[j*2];wave2[1][i][j]=prod2[j*2+1];
55         }
56     }
57     double dataout[][]=new double[wave1[0][0].length][wave1[0].length];
58     double dataout2[][] = new double[wave1[0][0].length][wave1[0].length];
59     double dataout3[][] = new double[wave1[0][0].length][wave1[0].length];
60     for(int i=0;i<wave1[0][0].length;i++)
61     {
62         for(int j=0;j<wave1[0].length;j++)
63         {
64             double cosp=(wave1[0][j][i]*wave2[0][j][i]+wave1[1][j][i]*wave2[1][j][i]);
65             double quad=(wave1[1][j][i]*wave2[0][j][i]-wave1[0][j][i]*wave2[1][j][i]);
66             dataout[i][j]=Math.atan2(quad,cosp);
67             dataout2[i][j]=((2./a.length*Math.sqrt(Math.pow(wave1[0][j][i], 2)+
68                 Math.pow(wave1[1][j][i], 2)))/Math.sqrt(scale[j]));
69             dataout3[i][j]=((2./a.length*Math.sqrt(Math.pow(wave2[0][j][i], 2)+
70                 Math.pow(wave2[1][j][i], 2)))/Math.sqrt(scale[j]));}
71     double[][] morlet=dataout,morletpower1 = dataout2,morletpower2 = dataout3;
72     int W=morlet.length,H=morlet[0].length;

```

```

73     double[] rightvar = new double[H],botvar = new double[W];
74     double[] rightvar2 = new double[H],botvar2 = new double[W];
75     double[] rightvar3 = new double[H],botvar3 = new double[W];
76     for(int h=0;h<H;h++)
77     {
78         for(int w=0;w<W;w++)
79         {
80             botvar[w] = morlet[w][h];botvar2[w] = morletpower1[w][h];
81             botvar3[w] = morletpower2[w][h];
82         }
83         rightvar[h]=variance(botvar);rightvar2[h]=sum(botvar2);rightvar3[h]=sum(botvar3);
84     }
85     ArrayList<Double> answerfinal1=new ArrayList<Double>();
86     ArrayList<Double> answerfinal2=new ArrayList<Double>();
87     for(int i=0;i<scale.length;i++)
88     {for(int j=i;j<scale.length;j++){
89         double answer=sumportionl(rightvar,i,j);
90         double answer2=sumportionpl(rightvar2,rightvar3,i,j);
91         answerfinal1.add(answer);answerfinal2.add(answer2);}}
92     double[][] matrixout= new double[answerfinal1.size()+2][answerfinal1.size()];
93     for(int i=0;i<answerfinal1.size();i++)
94     {matrixout[0][i]=answerfinal1.get(i)+2; matrixout[1][i]=answerfinal2.get(i)+2;}
95     for(int i=2;i<answerfinal1.size();i++)
96     {for(int j=0;j<answerfinal1.size();j++){
97         matrixout[i][j]=(answerfinal1.get(i)+2)*(answerfinal2.get(j)+2);}}
98     double[] answerfinal=new double[answerfinal1.size()];
99     for(int i=0;i<answerfinal.length;i++){answerfinal[i]=answerfinal1.get(i);}
100    return matrixout;
101 }
102 private double sumportionpl(double[] datapower,
103     double[] datapower2,int portiostart,
104     int portioend)
105 {
106     double rett=0,rett2=0;
107     double[] data11=datapower,data111=datapower2;
108     ArrayList<Double> d2=new ArrayList<Double>();
109     ArrayList<Double> d3=new ArrayList<Double>();
110     Euclidean_distance ed=new Euclidean_distance();
111     for(int i=(portiostart);i<(portioend);i++){d2.add(data11[i]);d3.add(data111[i]);}
112     double[] data2=new double[d2.size()];double[] data3=new double[d2.size()];
113     for(int i=0;i<d2.size();i++){data2[i]=d2.get(i);data3[i]=d3.get(i);}
114     return (ed.distance(data2,data3));
115 }
116 private double sumportionl(double[] data,int portiostart,int portioend)
117 {
118     double rett=0;double[] data1=data;
119     for(int i=(portiostart);i<=(portioend);i++){rett+=data1[i);}
120     return (rett);

```

```

121     }
122     private double variance(double[] data)
123     {
124         double mean=0;
125         for(int i=0;i<data.length;i++){ mean+=data[i];}
126         mean/=data.length;
127         double var=0;
128         for(int i=0;i<data.length;i++){var+=(data[i]-mean)*(data[i]-mean);}
129         var/=data.length-1;
130         return var;
131     }
132     private double sum(double[] data)
133     {
134         double sum=0;
135         for(int i=0;i<data.length;i++){sum+=data[i];}
136         return sum;
137     }
138 }

```

LISTING D.5: Morlet base

```

1 package cws;
2 /**
3  * Copyright (C) 1995-1998, Christopher Torrence and Gilbert P. Compo %
4  * University of Colorado, Program in Atmospheric and Oceanic Sciences. % This
5  * software may be used, copied, or redistributed as long as it is not % sold
6  * and this copyright notice is reproduced on each copy made. This % routine is
7  * provided as is without any express or implied warranties % whatsoever.
8  * %-----
9  *
10 * @author modified by Marc Pienaar
11 */
12 class morlet_base {
13     public double[] wave_bases(double[] k, double[] scale, int sampleCount, double k0, int a1) {
14         int n = k.length;double norm;
15         double[] daughter = new double[sampleCount],daughtertest = new double[sampleCount];
16         double[] expnt = new double[sampleCount];
17         for (int i = 0; i < sampleCount; i++) {
18             if (k[i] > 0){expnt[i] = -Math.pow((scale[a1] * k[i] - k0), 2.) / 2.;}
19             else {expnt[i] = 0;}}
20         norm = Math.sqrt(scale[a1] * k[1]) * (Math.pow(Math.PI, (-0.25)) * Math.sqrt(n));
21         for (int i = 0; i < sampleCount; i++) {daughtertest[i] = norm * Math.exp(expnt[i]);}
22         for (int i = 0; i < sampleCount; i++) {
23             if (k[i] > 0) {daughter[i] = daughtertest[i];}
24             else {daughter[i] = 0; }
25         }
26         return daughter;
27     }

```

28 }  
}

LISTING D.6: Euclidean distance

```

1 package cws;
2 /**
3  * This class is used to get the Euclidean distance between two arrays.
4  * @author Marc Pienaar
5  * @version 1.0 *
6  */
7 public class Euclidean_distance {
8     public double distance(double[] a, double[] b) {
9         double sum = 0;
10        for (int i=0; i < a.length; i++)
11            sum += (a[i] - b[i])*(a[i] - b[i]);
12        return Math.sqrt(sum);
13    }
14 }

```

LISTING D.7: DTW

```

1 package cws;
2 /**
3  * This class implements the Dynamic Time Warping algorithm
4  * given two sequences
5  * <pre>
6  *   X = x1, x2, ..., xi, ..., xn
7  *   Y = y1, y2, ..., yj, ..., ym
8  * </pre>
9  *
10 * @author Cheol-Woo Jung (cjung@gatech.edu)
11 * @version 1.0
12 */
13 public class DTW
14 {
15     protected double[] seq1, seq2;
16     protected int[][] warpingPath;
17     protected int n,m,K;
18     protected double warpingDistance;
19     /**
20     * Constructor
21     *
22     * @param query
23     * @param templete
24     */
25     public DTW(double[] sample, double[] templete)
26     {
27         seq1=sample; seq2=templete;

```

```

28     n=seq1.length;
29     m=seq2.length;
30     K=1;
31     warpingPath=new int[n+m][2];    // max(n, m) <= K < n + m
32     warpingDistance=0.0;
33     this.compute();
34 }
35 public void compute()
36 {
37     double accumulatedDistance=0.0;
38     double[][] d=new double[n][m]; // local distances
39     double[][] D=new double[n][m]; // global distances
40     for(int i=0;i<n;i++){for(int j=0;j<m;j++){d[i][j]=distanceBetween(seq1[i],seq2[j]);}}
41     D[0][0]=d[0][0];
42     for(int i=1;i<n;i++){ D[i][0]=d[i][0]+D[i-1][0];}
43     for(int j=1;j<m;j++){D[0][j]=d[0][j]+D[0][j-1];}
44     for(int i=1;i<n;i++){for(int j=1;j<m;j++){
45         accumulatedDistance=Math.min(Math.min(D[i-1][j],D[i-1][j-1]),
46                                     D[i][j-1]);
47         accumulatedDistance+=d[i][j];D[i][j]=accumulatedDistance;}
48     }
49     accumulatedDistance=D[n-1][m-1];
50     int i=n-1,j=m-1,minIndex=1;
51     warpingPath[K-1][0]=i;warpingPath[K-1][1]=j;
52     while((i+j)!=0){
53         if(i==0){j-=1;}
54         else if(j==0){ i-=1;}
55         else{
56             double[] array=
57             {
58                 D[i-1][j],D[i][j-1],D[i-1][j-1]
59             };
60             minIndex=this.getIndexOfMinimum(array);
61             if(minIndex==0){i-=1;}
62             else if(minIndex==1){j-=1;}
63             else if(minIndex==2){i-=1;j-=1;}
64         }
65         K++;warpingPath[K-1][0]=i;warpingPath[K-1][1]=j;
66     } // end while
67     warpingDistance=accumulatedDistance/K;
68     this.reversePath(warpingPath);
69 }
70 /**
71  * Changes the order of the warping path (increasing order)
72  *
73  * @param path    the warping path in reverse order
74  */
75 protected void reversePath(int[][] path)

```

```
76     {
77         int[] [] newPath=new int[K][2];
78         for(int i=0;i<K;i++){for(int j=0;j<2;j++)
79             {
80                 newPath[i][j]=path[K-i-1][j];
81             }}
82         warpingPath=newPath;
83     }
84     /**
85      * Returns the warping distance
86      *
87      * @return
88      */
89     public double getDistance(){return warpingDistance;}
90     /**
91      * Computes a distance between two points
92      *
93      * @param p1         the point 1
94      * @param p2         the point 2
95      * @return           the distance between two points
96      */
97     protected double distanceBetween(double p1,double p2){
98         return (p1-p2)*(p1-p2);
99     }
100    /**
101     * Finds the index of the minimum element from the given array
102     *
103     * @param array       the array containing numeric values
104     * @return            the min value among elements
105     */
106    protected int getIndexOfMinimum(double[] array)
107    {
108        int index=0;double val=array[0];
109        for(int i=1;i<array.length;i++){if(array[i]<val){val=array[i];index=i;}}
110        return index;
111    }
112    /**
113     * Returns a string that displays the warping distance and path
114     */
115    public String toString()
116    {
117        String retVal="Warping Distance: "+warpingDistance+"\n";
118        retVal+="Warping Path: {";
119        for(int i=0;i<K;i++)
120        {
121            retVal+="("+warpingPath[i][0]+", "+warpingPath[i][1]+")";
122            retVal+=(i==K-1?"}":"}, ";
123        }
124    }
```

```

124     return retVal;
125 }
126 /**
127  * Tests this class
128  *
129  * @param args    ignored
130  */
131 public static void main(String[] args)
132 {
133     //float[] n2 = {1.5f, 3.9f, 4.1f, 3.3f};
134     //float[] n1 = {2.1f, 2.45f, 3.673f, 4.32f, 2.05f, 1.93f, 5.67f, 6.01f};
135     //DTW dtw = new DTW(n1, n2);
136     //System.out.println(dtw.getDistance());
137 }
138 }

```

LISTING D.8: ComplexDoubleFFT\_Mixed

```

1 package cws;
2
3 //package jnt.FFT;
4
5 /** Computes FFT's of complex, double precision data of arbitrary length n.
6  * This class uses the Mixed Radix method; it has special methods to handle
7  * factors 2, 3, 4, 5, 6 and 7, as well as a general factor.
8  * <P>
9  * This method appears to be faster than the Radix2 method, when both methods apply,
10 * but requires extra storage (which ComplexDoubleFFT_Mixed manages itself).
11 * <P>
12 * See {@link ComplexDoubleFFT ComplexDoubleFFT} for details of data layout.
13 *
14 * @author Bruce R. Miller bruce.miller@nist.gov
15 * @author Contribution of the National Institute of Standards and Technology,
16 * @author not subject to copyright.
17 * @author Derived from GSL (Gnu Scientific Library)
18 * @author GSL's FFT Code by Brian Gough bjg@vsv.lanl.gov
19 * @author Since GSL is released under
20 * @author <H HREF="http://www.gnu.org/copyleft/gpl.html">GPL</A>,
21 * @author this package must also be.
22 */
23 public class ComplexDoubleFFT_Mixed extends ComplexDoubleFFT{
24     static final double PI = Math.PI;
25
26     public ComplexDoubleFFT_Mixed(int n){
27         super(n);
28         setup_wavetable(n);
29     }
30     public void transform(double data[], int i0, int stride) {

```

```

31     checkData(data,i0,stride);
32     transform_internal(data, i0, stride, -1); }
33 public void backtransform (double data[], int i0, int stride){
34     checkData(data,i0,stride);
35     transform_internal(data, i0, stride, +1); }
36 /*-----
37     Setting up the Wavetable */
38
39 private int factors[];
40 // Reversed the last 2 levels of the twiddle array compared to what the C version had.
41 private double twiddle[][][];
42 private int available_factors[]={7, 6, 5, 4, 3, 2};
43 void setup_wavetable(int n){
44     if (n <= 0) {throw new Error("mmm"+n); }
45     this.n = n;
46     factors = Factorize.factor(n, available_factors);
47     double d_theta = -2.0 * PI / (n);
48     int product = 1;
49     twiddle = new double[factors.length][][];
50     for (int i = 0; i < factors.length; i++) {
51         int factor = factors[i];
52         int product_1 = product;
53         product *= factor;int q = n / product;
54         twiddle[i] = new double[q+1][2*(factor-1)];double twid[][] = twiddle[i];
55         for(int j=1; j<factor; j++){twid[0][2*(j-1)] = 1.0;twid[0][2*(j-1)+1] = 0.0;}
56         for (int k = 1; k <= q; k++) {int m = 0;
57             for(int j=1; j<factor; j++){
58                 m += k*product_1;m %= n;double theta = d_theta * m;
59                 twid[k][2*(j-1)] = Math.cos(theta);twid[k][2*(j-1)+1] = Math.sin(theta);}}
60     }
61 }
62 /*-----
63     The main transformation driver */
64 void transform_internal(double data[], int i0, int stride, int sign){
65     if (n == 1) {return; /* FFT of 1 data point is the identity */}
66     double scratch[] = new double[2*n];
67     int product = 1;
68     int state = 0;
69     double in[], out[];
70     int istrate, ostride;
71     int in0, out0;
72     for (int i = 0; i < factors.length; i++) {
73         int factor = factors[i];
74         product *= factor;
75
76         if (state == 0) {
77             in = data;
78             in0 = i0;

```



```

79     istrade = stride;
80     out = scratch;
81     out0 = 0;
82     ostride = 2;
83     state = 1; }
84 else {
85     in = scratch;
86     in0 = 0;
87     istrade = 2;
88     out = data;
89     out0 = i0;
90     ostride = stride;
91     state = 0; }
92
93     switch(factor){
94     case 2: pass_2(i,in, in0, istrade, out, out0, ostride, sign, product); break;
95     case 3: pass_3(i,in, in0, istrade, out, out0, ostride, sign, product); break;
96     case 4: pass_4(i,in, in0, istrade, out, out0, ostride, sign, product); break;
97     case 5: pass_5(i,in, in0, istrade, out, out0, ostride, sign, product); break;
98     case 6: pass_6(i,in, in0, istrade, out, out0, ostride, sign, product); break;
99     case 7: pass_7(i,in, in0, istrade, out, out0, ostride, sign, product); break;
100    default:pass_n(i,in, in0, istrade, out, out0, ostride, sign, factor, product); }
101 }
102 if (state == 1){ /* copy results back from scratch to data */
103     for (int i = 0; i < n; i++) {
104         data[i0+stride*i] = scratch[2*i];
105         data[i0+stride*i+1] = scratch[2*i+1]; }}
106 }
107
108 /*-----*/
109
110 void pass_2(int fi,
111             double in[], int in0, int istrade,
112             double out[], int out0, int ostride,
113             int sign, int product) {
114     int k, k1;
115
116     int factor = 2;
117     int m = n / factor;
118     int q = n / product;
119     int product_1 = product / factor;
120
121     int di = istrade * m;
122     int dj = ostride * product_1;
123     int i = in0, j = out0;
124     double x_real, x_imag;
125     for (k = 0; k < q; k++) {
126         double twids[] = twiddle[fi][k];

```

```

127     double w_real =      twids[0];
128     double w_imag = -sign*twids[1];
129
130     for (k1 = 0; k1 < product_1; k1++) {
131         double z0_real = in[i];
132         double z0_imag = in[i+1];
133         double z1_real = in[i+di];
134         double z1_imag = in[i+di+1];
135         i += istride;
136
137         /* compute x = W(2) z */
138
139         /* apply twiddle factors */
140
141         /* out0 = 1 * (z0 + z1) */
142         out[j]   = z0_real + z1_real;
143         out[j+1] = z0_imag + z1_imag;
144
145         /* out1 = w * (z0 - z1) */
146         x_real = z0_real - z1_real;
147         x_imag = z0_imag - z1_imag;
148         out[j+dj]   = w_real * x_real - w_imag * x_imag;
149         out[j+dj+1] = w_real * x_imag + w_imag * x_real;
150
151         j += ostride;
152     }
153     j += (factor-1)*dj;
154 }}
155 /*-----*/
156
157 void pass_3(int fi,
158            double in[], int in0, int istride,
159            double out[], int out0, int ostride,
160            int sign, int product) {
161     int k, k1;
162
163     int factor = 3;
164     int m = n / factor;
165     int q = n / product;
166     int product_1 = product / factor;
167     double tau = sign * Math.sqrt(3.0) / 2.0;
168     int di = istride * m;
169     int dj = ostride * product_1;
170     int i = in0, j = out0;
171     double x_real, x_imag;
172     for (k = 0; k < q; k++) {
173         double twids[] = twiddle[fi][k];
174         double w1_real =      twids[0];

```

```
175     double w1_imag = -sign*twids[1];
176     double w2_real =      twids[2];
177     double w2_imag = -sign*twids[3];
178
179     for (k1 = 0; k1 < product_1; k1++) {
180         double z0_real = in[i];
181         double z0_imag = in[i+1];
182         double z1_real = in[i+di];
183         double z1_imag = in[i+di+1];
184         double z2_real = in[i+2*di];
185         double z2_imag = in[i+2*di+1];
186         i += istride;
187
188         /* compute x = W(3) z */
189
190         /* t1 = z1 + z2 */
191         double t1_real = z1_real + z2_real;
192         double t1_imag = z1_imag + z2_imag;
193
194         /* t2 = z0 - t1/2 */
195         double t2_real = z0_real - t1_real / 2.0;
196         double t2_imag = z0_imag - t1_imag / 2.0;
197
198         /* t3 = (+/-) sin(pi/3)*(z1 - z2) */
199         double t3_real = tau * (z1_real - z2_real);
200         double t3_imag = tau * (z1_imag - z2_imag);
201
202         /* apply twiddle factors */
203
204         /* out0 = 1 * (z0 + t1) */
205         out[j]   = z0_real + t1_real;
206         out[j+1] = z0_imag + t1_imag;
207
208         /* out1 = w1 * (t2 + i t3) */
209         x_real = t2_real - t3_imag;
210         x_imag = t2_imag + t3_real;
211         out[j+dj]   = w1_real * x_real - w1_imag * x_imag;
212         out[j+dj+1] = w1_real * x_imag + w1_imag * x_real;
213
214         /* out2 = w2 * (t2 - i t3) */
215         x_real = t2_real + t3_imag;
216         x_imag = t2_imag - t3_real;
217         out[j+2*dj]   = w2_real * x_real - w2_imag * x_imag;
218         out[j+2*dj+1] = w2_real * x_imag + w2_imag * x_real;
219
220         j += ostride;
221     }
222     j += (factor-1) * dj;
```

```
223     }}
224     /*-----*/
225
226 void pass_4(int fi,
227            double in[], int in0, int istrate,
228            double out[], int out0, int ostride,
229            int sign, int product) {
230     int k, k1;
231
232     int factor = 4;
233     int m = n / factor;
234     int q = n / product;
235     int p_1 = product / factor;
236     int i = in0, j = out0;
237     int di = istrate * m;
238     int dj = ostride * p_1;
239     double x_real, x_imag;
240     for (k = 0; k < q; k++) {
241         double twids[] = twiddle[fi][k];
242         double w1_real = twids[0];
243         double w1_imag = -sign*twids[1];
244         double w2_real = twids[2];
245         double w2_imag = -sign*twids[3];
246         double w3_real = twids[4];
247         double w3_imag = -sign*twids[5];
248
249         for (k1 = 0; k1 < p_1; k1++) {
250             double z0_real = in[i];
251             double z0_imag = in[i+1];
252             double z1_real = in[i+di];
253             double z1_imag = in[i+di+1];
254             double z2_real = in[i+2*di];
255             double z2_imag = in[i+2*di+1];
256             double z3_real = in[i+3*di];
257             double z3_imag = in[i+3*di+1];
258             i += istrate;
259
260             /* compute x = W(4) z */
261
262             /* t1 = z0 + z2 */
263             double t1_real = z0_real + z2_real;
264             double t1_imag = z0_imag + z2_imag;
265
266             /* t2 = z1 + z3 */
267             double t2_real = z1_real + z3_real;
268             double t2_imag = z1_imag + z3_imag;
269
270             /* t3 = z0 - z2 */
```

```
271     double t3_real = z0_real - z2_real;
272     double t3_imag = z0_imag - z2_imag;
273
274     /* t4 = (+/-) (z1 - z3) */
275     double t4_real = sign * (z1_real - z3_real);
276     double t4_imag = sign * (z1_imag - z3_imag);
277
278     /* apply twiddle factors */
279
280     /* out0 = 1 * (t1 + t2) */
281     out[j]   = t1_real + t2_real;
282     out[j+1] = t1_imag + t2_imag;
283
284     /* out1 = w1 * (t3 + i t4) */
285     x_real = t3_real - t4_imag;
286     x_imag = t3_imag + t4_real;
287     out[j + dj]   = w1_real * x_real - w1_imag * x_imag;
288     out[j + dj+1] = w1_real * x_imag + w1_imag * x_real;
289
290     /* out2 = w2 * (t1 - t2) */
291     x_real = t1_real - t2_real;
292     x_imag = t1_imag - t2_imag;
293     out[j + 2 * dj]   = w2_real * x_real - w2_imag * x_imag;
294     out[j + 2 * dj+1] = w2_real * x_imag + w2_imag * x_real;
295
296     /* out3 = w3 * (t3 - i t4) */
297     x_real = t3_real + t4_imag;
298     x_imag = t3_imag - t4_real;
299     out[j + 3 * dj]   = w3_real * x_real - w3_imag * x_imag;
300     out[j + 3 * dj+1] = w3_real * x_imag + w3_imag * x_real;
301
302     j += ostride;
303 }
304 j += (factor - 1)*dj;
305 }}
306 /*-----*/
307
308 void pass_5(int fi,
309            double in[], int in0, int istride,
310            double out[], int out0, int ostride,
311            int sign, int product) {
312     int k, k1;
313
314     int factor = 5;
315     int m = n / factor;
316     int q = n / product;
317     int p_1 = product / factor;
318     double tau = (Math.sqrt (5.0) / 4.0);
```

```
319 double sin_2pi_by_5 = sign * Math.sin (2.0 * PI / 5.0);
320 double sin_2pi_by_10 = sign * Math.sin (2.0 * PI / 10.0);
321 int i = in0, j = out0;
322 int di = istride * m;
323 int dj = ostride * p_1;
324 double x_real, x_imag;
325 for (k = 0; k < q; k++) {
326     double twids[] = twiddle[fi][k];
327     double w1_real = twids[0];
328     double w1_imag = -sign*twids[1];
329     double w2_real = twids[2];
330     double w2_imag = -sign*twids[3];
331     double w3_real = twids[4];
332     double w3_imag = -sign*twids[5];
333     double w4_real = twids[6];
334     double w4_imag = -sign*twids[7];
335
336     for (k1 = 0; k1 < p_1; k1++) {
337         double z0_real = in[i];
338         double z0_imag = in[i+1];
339         double z1_real = in[i + di];
340         double z1_imag = in[i + di+1];
341         double z2_real = in[i + 2*di];
342         double z2_imag = in[i + 2*di+1];
343         double z3_real = in[i + 3*di];
344         double z3_imag = in[i + 3*di+1];
345         double z4_real = in[i + 4*di];
346         double z4_imag = in[i + 4*di+1];
347         i += istride;
348
349         /* compute x = W(5) z */
350
351         /* t1 = z1 + z4 */
352         double t1_real = z1_real + z4_real;
353         double t1_imag = z1_imag + z4_imag;
354
355         /* t2 = z2 + z3 */
356         double t2_real = z2_real + z3_real;
357         double t2_imag = z2_imag + z3_imag;
358
359         /* t3 = z1 - z4 */
360         double t3_real = z1_real - z4_real;
361         double t3_imag = z1_imag - z4_imag;
362
363         /* t4 = z2 - z3 */
364         double t4_real = z2_real - z3_real;
365         double t4_imag = z2_imag - z3_imag;
366
```

```
367     /* t5 = t1 + t2 */
368     double t5_real = t1_real + t2_real;
369     double t5_imag = t1_imag + t2_imag;
370
371     /* t6 = (sqrt(5)/4)(t1 - t2) */
372     double t6_real = tau * (t1_real - t2_real);
373     double t6_imag = tau * (t1_imag - t2_imag);
374
375     /* t7 = z0 - ((t5)/4) */
376     double t7_real = z0_real - t5_real / 4.0;
377     double t7_imag = z0_imag - t5_imag / 4.0;
378
379     /* t8 = t7 + t6 */
380     double t8_real = t7_real + t6_real;
381     double t8_imag = t7_imag + t6_imag;
382
383     /* t9 = t7 - t6 */
384     double t9_real = t7_real - t6_real;
385     double t9_imag = t7_imag - t6_imag;
386
387     /* t10 = sin(2 pi/5) t3 + sin(2 pi/10) t4 */
388     double t10_real = sin_2pi_by_5 * t3_real + sin_2pi_by_10 * t4_real;
389     double t10_imag = sin_2pi_by_5 * t3_imag + sin_2pi_by_10 * t4_imag;
390
391     /* t11 = sin(2 pi/10) t3 - sin(2 pi/5) t4 */
392     double t11_real = sin_2pi_by_10 * t3_real - sin_2pi_by_5 * t4_real;
393     double t11_imag = sin_2pi_by_10 * t3_imag - sin_2pi_by_5 * t4_imag;
394
395     /* apply twiddle factors */
396
397     /* out0 = 1 * (z0 + t5) */
398     out[j] = z0_real + t5_real;
399     out[j+1] = z0_imag + t5_imag;
400
401     /* out1 = w1 * (t8 + i t10) */
402     x_real = t8_real - t10_imag;
403     x_imag = t8_imag + t10_real;
404     out[j + dj] = w1_real * x_real - w1_imag * x_imag;
405     out[j + dj+1] = w1_real * x_imag + w1_imag * x_real;
406
407     /* out2 = w2 * (t9 + i t11) */
408     x_real = t9_real - t11_imag;
409     x_imag = t9_imag + t11_real;
410     out[j+2*dj] = w2_real * x_real - w2_imag * x_imag;
411     out[j+2*dj+1] = w2_real * x_imag + w2_imag * x_real;
412
413     /* out3 = w3 * (t9 - i t11) */
414     x_real = t9_real + t11_imag;
```

```

415     x_imag = t9_imag - t11_real;
416     out[j+3*dj] = w3_real * x_real - w3_imag * x_imag;
417     out[j+3*dj+1] = w3_real * x_imag + w3_imag * x_real;
418
419     /* out4 = w4 * (t8 - i t10) */
420     x_real = t8_real + t10_imag;
421     x_imag = t8_imag - t10_real;
422     out[j+4*dj] = w4_real * x_real - w4_imag * x_imag;
423     out[j+4*dj+1] = w4_real * x_imag + w4_imag * x_real;
424
425     j += ostride;
426 }
427 j += (factor - 1)*dj;
428 }}
429 /*-----*/
430
431 void pass_6(int fi,
432            double in[], int in0, int istrate,
433            double out[], int out0, int ostride,
434            int sign, int product) {
435
436     int k, k1;
437
438     int factor = 6;
439     int m = n / factor;
440     int q = n / product;
441     int p_1 = product / factor;
442     double tau = sign * Math.sqrt (3.0) / 2.0;
443     int i = in0, j = out0;
444     int di = istrate * m;
445     int dj = ostride * p_1;
446     double x_real, x_imag;
447     for (k = 0; k < q; k++) {
448         double twids[] = twiddle[fi][k];
449         double w1_real = twids[0];
450         double w1_imag = -sign*twids[1];
451         double w2_real = twids[2];
452         double w2_imag = -sign*twids[3];
453         double w3_real = twids[4];
454         double w3_imag = -sign*twids[5];
455         double w4_real = twids[6];
456         double w4_imag = -sign*twids[7];
457         double w5_real = twids[8];
458         double w5_imag = -sign*twids[9];
459
460         for (k1 = 0; k1 < p_1; k1++) {
461             double z0_real = in[i];
462             double z0_imag = in[i+1];

```



```
463     double z1_real = in[i+di];
464     double z1_imag = in[i+di+1];
465     double z2_real = in[i+2*di];
466     double z2_imag = in[i+2*di+1];
467     double z3_real = in[i+3*di];
468     double z3_imag = in[i+3*di+1];
469     double z4_real = in[i+4*di];
470     double z4_imag = in[i+4*di+1];
471     double z5_real = in[i+5*di];
472     double z5_imag = in[i+5*di+1];
473     i += istride;
474
475     /* compute x = W(6) z */
476
477     /* W(6) is a combination of sums and differences of W(3) acting
478        on the even and odd elements of z */
479
480     /* ta1 = z2 + z4 */
481     double ta1_real = z2_real + z4_real;
482     double ta1_imag = z2_imag + z4_imag;
483
484     /* ta2 = z0 - ta1/2 */
485     double ta2_real = z0_real - ta1_real / 2;
486     double ta2_imag = z0_imag - ta1_imag / 2;
487
488     /* ta3 = (+/-) sin(pi/3)*(z2 - z4) */
489     double ta3_real = tau * (z2_real - z4_real);
490     double ta3_imag = tau * (z2_imag - z4_imag);
491
492     /* a0 = z0 + ta1 */
493     double a0_real = z0_real + ta1_real;
494     double a0_imag = z0_imag + ta1_imag;
495
496     /* a1 = ta2 + i ta3 */
497     double a1_real = ta2_real - ta3_imag;
498     double a1_imag = ta2_imag + ta3_real;
499
500     /* a2 = ta2 - i ta3 */
501     double a2_real = ta2_real + ta3_imag;
502     double a2_imag = ta2_imag - ta3_real;
503
504     /* tb1 = z5 + z1 */
505     double tb1_real = z5_real + z1_real;
506     double tb1_imag = z5_imag + z1_imag;
507
508     /* tb2 = z3 - tb1/2 */
509     double tb2_real = z3_real - tb1_real / 2;
510     double tb2_imag = z3_imag - tb1_imag / 2;
```

```
511
512     /* tb3 = (+/-) sin(pi/3)*(z5 - z1) */
513     double tb3_real = tau * (z5_real - z1_real);
514     double tb3_imag = tau * (z5_imag - z1_imag);
515
516     /* b0 = z3 + tb1 */
517     double b0_real = z3_real + tb1_real;
518     double b0_imag = z3_imag + tb1_imag;
519
520     /* b1 = tb2 + i tb3 */
521     double b1_real = tb2_real - tb3_imag;
522     double b1_imag = tb2_imag + tb3_real;
523
524     /* b2 = tb2 - i tb3 */
525     double b2_real = tb2_real + tb3_imag;
526     double b2_imag = tb2_imag - tb3_real;
527
528     /* apply twiddle factors */
529
530     /* out0 = 1 * (a0 + b0) */
531     out[j] = a0_real + b0_real;
532     out[j+1] = a0_imag + b0_imag;
533
534     /* out1 = w1 * (a1 - b1) */
535     x_real = a1_real - b1_real;
536     x_imag = a1_imag - b1_imag;
537     out[j+dj] = w1_real * x_real - w1_imag * x_imag;
538     out[j+dj+1] = w1_real * x_imag + w1_imag * x_real;
539
540     /* out2 = w2 * (a2 + b2) */
541     x_real = a2_real + b2_real;
542     x_imag = a2_imag + b2_imag;
543     out[j+2*dj] = w2_real * x_real - w2_imag * x_imag;
544     out[j+2*dj+1] = w2_real * x_imag + w2_imag * x_real;
545
546     /* out3 = w3 * (a0 - b0) */
547     x_real = a0_real - b0_real;
548     x_imag = a0_imag - b0_imag;
549     out[j+3*dj] = w3_real * x_real - w3_imag * x_imag;
550     out[j+3*dj+1] = w3_real * x_imag + w3_imag * x_real;
551
552     /* out4 = w4 * (a1 + b1) */
553     x_real = a1_real + b1_real;
554     x_imag = a1_imag + b1_imag;
555     out[j+4*dj] = w4_real * x_real - w4_imag * x_imag;
556     out[j+4*dj+1] = w4_real * x_imag + w4_imag * x_real;
557
558     /* out5 = w5 * (a2 - b2) */
```

```
559     x_real = a2_real - b2_real;
560     x_imag = a2_imag - b2_imag;
561     out[j+5*dj] = w5_real * x_real - w5_imag * x_imag;
562     out[j+5*dj+1] = w5_real * x_imag + w5_imag * x_real;
563
564     j += ostride;
565 }
566 j += (factor - 1)*dj;
567 }}
568 /*-----*/
569
570 void pass_7(int fi,
571            double in[], int in0, int istrate,
572            double out[], int out0, int ostride,
573            int sign, int product){
574
575     int k, k1;
576
577     int factor = 7;
578     int m = n / factor;
579     int q = n / product;
580     int p_1 = product / factor;
581     double c1 = Math.cos(1.0 * 2.0 * PI / 7.0);
582     double c2 = Math.cos(2.0 * 2.0 * PI / 7.0);
583     double c3 = Math.cos(3.0 * 2.0 * PI / 7.0);
584
585     double s1 = (-sign)*Math.sin(1.0 * 2.0 * PI / 7.0);
586     double s2 = (-sign)*Math.sin(2.0 * 2.0 * PI / 7.0);
587     double s3 = (-sign)*Math.sin(3.0 * 2.0 * PI / 7.0);
588     int i = in0, j = out0;
589     int di = istrate * m;
590     int dj = ostride * p_1;
591     double x_real, x_imag;
592     for (k = 0; k < q; k++) {
593         double twids[] = twiddle[fi][k];
594         double w1_real = twids[0];
595         double w1_imag = -sign*twids[1];
596         double w2_real = twids[2];
597         double w2_imag = -sign*twids[3];
598         double w3_real = twids[4];
599         double w3_imag = -sign*twids[5];
600         double w4_real = twids[6];
601         double w4_imag = -sign*twids[7];
602         double w5_real = twids[8];
603         double w5_imag = -sign*twids[9];
604         double w6_real = twids[10];
605         double w6_imag = -sign*twids[11];
606
```

```
607     for (k1 = 0; k1 < p_1; k1++) {
608         double z0_real = in[i];
609         double z0_imag = in[i+1];
610         double z1_real = in[i+di];
611         double z1_imag = in[i+di+1];
612         double z2_real = in[i+2*di];
613         double z2_imag = in[i+2*di+1];
614         double z3_real = in[i+3*di];
615         double z3_imag = in[i+3*di+1];
616         double z4_real = in[i+4*di];
617         double z4_imag = in[i+4*di+1];
618         double z5_real = in[i+5*di];
619         double z5_imag = in[i+5*di+1];
620         double z6_real = in[i+6*di];
621         double z6_imag = in[i+6*di+1];
622         i += istride;
623
624         /* compute x = W(7) z */
625
626         /* t0 = z1 + z6 */
627         double t0_real = z1_real + z6_real;
628         double t0_imag = z1_imag + z6_imag;
629
630         /* t1 = z1 - z6 */
631         double t1_real = z1_real - z6_real;
632         double t1_imag = z1_imag - z6_imag;
633
634         /* t2 = z2 + z5 */
635         double t2_real = z2_real + z5_real;
636         double t2_imag = z2_imag + z5_imag;
637
638         /* t3 = z2 - z5 */
639         double t3_real = z2_real - z5_real;
640         double t3_imag = z2_imag - z5_imag;
641
642         /* t4 = z4 + z3 */
643         double t4_real = z4_real + z3_real;
644         double t4_imag = z4_imag + z3_imag;
645
646         /* t5 = z4 - z3 */
647         double t5_real = z4_real - z3_real;
648         double t5_imag = z4_imag - z3_imag;
649
650         /* t6 = t2 + t0 */
651         double t6_real = t2_real + t0_real;
652         double t6_imag = t2_imag + t0_imag;
653
654         /* t7 = t5 + t3 */
```

```
655     double t7_real = t5_real + t3_real;
656     double t7_imag = t5_imag + t3_imag;
657
658     /* b0 = z0 + t6 + t4 */
659     double b0_real = z0_real + t6_real + t4_real;
660     double b0_imag = z0_imag + t6_imag + t4_imag;
661
662     /* b1 = ((cos(2pi/7) + cos(4pi/7) + cos(6pi/7))/3-1) (t6 + t4) */
663     double b1_real = (((c1 + c2 + c3)/3.0 - 1.0) * (t6_real + t4_real));
664     double b1_imag = (((c1 + c2 + c3)/3.0 - 1.0) * (t6_imag + t4_imag));
665
666     /* b2 = ((2*cos(2pi/7) - cos(4pi/7) - cos(6pi/7))/3) (t0 - t4) */
667     double b2_real = (((2.0 * c1 - c2 - c3)/3.0) * (t0_real - t4_real));
668     double b2_imag = (((2.0 * c1 - c2 - c3)/3.0) * (t0_imag - t4_imag));
669
670     /* b3 = ((cos(2pi/7) - 2*cos(4pi/7) + cos(6pi/7))/3) (t4 - t2) */
671     double b3_real = (((c1 - 2.0*c2 + c3)/3.0) * (t4_real - t2_real));
672     double b3_imag = (((c1 - 2.0*c2 + c3)/3.0) * (t4_imag - t2_imag));
673
674     /* b4 = ((cos(2pi/7) + cos(4pi/7) - 2*cos(6pi/7))/3) (t2 - t0) */
675     double b4_real = (((c1 + c2 - 2.0 * c3)/3.0) * (t2_real - t0_real));
676     double b4_imag = (((c1 + c2 - 2.0 * c3)/3.0) * (t2_imag - t0_imag));
677
678     /* b5 = sign * ((sin(2pi/7) + sin(4pi/7) - sin(6pi/7))/3) (t7 + t1) */
679     double b5_real = ((s1 + s2 - s3)/3.0) * (t7_real + t1_real);
680     double b5_imag = ((s1 + s2 - s3)/3.0) * (t7_imag + t1_imag);
681
682     /* b6 = sign * ((2sin(2pi/7) - sin(4pi/7) + sin(6pi/7))/3) (t1 - t5) */
683     double b6_real = ((2.0 * s1 - s2 + s3)/3.0) * (t1_real - t5_real);
684     double b6_imag = ((2.0 * s1 - s2 + s3)/3.0) * (t1_imag - t5_imag);
685
686     /* b7 = sign * ((sin(2pi/7) - 2sin(4pi/7) - sin(6pi/7))/3) (t5 - t3) */
687     double b7_real = ((s1 - 2.0 * s2 - s3)/3.0) * (t5_real - t3_real);
688     double b7_imag = ((s1 - 2.0 * s2 - s3)/3.0) * (t5_imag - t3_imag);
689
690     /* b8 = sign * ((sin(2pi/7) + sin(4pi/7) + 2sin(6pi/7))/3) (t3 - t1) */
691     double b8_real = ((s1 + s2 + 2.0 * s3)/3.0) * (t3_real - t1_real);
692     double b8_imag = ((s1 + s2 + 2.0 * s3)/3.0) * (t3_imag - t1_imag);
693
694
695     /* T0 = b0 + b1 */
696     double T0_real = b0_real + b1_real;
697     double T0_imag = b0_imag + b1_imag;
698
699     /* T1 = b2 + b3 */
700     double T1_real = b2_real + b3_real;
701     double T1_imag = b2_imag + b3_imag;
702
```

```
703     /* T2 = b4 - b3 */
704     double T2_real = b4_real - b3_real;
705     double T2_imag = b4_imag - b3_imag;
706
707     /* T3 = -b2 - b4 */
708     double T3_real = -b2_real - b4_real;
709     double T3_imag = -b2_imag - b4_imag;
710
711     /* T4 = b6 + b7 */
712     double T4_real = b6_real + b7_real;
713     double T4_imag = b6_imag + b7_imag;
714
715     /* T5 = b8 - b7 */
716     double T5_real = b8_real - b7_real;
717     double T5_imag = b8_imag - b7_imag;
718
719     /* T6 = -b8 - b6 */
720     double T6_real = -b8_real - b6_real;
721     double T6_imag = -b8_imag - b6_imag;
722
723     /* T7 = T0 + T1 */
724     double T7_real = T0_real + T1_real;
725     double T7_imag = T0_imag + T1_imag;
726
727     /* T8 = T0 + T2 */
728     double T8_real = T0_real + T2_real;
729     double T8_imag = T0_imag + T2_imag;
730
731     /* T9 = T0 + T3 */
732     double T9_real = T0_real + T3_real;
733     double T9_imag = T0_imag + T3_imag;
734
735     /* T10 = T4 + b5 */
736     double T10_real = T4_real + b5_real;
737     double T10_imag = T4_imag + b5_imag;
738
739     /* T11 = T5 + b5 */
740     double T11_real = T5_real + b5_real;
741     double T11_imag = T5_imag + b5_imag;
742
743     /* T12 = T6 + b5 */
744     double T12_real = T6_real + b5_real;
745     double T12_imag = T6_imag + b5_imag;
746
747     /* apply twiddle factors */
748
749     /* out0 = 1 * b0 */
750     out[j] = b0_real;
```

```

751     out[j+1] = b0_imag;
752
753     /* out1 = w1 * (T7 - i T10) */
754     x_real = T7_real + T10_imag;
755     x_imag = T7_imag - T10_real;
756     out[j+dj]   = w1_real * x_real - w1_imag * x_imag;
757     out[j+dj+1] = w1_real * x_imag + w1_imag * x_real;
758
759     /* out2 = w2 * (T9 - i T12) */
760     x_real = T9_real + T12_imag;
761     x_imag = T9_imag - T12_real;
762     out[j+2*dj]   = w2_real * x_real - w2_imag * x_imag;
763     out[j+2*dj+1] = w2_real * x_imag + w2_imag * x_real;
764
765     /* out3 = w3 * (T8 + i T11) */
766     x_real = T8_real - T11_imag;
767     x_imag = T8_imag + T11_real;
768     out[j+3*dj]   = w3_real * x_real - w3_imag * x_imag;
769     out[j+3*dj+1] = w3_real * x_imag + w3_imag * x_real;
770
771     /* out4 = w4 * (T8 - i T11) */
772     x_real = T8_real + T11_imag;
773     x_imag = T8_imag - T11_real;
774     out[j+4*dj]   = w4_real * x_real - w4_imag * x_imag;
775     out[j+4*dj+1] = w4_real * x_imag + w4_imag * x_real;
776
777     /* out5 = w5 * (T9 + i T12) */
778     x_real = T9_real - T12_imag;
779     x_imag = T9_imag + T12_real;
780     out[j+5*dj]   = w5_real * x_real - w5_imag * x_imag;
781     out[j+5*dj+1] = w5_real * x_imag + w5_imag * x_real;
782
783     /* out6 = w6 * (T7 + i T10) */
784     x_real = T7_real - T10_imag;
785     x_imag = T7_imag + T10_real;
786     out[j+6*dj]   = w6_real * x_real - w6_imag * x_imag;
787     out[j+6*dj+1] = w6_real * x_imag + w6_imag * x_real;
788
789     j += ostride;
790 }
791 j += (factor - 1)*dj;
792 }}
793 /*-----*/
794
795 void pass_n(int fi,
796            double in[], int in0, int istride,
797            double out[], int out0, int ostride,
798            int sign, int factor, int product){

```

```

799  int i = 0, j = 0;
800  int k, k1;
801
802  int m = n / factor;
803  int q = n / product;
804  int p_1 = product / factor;
805  int jump = (factor - 1) * p_1;
806  int e, e1;
807
808  for (i = 0; i < m; i++) {
809      out[out0+ostride*i] = in[in0+istride*i];
810      out[out0+ostride*i+1] = in[in0+istride*i+1]; }
811
812  for (e = 1; e < (factor - 1) / 2 + 1; e++) {
813      for (i = 0; i < m; i++) {
814          int idx = i + e * m;
815          int idxc = i + (factor - e) * m;
816          out[out0+ostride*idx] = in[in0+istride*idx] + in[in0+istride*idxc];
817          out[out0+ostride*idx+1] = in[in0+istride*idx+1] + in[in0+istride*idxc+1];
818          out[out0+ostride*idxc] = in[in0+istride*idx] - in[in0+istride*idxc];
819          out[out0+ostride*idxc+1] = in[in0+istride*idx+1] - in[in0+istride*idxc+1]; }}
820
821  /* e = 0 */
822
823  for (i=0; i<m; i++) {
824      in[in0+istride*i] = out[out0+ostride*i];
825      in[in0+istride*i+1] = out[out0+ostride*i+1]; }
826
827  for (e1 = 1; e1 < (factor - 1) / 2 + 1; e1++){
828      for (i = 0; i < m; i++){
829          in[in0+istride*i] += out[out0+ostride*(i + e1*m)];
830          in[in0+istride*i+1] += out[out0+ostride*(i + e1*m)+1]; }}
831
832  double twiddl[] = twiddle[fi][q];
833
834  for (e = 1; e < (factor-1)/2 + 1; e++){
835      int idx = e;
836      double w_real, w_imag;
837
838      int em = e * m;
839      int ecm = (factor - e) * m;
840
841      for (i = 0; i < m; i++) {
842          in[in0+istride*(i+em)] = out[out0+ostride*i];
843          in[in0+istride*(i+em)+1] = out[out0+ostride*i+1];
844          in[in0+istride*(i+ecm)] = out[out0+ostride*i];
845          in[in0+istride*(i+ecm)+1] = out[out0+ostride*i+1];
846      }

```



```

847
848   for (e1 = 1; e1 < (factor - 1) / 2 + 1; e1++) {
849       if (idx == 0) {
850           w_real = 1;
851           w_imag = 0; }
852       else {
853           w_real = twiddl[2*(idx-1)];
854           w_imag = -sign*twiddl[2*(idx-1)+1]; }
855       for (i = 0; i < m; i++) {
856           double ap = w_real * out[out0+ostride*(i + e1 * m)];
857           double am = w_imag * out[out0+ostride*(i + (factor - e1) *m)+1];
858
859           double bp = w_real * out[out0+ostride*(i + e1 * m)+1];
860           double bm = w_imag * out[out0+ostride*(i + (factor - e1) *m)];
861
862           in[in0+istride*(i + em)] += (ap - am);
863           in[in0+istride*(i + em)+1] += (bp + bm);
864           in[in0+istride*(i + ecm)] += (ap + am);
865           in[in0+istride*(i + ecm)+1] += (bp - bm);
866       }
867       idx += e;
868       idx %= factor;
869   }
870 }
871
872 i = 0;
873 j = 0;
874
875 /* k = 0 */
876 for (k1 = 0; k1 < p_1; k1++) {
877     out[out0+ostride*k1] = in[in0+istride*k1];
878     out[out0+ostride*k1+1] = in[in0+istride*k1+1]; }
879
880 for (e1 = 1; e1 < factor; e1++){
881     for (k1 = 0; k1 < p_1; k1++){
882         out[out0+ostride*(k1 + e1 * p_1)] = in[in0+istride*(k1 + e1 * m)];
883         out[out0+ostride*(k1 + e1 * p_1)+1] = in[in0+istride*(k1 + e1 * m)+1];
884     }}
885
886 i = p_1;
887 j = product;
888
889 for (k = 1; k < q; k++) {
890     for (k1 = 0; k1 < p_1; k1++) {
891         out[out0+ostride*j] = in[in0+istride*i];
892         out[out0+ostride*j+1] = in[in0+istride*i+1];
893         i++;
894         j++;

```

```

895     }
896     j += jump;
897 }
898
899 i = p_1;
900 j = product;
901
902 for (k = 1; k < q; k++) {
903     twiddl = twiddle[fi][k];
904     for (k1 = 0; k1 < p_1; k1++) {
905         for (e1 = 1; e1 < factor; e1++) {
906             double x_real = in[in0+istride*(i + e1 * m)];
907             double x_imag = in[in0+istride*(i + e1 * m)+1];
908
909             double w_real = twiddl[2*(e1-1)];
910             double w_imag = -sign*twiddl[2*(e1-1)+1];
911
912             out[out0+ostride*(j + e1 * p_1)] = w_real * x_real - w_imag * x_imag;
913             out[out0+ostride*(j + e1 * p_1)+1] = w_real * x_imag + w_imag * x_real;
914         }
915         i++;
916         j++;
917     }
918     j += jump;
919 }
920 }
921
922
923 }

```

LISTING D.9: ComplexDoubleFFT

```

1 package cws;
2 /** Abstract Class representing FFT's of complex, double precision data.
3  * Concrete classes are typically named ComplexDoubleFFT_<i>method</i>, implement the
4  * FFT using some particular method.
5  * <P>
6  * Complex data is represented by 2 double values in sequence: the real and imaginary
7  * parts. Thus, in the default case (i0=0, stride=2), N data points is represented
8  * by a double array dimensioned to 2*N. To support 2D (and higher) transforms,
9  * an offset, i0 (where the first element starts) and stride (the distance from the
10 * real part of one value, to the next: at least 2 for complex values) can be supplied.
11 * The physical layout in the array data, of the mathematical data d[i] is as follows:
12 *<PRE>
13 *   Re(d[i]) = data[i0 + stride*i]
14 *   Im(d[i]) = data[i0 + stride*i+1]
15 *</PRE>
16 * The transformed data is returned in the original data array in

```

```

17 * <a href="package-summary.html#wraparound">wrap-around</A> order.
18 *
19 * @author Bruce R. Miller bruce.miller@nist.gov
20 * @author Contribution of the National Institute of Standards and Technology,
21 * @author not subject to copyright.
22 */
23 public abstract class ComplexDoubleFFT {
24
25     int n;
26
27     /** Create an FFT for transforming n points of complex, double precision data. */
28     public ComplexDoubleFFT(int n){
29         if (n <= 0) {
30             throw new IllegalArgumentException("mmm"+n); //$NON-NLS-1$
31         }
32         this.n = n; }
33
34     /** Creates an instance of a subclass of ComplexDoubleFFT appropriate for data
35     * of n elements.*/
36     public ComplexDoubleFFT getInstance(int n){
37         return new ComplexDoubleFFT_Mixed(n); }
38
39     protected void checkData(double data[], int i0, int stride){
40         if (i0 < 0) {
41             throw new IllegalArgumentException("mmm"+i0); //$NON-NLS-1$
42         }
43         if (stride < 2) {
44             throw new IllegalArgumentException("mmm"+stride); //$NON-NLS-1$
45         }
46         if (i0+stride*(n-1)+2 > data.length) {
47             throw new IllegalArgumentException("mmm"+n+"mmm"+ //$NON-NLS-1$ //$NON-NLS-2$
48                 "mmm"+i0+"mmm"+stride+ //$NON-NLS-1$ //$NON-NLS-2$
49                 "mmm"+data.length); //$NON-NLS-1$
50         } }
51
52     /** Compute the Fast Fourier Transform of data leaving the result in data.
53     * The array data must be dimensioned (at least) 2*n, consisting of alternating
54     * real and imaginary parts. */
55     public void transform (double data[]) {
56         transform (data, 0,2); }
57
58     /** Compute the Fast Fourier Transform of data leaving the result in data.
59     * The array data must contain the data points in the following locations:
60     * <PRE>
61     *     Re(d[i]) = data[i0 + stride*i]
62     *     Im(d[i]) = data[i0 + stride*i+1]
63     * </PRE>
64     */

```

```
65 public abstract void transform (double data[], int i0, int stride);
66
67 /** Return data in wraparound order.
68  * @see <a href="package-summary.html#wraparound">wraparound format</A> */
69 public double[] toWraparoundOrder(double data[]){
70     return data; }
71
72 /** Return data in wraparound order.
73  * i0 and stride are used to traverse data; the new array is in
74  * packed (i0=0, stride=2) format.
75  * @see <a href="package-summary.html#wraparound">wraparound format</A> */
76 public double[] toWraparoundOrder(double data[], int i0, int stride) {
77     if ((i0==0)&&(stride==2)) {
78         return data;
79     }
80     double newdata[] = new double[2*n];
81     for(int i=0; i<n; i++){
82         newdata[2*i] = data[i0+stride*i];
83         newdata[2*i+1] = data[i0+stride*i+1]; }
84     return newdata; }
85
86 /** Compute the (unnormalized) inverse FFT of data, leaving it in place.*/
87 public void backtransform (double data[]){
88     backtransform(data,0,2); }
89
90 /** Compute the (unnormalized) inverse FFT of data, leaving it in place.
91  * The frequency domain data must be in wrap-around order, and be stored
92  * in the following locations:
93  *<PRE>
94  *   Re(D[i]) = data[i0 + stride*i]
95  *   Im(D[i]) = data[i0 + stride*i+1]
96  *</PRE>
97  */
98 public abstract void backtransform (double data[], int i0, int stride);
99
100 /** Return the normalization factor.
101  * Multiply the elements of the backtransform'ed data to get the normalized inverse.*/
102 public double normalization(){
103     return 1.0/n; }
104
105 /** Compute the (normalized) inverse FFT of data, leaving it in place.*/
106 public void inverse(double data[]) {
107     inverse(data,0,2); }
108
109 /** Compute the (normalized) inverse FFT of data, leaving it in place.
110  * The frequency domain data must be in wrap-around order, and be stored
111  * in the following locations:
112  *<PRE>
```

```

113     *   Re(D[i]) = data[i0 + stride*i]
114     *   Im(D[i]) = data[i0 + stride*i+1]
115     *</PRE>
116     */
117     public void inverse (double data[], int i0, int stride) {
118         backtransform(data, i0, stride);
119
120         /* normalize inverse fft with 1/n */
121         double norm = normalization();
122         for (int i = 0; i < n; i++) {
123             data[i0+stride*i] *= norm;
124             data[i0+stride*i+1] *= norm; }}
125 }

```

LISTING D.10: Factorize

```

1 package cws;
2
3 //package jnt.FFT;
4 /** Supplies static methods for factoring integers needed by various FFT classes.
5  *
6  * @author Bruce R. Miller bruce.miller@nist.gov
7  * @author Contribution of the National Institute of Standards and Technology,
8  * @author not subject to copyright.
9  * @author Derived from GSL (Gnu Scientific Library)
10 * @author GSL's FFT Code by Brian Gough bjg@vzv.lanl.gov
11 * @author Since GSL is released under
12 * @author <H HREF="http://www.gnu.org/copyleft/gpl.html">GPL</A>,
13 * @author this package must also be.
14 */
15 public class Factorize {
16
17     /** Return the prime factors of n.
18     * The method first extracts any factors in fromfactors, in order (which
19     * needn't actually be prime). Remaining factors in increasing order follow. */
20     public static int[] factor (int n, int fromfactors[]){
21         int factors[] = new int[64]; // Cant be more than 64 factors.
22         int nf = 0;
23         int ntest = n;
24         int factor;
25
26         if (n <= 0) {
27             throw new Error("mmm"+n+"mmm"); //$NON-NLS-1$ //$NON-NLS-2$
28         }
29
30         /* deal with the preferred factors first */
31         for(int i = 0; (i < fromfactors.length) && (ntest != 1); i++){
32             factor = fromfactors[i];

```

```
33     while ((ntest % factor) == 0) {
34         ntest /= factor;
35         factors[nf++] = factor; }}
36
37     /* deal with any other even prime factors (there is only one) */
38     factor = 2;
39     while (((ntest % factor) == 0) && (ntest != 1)) {
40         ntest /= factor;
41         factors[nf++] = factor; }
42
43     /* deal with any other odd prime factors */
44     factor = 3;
45     while (ntest != 1) {
46         while ((ntest % factor) != 0) {
47             factor += 2; }
48         ntest /= factor;
49         factors[nf++] = factor; }
50
51     /* check that the factorization is correct */
52     int product = 1;
53     for (int i = 0; i < nf; i++) {
54         product *= factors[i]; }
55     if (product != n) {
56         throw new Error("mmm"+n); //$NON-NLS-1$
57     }
58
59     /* Now, make an array of the right length containing the factors... */
60     int f[] = new int[nf];
61     System.arraycopy(factors,0,f,0,nf);
62     return f; }
63
64     /** Return the integer log, base 2, of n, or -1 if n is not an integral power of 2.*/
65     public static int log2 (int n){
66         int log = 0;
67
68         for(int k=1; k < n; k *= 2, log++) {
69             ;
70         }
71
72         if (n != (1 << log)) {
73             return -1 ; /* n is not a power of 2 */
74         }
75         return log; }
76 }
```

# E

## Application papers

### **E.1 A new approach to finding similarities between time series using Cross Wavelet Phase Variance**

# A new approach to finding similarities between time series using Cross Wavelet Phase Variance

Marc Pienaar

Department of Electrical Engineering  
University of Cape Town and the  
COUNCIL FOR SCIENTIFIC AND  
INDUSTRIAL RESEARCH  
(CSIR)

Pretoria, South Africa  
Email: mpienaar@csir.co.za

Jonathan Tapson

Department of Electrical Engineering  
University of Cape Town  
Cape Town, South Africa  
Email: Jonathan.Tapson@uct.ac.za

Frans van den Bergh  
and Stephan Woodborne  
COUNCIL FOR SCIENTIFIC AND  
INDUSTRIAL RESEARCH  
(CSIR)

Pretoria, South Africa  
Email: FvdBergh@csir.co.za  
Email: swoodbor@csir.co.za

**Abstract**—This study presents a method for class identification and classification of multiple time-series data using Cross Wavelet Phase variance (Pv). The Pv method can be used to emphasize regions of frequency commonality or regions of frequency dissimilarity between datasets. By focussing on similarities in the frequency domain, the technique performs better than traditional techniques such as Euclidean distance and the euclidean distance of FFT amplitude in classifying the University of California Riverside (UCR) benchmark time series. The possibility that the Pv method will accommodate lead and lag time is hypothesized for future testing.

## I. INTRODUCTION

A similarity function is a discrimination technique which can be used to classify or cluster elements of a dataset into classes according to similar characteristics using a normalized distance metric. A time series similarity framework can be formalized by defining the similarity metric within a *metric space*. In such a space the algorithm can be defined as a distance function  $d$ , where  $d$  is calculated using an appropriate function approximator such as nearest neighbor classifiers or R-trees. A simple time domain algorithm for  $d$  is the Euclidean distance ( $d = \sqrt{\sum (Xi - Yi)^2}$ ). Where  $Xi$  and  $Yi$  represent elements of the time series  $X$  and  $Y$ . Within this context, we define the concept of *metric space*. A *metric space*  $X$  denotes all valid objects within a database to match with the distance function  $d$  so that:  $\forall x, y \in X, d(x, y) \geq 0, d(x, y) = d(y, x); \forall x \in X, d(x, x) = 0$ ; and  $\forall x, y, z \in X, d(x, y) \leq d(x, z) + d(z, y)$ . If all these properties are satisfied then  $d$  is the distance function and  $(d, X)$  is the *metric space* [1].

Where a set of time series data in a metric space are known to share a common response pattern, they can be grouped into a single class - whereas data that are the result of processes that cause a greater variability between two or more time series may be classified into alternative classes. Collectively, these time series form a multi-class database.

A desirable distance function should assume no background knowledge of the underlying processes and patterns within a dataset and avoid optimizing the characteristics of a single class, thereby providing nondiscriminatory multi-class classification. During the classification process false clustering could

occur when similar items in a dataset have been grouped together incorrectly whereas false dismissals imply that not all the items with the same characteristics within  $(d, X)$  have been returned. To reduce the possibility of false dismissals it is important that the classifying scheme covers the entire range of the search area and the returns are an exact match to sequential scanning [2–4]. Conversely, if the distance function  $d$  cannot accommodate multiple class problems, then an alternative classifier function is required.

In this paper, we present a novel approach to similarity searching using cross wavelet phase variance and we design a framework to evaluate the class differential capability of the technique. We characterize the frequency components derived using the Morlet wavelet [5] that are common among time series to perform similarity clustering. The results are compared with other similarity metric's such as Euclidean distance, Dynamic Time Warping (DTW), the euclidean distance of Fast Fourier Transform (FFT) amplitude, and cosine distance in a one-nearest neighbor classifying scheme on publically available time series data [6]. Our method would be particularly useful in the earth sciences, where a comparison between spatially distinct time series in complex multi agency systems such as ecosystem processes are complicated by inherent time lag responses.

### A. Related work

A time series is a sequence of real numbers that typically represent real-world measurements or observations. Many time series classification problems consist of large databases that require some form of dimensionality reduction to reduce the computational time taken to map all objects within the search area. Dimensionality reduction occurs at a pre-processing stage prior to classifying the data. Some of the more common techniques include: the Discrete Fourier Transform (DFT) [2, 7–10]; the Discrete Wavelet Transform (DWT) [11–15]; Piecewise Aggregate Approximation (PAA) [16]; Piecewise Linear Approximation (PLA) [17, 18]; Chebyshev Polynomials (CP) [19]; and Singular Value Decomposition (SVD) [20, 21].



Signal processing techniques provide a good basis for dimensionality reduction. Similarity matching in the frequency domain is possible, according to Parseval's theorem [22], which states that the Euclidean distance is equivalent in both the time and the frequency domain. The most commonly used techniques are the Discrete Fourier Transform (DFT) and the Discrete Wavelet Transform (DWT). Agrawal *et al.* [7] proposed the use of the DFT for similarity indexing and introduced the concept called F-index. They tested their method on synthetic data, and showed significant gains when a higher number of sequences were introduced. The F-Index relates to only a few Fourier coefficients that are needed to successfully match time series. Faloutsos *et al.* [2] extended the work of Agrawal *et al.* [7] by analyzing a sliding data window in the time domain and then applying the DFT within each window on a selected stock price database. Rafiei [23] optimized the process by using the last few coefficients; this is possible because each  $n - \text{ith}$  coefficient of the DFT analysis of a given time series is the complex conjugate of the  $\text{ith}$  coefficient. With a slight loss of computational speed the results of the DFT similarity indexing can be improved by using the symmetry of Fourier transforms [10].

Chan and Fu [11] introduced similarity indexing using the Discrete Haar Wavelet, which seems to be the most time effective of the wavelet based techniques [3, 11–13, 15]. They experimented on both stock data from the Hong Kong stock market and synthetic data. The DWT approach was later optimized by Liabotis *et al.* [12] using a number of dimensions between 16 and 20.

## II. MATERIALS AND METHODS

### A. The Continuous Wavelet Transform

The Continuous Wavelet Transform (CWT) is a branch of harmonic analysis that provides a time-frequency representation of  $f(t)$ . The fundamental of the CWT is the Fourier Transform in which any  $2\pi$  periodic function  $f(t)$  can be represented as a superposition of harmonically related waves.

Typically, a Fast Fourier transform algorithm (FFT) [24] is applied by approximating the number of DFTs that are used to calculate the frequency coefficients at  $n$  number of sample points.

The Continuous Wavelet Transform (CWT) [5] has an advantage over the Fourier transform because it is possible to compare time series over a broad spectrum of wavelengths (periods) as a function of time. A major advantage of wavelets lies in the scaling function, that allows the multi-resolution representation of frequencies. The window or scaling function is called a mother wavelet; one example is the Morlet [5], defined by a Gaussian process so that the effect of energy loss is minimum across all scales and is given as,

$$\psi_0(t) = \pi^{1/4} e^{-i\omega_0 t} e^{-t^2/2} \quad (1)$$

Where  $\omega_0$  is the frequency parameter, usually taken as six, to satisfy the admissibility condition [25]. The admissibility condition implies that the Fourier transform of the wavelet

vanishes at a zero frequency. Normalization is another important property of the Morlet as it ensures that the chosen set of scales  $a$  are directly comparable with each other. The CWT is defined as the convolution of  $f(t)$  with a scaled and translated version of the mother wavelet  $\psi_0(t)$ . The CWT convolution is applied  $n$  times to the data in Fourier space, where all  $n$  convolutions are done simultaneously using the FFT. The equation that describes the CWT is given as,

$$W_f(b, a) = \frac{1}{a} \int_{-\infty}^{\infty} f(t) \psi^*\left(\frac{t-b}{a}\right) dt \quad (2)$$

Where  $\psi$  is the mother wavelet and  $*$  indicates the complex conjugation. The subscript 0 is dropped to indicate that  $\psi$  is normalized. A complex wavelet is used to ensure the phase content of a signal is maintained. The wavelet spectrum is a consistent estimator of the Fourier Spectrum over time; however, because of the properties of the reproducing kernel, the estimate is biased in either the time or scale (frequency) direction. The amount of independent scale information is limited by the Nyquist frequency and rate [26]. The Nyquist frequency is equivalent to half the sampling frequency and the Nyquist rate is equivalent to twice the sampling frequency. We therefore note that when the signal deviates from a  $2\pi$  periodic process, redundant frequencies are represented and deviation from the Nyquist frequency results in alias signals at frequencies lower than the required sampling rate. To limit redundancies produced by boundary effects, wavelet coefficients are plotted inside an envelope or cone of influence defined as the scale/time decay of  $1/\epsilon^2$ . As the Morlet is proportionally localized in both time and frequency the ability of the reproducing kernel to detect very time-localized structures, like jumps or frequency changes inside a time series, is retained and the frequency content is simply exaggerated.

### B. The Phase Variance Method

We propose a similarity metric based on the variance calculated from the phase modulus of the cross wavelet. The cross spectrum conveys predictive information of two processes by reinforcing the covariance found in the power spectrum of independent variables, according to scale [27]. This shows coherency between two variables normalized in a single spectrum defined as the modulus of the cross-wavelet spectrum. The functional form is defined as,

$$CS(b, a) = W_{f1}^*(b, a) W_{f2}(b, a) \quad (3)$$

Where  $W_{f1}$  and  $W_{f2}$  are the wavelet transform's of the two signals, calculated in (2), and  $*$  is the complex conjugate. The coherency of the cross modulus highlights frequency modulated (FM) and amplitude modulated (AM) components of each time series. The cross wavelet modulus provides a good metric of AM similarity between two time series datasets but is limited to a time reference to discern the degree of coherent FM between the time series. Conversely, the cross wavelet phase provides a good metric of the FM components but is completely void of amplitude.

We introduce the phase variance  $Pv$  method in this paper which is calculated as a function of wavelength, where the minimum of variance indicates the degree of FM similarity between two time series. The phase modulus is defined as,

$$\theta(b, a) = \tan^{-1} \frac{\Im[CS(b, a)]}{\Re[CS(b, a)]} \quad (4)$$

Where  $\Im[CS(b, a)]$  and  $\Re[CS(b, a)]$  are the Imaginary and Real parts of the cross-wavelet spectrum. The phase variance ( $Pv$ ) is calculated as,

$$Pv = \sum_{a_{min}}^{a_{max}} \frac{\sum_{b_{min}}^{b_{max}} (\theta(b, a) - \overline{\theta(b, a)})^2}{(n-1)} \quad (5)$$

Where  $\theta(b, a)$  is the phase modulus defined in (4),  $b_{min}$  and  $b_{max}$  are the limits of the time window to be analyzed and  $a_{min}$  and  $a_{max}$  are the set of scales over which to compute the phase variance. Phase coherence is assumed to reflect a common response to an underlying driving signal that is amplitude modulated in the time series being compared. The total of the phase coherence is assessed across all wavelengths that make up the time series datasets that are being compared. The greater the extents of phase coherency over a broad range of wavelengths, the more similar the two datasets are presumed to be. The simplest implementation of the  $Pv$  method is applied in a single time window that covers all the points in the time series, and  $a_{min}$  and  $a_{max}$  cover all the scales. In this approach computation time is controlled by the resolution of each scale, and the classification problem is assumed to be purely frequency related. The AM differences could be accounted for by the cross wavelet power spectrum. However, we prefer to use the Euclidean distance of the FFT amplitude.

The method matches time series, even if there is a lead/lag offset between the compared data, and the FM differences between time series datasets manifest as increased variances at particular frequency/wavelength bands of the cross wavelet phase variance. Accordingly, the phase variance is not always a simple sum of the variance. Instead, a unique set of wavelengths will characterize the similarity between different datasets. The wavelengths that are the best indication of the similarity between time series datasets will differ between datasets.

To illustrate this relationship consider the cross wavelet analysis in Figure. 1 of four time series that have been extracted from the Coffee database of the UCR time series datasets[6]. The time series represent two classes. The variance in the phase modulus of Figure. 1, highlights slight discrepancies at particular wavelengths whereas the power relationship (the domain of euclidean distance) is almost identical, an indication that a pure AM similarity metric would not perform well on this problem.

If the frequency characteristics, such as the wavelength band of the classification problem, are known then the dimensions can be dramatically reduced. Such instances are highly desirable. By focusing on the whole range of wavelengths when summing the phase variance, the metric is measuring both

the similar and the dissimilar components of the time series that are being compared. By focusing on limited wavelength ranges, it is more likely that the summed variance is reflecting either the similar or the dissimilar components of the time series been compared. Without *a priori* knowledge of the structure of the datasets in the frequency domain, it is not possible to determine the optimum wavelength range in which to match the comparison. However, by ranking the  $Pv$  values from smallest to largest it is possible to select the integration range to emphasize either similarities or differences (see Figure. 2B). We assume that summing over the half of the resulting vector that represents the similarity between the datasets gives the best FM similarities, regardless of variations within discrete frequency characteristics of multi-class problems. We suggest that the most appropriate approach is the  $Pv$  1/2 approach, whereby we rank the  $Pv$ , and normalize the smallest half by FFT amplitude (see Figure. 2B). We do note, however, that this approach includes low frequency alias signals that may or may not be relevant to the indexing problem.

### C. Data

We design our experiment around the publically available UCR time series datasets [2]. The data consists of twenty problems of various lengths and classes summarized in Table I. Our experiment is conducted in a 1 – *NearestNeighbor* framework against Euclidean distance, the euclidean distance of FFT amplitude, Cosine distance and Dynamic Time Warping (DTW).

TABLE I  
SUMMARY OF UCR DATASETS USED IN THIS ANALYSIS. EACH DATASET HAS A GIVEN NUMBER OF CLASSES AND A PRESCRIBED SUBSET THAT CAN BE USED TO VERIFY THE RETURNS OF A SIMILARITY METRIC ALGORITHM

Problem	Classes	Training sets	Test sets	Length
Synthetic Control	6	300	300	60
Gun-Point	2	50	150	150
CBF	3	30	900	128
Face (all)	14	560	1690	131
OSU Leaf	6	200	242	427
Swedish Leaf	15	500	625	128
50words	50	450	455	270
Trace	4	100	100	275
Two Patterns	4	1000	4000	128
Wafer	2	1000	6174	152
Face (four)	4	24	88	350
Lighting-2	2	60	61	637
Lighting-7	7	70	73	319
ECG	2	100	100	96
Adiac	37	390	391	176
Yoga	2	300	3000	426
Fish	7	175	175	463
Beef	5	30	30	470
Coffee	2	28	28	286
OliveOil	4	30	30	570

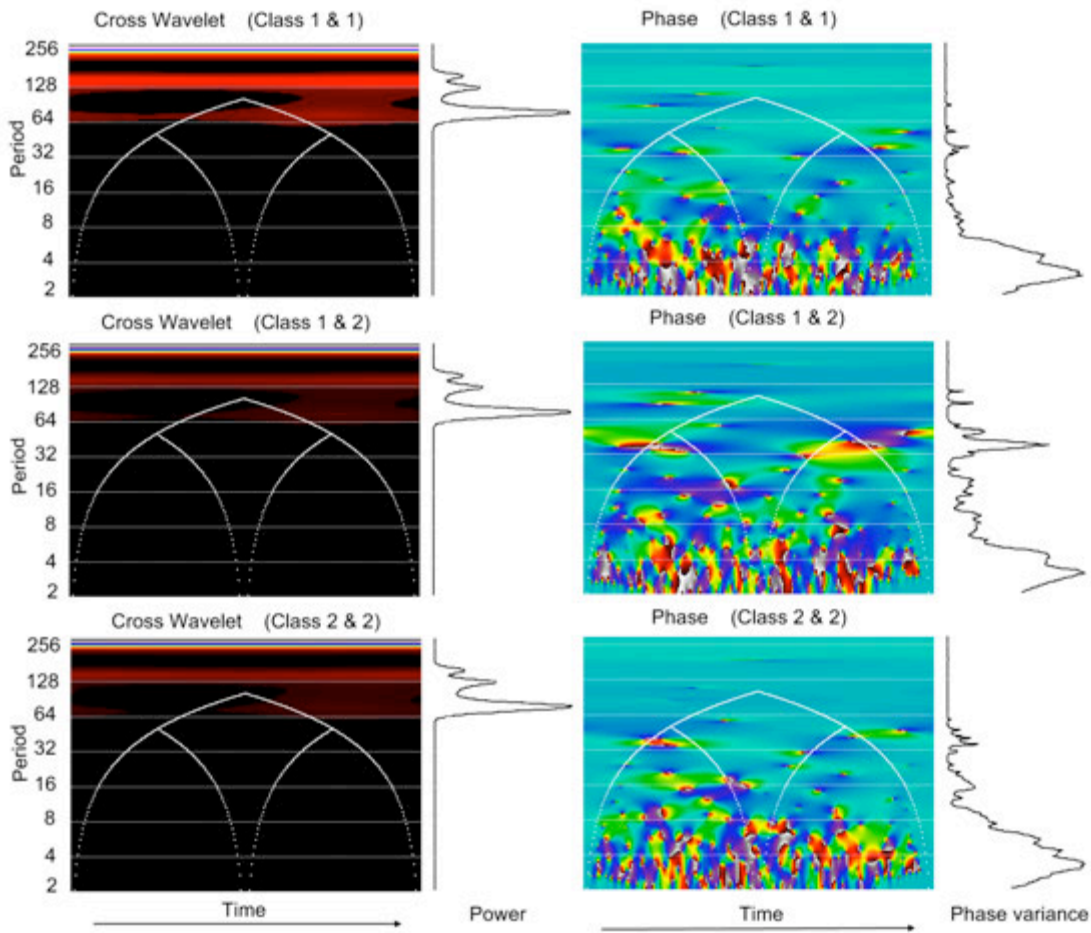


Figure 1. The cross wavelet method (left) illustrates power in the frequency domain that is common to two time series datasets. Integration across the scales (period) of the cross wavelet modulus provides coherency between the AM components of the two datasets. The cross wavelet phase analysis (right) provides an index of similar FM behavior between the datasets by calculating the variance of the cross wavelet phase as a function of time (shown as a graph on the right hand side). Low values indicate good synchronicity (and therefore, similarities between the datasets at those periods), whereas, high values indicate differences in the FM behavior of the datasets.

### III. RESULTS AND DISCUSSION

Table II provides a direct comparison of the classification skill of Euclidian distance, the euclidean distance of FFT amplitude, cosine distance, DTW and for the phase variance similarity metrics. The results were generated through a blind experiment with no a priori knowledge of the characteristics of each dataset. The results are reported as the number of time series that are assigned incorrect classification (errors) divided by the total number of time series in the database as,

$$\frac{\text{database.length} - \text{correct}}{\text{database.length}} \quad (6)$$

Phase variance results include the variance summed over all the wavelengths (full), and  $\frac{1}{2}$  the re-ordered coefficients. The  $P_v$  full approach was calculated as,

$$P_v = \sum_2^{256} \frac{\sum_{b_{min}}^{b_{max}} (\theta(b, a) - \overline{\theta(b, a)})^2}{(n-1)} * \sqrt{\sum (F_{ai} - F_{bi})^2} \quad (7)$$

Where,  $b_{min}$  and  $b_{max}$  are the start and end of each time series respectively, and  $F_{ai}$  and  $F_{bi}$  are the FFT amplitude coefficients of each time series. The results presented in Table II provide a good indication of the performance of the  $P_v$  method over other classification techniques. The  $P_v$  1/2 method out-performs the  $P_v$  Full method in 17 of the 20 examples. The  $P_v$  1/2 method also performs better than the Euclidean distance, FFT amplitude and Cosine techniques in all but 3 of the examples.

### IV. CONCLUSION

The phase variance method for the determination of class similarity is an improvement on traditional techniques such as Euclidean distance. Frequency variations within time series

TABLE II  
RESULTS. ED STANDS FOR EUCLIDEAN DISTANCE, AND FFT-A IS THE EUCLIDEAN DISTANCE OF THE FFT AMPLITUDE COEFFICIENTS. THE BEST RESULTS ARE HIGHLIGHTED

Problem	Ed	DTW (Best Warping Window)	DTW (no warping window)	FFT-A	Cosine	$P_v$ Full	$P_v$ 1/2
Synthetic Control	0.120	0.120	0.007	0.397	0.120	0.150	0.100
Gun-Point	0.087	0.087	0.093	0.027	0.087	0.013	0.027
CBF	0.147	0.004	0.003	0.387	0.147	0.266	0.148
Face (all)	0.287	0.192	0.192	0.257	0.286	0.243	0.228
OSU Leaf	0.479	0.384	0.409	0.430	0.483	0.442	0.413
Swedish Leaf	0.211	0.157	0.210	0.147	0.211	0.123	0.144
50words	0.369	0.242	0.310	0.411	0.369	0.371	0.341
Trace	0.250	0.010	0.000	0.140	0.250	0.140	0.120
Two Patterns	0.094	0.002	0.000	0.496	0.094	0.457	0.280
Wafer	0.005	0.005	0.020	0.003	0.005	0.002	0.002
Face (four)	0.216	0.114	0.170	0.239	0.216	0.125	0.068
Lighting-2	0.246	0.131	0.131	0.148	0.246	0.213	0.230
Lighting-7	0.425	0.288	0.274	0.301	0.425	0.315	0.301
ECG	0.120	0.120	0.230	0.160	0.120	0.110	0.100
Adiac	0.389	0.391	0.396	0.263	0.483	0.263	0.261
Yoga	0.169	0.155	0.164	0.160	0.171	0.147	0.140
Fish	0.217	0.160	0.167	0.229	0.709	0.154	0.131
Beef	0.467	0.467	0.500	0.500	0.800	0.433	0.367
Coffee	0.250	0.179	0.179	0.357	0.536	0.214	0.107
OliveOil	0.133	0.167	0.133	0.200	0.600	0.233	0.133

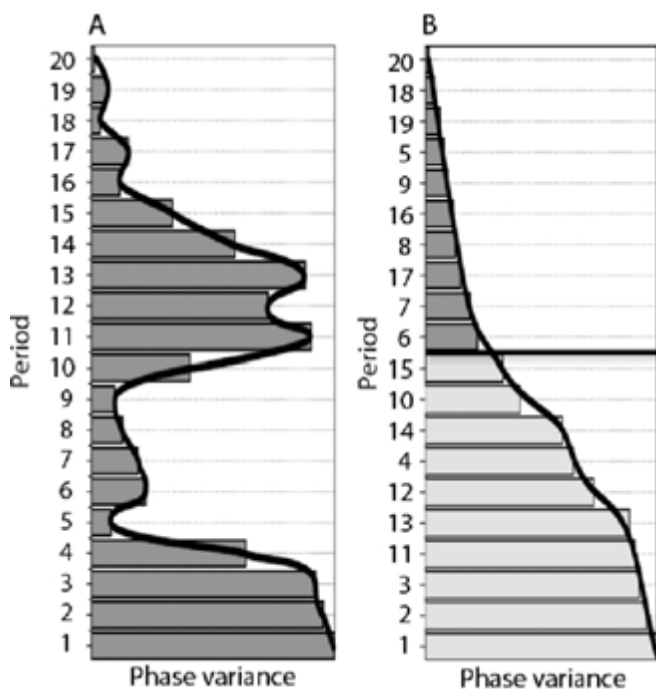


Figure 2. The  $P_v$  vector portrays similarities between datasets in the frequency domain (low  $P_v$  values) as well as differences (high  $P_v$  values). To illustrate the approach, a  $P_v$  vector is represented as a bar-graph (A). By integrating over different frequency ranges the resulting value will emphasize either similarities or differences. Ranking the  $P_v$  vector (B) emphasizes the similarities or differences between datasets. We integrate the 50% of the vector that represents common behavior.

databases imply the nearest neighbor approach is not optimal for this method and some initial optimization is needed to ensure that the classes and the correct variation of the phase variance method is used on the dataset problem. We are optimistic, that this method can be optimized on a relatively small training set in cases where there is a priori knowledge of the classes to be classified. The method will also work, but may require additional computational time, where there is no a priori knowledge of classes, and therefore may be used to define classes, based on similarities within arbitrary frequency bands.

The context of this research is to develop a metric to understand ecological trends and processes. The target research domain differs from the test applied in this study in that ecological processes often involve threshold responses and inherent time lag responses. Soil moisture storage, for example, will allow plant productivity to continue well after a rainfall event and the classification for this process would fail if threshold and lag responses were not accommodated. By working in the frequency domain the time-localization of the monitoring system is redundant, and so the  $P_v$  method should be applicable where lead and lag times characterize the target dataset. This quality offers an additional advantage of the  $P_v$  method over other similarity metrics.

#### ACKNOWLEDGMENT

This study was funded by the Hi-Tempo SRP project of the Meraka Institute, CSIR and CSIR HCD funds.

## REFERENCES

- [1] M. Li, X. Chen, X. Li, B. Ma, and P. M. B. Vitányi, "The similarity metric," *IEEE TRANSACTIONS ON INFORMATION THEORY*, vol. 50, pp. 3250–3264, 2004.
- [2] C. Faloutsos, M. Ranganathan, and Y. Manolopoulos, "Fast subsequence matching in time-series databases," *Proceedings of the 1994 ACM SIGMOD international conference on Management of data, Minneapolis, Minnesota, USA*, 1994.
- [3] E. Keogh, K. Chakrabarti, M. Pazzani, and S. Mehrotra, "Dimensionality reduction for fast similarity search in large time series databases," *Knowledge and Information Systems*, vol. 3, pp. 263–286, 2001.
- [4] C. A. Ratanamahatana and E. Keogh, "Everything you know about dynamic time warping is wrong," *Proceedings of the Tenth ACM SIGKDD International Conference on Knowledge Discovery and Data Mining*, 2004.
- [5] A. Grossman and J. Morlet, "Decomposition of hardy functions into square integrable wavelets of constant shape," *SIAM journal on mathematical analysis*, vol. 15, pp. 723–736, 1984.
- [6] E. Keogh, X. Xi, L. Wei, and C. Ratanamahatana, "The ucr time series classification/clustering homepage," [www.cs.ucr.edu/eamonn/time\\_series\\_data/](http://www.cs.ucr.edu/eamonn/time_series_data/), 2006.
- [7] R. Agrawal, C. Faloutsos, and A. Swami, "Efficient similarity search in sequence databases," *Proceedings of the 4th International Conference on Foundations of Data Organization and Algorithms, Chicago*, 1993.
- [8] K. K. W. Chu and M. H. Wong, "Fast time-series searching with scaling and shifting," *Proceedings of the eighteenth ACM SIGMOD-SIGACT-SIGART symposium on Principles of database systems, Philadelphia, Pennsylvania, USA*, 1999.
- [9] D. Rafiei and A. Mendelzon, "Similarity-based queries for time series data," *Proceedings of the ACM SIGMOD International Conference on Management of Data, Tucson, Arizona, USA*, 1997.
- [10] A. Rafiei, D. and Mendelzon, "Efficient retrieval of similar time sequences using dft," *Proceedings of the 5th International Conference on Foundations of Data Organization (FODO'98), Kobe, Japan*, 1998.
- [11] K.-P. Chan and A. W.-C. Fu, "Efficient time series matching by wavelets," *Proceedings of the 15th International Conference on Data Engineering, Sydney, Australia*, 1999.
- [12] I. Liabotis, B. Theodoulidis, and M. Saraee, "Improving similarity search in time series using wavelets," *International Journal of Data Warehousing and Mining*, vol. 2, pp. 55–81, 2006.
- [13] I. Popivanov and R. J. Miller, "Similarity search over time-series data using wavelets," *Proceedings of the 18th International Conference on Data Engineering (ICDE'02)*, 2002.
- [14] M. Saeed and R. Mark, "A novel method for the efficient retrieval of similar multiparameter physiologic time series using wavelet-based symbolic representations," *AMIA 2006 Symposium Proceedings*, 2006.
- [15] Y.-L. Wu, D. Agrawal, and E. Abbadi, "A comparison of dft and dwt based similarity search in time-series databases," *Proceedings of the International Conference on Information and Knowledge Management*, 2000.
- [16] B.-K. Yi and C. Faloutsos, "Fast time sequence indexing for arbitrary  $l_p$  norms," *Proceedings of the 26th Very Large Data Base Conference, Cairo, Egypt*, 2000.
- [17] E. J. Keogh and M. J. Pazzani, "An enhanced representation of time series which allows fast and accurate classification, clustering and relevance feedback," *Proceedings of the 4th International Conference of Knowledge Discovery and Data Mining*, 1998.
- [18] Q. Chen, L. Chen, X. Lian, Y. Liu, and J. X. Yu, "Indexable pla for efficient similarity search," in *Proceedings of the 33rd international conference on Very Large Data Bases, Vienna, Austria*, 2007.
- [19] Y. Cai and R. Ng, "Indexing spatio-temporal trajectories with chebyshev polynomials," in *Proceedings of the 2004 ACM SIGMOD international conference on Management of data, Paris, France*, 2004.
- [20] K. V. R. Kanth, D. Agrawal, and A. Singh, "Dimensionality reduction for similarity in dynamic databases," *ACM SIGMOD Record*, vol. 27, pp. 166–176, 1998.
- [21] F. Korn, H. V. Jagadish, and C. Faloutsos, "Efficiently supporting ad hoc queries in large datasets of time sequences," in *Proceedings of the 1997 ACM SIGMOD international conference on Management of data, Tucson, Arizona, USA*, 1997.
- [22] M.-A. Parseval des Chênes, "Mémoire sur les séries et sur l'intégration complète d'une équation aux différences partielle linéaire du second ordre, à coefficients constants," *Mémoires présentés à l'Institut des Sciences, Lettres et Arts, par divers savans, et lus dans ses assemblées. Sciences, mathématiques et physiques. (Savans étrangers.)*, vol. 1, pp. 638–648, 1806.
- [23] D. Rafiei, "Fourier-transform based techniques in efficient retrieval of similar time sequences," Ph.D. dissertation, Department of Computer Science, University of Toronto, 1999.
- [24] J. W. Cooley and J. W. Tukey, "An algorithm for the machine calculation of complex fourier series," *Mathematics of Computation*, vol. 19, pp. 297–301, 1965.
- [25] M. Farge, "Wavelet transforms and their applications to turbulence," *Annual Review of Fluid Mechanics*, vol. 24, pp. 395–457, 1992.
- [26] H. Nyquist, "Certain topics in telegraph transmission theory," *Transactions of the American Institute of Electrical Engineers*, vol. 47, no. 2, pp. 617–644, 1928.
- [27] L. Hudgins, C. A. Friehe, and M. E. Mayer, "Wavelet transforms and atmospheric turbulence," *Physical Review Letters*, vol. 71, pp. 3279–3282, 1993.

# Bibliography

- [1] A. Graps, “An introduction to wavelets,” *IEEE Computational Sciences and Engineering*, vol. 2, pp. 50–61, 1995.
- [2] L. Hudgins, C. A. Friehe, and M. E. Mayer, “Wavelet transforms and atmospheric turbulence,” *Physical Review Letters*, vol. 71, pp. 3279–3282, 1993.
- [3] C. Torrence and G. Compo, “A practical guide to wavelet analysis,” *Bulletin of the American Meteorological Society*, vol. 79, no. 1, pp. 62–78, 1998.
- [4] E. Keogh, Q. Zhu, B. Hu, Y. Hao, X. Xi, L. Wei, and C. Ratanamahatana, “The ucr time series classification/clustering homepage: [www.cs.ucr.edu/~eamonn/time-seriesdata/](http://www.cs.ucr.edu/~eamonn/time-seriesdata/),” 2011.
- [5] Y. Chen, E. Keogh, N. Hu, B. Begum, A. Bagnall, A. Mueen, and G. Batista. The ucr time series classification archive (2015). [Online]. Available: [www.cs.ucr.edu/~eamonn/time\\_series\\_data/](http://www.cs.ucr.edu/~eamonn/time_series_data/)
- [6] M. Pienaar, J. Tapson, and F. Van den Bergh, “A new approach to finding similarities between time series using cross wavelet phase variance,” *In F. Nicolls (ed.), Proceedings of the Twenty-First Annual Symposium of the Pattern Recognition Association of South Africa (PRASA)*, 22-23 November 2010. Stellenbosch, South Africa. Cape Town: PRASA 2010. ISBN 9780799224702.

- 
- [7] J. Fourier (translated By Alexander Freeman), *Analytical Theory of Heat*. Cambridge University Press, 1878.
- [8] P. G. L. Dirichlet, “Sur la convergence des séries trigonométriques qui servent à représenter une fonction arbitraire entre des limites données,” *Journal für die reine und angewandte Mathematik (Journal de Crelle)*, vol. 4, pp. 157–169, 1829.
- [9] I. Fredholm, “Sur une classe d’équations fonctionnelles,” *Acta Mathematica*, vol. 27, pp. 365–390, 1903.
- [10] H. Lebesgue, “Intégrale, longueur, aire (thèse),” *Annali di Matematica Pura ed Applicata*, vol. 7, pp. 231–359, 1902.
- [11] G. Cantor, “über die ausdehnung eines satzes aus der theorie der trigonometrischen reihen,” *Mathematische Annalen*, vol. 5, pp. 123–132, 1872.
- [12] M. Fréchet, “Sur quelques points du calcul fonctionnel,” *Rendiconti del Circolo Matematico di Palermo*, vol. 74, pp. 1–74, 1906.
- [13] D. Hilbert, *Grundzüge einer allgemeinen Theorie der linearen Integralgleichungen*. Cornell University Library, 1912.
- [14] D. Gabor, “Theory of communication.” *Journal of the Institute of Electrical Engineers*, vol. 93, pp. 429–457, 1946.
- [15] J. Morlet, G. Arens, I. Fourgeau, and D. Giard, “Wave propagation and sampling theory,” *Geophysics*, vol. 47, pp. 203–236, 1982.
- [16] W. W. Rouse Ball, *A Short Account of the History of Mathematics*. the University of Michigan, 1888.
- [17] T. L. Heath, *Euclid’s Elements translated by Thomas. L. Heath*. Green Lion Press, 2007.
- [18] *The Almagest: I-V*. Encyclopedia Britannica, 1952, vol. 15, ch. Great Books of the Western World, pp. 5–24.
- [19] U. C. Merzbach and C. B. Boyer, *A History of Mathematics. Third edition*. John Wiley and Sons, 2011.

- [20] J. Muir, *Of Men and Numbers: The Story of the Great Mathematicians*. Dover Publications, New York, 1996.
- [21] N. Copernicus, *De Revolutionibus Orbium Coelestium (On the Revolutions of the Heavenly Spheres)*. Johannes Petreius, Nuremberg, 1543.
- [22] I. Newton, *The Principia / Isaac Newton (translated by Andrew Motte)*, ser. Great Minds, A. Motte, Ed. Prometheus Books, New York, 1995.
- [23] J.-P. Kahane and P. G. Lemarié-Rieusset, *Fourier series and wavelets: Studies in the development of modern mathematics, v. 3*. Luxembourg : Gordon and Breach Publishers, 1995.
- [24] B. B. Hubbard, *The World According to Wavelets: The Story of a Mathematical Technique in the Making*. A K Peters, 1996.
- [25] E. Prestini, *The evolution of Applied Harmonic Analysis: Models of the Real World*, ser. Applied and Numerical Harmonic Analysis. Birkhauser, Boston, 2004.
- [26] J. I. R. d'Alembert, *Acoustics: Historical and Philosophical Development*. Dowden, Hutchinson & Ross, Stroudsburg, 1973, ch. Investigation of the curve formed by a vibrating string, 1747, pp. 119–123.
- [27] T. N. Narasimhan, “Fourier’s heat conduction equation: History, influence, and connections,” *Reviews of Geophysics*, vol. 37, pp. 151–172, 1999.
- [28] D. Bernoulli, “*réflexions et éclaircissemens sur les noucelles vibrations des cordes exposées dans les mémoires de l’académie de 1747 et 1748*,” *Mémoires de l’Académie Rouale de Berlin*, vol. 9, pp. 147–172, 1755.
- [29] S. G. Krantz and L. Lee, *Explorations in Harmonic Analysis with Applications to Complex Function Theory and the Heisenberg Group*, ser. Applied and Numerical Harmonic Analysis. Birkhauser Boston, 2007.
- [30] P. Brémaud, *Mathematical Principles of Signal Processing: Fourier and Wavelet Analysis*. Springer, New York, 2001.



- [31] U. Dini, *Serie di Fourier e altre rappresentazioni analitiche delle funzioni di una variabile reale*. Pisa, 1880.
- [32] H. Weber and R. Dedekind, *The Collected Works of Riemann*. New York, Dover Publications, 1953.
- [33] F. Riesz, “Sur une espèce de géométrie analytique des systèmes de fonctions sommables,” *Comptes rendus de l’Académie des Sciences*, vol. 144, pp. 1409–1411, 1907.
- [34] E. Fischer, “Sur la convergence en moyenne,” *Comptes rendus de l’Académie des Sciences*, vol. 144, pp. 1022–1024, 1907.
- [35] S. Banach, “Sur les opérations dans les ensembles abstraits et leur application aux équations intégrales,” *Fundamenta Mathematicae*, vol. 3, pp. 133–181, 1922.
- [36] A. Haar, “Zur theorie der orthogonalen funktionensysteme,” *Mathematische Annalen*, vol. 69, no. 3, pp. 331–371, 1910.
- [37] J. Marcinkiewics, “Sur une propriete de la loi de gauss,” *Mathematische Zeitschrift*, vol. 44, pp. 612–618, 1938.
- [38] I. Daubechies, *Ten Lectures on Wavelets*. Society fo Industrial and Applied Mathematics, 1992.
- [39] G. Faber, “über die orthoganal funktionen des herrn haar,” *Jahresber. Deutsch. Math.-Verein*, vol. 19, pp. 104–112, 1910.
- [40] J. Schauder, “Zur theorie stetiger abbildungen in funktionalräumen,” *Mathematische Zeitschrift*, vol. 26, pp. 47–65, 1927.
- [41] P. Levy, *Théorie de l’addition des variables aléatoires*. Gauthier-Villars, Paris, 1937.
- [42] J. E. Littlewood and R. E. A. C. Paley, “Theorems on fourier series and power series,” *Journal of the London Mathematical Society*, vol. 6, no. 3, pp. 230–233, 1931.

- [43] ———, “Theorems on fourier series and power series (ii),” *Proceedings of the London Mathematical Society*, vol. 43, no. 2, pp. 105–126, 1938.
- [44] ———, “Theorems on fourier series and power series (ii),” *Proceedings of the London Mathematical Society*, vol. 42, no. 1, pp. 52–89, 1937.
- [45] Y. Meyer, *Wavelets: algorithms & applications*. Philadelphia: Society for Industrial and Applied Mathematics, 1993.
- [46] E. P. Wigner, “On the quantum correction for thermodynamic equilibrium,” *Physics Reviews*, vol. 40, pp. 749–759, 1932.
- [47] J. Ville, “Théorie et applications de la notion de signal analytique,” *Câbles et Transmissions*, vol. 2, no. 1, pp. 61–74, 1948.
- [48] A. P. Calderón, “Intermediate spaces and interpolation, the complex method,” *Studia Math*, vol. 24, pp. 113–190, 1964.
- [49] A. Grossmann and J. Morlet, “Decomposition of hardy functions into square integrable wavelets of constant shape,” *SIAM Journal of Mathematical Analysis and Applications*, vol. 15, pp. 723–736, 1984.
- [50] Y. Meyer, “Principe d’incertitude, bases hilbertiennes et algèbres d’opérateurs [uncertainty principle, hilbert bases, and algebras of operators],” *Séminaire Bourbaki*, vol. 145-146, pp. 209–223, 1985/86.
- [51] P. G. Lemarie and Y. Meyer, “Ondelettes et bases hilbertiennes [wavelets and hilbert bases],” *Revista Matemática Iberoamericana*, vol. 2, pp. 1–18, 1986.
- [52] S. Mallet, “Multiresolution approximations and wavelet orthonormal bases of  $l^2(\mathbb{R})$ ,” *Transactions of the American Mathematical Society*, vol. 315, pp. 69–87, 1989.
- [53] ———, “Multifrequency channel decompositions of images and wavelet models,” *IEEE Transactions on Acoustics, Speech and Signal Processing*, vol. 37, pp. 2091–2110, 1989.

- [54] ———, “A theory for multiresolution signal decomposition: The wavelet representation,” *IEEE Transactions on Pattern Analysis and Machine Intelligence*, vol. 11, no. 7, pp. 674–639, 1989.
- [55] I. Daubechies, “Orthonormal bases of compactly supported wavelets,” *Communications on Pure and Applied Mathematics*, vol. 41, pp. 909–966, 1988.
- [56] M. Plancherel and M. Leffler, “Contribution l’étude de la représentation d’une fonction arbitraire par les intégrales définies,” *Rendiconti del Circolo Matematico di Palermo*, vol. 30, no. 1, pp. 289–335, 1910.
- [57] M.-A. Parseval des Chenes, “Mémoire sur les séries et sur l’intégration complète d’une équation aux différences partielles linéaire du second ordre, coefficients constants,” *Mémoires présentés à l’Institut des Sciences, Lettres et Arts, par divers savans, et lus dans ses assemblées. Sciences, mathématiques et physiques. (Savans étrangers.)*, vol. 1, pp. 638–648, 1806.
- [58] S. Mallat, *A Wavelet Tour of Signal Processing*, 2nd ed. Academic Press, 1999.
- [59] H. Nyquist, “Certain topics in telegraph transmission theory,” *Transactions of the American Institute of Electrical Engineers*, vol. 47, no. 2, pp. 617–644, 1928.
- [60] C. E. Shannon, “Communication in the presence of noise,” *Proceedings of the Institute of Radio Engineers*, vol. 37, no. 1, pp. 10–21, 1949.
- [61] M. T. Heideman, D. H. Johnson, and C. S. Burrus, “Gauss and the history of the fast Fourier transform,” *IEEE ASSP Magazine*, vol. 1, pp. 14–21, 1984.
- [62] F. Yates, “The design and analysis of factorial experiments,” *Imperial Bureau of Soil Science. Technical communication 35*, vol. 35, 1937.
- [63] G. C. Danielson and C. Lanczos, “Some improvements in practical Fourier analysis and their application to x-ray scattering from liquids,” *Journal of The Franklin Institute*, vol. 233, pp. 365–380 and 432–452, 1942.
- [64] J. W. Cooley and J. W. Tukey, “An algorithm for the machine calculation of complex Fourier series,” *Mathematics of Computation*, vol. 19, pp. 297–301, 1965.

- [65] M. Frigo and S. G. Johnson, “The fastest fourier transform in the west. technical report mit-lcs-tr-728,” Laboratory for Computer Science, MIT, Cambridge, MA, Tech. Rep., 1997.
- [66] —, “The design and implementation of fftw3,” *Proceedings of the IEEE*, vol. 93, p. 216:231, 2005.
- [67] J. Allen and L. Rabiner, “A unified approach to short-time fourier analysis and synthesis,” *Proceedings of the IEEE*, vol. 65, no. 11, pp. 1558–1564, 1977.
- [68] W. Heisenberg, *The Physical Principles of the Quantum Theory (Translated By C. Eckart And FC Hoyt)*. Universtiy of Chigao Press, 1930.
- [69] H. Wilbraham, “On certian periodic function,” *Cambridge and Dunlin Mathematical Journal*, vol. 3, pp. 198–201, 1848.
- [70] J. W. Gibbs, “Fourier series,” *Nature*, vol. 59, p. 200 and 606, 1899.
- [71] H. Bocher, “Introduction to the theory of fourier’s series,” *Annals of Mathematics*, vol. 7, pp. 81–152, 1906.
- [72] J. Morlet, *Issues in Acoustic signal/Image processing and recognition.*, ser. NATO ASI series. Springer-Verlag, Berlin, 1983, vol. 1, ch. Sampling theory and wave propagaton, pp. 233–261.
- [73] *Mathematica, Version 8.0*. Wolfram Research, Inc. Champaign, Illinois, 2010.
- [74] E. B. Delprat, N., P. Guillemain, R. Kronland-Martinet, P. Tchamitchian, and B. Torr sani, “Asymptotic wavelet and gabor analysis: extraction of instantaneous frequencies.” *IEEE Transactions on Information Theory*, vol. 38, no. 2, pp. 644–664, 1992.
- [75] S. Mallet and W. L. Hwang, “Characterization of signals from multiscale edges,” *IEEE Transactions on Information Theory*, vol. 38, pp. 617–643, 1992.
- [76] C. Torrence and P. J. Webster, “Interdecadal changes in the enso-monsoon system,” *American Meteorological Society*, vol. 12, pp. 2679–2690, 1999.

- [77] A. Grinsted, J. Moore, and S. Jevrejeva, "Application of the cross wavelet transform and wavelet coherence to geophysical time series," *Nonlinear Processes in Geophysics*, vol. 11, pp. 561–566, 2004.
- [78] D. Maraun and J. Kurths, "Cross wavelet analysis. significance testing and pitfalls," *Nonlinear Processes in Geophysics*, vol. 11, no. 4, pp. 505–514, 2004.
- [79] A. Prokoph and H. El Bilali, "Cross-wavelet analysis: a tool for detection of relationships between paleoclimate proxy records," *Mathematical Geosciences*, vol. 40, no. 5, pp. 575–586, 2008.
- [80] G. Zhang, "Time series forecasting using a hybrid arima and neural network model," *Neurocomputing*, vol. 50, pp. 159–175., 2003.
- [81] J. Barnett. (2011). origins of boolean algebra in the logic of classes: George boole, john venn and cs peirce. available from the webpage <http://www.cs.nmsu.edu/historical-projects>.
- [82] B. Carpenter and R. Doran, Eds., *A. M. Turing's ACE Report and Other Papers*. MIT Press, Cambridge, MA, 1986.
- [83] D. Michie, D. J. Spiegelhalter, and C. C. Taylor, *machine learning, neural and statistical classification*. Citeseer, 1994.
- [84] S. Muggleton, *Machine Intellegence*. Oxford University Press, Oxford. Oxford University Press, Oxford. Oxford University Press, Oxford, 1993, vol. 13, ch. Logic and learning: Turing's legacy.
- [85] T. Cover and P. Hart, "Nearest neighbor pattern classification," *IEEE Transactions on Information Theory*, vol. 13, no. 1, pp. 21–27, 1967.
- [86] J. McCarthy, M. Minsky, N. Rochester, and C. E. Shannon, "A proposal for the dartmouth summer research project on artificial intelligence. august 31, 1955," *AI Magazine*, vol. 27, no. 4, 2006.
- [87] N. Rashevsky, "An approach to the mathematical biophysics of biological self-regulation and of cell polarity," *The Bulletin of Mathematical Biophysics.*, vol. 2, 1940.

- 
- [88] W. S. McCulloch and W. Pitts, “A logical calculus of the ideas immanent in nervous activity,” *The Bulletin of Mathematical Biophysics*, vol. 5, no. 4, pp. 115–113, 1943.
- [89] F. Rosenblatt, “The perceptron: a probabilistic model for information storage and organization in the brain,” *Psychological review*, vol. 65, no. 6, p. 386, 1958.
- [90] W. Ashby, *Design for a Brain*. Springer Science & Business Media, 1960.
- [91] F. Rosenblatt, “Principles of neurodynamics. perceptrons and the theory of brain mechanisms,” DTIC Document, Tech. Rep., 1961.
- [92] H. Block, “The perceptron: A model for brain functioning,” *Reviews of Modern Physics*, vol. 34, no. 1, p. 123, 1962.
- [93] M. Yovits, Ed., *Self organizing systems*. Spartan Books, 1962.
- [94] M. Minsky and S. Papert, *Perceptrons*. MIT Press, 1969.
- [95] F. Rosenblatt, *Principles of neurodynamics*. Spartan Books, 1962.
- [96] J. G. Carbonell, R. S. Michalski, and T. M. Mitchell, “Machine learning: a historical and methodological analysis,” *AI Magazine*, vol. 4, no. 3, 1983.
- [97] J. W. Shavlik and T. G. Dietterich, *Readings in machine learning*. Morgan Kaufmann., 1990.
- [98] N. J. Nilsson, *The quest for artificial intelligence*. Cambridge University Press, 2009.
- [99] V. Vapnik, *The nature of statistical learning theory*. Springer Science and Business Media, 2013.
- [100] [Online]. Available: <http://history-computer.com/MechanicalCalculators/Pioneers/Schickard.html>
- [101] T. Koetsier, “On the prehistory of programmable machines: musical automata, looms, calculators,” *Mechanism and Machine theory*, vol. 36, no. 5, pp. 589–603, 2001.

- [102] M. Bayes and M. Price, “An essay towards solving a problem in the doctrine of chances. by the late rev. mr. bayes, frs communicated by mr. price, in a letter to john canton, amfrs,” *Philosophical Transactions (1683-1775)*, pp. 370–418, 1963.
- [103] A. Legendre, *Sur la Méthode des moindres quarrés*. Firmin Didot, Paris, 1805, ch. Nouvelles méthodes pour la détermination des orbites des comètes.
- [104] C. Gauss, *Theoria Motus Corporum Coelestium in Sectionibus Conicis Solem Ambientum*, 1809.
- [105] R. Harley, “The stanhope demonstrator,” *Mind*, vol. 4, pp. 192–210, 1879.
- [106] J. Delve, “Joseph marie jacquard: Inventor of the jacquard loom,” *IEEE Annals of the History of Computing*, vol. 29, no. 4, 2007.
- [107] D. Halacy, *Charles Babbage, Father of the Computer*. Crowell-Collier Press, 1970.
- [108] G. Boole, *An Investigation of the Laws of Thought on Which are Founded the Mathematical Theories of Logic and Probabilities*. Dover Publications, 1854.
- [109] G. Currie, *Frege: An Introduction to His Philosophy*. Harvester Press, 1982.
- [110] M. Cambell-Kelly and W. Aspray, *Computer: a history of the information machine*. Basic Books, 1996.
- [111] J. Brittain, “Electrical engineering hall of fame: Vannevar bush,” *Proceedings of the IEEE*, vol. 96, no. 12, 2008.
- [112] G. K, “Ueber formal unentscheidbare saetze der principia mathematica und verwandter systeme,” *Monatshefte fuer Mathematik und Physik*, vol. 38, pp. 173–198, 1931.
- [113] G. Kriesal, “Kurt godel. 28 april 1906-14 january 1978,” *Biographical Memoirs of Fellows of the Royal Society*, vol. 26, 1980.
- [114] A. M. Turing, “On computable numbers, with an application to the entscheidungsproblem,” *Journal of Math*, vol. 58, no. 5, pp. 345–363, 1936.

- [115] R. Fisher, "The use of multiple measures in taxonomic problems," *Ann. Eugenics*, vol. 7, 1937.
- [116] C. R. Rao, "The utilization of multiple measurements in problems of biological classification," *Journal of the Royal Statistical Society. Series B (Methodological)*, vol. 10, no. 2, pp. 159–203, 1948.
- [117] K. Pearson, "On lines and planes of closest fit to systems of points in space," *Philosophical Magazine*, vol. 11, no. 2, pp. 559–572, 1901.
- [118] R. Kurzweil, *The age of intelligent machines*. Cambridge: MIT press, 1990.
- [119] C. E. Shannon, "A mathematical theory of communication," *Bell System Technical Journal*, vol. 27, no. 4, pp. 379–423, 1948.
- [120] N. Wiener, *Cybernetics: Or Control and Communication in the Animal and the Machine*. Hertmann, Paris, 1948.
- [121] E. Weiss, "Arthur lee samuel (1901-90)," *IEEE Annals of the History of Computing*, vol. 14, no. 3, pp. 55–69, 1992.
- [122] N. J. Nilsson, *Learning machines: foundations of trainable pattern-classifying systems*. McGraw-Hill, 1965.
- [123] P. Werbos, "Applications of advances in nonlinear sensitivity analysis," in *In Proceedings of the 10th IFIP Conference, 31.8 - 4.9, NYC.*, 1981, pp. 762–770.
- [124] S. Linnainmaa, "The representation of the cumulative rounding error of an algorithm as a taylor expansion of the local rounding errors." Master's thesis, University of Helsinki, 1970.
- [125] J. R. Quinlan, "Induction of decision trees," *Machine learning*, vol. 1, no. 1, pp. 81–106, 1986.
- [126] —, "Simplifying decision trees," *International Journal of Man-Machine Studies*, vol. 27, no. 3, p. 221, 1987.
- [127] J. Mena, *Machine learning forensics for law enforcement, security, and intelligence*. CRC Press, 2011.



- [128] G. Piatetsky-Shapiro, “Knowledge discovery in databases: 10 years after,” *ACM SIGKDD Explorations Newsletter*, vol. 1, no. 2, pp. 59–61, 2000.
- [129] S. McPherson, *Tim Berners-Lee: Inventor of the World Wide Web*. Twenty-First Century Books, 2009.
- [130] C. Cortes and V. Vapnik, “Support-vector networks,” *Machine Learning*, vol. 20, no. 3, pp. 273–197, 1995.
- [131] C. Kleist, “Time series data mining methods,” Master’s thesis, umboldt-Universität zu Berlin, Wirtschaftswissenschaftliche Fakultät, 2015.
- [132] X. Wang, A. Mueen, H. Ding, G. Trajcevski, P. Scheuermann, and E. Keogh, “Experimental comparison of representation methods and distance measures for time series data,” *Data Mining and Knowledge Discovery*, vol. 26, no. 2, pp. 275–309, 2013.
- [133] I. Alles, “Time series clustering in the field of agronomy: Cluster analyse agronomischer zeitreihen,” Ph.D. dissertation, Department of computer science. Technische Universität Darmstadt, 2013.
- [134] R. Agrawal, C. Faloutsos, and A. Swami, “Efficient similarity search in sequence databases,” in *Proceedings of the 4th International Conference on Foundations of Data Organization and Algorithms, Chicago.*, 1993.
- [135] K.-P. Chan and A. W.-C. Fu, “Efficient time series matching by wavelets.” in *Proceedings of the 15th International Conference on Data Engineering, Sydney, Australia.*, 1999.
- [136] Y.-L. Wu, D. Agrawal, and E. Abbadi, “A comparison of dft and dwt based similarity search in time-series databases.” in *Proceedings of the International Conference on Information and Knowledge Management.*, 2000.
- [137] E. Keogh, K. Chakrabarti, M. Pazzani, and S. Mehrotra, “Dimensionality reduction for fast similarity search in large time series databases.” *Knowledge and Information Systems.*, vol. 3, pp. 263–286, 2001.

- [138] I. Popivanov and R. Miller, “Similarity search over time-series data using wavelets,” in *Proceedings of the 18th International Conference on Data Engineering (ICDE02)*., 2002.
- [139] I. Liabotis, B. Theodoulidis, and M. Saraee, “Improving similarity search in time series using wavelets.” *International Journal of Data Warehousing and Mining*, vol. 2, pp. 55–81, 2006.
- [140] C. Faloutsos, M. Ranganathan, and Y. Manolopoulos, “Fast sub sequence matching in time-series databases,” in *Proceedings of the 1994 ACM SIGMOD international conference on Management of data, Minneapolis, Minnesota, USA*, 1994.
- [141] D. Rafiei and A. Mendelzon, “Similarity-based queries for time series data.” in *Proceedings of the ACM SIGMOD International Conference on Management of Data, Tucson, Arizona, USA.*, 1997.
- [142] —, “Efficient retrieval of similar time sequences using dft.” in *Proceedings of the 5th International Conference on Foundations of Data Organization (FODO’98), Kobe, Japan.*, 1998.
- [143] K. Chu and M. Wong, “Fast time-series searching with scaling and shifting,” in *Proceedings of the eighteenth ACM SIGMOD-SIGACT-SIGART symposium on Principles of database systems, Philadelphia, Pennsylvania, USA.*, 1999.
- [144] B. Yi and C. Faloutsos, “Fast time sequence indexing for arbitrary  $l_p$  norms,” in *Proceedings of the 26th Very Large Data Base Conference, Cairo, Egypt.*, 2000.
- [145] E. J. Keogh and M. J. Pazzani, “An enhanced representation of time series which allows fast and accurate classification, clustering and relevance feedback.” in *Proceedings of the 4th International Conference of Knowledge Discovery and Data Mining.*, 1998.
- [146] Q. Chen, L. Chen, X. Lian, Y. Lui, and J. yu, “Indexable pla for efficient similarity search.” in *Proceedings of the 33rd international conference on Very Large Data Bases, Vienna, Austria.*, 2007.

- [147] Y. Cai and R. Ng, “Indexing spatio-temporal trajectories with chebyshev polynomials.” in *Proceedings of the 2004 ACM SIGMOD international conference on Management of data, Paris, France.*, 2004.
- [148] C. Eckart and G. Young, “The approximation of one matrix by another of lower rank,” *Psychometrika*, vol. 1, no. 3, pp. 211–218, 1936.
- [149] M. R. Hestenes, “Inversion of matrices by biorthogonalization and related results,” *Journal of the Society for Industrial and Applied Mathematics*, vol. 6, no. 1, pp. 51–90, 1958.
- [150] G. H. Golub and W. Kahan, “Calculating the singular values and pseudo-inverse of a matrix,” *Journal of the Society for Industrial and Applied Mathematics: Series B, Numerical Analysis*, vol. 2, no. 2, pp. 205–224, 1965.
- [151] G. H. Golub and C. Reinsch, “Singular value decomposition and least squares solutions,” *Numerische Mathematik*, vol. 14, no. 5, pp. 403–420, 1970.
- [152] F. Korn, H. Jagadish, and C. Faloutsos, “Efficiently supporting ad hoc queries in large datasets of time sequences.” in *Proceedings of the 1997 ACM SIGMOD international conference on Management of data, Tuscan, Arizona, USA.*, 1997.
- [153] K. Kanth, D. Agrawal, and A. Singh, “Dimensionality reduction for similarity in dynamic databases.” *ACM SIGMOD Record*, vol. 27, pp. 166–176, 1998.
- [154] H. Hotelling, “Analysis of a complex of statistical variables into principal components,” *Journal of educational psychology*, vol. 24, no. 6, p. 417, 1933.
- [155] J. M. Raychaudhuri, S. and Stuart and R. B. Altman, “rincipal components analysis to summarize microarray experiments: application to sporulation time series,” in *Pacific Symposium on Biocomputing. Pacific Symposium on Biocomputing.* NIH Public Access, 2000, p. 455.
- [156] K. Yang and C. Shahabi, “On the stationarity of multivariate time series for correlation-based data analysis.” in *Fifth IEEE International Conference on Data Mining, IEEE*, 2005, p. 4.

- [157] H. Li, “Asynchronism-based principal component analysis for time series data mining.” *Expert Systems with Applications*, vol. 41, no. 6, pp. 2842–2850, 2014.
- [158] J.-P. Benzécri, “L’analyse des données,” *L’Analyse des Correspondences, Parris*, vol. 2, 1973.
- [159] E. J. Keogh and M. J. Pazzani, *Knowledge Discovery and Data Mining. Current Issues and New Applications*. Springer, 2000, ch. A simple dimensionality reduction technique for fast similarity search in large time series databases, pp. 122–133.
- [160] E. Keogh, K. Chakrabarti, M. Pazzani, and S. Mehrotra, “Locally adaptive dimensionality reduction for indexing large time series databases,” *ACM SIGMOD Record*, vol. 30, no. 2, pp. 151–162, 2001.
- [161] T.-c. Fu, “A review on time series data mining,” *Engineering Applications of Artificial Intelligence*, vol. 24, no. 1, pp. 164–181, 2011.
- [162] S. Lee, D. Kwon, and S. Lee, “Dimensionality reduction for indexing time series based on the minimum distance,” *Journal of Information Science and Engineering*, vol. 19, pp. 697–711, 2003.
- [163] H. Shatkay and S. Zdonik, “Approximate queries and representations for large data sequences,” in *Proceedings of the 12th IEEE International Conference on Data Engineering*, 1996, pp. 536–545.
- [164] F. Chung, T. Fu, R. Luk, and V. Ng, “Flexible time series pattern matching based on perceptually important points,” in *International Joint Conference on Artificial Intelligence Workshop on Learning from Temporal and Spatial Data*, 2001, pp. 1–7.
- [165] Z. Yang and G. Zhao, “Application of symbolic techniques in detecting determinism in time series,” in *Proceedings of the 20th Annual International Conference of the IEEE Engineering in Medicine and Biology Society*, vol. 20, no. 5, 1998, pp. 2670–2673.
- [166] J. Lin, E. Keogh, S. Lonardi, and B. Chiu, “A symbolic representation of time series, with implications for streaming algorithms,” in *Proceedings of the 8th ACM*

- SIGMOD workshop on Research issues in data mining and knowledge discovery.*, 2003, pp. 2–11.
- [167] C. Ratanamahatana, J. Lin, D. Gunopulos, E. Keogh, M. Vlachos, and G. Das, *Data Mining and Knowledge Discovery Handbook*, 2nd ed. Springer, New York, 2010, ch. Mining Time Series Data, pp. 1049–1077.
- [168] J. Shieh and E. Keogh, “i sax: indexing and mining terabyte sized time series,” in *Proceedings of the 14th ACM SIGKDD international conference on Knowledge discovery and data mining*. ACM, 2008, pp. 623–631.
- [169] B. Li, L. Tan, J. Zhang, and Z. Zhuang, “Using fuzzy neural network clustering algorithm in the symbolization of time series,” in *IEEE APCCAS*. IEEE, 2000, pp. 379–382.
- [170] V. Megalooikonomou, Q. Wang, G. Li, and C. Faloutsos, “A multiresolution symbolic representation of time series,” in *ICDE Proceedings. 21st International Conference on Data Engineering*. IEEE, 2005, pp. 668–679.
- [171] F. Morchen and A. Ultsch, “Optimizing time series discretization for knowledge discovery,” in *Proceedings of the eleventh ACM SIGKDD international conference on Knowledge discovery in data mining*, 2005, pp. 660–665.
- [172] L. Ye and E. Keogh, “Time series shapelets: a new primitive for data mining,” in *Proceedings of the 15th ACM SIGKDD international conference on Knowledge discovery and data mining*. ACM, 2009, pp. 947–956.
- [173] C. Ratanamahatana, E. Keogh, A. J. Bagnall, and S. Lonardi, *Advances in knowledge discovery and data mining*. Springer, 2005, ch. A novel bit level time series representation with implication of similarity search and clustering, pp. 771–777.
- [174] A. Bagnall, E. Keogh, S. Lonardi, and G. Janacek, “A bit level representation for time series data mining with shape based similarity,” *Data Mining and Knowledge Discovery*, vol. 13, no. 1, pp. 11–40, 2006.
- [175] D. Pollock, “Methods of time-series analysis,” *Interdisciplinary Science Reviews*, vol. 12, no. 2, 1987.

- [176] M. B. Priestley, *Non-Linear and Non-Stationary Time Series*. London: Academic Press, 1988.
- [177] M. Azzouzi and I. Nabney, "Analysing time series structure with hidden markov models," in *Proceedings of the IEEE Conference on Neural Networks and Signal Processing*, 1998, pp. 402–408.
- [178] G. Box and J. G.M., *Time series analysis: Forecasting and control*. Holden-Day inc, San Francisco., 1970.
- [179] S. Makridas, S. Wheelwright, and R. Hyndman, *Forecasting methods and applications*. New York: John Wiley and Sons, 1998.
- [180] J. Brocklebank and D. Dickney, *SAS for forecasting time series*, 2nd, Ed. Hoboken (NJ): John Wiley and Sons, 2003.
- [181] J. Armstrong, *Principles of forecasting*. Dordrecht: Kluwer Academic Publishers, 2001.
- [182] A. Guttman, "R-trees. a dynamic index structure for spatial searching." in *Proceedings of the 1984 ACM SIGMOD international conference on Management of data - SIGMOD '84*, 1984, p. 47.
- [183] N. Beckmann, H.-P. Kriegel, R. Schneider, and B. Seeger, "The  $r^*$ -tree: an efficient and robust access method for points and rectangles," *ACM*, vol. 19, 1990.
- [184] G. Janacek, A. Bagnall, and M. Powell, "Likelihood ratio distance measure for the similarity between the fourier transform of time series," in *Proceedings of the Ninth Pacific-Asia Conference on Knowledge Discovery and Data Mining*, 2005, pp. 737–743.
- [185] C. S. Burrus, R. A. Gopinath, and H. Guo, *Introduction to wavelets and wavelet transforms*. Prentice Hall, New Jersey, 1998, vol. 998.
- [186] Z. R. Struzik and A. Siebes, *Principles of Data Mining and Knowledge Discovery*. Springer, 1999, ch. The haar wavelet transform in the time series similarity paradigm, pp. 12–22.

- [187] P. Dasha, M. Nayaka, M. Senapatia, and I. Lee, “Mining for similarities in time series data using wavelet-based feature vectors and neural networks.” *Engineering Applications of Artificial Intelligence*, vol. 20, no. 2, 2007.
- [188] P. Chaovalit, A. Gangopadhyay, G. Karabatis, and Z. Chen, “Discrete wavelet transform-based time series analysis and mining,” *ACM Computing Surveys (CSUR)*, vol. 43, no. 2, p. 6, 2011.
- [189] C. M. Bishop, *In the terminology of statistics, this model is known as logistic regression, although it should be emphasized that this is a model for classification rather than regression.* Springer, 2006.
- [190] B. D. Fulcher and N. S. Jones, “Highly comparative feature-based time-series classification,” *IEEE Transactions on Knowledge and Data Engineering*, vol. 26, no. 12, pp. 3026–3037, 2014.
- [191] P. Montalto, M. Aliotta, A. Cannata, C. Cassisi, and A. Pulvirenti, *Similarity Measures and Dimensionality Reduction Techniques for Time Series Data Mining*, ser. Advances in Data Mining Knowledge Discovery and Applications, 2012.
- [192] M. Li, X. Chen, X. Li, B. Ma, and P. Vitnyi, “The similarity metric,” *IEEE transactions on information theory*, vol. 50, pp. 3250–3264, 2004.
- [193] M. Halkidi and M. Vazirgiannis, *Data Mining and Knowledge Discovery Handbook*, 2nd ed. Springer, New York, 2010, ch. 31. Quality Assessment Approaches in Data Mining, pp. 613–639.
- [194] L. Rokach and O. Maimon, *Data Mining and Knowledge Discovery Handbook*, 2nd ed. Springer, New York, 2010, ch. 8. Supervised Learning, pp. 133–147.
- [195] P. Senin and S. Malinchik, “Sax-vsm: Interpretable time series classification using sax and vector space model,” in *2013 IEEE 13th International Conference on Data Mining (ICDM)*. IEEE, 2013, pp. 1175–1180.
- [196] V. Velicho and N. Zagoruyko, “Automatic recognition of 200 words.” *International Journal of Man-Machine Studies*, vol. 2, pp. 223–234, 1970.

- [197] H. Sakoe and S. Chiba, "A dynamic programming approach to continuous speech recognition," in *Proceedings of the Seventh International Congress on Acoustics*, vol. 3. Akademiai Kiado, Budapest, 1971, pp. 65–69.
- [198] D. Berndt and J. Clifford, "Using dynamic time warping to find patterns in time series," Tech. Rep., 1994.
- [199] K. Gollmer and C. Posten, "Supervision of bioprocesses using a dynamic time warping algorithm," *Control Engineering Practice*, vol. 4, no. 9, pp. 1287–1295, 1996.
- [200] J. Aach and G. Church, "Aligning gene expression time series with time warping algorithms," *Bioinformatics*, vol. 17, no. 6, pp. 495–508., 2001.
- [201] B. Huang and W. Kinsner, "Ecg frame classification using dynamic time warping." in *Proceedings of the Canadian Conference on Electrical and Computer Engineering - IEEE CCECE 2002*, vol. 2. Computer Society, Los Alamitos, CA, USA., 2002, pp. 1105–1110.
- [202] T. Rath and R. Manmatha, "Word image matching using dynamic time warping," in *Proceedings of the IEEE Computer Society Conference on Computer Vision and Pattern Recognition*, R. Manmatha, Ed., vol. 2. IEEE Computer Society, Los Alamitos, CA, USA, 2003, pp. 521–527.
- [203] V. Tuzcu and S. Nas, "Dynamic time warping as a novel tool in pattern recognition of ecg changes in heart rhythm disturbances." in *Proceedings of the IEEE International Conference on Systems, Man and Cybernetics*, M. Jamshidi, M. Johnston, and P. Chen, Eds., vol. 1. IEEE Computer Society, Los Alamitos, CA, USA., 2005, pp. 182–186.
- [204] M. Faundez-Zanuy, "On-line signature recognition based on vq-dtw." *Pattern Recognition*, vol. 40, no. 3, pp. 981–992, 2007.
- [205] F. Hermans and E. Tsiporkova, "Merging microarray cell synchronization experiments through curve alignment." *Bioinformatics*, vol. 23, no. 2, pp. 64–70, 2007.



- [206] T. Syeda-Mahmood, D. Beymer, and F. Wang, "Shape-based matching of ecg recordings," in *29th Annual International Conference of the IEEE*, ser. Engineering in Medicine and Biology Society, 2007. EMBS 2007, A. Dittmar, J. Clark, E. McAdams, and N. Lovell, Eds. IEEE Computer Society, Los Alamitos, CA, USA., 2007, pp. 2012–218.
- [207] X. Wang, A. Mueen, H. Ding, G. Trajcevski, P. Scheuermann, and E. Keogh, "Experimental comparison of representation methods and distance measures for time series data," *Data Mining and Knowledge Discovery*, vol. 26, no. 2, pp. 275–309, 2012.
- [208] T. Giorgino, "Computing and visualizing dynamic time warping alignments in r: The dtw package," *Journal of Statistical Software*, vol. 31, no. 7, 2009.
- [209] C. Ratanamahatana and E. Keogh, "Everything you know about dynamic time warping is wrong." in *Third Workshop on Mining Temporal and Sequential Data, in conjunction with the Tenth ACM SIGKDD International Conference on Knowledge Discovery and Data Mining.*, Seattle, WA, August 2004.
- [210] S. Spiegel, B. J. Jain, and S. Albayrak, "Fast time series classification under lucky time warping distance," in *Proceedings of the 29th Annual ACM Symposium on Applied Computing*. ACM, 2014, pp. 71–78.
- [211] M. K. Jeong, Y-S. Jeong and O. Omitaomu, "Weighted dynamic time warping for time series classification," *Pattern Recognition*, vol. 44, no. 9, pp. 2231–2240, 2011.
- [212] K. Kawagoe and A. Al-Maruf, "Searching time series using textual approximation," in *The Third International Conference on Emerging Databases (EDB 2011)*. EDB, 2011, pp. 121–132.
- [213] A. A. Maruf, H. H. Huang, and K. Kawagoe, "Textual approximation methods for time series classification: Tax and l-tax," *IEICE Transactions on Information and Systems*, vol. 97, no. 4, pp. 798–810, 2014.

- [214] D. E. Zhuang, G. C. Li, and A. K. Wong, "Discovery of temporal associations in multivariate time series," *IEEE Transactions on associations in multivariate time series. Knowledge and Data Engineering*, vol. 26, no. 12, pp. 2969–2982, 2014.
- [215] U. Kamath, J. Lin, and K. De Jong, "Sax-efg: an evolutionary feature generation framework for time series classification," in *Proceedings of the 2014 conference on Genetic and evolutionary computation*, 2014, pp. 533–540.
- [216] G. Salton, A. Wong, and Y. C-S., "A vector space model for automatic indexing," *Communications of the ACM*, vol. 18, no. 11, pp. 613–620, 1975.
- [217] M. M. M. Fuad, "One-step or two-step optimization and the overfitting phenomenon: A case study on time series classification," *arXiv*, 2014.
- [218] J. Lin, R. Khade, and Y. Li, "Rotation-invariant similarity in time series using bag-of-patterns representation," *ournal of Intelligent Information Systems*, vol. 39, no. 2, pp. 287–315, 2012.
- [219] M. G. Baydogan, G. Runger, and E. Tuv, "A bag-of-features framework to classify time series," *IEEE Transactions on Pattern Analysis and Machine Intelligence.*, vol. 35, no. 11, pp. 2796–2802, 2013.
- [220] J. Hills, J. Lines, E. Baranauskas, J. Mapp, and A. Bagnall, "Classification of time series by shapelet transformation," *Data Mining and Knowledge Discovery*, vol. 28, no. 4, pp. 851–881, 2014.
- [221] T. Rakthanmanon and E. Keogh, "Fast shapelets: A scalable algorithm for discovering time series shapelets," in *Proceedings of the thirteenth SIAM conference on data mining (SDM)*, 2013.
- [222] M. Wistuba, J. Grabocka, and L. Schmidt-Thieme, "Ultra-fast shapelets for time series classification," *arXiv*, vol. cs.lg, 2015.
- [223] J. P. Eckmann, O. S. Kamphorst, and D. Ruelle, "Recurrence plots of dynamical systems," *Europhysics Letters*, vol. 4, no. 9, pp. 973–977, 1987.

- [224] D. F. Silva, V. M. De Souza, and G. E. Batista, "Time series classification using compression distance of recurrence plots," in *2013 IEEE 13th International Conference on Data Mining (ICDM)*. IEEE, 2013, pp. 687–696.
- [225] B. J. L. Campana and E. J. Keogh, "A compression based distance measure for texture," in *Proceedings of the 10th SIAM International Conference on Data Mining*, 2010, pp. 850–861.
- [226] F. Mörchen, "Time series feature extraction for data mining using dwt and dft," Philipps-University Marburg.
- [227] F. K. P. Chan, A. W. C. Fu, and C. Yu, "Haar wavelets for efficient similarity search of time-series: with and without time warping," *IEEE Transactions on Knowledge and Data Engineering*, vol. 15, no. 3, pp. 686–705, 2003.
- [228] R. Gupta, A. Mittal, and K. Singh, "A time-series-based feature extraction approach for prediction of protein structural class," *EURASIP Journal on Bioinformatics and Systems Biology*, vol. 2, 2008.
- [229] P. Fryzlewicz and H. Ombao, "Consistent classification of nonstationary time series using stochastic wavelet representations," *Journal of the American Statistical Association*, vol. 104, 2009.
- [230] S. Banerjee and M. Mitra, "Application of crosswavelet transform and wavelet coherence for classification of ecg patterns," in *Third International Conference on Emerging Applications of Information Technology (EAIT)*. IEEE, 2012, pp. 89–92.
- [231] A. Kumar and S. Tale, "Similarity measurement technique of two ecg signals analysis and pattern classification," *International journal of scientific Engineering and technology research*, vol. 4, no. 21, pp. 4023–4030, 2015.
- [232] E. Keogh and S. Kasetty, "On the need for time series data mining benchmarks: a survey and empirical demonstration," *Data Mining and knowledge discovery*, vol. 7, no. 4, pp. 349–371, 2003.

- [233] J. Paparrizos and E. Keogh, “A note on the z-normalization of some ucr time-series datasets,” [http://www.cs.columbia.edu/~jopa/Papers/note\\_about\\_UCR\\_archive\\_values.pdf](http://www.cs.columbia.edu/~jopa/Papers/note_about_UCR_archive_values.pdf), September 2015.
- [234] J. Serrà and J. L. Arcos, “An empirical evaluation of similarity measures for time series classification,” *Knowledge-Based Systems*, vol. 67, pp. 305–314, 2014.
- [235] A. Bagnall, L. Davis, J. Hills, and J. Lines, “Transformation based ensembles for time series classification,” in *Proceedings of the Twelfth SIAM International Conference on Data Mining*, Anaheim, California, USA, 2012, pp. 307–318.
- [236] G. E. Batista, X. Wang, and E. J. Keogh, “A complexity-invariant distance measure for time series,” in *Proceedings of the SIAM International Conference on Data Mining.*, 2011, pp. 699–710.
- [237] W. C. Thompson, “Painting the target around the matching profile: the texas sharpshooter fallacy in forensic dna interpretation,” *Law, Probability and Risk*, vol. 8, no. 3, pp. 257–276, 2009.
- [238] D. Pham and A. Chan, “Control chart pattern recognition using a new type of self-organizing neural network,” *Proceedings of the Institution of Mechanical Engineers, Part I: Journal of Systems and Control Engineering*, vol. 212, pp. 115–127, 1998.
- [239] M. Chris, S. Banerjee, and A. E. Hassanien, “Clustering time series data: An evolutionary approach,” *Foundations of computational intelligence*, vol. 6, pp. 193–207, 2009.
- [240] *Making Time-series Classification More Accurate Using Learned Constraints*. SIAM International Conference on DATA MINING, 2004.
- [241] N. Saito, “Local feature extraction and its applications using a library of bases,” Ph.D. dissertation, Yale University, New Haven, USA, 1994.
- [242] E. Keogh, L. Wei, X. Xi, L. Sang-hee, and M. Vlachos, “Lb\_keogh supports exact indexing of shapes under rotation invariance with arbitrary representations and distance measures.” *Very large Databases*, 2006.

- [243] A. Gandhi, "Content-based image retrieval: Plant species identification," Master's thesis, Oregon State University, September 2002.
- [244] O. J. O. Soderkvist, "Computer vision classification of leaves from swedish trees," Master's thesis, Linkoping University, Sweden, 2001.
- [245] D. Roverso, "Multivariate temporal classification by windowed wavelet decomposition and recurrent neural networks," Washington, DC, 2000, pp. 2–8.
- [246] P. Geurts, "Contributions to decision tree induction: bias/variance tradeoff and time series classification," Ph.D. dissertation, Department of Electrical Engineering, University of Liege, Belgium, 2002.
- [247] D. Eads, S. Hill, S. Davis, J. Perkins, R. Porter, and J. Theiler, "Genetic algorithms and support vector machines for time series classification," in *SPIE*, vol. 4787, 2002, pp. 74–85.
- [248] R. Olszewski, "Generalized feature extraction for structural pattern recognition in time-series data," Ph.D. dissertation, Carnegie Mellon University, Pittsburgh, 2001.
- [249] A. Jalba, M. Wilkinson, J. Roerdink, M. Bayer, and S. Juggins, "Automatic diatom identification using contour analysis by morphological curvature scale spaces," *Machine Vision and Applications*, vol. 16, no. 4, pp. 217–228, 2005.
- [250] L. Wei and E. Keogh, "Semi-supervised time series classification," in *12th ACM SIGKDD International Conference on Knowledge Discovery and Data Mining (KDD 2006)*, 2006, pp. 748–753.
- [251] D.-j. Lee, R. B. Schoenberger, D. Shiozawa, and X. Xu, "Contour matching for a fish recognition and migration-monitoring system," *Proceedings of the SPIE*, vol. 5606, pp. 37–48, 2004.
- [252] O. AlJowder, E. Kemsley, and R. Wilson, "Detection of adulteration in cooked meat products by mid-infrared spectroscopy," *Journal of agricultural and food chemistry*, vol. 50, 2003.